

PYRROLIC PIGMENTS

by

CHRISTIAN BRÜCKNER

Dipl.Chem., Rheinisch-Westfälisch Technische Hochschule Aachen, Germany, 1991

A THESIS SUBMITTED IN PARTIAL FULFILLMENT OF
THE REQUIREMENTS FOR THE DEGREE OF
DOCTOR OF PHILOSOPHY

in

THE FACULTY OF GRADUATE STUDIES
DEPARTMENT OF CHEMISTRY

We accept this thesis as conforming to the required standard

THE UNIVERSITY OF BRITISH COLUMBIA, VANCOUVER

March 1996

© Christian Brückner, 1996

In presenting this thesis in partial fulfilment of the requirements for an advanced degree at the University of British Columbia, I agree that the Library shall make it freely available for reference and study. I further agree that permission for extensive copying of this thesis for scholarly purposes may be granted by the head of my department or by his or her representatives. It is understood that copying or publication of this thesis for financial gain shall not be allowed without my written permission.

Department of CHEMISTRY

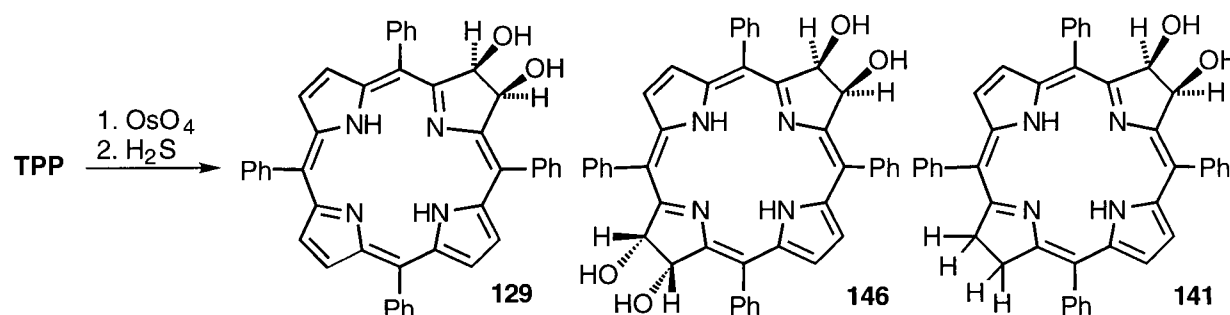
The University of British Columbia
Vancouver, Canada

Date 12/3/96

ABSTRACT

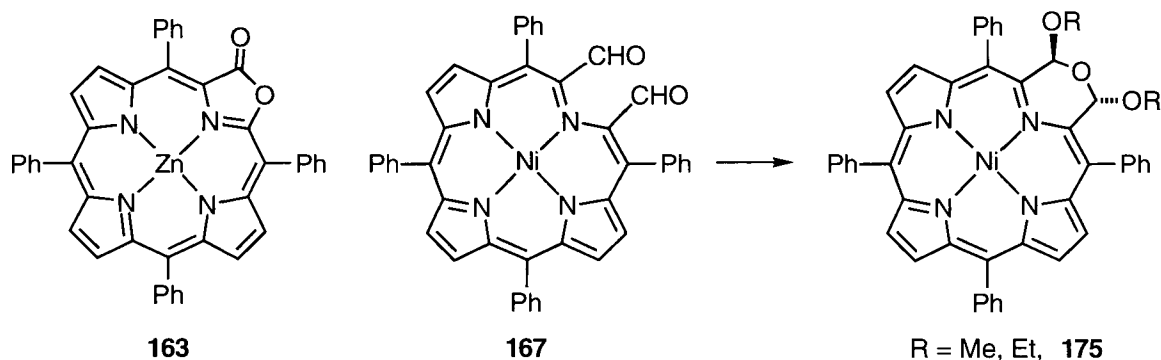
Part 1 presents studies aimed at the synthesis of novel aromatic tetra- and pentapyrrolic pigments with *meso*-phenyl substituents and with long wavelengths of absorption. Such compounds are potential photosensitizers for use in photodynamic therapy (PDT). Several approaches are described:

1. The osmium tetroxide mediated dihydroxylation of variously substituted *meso*-tetraphenylporphyrins (**TPP**) to provide novel stable chlorins such as **129** and bacteriochlorins such as **141** and **146** is reported. The directing effect of the central metal zinc in the stereo- and regiochemical outcome of the dihydroxylation of *meso*-tetraphenylchlorins is outlined. The resulting β,β' -dihydroxylated amphiphilic chlorins are characterized by spectroscopic and analytical techniques. Preliminary *in vitro* biological results of their potency as drugs in PDT have been encouraging. One side-product of the osmylation reaction, the 2-oxa-3-oxochlorin **163**, was structurally characterized by X-ray crystallography.

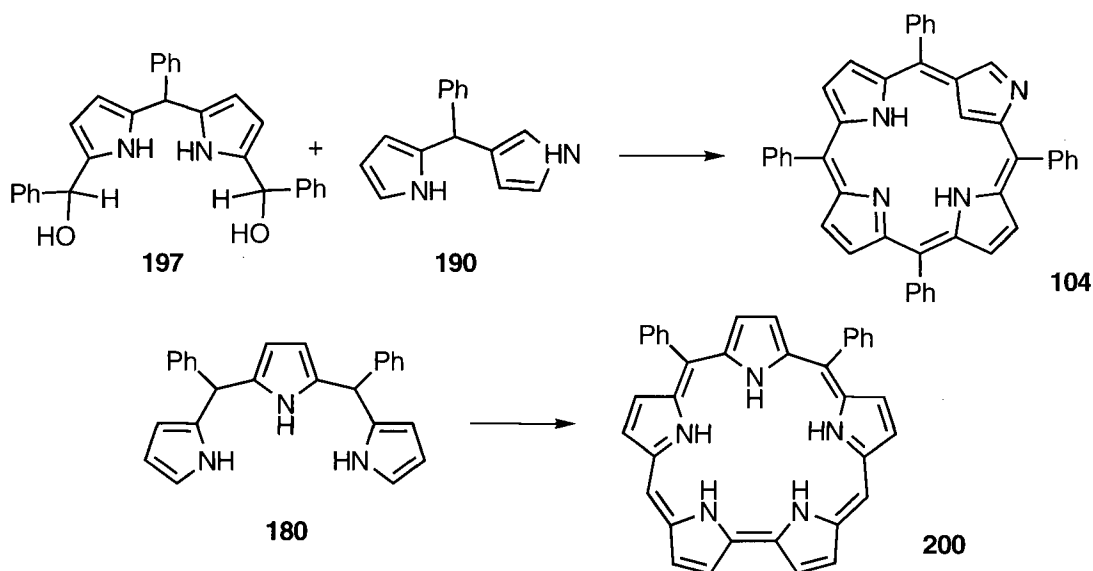


Some unique physical (observable rotation of the phenyl groups) and chemical properties of the β,β' -diolchlorins are reported. For instance, *meso*-tetraphenyl-2,3-*vic*-dihydroxy-2,3-chlorinato)nickel(II) can be converted oxidatively into the corresponding 2,3-secochlorin-2,3-dialdehyde **167**. This compound can ring-close to the novel double ketal

175. This severely distorted pigment has been structurally characterized by X-ray crystallography and is without precedent.

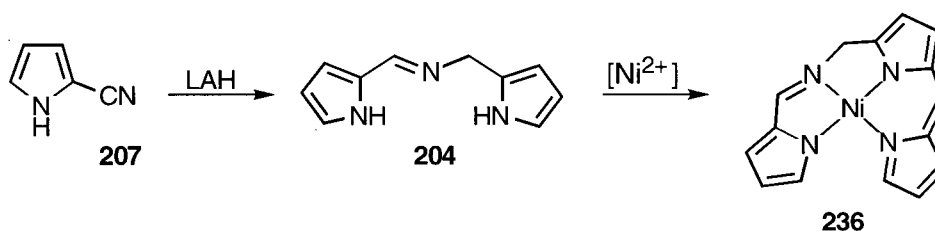


2. A directed synthesis of N-confused porphyrin **104** was developed. The key step in the synthesis was a 2+2-type condensation of dipyrrromethane **197** with the novel α,β -linked dipyrrromethane **190**. Although the goal of producing **104** in high yields could not be met, this study provided valuable insight into the chemistry of dipyrrromethanes and provided through fortuitous circumstance tripyrrane **180**.

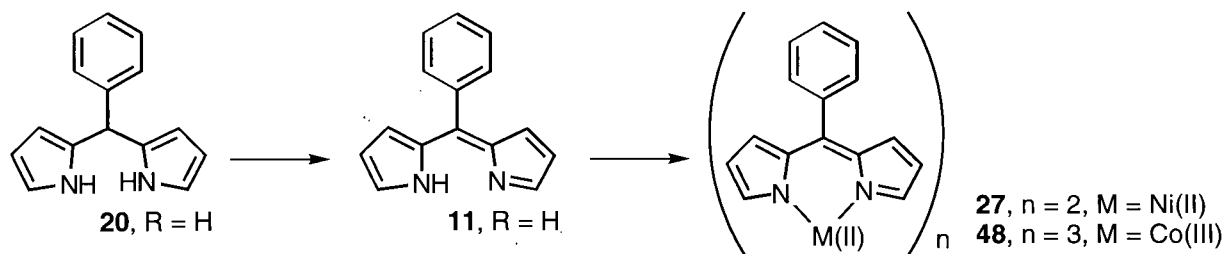


3. Tripyrrane **180** is the key reagent in the directed high-yield synthesis of *meso*-phenyl-sapphyrins such as **200**. As inferred from spectroscopic properties, the protonation dependent conformation of **200** is described.

4. Studies towards the elucidation of the mechanism of formation of porphycyanines *via* the lithium aluminum hydride (LAH) reduction pathway of 2-cyanodipyrromethanes are presented. To this end, variously substituted 2-cyanopyrroles were prepared and reduced by LAH. It was found that imine linked dimers such as **204** are directly formed during this reduction. A mechanistic proposal for this outcome is presented. A unique reaction of **204** with nickel(II) to form the tripyrrolic complex **236** is described. The complex was structurally characterized by X-ray crystallography and its mode of formation has been rationalized.



Part 2 describes the synthesis of 5-phenyldipyrromethane (**20**) and the conversion into the corresponding *meso*-phenyldipyrins (**11**). Their ability to complex to transition metals is described and the optical spectra of the resulting dipyrinat^o complexes of nickel(II), copper(II), and zinc(II) are discussed in depth, compared to known alkyldipyrinat^o complexes and correlated to their structure. The special steric properties of the novel *meso*-phenyl dipyrins are highlighted by the structural characterization of two unusual complexes, namely the square planar diamagnetic nickel(II) complex **27** and octahedral copper(III) complex **48**.



Part 3 describes the improved preparation of dipyrromethane **2** by direct hydrodesulfurization of thione **7** with Raney-nickel/H₂. It was also found that 2-pyrrolylthiones chelate in an N,S-bidentate fashion to a variety of transition metals. The preparation of, for instance, the square planar nickel(II) (**29**), octahedral copper(III) (**33**, two isomers) and tetrahedral mercury(II) (**32**) chelates of **7** are described and their spectroscopic properties are correlated to their structures. The steric requirements for the dipyrrolylthione ligand were determined. These complexes as well as the free base **7** were structurally characterized by X-ray crystallography. Furthermore, the synthesis of the 2-thioacetylpyrrole and 2-thiobenzoylpyrrole and their nickel(II) and cobalt(III) complexes is described. This is the first report of the complexing ability of the 2-pyrrolyl moiety.

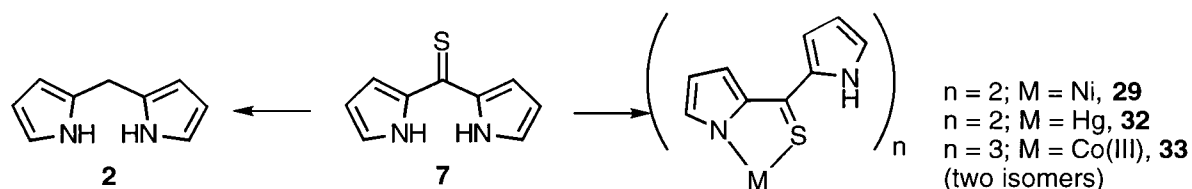


TABLE OF CONTENTS

ABSTRACT	ii
TABLE OF CONTENTS	vi
LIST OF TABLES	xii
LIST OF FIGURES	xiv
LIST OF SCHEMES	xvii
LIST OF ABBREVIATIONS	xxi
NOMENCLATURE	xxii
References	xxviii
ACKNOWLEDGMENTS	xxix
GENERAL INTRODUCTION TO PYRROLIC PIGMENTS	1
Part 1: SYNTHESIS AND STUDY OF PYRROLIC PIGMENTS FOR USE IN PHOTODYNAMIC THERAPY (PDT)	
1. INTRODUCTION AND LITERATURE REVIEW	5
1.1 Photodynamic Therapy (PDT)	5
1.1.1 History and General Introduction	5
1.1.2 Photophysical and Photochemical Basis of PDT	9
1.1.3 The Profile of the Ideal PDT Drug	13
1.2 Research Objective	15
1.3 Review of Synthesis and Properties of Pyrrolic Pigments Potentially Useful in PDT	16
1.3.1 Porphyrins	16

1.3.1.1	Naturally Occurring Porphyrins	16
1.3.1.2	Synthetic Porphyrins	17
1.3.2	Chlorins, Bacterio- and Isobacteriochlorins	21
1.3.2.1	The Optical Properties of Chlorins	21
1.3.2.2	Naturally Occurring Chlorins	24
1.3.2.3	The Total Synthesis of Chlorins	24
1.3.2.4	The Conversion of Porphyrins into Chlorins by Reduction	27
1.3.2.5	Non-Reversible Conversions of Porphyrins into Chlorins	31
1.3.3	Synthesis of β -Hydroxychlorins	38
1.3.3.1	The Osmium Tetroxide Oxidation in General	38
1.3.3.2	The Mechanism of the Osmium Tetroxide Addition to Double bonds	41
1.3.3.3	The Osmium Tetroxide Oxidation of Aromatic Systems	43
1.3.3.4	The Osmium Tetroxide Oxidation of Porphyrins	46
1.3.3.5	Reactivity of <i>vic</i> -Diol Chlorins	51
1.3.3.6	β -Hydroxychlorins not Derived from an Osmium Tetroxide Oxidation	52
1.3.3.7	β -Oxochlorins and Related Pigments	55
1.3.4	Porphyrin Isomers	62
1.3.5	Expanded Porphyrins	67
2.	RESULTS AND DISCUSSION	74
2.1	The Osmium Tetroxide-Mediated Dihydroxylation of <i>meso</i> -Phenylporphyrins and -chlorins	74
2.1.1	The Osmylation of TPP - The Principal Reaction	75

2.1.2	The Osmylation of <i>meso</i> -Tetraphenylchlorins	85
2.1.2	The Osmylation of <i>meso</i> -Tetraphenyl-2,3-dihydroxy-2,3- chlorins and -metallochlorins	88
2.1.3	Comments on the Optical Spectra of the β,β' -Diolchlorins	91
2.1.4	Preliminary Results of the Biological Activity of Diolchlorin 137	92
2.1.5	Rotation of Phenyl Rings in <i>meso</i> -Tetraphenyl- β,β' - <i>vic</i> -diolchlorins and -metallochlorins	95
2.1.6	The Reactivity of the <i>meso</i> -Tetraphenyl- <i>vic</i> -diolchlorins	101
2.1.6.1	Formation of Isopropylidene Ketal 150	101
2.1.6.2	Formation of β -Oxo-Derivatized Pigments	102
2.1.6.3	Formation of 2-Oxa-3-oxochlorin 163	108
2.1.6.4	Formation of a Secochlorin and Subsequent Ring- Closure Reactions	115
2.2	Studies Towards the Directed Synthesis of N-confused TPP	124
2.2.1	Retrosynthetic Analysis of N-Confused Porphyrin	124
2.2.2	The Directed Synthesis of N-Confused Porphyrin	126
2.3	The Directed Synthesis of <i>meso</i> -Phenylsapphyrins	134
2.4	The Reductive Coupling of 2-Cyanopyrroles	141
2.5	The Unexpected Formation of a Tripyrrolic Tetradentate Nickel Chelate (236)	149
3.	EXPERIMENTAL	156
3.1	Instrumentation and Materials	156
3.1	<i>meso</i> -Aryl- <i>vic</i> -diolchlorins, -bacteriochlorins and -isobacteriochlorins	159
3.2	Reactions of the <i>meso</i> -Tetraphenyl- <i>vic</i> -diol-chlorins	169

3.3	The Directed Synthesis of N-Confused TPP	174
3.4	The Directed Synthesis of Sapphyrins	180
3.5	The Preparation of Cyanopyrroles	184
3.6	The Reductive Coupling of 2-Cyanopyrroles	188
3.7	The Formation of Complex 236	191
3.8	Crystal Structure Analyses of 163 -pyridine, 175 and 236	192
4.	REFERENCES	202

Part 2: *meso*-PHENYLDIPYRRINS - SYNTHESIS AND METAL COMPLEX FORMATION

1.	INTRODUCTION	223
1.1	Alkyldipyrins and Their Metal Complexes	223
1.2	<i>meso</i> -Substituted 4,6-Dipyrins	226
1.3	4,7-Dipyrins	228
1.4	Tripyrins and Related Tripyrrolic Pigments	229
2.	RESULTS AND DISCUSSION	230
2.1	Synthesis of 5-Phenyldipyrromethanes	230
2.2	Preparation and Characterization of <i>meso</i> -Phenyldipyrins	231
2.3	Formation and Characterization of Transition Metal Chelates of <i>meso</i> -Phenyldipyrins	234
2.3.1	The Complexes of Ni(II), Cu(II), and Zn(II)	234
2.3.2	Crystal Structure Analysis of bis(<i>meso</i> -Phenyl- dipyrinato)Ni(II) (27)	244
2.3.3	The Complexes of Cobalt(II) and Cobalt(III)	248
2.3.4	Crystal Structure Analysis of tris(<i>meso</i> -Phenyl-	

	dipyrinato)cobalt(III) (48)	251
2.4	The DDQ-Oxidation of <i>meso</i> -Diphenyltripyrane (49)	253
3.	CONCLUSIONS	257
4.	EXPERIMENTAL SECTION	258
4.1	Dipyrromethanes, Dipyrins and their Metal Complexes	259
4.2	Crystal Structure Analysis of 27 and 48	265
5.	LIST OF REFERENCES	270

Part 3: 2-PYRROLYLTHIONES AS N,S-BIDENTATE CHELATORS

1.	INTRODUCTION	275
1.1	2-Pyrrolylthiones as Common Precursors Used in a Porphyrin Synthesis	275
1.2	Thiocarbonyl Compounds	278
1.3	Sulfur Donor-Metal Complexes in Biological Systems	280
1.4	Sulfur-Nitrogen Chelating Agents and their Metal Complexes	281
2.	RESULTS AND DISCUSSION	283
2.1	Synthesis of di-2-Pyrrolylthiones	283
2.2	Hydrodesulfurization of di-2-Pyrrolylthiones	284
2.3	Reaction of di-2-Pyrrolylthione (7) with Nickel(II)	286
2.4.	Solution and Solid State Conformation of di-2-Pyrrolylthione (7) and -ketone (6)	288
2.5	Spectroscopic Properties of Complex 29	291
2.6	Structural Characterization of Complex 29	293

2.7	Transformations of Complex 29	297
2.8	The Reaction of di-2-Pyrrolylthione (7) with Various Metal Ions, and Structural Characterization of Selected Complexes	299
2.8.1	Reaction of Thione 7 with Mercury(II)	299
2.8.2	Reaction of Thione 7 with Cobalt(II) and Cobalt(III)	302
2.8.3	Reaction of Thione 7 with Various Metal Ions	306
2.9	Establishment of the Steric Requirements of the 2-Pyrrolylthionato- moiety	307
2.10	Synthesis of 2-Thioacetyl- (37) and 2-Thiobenzoylpyrrole (38), and Formation of the Nickel(II) and Cobalt(III) Complexes thereof	310
2.11	Preliminary Reports on the Formation of Tetradentate Ligands Containing the 2-pyrrolylthione Motif, and their Nickel(II) complexes	313
3.	CONCLUSION AND FUTURE WORK	316
4.	EXPERIMENTAL	317
3.1	Instrumentation and Materials	317
3.2	2-Pyrrolylketones	319
3.3	2-Pyrrolylthiones	320
3.4	2-Pyrrolylthionatometal Complexes	324
3.5	Hydrodesulfurization of 2-Pyrrolylthiones	332
3.6	Crystal Structure Analyses of 6 , 7 , 29 , 33-I , and 32	334
5.	LIST OF REFERENCES	343

LIST OF TABLES

Table 0-1	Fischer nomenclature for selected naturally occurring porphyrins	xxvi
Table 1-1	Optical spectra of the novel diol chlorins in comparison to their non-dihydroxylated analogs	92
Table 1-2	Crystallographic data for 163 -pyridine, 175 , and 236	193
Table 1-7	Atomic coordinates and B_{eq} [\AA^2] for 163 -pyridine	194
Table 1-4	Selected bond lengths [\AA] in 163 -pyridine with estimated standard deviations in parentheses	196
Table 1-7	Atomic coordinates and B_{eq} [\AA^2] for 175	197
Table 1-6	Selected bond lengths [\AA] in 175 with estimated standard deviations in parentheses	199
Table 1-7	Atomic coordinates and B_{eq} [\AA^2] for 236	200
Table 1-8	Bond lengths in 236 [\AA]	201
Table 2-1	UV-visible data and dihedral angles of literature known and novel dipyrinato-complexes	238
Table 2-2	Selected bond lengths in 27	245
Table 2-3	Nickel-nitrogen bond lengths in selected tetrapyrrolic pigments	246
Table 2-4	Crystallographic data of compounds 27 and 48	267
Table 2-5	Atomic coordinates and B_{eq} [\AA^2] for 27	268
Table 2-6	Atomic coordinates and B_{eq} [\AA^2] for 48	268
Table 3-1	Crystallographic data for 6 and 7	335
Table 3-2	Crystallographic data for 29 , 33-I , and 32	336
Table 3-3	Atomic coordinates and B_{eq} [\AA^2] for 7	337

Table 3-4	Atomic coordinates and $B_{eq}[\text{\AA}^2]$ for 6	337
Table 3-5	Atomic coordinates and $B_{eq}[\text{\AA}^2]$ for 29	338
Table 3-6	Atomic coordinates and $B_{eq}[\text{\AA}^2]$ for 32	339
Table 3-7	Atomic coordinates and $B_{eq}[\text{\AA}^2]$ for 33-I	340
Table 3-8	Selected bond lengths in 7 with estimated standard deviations in parentheses	341
Table 3-9	Selected bond lengths in 6 with estimated standard deviations in parentheses	342
Table 3-10	Selected bond lengths in 29 with estimated standard deviations in parentheses	342

LIST OF FIGURES

Figure 1-1	Structures of selected second generation photosensitizers	9
Figure 1-2	Modified Jablonski diagram for a typical photosensitizer	10
Figure 1-3	Type I photoprocesses	12
Figure 1-4	Type II photoprocesses	12
Figure 1-5	Optical (CHCl ₃) spectrum of protoporphyrin IX dimethyl ester	16
Figure 1-6	The different concepts of porphyrin synthesis	17
Figure 1-7	UV-visible spectrum of chlorin 1 and bacteriochlorin TPBC	21
Figure 1-8	Energy level diagram for the frontier orbitals of the four generic metalloporphyrin classes	22
Figure 1-9	X-Ray crystal structure of C ₆₀ -buckminsterfullerene osmate ester (from Hawkin <i>et al.</i> ^{186b})	45
Figure 1-10	X-Ray crystal structure of 53 (from Barkingia <i>et al.</i> ^{241b})	48
Figure 1-11	18 π -Electron delocalization pathway in porphyrins, chlorins and metallochlorins	49
Figure 1-12	Porphine - isoporphine tautomerism	66
Figure 1-13	¹ H-NMR spectra of 125 (bottom trace) and NOE difference spectrum of 125 (top trace)	76
Figure 1-14	Optical spectrum (CH ₂ Cl ₂ /0.5% MeOH) of 129 and 130	80
Figure 1-15	¹ H-NMR of 134 (bottom trace) and of 135 (top trace)	83
Figure 1-16	Measured (A) ¹ H-NMR signal of the pyrroline protons in 141 and coupling constants determined by simulation (B)	86
Figure 1-17	Optical spectrum (CH ₂ Cl ₂ /0.5%MeOH) of 141 and 144	86
Figure 1-18	Optical spectrum (CH ₂ Cl ₂ /0.5%MeOH) of 146 and 149	88

Figure 1-19	Schematic representation of the face differentiation in <i>meso</i> -tetraphenylmetalloporphyrins with additional ligands (A) and in β,β' - <i>vic</i> -diolchlorins (B)	96
Figure 1-20	Temperature dependent $^1\text{H-NMR}$ spectrum of 129	99
Figure 1-21	Temperature dependent $^1\text{H-NMR}$ spectrum of 130	100
Figure 1-22	Normalized optical spectra (CH_2Cl_2) of 151 and 152	102
Figure 1-23	Optical spectra (CH_2Cl_2) of 163 and 164	109
Figure 1-24	$^1\text{H-NMR}$ spectrum of 163 and 164	110
Figure 1-25	ORTEP representation (33% probability level) and side view of 163 ·pyridine	112
Figure 1-26	Normalized optical spectra (CH_2Cl_2) of 167 and 168	116
Figure 1-27	Optical spectrum (CH_2Cl_2) of 173	118
Figure 1-28	ORTEP representation (33% probability level) of 175	121
Figure 1-29	Side view and stereo view of the crystal structure of 175	122
Figure 1-30	Optical spectrum (CH_2Cl_2) of 200 and 200 ·2HCl	136
Figure 1-31	$^1\text{H-NMR}$ of 200 and 200 ·2HCl	138
Figure 1-32	Conformation of diphenylsapphyrin 200 as free base and as diprotonated species	139
Figure 1-33	Optical spectrum (CHCl_3) of 236	149
Figure 1-34	$^1\text{H NMR}$ spectrum of 236	150
Figure 2-1	<i>meso</i> -Methyldipyrin - <i>meso</i> -ylidenedipyrane equilibrium	226
Figure 2-2	UV-visible spectrum of 11 in MeOH, and in MeOH/trace HCl, and 23 in MeOH/trace HCl	231
Figure 2-3	UV-visible spectra (CH_2Cl_2) of 27 and 26	235
Figure 2-4	UV-visible spectra of 25 and 24 in CH_2Cl_2 , and of 24 in $\text{CH}_2\text{Cl}_2/20\%$ pyridine	236
Figure 2-5	$^1\text{H-NMR}$ spectrum of 26	242

Figure 2-6	ORTEP representation (33% probability level) of 27	245
Figure 2-7	Limiting resonance forms of the dipyrinato ligands	247
Figure 2-8	Optical spectrum (CHCl ₃) of 46 and 48 in	248
Figure 2-9	ORTEP representation (33% probability level) of 48	251
Figure 2-10	Optical spectrum of equal concentrations of 50	253
Figure 2-11	¹ H-NMR spectrum of 50	254
Figure 3-1	Normalized optical spectra (MeOH) of 2-pyrrolylketone (6) and 2-pyrrolylthione (7)	279
Figure 3-2	Optical (CH ₂ Cl ₂) spectrum of 29	286
Figure 3-3	ORTEP representation (33% probability level) and unit cell of 6	290
Figure 3-4	ORTEP representation (33% probability level) and unit cell of 7	290
Figure 3-5	C,H-COSY (500, 125 MHz, acetone-d ₆) of 29	292
Figure 3-6	ORTEP representation (33% probability level) and side view of 29 ..	294
Figure 3-7	Bond lengths and angle changes of the ligand 7 upon metallation	295
Figure 3-8	Intermolecular interaction as seen in the crystal of 29	295
Figure 3-9	Optical spectrum (CH ₂ Cl ₂) of mercury complex 32	230
Figure 3-10	Stereoscopic view of the mercury complex 32	301
Figure 3-11	Optical spectra (CH ₂ Cl ₂) of the cobalt complexes 33-I	302
Figure 3-12	¹ H-NMR spectrum of the two isomeric complexes 40-I and 40-II	303
Figure 3-13	ORTEP representation (33% probability level) of 33-I (as its acetone solvate)	305
Figure 3-14	Computer generated model of a hypothetical nickel(II) complex with an α-methylthionato ligand	308
Figure 3-15	Optical spectrum (CH ₂ Cl ₂) of 41 and 42	311
Figure 3-16	Normalized optical spectra (CH ₂ Cl ₂) of 44-I , 44-II and 43	312
Figure 3-17	Optical spectrum (CH ₂ Cl ₂) of 47	314

LIST OF SCHEMES

Scheme 1-1	Rothemund synthesis of <i>meso</i> -tetraphenylporphyrin (6)	19
Scheme 1-2	Rothemund-type synthesis of <i>meso</i> -tetraalkylmetallochlorins 13	25
Scheme 1-3	MacDonald 2+2 synthesis of metallochlorin 17	26
Scheme 1-4	Diimide reduction of TPP (6)	28
Scheme 1-5	Reduction of 2-nitro-TPP (25)	30
Scheme 1-6	Diels-Alder reactions of protoporphyrin IX dimethyl ester (27).	32
Scheme 1-7	Preparation of BPD-MA	33
Scheme 1-8	Cyclopropanation of TPP with a carbene	34
Scheme 1-9	Formation of octaethylpurpurin (36) and octaethylbenzochlorin (37)	36
Scheme 1-10	Claisen-type rearrangement of a hydroxyethyl-substituted porphyrin	37
Scheme 1-11	Osmium tetroxide mediated dihydroxylation of alkenes	39
Scheme 1-12	Mechanistic alternatives for the osmylation of olefins	41
Scheme 1-13	Osmium tetroxide mediated dihydroxylation of polycyclic aromatics	43
Scheme 1-14	Osmylation of C ₆₀ -buckminsterfullerene	44
Scheme 1-15	Osmium tetroxide mediated dihydroxylation of deuterio- porphyrin dimethylester (48)	46
Scheme 1-16	Osmium tetroxide mediated dihydroxylation of OEP	47
Scheme 1-17	Stepwise reaction of benzoporphyrin derivative (56) with osmium tetroxide	50

Scheme 1-18	Pinacol-pinacolone-type rearrangement of the <i>vic</i> -diolalkyl-chlorins	51
Scheme 1-19	Dehydration and rearrangement of <i>vic</i> -dihydroxy-octaethylchlorin 53	51
Scheme 1-20	Photochemical synthesis of bacteriodiol-monomethyl ether 67	53
Scheme 1-21	Formation of photoporphyrin (73)	54
Scheme 1-22	Hydroxylation and rearrangement of β -oxochlorins and β -oxometallochlorins	56
Scheme 1-23	Preparation of Bonnett's chlorins with graded amphiphilicity	57
Scheme 1-24	Hydroxylation of keto-chlorin 86 and its reduction to triol 87	58
Scheme 1-25	Formation of <i>meso</i> -hydroxyoctaethylporphyrin	60
Scheme 1-26	Formation of octaethylporphycene (100)	63
Scheme 1-27	Formation of sapphyrin (105), pentaphyrin (106), and hexaphyrin (107)	69
Scheme 1-28	Formation of porphocyanine (115)	69
Scheme 1-29	Formation of <i>meso</i> -phenyl substituted porphocyanines	73
Scheme 1-30	Osmylation of TPP to form the corresponding osmate ester chlorins	78
Scheme 1-31	Reduction of the osmate ester chlorins to form the corresponding diol chlorins and the one-step conversion of porphyrins into diol chlorins	79
Scheme 1-32	Preparation of diolbacteriochlorin 141	85
Scheme 1-33	Preparation of the diolisobacteriochlorins 143 and 144	87
Scheme 1-34	Preparation of the tetraolbacterio- and tetraolisobacteriochlorins 145-149	89
Scheme 1-35	Formation of acetonide 150	101

Scheme 1-36	Dehydration of the β,β' -diolchlorins to give the corresponding ketochlorins 151	103
Scheme 1-37	Formation of 154	104
Scheme 1-38	Formation of β,β' -dione chlorin 156 and 157	105
Scheme 1-39	Proposed formation of dioxobacterio and -isobacteriochlorins	107
Scheme 1-40	Proposed autooxidation mechanism for the formation of 163	114
Scheme 1-41	Crossley's synthesis of lactone 164	114
Scheme 1-42	Formation of <i>meso</i> -phenylsecochlorin bisaldehydes 167 and 168	115
Scheme 1-43	Formation of furochlorophin (70)	117
Scheme 1-44	Formation of octaethyl-2,3-secochlorin-2,3-dione (171)	117
Scheme 1-45	Formation of 172 and 173	119
Scheme 1-46	Formation of aldol condensation product 176	123
Scheme 1-47	Retrosynthetic analysis of N-confused porphyrin (104)	125
Scheme 1-48	Directed synthesis of N-confused TPP (104)	128
Scheme 1-49	Rationalization of the findings of the benzylation experiments of 179	129
Scheme 1-50	Proposed mechanism of formation of N-confused porphyrin	132
Scheme 1-51	Alternative retrosynthetic analysis of N-confused porphyrin	133
Scheme 1-52	Synthesis of the <i>meso</i> -phenylsapphyrins 114 , 199 , and 200	135
Scheme 1-52	Proposed alternative synthetic pathway for the formation of <i>meso</i> -phenylporphocyanines	141
Scheme 1-53	Formation of imine-linked dipyrrolic compound 204	142
Scheme 1-54	Syntheses of the cyanopyrroles	144
Scheme 1-55	Outcome of the LiAlH_4 reduction of various cyanopyrroles	145
Scheme 1-56	Mechanism of the LAH coupling of benzaldoxime	147
Scheme 1-57	Hypothetical mechanistic scheme of formation of 204 through the LiAlH_4 reduction of cyanopyrrole 207	148

Scheme 1-58	Proposed mechanism of formation and structure of 236	151
Scheme 1-59	Fragmentation of 236 in the EI mass spectrometer	155
Scheme 2-1	Synthetic pathways towards dipyrrens	224
Scheme 2-2	Formation of <i>meso</i> -phenyldipyrrens	227
Scheme 2-3	Synthesis of <i>meso</i> -phenyldipyrrenes and <i>meso</i> -phenyldipyrrens	230
Scheme 2-4	Formation of dipyrrenato complexes from dipyrrens	234
Scheme 2-5	Formation of cobalt(II) and cobalt(III) dipyrrenato complexes	250
Scheme 2-6	DDQ oxidation of <i>meso</i> -diphenyltripyrrene (49)	255
Scheme 2-7	Classic method for the synthesis of tripyrrenones.	256
Scheme 3-1	Principal pathways for the formation of 5,10- <i>meso</i> -diphenyl- porphyrin (x)	276
Scheme 3-2	Synthesis of di-2-dipyrrolylmethane	276
Scheme 3-3	Formation of dipyrrolylthiones and pyrrolylthione esters	283
Scheme 3-4	Hydrodesulfurization of 7	284
Scheme 3-5	Possible conformers and tautomers of di-2-pyrrolylcarbonyl compounds	288
Scheme 3-6	N-methylation of complex 29	297
Scheme 3-7	Attempted formation of complex 35 and formation of 34	307
Scheme 3-8	Formation of nickel(II) complex 36	309
Scheme 3-9	Synthesis of 2-pyrrolylthiones 37 and 38 , and their nickel(II) and cobalt(III) complex formation	310
Scheme 3-10	Formation of tetradentate 2-pyrrolylthione and -ketone ligands, and their nickel(II) complexes	313

LIST OF ABBREVIATIONS

BPD-MA	benzoporphyrin derivative monoacid
CSI	chlorosulfonylisocyanate
DDQ	2,3-dichloro-5,6-dicyano-1,4-benzoquinone
DMAD	dimethylacetylene dicarboxylate
FGI	functional group interconversion
HMPA	hexamethylphosphoramide
HR-MS	high-resolution mass spectroscopy
LAH	lithium aluminum hydride
LR-MS	low-resolution mass spectroscopy
MCPBA	<i>meta</i> -chloroperbenzoic acid
MO	molecular orbital
MRI	magnetic resonance imaging
NOE	nuclear Overhauser effect
OEP	2,3,7,8,12,13,17,18-octaethylporphyrin
PDT	photodynamic therapy
<i>p</i> -Ts	<i>para</i> -toluenesulfonyl-
TFA	trifluoroacetic acid
TPC	<i>meso</i> -tetraphenylchlorin
TPBC	<i>meso</i> -tetraphenylbacteriochlorin
TPiBC	<i>meso</i> -tetraphenylisobacteriochlorin
TPP	<i>meso</i> -tetraphenylporphyrin

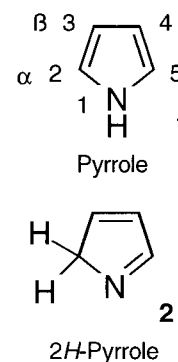
All other abbreviations were used as defined in the "Standard List of Abbreviations" *J. Org. Chem.* **1995**, 60(1), 12A.

NOMENCLATURE

The nomenclature of pyrrolic compounds (pigments and non-pigments) has undergone much revision over the past several decades.¹ The most current IUPAC recommendations² are adopted here. The formal nomenclature is, where appropriate, supplemented with IUPAC accepted trivial names, which continue to be widely used because of their brevity and historic significance. For example, the Fischer³ system for naming the naturally occurring tetrapyrrols and their isomers (Table 1). The abbreviations used for porphyrins are defined in this section.

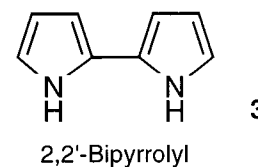
MONOPYRROLIC SYSTEMS⁴

The parent monocyclic system, pyrrole (1), is numbered as shown at right. The Greek letters α and β are used to distinguish between the two types of carbon positions in all pyrrolic pigments. The pyrrole moiety is named '-pyrrolyl'. The isopyrrole structure 2 is the base of the formal nomenclature of dipyrins and related pigments.

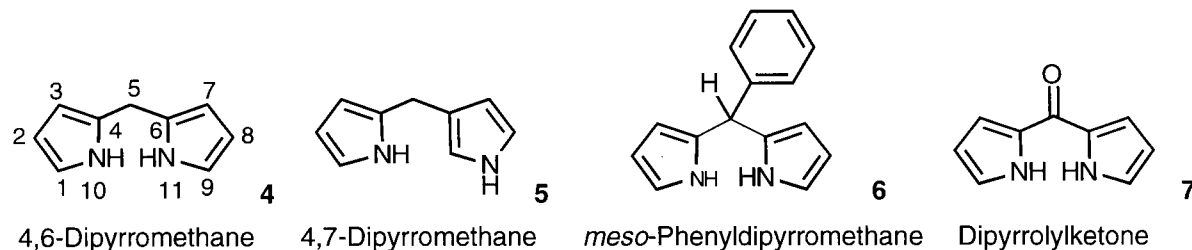


DIPYRROLIC SYSTEMS

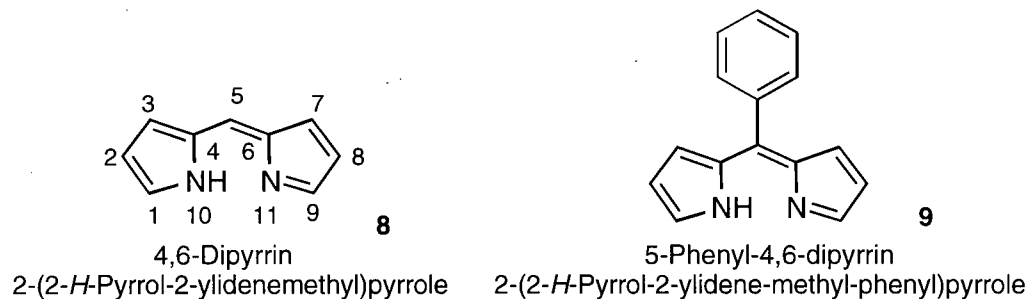
The most simple structure, 3, containing two directly-linked pyrrole rings is named 2,2'-bipyrrolyl. It is commonly referred to as bipyrrole.



The most important dipyrrolic molecules for this work are those comprised of two pyrrole moieties joined by a single carbon bridge, the so called *meso*-carbon.



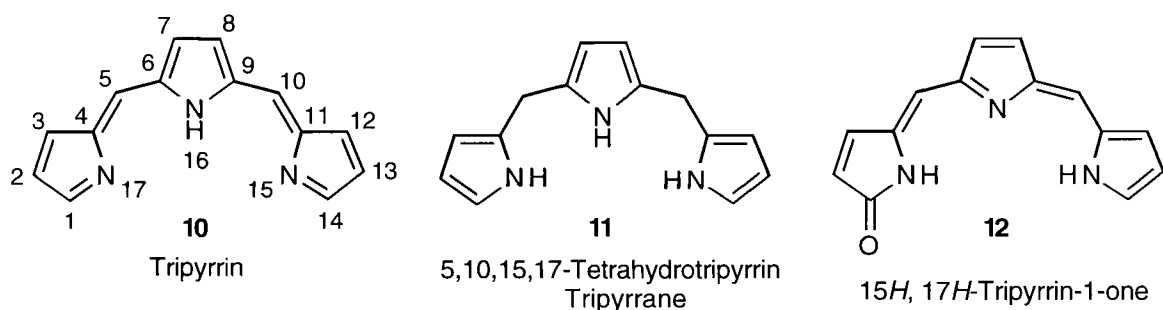
Their numbering scheme and nomenclature is shown above. The parent compound **4** is named 4,6-dipyrromethane. Compound **5** is an isomer of **4**. In this work, discussion of dipyrromethanes refer to the 4,6-isomer, unless otherwise specified. Ketone **7** will be referred to as dipyrrolylketone. The, formally, dehydro-4,6-dipyrromethane **8** is named dipyrrin. This pigment is known in the older literature as dipyrromethene.



In the case of a symmetrically substituted systems, the fast tautomeric exchange of the NH-proton renders the two pyrrolic rings in dipyrins equivalent. In this work, the 4,6-dipyrins will simply be referred to as dipyrins. The 5-position of dipyrins is also referred to as the *meso*-position.

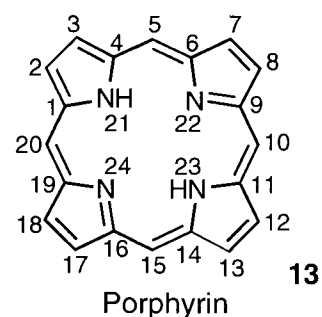
TRIPYRROLIC SYSTEMS⁵

Tripyrrolic systems with directly-linked pyrroles are called terpyrroles.⁶ Most important to this work are tripyrrolic systems with a bridging single carbon unit. The parent compound tripyrrin (**10**) is the most unsaturated system. The reduced tripyrrins are named as dihydro, tetrahydro etc. tripyrrins, with numbers used to denote the positions of saturation. The fully reduced form **11** is named tripyrrane. Positions 5 and 10 are the *meso*-positions.



PORPHYRINS AND RELATED TETRAPYRROLIC SYSTEMS

The fundamental system is the fully unsaturated, cyclic tetrapyrrolic pigment porphyrin (**13**). Positions 2,3,7,8,12,13,17, and 18 are referred to as the β -positions; positions 5,10,15, and 20 as the *meso*-positions; positions 1,4,6,9,11,14,16, and 19 are the α -positions. The structure is tautomeric with



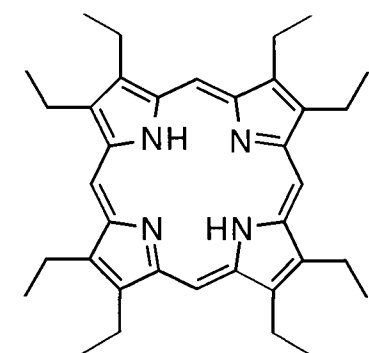
respect to the location of the two inner hydrogens, which may be associated with any two of the four nitrogens. All substituted porphyrins can be named systematically with this system, but for convenience, the naturally occurring porphyrins are named according to the trivial Fischer nomenclature. A selection is presented in Table 1. Trivial names for other porphyrins that have not been sanctioned by the IUPAC will be defined in the text.

Two synthetic porphyrins, octaethylporphyrin (**14**) and *meso*-tetraphenylporphyrin (**15**) are simply named as OEP and TPP, respectively. Metal complexes of these compounds are abbreviated as TPPZn or OEPFe(III)Cl, for example.

Table 0-1 Fischer nomenclature for selected naturally occurring porphyrins

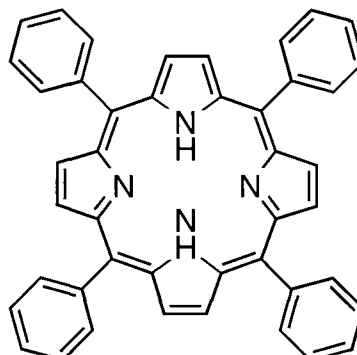
Trivial Name	Substituents ^a and Locants ^b							
	2	3	7	8	12	13	17	18
Deuteroporphyrin	Me	H	Me	H	Me	P ^H	Me	P ^H
Hematoporphyrin	Me	Et(OH)	Me	Et(OH)	Me	P ^H	Me	P ^H
Mesoporphyrin	Me	Et	Me	Et	Me	P ^H	Me	P ^H
Protoporphyrin IX ^c	Me	Vn	Me	Vn	Me	P ^H	Me	P ^H
Uroporphyrin	A ^H	P ^H	A ^H	P ^H	A ^H	P ^H	A ^H	P ^H

^a Et(OH) = -CH(OH)CH₃, Vn = -CHCH₂, A^H = -CH₂COOH, P^H = -CH₂CH₂COOH; ^b see numbering scheme as outlined in Figure 7; ^c the roman numerals refer to Fischer's type nomenclature for naming all the possible regioisomers of one set of substituents.



14

2,3,7,8,12,13,17,18-Octaethylporphyrin
OEP



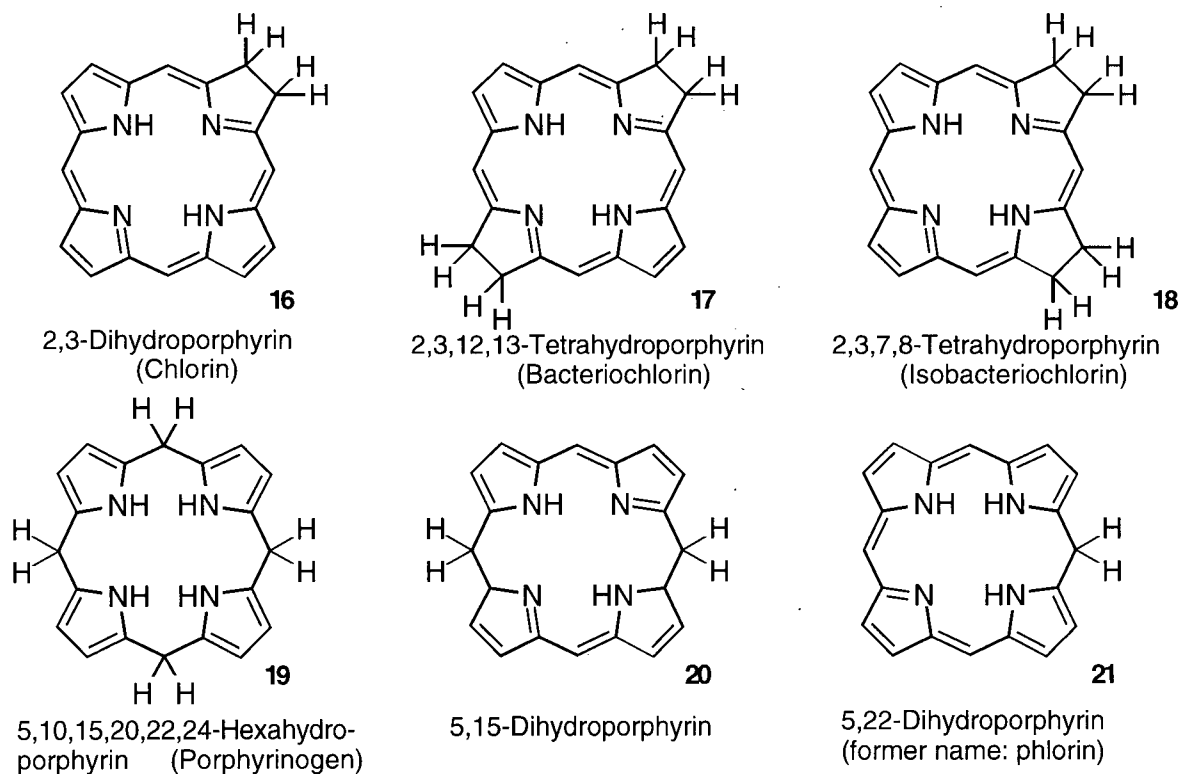
15

5,10,15,20-Tetraphenylporphyrin
meso-Tetraphenylporphyrin
TPP

REDUCED PORPHYRINS

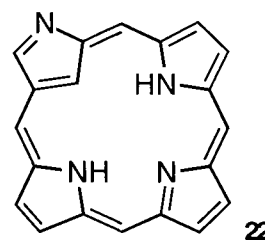
Reduced porphyrins are named systematically as hydroporphyrins, or they can be named trivially. Both naming possibilities are shown. The parent reduced porphyrin is the 2,3-dihydroporphyrin (**16**), also named chlorin. The tetrahydro-system with two opposite reduced pyrrolic units is called a bacteriochlorin (**17**), whilst the regioisomer with two adjacent reduced pyrrolic units is called isobacteriochlorin (**18**). All other reduced porphyrins are, with the exception of porphyrinogen (**19**) named systematically.

It has been pointed out⁷ that the name 2,3-dihydroporphyrin (**16**) for the chlorin chromophore implies that the inner hydrogens are at the nitrogen atoms at positions 21 and 23. However, it has been found in solution state NMR investigations⁷ that the actual structure of chlorins is not consistent with this nomenclature. Therefore, chlorins should be named 2,3-dihydro-22*H*-,24*H*-porphyrins. Only in cases where this nomenclature will contribute to any clarification of the issues to be discussed in this thesis it will be used.



PORPHYRIN ISOMERS

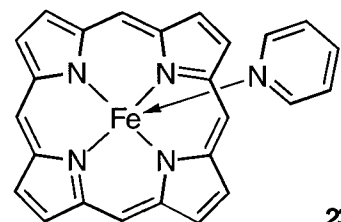
One porphyrin isomer is of relevance: The porphyrin with an inverted pyrrolic unit (**22**) is, following a suggestion of the discoverers of this pigment, referred to as 'N-confused' porphyrin.⁸



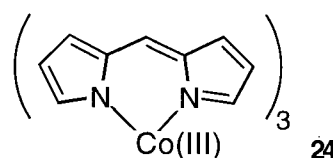
'N-confused' porphyrin
2-aza-21-carba-porphyrin

METAL COMPLEXES OF THE PYRROLIC SYSTEMS

The IUPAC recommended "Rules for Coordination Compounds"⁹ are followed. The name of the ligand precedes the name of the metal. The organic ligand(s) is (are) placed in brackets, listed in alphabetical order and the (anionic) ligand name takes the ending '-ato'. The name of the metal is followed by its oxidation number (Roman numerals in parenthesis). Coordination of the four central nitrogens is the common structural pattern of porphyrinic compounds, and need not be specifically designated. In more ambiguous cases the kappa (κ) notation is used, demonstrated at structure **24**.



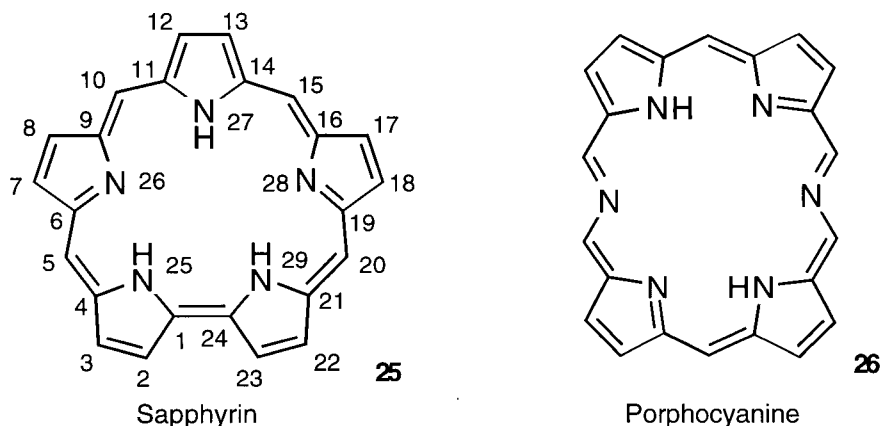
[Porphyrinato](pyridine)iron(II)



Tris(dipyrrinato- κ^2 -N¹⁰,N¹¹)cobalt(III)

'EXPANDED' PORPHYRINS

'Expanded' porphyrins are porphyrinic compounds containing either more than four pyrrolic units or more than one single carbon linking unit between these pyrrols, or both.¹¹ Their nomenclature is not homogenous, and the use of trivial names widespread. Here, only 'expanded' systems with relevance to this work will be defined as shown below.



REFERENCES

- (1) Bonnett, R. In *The Porphyrins*; D. Dolphin, Ed.; Academic Press: New York, 1978; Vol. 1; Chapter 1.
- (2) IUPAC-IUB Joint Commission on Biochemical Nomenclature (JCBN), *Pure Appl. Chem.* **1987**, 59, 779.
- (3) Fischer, H.; Orth, H. *Die Chemie des Pyrrols*; Akademische Verlagsgesellschaft: Leipzig, 1937; Vol. II, p 269.
- (4) (a) *Pyrroles: Part 1: The Synthesis and the Physical and Chemical Properties of the Pyrrole Ring*; Jones, A., Ed.; John Wiley & Sons: New York, 1990; Vol. 48. (b) *Pyrroles: Part 2: The Synthesis, Reactivity, and Physical Properties of Substituted Pyrroles*; Jones, A., Ed.; John Wiley & Sons: New York, 1992; Vol. 48.
- (5) Falk, H. *The Chemistry of Linear Oligopyrroles and Bile Pigments*; Springer Verlag: Wien, New York, 1989, Chapter 2.
- (6) Sessler, J. L.; Weghorn, S. J.; Hiseada, Y.; Lynch, V. *Eur. J. Chem.* **1995**, 1, 56.
- (7) (a) Crossley, M. J.; King, L. G. *J. Org. Chem.* **1993**, 58, 4370. (b) Crossley, M. J.; Harding, M. M.; Sternhell, S. *J. Org. Chem.* **1988**, 53, 1132.
- (8) Furuta, H.; Asano, T.; Ogawa, T. *J. Am. Chem. Soc.* **1994**, 116, 767.
- (9) (a) Commission on the Nomenclature of Inorganic Compounds (CNIC), *Pure Appl. Chem.* **1971**, 28, 39. (b) Sloan, T.E. In *Comprehensive Coordination Chemistry*, Wilkinson, G., Gillard, R.D., McCleverty, J.A., Eds., Pergamon:Oxford, 1987, Vol.1, Chapter 3.
- (10) Sessler, J. L. *Top. Curr. Chem.* **1991**, 161, 177.

ACKNOWLEDGMENTS

I wish to express my sincere thanks to Prof. David Dolphin for his guidance and the academic freedom he offered. I can only hope that I have made most out of the opportunities he provided.

Special tribute goes to my parents for their continued support and encouragement to develop my exploratory nature.

It is my pleasure to thank the past and present colleagues of my own and other research groups for their help and entertainment over the years. Mr. Andrew Tovey and Ms. Claire Johnson diligently proof-read the manuscript. I would like to thank especially Dr. Ethan Sternberg. He introduced me to Vancouver and the Pacific North-West and he was an invaluable consultant in chemical issues. I credit thanks to Dr. Ross Boyle and Ms. Huguette Savoie for not only having performed the biological tests on some of the compounds prepared in this thesis but also for having shared their excellent home-cooked foods.

This work would not have been possible with the help of the many people in the Department: my teachers, my advisory committee, the secretarial staff, the technicians in the machine shop and the crew in Chem-Stores, to list only a few. Sincere thanks go to the staff of the NMR facility for the crucial help, training and service provided, and the crew in the Mass Spectroscopy Department. Mr. Peter Boda incinerated some of my finest samples - and I thank him for having done that. Special thanks go to Dr. Steve Rettig for the X-ray crystal structures appearing in this thesis. It was always a pleasure to share the excitement when presenting my perfect crystals, and it was never too harshly put when their perfection crumbled upon closer investigation.

Financial support in the form of a year-round research assistantship from Prof. David Dolphin (September 1991 to present) is greatly appreciated.

And, hey, thank you, Mary-Lynn, for your unfaltering faith and support.

This is
another specimen
in the ongoing collection
of
stamps, stones,
bones and feathers.

PYRROLIC PIGMENTS

GENERAL INTRODUCTION

pigment (pig'mənt)

n. **1.** Any of a class of finely powdered, insoluble coloring matters suitable for making paints, enamels, oil colors, etc. **2.** Any substance that imparts color to animal or vegetable tissues such as melanin and chlorophyll. **3.** Any substance used for coloring. [L < *pigmentum* < *pingere* to paint]

(Funk & Wagnalls Canadian College Dictionary, Fitzhenry & Whiteside, Toronto: 1989)

Pyrrolic pigments contain one or more, typically conjugated, pyrrolic units. Cyclic tetrapyrrolic pigments are ubiquitous in nature and are found, for example, as chlorophylls, hemes and corroles. Due to their fundamental importance to life they have been dubbed "the pigments of life". Naturally occurring linear pyrrolic pigments are, for instance, the phytochromes whilst others are the source of bioluminescence, metabolic diseases or antimicrobial activities. Recent advances in medicinal chemistry have introduced pyrrolic pigments as photosensitizers in tumor therapy and as chelators for metals used in diagnostic medicine. In addition, they are utilized as ligands for metals used in transition metal catalysis, as paints, in dyes for optical recording media, as well as insecticides. They are also players in a host of basic research areas.

Thus it becomes apparent that this thesis can focus only on partial aspects of the wide field of pyrrolic pigments. However, despite this natural limitation, the number of different subjects touched and the structural variety of the pigments displayed herein will, perhaps, give some reflection of the breadth of the field. The various topics are presented in three independent and unequally weighted parts, each containing their own introductory, results and experimental sections as well as references. These parts are defined as follows:

Part 1

Synthesis and Study of Pyrrolic Pigments for Use in Photodynamic Therapy (PDT)

This part discusses the synthetic aspects of cyclic, aromatic pigments such as *meso*-phenyl substituted porphyrins, chlorins and saphyrins. The aim of the research was to develop rational syntheses for potential drugs for PDT. This, in turn, has led to the investigation of the physical, chemical and biological properties of the novel compounds prepared. Truly unique (and unexpected) pigments were synthesized in due course of these studies.

The opening chapter of Part 1 presents an introduction to the principles of PDT and a review of selected compounds which are potentially interesting compounds for use as photosensitizers. Special focus is placed on the synthesis of hydroxylated porphyrins and chlorins in general, and the osmium tetroxide mediated dihydroxylation of porphyrins and other aromatic systems in particular.

Part 2

meso-Phenyldipyrrens - Synthesis and Metal Complex Formation

This part describes the oxidation of bi- and tripyrrolic non-colored matter to their corresponding pigments and the metal chelating properties of these pigments. This mainly curiosity driven project was made possible by the availability of large quantities of *meso*-phenyldipyrromethane and -tripyrane. This stemmed from the result of one of the rational synthetic approaches described in Part 1.

Part 3

2-Pyrrolylthiones as Bidentate N,S Chelators

This part introduces mainly the use of monopyrrolic pigments containing the 2-pyrrolylthione moiety as transition metal chelators. This part describes work which emerged by serendipity while attempting (eventually successfully) to find an improved synthesis for *meso*-diphenylporphyrin used as starting material in Part 1.

PART 1

**SYNTHESIS AND STUDY
OF
PYRROLIC PIGMENTS
FOR USE IN
PHOTODYNAMIC THERAPY (PDT)**

1. INTRODUCTION AND LITERATURE REVIEW

1.1 PHOTODYNAMIC THERAPY (PDT)

1.1.1 HISTORY AND GENERAL INTRODUCTION¹⁻³

Photodynamic therapy is a medical treatment which employs the combination of light and drug to bring about a (lethal) cytotoxic effect to cancerous or otherwise unwanted tissue. It derives great promise from an idealized mode of action: A drug (photosensitizer) of negligible dark toxicity is introduced into a body and accumulates preferentially in cancerous cells. When the drug reaches its highest ratio of accumulation in diseased *versus* healthy tissue, a carefully regulated light dose is shone onto the diseased tissue. Light activates the drug and elicits the toxic action. The amount of light is large enough to cause a lethal response in the tissue with high levels of photosensitizer, but small enough to spare the surrounding healthy tissue from extensive damage. Shortly after the treatment, the lethally damaged cells become necrotic, and are rejected or absorbed by the body. The photosensitizer clears rapidly out of the body after light treatment. It is worth pointing out that PDT is ideally curative, whereas many traditional cancer treatments aim merely to prevent further growth or the spread of cancer. PDT can, due to fiber optic technology, be applied at almost any location in the body, either with or without accompanying surgical treatment. In addition, extracorporeal treatments of blood for virus deactivation are under investigation.⁴

While the term PDT is relatively modern, this binary modality of treating diseases can be traced far back in history. The ancient Egyptians used the combination of orally ingested plants (containing light-activated psoralens) and sunlight to successfully treat vitiligo over 4000 years ago.⁵ Contemporary PDT began when Raab described in 1900 the toxic action of acridine dyes and light on *Paramecia*, and he also showed that these unicellular organisms could be effectively killed with this combination.⁶ Jesionek and Trappeiner treated, in 1903, a skin cancer with topically applied eosin and light.⁷ In 1925 Policard examined the ability of porphyrins to produce a phototoxic effect.⁸ One unusual experiment highlighted the potency of drug-induced photosensitivity. Mayer-Betz injected himself in 1913 with 200 milligrams hematoporphyrin and registered no ill effects until he exposed himself to sun-light, whereupon he suffered extreme swelling and photosensitivity remained for several months.^{9,10}

The modern age of PDT began when a mixture, called 'hematoporphyrin derivative' (HpD) was used in 1960 by Lipson and Baldes.¹¹ This multi-component photosensitizer was, and currently is, prepared by the treatment of hematoporphyrin with sulfuric acid in acetic acid followed by an alkaline hydrolysis. A number of monomeric, dimeric and polymeric porphyrins containing ether, ester and carbon-carbon linkages are thus formed.³ HpD was originally tried as a fluorescent tumor imaging agent and the preferential accumulation of HpD in certain cancerous tissues (in animal models) was found.¹² The potential to use HpD as an anti-cancer drug was investigated by Dougherty *et al.*, and this led to the discovery of HpD as the first generation PDT drug.¹³⁻¹⁵ Several attempts to define the active compound(s) in this mixture failed, but these investigations did determine that neither the monomers nor the dimers of hematoporphyrin are the most active species.¹⁶ A somewhat purified, synthetically reproducible version of HpD, known under the trade name Photofrin[®], has, in the past few years, received regulatory approval for the treatment of selected cancers in several countries.¹

In spite of this approval, Photofrin[®] exhibits several drawbacks. First and foremost, it is a complex mixture of compounds. This complexity makes characterization, as well as physical and biological studies very complicated, and regulatory approval for drugs consisting of mixtures is becoming increasingly more difficult. These obstacles may explain the fact that it has taken over twenty years from initial biological testing to final approval of Photofrin[®]. Secondly, the longest wavelength of absorption of Photofrin[®], that is the longest wavelength at which the drug can be photoactivated, is at 630 nm. At this wavelength, effective light penetration through tissue due to endogenous chromophores, mainly hemoglobin, and light scattering is quite low (~4 mm).¹⁷ Thirdly, the clearance rate for Photofrin[®] is slow. As a consequence, a patient must remain in subdued light for several weeks post-injection of the drug to prevent skin damage.¹⁸

The above drawbacks provided the benchmarks for the development of the so called second-generation photodynamic drugs. These components are generally single substances with longer wavelengths of absorption. These longer wavelength are desired because tissue has a 'spectral window' between around 650 nm and 800 nm. In this range, light penetration is deepest and, hence, deeper-seated tumors can be treated with these drugs.¹⁹ Also, the pharmacokinetic patterns of the second-generation drugs are better adjusted for their uses. Several of these second-generation drugs are currently in clinical trials.³ However, many of these are difficult to synthesize or have other drawbacks. Selected second-generation drugs will be discussed in more detail in the following chapters. The third-generation of drugs are currently in pre-clinical stages of investigation and they aim at eliminating the disadvantages of the preceding generations. They also will be discussed in more detail in the following chapters.

The development of novel PDT drugs is complicated by the nature of the mode of action of PDT. The drugs used are non-specific in the sense that they do not target a specific

enzyme or DNA sequence or even organ. Their mechanism of accumulation is believed to be an interaction with various lipoproteins found in plasma, in cell membranes and elsewhere.¹ This non-specificity makes the development of structure-function relationships, according to which a development of an improved drug could be directed, very difficult.

The achievement of the desired photophysical properties seems not to be an impediment to the development of new drugs as the plethora of long-wavelength absorbing dyes to be discussed below will show. On the other hand, the delivery system of a PDT drug, or of any drug, has a great influence on the efficiency of the drug, implying that a good drug might give a bad biological response due to delivery problems. Consequently, a rigorous and time-consuming (biological) testing program has to accompany any PDT drug development.²⁰

As more drugs are being developed and tested, certain trends common to promising PDT drugs can be recognized. Most prominent of these trends is that all have pronounced amphiphilicity. A selection of the second-generation photosensitizers is shown below (Figure 1-1). The diversity of these second-generation drugs illustrates this lack of a generally valid baseline structure. The development of BPD-MA (**1**) illustrates also that fortuitous circumstances are often involved in finding the 'optimal' drug, as neither the diacid nor the diester derivative of this drug show the high biological activity of the monoacid monoester (**1**).¹ Although this review will be restricted to tetrapyrrolic (porphyrinic) pigments, it must be stressed that the effect of photosensitization is not restricted to these pigments (*vide supra*), and other substance classes might be suitable candidates for PDT.⁹

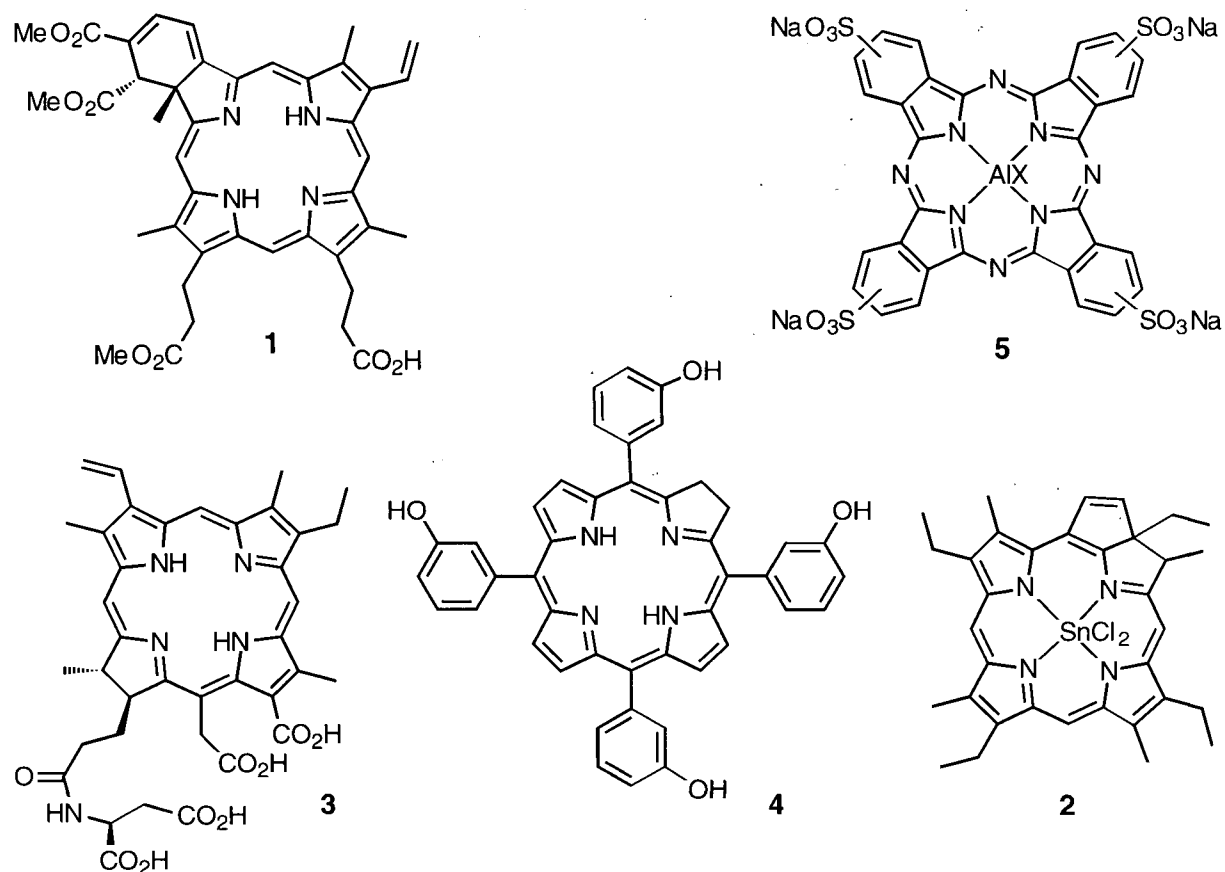


Figure 1-1 Structures of selected second generation photosensitizers: **1** benzoporphyrin derivative monoacid (BPD-MA)²¹, **2** tin etiopurpurin²²; **3** mono-L-aspartyl chlorin *e6*³; **4** meso-tetra(*m*-hydroxy)phenylchlorin²³; **5** aluminum phthalocyanine tetrasulfonate²⁴

1.1.2 PHOTOPHYSICAL AND PHOTOCHEMICAL BASIS OF PDT ²⁵

PDT is largely dependent on the presence of molecular oxygen.²⁶ PDT performed in molecular oxygen-free systems was found to be ineffective.²⁷ This suggests that singlet oxygen generated by the photosensitization of molecular triplet oxygen (or other reactive species) is the principal toxic species formed during PDT, although the extent to which this species is responsible for the photodynamic effect is under debate. Nonetheless, the generation of singlet oxygen is extremely crucial to the success of PDT, and one of the first

tests performed on new PDT drugs is to probe their capability of singlet oxygen generation.²⁸

The principal photophysics of photosensitization are illustrated in a modified Jablonski diagram, shown in Figure 1-2. The sensitizing compound in its singlet ground state (S_0) absorbs a photon to place it in an excited singlet state (S_1 - S_n). Depending on the energy of the exciting photon, a higher or lower state may be reached (1). In a porphyrin, this transition corresponds to a $\pi^* \leftarrow \pi$ transition. A compound in a higher S-state may lose the energy radiatively through fluorescence (2) or non-radiatively (thermally) through internal conversion (3) and, thereby, returns to its ground state. Both transitions are spin-allowed processes and, therefore, the lifetime of the excited singlet states is very short, typically in the nanosecond range.

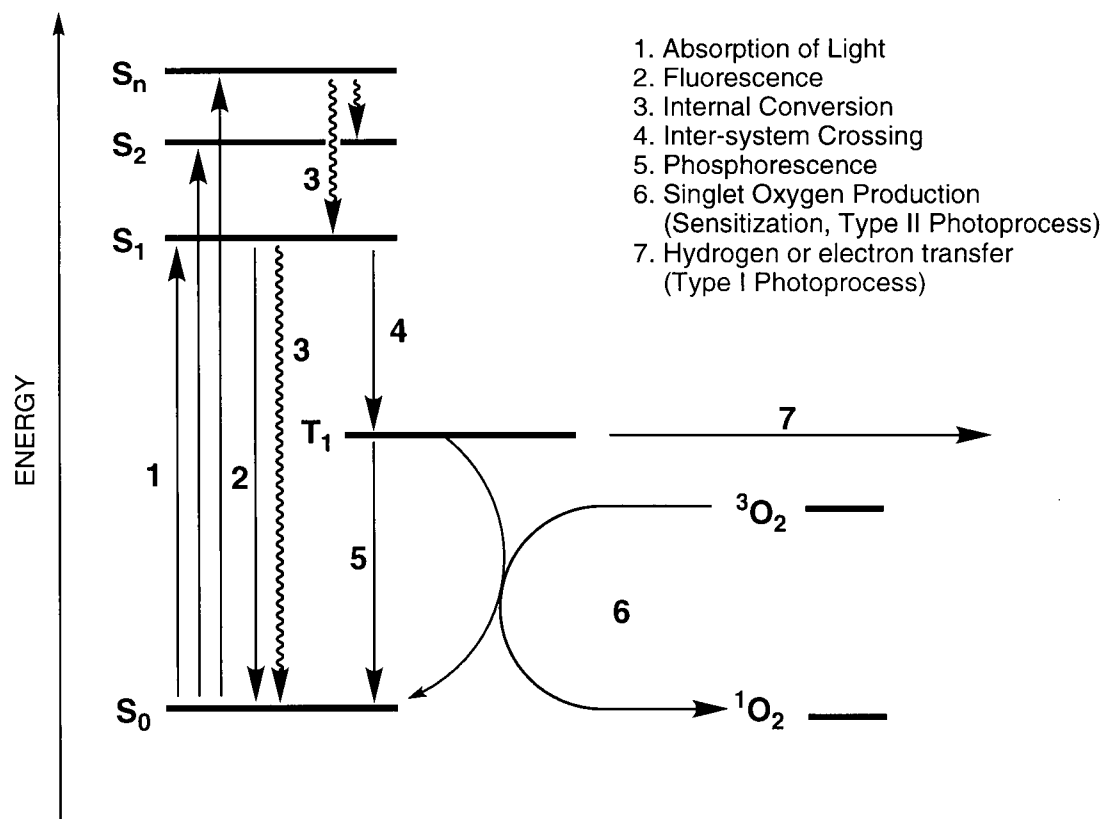


Figure 1-2 Modified Jablonski diagram for a typical Photosensitizer

Of particular importance with regard to PDT is that the excited species can undergo the non-radiative process of inter-system crossing (ISC) (4). This process is a so called spin-forbidden process as it requires spin inversion, thereby converting the photosensitizer to a triplet state (T_1). Any 'forbidden' pathway is less likely than an 'allowed' process, but a good photosensitizer undergoes the 'forbidden' ISC pathway with very high efficiency. The molecule can relax from the triplet state *via* two pathways: radiatively by phosphorescence (5), and non-radiatively by spin exchange with another triplet state molecule. Phosphorescence involves a spin-inversion and thus is also spin-forbidden, imposing a relatively long lifetime on the triplet state, typically measured in microseconds, thus allowing the interaction with molecules in the vicinity of the sensitizer.

Spin exchange (also corresponding to energy transfer) with triplet oxygen generates the highly reactive species singlet oxygen (6). This process is called a Type II photoprocess. Another type of interaction with other molecules can bring about electron or hydrogen transfers, converting the sensitizer into a novel chemical species (7). These latter processes are called Type I photoprocesses. The prevalence of these processes is dictated by many factors such as substrate and oxygen concentration, substrate types and many physical parameters of the solution in which these processes are taking place. As shown below, both processes have the potential to cause detrimental damage to a cell by altering the chemical structure of its vital components.

Type I Photoprocesses

A sensitizer (SENS) in its triplet state ($^3\text{SENS}$) is often a strong oxidant and, as is shown in Figure 1-3, capable of abstracting electrons or hydrogens from a particular substrate (SUB). The reduced forms of the sensitizer can react in many ways, such as with ground state oxygen to form the cytotoxic superoxide radical (Pathway A) or its protonated

form (Pathway B). In either case, the sensitizer relaxes to its ground state and is available for another photosensitization cycle.

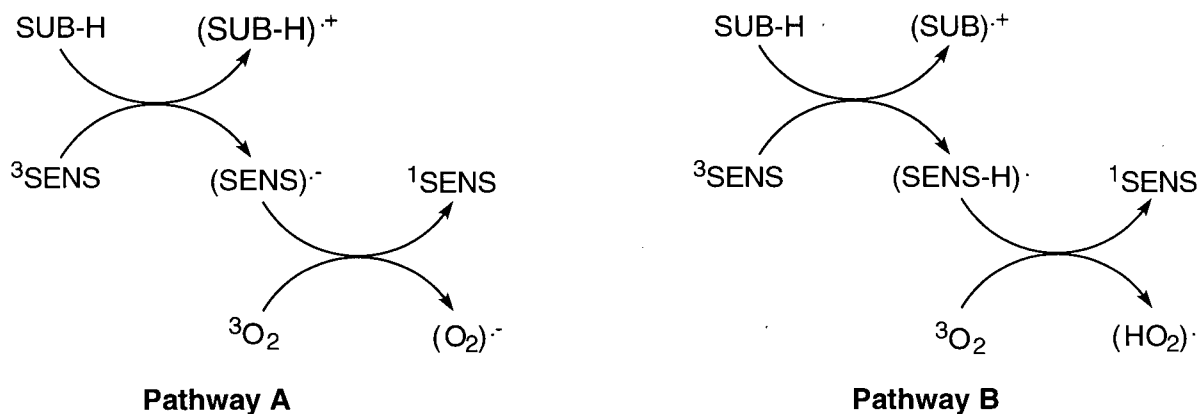


Figure 1-3 Type I photoprocesses

Type II Photoprocesses

The singlet oxygen generated by the sensitizing action is a very reactive species with a lifetime in water of roughly four microseconds. It undergoes several reactions with biological substrates such as oxidations and cycloadditions, as shown in Figure 1-4.

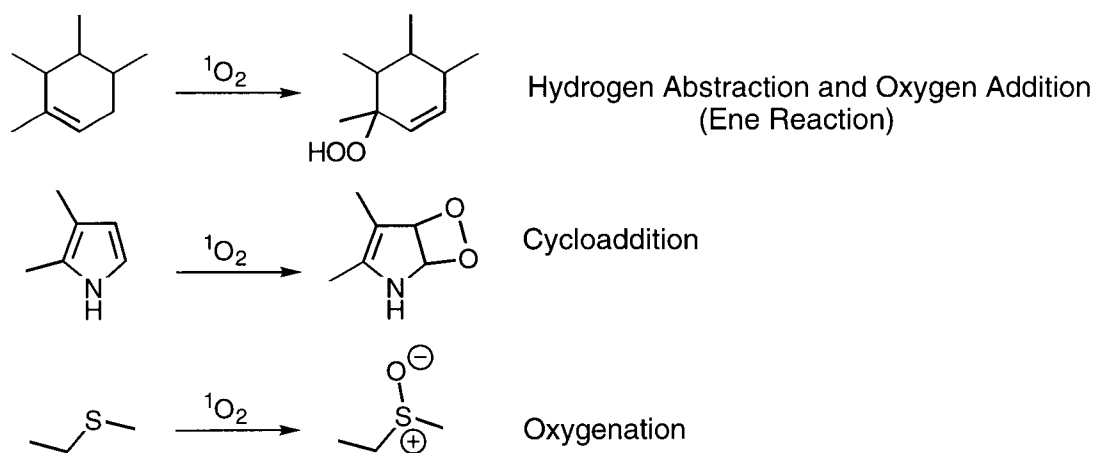


Figure 1-4 Type II photoprocesses

1.1.3 THE PROFILE OF THE IDEAL PDT DRUG

Using the aforementioned principles of PDT and general considerations for the synthesis and marketing of any drug, the profile for the ideal PDT drug can be constructed:²⁹ (The order of points does not necessarily reflect a ranking of their importance.)

- The photosensitizer should have strong absorption in the red part of the visible spectrum (≤ 650 nm), where light penetration into tissue is the greatest.
- For type I photosensitizers, the photophysical properties should be such that the quantum yield of triplet formation is high, with a triplet energy greater than 94 kJmol^{-1} , and that the triplet energy is effectively transferred to the triplet oxygen.
- The photosensitizer should have a negligible or very low toxicity in the dark.
- The drug must exhibit a large selectivity for enrichment in tumorous tissue vs. healthy tissue, particularly skin. General skin sensitization must be avoided. However, certain treatment modalities call for skin sensitization, *e.g.* the treatment of psoriasis. In that case, rapid and selective sensitization and desensitization of the skin should be achieved.
- The solution state properties such as solubility, partition coefficients, aggregation behavior and ionic charges of the drug should allow easy formulation (in solutions, creams, etc.), and should confer the above mentioned selectivity.
- The drug should be excreted or metabolized quickly post-treatment (within hours or maximum days) in a way that does not generate toxic metabolites of any kind.
- The drug should be a single, enantiomerically and diastereomerically pure substance.
- The drug should contain a functionality or moiety such as the phenyl group which allows easy derivatization or variation in order to optimize various properties of the drug.

-
- The compound should be synthetically easily attainable from readily available starting materials. The process to yield the drug must bear the potential for upscaling to industrial (multi-kilogram) scales. This severely limits, for example, the number of separations by chromatography. The necessarily simple process of production will, to a large degree, determine the price of the drug. This is a point of consideration in a highly competitive market place with increasing pressure on health costs.
 - The overall costs for a PDT treatment are also reduced by the use of light emitting diodes (LEDs) as light source. Hence, a wavelength of activation suitable for the use of LEDs would be advantageous.
 - The formulated drug should be stable, *i.e.* possess a long shelf life. The preparation of the administered form of the drug should be simple, *e.g.* by dissolution in physiological sodium chloride solution for any injectable form of the drug.
 - Last, but not least, the development of any drug with the enormous investment required is only worthwhile, *i.e.* profitable, for the developer if the patent rights for the drug and their use are exclusively in the hands of the developer. The development of drugs solely for the improvement of humankind is, apart from notable exceptions, an illusion.

1.2 RESEARCH OBJECTIVE

The aim of this work is the rational development of drugs intended for PDT, focusing primarily on *meso*-phenyl substituted pigments. The rationale for this focus is as follows:

1. Certain *meso*-phenylporphyrins and -chlorins have shown some promise as photosensitizers for use in PDT, although only a few *meso*-phenyl substituted photosensitizers have been tested for PDT. Consequently, this area has the potential for development.
2. The chemical nature of these pigments will allow facile derivatization (to hone pharmacokinetic or other properties of the drug) should a promising lead drug be found.
3. Many pigment classes such as the sapphyrins had not been synthesized or characterized with *meso*-phenyl substituents at the time these studies were initiated.
4. The *meso*-phenylporphyrins are favorable starting compounds for development of PDT drugs as they are available *via* single step syntheses in large quantities.
5. Concurrent with this investigation a novel class of *meso*-phenyl substituted pigment (N-confused porphyrin) with promising photophysical properties appeared in the literature, however, its synthesis was not suited to generate larger quantities of this pigment and, hence, a novel synthetic pathway to access this pigment was desirable.

The work focuses on the elucidation of synthetic and other chemical aspects of the potential drugs rather than on their biological properties, albeit some preliminary biological results will be reported. The chemical aspects are three-fold: one aspect is the synthesis of novel compound classes, and study of their chemical and physical properties; the second and third aspects are the elucidation of the mechanism of synthesis and the synthesis *via* novel pathways of known compounds, respectively.

1.3 REVIEW OF SYNTHESIS AND PROPERTIES OF PYRROLIC PIGMENTS POTENTIALLY USEFUL IN PDT

1.3.1 PORPHYRINS

1.3.1.1 NATURALLY OCCURRING PORPHYRINS

Porphyrins occur naturally as prosthetic groups in enzymes³⁰, as dyes in various egg shells³¹ or feathers³², and are found in crude oils³³ and in the urine of humans or cattle suffering from congenital porphyria³⁴. The only readily available source of porphyrins is blood from which, depending on the procedure of isolation, protoporphyrin IX and hematoporphyrin IX as their diacids or diesters can be isolated in bulk quantities.^{35,36} The UV-visible spectrum of protoporphyrin dimethyl ester is shown in Figure 1-5. This spectrum exhibiting a very strong ($\log \epsilon = 5-5.5$) absorption around 400 nm, known as Soret-band, and four low intensity bands, known as Q-bands, is characteristic of porphyrins. The weak absorption in the long wavelength region indicates that porphyrins are not ideal PDT drugs, although, as mentioned, they may cause strong photosensitization.

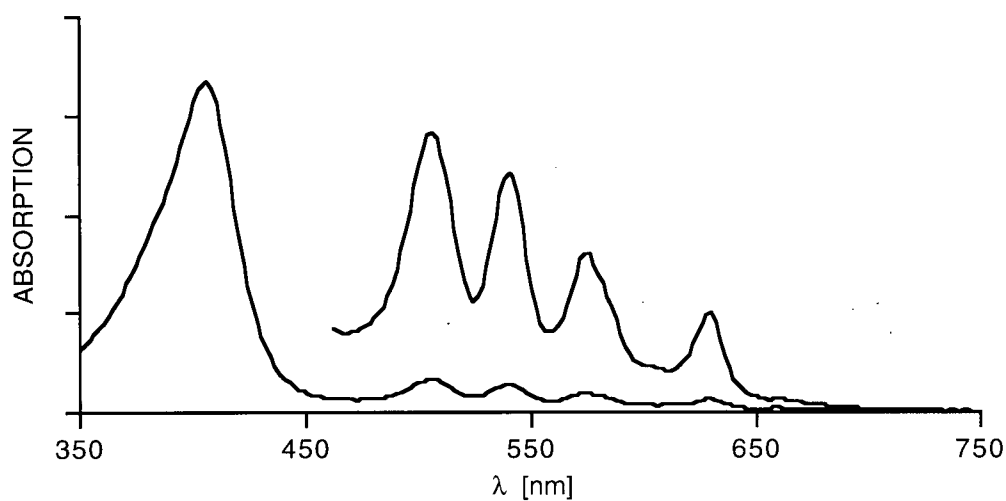


Figure 1-5 Optical (CHCl₃) spectrum of protoporphyrin IX dimethyl ester

The chemistry of naturally occurring porphyrins has been reviewed in depth.^{31,36-38} Their importance within the realm of this review does not go beyond their use as starting materials in the synthesis of certain PDT drugs, as mentioned above and detailed below.

1.3.1.2 SYNTHETIC PORPHYRINS

Synthetic porphyrins fall primarily into two classes. There are those with all β -positions alkylated, the archetype of which is octaethylporphyrin (OEP), and those with all *meso*-positions arylated, the archetype of which is *meso*-tetraphenylporphyrin (TPP). As in nature, synthetic porphyrins are built up from pyrrolic precursors. OEP and TPP can, due to their symmetric structures, be synthesized from one monopyrrolic precursor in a one-step 4×1 -type condensation reaction (Figure 1-6), although this type of reaction is much more common for the TPP-type porphyrins than it is for the OEP. The pyrrolic units may (as in most OEP syntheses) or may not (as in most TPP syntheses) carry the linking carbon.

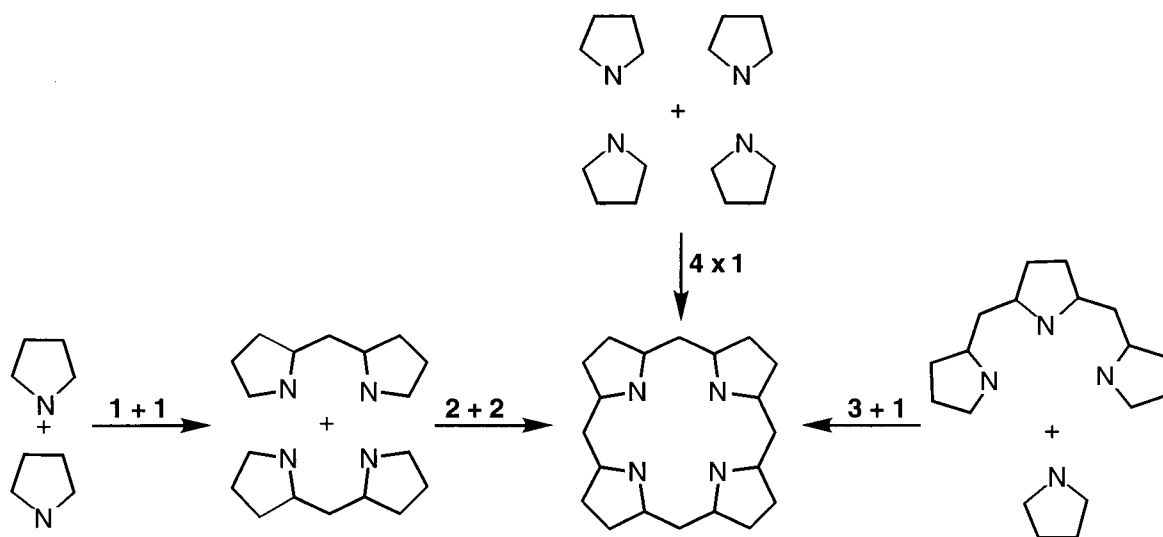
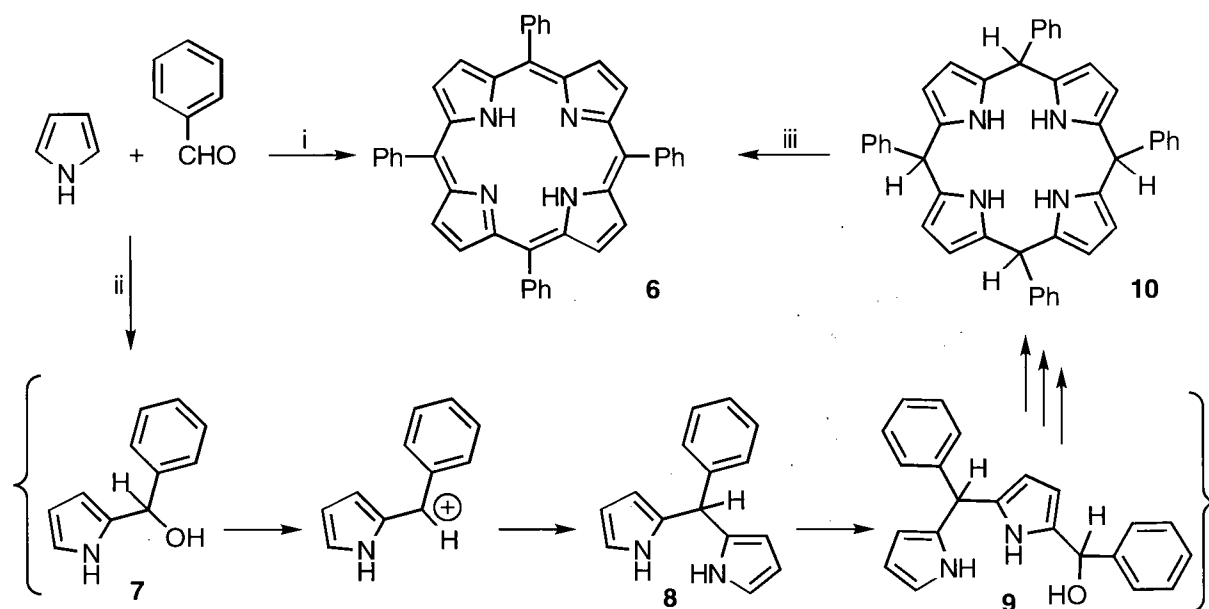


Figure 1-6 The different concepts of porphyrin synthesis

All other porphyrin syntheses have to be accomplished step-by-step. Conceptually, many approaches are possible, all of which have precedent in the literature. A 2 + 2 approach joins two bipyrrrolic precursors.³⁹ The two bipyrrrolic precursors are generated by a 1 + 1 addition. They may be, depending on the particular porphyrin desired, the same or different. They can be set up to condense in only one orientation, or in both orientations. They can be joined in one step to form the cyclic tetrapyrrolic pigment, or first joined into a linear tetrapyrrolic species which is cyclized in a second, independent, step. A rarely performed 3 + 1 approach inserts the fourth pyrrolic unit into a tripyrrrolic precursor. The particular modes are chosen depending on the porphyrin required and the starting materials available. The various methods of synthesis have been reviewed³⁰ and only those of particular importance for the understanding of this work will be briefly outlined.

The Synthesis of TPP

The classic preparation of *meso*-tetraarylporphyrins is *via* a 4 x 1-type methodology as originally developed by Rothmund^{40,41} and improved by Adler *et al.*⁴², Gonsalves⁴³, and then Lindsey *et al.*⁴⁴⁻⁴⁶ The mechanism of the TPP formation has been elucidated.^{47,48} Benzaldehyde reacts under acid catalysis with pyrrole to form an intermediate arylpyrrolyl-carbinol (**7**).⁴⁹ This carbinol is set up to form a resonance stabilized cation (**8**) which reacts with another equivalent of pyrrole to yield the dipyrromethane **9**. To this is added another benzaldehyde moiety and repetition of this reaction sequence occurs. Ultimately a ring-closure condensation forms the porphyrinogen (**10**), which is oxidized *in situ* to the corresponding fully unsaturated porphyrin (**6**). The Rothmund-type TPP synthesis has been applied to a wide variety of aryl^{41,50-52} and alkyl⁵³ aldehydes. Several solid^{54,55} and, more traditionally, liquid acid catalysts are suitable to catalyze the reaction. Under a standard set of conditions, yields of over 30% for this condensation are regularly observed. Until 1995 it was believed that TPP was the only macrocyclic pyrrolic pigment formed in this reaction. Chapter 1.3.4 and 1.3.5.1 discuss findings which led to the correction of this view.



Scheme 1-1 Rothemund synthesis of *meso*-tetraphenylporphyrins **6**

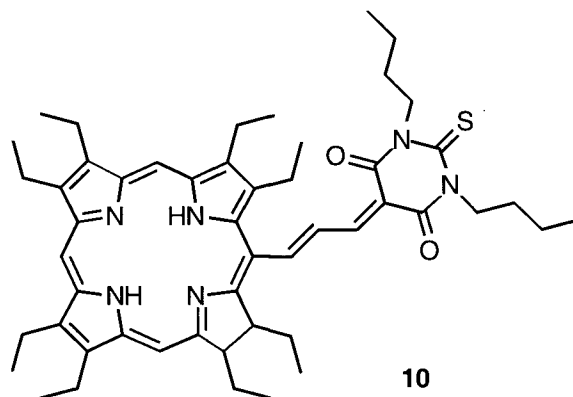
Reaction conditions: (i) 1. catalytic H^+ ; 2. oxidant (ii) catalytic H^+
(iii) oxidant

meso-Tetraarylporphyrins which are less symmetric than TPP have to be synthesized in a step-wise manner, either along a 2 + 2 or a fully stepwise approach.^{56,57} This step-wise approach results in a drastic reduction in overall yield of the final porphyrin.

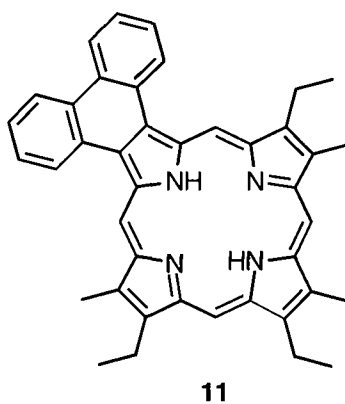
Porphyrins with Extended π -Systems

The optical properties of regular porphyrins are, as mentioned, not ideal for their application in PDT. However, certain porphyrins with extended π -systems have significantly bathochromically shifted spectra. Robinson and Morgan prepared porphyrins bearing thiobarbituric and barbituric acid functionalities at the *meso*-position, for instance compound **10**.⁵⁸ Somewhat unexpectedly, its electronic spectrum exhibits one broad and strong band at ~ 710 nm. The NMR of **10** indicates a certain loss of aromaticity of the porphyrin chromophore. Without any details, the researchers remarked that biological

studies with these compounds looked promising with respect to their further refinement for their use in PDT.⁵⁸



Lash and co-workers introduced recently a series of porphyrins in which one or more pyrrolic units were replaced by pyrroles fused to larger aromatic systems, for instance phenanthrene system **11**.⁵⁹⁻⁶¹ Their UV-Vis spectra are reportedly bathochromically shifted as compared to regular porphyrins, however, the scarce data available as of now indicate that they are not shifted to an extent that they are suited as PDT agents.



This finding is matched by evaluations for similar systems such as monobenzoporphyrins^{62,63}, dibenzoporphyrins⁶⁴, or tetrabenzoporphyrins⁶⁵.

3.2 CHLORINS, BACTERIO- AND ISOBACTERIOCHLORINS

1.3.2.1 THE OPTICAL PROPERTIES OF CHLORINS

Chlorins are distinguished from their parent porphyrin by the presence of one reduced peripheral double bond, and this leads to an altered optical spectrum of these compounds. Figure 1-7 shows the spectrum of BPD-MA (1) which exhibits the general features of chlorin spectra. Most importantly in the context of PDT, they have a strong absorption in the long wavelength portion of the visible spectrum, and this feature makes them very attractive as photosensitizers.

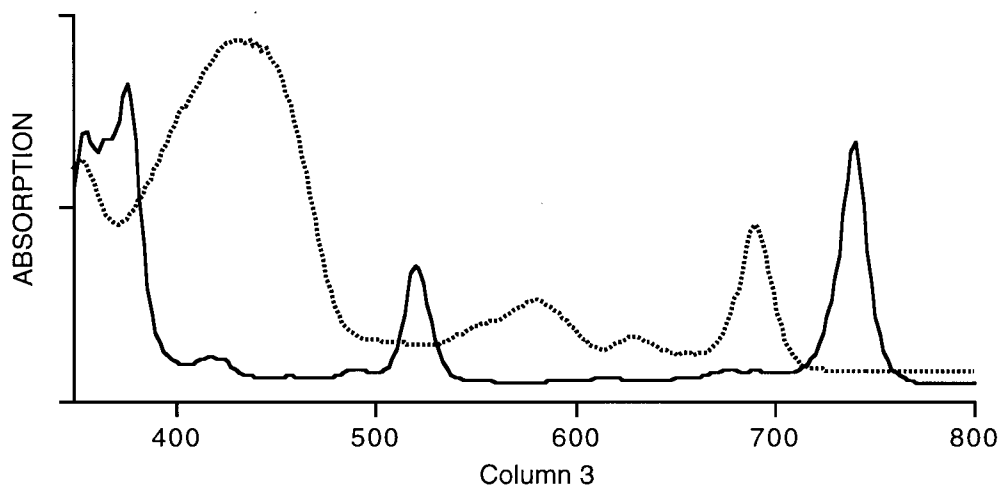


Figure 1-7 UV-visible spectrum of chlorin 1 (.....) and bacteriochlorin TPBC (—)

Also shown in Figure 1-7 is the spectrum of a bacteriochlorin (*meso*-tetraphenyl-bacteriochlorin, TPBC). Its optical spectrum is even further bathochromically shifted, and its long-wavelength absorption is within the 'ideal'¹⁹ region for PDT. Isobacteriochlorins have spectra very similar to chlorins and the synthetic effort to establish a second reduced

site is not rewarded with an improved spectrum and, consequently, research toward novel photosensitizers has been focused on the preparation of chlorins and bacteriochlorins.

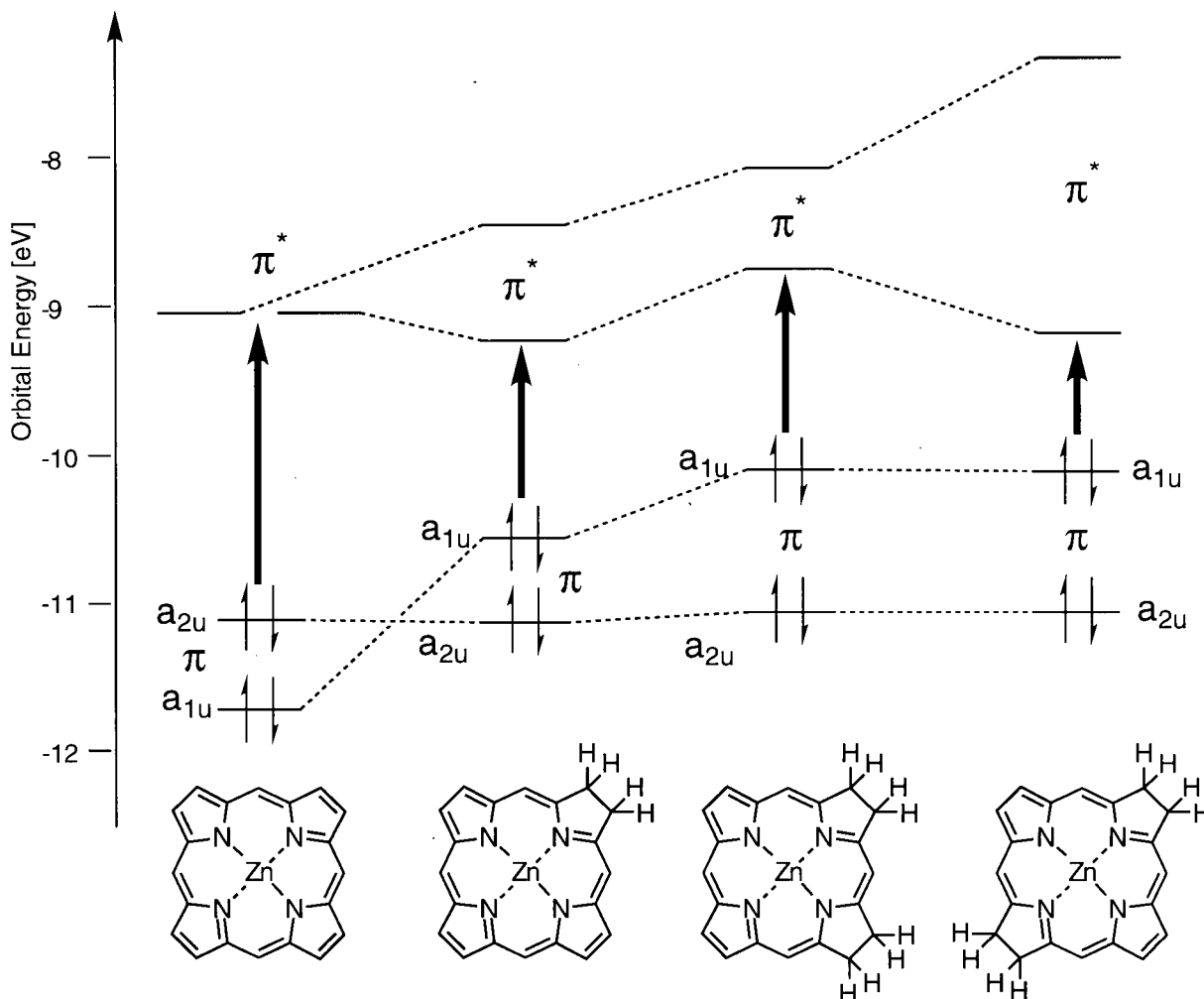


Figure 1-8 Energy level diagram for the frontier orbitals of the four generic metalloporphyrin classes (adapted from Fajer⁶⁶)

Gouterman laid the theoretical foundation of porphyrin optical spectroscopy.⁶⁷ Figure 1-8 presents a scheme based on extended Hückel calculations of the frontier orbitals of the four generic metalloporphyrin* classes. The longest wavelength absorption in

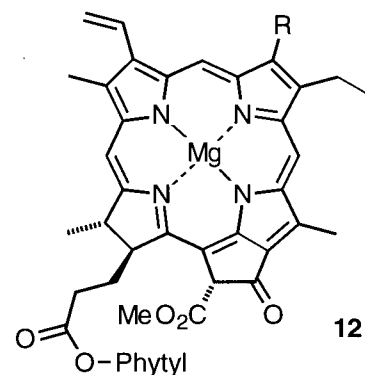
* Metalloporphyrins and chlorins are chosen here as example for reasons of simplicity. An equivalent trend is valid for the free bases of the pigments.

porphyrins and chlorins can be assigned to a HOMO-LUMO transition. This is shown here as a $\pi^* \leftarrow \pi$ transition, indicated by a dark arrow. With increasing saturation of the porphyrin macrocycle, the energy of the so called a_{1u} orbitals, the HOMOs, are progressively raised. The LUMOs of porphyrin, chlorin and bacteriochlorin remain largely isoenergetic, whereas those of the isobacteriochlorin are raised. The size of the HOMO-LUMO gap corresponds to the energy for this transition: the larger the gap, the higher the energy needed for the transition, and *vice versa*. The trends seen in the electronic spectra of porphyrins and the reduced species reflect this clearly: the higher the energy, the shorter the wavelength of the corresponding absorption band, the lower the energy, the longer the wavelength of the absorption band. The theoretical picture corresponds even further with the chemistry of these pigments. Since (electrochemical) oxidation corresponds to an abstraction of an electron from the HOMO, and reduction to the filling of a LUMO, it can be expected that it becomes increasingly harder to perform an oxidation the more saturated the system is, and that it is easier to reduce a chlorin and a bacteriochlorin than it is to reduce a porphyrin or an isobacteriochlorin. This trend can, indeed, be confirmed experimentally.^{68,69}

In the remainder of this introduction, the synthesis and properties of various chlorins and related long wavelength absorbing dyes will be discussed.

1.3.2.2 NATURALLY OCCURRING CHLORINS: CHLOROPHYLLS

Chlorophylls *a* and *b* (**12**) are the pigments of photosynthesis, and, consequently, they are ubiquitous. Demetallated chlorophylls have a strong absorption at ~660 nm and for that reason are suitable for PDT. However, their isolation and purification is non-trivial and they are chemically very unstable substances. Nonetheless, their use as PDT agents has been proposed and investigated by numerous workers.⁷⁰ This review is focused on the chemistry of synthetic chlorins.



R = -CH₃; Chlorophyll *a*
R = -CHO; Chlorophyll *b*

The chemistry of chlorophylls, their isolation and modification have been reviewed extensively.^{31,71-73}

1.3.2.3 THE TOTAL SYNTHESIS OF CHLORINS

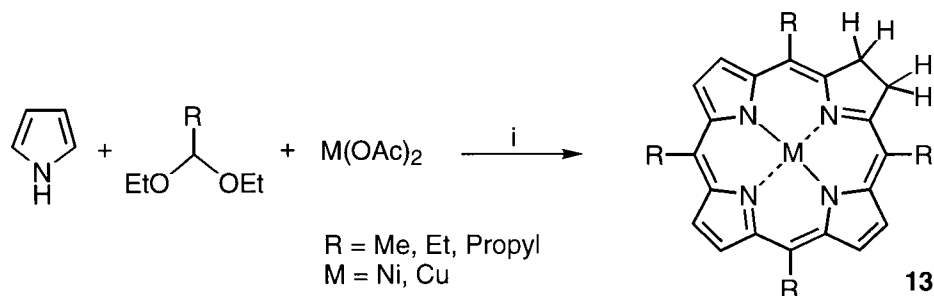
The 'Classical' Total Synthesis of Chlorins

The total synthesis of chlorins follows conceptually the same routes as the total synthesis of porphyrins, but includes additional steps to introduce a hydropyrrolic unit. This necessitates synthetic strategies unknown in porphyrin chemistry and often complicates the synthesis enormously. In fact, the crucial steps in some chlorin total syntheses are more reminiscent of corrin syntheses as they are adapted from synthetic strategies devised by Eschenmoser, Woodward, and Battersby for the total synthesis of corrins.⁷⁴ The total synthesis of chlorophyll *a* by Woodward *et al.*^{75,76} is the prime example of the total synthesis of a chlorin. This chlorophyll synthesis was at its time (and still is) of such monumental

scale that it was cited as one of the reasons why Woodward was awarded in 1965 the Nobel Prize. It is, therefore, obvious that a chlorin total synthesis can be excluded as a viable way to produce a commercial product such as a PDT drug. Total syntheses have been performed solely for the purpose of structure elucidation and verification or the demonstration of the power of a novel synthetic strategy, as illustrated with the total synthesis of bonnelin^{77,78} and sirohydrochlorin⁷⁹. A review published in 1994, entitled "Discovery and Synthesis of Less Common Natural Hydroporphyrins", cites more examples.⁸⁰

Chlorins through a Rothemund-type condensation

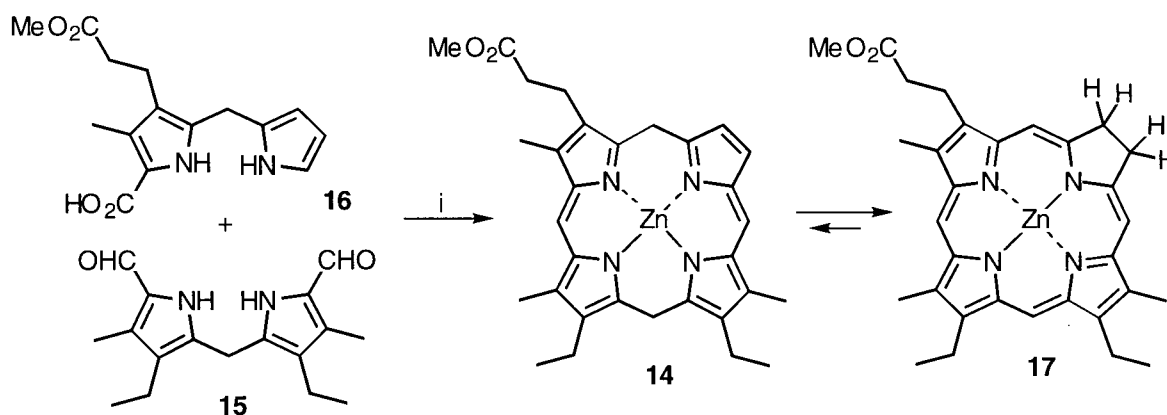
In 1946, Calvin *et al.* identified the pigment generally present as a contaminant in TPP when produced by a Rothemund-type synthesis, as *meso*-tetraphenylchlorin (TPC).⁸¹ Separation of these traces of TPC from the bulk material TPP is possible by chromatographic means however, this is a highly inefficient method to prepare this chlorin.⁸² Extraction or fractional crystallization techniques are not much more efficient.⁸³ A Rothemund condensation designed to generate *meso*-tetramethylporphyrin reportedly contained large amounts of the chlorin contaminant (**13**),^{40,84,85} presumably due to a higher oxidation potential of this chlorin *versus* TPC. Ulman, Ibers and co-workers found conditions under which this contamination could be, albeit in low total yields (2-4 %), formed as the exclusive product (Scheme 1-2).⁸⁶ Demetallation of these metallochlorins under strict exclusion of oxygen gave the free base chlorins.



Scheme 1-2 Rothemund-type synthesis of *meso*-tetraalkylmetallochlorins **13**
Reaction conditions: (i) 1. AcOH, 2% Ac₂O, M(OAc)₂, Δ

Chlorins via 2 + 2 Synthesis

Burns *et al.* succeeded recently in synthesizing in an astounding yield of 24-27 % a chlorin *via* a 2 + 2 MacDonald-type condensation in a two-step one-pot procedure.⁸⁷ The researchers based their synthesis on the previous findings of Closs⁸⁸, Buchler⁸⁹, and Whitlock and their co-workers.⁹⁰ They described the tautomeric equilibrium between the anion of a metallo-5,23-dihydroporphyrin and the corresponding metallated chlorin anion. The phlorin anion seemed to be the equivalent of the monoanion of a 5,15-dihydroporphyrin. Phlorins, such as **14**, can be prepared by a MacDonald 2 + 2 condensation of a dipyrromethane bisaldehyde **15** with a dipyrromethane **16**, if care is taken to exclude oxygen (Scheme 1-3). Upon metallation with zinc, **14** tautomerized, to the surprise of Burns *et al.*, over the course of several hours quantitatively to metallochlorin **17**, without the need to form the anion first. For reasons not entirely clear, zinc ions seem to be exceptional in stabilizing chlorins and/or in promoting the rearrangement of *meso*-hydrogenated porphyrins into chlorins.⁷² Even more surprising, one chlorin isomer is almost exclusively formed. The mechanism and regioselectivity of this interesting chlorin synthesis are, according to Burns *et al.*, currently under investigation and thus no evaluation of this reaction for the production of PDT agents can be made.



Scheme 1-3

MacDonalld 2 + 2 synthesis of metallochlorin **17**⁸⁷

Reaction conditions: (i) 1. N₂, *p*-TsOH, CHCl₃; 2. aqueous NaHCO₃ wash; 2. Zn(OAc)₂, MeOH

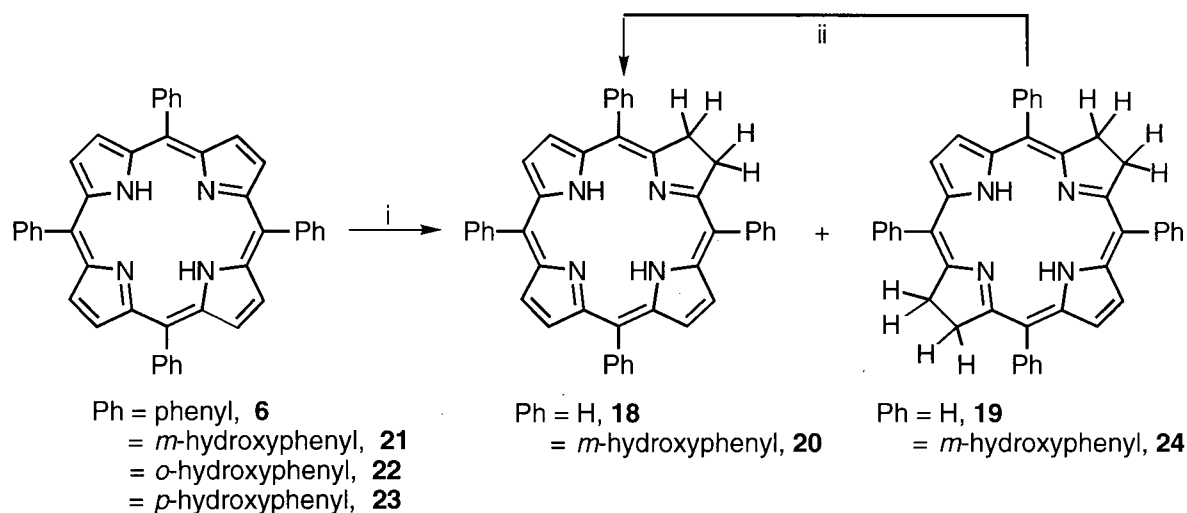
1.3.2.4 THE CONVERSION OF PORPHYRINS INTO CHLORINS BY REDUCTION

The importance of chlorins as model systems for certain biological systems and for their use in PDT, coupled with the lack of simple or general methods for their total synthesis, resulted in profuse efforts to convert porphyrins into their reduced forms. Theoretically, this corresponds to the mere addition of one (or two) pairs of (molecular) hydrogen to the β -positions of porphyrins. In practice, this turns out to be non-trivial. All eleven double bonds of a porphyrin are potentially reducible, and the conversion of porphyrins into chlorins is, therefore, a matter of delicate chemical selectivity. In practice, however, only a few of the double bonds will react with a given reagent. Calculations have shown that the *meso*- and the β -carbons are, in comparison to the others, the most reactive, a finding which is confirmed by the reduction reactions. Phlorins are often formed as primary (kinetic) products which subsequently rearrange into chlorins (thermodynamic products). Once the non-aromatic phlorin is formed, it is prone to further reduction. Metallation of a porphyrin often has profound consequences for the outcome of the reduction. Reactions which transfer dihydrogen are advantageous as this transfer can occur for steric reasons much more easily at the periphery of the porphyrin, *i.e.* at the β -positions than at any other position, leading directly to the formation of chlorins.

The common hydride containing reducing agents are generally inactive with the noticeable exception of diborane. Hydroboration of OEP results in the formation of a 5:1 mixture of the *cis*- and *trans*-isomers of the octaethylchlorin (OEC), possibly due to two competing pathways.^{72,91} Pure *trans*-OEC is best prepared by the sodium reduction of OEPFe(III)Cl in isoamyl alcohol. Catalytic reductions such as hydrogen over palladium or

platinum/charcoal form the *cis*-isomer but tend to over-reduce the porphyrin to the corresponding leuco-form, *i.e.* the porphyrinogen.

The most common, in fact the only reagent known to generally convert porphyrins into chlorins, is diimide (Scheme 1-4).⁹² This reduction method was introduced in 1969 by Whitlock *et al.* and is performed today essentially as described in the original report.⁸³ The diimide is generated *in situ* from *p*-toluenesulfonylhydrazide in refluxing pyridine. This reduction of a porphyrin, however, produces a mixture of reduced products. For instance in the diimide reduction of TPP are starting material **6**, chlorin **18** and bacteriochlorin **19** isolated by extraction techniques utilizing the different basicity of the compounds, and then these are finally purified by chromatography. The chromatography steps have severe practical disadvantages. The R_f -values of these chlorins, bacteriochlorins and porphyrins are only marginally different and require chromatography columns with extremely large compound to solid phase ratios or preparative HPLC or TLC techniques. This practical disadvantage can be mitigated somewhat by the possibility of selectively oxidizing the bacteriochlorin to the chlorin and thereby simplifying the mixture.^{93,94}



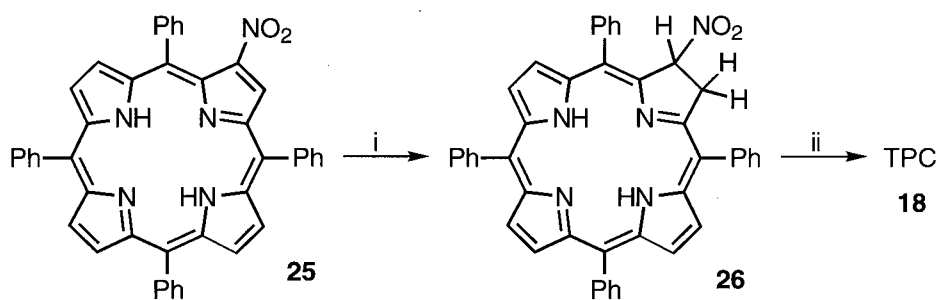
Scheme 1-4

Diimide reduction of TPP (**6**)Reaction conditions: (i) K_2CO_3 , *p*-toluenesulfonylhydrazide, Δ (ii) *p*-chloranil

The diimide reduction exhibits an interesting selectivity. Metallochlorins are converted selectively into metalloisobacteriochlorins, whereas chlorins are converted selectively into bacteriochlorins. The basis for this and related selectivities is discussed in section 1.3.3.4.

Regardless of the practical difficulties, Bonnett hails the use of *meso*-tetra-(*m*-hydroxyphenyl)chlorin **20**, prepared by the diimide reduction of the corresponding porphyrin, as the next generation PDT drug.³ Following the discovery that TPPs with hydroxy substitution (**21-23**) are good *in vivo* photosensitizers, Berenbaum, Bonnett and co-workers tested the analogous chlorins and bacteriochlorins.^{23,95,96} And, as expected, their *in vivo* activity as measured by dose of sensitizer required to cause photonecrosis reaching 5 mm deep into a rat tumor model increases in the sequence porphyrin **21** << chlorin **20** < bacteriochlorin **24**.²³ Since the bacteriochlorin is labile, the research efforts have been focused on the chlorin **20**.^{23,96} Also, a cost-benefit analysis, *i.e.* a comparative analysis of the benefit of desired tumor photonecrosis *versus* the cost of photodamage of healthy tissue under the same irradiation conditions, has singled out chlorin **20** as the most promising drug.⁹⁷ It possesses the required photophysical properties (λ_{\max} (MeOH) = 650 nm, $\log \epsilon = 4.52$), is a single compound accessible in a few steps from simple starting materials, is non-mutagenic and has minimal dark toxicity.^{3,98} Its therapeutic index has been optimized.⁹⁹ As a result of these favorable characteristics, clinical studies with this drug have been conducted or are underway and their initial results have been promising.^{3,100,101}

The reduction of non-symmetric porphyrins results generally in the formation of all four regioisomeric chlorins. Only in exceptional cases has a selective reduction been observed and steric^{72,76,102,103} as well as electronic¹⁰⁴ reasons have been cited for the observed selectivity. Another case is the specific hydride reduction of 2-nitro-TPP (**25**)¹⁰⁵ (Scheme 1-5).



Scheme 1-5 Reduction of 2-nitro-TPP (**25**)¹⁰⁵
Reaction conditions: (i) 1. NaBH₄; 2. H₂O (ii) Bu₃SnH/AIBN, benzene, Δ

2-Nitro-TPP (**25**) can be reduced with sodium borohydride to the nitro-chlorin **26**.¹⁰⁶⁻¹⁰⁸ TPP itself is inert under the very same conditions. Apparently the presence of the nitro group activates the porphyrin towards a nucleophilic attack of the hydride ion such that the nitrated β,β' -bond resembles in its activity an isolated nitroene system.^{109,110} Radical denitration yields the desired chlorin (**18**).

Photochemical, electrochemical and other special reduction methods have also been utilized.⁷² The limited selection of effective reducing reagents and the reversible nature and general non-selectivity of the reductions, have led to the development of many non-reversible chlorin syntheses.^{111,112}

1.3.2.5 NON-REVERSIBLE CONVERSION OF PORPHYRINS INTO CHLORINS

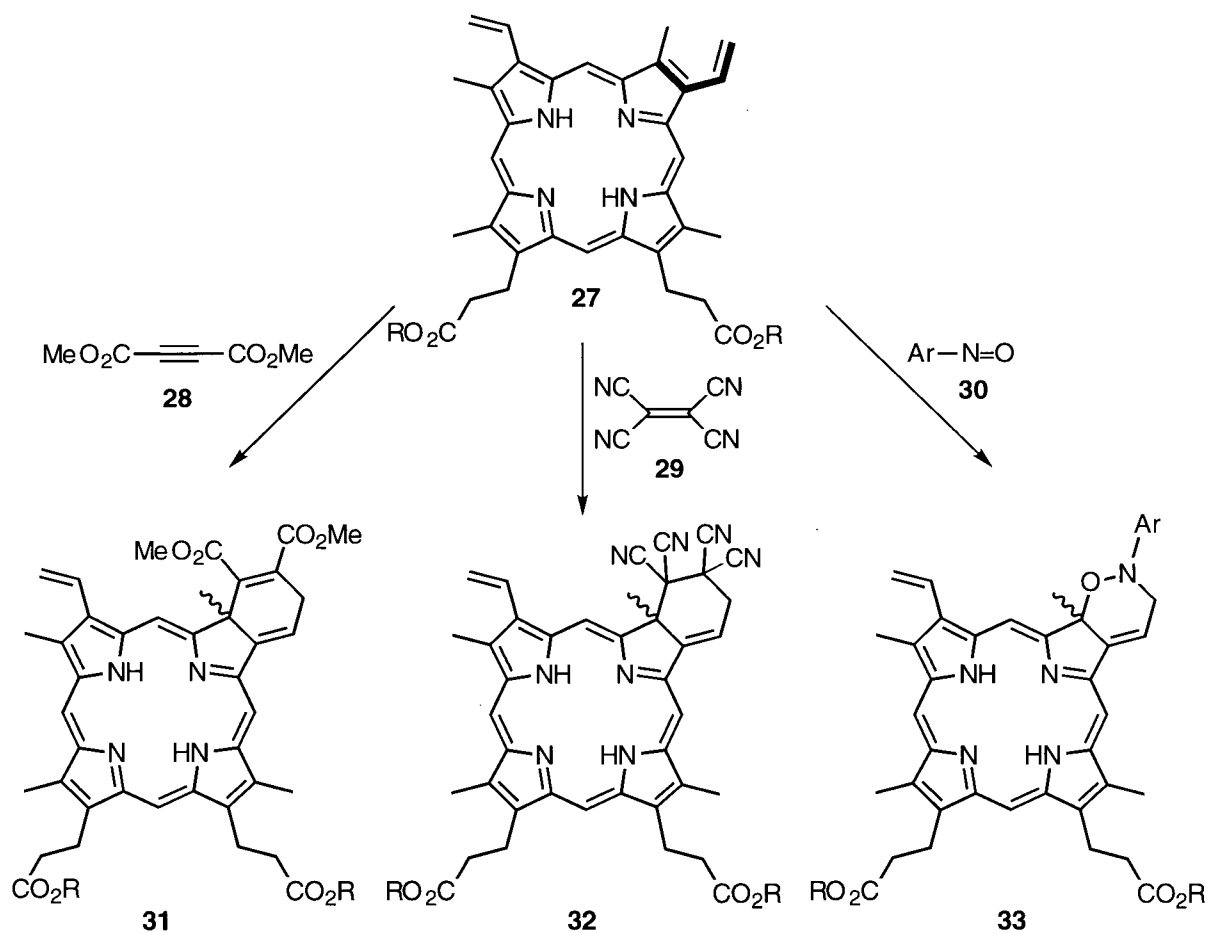
Diels-Alder Reactions of β -Vinylporphyrins

The β -vinyl group of a porphyrin, for instance protoporphyrin IX (**27**), in cooperation with a β,β' -double bond, can act as a diene in a [4+2]-Diels-Alder cycloaddition with activated dienophiles.^{113,114} Dimethylacetylene dicarboxylate¹¹⁵⁻¹¹⁸ (DMAD) (**28**), tetracyano-ethylene (**29**)¹¹⁹, β -(phenylsulfonyl)propionic acid¹¹⁶, and nitrosobenzene (**30**)¹²⁰ have been used successfully as dienophiles (cf. to the [4+2]-cycloaddition of singlet oxygen with protoporphyrin IX as described in section 1.3.3.5). In the course of the reaction, the β,β' -double bond of the porphyrin is lost and a stable chlorin (**31-33**) is generated (Scheme 1-6).

This reaction has the great advantage of being capable of utilizing a naturally-occurring vinyl substituted porphyrin which also is available in large amounts, namely protoporphyrin IX (**27**).¹²¹ This advantage has a flip-side: protoporphyrin IX is not symmetric, *i.e.* the two vinyl groups are non-equivalent and any Diels-Alder reaction occurs in a roughly 1:1 ratio at both vinyl groups, generating a mixture of so called ring A and ring B isomers, or it may even react with both vinyl groups to generate an isobacteriochlorin.¹¹⁹ The generated diastereomers are separable by chromatography. Moreover, the attack of the dienophile can proceed from above the plane of the porphyrin or from below the plane, resulting in a mixture of enantiomers which are much more difficult to separate.

The primary Diels-Alder adduct of **27** when treated with DMAD, the 1,4 diene (**31**), is prone to undergo base catalyzed rearrangement to the corresponding 1,3-diene (**1**) (Scheme 1-7). This rearrangement yields a chlorin chromophore with an extension of the

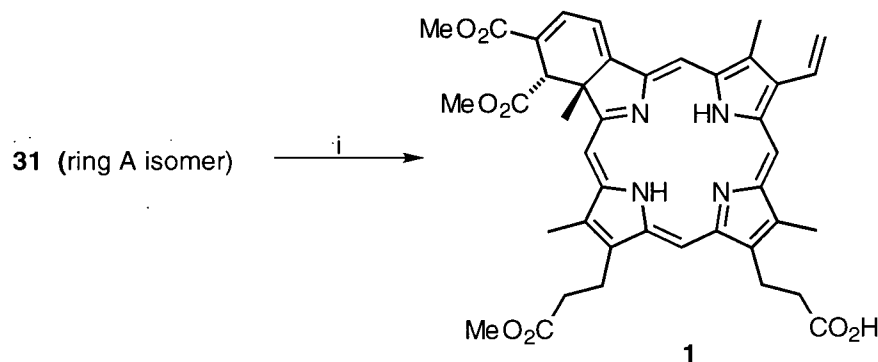
π -system. This leads to a bathochromic shift of the longest wavelength absorption (from $\lambda_{\max}(\text{CHCl}_3) = 666 \text{ nm}$ for **31** to $\lambda_{\max}(\text{MeOH}) = 686 \text{ nm}$, $\log \epsilon = 4.53$ for **1**).¹²² This absorption is within the 'ideal' region for PDT. Other photophysical parameters of **1** such as singlet oxygen quantum yield *etc.* are also adequate for use as a PDT drug.¹²²



Scheme 1-6 Diels-Alder reactions of protoporphyrin IX dimethyl ester (**27**). For clarity only one of the two possible regioisomers (ring A and ring B isomers) is shown. The diene moiety is shown in bold.

Acid-catalyzed hydrolysis of the propionic acid esters to the free acids generates a highly cytophototoxic compound (Scheme 1-7).²¹ It was, however, the discovery that the partially hydrolyzed regioisomeric monoester monoacid (**1**), now known as BPD-MA (benzoporphyrin derivative ring A mono acid), exhibited an even larger cytotoxicity when

tested against a variety of normal and malignant cell lines which led to its evolution into a promising PDT drug.¹²³

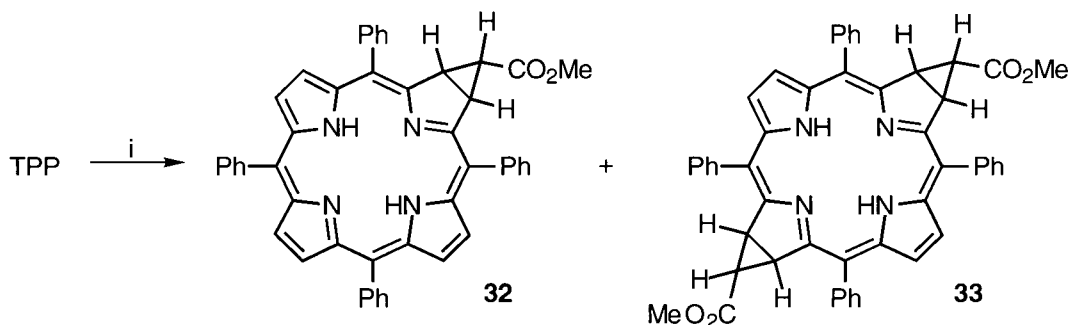


Scheme 1-7 The preparation of BPD-MA. Only one possible enantiomer of the regioisomeric monoesters is shown.
Reaction conditions: (i) 1. DBU; 2. HCl

While **1** does not show specific affinity for tumors, it exhibits significantly higher concentration in tumors than in the surrounding healthy tissue.¹²⁴ BPD-MA demonstrated a lower skin photosensitivity than that given by Photofrin®. BPD-MA also clears, post administration, rapidly from the system, which is another advantage. The presence of stereo- and regioisomers in the drug impels laborious experimentation in order to meet the regulatory requirements for the approval of new drugs. To this end, clinical trials are now well under way and this drug has been approved by some national regulatory agencies for its clinical use in PDT.¹ Further derivatization of BPD for its use in, for instance, topical applications, is still in progress.¹²⁵ The development of BPD-MA as a PDT drug has recently been reviewed in a (printed) lecture.¹

Reactions of TPP with Carbenes

The exocyclic double bonds in porphyrins have been shown to be susceptible to cyclopropanation with carbenes from sources such as diazomethane or diazoesters. TPP, for example, combines with diazoesters in the presence of copper(I) iodide to form the chlorin **32** ($\lambda_{\max}(\text{CH}_2\text{Cl}_2) = 650 \text{ nm}$, $\log \epsilon = 4.25$) as a separable mixture of *endo*- (5 %) and *exo*- isomers (20 %) and bacteriochlorins **33** ($\lambda_{\max}(\text{CH}_2\text{Cl}_2) = 720 \text{ nm}$, $\log \epsilon = 3.6$). Although Callot reports the isolation of the two possible *exo/exo* isomers of **33**, it is reasonable to assume the presence of other isomers.¹²⁶

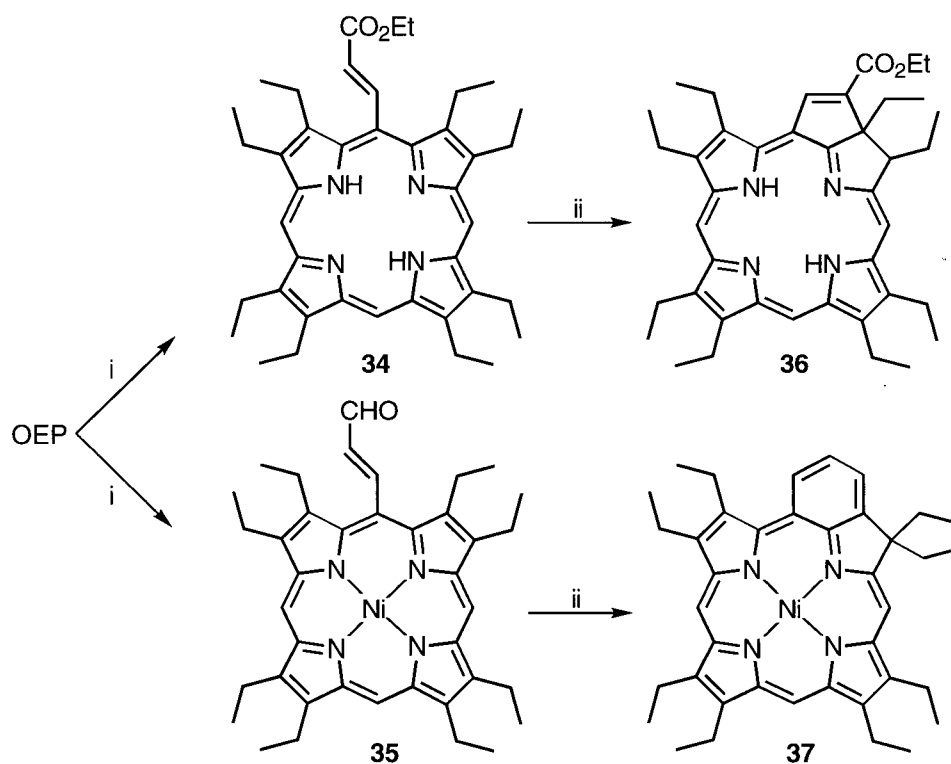


Scheme 1-8 Cyclopropanation of TPP with a carbene
Reaction condition: (i) diazoethylacetate/CuCl

N-Alkylated products are the sole products of the equivalent reaction with TPPZn. Callot's report has been the only one of this kind, and with a respectable yield of 30 % for the chlorin resulting from the reaction with diazoethylmalonate, this is surprising. The cyclopropane entity is apparently stable, introduces amphiphilicity, could be cleaved to the free acid and the reaction is theoretically compatible with a variety of possible phenyl substituents. The reaction of OEP with carbenes generates lower yields and more side products, but the cyclopropane chlorin of OEP is known.¹¹⁵

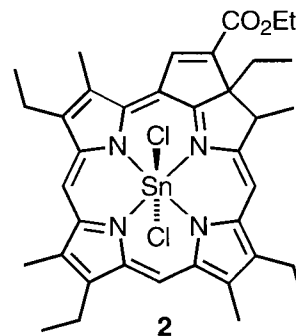
Benzochlorins and Purpurins¹²⁷

Both benzochlorins and purpurins are products of an intramolecular cyclization of *meso*-alkene substituted porphyrins, such as **34** or **35** (Scheme 1-9). They are, typically derived from consecutive Vilsmeier-Haak and Wittig reactions.



Scheme 1-9 Formation of octaethylpurpurin (**36**) and octaethylbenzochlorin (**37**)
Reaction conditions: (i) Me_2NCHCHR , POCl_3 ; (ii) strong H^+

Acid catalyzed cyclization of acrylate substituted nickel porphyrin **34** yields purpurin **36**.^{128,129} This compound exhibits the typical spectroscopic characteristics of a chlorin. A number of purpurins have shown photodynamic activity.¹²⁷ The dichloro tin(IV) complex of an etiopurpurin, **2**, has turned out to be an



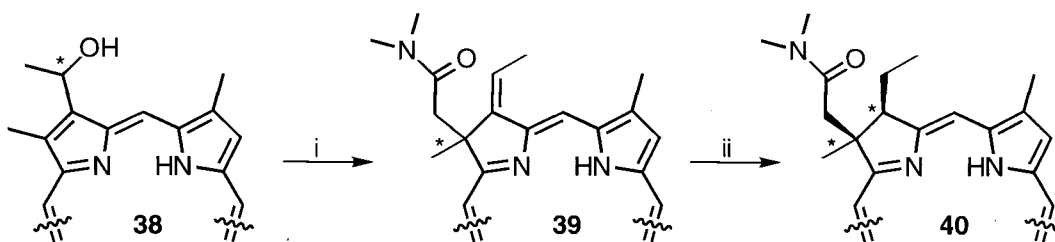
attractive candidate as an PDT agent. Of special note is the fact that administration of this compound elicits only minimal skin sensitization in a rat model.¹³⁰ Clinical trials for treatment of cutaneous carcinoma are under way.¹³¹ Purpurins with various *meso*-phenyl substituents have been prepared, however, no biological data are available.¹³²

Metallobenzochlorins, like **37**, are available through the acid-catalyzed cyclization of a *meso*-acrolein substituted¹³³ metalloporphyrin such as **35** (Scheme 1-9).^{127,128} Removal of the metal from these chlorins creates biologically active photosensitizers.¹³⁴ Several 'improved' (metallo)benzochlorins with either *meso*-phenyl substituents¹³⁵ or a *meso*-iminium salt moiety¹³⁶ have been prepared. The copper complex of the latter was shown to be a photosensitizer acting *via* a Type I mechanism, whereas its free base showed, due a prolonged triplet life time, Type II characteristics.¹³⁷

Compounds integrating the characteristics of purpurins and benzochlorins are known but their synthesis is much more involved. It is doubtful that they will become any option for larger scale syntheses.¹³¹

Chlorins by Claisen Rearrangement

Montforts and Zimmermann introduced in 1986 an interesting conversion of a hydroxyethyl substituted porphyrin (**38**) as shown in Scheme 1-10.^{138,139} Compound **38** undergoes a Claisen-type rearrangement if treated with *N,N*-dimethylacetamide dimethyl-acetal at elevated temperatures. The resulting chlorin **39** can be reduced to the closely related chlorin **40**. Both chlorins have satisfactory photophysical properties (for **39**: λ_{\max} (CHCl₃) = 660 nm, $\log \epsilon = 4.62$; for **40**: λ_{\max} (CHCl₃) = 645 nm, $\log \epsilon = 4.67$)¹⁴⁰, but the procedure introduces two chiral centers into the porphyrin and generates a mixture of stereoisomers. In addition to this conversion, some variations of this rearrangement pathway have been published.^{141,142}



Scheme 1-10 Claisen-type rearrangement of a hydroxyethyl substituted porphyrin with *N,N*-dimethylacetamide dimethylacetal. Only one set of possible stereoisomers shown.
Reaction conditions: (i) CH₃C(OCH₃)₂N(CH₃)₂, *o*-xylene, 160°, mol-sieves 3 Å (ii) H₂, Pd/C, methanol

With hematoporphyrin as the substrate, an isobacteriochlorin is produced and the regio- and stereochemistry of this compound are complex.¹⁴³ The researchers have, therefore, settled for the development of PDT drugs from the rearrangement of mono-substituted deuteroporphyrins, which cuts down on the final number of isomers but introduces several non-trivial steps to the total synthetic pathway as these mono-substituted deuteroporphyrins have to be synthesized, typically from hemato- or protoporphyrin.¹³⁹

1.3.3 SYNTHESIS OF β -HYDROXY CHLORINS

β -Hydroxychlorins are a central topic of this thesis and, hence, will be discussed in some detail. As will be shown, most β -hydroxychlorins are synthesized *via* the osmium tetroxide mediated oxidation of a peripheral double bond in porphyrins. For a better understanding of these reactions, some aspects of the osmium tetroxide oxidation will be discussed first.

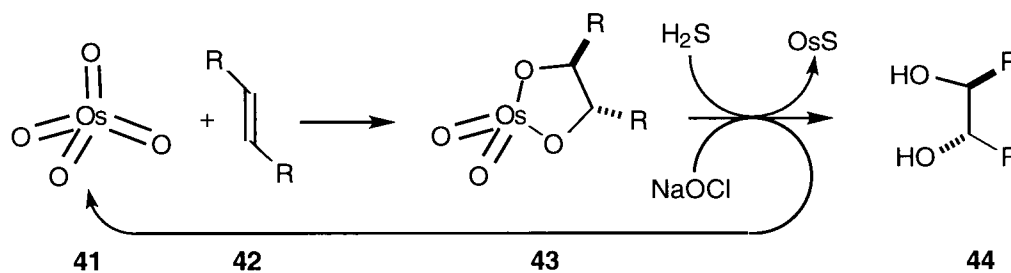
1.3.3.1 THE OSMIUM TETROXIDE OXIDATION IN GENERAL

It has been stated in a review¹⁴⁴ that the first research paper describing the reduction of osmium tetroxide by unsaturated species was published in 1908 by Makowka,¹⁴⁵ however, in an historical account¹⁴⁶ it was noted that Butlerov mentioned, in his 1851 Masters Thesis, the oxidation of organic compounds by osmic acid. Hofmann showed in 1912 that osmium tetroxide could, in the presence of a co-oxidant, be used catalytically to hydroxylate double bonds.¹⁴⁷ In 1936, Criegee¹⁴⁸ developed the dihydroxylation of alkenes with stoichiometric amounts of osmium tetroxide and recognized the intermediate formation of an osmate ester.

“The stoichiometric osmylation of olefins as perfected by Criegee ... is generally regarded as the most reliable synthetic transformation available to organic chemists. The reasons are simple: OsO_4 reacts with *all* olefins, and it reacts *only* with olefins. Admittedly, the “all” and “only” in this latter statement are used with some poetic license; however, no other known organic reaction comes close to achieving such enormous scope coupled with such great selectivity.”¹⁴⁹

This strong statement about the osmium tetroxide oxidation of olefins is a quote from a recent review by Kolb, Van Nieuwenhze and Sharpless. This chapter will describe the general mechanism of the osmylation and will detail the “poetic license” of this reaction.

Figure 1-11 illustrates in a schematic way the fundamental steps of the catalytic and stoichiometric osmium tetroxide dihydroxylation.



Scheme 1-11 Osmium tetroxide mediated dihydroxylation of alkenes

Osmium tetroxide (41) adds to a double bond (42) to form the stable osmate ester (43). This osmate ester can be cleaved reductively (with *e.g.* hydrogen sulfide, lithium aluminum hydride, mannitol or sodium bisulfite) to form an insoluble osmium salt, or can be oxidatively cleaved (*e.g.* with *tert*-butyl hydroperoxide, morpholino N-oxide, sodium hypochlorite) to regenerate the osmium tetroxide thus opening up a pathway in which the osmium tetroxide can be used in catalytic amounts. In either case, the *cis*-diol (44) is formed in good yields. The structure of species 43 is only a formal representation. In the absence of any amine ligand it exists either as a dimer containing five-coordinate square-based pyramidal osmium(VI) with cyclic ester rings¹⁵⁰ or it reacts with a second equivalent of alkene to form a monomeric diester complex in which the osmium is coordinated in an analogous fashion.¹⁵¹ In the presence of an amine ligand it exists as a bis-amine complex.

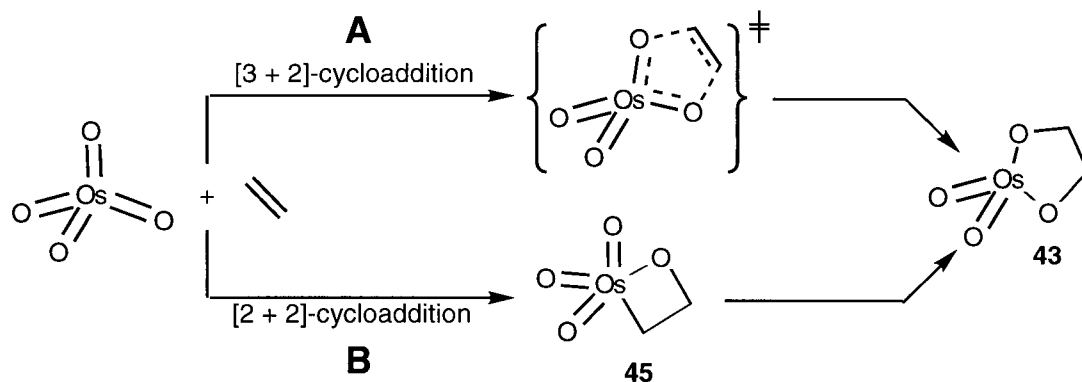
Generally, isolated and conjugated double and triple bonds are susceptible to the dihydroxylation and aromatic systems are inert, with the notable exceptions discussed below.

The osmylation reaction has found a wide field of application, ranging from its use in electron microscopy as a staining and fixative agent for biological tissue¹⁵² (unsaturated lipids are proposed to be osmylated, thus crosslinked and permeated with the electron-rich metal) to the preparation of fine chemicals¹⁴⁴. Crystal structures of the intermediate osmate esters have been determined^{153,154}, their rates of formation and hydrolysis have been studied^{144,155}, electron-poor substrates such as partially and fully fluorinated olefins have been osmylated^{154,156,157}, and heterogeneous osmium tetroxide oxidation catalysts have been prepared.¹⁵⁸ The rate of the osmium tetroxide-catalyzed dihydroxylation is considerably accelerated by the additions of amine ligands^{159,160} and this metal-ligand interaction has been utilized to impose enantioselectivity on the dihydroxylation through the use of chiral amine ligands.^{161,162,163} Reviews pertaining to the various aspects of the osmium tetroxide hydroxylations have been published.^{144,164,165}

1.3.3.2 THE MECHANISM OF THE OSMIUM TETROXIDE ADDITION TO DOUBLE BONDS

In light of the aforementioned, it seems astonishing that the mechanism of the osmylation is still under debate. The alternatives are shown below:

- A** A one step concerted mechanism in the form of a [3+2]-cycloaddition of the osmium tetroxide to the olefin to form the glycol ester **43**.
- B** A two step mechanism involving the metallaoxetane formation (**45**) in the form of a [2+2]-cycloaddition and subsequent rearrangement into the glycolate complex **43**.



Scheme 1-12 Mechanistic alternatives for the osmylation of olefins. Possible ligation by amine ligands at any stage has been omitted for clarity.

In an attempt to clarify the situation, Göbel and Sharpless published in 1993 a kinetic study on the influence of the reaction temperature on the enantioselectivity of the asymmetric hydroxylation of olefins with chirally modified alkaloid-osmium tetroxide complexes.¹⁶⁶ They evaluated the modified Eyring-plots according to the isoinversion principle, a model of chemical selectivity.¹⁶⁷ Clear indications of a multi-step mechanism with at least two rate-determining diastereoselective steps were thus provided. This finding rules out the one step [3+2]-addition mechanism. Although this is strong evidence for the two step mechanism shown above, it is not proof. The findings are consistent with any two-

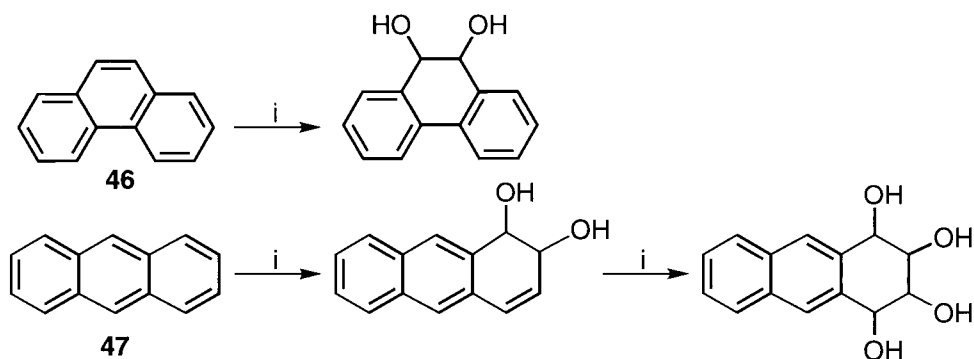
step mechanism. However, several other indications support the [2+2]-pathway which was initially proposed as a result of the comparison of the reactivity of alkenes with the permanganate ion and osmium tetroxide:¹⁶⁸

- A C=C bond, albeit only a weak nucleophile, would be expected to attack at the more electropositive end of the Os=O bond, thus forming **45**.¹⁶⁹ In accord with this, osmium tetroxide reacts with the stronger nucleophile *tert*-butylamine at the metal centre.¹⁷⁰
- It has been repeatedly observed that electron-withdrawing groups on the alkene retard its reactivity toward osmium tetroxide presumably because of the lowering of the nucleophilicity of the double bond.¹⁴⁴,
- Aromatic substrates (*vide infra*) react with osmium tetroxide at their site of greatest electron density¹⁷¹, *i.e.* the bond with the highest degree of bond localization and, therefore, greatest nucleophilicity. The following section will present an extended discourse of this reaction type.
- The dramatic increase in the rate of formation of the osmate ester **43** on addition of amines like pyridine might be explained by an increase of the rate of the rearrangement due to the electron-donating effect of the amine ligand.¹⁴⁴
- Theoretical approaches calculate a lower transition state energy for the [2+2]-pathway as compared to the [3+2]-pathway.¹⁶³

Collectively, these indications are highly supportive of the [2+2]-addition with subsequent rearrangement of the metallacycle and, consequently, this can be considered the most likely mechanism.

1.3.3.3 THE OSMIUM TETROXIDE OXIDATION OF AROMATIC SYSTEMS

The osmium tetroxide-catalyzed dihydroxylation of olefins is considered a mild and highly selective oxidation and is routinely performed in the presence of aromatic systems.¹⁶⁵ However, osmium tetroxide oxidations of aromatic systems were described as early as 1942¹⁷² and have been studied in detail since.¹⁷³⁻¹⁸⁰ This apparent paradox finds its explanation in the rate of the oxidation of alkenes as compared to that of aromatic systems. Whereas a reaction time of some hours is sufficient to achieve quantitative turnover for the former, the latter requires days, weeks, and in extreme cases months for reasonably high yields. As will later be shown with the osmium tetroxide oxidation of a benzoporphyrin derivative (Scheme 1-17), in substrates containing both double bonds and aromatic systems, any available double bond will be oxidized first before the oxidation of the aromatic system becomes appreciable. This kinetic differentiation explains the high degree of selectivity of the osmylation reaction.



Scheme 1-13 Osmium tetroxide mediated dihydroxylation of polycyclic aromatics
Reaction conditions: (i) 1. 1 equiv. OsO₄/3%pyridine/benzene, several days to one week; 2. mannitol/KOH

Aromatic systems undergo ring cleavage only in extreme cases.¹⁷⁸ Generally, osmium tetroxide attacks polycyclic aromatics regioselectively at the site where the addition to the double bonds results in minimal electron reorganization.^{181,182}

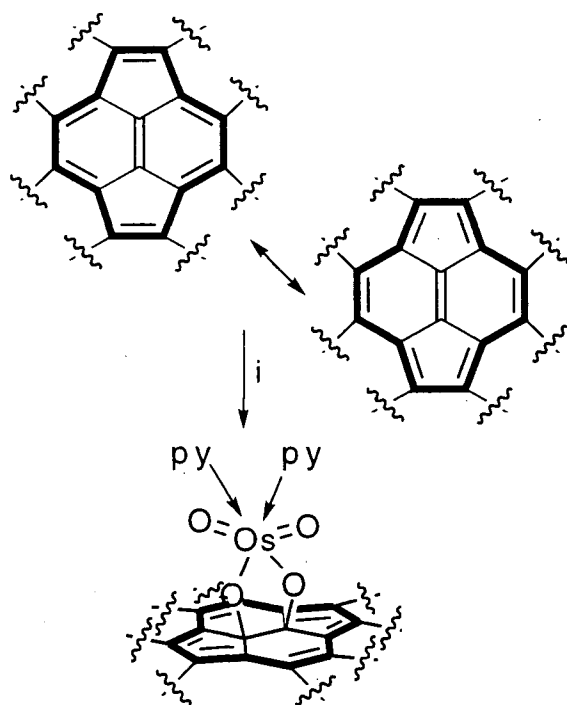
For example, phenanthrene (**46**) reacts at the 9- and 10-position, maintaining the aromaticity of two phenyl rings^{172,180}, and anthracene (**47**) adds the first equivalent to the 1,2-bond, maintaining a fully conjugated naphthalene system, and a second equivalent adds to the conjugated, yet non-aromatic 3,4-bond (Scheme 1-13).^{176,177} The site of addition in the phenanthrene case correlates with the site of highest electron density; in the anthracene case it does not, however, in both cases the attack occurs at the bond with the lowest localization energy $L(i)$, defined as

$$L(i) = E_{\pi}(S) - E_{\pi}(S - i) \quad \text{Equation 1-1}$$

where $E_{\pi}(S)$ is the π -electron energy computed, for instance, by HMO calculations, for the aromatic substrate S, and $E_{\pi}(S - i)$ is the computed π -electron energy of aromatic substrate without the bond at which the addition reaction took place.¹⁸¹ $L(i)$ is then an index which quantifies the extent to which the bond is delocalized. As a result, the smaller the value of $L(i)$, the greater the probability of the addition reaction occurring at the bond i . In other words, the bond with the highest (localized) double bond character will be the site of reaction. This sums up the interpretation of the "poetic license" in the statement regarding the selectivity of osmium tetroxide oxidations of alkenes.

The above bond localization energy argument as put forward by Dewar and Dougherty¹⁸³ has been formulated over the years as 'the principle of least motion or minimum electron reorganization'¹⁸² and is known for many reaction types, being exemplified in a formidable way by the osmylation of C₆₀-buckminsterfullerene. Buckminsterfullerene has a spherical C₆₀-frame work which resembles the seams of a soccer ball, *i.e.* it is composed of five- and six-membered rings. All vertices of the five-membered rings are connected to six-membered rings, and every second vertex of the six-membered rings is connected to another six-membered ring. This renders all carbons equivalent but

results in two bond types, namely those between two six-membered rings and those between six- and five-membered rings. Buckminsterfullerene regioselectively adds osmium tetroxide to the bonds connecting two six-membered rings¹⁸⁴⁻¹⁸⁶ (Scheme 1-14), a finding which has been confirmed by the X-ray crystal structure analysis of the buckminsterfullerene monoosmate ester bispyridine adduct (Figure 1-8)^{186b}.



Scheme 1-14 The osmylation of buckminsterfullerene

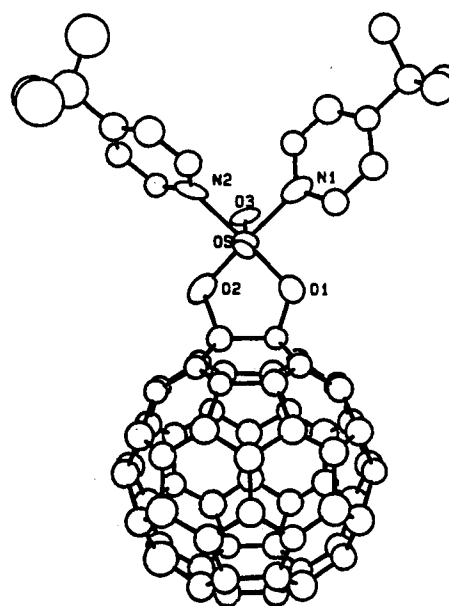


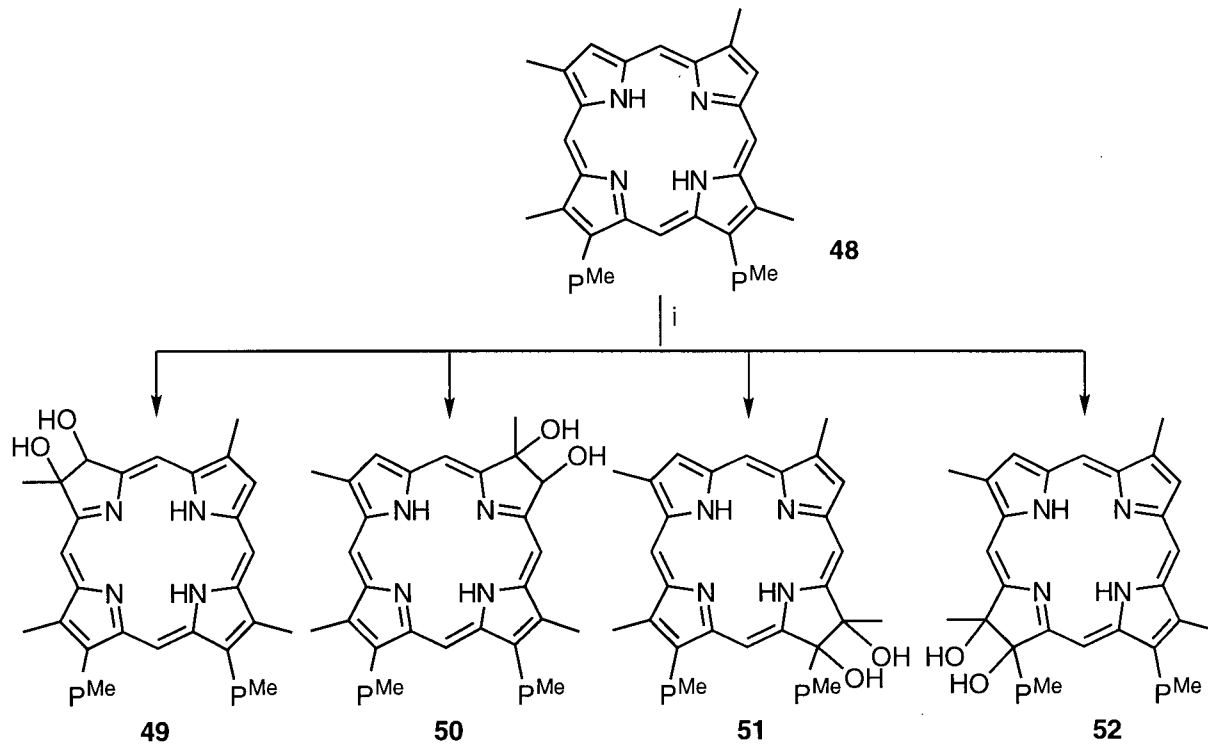
Figure 1-9 X-ray crystal structure of the buckminsterfullerene-osmium tetroxide adduct (from Hawkins *et al.*^{186b})

Wudl has rationalized this on the basis of defining buckminsterfullerene as a cluster of pyracycles, *i.e.* cyclic conjugated $4n-\pi$ -systems, shown in Scheme 1-14 in bold.¹⁸⁷ These cyclic systems 'freeze' the inner double bond in place. Consistent with Wudl's picture, this bond is also calculated to have a lower bond localization energy than the alternative bond¹⁸¹ and extended Hückel calculations also assign it a higher electron density¹⁸⁵. In light of this, it is expected that osmium tetroxide adds to this 'frozen' double bond.

1.3.3.4 THE OSMIUM TETROXIDE OXIDATION OF PORPHYRINS

Another large aromatic polycyclic system which has been successfully osmylated is the octaalkylporphyrin nucleus. To anticipate the conclusions, it can be stated that, as expected, the osmium tetroxide attacks the bond of highest double bond character, namely the β,β' -bond.¹⁸⁸ These bonds have also been described as "cryptoolefinic"¹¹¹.

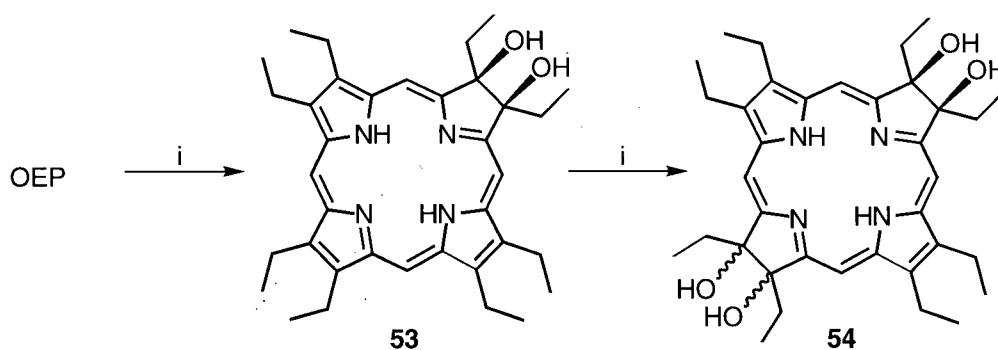
Fischer *et al.* reported in 1940 the oxidation of naturally occurring octaalkylporphyrins with osmium tetroxide to yield the corresponding *vic*-dihydroxy-chlorins.^{189,190} It was noticed¹⁹¹ that the reaction with naturally occurring non-symmetrical substituted porphyrins did not yield a single product, but the chlorin-type spectrum of the products revealed formation of the diol at the β,β' -positions.



Scheme 1-15 Osmium tetroxide mediated dihydroxylation of deuteroporphyrin dimethylester (**48**). PMe = methyl propionate side chain
Reaction condition: (i) 1. 1 equiv. OsO₄, pyridine, 2. H₂S

Porphyrins provide four such positions and this may give rise to the observed formation of regioisomers. Scheme 1-15 shows the four possible regioisomers (**49-52**) of the osmium tetroxide-mediated dihydroxylation of deuteroporphyrin dimethylester (**48**).¹⁹²

The separation of the regioisomers is cumbersome and, moreover, each regioisomer is formed as a pair of stereoisomers as a result of attack from above and below the plane of the porphyrin. The products are formed in a non-statistical manner. Steric as well as electronic influences are responsible for this. Oxidation takes place preferentially at the subunit in the quadrant opposite to a electronegative group.¹⁹³ MO calculations on this type of porphyrins have not been published, so any explanations following the principles of minimal electron reorganization or the like would be presumptuous. The osmylation of highly symmetric porphyrin, such as synthetic etioporphyrin I or OEP, provides only one isomer (Scheme 1-16).¹⁹⁴ The structure of **53** has been proven by X-ray crystallography (Figure 1-10). The diol functionality introduces some amphiphilicity into the molecule and generates a stable chlorin chromophore (**53**) (λ_{\max} (CHCl₃) = 643 nm, log ϵ = 4.62) fulfilling some of the photophysical criteria listed in section 1.1.3. Therefore, it is not surprising that these compounds have been suggested as third generation PDT agents.^{3,29,195-197} The skeleton of OEP allows no simple functionalization, so fine-tuning of the solubility and other physical properties is limited.



Scheme 1-16 Osmium tetroxide mediated dihydroxylation of OEP
Reaction condition: (i) 1. OsO₄/pyridine, 2. Reduction

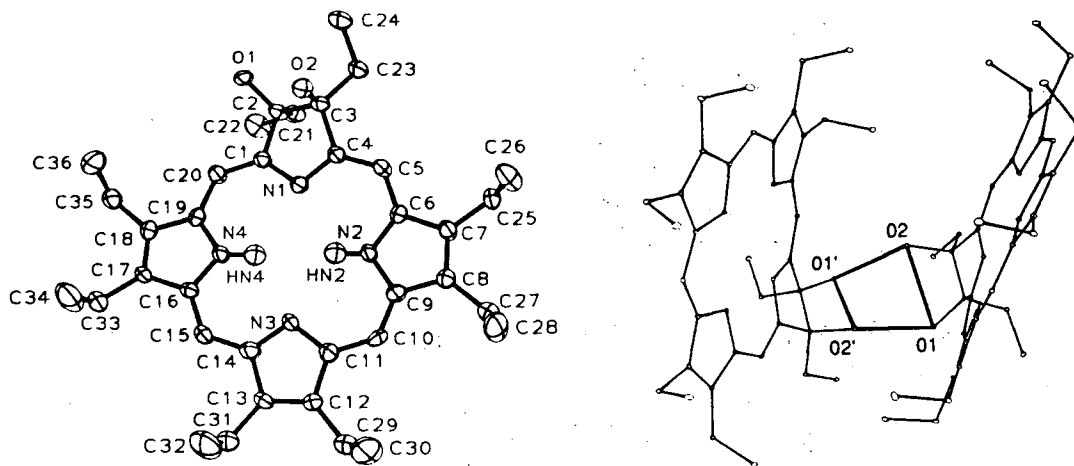


Figure 1-10 X-ray structure of **53** (from Barkigia *et al.*^{241b}). **53** forms a hydrogen bonded dimer in the solid state.

A second equivalent of osmium tetroxide oxidizes the diol chlorin selectively to the tetraol bacteriochlorin **54** (λ_{\max} (CHCl₃) = 715 nm, log ϵ = 4.72) as a mixture of stereoisomers.¹⁹⁵ This selectivity is general for all types of chlorins.^{198,199}

Insertion of a metal into the chlorin changes the outcome of the reaction drastically: Dihydroxylation of a metallochlorin results selectively in the formation of an isobacteriochlorin.¹⁹² The pronounced directing effect of the central metal has been observed before and appears to be general, *e.g.* in the diimide reduction of TPC⁸³, in the Raney nickel catalyzed reduction of nickel(II)pheophorbides²⁰⁰ and in the osmium tetroxide oxidation of pheophorbides¹⁹³ and *meso*-azachlorins²⁰¹. It has been suggested^{83,192} that the reduced double bond in a chlorin induces a pathway for the delocalized π -electrons that 'isolates' the diametrically opposed cross-conjugated pyrrolic double bond such that attack of this bond is favored over the attack of the double bond in the adjacent pyrrolic unit, resulting in a minimal loss of π -energy. Introduction of a metal (or protonation of the chlorin) changes the preferred π -delocalizing pattern, making the double bond in an adjacent

pyrrolic unit more reactive. Figure 1-10 shows the preferred π -electron delocalization pathway (bold) in chlorins and metallochlorins as inferred from the experimental findings.

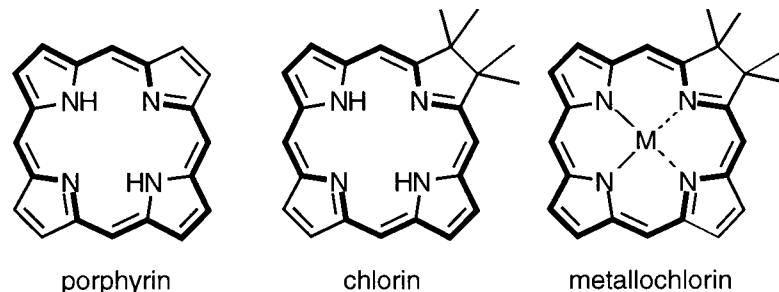
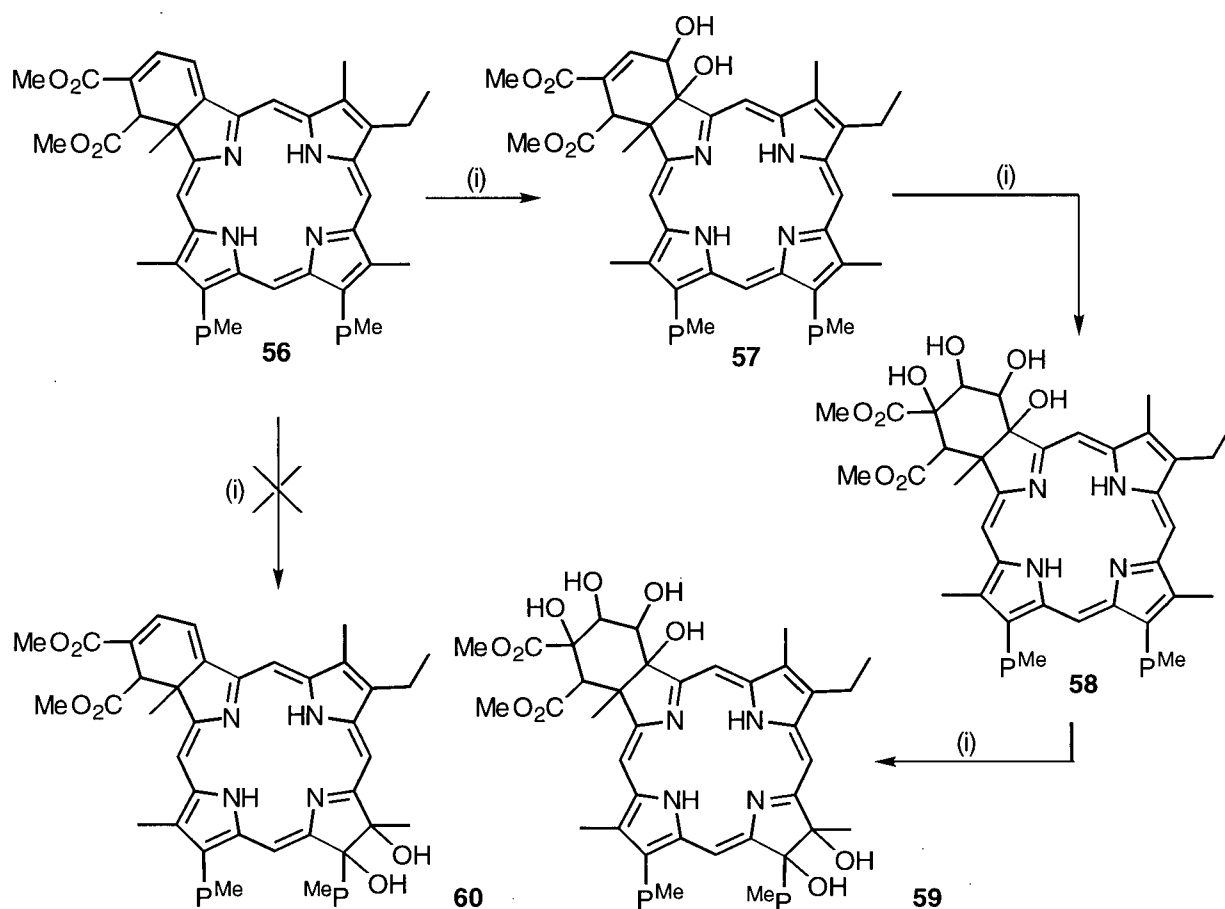


Figure 1-11 18 π -Electron delocalization pathway in porphyrins, chlorins and metallochlorins

Fischer reported in a publication from 1940 that multiple additions of osmium tetroxide form pigments with a red-shifted spectrum¹⁸⁹, but he was unable to isolate and characterize these pigments. Without realizing it, he surely was the first to observe this directing effect in chlorins.

With this and the above mentioned substituent directing effect and the relative rates of reaction of aromatic and non-aromatic double bonds in mind, the outcome of an osmium tetroxide mediated dihydroxylation on any porphyrin is predictable. The example of the dihydroxylation of the benzoporphyrin derivative **56** in Scheme 1-17 illustrates this. The non-aromatic double bonds will, upon exposure to osmium tetroxide, react first to yield the pigments **57** and **58**. At this stage a bacteriochlorin derivative **59** is formed. The direct formation of any bacteriochlorin **60** was not observed.²⁰² Despite the favorable photophysical properties and possible amphiphilic properties of **59**, any large scale use for this potential PDT drug can be ruled out on the basis of the mixture of stereoisomers formed and the many synthetic steps required.

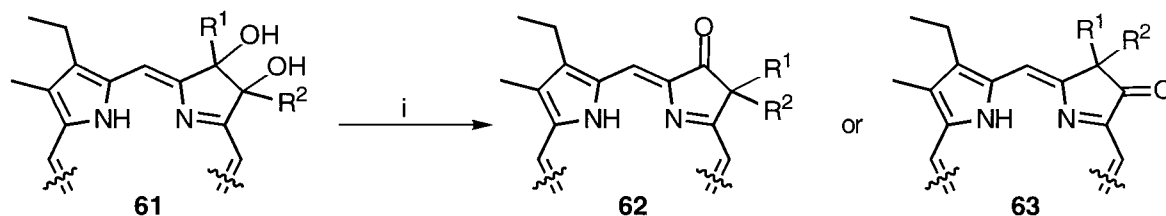


Scheme 1-17 Stepwise reaction of benzoporphyrin derivative (56) with osmium tetroxide. Stereochemistry was not specified.²⁰²
Reaction condition: (i) 1. OsO₄, 2. reduction

It should also be noted that the osmium tetroxide oxidation has been applied to *meso*-azaporphyrins to yield chlorins and bacteriochlorins.²⁰¹ Their complex synthesis, however, again precludes their practical use as drugs in PDT.

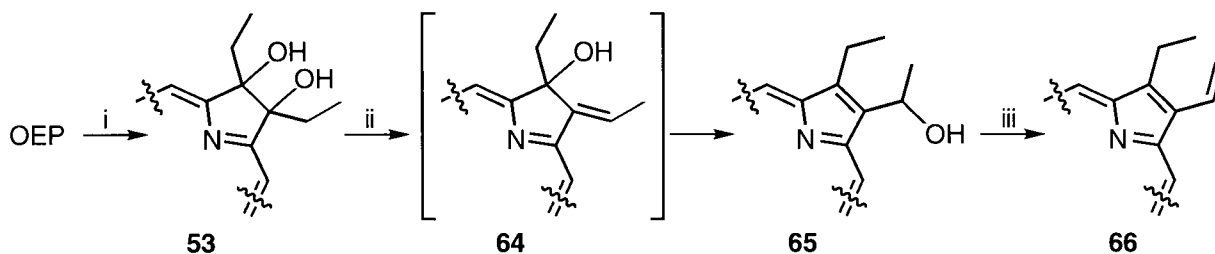
1.3.3.5 REACTIVITY OF VIC-DIOL CHLORINS

The chlorin diols undergo an acid-catalyzed pinacol-pinacolone-type rearrangement to yield β -oxochlorins. For non-symmetric substitution patterns on the porphyrin, the outcome of the rearrangement carries a regiochemical bias, as shown in Scheme 1-18. The diol **61** may rearrange into the two different oxo-chlorins **62** or **63**, depending on the migratory aptitude of the substituents. The migratory aptitude of the substituents has been established.²⁰³ The *gem*-dialkyl oxo-chlorins are, due to the lack of enolizable hydrogens, true chlorins.



Scheme 1-18 Pinacol-pinacolone-type rearrangement of the *vic*-diolalkylchlorins
Reaction condition: (i) benzene, trace HClO₄/ Δ .

Under carefully controlled conditions, the diol does not undergo the pinacolonic rearrangement but dehydration with subsequent rearrangement, as illustrated in Scheme 1-19.²⁰⁴



Scheme 1-19 Dehydration and rearrangement of *vic*-dihydroxyoctaethylchlorin **53**
Reaction Conditions: (i) 1. OsO₄, 2. H₂S; (ii) dioxane/water/HCl conc./ Δ ; (iii) benzene/trace HCl conc./ Δ

Diol **53** presumably dehydrates to the unstable ethenylhydroxychlorin **64**, which, with reconstitution of the fully-conjugated porphyrin system, rearranges to **65**. This hydroxyethylporphyrin can further be dehydrated to the heptaethylvinylporphyrin (**66**). This reaction sequence is of importance as it is otherwise very difficult to derivatize the ethyl side chains in OEP.

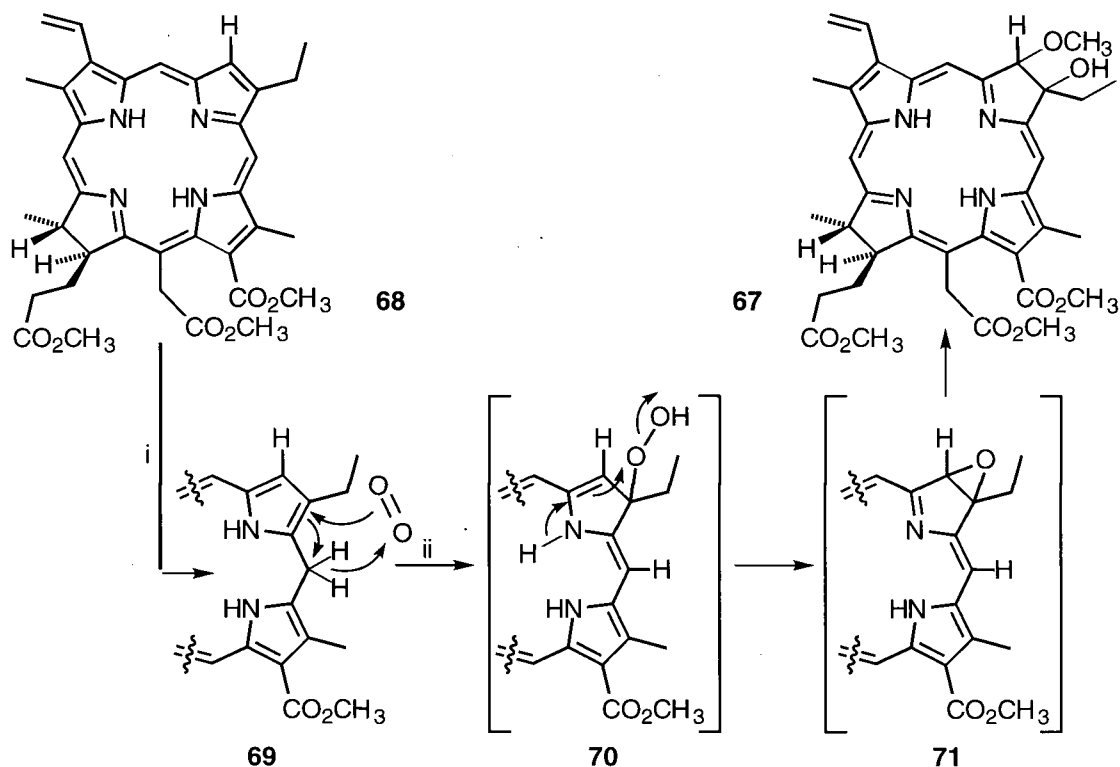
1.3.3.6 β -HYDROXYCHLORINS NOT DERIVED FROM AN OSMIUM TETROXIDE OXIDATION

Inhoffen's β,β' -Diol Monomethylether Bacteriochlorin

The osmium tetroxide oxidation of porphyrins is possibly the most versatile but not the only way to access β,β' -diol-type chlorins. The synthesis of a β,β' -diol monomethyl ether **67** by an intriguing photochemical pathway, shown in Scheme 1-20, was detailed by Inhoffen and co-workers.^{205,206}

Electrochemical reduction of chlorin- e_6 -trimethyl ester (**68**) resulted in the generation of the 10,22-dihydrochlorin- e_6 -trimethyl ester (**69**). Irradiation with light in the presence of oxygen and methanol led selectively to the formation of the diol monomethyl ether bacteriochlorin **67**. This finding can be rationalized by the mechanism of Scheme 1-20. Photooxidation of **68** leads to the formation of hydroperoxide **70**. Its dehydration leads to epoxide **71**, which opens in the presence of methanol to give the final product **67**. The configuration at C3 and C4 has not been determined, but according to the proposed mechanism, the diol ought to be a *trans*-diol. This pathway appears to be an attractive method to reduce a chlorin to a bacteriochlorin with concomitant selective introduction of,

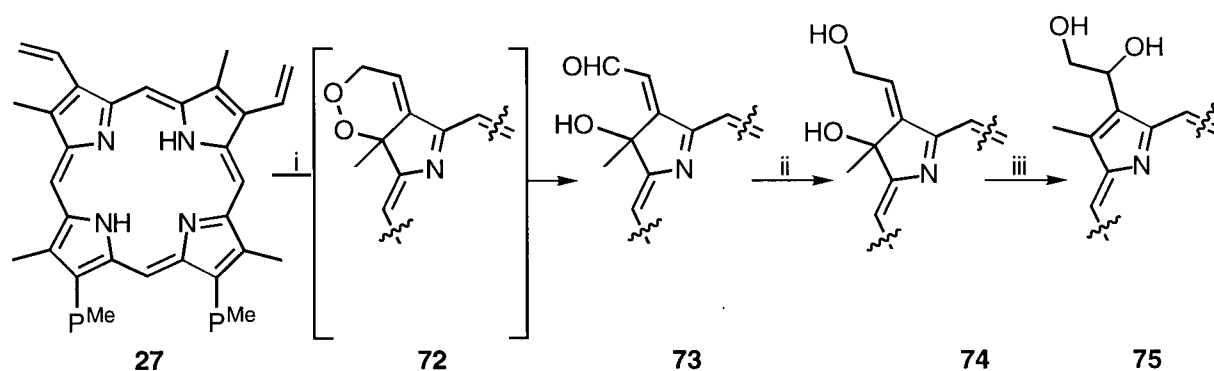
from the view point of designing PDT agents, desirable substituents. Unfortunately, this pathway cannot be considered general for variously substituted chlorins.



Scheme 1-20 Photochemical synthesis of bacteriodiol-monomethylether **67**. Configuration at C3 and C4 was not determined.
Reaction conditions: (i) electrolytic reduction; (ii) 1. O₂/hν, 2. MeOH

Photoporphyrin

Protoporphyrin (**27**) exposed to light and oxygen forms, most likely *via* an intermediate endoperoxide (**72**), the so called photoporphyrin (**73**) (Scheme 1-21).^{113,207-209} This name is a misnomer in the sense that photoporphyrin is a chlorin. Only one of the two available vinyl groups of the protoporphyrin reacts, thus forming two regioisomers, and owing to the chiral centre at C2/C7, each as pairs of stereoisomers. Upon reduction, it forms the allyl-diol **74**.

**Scheme 1-21** Formation of photoporphyrin **73**

Reaction conditions: (i) $O_2/h\nu$; (ii) $NaBH_4$; (iii) trace H^+/Δ

Assessing the viability of chlorin **73** and **74** as photosensitizers for PDT reveals that **73** has the disadvantage of necessitating a large scale photo-reaction, a less common modus for the industrial preparation of chemicals. Of greater practical disadvantage, however, is the formation of a mixture of stereo- and regioisomers, which require costly and cumbersome separation. The conjugated aldehyde functionality might also prove to be too reactive under physiological conditions. Its reduction to **74** may solve this, but **74** is acid labile. It rearranges readily to porphyrin **75**, obviating the spectral advantages of the chlorin. In short, photoporphyrin strikes one, for practical and reactivity reasons, as a less than ideal photosensitizer.

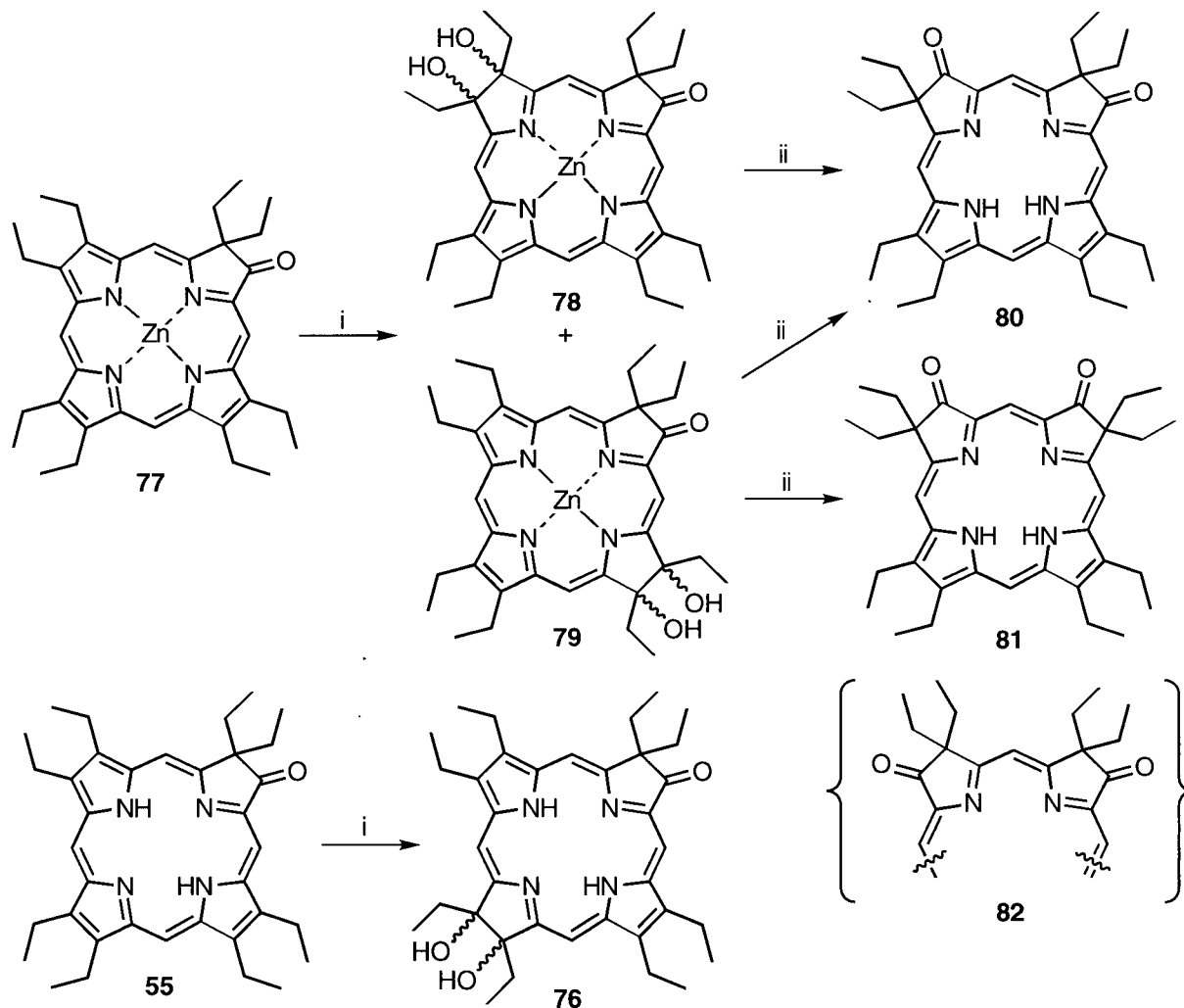
1.3.3.7 β -OXOCHLORINS AND RELATED PIGMENTS

β -Oxochlorins

As mentioned in a previous section, β,β' -dihydroxyoctaalkylchlorins can be rearranged into β -oxochlorins, such as **63**.^{203,210} The β -oxochlorin **55** (derived from the rearrangement of diol **53**, Scheme 1-23) shows the typical selectivity of chlorins upon further dihydroxylation, *i.e.* the selective formation of a bacteriochlorin chromophore **76**, and in a corresponding fashion, the β -oxometallochlorin **77** forms the metalloisobacteriochlorins **78** (major) and **79** (minor) (Scheme 1-22). The rearrangement into **80** and **81** is characterized by a distinct selectivity in favor of the former. None of the third isomer **82** could be detected. The rearrangement of **76** has not been reported.

A second, much older route to these β -oxochlorins is the hydrogen peroxide-sulfuric acid oxidation of porphyrins as developed by Fischer *et al.* (Scheme 1-23).^{211,212} He mistakenly assigned these pigments a β,β' -epoxide structure but this misinterpretation was later corrected by Stephenson and co-workers.²¹⁰ The generation of β -oxoporphyrins *via* the hydrogen peroxide oxidation is somewhat in contrast to the mild, fairly selective and high yield synthesis *via* the osmylation-rearrangement pathway. It is extremely harsh, non-selective and it necessitates excruciating column chromatographic separations of the product mixtures. Inhoffen and Nolte reported the oxidation of 10.0 g OEP to yield monoketone **55** in 18.5% yield, five isomeric diketones in yields between 2.2 and 0.3%, and two triketones in 1.3 and 0.9% yield^{213,214}, which are respectable yields compared to the results reported elsewhere using less symmetric porphyrins^{215,216}. As some of these pigments serve as heme *dI* models, they have been, regardless of their cumbersome synthesis, studied in depth.²¹⁷⁻²²¹ Due to the low synthetic yield and the excessive efforts to separate the products, they are not

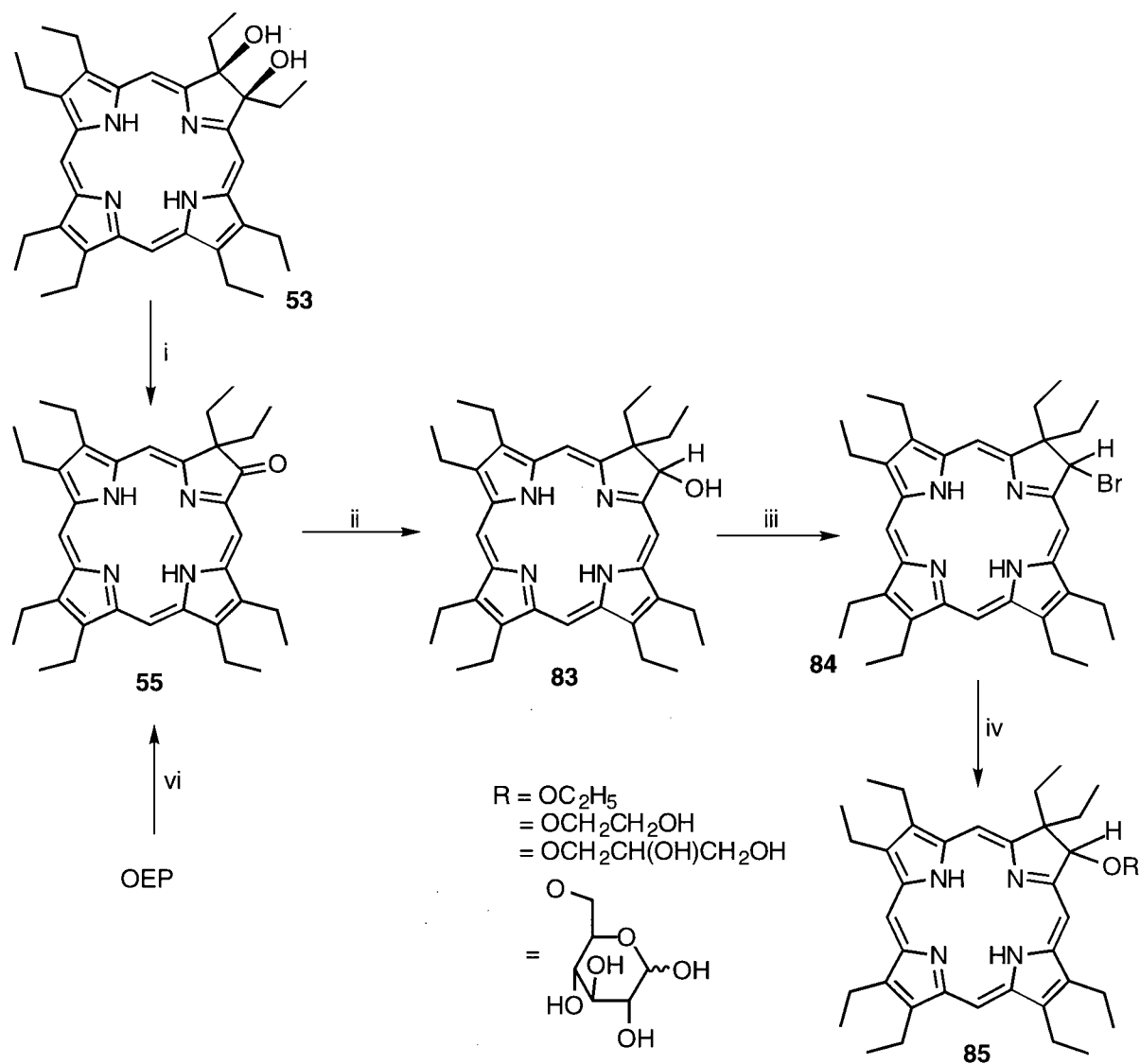
a practical option for drugs in PDT although some pigments meet certain of the desired criteria.



Scheme 1-22 Hydroxylation and rearrangement of β -oxochlorins and β -oxometallochlorins
Reaction conditions: (i) 1. $\text{OsO}_4/\text{pyridine}$ 2. H_2S (ii) H_2SO_4

The elegant access to oxochlorins such as **55** via the acid-catalyzed pinacol-pinacolone type rearrangement of the corresponding dihydroxychlorin **53** avoids the practical obstacle of separating the complex mixtures which are derived from the direct sulfuric acid-hydrogen peroxide oxidation of OEP. The oxochlorin can be reduced to the corresponding

alcohol **83** which can be further converted to the bromide **84**. Nucleophilic exchange of this benzylic bromide with a variety of alcohols generates a host of chlorins (**85**) with graded amphiphilic character.^{29,195} Some of these stable chlorins have been tested in an *in vivo* tumor assay and have shown considerable activity.¹⁹⁵

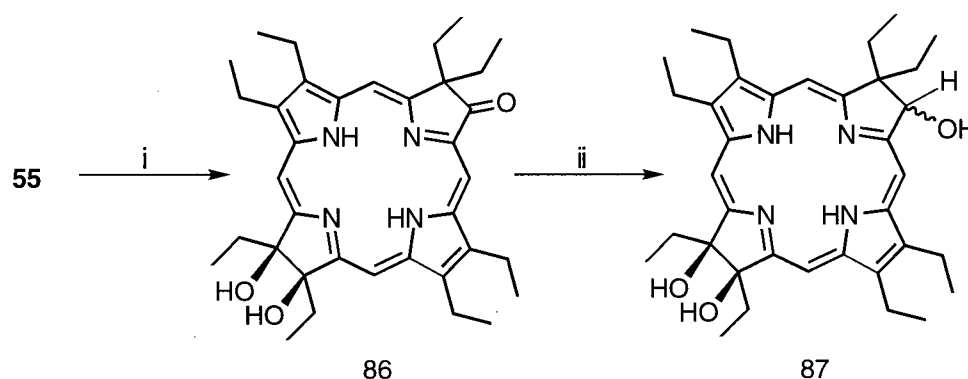


Scheme 1-23

The preparation of Bonnett's chlorins with graded amphiphilicity²⁹
 Reaction conditions: (i) $\text{HClO}_4/\text{CH}_2\text{Cl}_2$ (ii) 1. $\text{NaBH}_4/\text{EtOH}$; 2. H_2O (iii) HBr/HOAc (vi) HOR (vi) 1. $\text{H}_2\text{O}_2/\text{H}_2\text{SO}_4$; 2. chromatography

With respect to their use as practical PDT drugs, the assessment of compounds **85** is unfavorable. While they meet the photophysical criteria and their amphiphilicity and solubility can be fine-tuned to a wide degree, and they exhibit appreciable *in vivo* activity,^{3,197} they have been shown to exhibit poor tumor selectivity. When tested compound **85**, R=glucose, was shown to be an effective tumor photosensitizer but also a very effective skin and muscle photosensitizer, causing severe edema in the test animals upon radiation of the healthy tissue.²⁹ This lack of sensitivity lead Bonnett and co-workers to the conclusion that this substance cannot be regarded as promising drug for PDT. Certain other hydroxy-functionalized chain derivatives, seem to give better tumor to healthy tissue discrimination. Further downsides are the multistep syntheses and the introduction of stereocenters.

The carbonyl group in **55** reacts readily with Wittig reagents and magnesium or lithium alkyls.^{222,223} None of these reactions, however, furnished products that could be ideal PDT agents. A different set of manipulations of **55** was more promising. Bonnett and co-workers have taken the oxochlorin **55** and hydroxylated it to yield the bacteriochlorin **86** (λ_{\max} (CHCl₃) = 693 nm, log ϵ = 4.71) (Scheme 1-24).²⁹ Reduction of the ketone functionality in **86** gave the corresponding triol derivative **87**, which proved, however, to be very labile. This predicated a poor shelf-life time and further work was, therefore, discontinued.



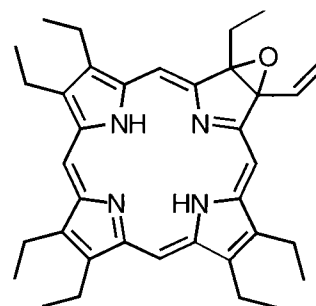
Scheme 1-24 The hydroxylation of keto-chlorin **86** and its reduction to triol **87**
Reaction conditions: (i) 1. OsO₄, 2. H₂S; (ii) NaBH₄/EtOH

Alcohol **83** gave erratic biological results, presumably due to a lack of solubility in aqueous solvents. Octaethyl-dihydroxychlorin **53**, **86**, as well as the 2,3,7,8,12,13,17,18-octaethyl-7,8,17,18-tetrahydroxybacteriochlorin (**54**) (undetermined stereochemistry) (λ_{\max} (CHCl₃) = 715 nm, log ϵ = 4.72) were tested *in vivo* and these compounds were potent photosensitizers, in fact, based on the dose given, more effective than Photofrin[®]. However, these compounds displayed poor selectivity with respect to photodamage.

Epoxychlorins

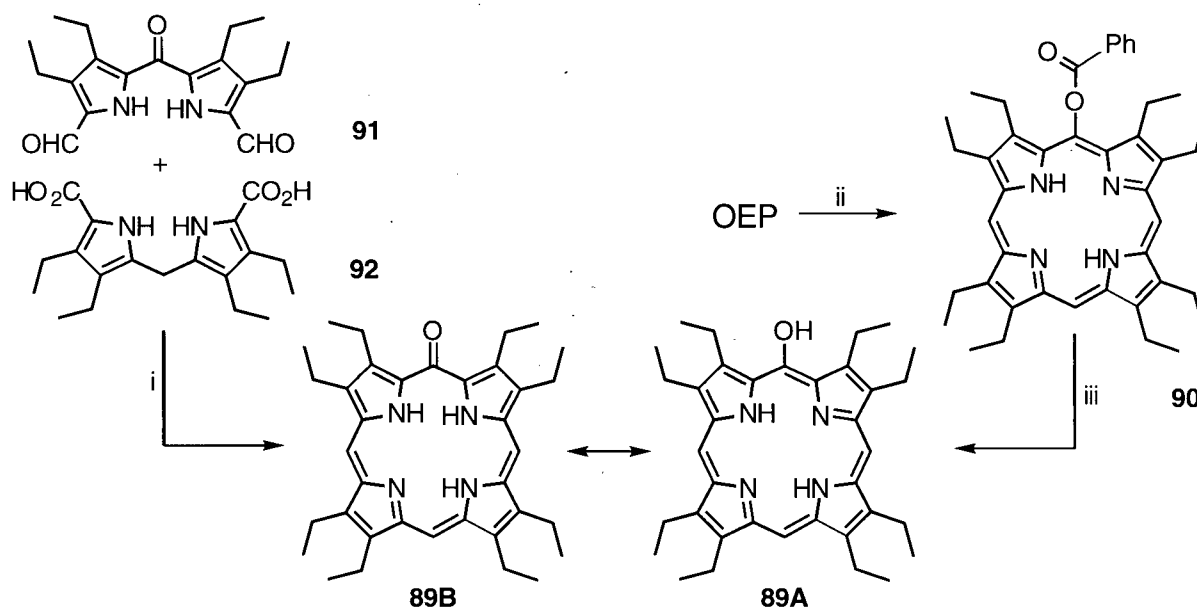
The, albeit fleeting, occurrence of an epoxychlorin during the hydrogen peroxide-sulfuric acid oxidation of OEP seems reasonable, though it has not been directly observed. The two reports in the literature claiming the existence of epoxychlorins were both proven wrong. The first were compounds reported by Fischer and co-workers^{211,212}, which were, as already mentioned, later proven to be oxo-chlorins.²¹⁰ The second example, claimed by the Johnson group^{224,225}, proved to be a pigment belonging to the secochlorin class.²²⁶ This, and other secochlorins, will be discussed in section 2.1.7.4.

There is, however, one synthetic procedure to form chlorin epoxides in the literature. With the goal of forming oxygen analogies of sulfchlorins^{227,228}, naturally occurring episulfides of protoporphyrin IX, Iakovides and Smith published the synthesis of chlorin epoxides *via* a modified Mitsunobu reaction.²²⁹ Its non-trivial multi-step synthesis cannot be generalized.

**88**

Oxophlorins²³⁰ and *meso*-Hydroxyporphyrins

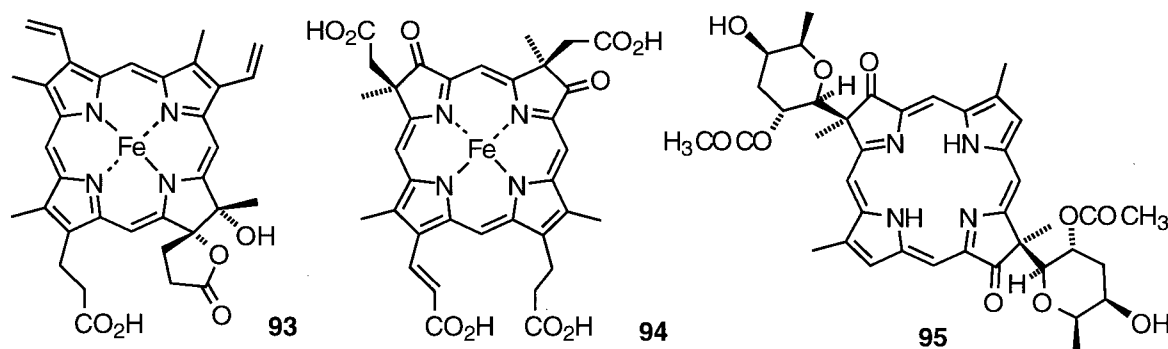
A second site to introduce hydroxy-substituents onto the porphyrin periphery is the *meso*-position. *Meso*-hydroxy substituted porphyrins, such as **89A**, have been known for some time.^{72,231} Scheme 1-25 shows two out of several syntheses of these systems, one being the oxidation of porphyrins with peracids²³² (OEP to **90**, followed by hydrolysis) and the other being the MacDonald-type condensation of a dipyrromethane diacid (**91**) with a dipyrroketone dialdehyde (**92**)^{233,234}. *Meso*-hydroxyporphyrin **89A** is in equilibrium with its tautomer **89B**, a so called oxophlorin. In fact, the equilibrium is, in the case of an octaalkyl substitution pattern, on the side of the oxophlorin form. The name oxophlorin expresses the similarity of its optical spectrum with that of 5,22-dihydroporphyrins, and, consequently, make its use as sensitizers for PDT uninteresting.



Scheme 1-25 Formation of *meso*-hydroxy-octaethylporphyrin
Reaction conditions: (i) H^+ ; (ii) MCPBA; (iii) H_2O

β -Hydroxy- and β -oxochlorins

Some naturally occurring β -hydroxy- and oxochlorins have been characterized. Among them are: Heme *d* (**93**), the prosthetic group of bacterial terminal oxidases^{235,236}, and formally a [5,6-*trans*-dihydroxychlorinato]Fe(III). It is not known whether the γ -spirolactone or the corresponding open structure is that of the native pigment.²³⁶ Heme *dI* (**94**) is the prosthetic group of bacterial dissimilatory nitrite reductase^{207,238,239}, a [7,12-dioxoisobacteriochlorinato]Fe(III).^{217,237-241} Tolyporphine (**95**) is a pigment with unknown function isolated from a blue-green algae²⁴², and formally a 8,18-dioxobacteriochlorin. Recently, eight more tolyporphyin-like porphyrinoids have been described.²⁴³



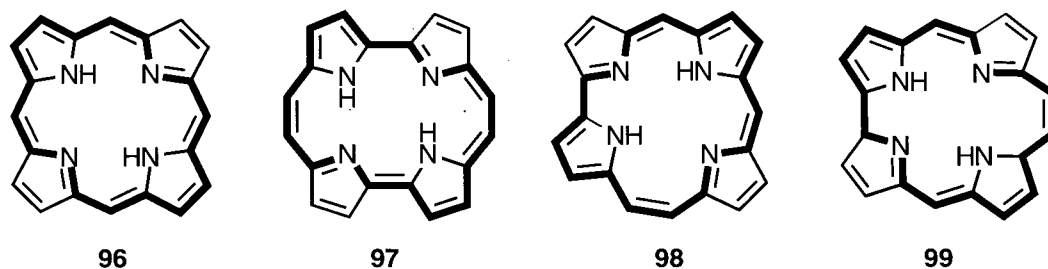
These naturally occurring pigments are uninteresting for large scale use as drugs for PDT as their isolation from the natural source is much too tedious. Consider, for example, the case of the pigment with the most ideal optical spectroscopic properties, *i.e.* the bacteriochlorin **95**. The organic extract of the cultured algae was fractionated by several consecutive reverse phase and silica gel columns to give 0.03 % yield of tolyporphin (**95**).²⁴² Total and partial syntheses of the free bases of **93**²⁴⁴ and **94**^{142,204,239} have been published, but again, they are, due to their length and associated low yields (*e.g.* \approx 1-2 % from protoporphyrin dimethylester for the non-stereoselective synthesis of **93**²⁴⁵) as well as their complexity, only of academic value. The syntheses of naturally occurring hydroporphyrins have been elaborated in a recently published review by Montforts *et al.*⁸⁰

1.3.4 PORPHYRIN ISOMERS

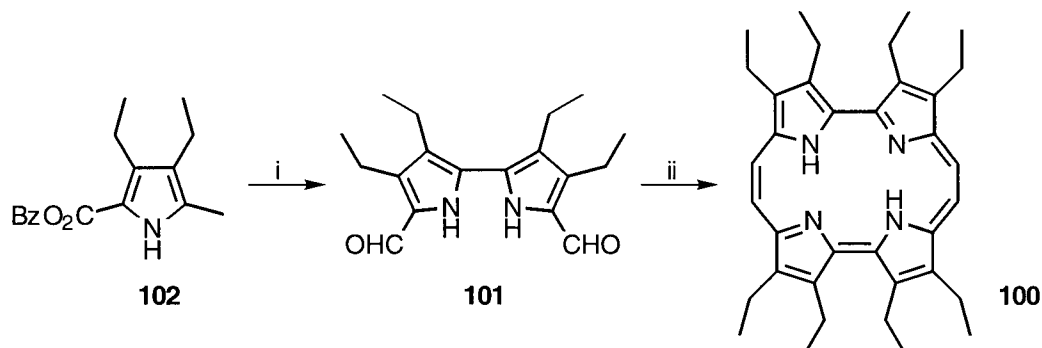
For the longest time, no structural isomers of porphyrins were known. This has changed recently with the appearance of several such isomers, opening up a new direction in porphyrin-related research.²⁴⁶ Many research papers have appeared in quick succession describing these fascinating compounds, and although many resemble in their activity the parent porphyrin, they differ significantly in other aspects and, hence, constitute a compound class in their own right.²⁴⁷ As some of these isomers show strong absorption in the red part of the visible spectrum and have also been shown to be capable of photo-generating singlet oxygen, they have become viewed as potential drugs for PDT. Here the syntheses, visible spectra and potential as PDT drugs as well other interesting aspects of the selected porphyrin isomers will be briefly reviewed.

Porphycene and Related Pigments

Porphyrin is a cyclic, aromatic tetrapyrrolic pigment with 18 π -electrons in a closed delocalization pathway in which the pyrrole units are linked by methine bridges. A reshuffling of the pyrrolic units and the bridges generates theoretically a host of porphyrin isomers as illustrated below, and all of them should be 18 π -electron aromatic compounds. A theoretical analysis of all conceivable isomers containing an N4 coordination site and [18]-annulene conjugation performed by Waluk and Michl gave credence to the supposition that isomers other than **96** could be porphyrin-like.²⁴⁸ And indeed, porphycene (**97**)²⁴⁹, synthesized in 1986 by Vogel *et al.*, hemiporphycene (**98**)²⁵⁰ and corphycene^{251,252} (**99**) synthesized jointly by Sessler and Vogel, have since been investigated and proven to be porphyrin-like, and they fulfill Michl's predictions satisfactorily. The remaining isomers are to this point unknown. Here, further discussion will be restricted to the porphycenes.



Porphycene, its alkyl substituted analogs such as **100**^{253,254}, and the 2,7,12,17-tetra-phenylporphycene (**103**) are synthesized *via* the McMurry coupling of two bipyrrole dialdehydes (**101**), as illustrated in Scheme 1-26. The dialdehydes were prepared through the Vilsmeier-Haak formylation of the corresponding α -free bipyrroles, which themselves are the product of an Ullmann coupling of two α -iodopyrroles (**102**).

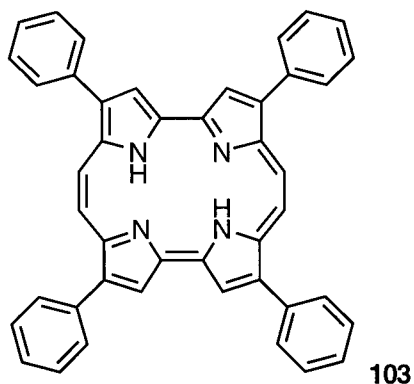


Scheme 1-26 Formation of octaethylporphycene²⁵³
Reaction conditions: (i) 1. SO_2Cl_2 , diethyl ether; 2. $\text{H}_2\text{O}/\text{NaOAc}$; 3. I_2/KI ; 4. Cu/DMF , Δ ; 5. H_2 , Pd/C ; 6. Δ ; 7. POCl_3/DMF ; 4. $\text{H}_2\text{O}/\text{NaOAc}$;
 (ii) 1. $\text{Zn}/\text{CuCl}/\text{TiCl}_4$, THF; 2. O_2

The greatest drawback of the porphycene synthesis is the low yield of the McMurry coupling, which is, in the case of the synthesis of **97**, only 4%. Porphycene itself is, in strong analogy to porphyrin, a very nonpolar compound with a porphyrin-like nature (λ_{max} (benzene) = 630 nm, $\log \epsilon = 4.71$).²⁴⁹ The longest wavelength absorption band of the octaethyl derivative **100** is, as compared to **96**, 35 nm bathochromically shifted

(λ_{\max} (CHCl₃) = 665 nm, log ϵ = 4.48)²⁵³. Porphycenes, N,N'-bridged porphycenes²⁵⁵ and metalloporphycenes^{253,254,256,257} have been studied in depth.²⁵⁸⁻²⁶⁵ Porphycene **100** generates singlet oxygen but, mainly due to its solubility and relatively short longest wavelength absorption, does not fulfill the basic criteria for PDT agents. Porphycene can be reduced to 2,3-dihydroporphycene, nominally a chlorin isomer.²⁶⁶ Its UV-Vis spectrum has a similar band pattern as the parent unsaturated compound - this is analogous to chlorins - but it does not exhibit the pronounced increase of the longest wavelength band (λ_{\max} (benzene) = 595 nm, log ϵ = 4.48) - this is in sharp contrast to chlorins.

Nonell *et al.* have prepared the TPP isomer **103** along an analogous synthetic pathway to that described for **100**.²⁶⁷ The photophysics of **103** are consistent with its proposed use as PDT agent (λ_{\max} (toluene) = 659 nm, log ϵ = 4.70) and it photoproduces singlet oxygen with a quantum yield of roughly 0.25. This ability translates into a high

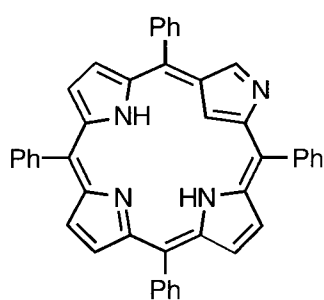


phototoxicity in cells and the compound has low dark toxicity. Details of the biological activity of this compound were not given, so any comparison of the efficacy or other properties with other photosensitizers cannot be made. The phenyl substituents can be functionalized to optimize the activity index of this compound. These pigments have the

potential to be useful as novel therapeutic agents for PDT, however, further research to significantly improve the McMurry coupling reaction and a short-cut synthetic pathway would be the minimal improvement mandatory if these compounds are to be amenable to larger scale preparations.

N-Confused Porphyrins

Porphyrin isomers could also be prepared, conceptually, by changing the orientation of the pyrrole moieties within the porphyrin framework. This simple concept found its experimental verification recently in two independent and serendipitous discoveries. Furuta *et al.*²⁶⁸ reported the preparation and crystal structure of *meso*-tetraphenyl-2-aza-21-carbaporphyrin (**104**), which they dubbed “N-confused porphyrin”, and Latos-Grazynski

**104**

and co-workers²⁶⁹ reported independently the synthesis and structure of an analogous isomer of tetra-*p*-tolylporphyrin. Both porphyrinoids are prepared in low yields (4-8%) *via* variations of classic pyrrole and aldehyde condensations, followed by oxidation, as side products of the regular *meso*-tetraarylporphyrin.

N-Confused porphyrins are intrinsically interesting as potential PDT agents: They are accessible in a one step reaction, the UV-Vis spectrum of the non-protonated species displays strong absorption in the red region ($\lambda_{\max}(\text{CH}_2\text{Cl}_2) = 725 \text{ nm}$, $\log \epsilon = 4.04$)²⁶⁸, ($\lambda_{\max}(\text{CH}_2\text{Cl}_2) = 730 \text{ nm}$, $\log \epsilon = 3.98$)²⁶⁹. The phenyl substituents can, presumably, be widely varied, and the (basic) nitrogen at the periphery of the compound introduces some amphiphilicity into the molecule. At this time, the low yield and non-directed synthesis and the demanding chromatographic purification of the compound are at odds with any large scale preparation. To overcome this, reaction conditions for the formation of N-confused porphyrin could be optimized, or a more directed approach towards its synthesis could be developed. Studies towards the directed synthesis of N-confused *meso*-phenylporphyrins will be described and discussed in section 2.2.

N-Confused porphyrins have also aroused interest through their unusual way of forming metal complexes. They form nickel(II) complexes in which the inner carbon has lost a proton, forming a carbon-metal bond.²⁶⁹ They have, therefore, the character of metal stabilized Arduengo-type,²⁷⁰⁻²⁷⁴ "bottleable" carbenes.²⁷⁵ The synthesis and step-wise protonation of a second derivative of **2**, namely the outer N-methylated derivative 2-methyl-2-aza-*meso*-tetraphenyl-21-carbaporphyrin, has been recently reported.²⁷⁶

Isoporphyrins

Woodward predicted in 1962 the existence of the isoporphyrin (**96B**) tautomer of porphine (**96A**).²⁷⁷ The [18]-annulene aromatic system is interrupted in this pigment owing to the presence of a saturated *meso*-carbon. The optical spectrum is characterized by a broad absorption in the long wavelength range.

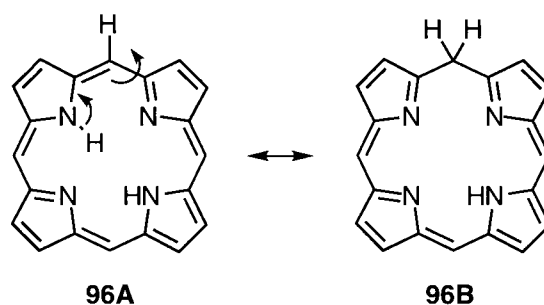


Figure 1-12 Porphine - isoporphine tautomerism

The first isoporphyrin was synthesized by Dolphin *et al.*²⁷⁸ by way of electrochemical oxidation, and since then a series of isoporphyrins has been prepared.²⁷⁹⁻²⁸⁸ However, they all suffer from severe instability and tend to revert to the parent porphyrin. Consequently, they will find no use in applications such as PDT.

1.3.5 EXPANDED PORPHYRINS

Any system larger than a porphyrin, *i.e.* containing more than one atom between the pyrrolic units, or containing more than four pyrrolic units, is called an 'expanded porphyrin'. By virtue of containing a larger number of π -electrons than porphyrins, their electronic spectra are considerably bathochromically shifted as compared to porphyrins and even bacteriochlorins. The long wavelength bands and their high extinction coefficient make these expanded porphyrins appealing candidates for application as photosensitizers in PDT. Expanded porphyrins have received tremendous attention in the last few years as they also offer a larger central binding core and additional coordinating heteroatoms than their congener porphyrins. This opens up the opportunity to bind very large metals, gadolinium, for instance, which is of biomedical interest as an imaging agent in magnetic resonance imaging (MRI).²⁸⁹⁻²⁹¹ Some radiopharmaceuticals also rely on the complexation of large metals, such as technetium. Recent reviews have given an overview of the rapidly expanding field.^{292,293} Here, only selected classes of expanded porphyrins with particular relevance to this thesis will be discussed.

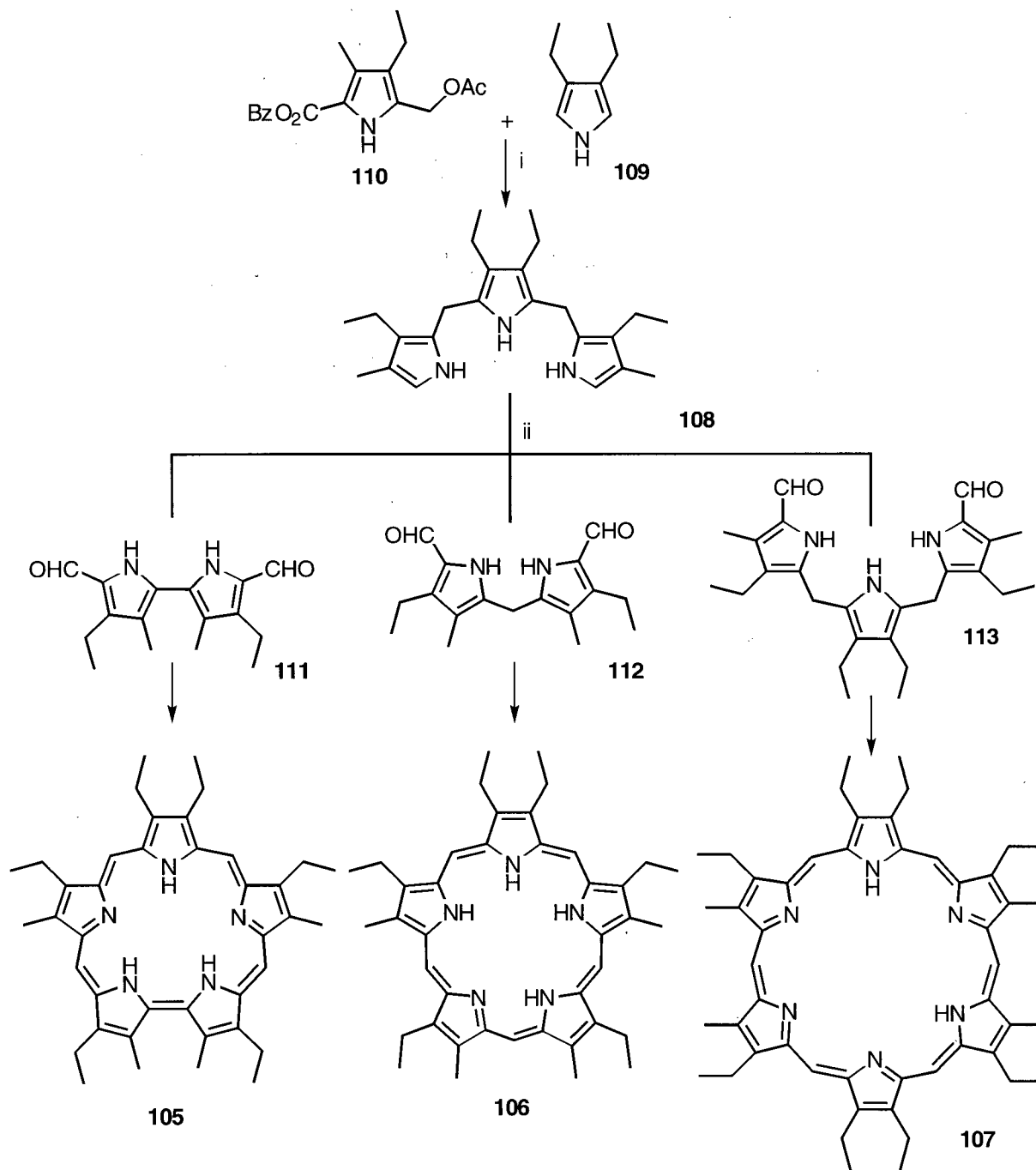
Sapphyrins, Pentaphyrins and Hexaphyrins

The first expanded porphyrin to be reported was a sapphyrin (**105**), a pentapyrrolic [22]-annulene with a direct pyrrole-pyrrole linkage.²⁹⁴ First report by Woodward in 1966, these compounds have attracted the most attention of all expanded porphyrins,²⁹² partially, perhaps, because their synthesis has been optimized²⁹⁵ since the original preparation.²⁹⁶⁻²⁹⁸ They were shown to be active in PDT and, as their gadolinium(III) complexes, as MRI agents.²⁹² They also show unexpected properties such as neutral substrate²⁹⁹ and anion recognition properties³⁰⁰⁻³⁰² as well as interactions with nucleic acids.³⁰³ Sapphyrins feature strong ($\log \epsilon = 4.32$ and 4.17) long wavelength absorptions at $\lambda_{\max}(\text{CH}_2\text{Cl}_2) = 668$ and

711 nm, respectively.²⁹⁵ Their solution state properties have been modified through variation of the alkyl side chains. Heterosapphyrins^{295,297,298,304,305} have been known for several years and very recently, the synthesis of a sapphyrin isomer³⁰⁶ has been communicated.

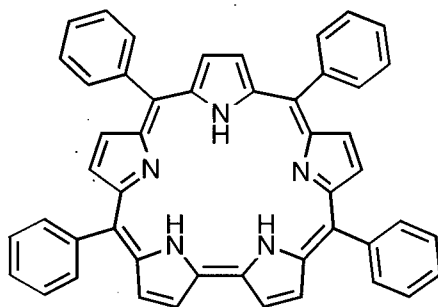
The syntheses of pentaphyrin³⁰⁷⁻³¹² (**106**), and its next higher homologue hexaphyrin (**107**),^{308,309,313} a hexapyrrolic [26]-annulene with six methine bridges, have been reported, but, compared to the aforementioned sapphyrin syntheses, they are still in their infancy. Pentaphyrins have strong long wavelength absorption bands,³¹² but lack of data on these types of compounds, especially with respect to photosensitization ability, stability or toxicity rules out any evaluation of their potential as drugs for PDT. Hexaphyrin has only a weak long wavelength absorption (λ_{\max} (CH₂Cl₂) = 789 nm, log ϵ = 3.60), but again, the lack of any more data prohibits any reasoned evaluation.

The key intermediate in the synthesis of all three macrocycles is the tripyrrane **108** (Scheme 1-27). Its synthesis involves the acid-catalyzed condensation of one equivalent of dialkylpyrrole (**109**) with two equivalents of (acetoxymethyl)pyrrole (**110**). Debenzylation of the resulting tripyrrane diester is followed by decarboxylation **108**.²⁹⁵ Acid catalyzed condensation of **108** with an α,α' -diformyl dipyrane (**111**), dipyrromethane (**112**), or tripyrrane (**113**), followed by oxidation of the initially formed macrocycle to the fully aromatic compound, completes the synthesis of sapphyrins (**105**), pentaphyrins (**106**), or hexaphyrins (**107**), respectively. Typically, a sapphyrin synthesis is a seventeen step procedure starting from a single pyrrole precursor.²⁹⁸ A similar length synthesis is required for the pentaphyrins, while the hexaphyrins, due to being composed of two identical halves, require fewer steps. An improved synthesis for the precursors has been published,^{295,314} but nevertheless, more than ten steps, some requiring expensive reagents, are necessary to access sapphyrins. This might be the strongest impediment for their biomedical use.



Scheme 1-27 Formation of sapphyrin (**105**), pentaphyrin (**106**), and hexaphyrin (**107**)
Reaction conditions: (i) 1. HOAc, &, 2. H₂, Pd/C; 3. &; (ii) catalytic H⁺

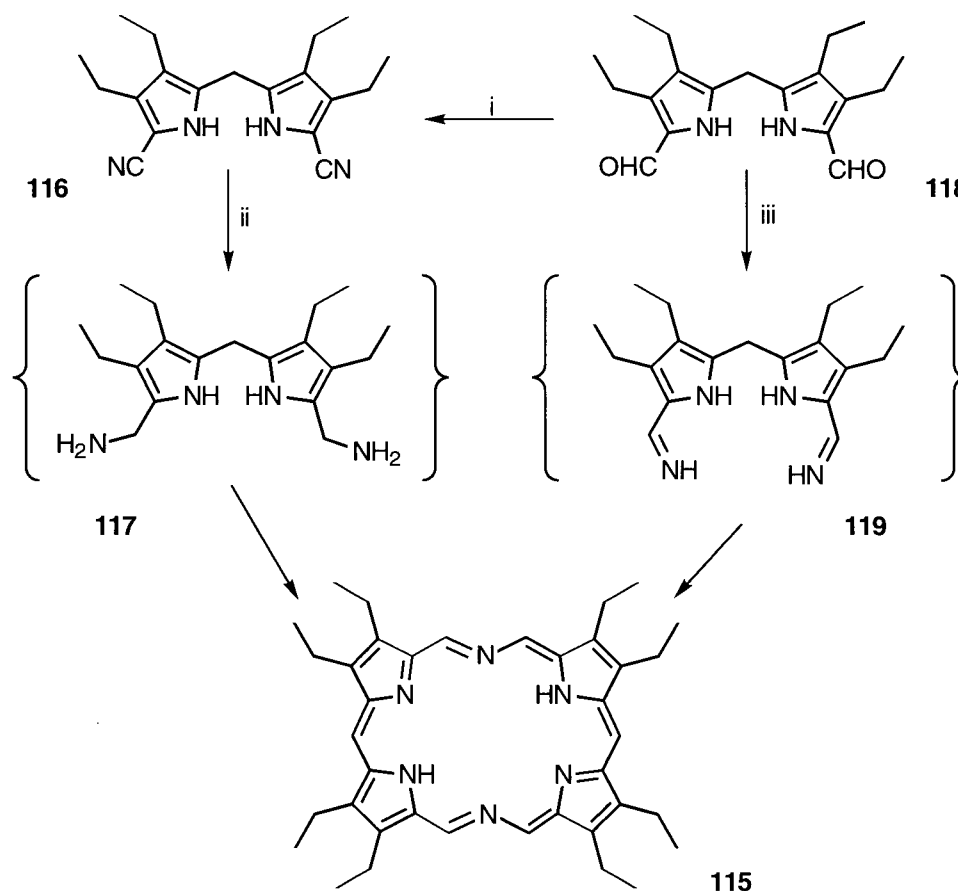
meso-Tetraphenyl substituted sapphyrin **114** has been isolated as a minor side product of the Rothmund-type TPP synthesis.³¹⁵ This was the first report showing the formation of a direct pyrrole-pyrrole linkage under the original Rothmund^{316,317} conditions or variations of it^{42,44}, and the first report of *meso*-substituted sapphyrins in general. An alternative synthesis of **114** and related *meso*-phenylsapphyrins will be discussed in section 2.3.

**114**

It is noteworthy that all but the *meso*-tetraphenylsapphyrin of the above mentioned expanded macrocycles have one common key intermediate: the tripyrrane **108**. This tripyrrane is also a crucial intermediate in the synthesis of other aromatic³¹⁸ and non-aromatic macrocycles.³¹⁹⁻³²¹

Porphocyanine

Dolphin *et al.* introduced, in 1993, a novel class of \equiv expanded porphyrins, the porphocyanines.³²² Their structure and synthesis is shown in Scheme 1-28.



Scheme 1-28 Formation of porphocyanine **115**
Reaction conditions: (i) 1. NH_2OH , NaOAc , EtOH , &; 2. Ac_2O , &; (ii) 1. LiAlH_4 , THF ; 2. H_2O ; 3. O_2 (iii) NH_3 , EtOH , &, O_2

Two different approaches towards this expanded system are available:

The lithium aluminum hydride reduction of a 1,9-dicyanodipyrromethane (**116**) to, possibly, the corresponding methylamino derivative **117**. This labile compound was not isolated but immediately self-condensed and oxidized by air to give porphocyanine **115** ($\lambda_{\text{max}} (\text{CHCl}_3) = 797 \text{ nm}$, $\log \epsilon = 4.43$).³²² The yield of this reduction and condensation

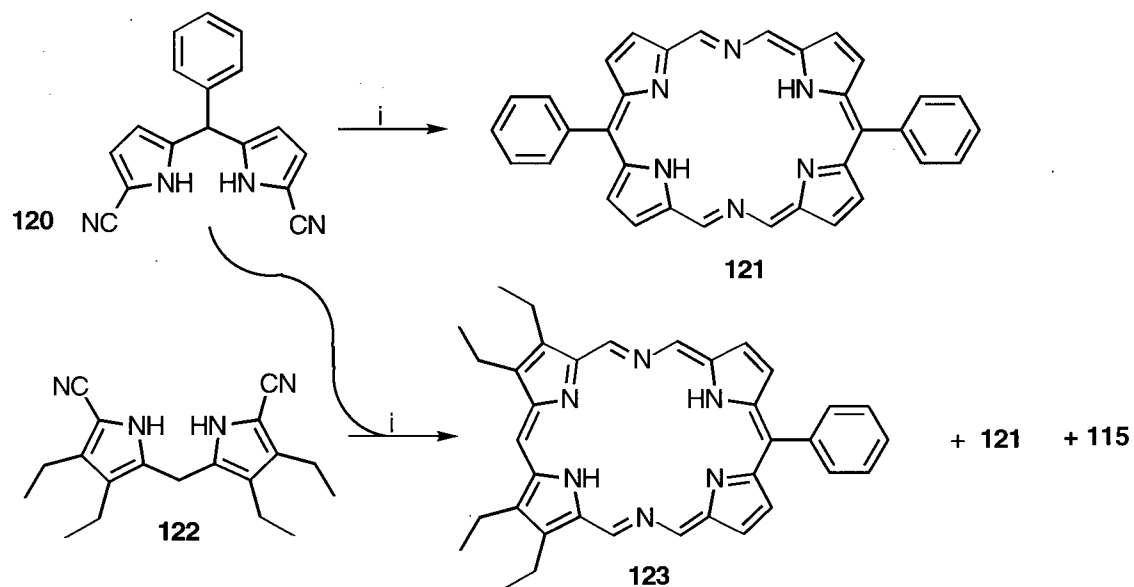
reaction is 24 %, a very respectable yield for the formation of macrocycles through a condensation reaction.

The condensation of an 1,9-diformyldipyrromethane (**118**) with ammonia to form, presumably, the intermediate diimine **119**. This diimine, presumably, condenses to a reduced, imine linked macrocycle which is then air oxidized to the final product in 26 % yield.³²³ There are precedents in the literature for such a condensation.³²⁴

Studies related to the elucidation of the mechanism of formation of sapphyrins *via* the reduction of cyanodipyrromethanes will be presented in section 2.4.

The long wavelength absorption bands of porphocyanine make these compounds interesting as potential PDT agents. An extension of the work to *meso*-substituted porphocyanines was reported shortly after the initial publication (Scheme 1-29).³²⁵ *meso*-Phenyl-1,9-dicyanodipyrromethanes (**120**) can be reduced and condensed to the diphenylporphocyanines (**121**) (λ_{\max} (CHCl₃) = 814 nm), and a mixed condensation of the *meso*-phenyldipyrromethane **120** and the tetraalkyldipyrromethane **122** produces a mixture of **115**, **121**, and the desired mono-*meso*-phenyltetraalkylporphocyanine **123** (λ_{\max} (CHCl₃) = 804 nm). This mixture had to be separated by preparative HPLC. **123** comes closest to the ideal of a strongly amphiphilic drug, particularly when polar substituents are attached to the phenyl ring.

The *meso*-phenyl substituents allow a facile interchange of functional groups on the long wavelength absorbing core. Their *in vitro* ability to generate singlet oxygen when irradiated with light of wavelengths longer than 600 nm has been shown. No biological data are presently known and thus, it is too early to evaluate these compounds as PDT agents. Their fairly long synthetic pathway and the need to separate compound mixtures when synthesizing the compounds of type **123** make these compounds initially appear to be less than ideal as practical PDT agents.



Scheme 1-29 Formation of *meso*-phenyl substituted porphocyanines
Reaction conditions: (i) 1. LiAlH₄, THF; 2. H₂O; 3. DDQ

2. RESULTS AND DISCUSSION

2.1 THE OSMIUM TETROXIDE-MEDIATED DIHYDROXYLATION OF *meso*-PHENYLPORPHYRINS AND -CHLORINS

Some *meso*-tetraphenylchlorins have shown promising activities in the field of PDT.^{23,96,196} It appeared to us that efficient syntheses of these and related *meso*-phenyl substituted long wavelength photosensitizers must be developed if these compounds were ever to be produced in large quantities. Inspection of the literature showed that syntheses of the porphyrin precursors had been optimized to a great extent but the yields to the corresponding chlorins were quite poor, due primarily to the laborious separations required. Development of an efficient method to convert the porphyrin to chlorin was seen as extremely crucial to the further advancement of research on this promising class of compounds. To this end, we decided to develop and exploit an alternative route to the large-scale production of stable *meso*-phenyl chlorins. Emphasis was placed on the route that would produce oxidation stable compounds and which would also allow introduction of potentially useful substituents to the chlorin periphery.

Study of the literature singled out the osmium tetroxide-mediated dihydroxylation as the most promising direction of research. The introductory chapter reviewed the conversion of OEP into octaethyl-2,3-diol-2,3-chlorins by means of the osmium tetroxide mediated

dihydroxylation. However, it was not obvious whether this method of preparing chlorins could be applied to TPP. In other words, it was not immediately apparent whether the resulting β,β' -diol chlorins produced from TPPs would be stable towards, for instance, spontaneous dehydration or if they would form at all. Steric as well as electronic factors may prevent the envisioned osmylation.

This portion of research shows that the conversion of TPPs to the corresponding dihydroxychlorins is indeed possible with the use of osmium tetroxide. The chlorins thus produced are stable, have the desired photophysical properties, can be widely derivatized and, hence, they are promising drugs for PDT. The resulting diol functionality confers unique chemical, biological and physical properties onto these chlorins. The following chapter details the studies of these *meso*-tetraphenyl-2,3-dihydroxy-2,3-chlorins.

2.1.1 THE OSMYLATION OF TPP - THE PRINCIPAL REACTION

A chloroform solution of TPPZn or its free base TPP containing pyridine and one equivalent of osmium tetroxide produces in the course of three to five days one major polar product **125** or **124**, respectively, which can be isolated from the relatively non-polar starting materials in satisfying yields by column chromatography. While considerable amounts of recyclable starting material are still present after this time, little decomposition or by-products are observed. The optical spectrum of compound **125** exhibits a more intense and 24 nm bathochromically shifted longest wavelength absorption whereas **124** shows a more intense but moderately shifted longest wavelength absorption when compared to the starting compounds. This is typical for the formation of a (metallo)chlorin and, thus, was the first indication of the successful conversion of TPPZn and TPP into the corresponding chlorin osmate esters **125** and **124**, respectively. The $^1\text{H-NMR}$ of **125** is shown in Figure 1-13.

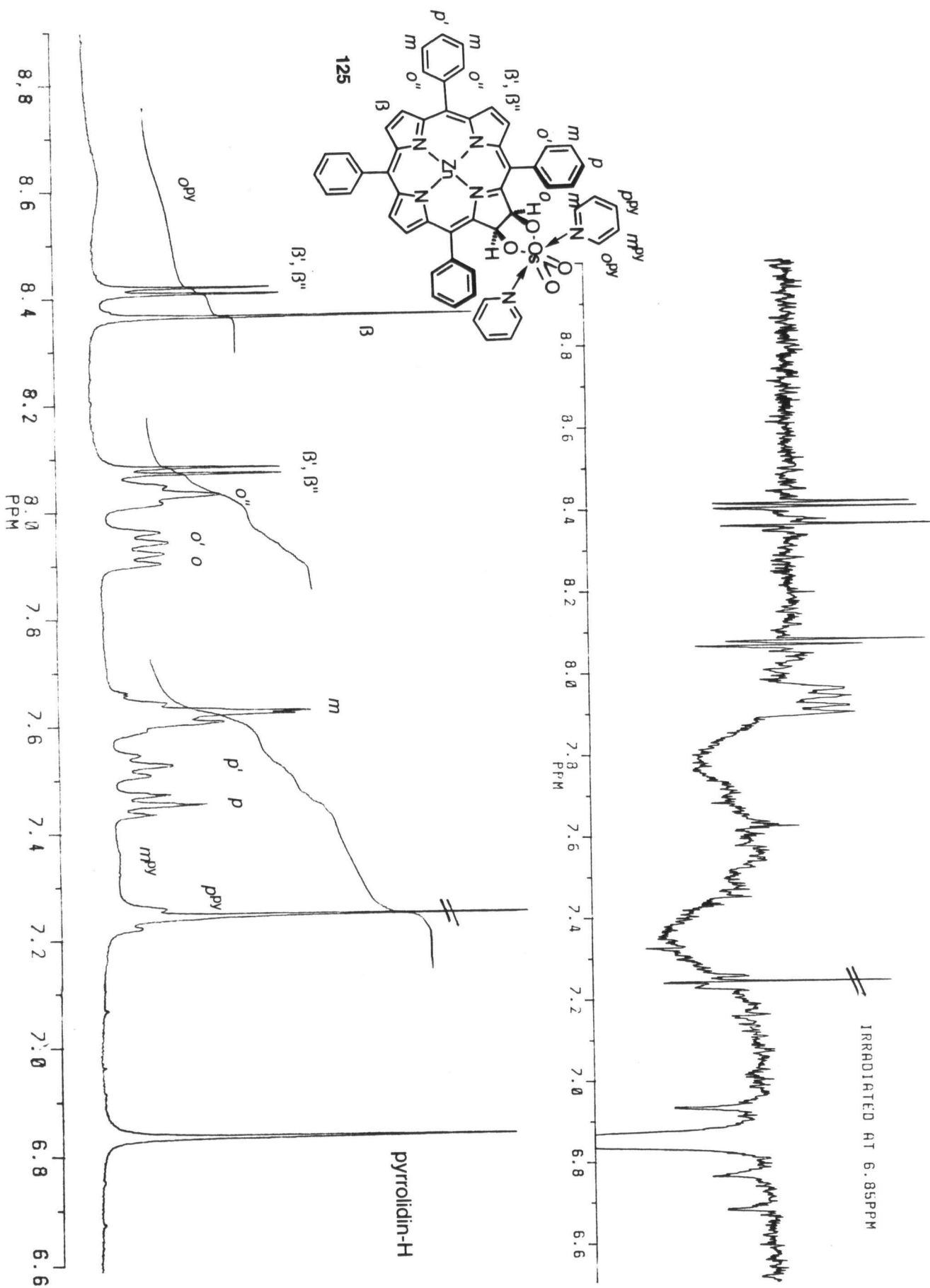
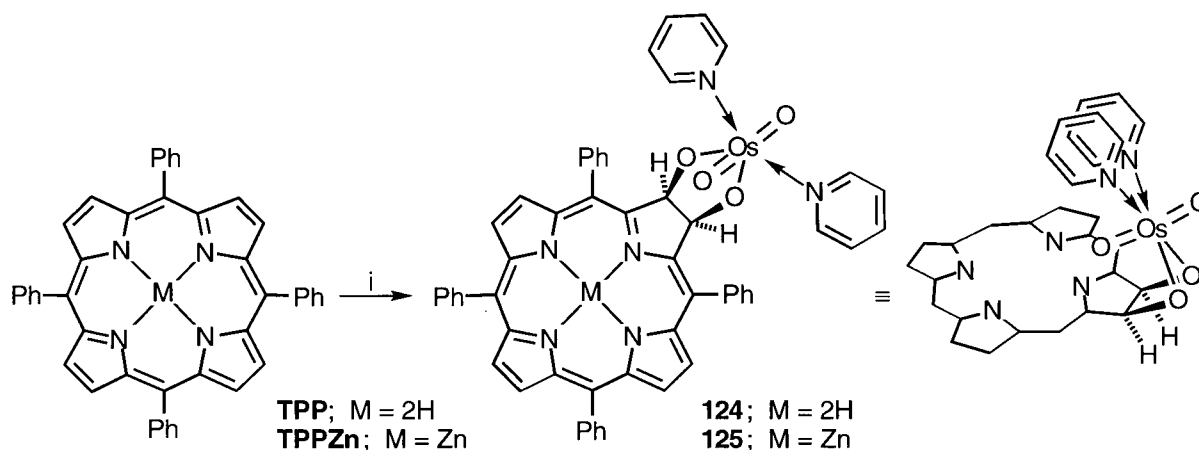


Figure 1-13 ¹H-NMR spectra of 125 (bottom trace) and NOE difference spectrum of 125 (top trace)

Osmylation experiments performed with deuterated pyridine- d_5 and H,H-COSY experiments led to the assignment of the signals at 7.25, 7.35 (v br), and 8.6 (v br) to the coordinated pyridines. Their presence is in accord with previous knowledge about osmate esters.¹⁴⁴ The remaining signals allow several conclusions. Firstly, the four-fold symmetry of the starting material (8.90, s, 8H (β -H); 8.25, m, 8H (o -H); 7.75, m, 12H ($m+p$ -H)) has been lost but an aromatic porphyrinic system is still maintained. Secondly, the signals for the o -protons have split into three sets with 4:2:2 intensity and, together with the number and splitting pattern of the signals attributable to the β -protons (2 d, 1 s, 2H each) clearly identify the β -positions as the location of addition. According to the nature of the addition of osmium tetroxide to a double bond, the formed osmate ester differentiates the porphyrin into one face bearing this group, and one face opposite of this group, thus differentiating the o -protons on the phenyl group into two non-equivalent sets. Whereas this differentiation is large enough to separate the signals for the two *ortho*-protons next to the osmate ester, it is too minor to be seen for the signals for the o -protons on the far side of the osmate ester. The singlet at 6.85 ppm can be attributed to the protons attached to the reduced pyrrolic unit. Irradiation of this signal causes a weak NOE-effect for both neighboring o -protons (Figure 1-13). This may show the slow rotation of the phenyl group. This rotation is subject to investigations to be described in section 2.1.6. The remaining multiplets integrating for 12H are due to the *meta*- and *para*-hydrogens of the phenyl groups. The presence of a high-field signal at -1.72 ppm in **124**, attributed to the inner NH-protons, shows that the osmium, as expected,³²⁶ did not insert into the porphyrin core of the free base porphyrin.

Scheme 1-30 shows the reaction scheme and the likely conformation of the resulting osmate ester. The *trans*-orientation of the oxo-substituents in the osmyl-moiety is typical for osmium(VI) complexes.¹⁵⁴ This enables the coordination of two pyridines at two equivalent positions, a finding supported by their equivalent NMR-signals. Their location above the porphyrin ring is based on steric considerations. The finding that the pyridine proton signals

are not drastically shifted by the porphyrin ring current effect when compared to those of free pyridine may be explained by distance from the ring or by their location in the 'neutral shift region' of the ring. The broadness of the signals attributed to the *o*- and *m*-pyridine hydrogens may indicate rotation of the pyridines along the Os-N axis.

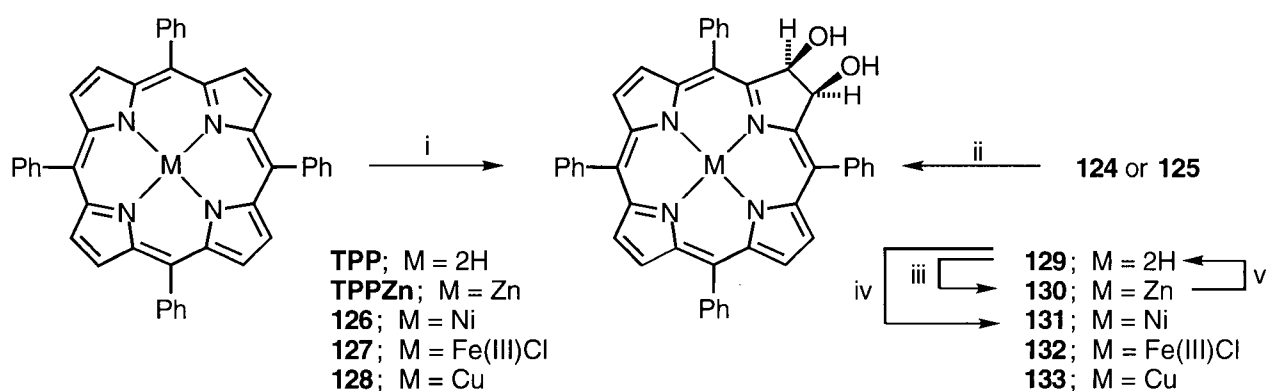


Scheme 1-30 Osmylation of TPP to form the corresponding osmate ester chlorin
 Reaction conditions: (i) 1. 1.1 equiv. OsO₄, CHCl₃/10% pyridine, several days, r.t., 2. column chromatography

These findings prove that osmylation of a peripheral double bond in TPP is a viable way to convert this porphyrin into a chlorin. The occurrence of monomeric osmium diesters or dimeric diesters¹⁴⁴ could not, presumably for steric reasons, be observed. The reaction was, depending on the substituents present at the phenyl groups (*vide infra*), performed in mixtures of ethyl acetate, water, acetone, THF, chloroform (for obvious reasons, pentene stabilized chloroform must not be used), or benzene with pyridine. The addition of pyridine to the reaction mixtures serves two purposes. The osmylation is subject to a ligand acceleration effect:¹⁷² that is, the osmylation proceeds much faster when a suitable ligand for the stabilization of the osmate ester is present. Several amine-type ligands are suitable for this acceleration.^{144,161,327} In addition, the rate of the reaction is also directly dependent on the concentrations of the reactants in solution. The solubility of *meso*-phenylporphyrins, particularly of TPP, is, even in the best of solvents, low when compared to the solubility of

other organic substrates. This alone predicts a slow reaction rate for the osmylation. Experimentation resulted in the choice of a mixture of 10% pyridine in chloroform, a solvent mixture which not only exploited the ligand acceleration effect but dramatically increased the solubility of the TPP to increase the overall reaction rate.

Osmate esters of type **124** can be reduced by a wide variety of reductants to the corresponding diols.¹⁴⁴ In fact, osmate esters produced by osmium tetroxide-mediated dihydroxylation procedures are generally not isolated, but are directly reductively (or oxidatively) cleaved. We found that hydrogen sulfide gas as reductant is the most convenient method of reduction, although sodium borohydride, sodium bisulfite or LAH are suitable for this transformation. This leads to a one-pot procedure for the production of the chlorin diols **129** to **133** (Scheme 1-31). After no further change in the osmium tetroxide reaction mixture can be detected by TLC or optical spectroscopy, hydrogen sulfide is bubbled through the mixture. The precipitated black osmium sulfides are filtered off, and the mixture is purified by chromatography.



Scheme 1-31 Reduction of the osmate ester chlorins to form the corresponding diol chlorins and one-step conversion of porphyrins into diol chlorins
Reaction conditions: (i) 1. 1.1 equiv. OsO₄, CHCl₃/10% pyridine, 3-5d, r.t.; 2. H₂S bubble; 3. chromatography; (ii) H₂S (iii) Zn-acetate/MeOH/CHCl₃/Δ; (iv) Ni(II)acetate/ MeOH/ CHCl₃/Δ (v) 5% TFA/CHCl₃.

The diols have, like their osmate esters, pronounced chlorin or metallochlorin-character. The optical spectra of the brown-purple **129** and the green **130** are shown in

Figure 1-14. The trends seen in optical spectra of several β,β' -diol chlorins as compared to their non-hydroxylated analogs will be discussed in section 2.1.4.

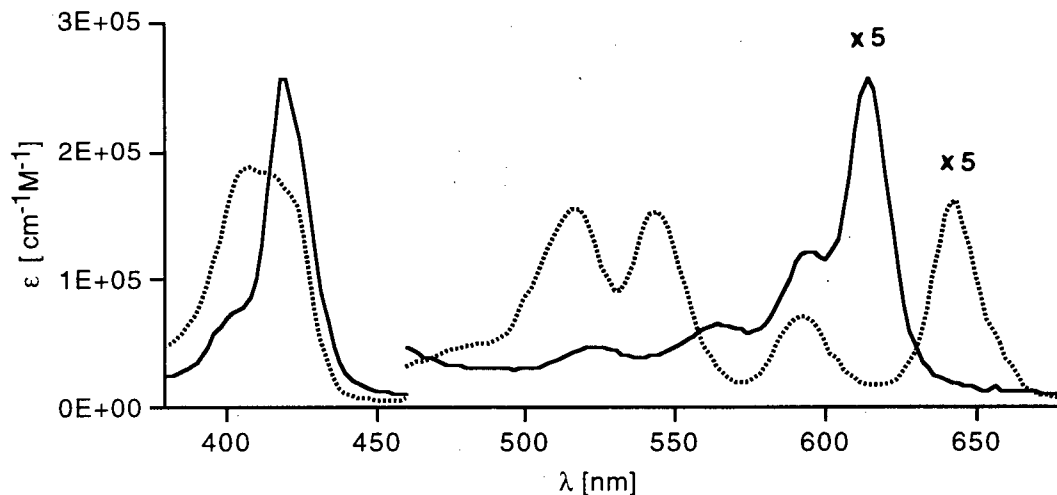


Figure 1-14 Optical spectrum ($\text{CH}_2\text{Cl}_2/0.5\% \text{ MeOH}$) of **129** (.....) and **130** (—)

The $^1\text{H-NMR}$ spectra of the diols are very similar to those of the osmate esters, without, of course, the signals attributed to the coordinated pyridines and with an additional signal for the hydroxy-hydrogens. The dynamic behavior of the proton spectra will be discussed in section 2.1.6. Metallochlorin **130** can also be prepared as its pyridine adduct. Such adducts are common for zinc(II) porphyrins and chlorins. The axial coordinated pyridine groups exhibit additional signals in the $^1\text{H-NMR}$ spectrum at 3.08 (br s, 2H), 5.95 (t, 2H), and 6.7 (t, 1H). Their drastically altered chemical shifts, compared to uncoordinated pyridine, are explained by the ring current effect of the porphyrin. Neither the shifts nor the coupling patterns conclusively indicate that the pyridines coordinate selectively on one side of the porphyrins or the other.

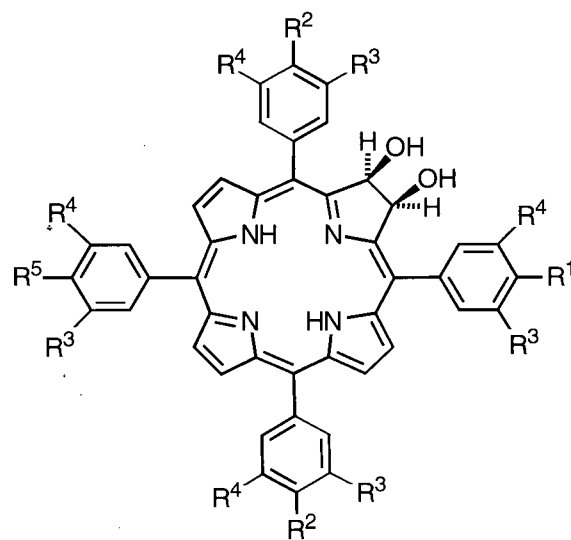
The diols are stable compounds in the solid state. No decomposition or re-oxidation to a porphyrin chromophore could be detected after storage at room temperature and protection from light for several years. Solutions of these chlorins are also stable under mild

conditions. Although they were generally handled under subdued light, they do not appear to be extremely light-sensitive. However, silica gel seems to promote the light-sensitivity of these compounds. Their dehydration and other reactions will be described in section 2.1.7. Also, the diol chlorins dehydrate under the conditions of electron ionization (EI) mass spectrometry and, as a result of that, no or a very little signal corresponding to the expected m/e can be seen. However, the milder conditions prevalent in fast atom bombardment (FAB) mass spectrometry allows the detection of the expected molecular ion peak. The first fragmentation pattern visible results, in all cases studied, from the dehydration.

The osmylation/dihydroxylation reaction can be performed on various metalloporphyrins, such as TPPZn, and **126** to **128**. However, the solubility of the zinc chelate is higher in the solvents used than that of, for instance, the nickel chelate, and on this basis the zinc chlorin is produced at a much faster rate than the corresponding nickel chlorin. This higher solubility reflects the higher tendency for zinc porphyrins to coordinate to an additional ligand to form a penta-coordinated complex than, for instance, the nickel porphyrins.³²⁸ Acid-catalyzed demetallation of the zinc chlorin **130** forms the free base **129**. We found that various mild techniques used to insert central metals such as copper and nickel are suitable to produce the corresponding metal complexes of the diol chlorin **129**.³²⁸ The route *via* the intermediate zinc-complexes was found to be more efficient and convenient to get to, for example, the nickel complex or, in fact, the free base chlorin **129**.

As a method of synthesizing a 'library' of differently substituted *meso*-tetraphenyl-based diolchlorins to be tested as photosensitizers in PDT, the dihydroxylation reaction was found to be successful with those compounds with hydroxy- and methoxy-substituents present on the phenyl group (**134** to **138**). Due to the known biological activity of hydroxy-substituted porphyrins,⁹⁶ we focused on this type of compounds. In addition to the compounds listed above, spectral evidence for the successful formation of diol chlorins was

gathered for compounds with phenyl substituents as diverse as 2,5-dichlorophenyl, 4-nitrophenyl, 4-cyanophenyl, 4-carbomethoxyphenyl, 4-sulfonatophenyl, 4-pyridyl, 3-, and 4-propioyloxy, and pentafluorophenyl. Hence, the osmium tetroxide oxidation can be considered to be general for *meso*-arylporphyrins and their metal complexes.



	R ¹	R ²	R ³	R ⁴	R ⁵
134	-OH	-H	-H	-H	-H
135	-H	-H	-H	-H	-OH
136	-OH	-OH	-H	-H	-OH
137	-H	-H	-OH	-H	-H
138	-OMe	-OMe	-OMe	-OMe	-OMe

Figure 1-15 shows the ¹H-NMR spectra of the two isomeric compounds 10,15,20-triphenyl-5-(4-hydroxyphenyl)-2,3-dihydroxy-2,3-chlorin (**134**) and 5,15,20-triphenyl-10-(4-hydroxyphenyl)-2,3-dihydroxy-2,3-chlorin (**135**). They were prepared by osmylation of the corresponding 10,15,20-triphenyl-5-(4-hydroxyphenyl)-porphyrin³²⁹, and the two isomers formed were separated by preparative TLC. The two spectra illustrate the side- and face-differentiation of the proton signals due to the β,β'-diol substituents, and the effects substituents located on the phenyl groups have on, for example, the β-protons in relation to the distance that separates them.

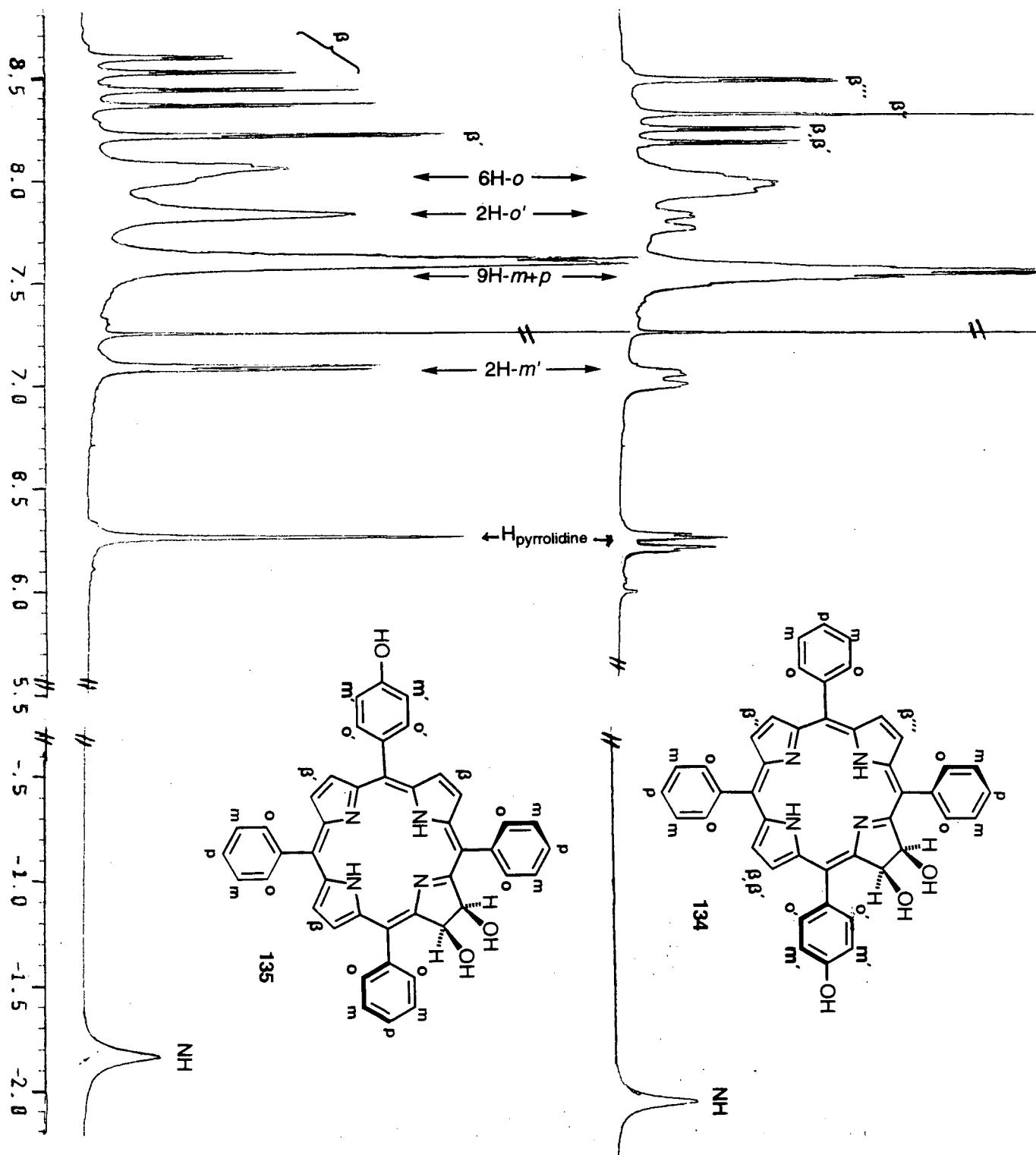
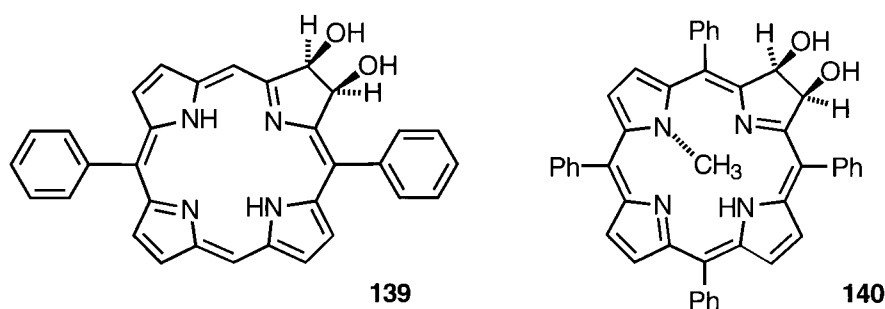


Figure 1-15 $^1\text{H-NMR}$ (400 MHz, $\text{CDCl}_3/10\%$ acetone- d_6) of **135** (bottom trace) and of **134** (top trace)

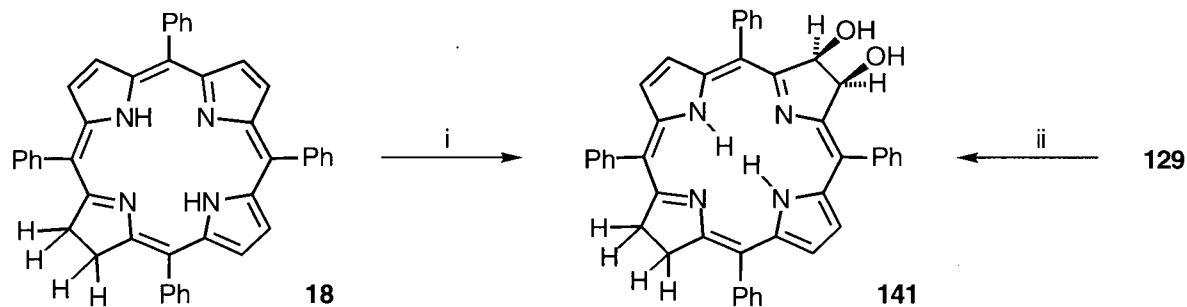
Compared to the corresponding OEP oxidation (reaction time 2 days, 66% yield diol, 17% OEP recovery)¹¹⁸ the oxidation of TPP is slower (up to one week reaction time, ~50% diol, 40% TPP recovery). Steric hindrance of the attack of the bulky osmium tetroxide-pyridine complex at the β -positions by the phenyl groups, as well as electronic reasons, are responsible for this. The oxidation of the less hindered yet electronically approximately equivalent 5,15-diphenyl-porphyrin to give **139** proceeds under similar conditions within hours in high yields. *meso*-Tetraphenyl-N-methylporphyrin³³⁰ reacts equally fast, producing **140**. We assume that N-methylporphyrin is, by virtue of its distortion, electronically activated. The latter reaction is under study by other members of the research group of Prof. Dolphin, and will not be discussed further. The sluggish reaction rate of the stoichiometric osmylation of TPP is responsible for our inability to perform the reaction with catalytic amounts of osmium tetroxide.^{144,160} It remains to be seen, however, whether the more reactive porphyrins like the two examples cited above, make a catalytic osmium tetroxide-mediated dihydroxylation possible. Such process improvement would be, due to the high costs and toxicity of osmium tetroxide, of great economical and practical interest.



The first experiment to evaluate a prospective photosensitizer for use in PDT is to test whether it generates singlet oxygen upon radiation with visible light. Compounds **129** and **146** (page 89), as assayed by their light-mediated aerial oxidation of cholesterol to 5 α -hydro-peroxycholesterol, were found to be efficient photosensitizers in organic solvents²⁸ when irradiated with light of ≥ 600 nm.

2.1.2 THE OSMYLATION OF *meso*-TETRAPHENYLCHLORINS

Reaction of *meso*-phenylchlorin (**18**)⁸³ with a stoichiometric amount of osmium tetroxide under the conditions described above, gives selectively the pink 2,3-*vic*-dihydroxy-*meso*-tetraphenylbacteriochlorin **141**, in good yield (Scheme 1-32). The optical spectrum of **141** is shown in Figure 1-17. Its spectrum unequivocally proves its bacteriochlorin structure. Alternatively, diol chlorin **129** can be reduced with diimide to also give **141**, albeit in poor yields.



Scheme 1-32

Preparation of diolbacteriochlorin **141**

Reaction conditions: (i) 1. 1.1 equiv. OsO₄, CHCl₃/10% pyridine, 2d, r.t.; 2. H₂S bubble; 3. chromatography; (ii) pyridine, K₂CO₃-anhydrous, excess p-toluenesulfonylhydrazine, Δ.

The bacteriochlorin structure is also clearly visible in the ¹H-NMR. The two sets of non-equivalent β-protons show as doublets of doublets with ³J = 5 Hz, a typical value for such β,β'-couplings, and ⁴J = 1.5 Hz, a typical value for couplings with the inner NH-proton. Inspection of the possible tautomers for bacteriochlorin chromophores reveals that the NH-protons are fixed to non-reduced pyrrolic units, and this shows their coupling with the β-protons. All other protons are detected at their expected chemical shifts.

One particularly beautiful and illustrative feature of the spectrum of bacteriochlorin **141** is shown in Figure 1-16. It is the expansion of the signal for the four protons attached to

the reduced pyrrolic unit opposite the diol moiety. The chemical shift is typical for this kind of proton. By virtue of their coupling pattern they show the face-differentiation of the diol moiety. The two hydrogens located on the same face as the diols are non-equivalent to those on the opposite side. This leads to a *vicinal* and a *geminal* coupling of each proton with the protons of the opposing side. As the chemical shift difference of the two proton sets is in the same range as their coupling constants, the complex non-first order spectrum is observed. This pattern was reproduced by a computer simulation³³¹ with the values as indicated in (B). These values are typical for *vic*- as well as *gem*-coupling constants.

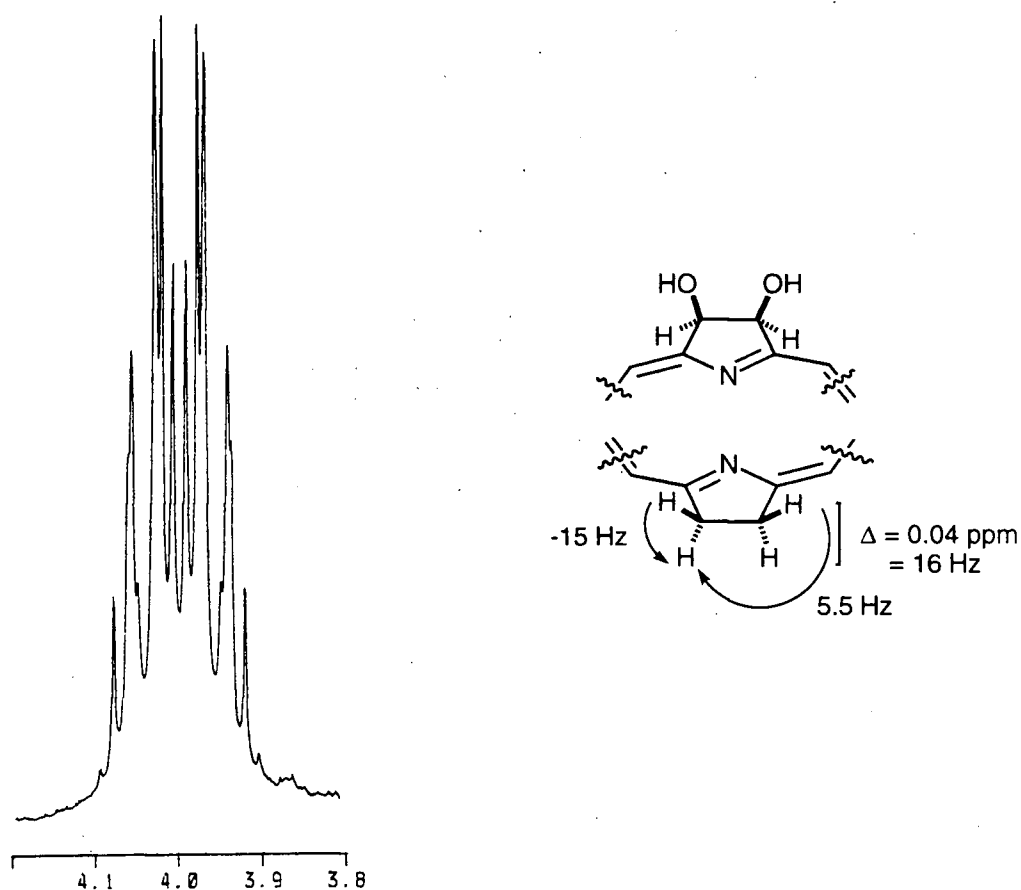
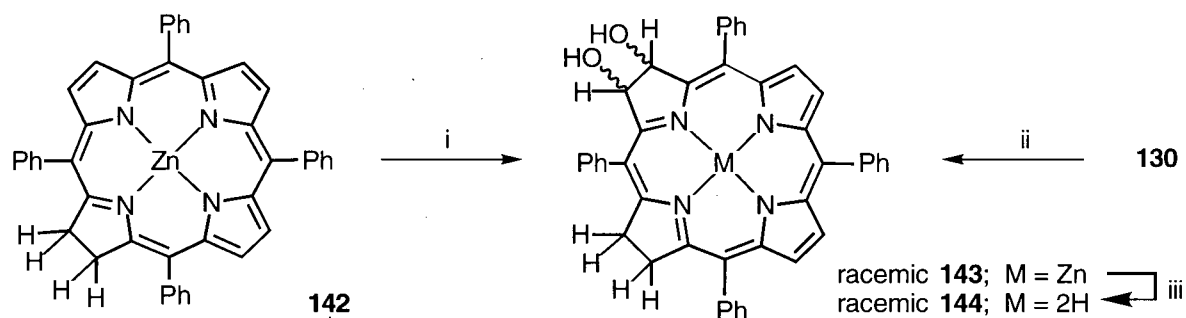


Figure 1-16 Measured ¹H-NMR (400 MHz) signal of the pyrroline protons in **141**(A) and coupling constants determined by simulation (B)

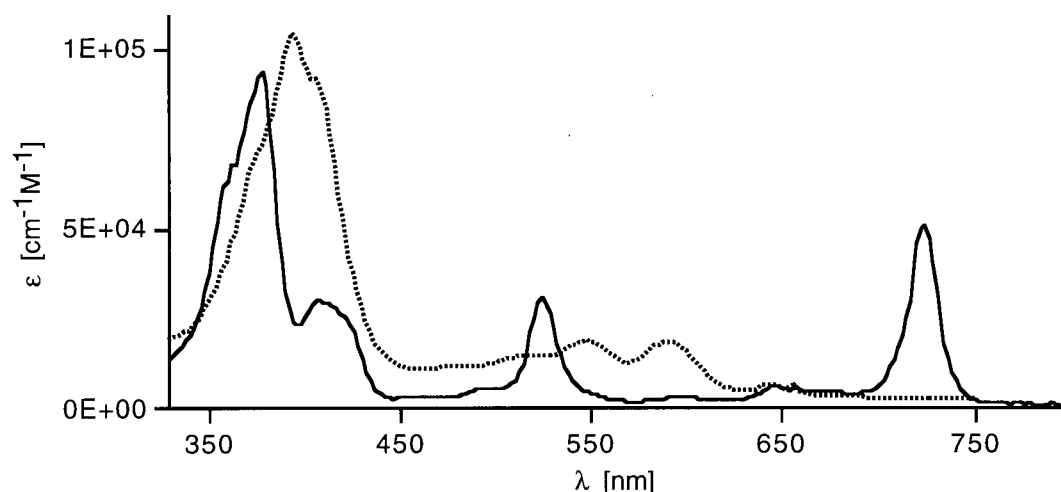
Insertion of zinc into the chlorin completely changes the outcome of the reaction. Thus, hydroxylation of (*meso*-phenylchlorinato)zinc **142** gave only the (2,3-*vic*-dihydroxy-

meso-tetraphenylisobacteriochlorinato)zinc **143**. The basis for this astonishing selectivity was discussed in Section 1.3.3.4. Demetallation afforded the 2,3-*vic*-dihydroxy-isobacteriochlorin **144**. The identities of the isobacteriochlorins were determined by their mass, optical (Figure 1-17) and $^1\text{H-NMR}$ spectra. The symmetry of these pigments (point group C_i) infers the existence of two enantiomeric forms. Due to the lack of any possible chiral induction, they are formed as a racemic mixtures.

**Scheme 1-33**Preparation of the diisobacteriochlorins **143** and **144**

Reaction conditions: (i) 1. 1.1 equiv. OsO_4 , $\text{CHCl}_3/10\%$ pyridine, 2-3 d, r.t.; 2. chromatography; 3. H_2S ; 4. chromatography; (ii) pyridine, K_2CO_3 , *p*-toluenesulfonylhydrazine, Δ .

The optical spectra of **141** and **144** again illustrate the greater potential of bacteriochlorin chromophores for use in PDT as compared to the corresponding isobacteriochlorin chromophores.

**Figure 1-17** Optical spectrum ($\text{CH}_2\text{Cl}_2/0.5\%\text{MeOH}$) of **141** (—) and **144** (····)

2.1.2 THE OSMYLATION OF *meso*-TETRAPHENYL-2,3-DIHYDROXY-2,3-CHLORINS AND -METALLOCHLORINS

The dihydroxylation of the diol chlorin **129** and diol metallochlorin **130** follow the same selectivities as the above pigments. **129** forms a *meso*-phenyl-2,3,12,13-tetrahydroxy-2,3,12,13-tetraolbacteriochlorin, and **130** forms a (*meso*-phenyl-2,3,7,8-tetrahydroxy-2,3,7,8-isobacteriochlorinato)zinc chromophore (Scheme 1-34). The same products can, albeit with lowered yields, be produced by the treatment of TPP or TPPZn with (at least) two equivalents of osmium tetroxide. The optical spectra of the tetraolbacteriochlorin **145** and the tetraolisobacteriochlorin **149** are shown in Figure 1-18.

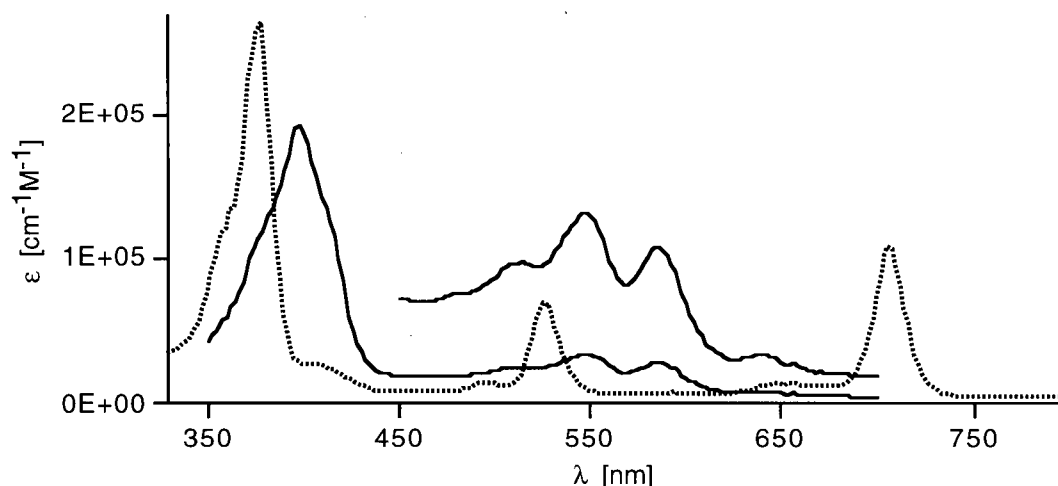
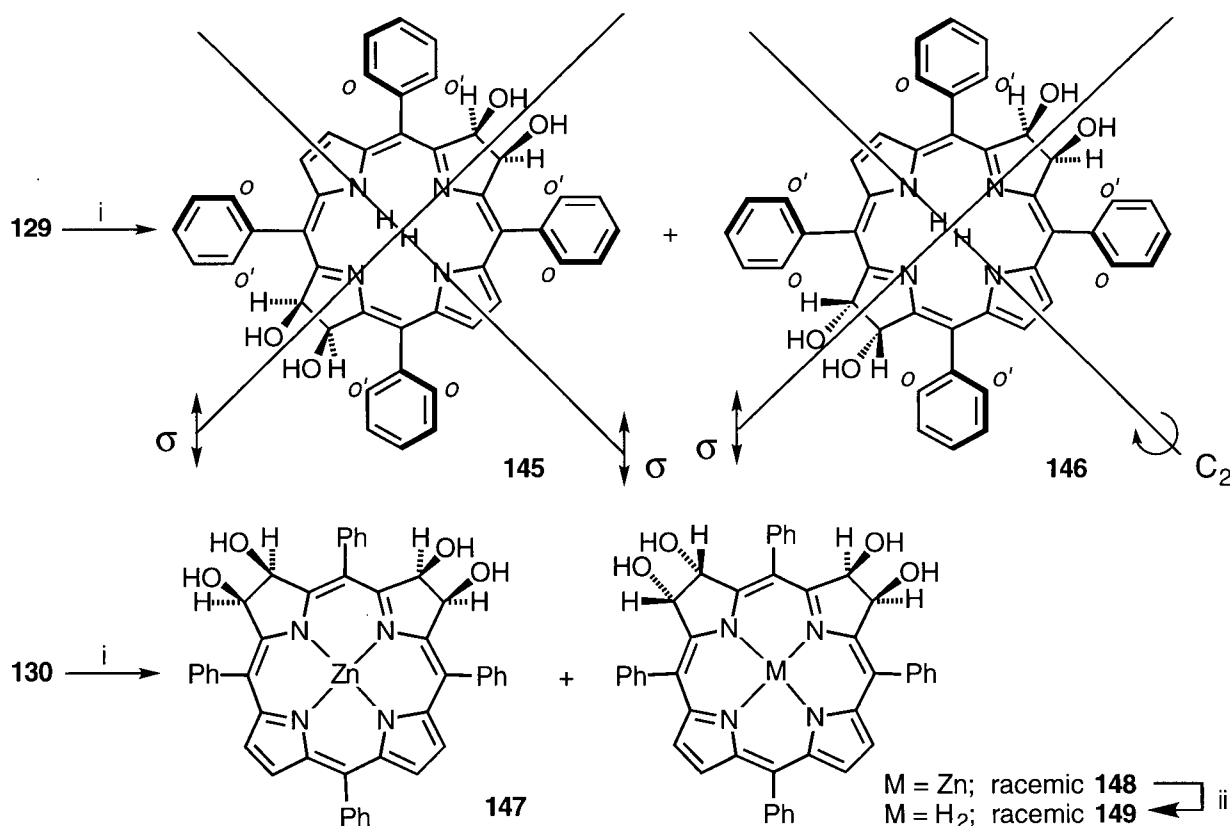


Figure 1-18 Optical spectrum (CH₂Cl₂/0.5%MeOH) of **146** (.....) and **149** (—)

The introduction of a second diol functionality into these pigments has several implications. Firstly, they impose such hydrophilicity on the pigments that their solubility in chloroform is not sufficient as to allow ¹H-NMR spectroscopic investigations. The more hydrophilic solvents methanol, methanol/chloroform mixtures or DMSO have to be used for that purpose. Secondly, their arrangement with respect to the already present diol moiety

can be one of two ways. Either the second diol group is attached on the same face as the first group, or on the opposite face. The formation of both isomers is observed in different ratios. The two pink bacteriochlorin isomers **145** and **146** form as a ~0.9:1 mixture, whereas the two blue-green isobacteriometallochlorins **147** and **148** form in favor of the '*trans*'-isomer **148** (as a racemic mixture), in a ~1:6 mixture. Demetallation of **148** afforded the 2,3-*vic*-dihydroxy-isobacteriochlorins **149** (as a racemic mixture). The difference of the two ratios in which these pigments are formed might be explained by steric effects. The incoming bulky osmate esters might show a preference to be attached on different faces of the molecule. This preference would be the more pronounced the closer the reactive sites are. Hence, the strong face preference in the isobacteriochlorins and the weak effect in the bacteriochlorins.



Scheme 1-34

Preparation of the tetraolbacterio- and tetraolisobacteriochlorins **145-149**
Reaction conditions: (i) 1. 1.1 equiv. OsO₄, CHCl₃/10% pyridine, ~2 d, r.t.;
 2. chromatography; 3. H₂S; 4. chromatography; (ii) 10% TFA/CHCl₃.

All isomers can be separated by preparative TLC and can be identified by their proton NMR spectra. These assignments rely on the recognition of the subtle differences in the region for the *ortho*-protons. For instance, the symmetry elements of structure **145** (point group C_{2v}), in which the diol moieties are on the same side of the molecule, result in a splitting of the *ortho*-protons into two sets, the *o*- *o'*-Hs (Scheme 1-34). The faces of this molecule are non-equivalent but the two sides ('north- and south-side') are equivalent. The symmetry elements in **146** (point group C_{2d}) have a similar effect in that they differentiate between *o*- and *o'*-Hs. The two faces of the molecule are equivalent but the two sides are not. The *o*- and *o'*-Hs in **145** are subject to the double face differentiation by two sets of diols and, thus, their chemical shift difference is more pronounced than that for the analogous protons in **146**, which experience merely a side differentiation. In other words, the *ortho*-protons in **145** experience the effect of four hydroxy groups situated either on the same (*o*-H) or the opposite face (*o'*-H), respectively, whereas all *ortho*-protons in **146** experience the effect of two hydroxy groups located on their respective sides. The slight difference between the *o*- and *o'*-Hs results because the hydroxy-groups on the same side as the respective *ortho*-protons are in one case closer (*o*-H), and in the other case further away (*o'*-H). This all translates into the observation of two separate signals of equal intensity (for 4H) for the *o*- and the *o'*-H signals in **145** as opposed to the lone broadened signal (for 8H) for those in **146**.

In further support of this assignment, **145** is much more polar as seen by its lower R_f -value ($R_f = 0.31$ (silica/5% MeOH/ CH_2Cl_2)) than **146** ($R_f = 0.51$ (silica/5% MeOH/ CH_2Cl_2)). This is expected for this type of rigid, flat molecule as **145** can provide simultaneously two sets of diols for the interaction with the silica gel surface, whereas **146** can provide only one set at a time. The steric protection evidently does not mask this effect.

A similar string of arguments can be used for the assignment of the structures of the isobacteriochlorins **147** and **148** and the demetallated complex **149**, although their NMR spectra are, due to their lower symmetries, more complex than those of the bacteriochlorins. Also, only a small amount of **147** was available and, thus, its structural assignment is more ambiguous than for the bacteriochlorins.

No spontaneous oxidation or dehydration to a chlorin or porphyrin is observed during handling or storage of the tetraol-bacteriochlorins. This is a significant improvement as compared to the very labile TPBC chromophore.

2.1.3 COMMENTS ON THE OPTICAL SPECTRA OF THE β,β' -DIOLCHLORINS

The optical spectra of the novel β,β' -diol derivatized compounds **129**, **141**, **144**, **145**, **146**, and **149** clearly demonstrate their respective chlorin, bacteriochlorin or isobacteriochlorin character.⁶⁷ Table 1-1 lists their spectral data in comparison with the spectral data of their non-dihydroxylated analogs.

The substitution of hydrogens by a set of *vic*-diols causes, in the bacteriochlorin series, a ~ 20 nm hypsochromic shift of the longest wavelength absorption, alters the extinction coefficients of all bands, and, in the bacteriochlorin series, sharpens the Soret-band as compared to the parent TPBC. The two isomeric bacteriochlorins **145** and **146** show identical electronic spectra. Both electronic and conformational effects cause variations in the optical spectra of porphyrinic molecules.³³² Molecular modeling of **129**, **145** and **146**

146 does not suggest an appreciable distortion of the porphyrin core due to introduction of pairs of hydroxy groups.³³³ Hence, the observed hypsochromic shifts seem to be associated with electronic interactions of the substituents with the π -system of the pigments. The nature of the spectra of the tetrahydroxy isomers **145** and **146** seems to support this prediction. A similar effect, though not as pronounced as in the bacteriochlorin series, can be seen in the isobacteriochlorin series (**144** and **149** as compared to TPiBC).

Table 1-1 Optical spectra of the novel diol chlorins in comparison to those of their non-dihydroxylated analogs

Compound	λ_{\max} [nm] (log ϵ)	Solvent ^a	Reference
TPP 6	420 (5.68), 515 (4.30), 549 (3.92), 595 (3.92), 653 (3.78)	A	41
TPC 18	419 (5.28), 517 (4.20), 542 (4.08), 598 (3.79), 652 (4.62)	A	83
129	408 (5.27), 518 (4.19), 544 (4.19), 592 (3.85), 644 (4.38)	B	this work
TPBC	356 (5.11), 378 (5.20), 520 (4.78), 742 (5.07)	A	83
141	378 (4.96), 524 (4.49), 724 (4.71)	B	this work
145/146	376 (5.42), 528 (5.08), 708 (4.89)	B	this work
TPiBC	390 (5.00), 408 (4.90), 516 (4.00), 552 (4.28), 516 (4.08)	A	83
144	394 (5.02), 408(sh), 389(sh), 514 (4.03), 546 (4.19), 590 (4.20)	B	this work
149	398 (5.17), 408(sh), 480(sh), 514 (4.12), 548 (4.29), 586 (4.20)	B	this work

^a The optical spectra of the novel compounds do not show to a large extent (≤ 2 nm) solvent dependent shifts; A = benzene; B = CH₂Cl₂/0.5% MeOH

2.1.4 PRELIMINARY RESULTS OF THE BIOLOGICAL ACTIVITY OF *vic*-DIOL CHLORIN **137**

The first level of testing revealed that diol chlorins have the ability to generate singlet oxygen (Section 2.1.1). The next level of testing is *in vitro* experiments in which defined carcinoma cell lines are irradiated with a controlled dose of light after they are allowed to soak in solutions containing with various concentrations of photosensitizers. The cell survival after certain time intervals is monitored. The better the photosensitizer, the lower the concentration of photosensitizer at which a high and fast cell killing rate is observed. There is, however, an ongoing debate about how indicative these type of *in vitro* tests are for the evaluation of a photosensitizer. For instance, Bonnett's chlorin **4** is reportedly very active when tested *in vivo*,²³ while our *in vitro* tests do not indicate such high activity.³³⁴

Several compounds were tested in-house by Mrs. Savoie of our group. The testing work is still in progress and it is too early to derive any final conclusions. *meso*-Tetra(3-hydroxyphenyl)-2,3-*vic*-dihydroxy-2,3-chlorin **137** has been tested the most thoroughly as the results derived from this compound could be set against the results published for the analogous chlorin **4** lacking the diol functionality. **137** proved in tests against the P-815 mouse mastocytoma cell lines to be not as active as BPD-MA (**1**) under the same conditions.

To gain further insight into the activity and possibly the mechanism of action of the diol chlorins *versus* the mechanism of action of their undihydroxylated counterparts and other photosensitizers, their photodynamic potential was tested by Dr. Ross Boyle of our laboratory in a collaboration with Prof. Matthews from the Pharmacology Department, University of Cambridge, England. Two sophisticated *in vitro* test techniques were employed. The first technique employed was cell assays against, firstly, pancreatic acini

freshly isolated from male Sprague-Dawley rats, secondly, AR4-2J cells derived from an azaserine-induced carcinoma in rat pancreas, and, thirdly, MIA cells derived from a human pancreatic adeno-carcinoma.³³⁵⁻³³⁸

These *in vitro* assays were performed to ascertain the efficacy of the drugs particularly in photoinactivation of pancreatic carcinoma. Pancreatic carcinoma is the fourth most common cause of death by cancer, and the five year survival rate is only 3%.³³⁹ The screening of healthy rat acini allows the therapeutic window for PDT with this drug to be determined. This is especially important for pancreatic cancer which, being diffuse, requires irradiation of the tumor and peritumoral tissue simultaneously. Preliminary results with **137** as photosensitizer indicate that the drug is more potent than the standard employed, BPD-MA (**1**), but because experiments are still in progress, it is too early to speculate on the magnitude of the therapeutic window.

The second technique employed was the measurement of the photodynamically mediated response (contraction upon irradiation) of freshly isolated superfused Guinea pig smooth muscle (Taenia Caecum) in the presence of the photosensitizers. The smooth muscle experiments can give insight into the mechanism by which the activated photosensitizer exerts its effect on cells.³⁴⁰ Compared with **1**, **137** seems to operate by a different, and distinct, mechanism, which causes contraction of the smooth muscle tissue, but in a much more reversible manner. This drug is also more sparing of the cell membrane suggesting a different pattern of intracellular localization.

Whether these effects are specifically attributable to the presence of the diol moiety remains to be elucidated. However, the initial results of the photodynamic activity of the diol chlorins are very encouraging.

2.1.5 ROTATION OF PHENYL RINGS IN *meso*-TETRAPHENYL- β,β' -DIHYDROXY-CHLORINS

Restricted rotation of phenyl rings resulting from steric interactions with neighboring groups has been the subject of considerable investigation since the early work on optically active biphenyls. *meso*-Tetraphenylporphyrins are in that respect an interesting case study. Although maximum delocalization between the porphyrin ring and the *meso*-phenyl substituent in TPP would be achieved through co-planarity, steric interactions between the β -hydrogens and the ortho-hydrogens on the phenyl rings prevent this conformation and force the phenyl plane to be placed approximately perpendicular to the porphyrin mean plane. Crystal structures have determined the dihedral angle to range from 90° ³⁴¹ to as small as 69° ³⁴² for most free base and metalloporphyrins.

The steric interaction of the *ortho*-substituents with the β -protons allows the isolation of atropisomers of *ortho*-phenyl substituted TPPs.³⁴³⁻³⁴⁵ However, rotation of the phenyl group is, albeit at a low rate, possible for TPPs with relatively small *ortho*-substituents.^{343,346} As can be readily shown with molecular models of TPP, the plane of the porphyrin has to undergo some distortion to allow any phenyl rotation to occur, even if the *ortho*-substituent is as small as hydrogen. The rigidity of a metalloporphyrin is controlled by the type of metal. Consequently, the rate of rotation in metallo-TPPs is a function of the size of the *ortho*-substituent, the type of metal present and possibly the presence of other substituents on the phenyl ring. All the factors mentioned have, mainly by work of Eaton and Eaton, been studied in fair detail.³⁴⁷⁻³⁵⁰

These studies depended, with no exception, upon the use of penta-coordinated metalloporphyrins. Given the right choice of a ligand inert towards substitution, this ligand

introduces a face differentiation to the metalloporphyrin such that the *ortho*- and *ortho'*-protons become non-equivalent and, consequently, separate signals in the $^1\text{H-NMR}$ spectra for these protons can be observed (**A** in Figure 1-19). The analysis of the temperature dependency of the NMR spectra reveals the activation parameters for variously substituted metallo-TPPs.

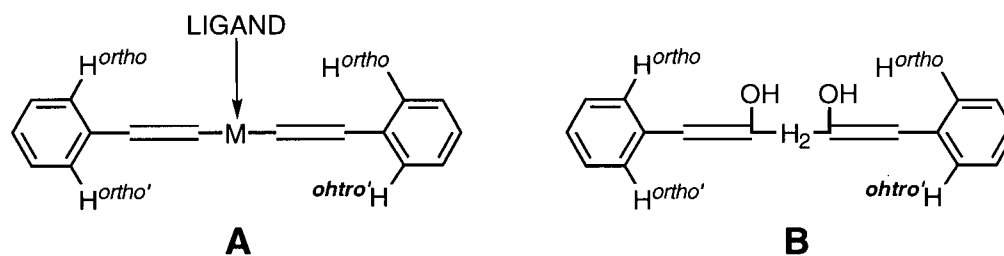


Figure 1-19 Schematic representation of the face differentiation in tetraphenyl metallo-chlorins with additional ligands (**A**) and in *vic*- β,β' -diolchlorins (**B**).

The use of metalloporphyrins is intrinsic to this methodology, and therefore, no activation parameters have been described for free base porphyrins (or chlorins). The *vic*-diol group in diol chlorin **129** is situated on one side of the chlorin plane and, as discussed earlier, brings about a face (and side) differentiation (**B** in Figure 1-19). This fact prompted the investigation of the temperature dependent NMR spectra of **129**, **130** and **138** as we reasoned that this face differentiation should enable the measurement of the rotational barriers of the phenyl substituents in these free base chlorins.

Figure 1-20 shows the low-field portion of the $^1\text{H-NMR}$ (400 MHz, DMSO-d_6) of **129** in the temperature range from room temperature to 140°C . Whereas the signals assigned to the β -protons remain unchanged, those associated with the phenyl protons undergo temperature dependent changes. The broad peaks at 8.08, 8.05, and 7.88, integrating for 4, 2, and 2 protons, respectively are assigned to the *ortho*-protons as indicated. The separation of the signals for the two non-equivalent *ortho*-protons attached to the phenyls next to the dihydroxylated pyrrolic unit (*o*- and *o'*-H near side) indicates that the phenyl groups rotate at

room temperature slowly on the NMR time scale. The broad feature may indicate rotation to some extent, and indeed, cooling of a sample of **129** in CHCl_3 to -20°C sharpens the peaks up a little (no shown), but this broadening could also be due to non-resolved couplings by all other hydrogens in the phenyl ring. Heating the sample to 50°C causes complete coalescence of the *o*- and *o'*-peaks, indicative of the rotation of the phenyl groups at a rate comparable to the NMR time scale. Further heating accelerates the rate of rotation and the two *ortho*-protons become indistinguishable. Finally, at 140°C (the technical limit for the spectrometer used), face differentiation due to the hydroxy substituents can no longer be seen. Merely their side-differentiation is visible by virtue of the two signals corresponding to the two sets (5-, 20-phenyl and 10-, 15-phenyl) of equivalent phenyl groups. The higher temperature of the coalescence of the peaks attributed to the *o*- and *o'*- near side as compared to that for the *o*- and *o'*- far side is the basis for the conclusion that the phenyl groups situated next to the diol moieties have a higher barrier of rotation than those phenyls on the far side of the diol moiety.

The analogous spectrum for the zinc diolchlorin **130** essentially shows the same effects as seen for the spectrum of the free base chlorin **129**, albeit the peaks for the *ortho*-protons are not as well resolved due to some overlap with peaks for the β -protons. There is one important difference, however. Even at 140°C , the peaks for the *o*- and *o'*- near side are not fully recovered, suggesting that the phenyl groups (5-, 20-phenyl) still rotate at a slow rate. We attribute this effect to the stiffening effect of the central metal, in other words, the metallochlorin moiety has a higher barrier of distortion so as to allow a rotation of the phenyl groups as the free base chlorin has. The shift of the peak for the OH-protons in **130** is attributable to the a change of water concentration (present as minor impurity in the DMSO-d_6) during the experiment. The sample was heated for several hours in excess of 100°C and this led to the evaporation of some of the moist in the solvent.

Not shown are the results of the temperature dependent NMR spectra for the *meso*-tetra(3,4,5-trimethoxyphenyl)-2,3-dihydroxy-2,3-chlorin (**138**). Its spectrum is, due to reduction of the number of intra-phenyl H,H-couplings, much simpler than that of the previous examples. Presumably due to the bulk of the methoxy-substituents, coalescence of the *o*- *o'*-H far side is observed at ~110°C, and coalescence of the near side-protons is observed at ~140°C. Consequently, no spectrum for the fast rotation limit could be obtained.

The single run experiments, the inaccuracy of the temperature measurements, and the uncertainty associated with the necessary estimate of the signal positions for the non-rotation limiting case due to the impossibility of measuring low temperature NMR spectra in the same solvent (DMSO- d_6) as in the high temperature runs, precluded the calculation of the activation parameters associated with the phenyl rotations. However, the observed trends fit well into what is known from previous studies about this kind of dynamic process.³⁴⁸⁻³⁵⁰ The significance of the experiments lay in showing that the unique face-differentiating nature of the diol functionality can serve as a tool for the measurement of parameters previously not measured due to the lack of suitable compounds.

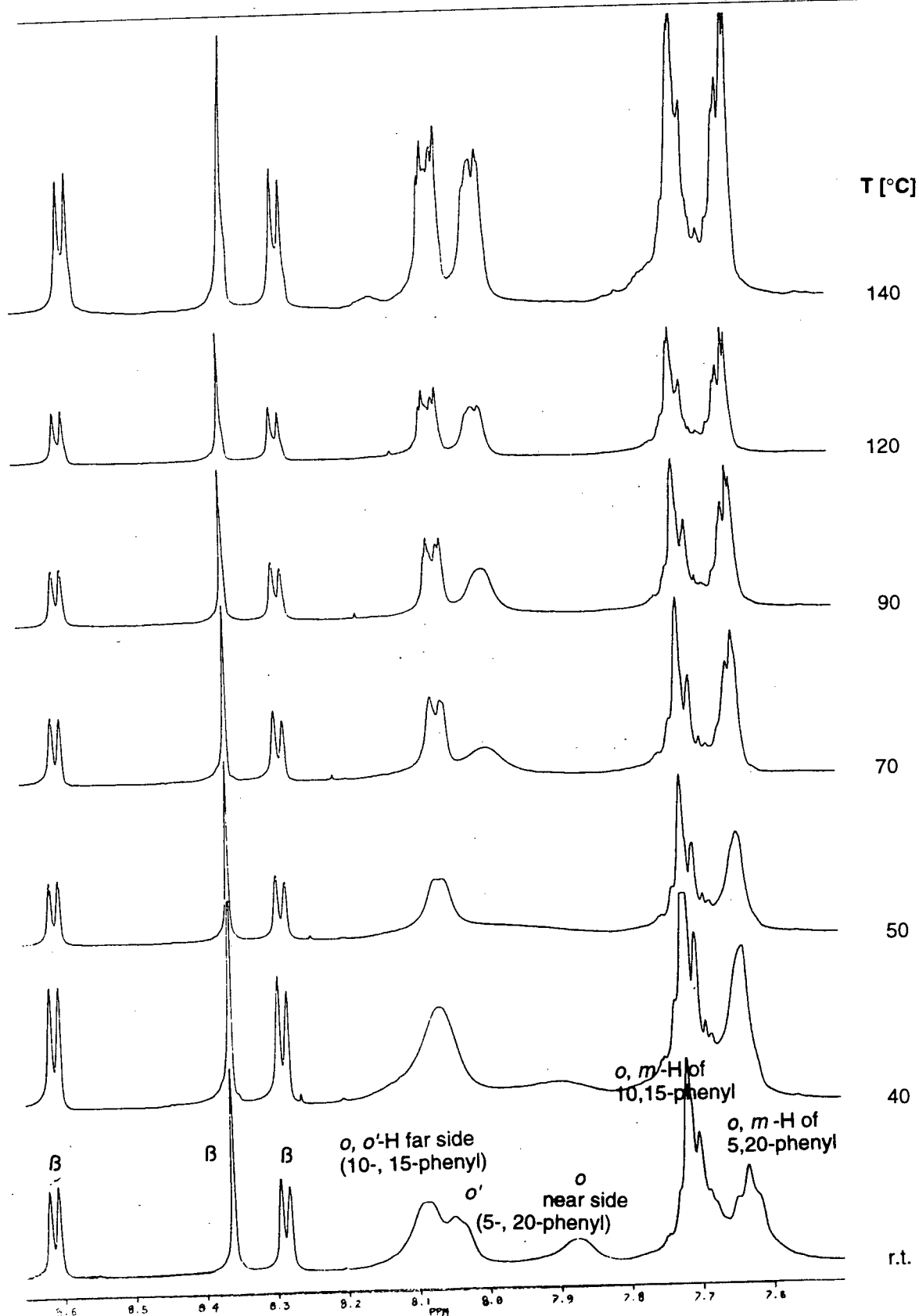
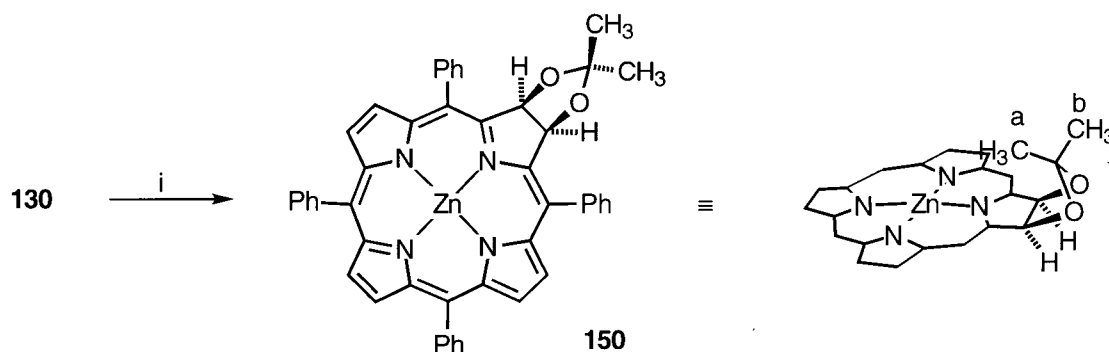


Figure 1-20 Temperature dependent $^1\text{H-NMR}$ (400 MHz, DMSO- d_6 , 38mM) of 129

2.1.6 THE REACTIVITY OF THE *meso*-TETRAPHENYL-*vic*-DIOLCHLORINS

2.1.6.1 FORMATION OF ISOPROPYLIDENE KETAL **150**

The formation of isopropylidene ketals from acetone and 1,2- and 1,3-diols is a common reaction to protect diols in, for example, sugars.³⁵¹ The reaction is generally acid-catalyzed. Diol **130** is, as shown below, sensitive to strong acids and, consequently, dry zinc(II) chloride was chosen as the relatively mild Lewis acid to catalyze the acetonide formation, shown in Scheme 1-35. Reaction of **130** in dry acetone containing freshly fused zinc(II) chloride produced a less polar product **150** as compared to the starting material, but, **150** displays virtually the same optical spectrum as the starting compound.



Scheme 1-35 Formation of acetonide **150**
Reaction condition: (i) freshly fused ZnCl_2 /acetone/ Δ ;

The $^1\text{H-NMR}$ of **150** readily allows for confirmation of the expected acetonide structure. The low-field signals of the starting material are essentially maintained. The signals for the diol hydrogens have vanished, no coupling is observed for the pyrrolidine hydrogens and two new signals at δ 0.61 (for $-\text{CH}_3^{\text{a}}$) and 1.35 ppm (for $-\text{CH}_3^{\text{b}}$) appeared, with the relative intensities corresponding to three hydrogens each. These signals can be assigned to the methyl-groups of the isopropylidene moiety.

2.1.6.2 FORMATION OF β -OXO-DERIVATIZED PIGMENTS β -Oxochlorins

The above mentioned stability of the diol chlorins towards dehydration has limits. Reflux of these chlorins with traces of strong acids such as perchloric or sulfuric acid rapidly and cleanly produces one purple pigment of low polarity and the expected mass spectral and analytical data for a compound corresponding to the starting compound minus one equivalent of water. It appears unimportant whether the zinc metallated or the free base is used for this dehydration as the conditions are harsh enough to induce demetallation, thus forming in both cases the metal-free compound **151** (Scheme 1-36). If, however, the diol chlorins are treated for several hours at reflux temperatures with the Lewis-acid zinc chloride in chloroform/methanol or tetrahydrofuran, the formation of the metallated analog **152** can be observed. The metallated and demetallated species can also be interconverted by standard methodologies. Their optical spectra are shown in Figure 1-22. Both spectra are surprisingly not chlorin- but porphyrin- or metalloporphyrin-like.

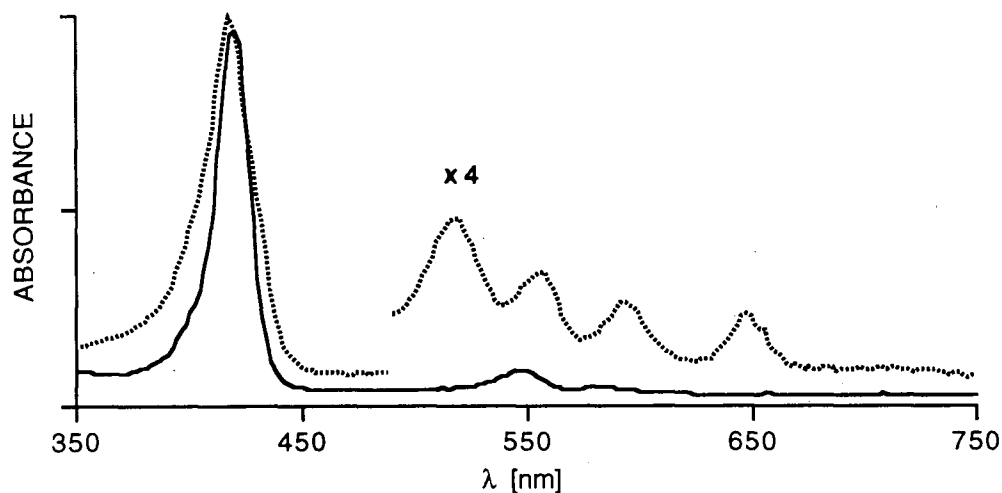
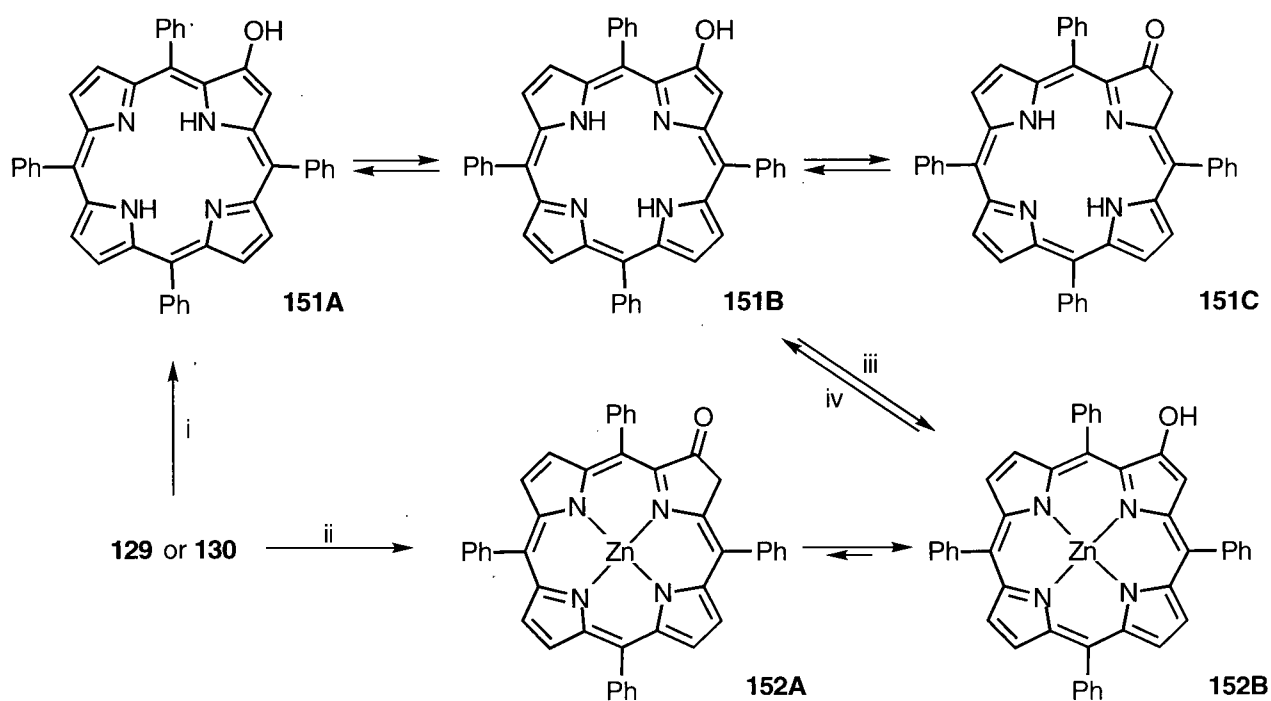


Figure 1-22 Normalized optical spectra (CH₂Cl₂) of **151** (.....) and **152** (—)

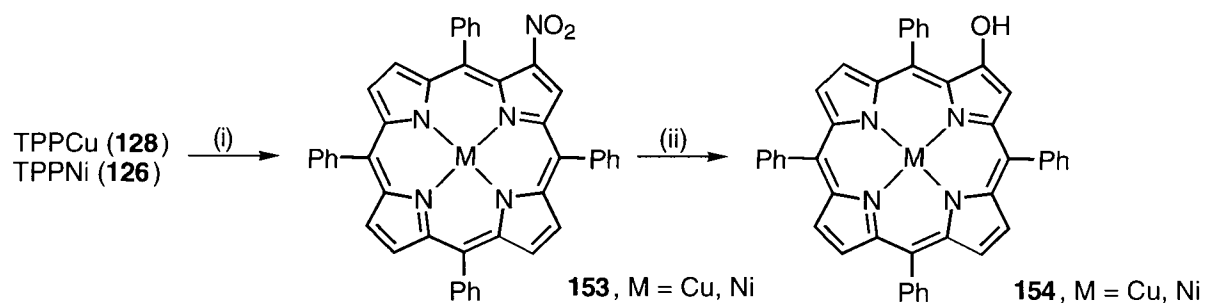


Scheme 1-36 Dehydration of diol **129** or **130** to give ketochlorins **151** and **152**
 Reaction conditions: (i) catalytic amount HClO_4 /benzene/ Δ ; (ii) ZnCl_2 /THF/ Δ ; (iii) $\text{Zn(II)acetate/MeOH/CHCl}_3$ / Δ ; (iv) TFA

The $^1\text{H-NMR}$ spectrum of **151** is surprisingly complex. This is due to the occurrence of three different tautomers (**151A** - **151C**). The tautomeric equilibria for **151** and **152** have been studied in detail by Crossley *et al.*³⁵² The $^1\text{H-NMR}$ spectrum for **152** is much simpler than that for **151**. It indicates the occurrence of **152B** as the main species in solution.

Crossley and co-workers have synthesized **151** and **152** previously.³⁵²⁻³⁵⁴ One of two possible synthetic routes is shown in Scheme 1-37. It is the optimal route known to date, namely the nucleophilic displacement of the nitro group in **153** by the anion of benzaldoxime with subsequent aqueous work-up.³⁵⁴ This method suffers from the disadvantage that it requires the use of the copper(II), nickel(II) or palladium(II) derivatives of TPP. To produce the metal-free 2-oxochlorin **151**, for example, a harsh demetallation step (two-phase system of conc. sulfuric acid and methylene chloride) has to be included in the synthesis. The synthesis of **151** *via* the dehydration of diol **129**, on the other hand, is a

convenient, mild, and high yield two-step process (starting from TPP) and can be performed on the metal-free systems. Thus, it represents an excellent alternative synthetic pathway for the formation of **151** and related pigments.

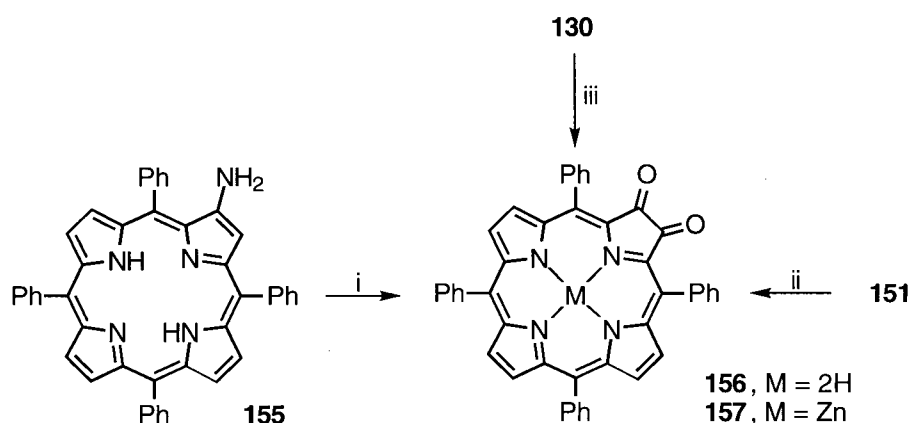


Scheme 1-37 Formation of **154**

Reaction conditions: (i) NO₂;¹⁰⁸ (ii)³⁵⁴ 1. Na-salt of benzaldoxime,
2. aqueous work-up³⁵⁴

β,β' -Dioxochlorins

The 2-oxo-TPP **151** is not only an interesting compound in its own right, but has also been used as starting material for the synthesis of β,β' -dioxo compounds such as **156** (Scheme 1-38). Two different syntheses^{355,356} of this diketone have been published and interesting porphyrin dimers and oligomers have been formed from them³⁵⁷ or from tetraoxobacterio- and isobacteriochlorins³⁵⁸ derived from **156**.



Scheme 1-38 Formation of β,β' -dione chlorins **156** and **157**

Reaction conditions: (i)^{355,356} 1. light/O₂, 2. H⁺/H₂O; (ii)³⁵⁶ 4 equiv. SeO₂/dioxan, Δ ; (iii) 2.2 equivalents DDQ/benzene

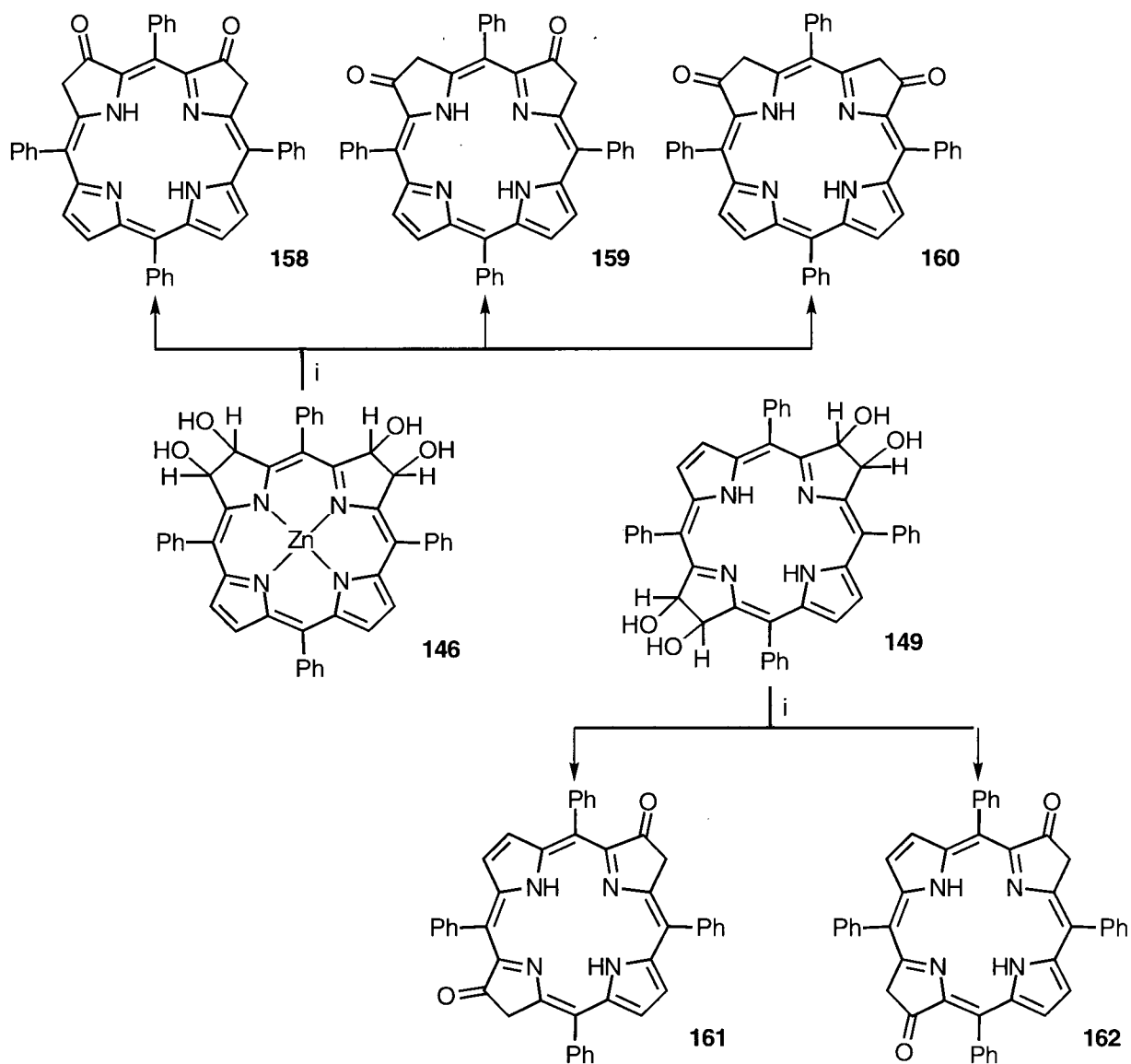
We found that oxidation of **130** with 2 equivalents of DDQ in dry benzene produces a non-polar yellow-brown pigment in excellent yields with spectroscopic and analytical properties identifying it as **157**. In particular, the symmetry inherent to this compound was clearly seen in the ¹H-NMR. The face-differentiation seen in the starting compound **130** had vanished and no signal other than those for three sets (two doublets, one singlet) of β - and one set for the phenyl protons could be detected. Due to time constraints, **157** and its reactions were not further investigated. In the 1984³⁵⁵ and 1991³⁵⁶ communications by Crossley and co-workers initially reported **157**, no analytical data were given, nor did the authors publish a full paper detailing their findings. Hence, any comparison of their data for the diones and those found by us is unfortunately not possible.

β -Dioxobacterio- and Isobacteriochlorins

The dehydration of diol **129** to give the oxochlorin **151** points to a synthetic path to produce dioxobacteriochlorins and -isobacteriochlorins by double dehydration of the corresponding tetraolbacteriochlorins and -isobacteriochlorins. The relative stereochemistry of the tetraols used should have no effect on the outcome of the dehydration products but each dehydration may produce several regioisomers of the resulting dioxo-compounds. These possible regioisomers are shown in Scheme 1-39.

No directing effect as seen, for instance, in the pinacol-pinacolone-type rearrangements of β,β' -diol- β -alkylchlorins (cf. Section 1.3.3.5), is expected to govern these dehydrations. This is basically what is found by experiment. Acid treatment of the tetraols **146** or **149** produces a mixture of three and two products, respectively. Mass spectral analysis of the crude mixture resulting from the dehydration of isobacteriochlorin **146** showed the presence of the expected mass (m/e (EI) = 647 for MH^+), however, the compounds proved in our hands to be impossible to separate by preparative TLC. Furthermore, this dehydration was associated with extensive decomposition, and thus, this reaction was not further investigated.

The dehydration of bacteriochlorin **149** is not corrupted by extensive decomposition, but produces two compounds relatively cleanly with the expected mass. Again, we did not succeed in separating these regioisomers in amounts which would have allowed their individual characterization.

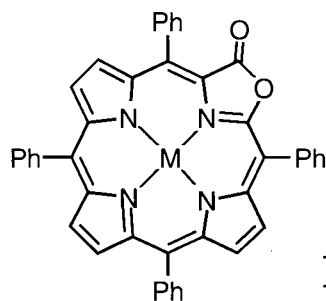


Scheme 1-39 Proposed formation of dioxobacterio and -isobacteriochlorins
Reaction condition: (i) trace HClO_4 /benzene, Δ

2.1.6.3 FORMATION OF 2-OXA-3-OXO-CHLORIN **163**

As noted above, the dihydroxylation of TPP derivatives is a 'clean' reaction, in other words, only few undesired by-products form during this reaction. Nonetheless, one by-product which formed in very small ($\leq 2\%$) amounts during the dihydroxylation of TPPZn is a non-polar (R_f between the diol and TPPZn) green pigment (**163**) which in dilute methylene chloride solution displays a remarkable blue-green color with a strong red fluorescence. This pigment was readily separated from the desired diol and the starting material during the column chromatography step. It was furthermore observed that more of this pigment formed the longer the TPPZn was allowed to react with the osmium tetroxide, but in no case was the yield higher than a few percent. Repeated execution of the dihydroxylation reaction led to the accumulation of enough material such that full characterization could be attained.

The pigment can be demetallated with 10%TFA in methylene chloride, and reaction of the demetallated product with zinc(II) under typical metallation conditions reconstituted the native pigment, thus proving that the pigment did not decompose during the acid treatment. The optical spectra of the zinc-containing (**163**) and metal-free pigment (**164**) are shown in Figure 1-23.



The Soret-bands and the well defined Q-bands of this spectrum clearly attest to the porphyrinic nature of this compound. The mass spectral analysis specified the composition of $C_{43}H_{26}N_4O_2Zn$ and $C_{43}H_{28}N_4O_2$ for **163** and **164**, respectively. This highly unusual composition indicated the loss of one carbon and the uptake of two oxygen atoms as

compared to TPPZn ($C_{44}H_{28}N_4Zn$). As the loss of a carbon from the phenyl moieties is highly unlikely, this loss had to have occurred in the porphine framework. Certain bile pigments can be derived from porphyrins by excision of a *meso*-proton and the introduction of ketone-functionalities at the 'exposed' α -carbons, but this implies in the case of *meso*-tetraphenyl pigments also a loss of a phenyl group which, based on the mass, is not observed, nor does the optical spectrum support the presence of an open-chain pigment. The loss of an α -carbon with retention of the macrocycle also seems very unlikely. That leaves only the loss of a β -carbon as the viable explanation for the observed data. Several positions for the oxygen atoms are conceivable and the 1H -NMR spectrum of the compound is expected to give clues to where the oxygens are situated. This, indeed, is the case. The 1H -NMR for **163** and **164** are shown in Figure 1-24.

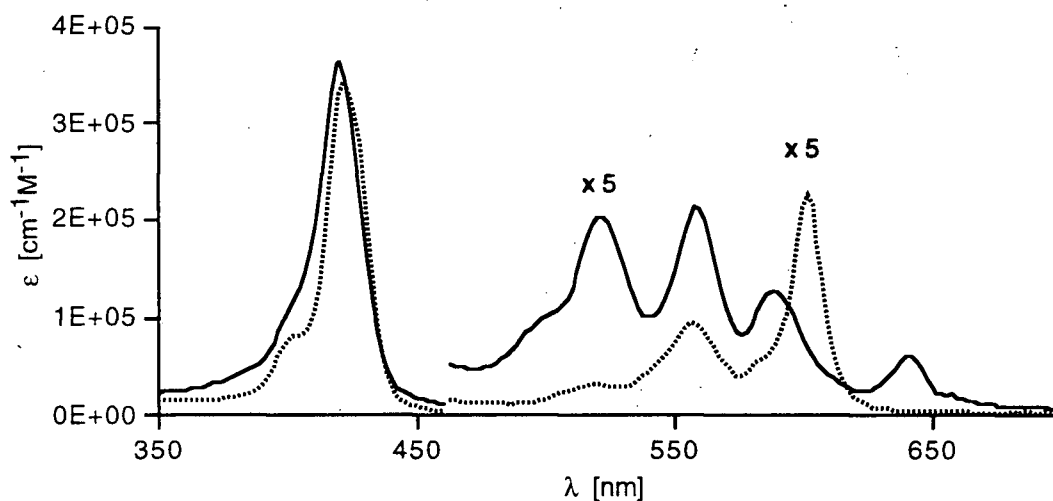


Figure 1-23 Optical spectra (CH_2Cl_2) of **163** (.....) and **164** (—)

Four clusters of peaks, each with unique patterns characteristic for certain hydrogens in TPP-derived compounds can be distinguished. The signals at -2.04 and -1.69 ppm with the relative integration for two hydrogens are in the typical region for the inner NH-protons. The occurrence of two signals is, given a slow tautomeric exchange on the NMR time scale, indicative of a porphyrin without any rotational symmetry. One example for this pattern is the above mentioned 2-oxo-TPP tautomer of compound **151**. The complex peak cluster

between 7.6 and 7.8 ppm can, by comparison with the spectra of related compounds and the total integration of twelve hydrogens, be attributed to the *meta*- and *para*-protons of the phenyl groups, and the peaks centered at 7.9 and 8.7 ppm to the corresponding *ortho*-protons. Most illustrative are the peaks above 8.5 ppm, the region for the β -hydrogens. Their total integration for six protons, the recognition of the typical AB-patterns with $^3J = 4.5$ Hz for adjacent non-equivalent β -hydrogens and the presence of a coupling of 1.5 Hz, typical for the 4J coupling of β -hydrogens with an NH-hydrogens, lead to the assignment indicated in Figure 1-24. Further plausibility of this is gained from the $^1\text{H-NMR}$ spectrum of the metallated pigment **163**, the low-field region of which is also shown in Figure 1-24. It shows essentially the same pattern as the spectrum for **164**, only simplified by the absence of the 4J coupling (and the signals for the NH protons).

These data indicate the presence of the structural unit shown in Figure 1-24. The wedge in the structural drawing indicates the non-symmetric moiety which contains both oxygens and one more carbon atom. The structure **163** (and **164**) incorporates these elements in a plausible fashion. Formally, a β, β' -link in TPPZn has been replaced with a lactone functionality. The $^{13}\text{C-NMR}$ spectrum of **163** shows a signal at 173 ppm, and the IR spectrum (film) a strong peak at 1740 cm^{-1} . Both facts support the presence of a lactone group.

The ultimate proof of the structural assignment of **163** as (*meso*-tetraphenyl-2-oxa-3-oxo-chlorinato)zinc(II) was provided by its X-ray crystal structure. The ORTEP representation of **163** (as its pyridine complex) is shown in Figure 1-25, the final atom coordinates, selected bond lengths and experimental details are listed in Tables 1-2, 1-3, and 1-4, respectively.

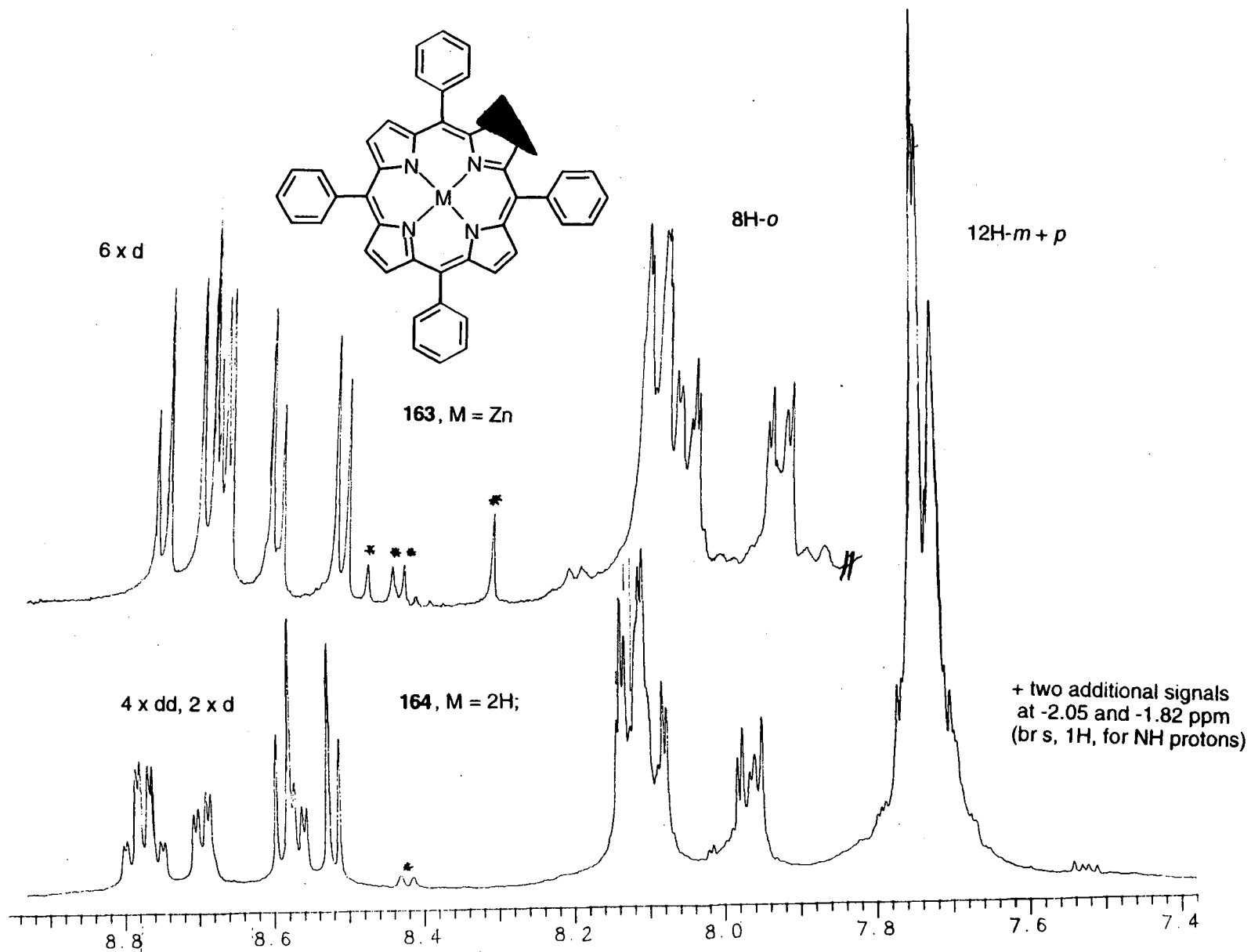


Figure 1-24 $^1\text{H-NMR}$ (300 MHz, CDCl_3) of 163 and 164 * impurity
Wedge symbolizes any non-symmetric moiety

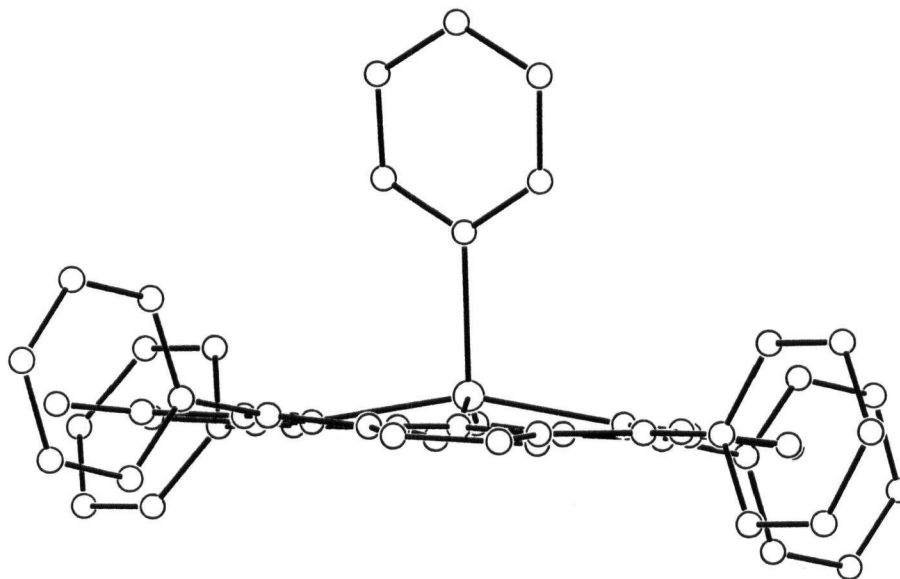
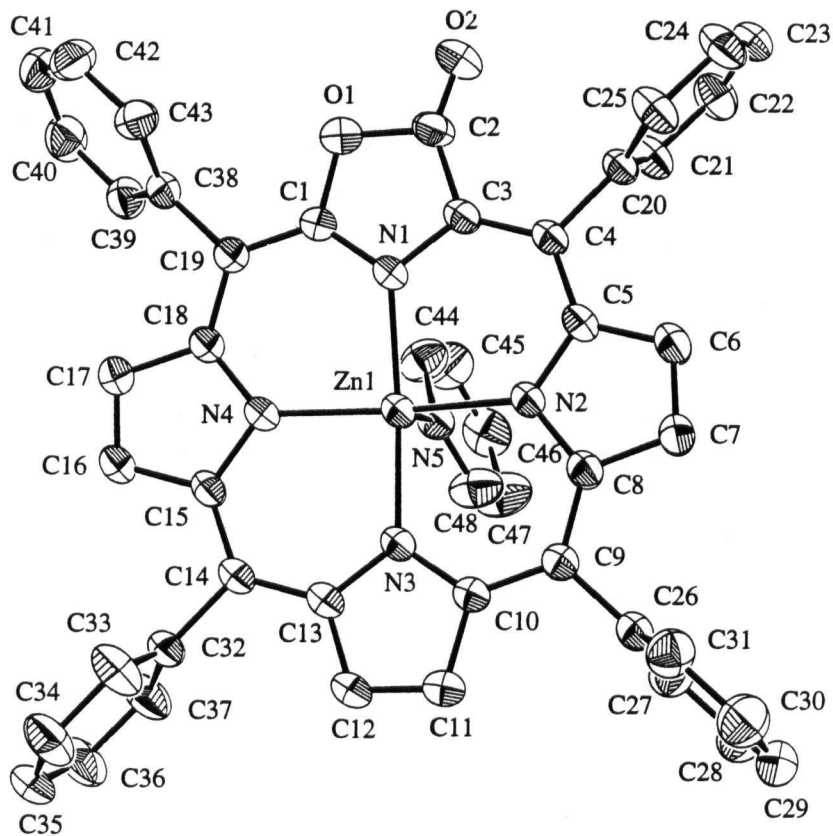
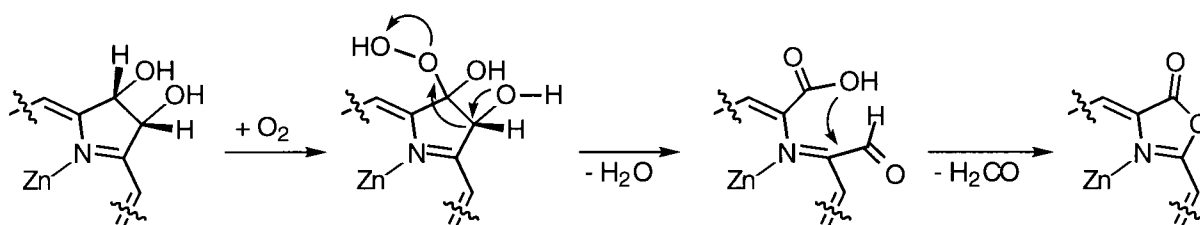


Figure 1-25 ORTEP representation (33% probability level) and side view of 163-pyridine

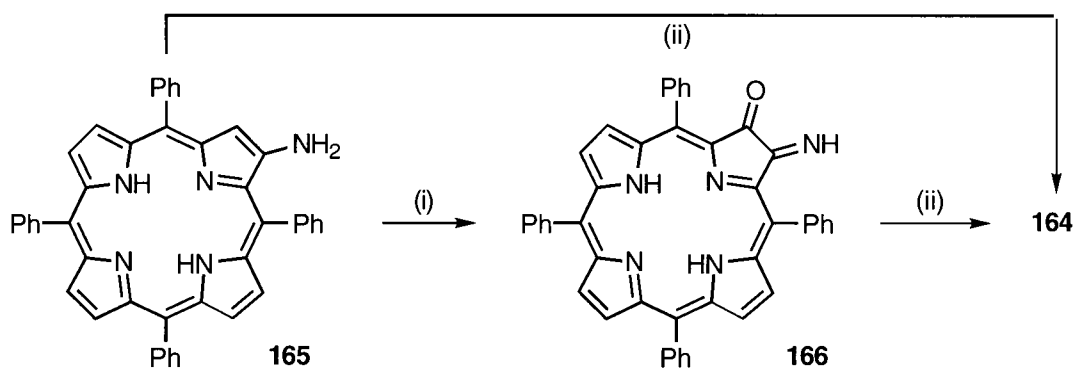
The crystal was disordered in respect to the rotational orientation of the individual porphyrins along the axis passing through the pyridine nitrogen and the central zinc atom. This shows that the crystal packing is more determined by the bulky phenyl groups, the pyridine coordinated to the zinc and the planarity of the porphyrin than the comparatively small β -substituents. However, 45% of the molecules are oriented in a unique way. The formal replacement of the pyrrole unit by a five-membered lactone-containing nitrogen heterocycle in **163** does not lead to any appreciable distortion of the mean plane of the macrocycle. The zinc atom is a little out of the porphyrin plane, a finding typical for zinc pyridine porphyrins.³⁵⁹ All bond lengths testify to the presence of a highly delocalized system. As expected for metallochlorins, the β, β' -bonds in the pyrrolic units adjacent to the 'reduced' pyrrolic unit are slightly shorter (C6-C7 = 1.352(3) and C16-C17 = 1.354(3) Å) than those in the opposite unit (C11-C12 = 1.378(3) Å). Perhaps unusual is the fairly short bond length between the carbonyl carbon and the connecting α -carbon (C2-C3 = 1.427(3) Å), the ring oxygen and the α -carbon (C1-O1 = 1.397(3) Å) and the C=O bond itself (C2-O2 = 1.148 Å). This may indicate some contribution of hyperconjugated structures to the overall structure.

The details of its formation remain unclear. It can be shown that the lactone is not a photooxidation product. Earlier reports of the osmium tetroxide oxidation of aromatic systems have shown that this oxidation may result in some ring cleavage.¹⁷⁹ Treatment of TPPZn with a large excess of osmium tetroxide leads to extensive decomposition of the porphyrin and the formation of **163** cannot be observed. It is reasonable to assume an autooxidation mechanism as shown in Scheme 1-40, but it is not clear whether the osmate ester or the diol is the more activated starting material for such an oxidation or whether the expelled carbon is formally in the oxidation state of formaldehyde or, following another oxidation, of carbon dioxide.



Scheme 1-40 Proposed autooxidation mechanism for the formation of **163**

It must be noted that **164** was reported in 1984 in a communication.³⁵⁵ The authors claimed the preparation of this pigment either by photo-oxidation of 2-amino-TPP (**165**) and subsequent MCPBA oxidation of the photooxidation product **166**, or by direct MCPBA oxidation of **165** (Scheme 1-41). The mechanism for this transformation also remains speculative. The authors reported only the optical spectrum and the mass, as determined by mass spectroscopy, for **164** and, to the best of our knowledge, they failed to substantiate their claims in a full paper. However, we find that their reported λ_{\max} and $\log \epsilon$ deviate only little ($\Delta \lambda_{\max} = 4 \text{ nm}$; $\Delta \log \epsilon \approx 0.1$) from our findings.

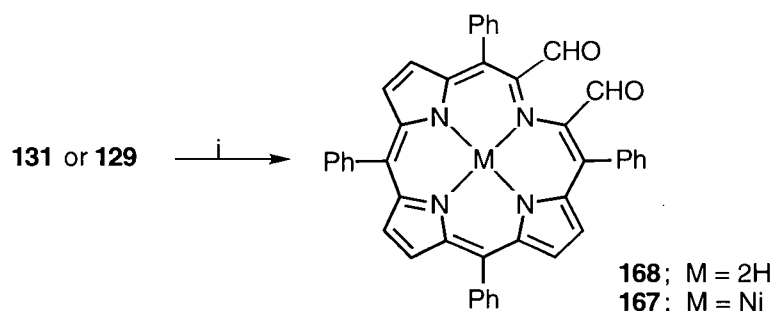


Scheme 1-41 Crossley's synthesis of lactone **164**³⁵⁵
Reaction conditions: (i) $\text{O}_2/h\nu$; (ii) MCPBA

2.1.6.4 FORMATION OF A SECOCHLORIN AND SUBSEQUENT RING-CLOSURE REACTIONS

Formation of a *meso*-Tetraphenylsecochlorin

The cleavage of a 1,2-glycol into two carbonyl compounds is performed classically either by periodate or lead tetraacetate.³⁶⁰ While the attempted oxidation of nickel diol **131** with periodate led to a complex mixture, the oxidation with a stoichiometric amount of lead tetraacetate gave cleanly the beige-brown pigment **167** (Scheme 1-42). Its optical spectrum is shown in Figure 1-26.



Scheme 1-42 Formation of *meso*-phenylsecochlorin bisaldehydes **167** and **168**
Reaction condition: (i) 1. 1 equiv. Pb(IV)acetate, THF, r.t.

This optical spectrum featuring the split and bathochromically shifted Soret-band as compared to the starting material and the broad Q-bands does not allow an immediate conclusion about the type of chromophore present, but any conventional chlorin or porphyrin can be excluded. High-resolution mass spectroscopy (found m/e 703.16394, corresponding to $C_{44}H_{29}O_2N_4Ni$), 1H - and ^{13}C -NMR (singlet at 9.7 ppm and 188.7 ppm, respectively), and IR spectroscopy ($C=O$ stretch at 1684 cm^{-1}) readily identify this product as the (*meso*-tetraphenyl-2,3-dicarboxaldehyde-2,3-secochlorinato)nickel(II) (**167**). The analogous conversion of the metal-free chlorin **129** produces a pigment with spectroscopic properties which allow its preliminary characterization as the metal-free analog **168** of **167**, but this

product is much less stable than **167** and largely converts in CHCl_3 within several hours into a pigment of unknown structure. The investigation of **168** and its reactions was reserved for future studies. The observed optical spectrum is attributed to the presence of the strongly electron-withdrawing and conjugated aldehyde groups and the greater flexibility of the porphyrin ring.

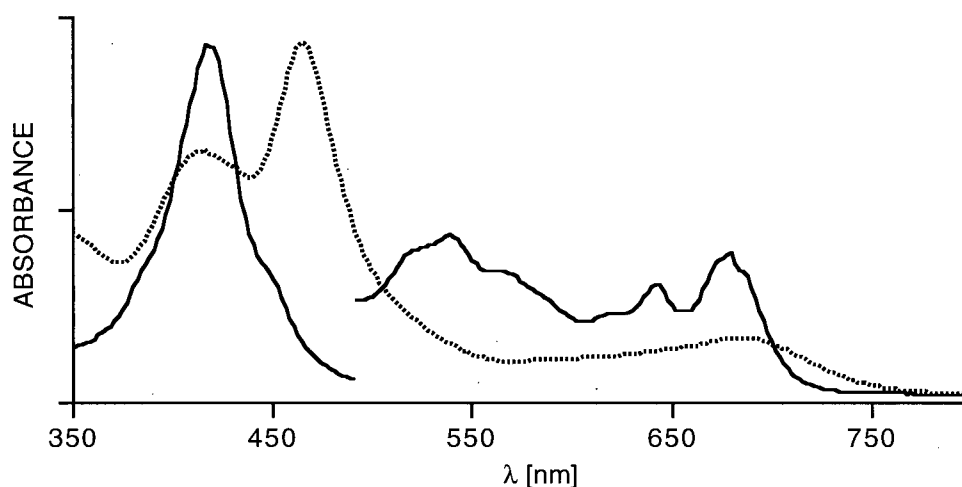
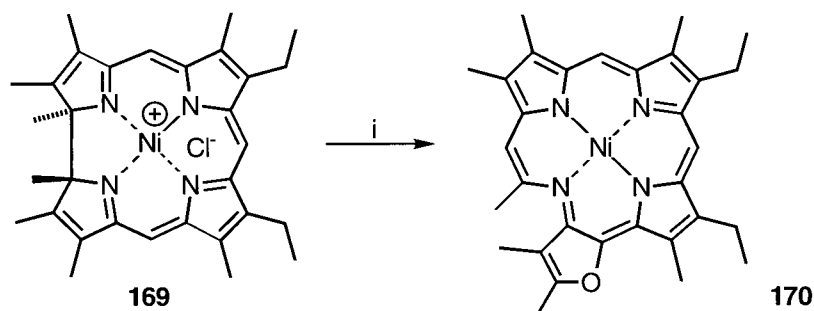


Figure 1-26 Normalized optical spectra (CH_2Cl_2) of **167** (.....) and **168** (—)

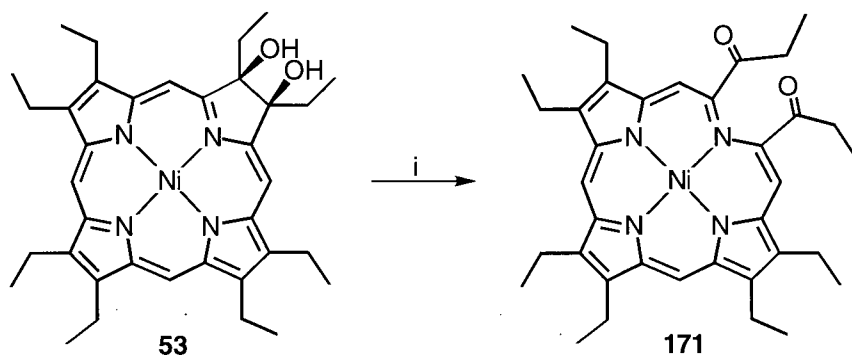
The formation of secochlorins is rare. Chang, Peng and co-workers²²⁶ reproduced in 1992 the alleged formation of an epoxychlorin from (dimethyloctadehydrocorrinato)-nickel(II) **169** as reported in 1969 by Johnson and co-workers^{224,225} (Scheme 1-43). They were able to confirm the spectral properties of the pigment formed, but also realized that some chemical properties were inconsistent with the formulation of the pigment as an epoxychlorin. Single crystal X-ray crystallography finally revealed the unusual structure of pigment **170** they dubbed furochlorophin. Its structure implies the series of rearrangements which apparently had taken place upon heating corrin **169**. The corrin frame has expanded and one angular methyl group has become a methine link. One pyrrole α - β -bond was broken and the vinylic appendage of the broken pyrrole turned 180° to reattach itself to the macrocyclic frame through an ether linkage. Molecular oxygen must be assumed to be the

source of the ether-oxygen. Several other porphyrins are also formed during the reaction. The free base of **170** shows a chlorin-type optical spectrum ($\lambda_{\text{max}} = 699 \text{ nm}$, $\log \epsilon = 4.11$). From the highly specific mode of formation of **170** it is evident that any use of the furochlorophins as PDT agents can be excluded, but the optical spectra make more general methods to prepare secochlorins an attractive field of study.



Scheme 1-43 Formation of furochlorophin
Reaction conditions: *o*-dichlorobenzene, 160°C, O₂

Apart from the first example, only two more examples of secochlorins are known to us. One is derived from the serendipitous singlet oxygen-mediated ring scission of an octakis(dimethylamino)porphyrazine. This secochlorin was communicated in 1994 by Barrett and Hoffman and co-workers.³⁶¹ The second, and closely related example, is the lead tetraacetate cleavage of the OEP derived diol chlorin **53** to give the octaethyl-2,3-secochlorin-2,3-dione **171**, reported in 1993 by Adams *et al.* (Scheme 1-44).³⁶²



Scheme 1-44 Formation of octaethyl-2,3-secochlorin-2,3-dione **171**³⁶²
Reaction condition: (i) 1. Pb(IV)acetate, 2. chromatography

Formation of the Novel Pigments 173 and 175

During recrystallizations of **167** from chloroform and methylene chloride solutions containing methanol, the slow formation of two green pigments, **172** and **173**, was observed. The halogenated solvents used are prone to the formation of small amounts of hydrochloric acid and, hence, we assumed the observed pigment formation to be an acid-catalyzed reaction. And indeed, treatment of a methanol/chloroform solution of **167** with gaseous hydrochloric acid resulted in complete and rapid disappearance of this pigment and the appearance of the two compounds **172** and **173**. Further treatment with acid finally resulted, at the expense of **172**, in the formation of **173** as the sole product (Scheme 1-45). The optical spectrum of **173** is shown in Figure 1-27. The optical spectrum of **172** and that found for **173** are almost identical. The spectra are reminiscent of metallochlorins but they are considerably broadened and bathochromically shifted.

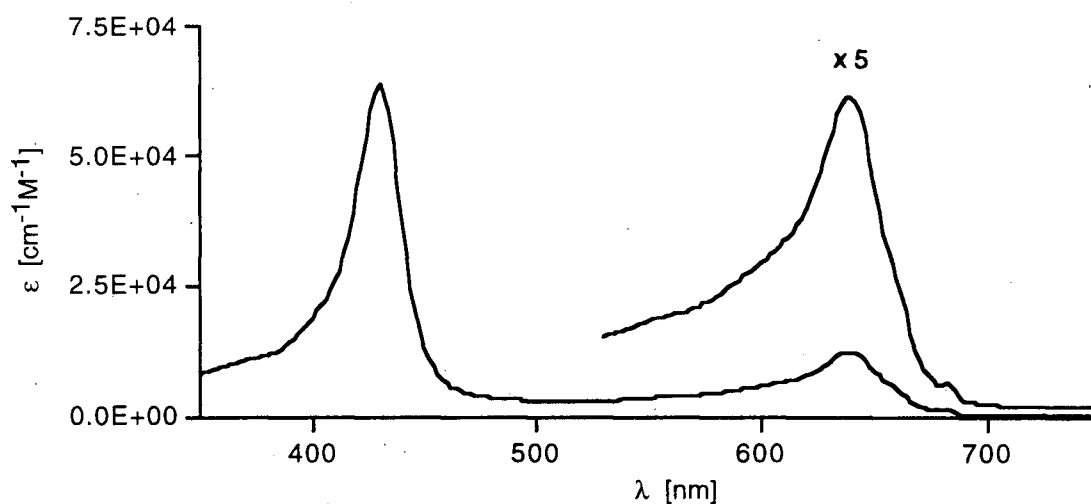
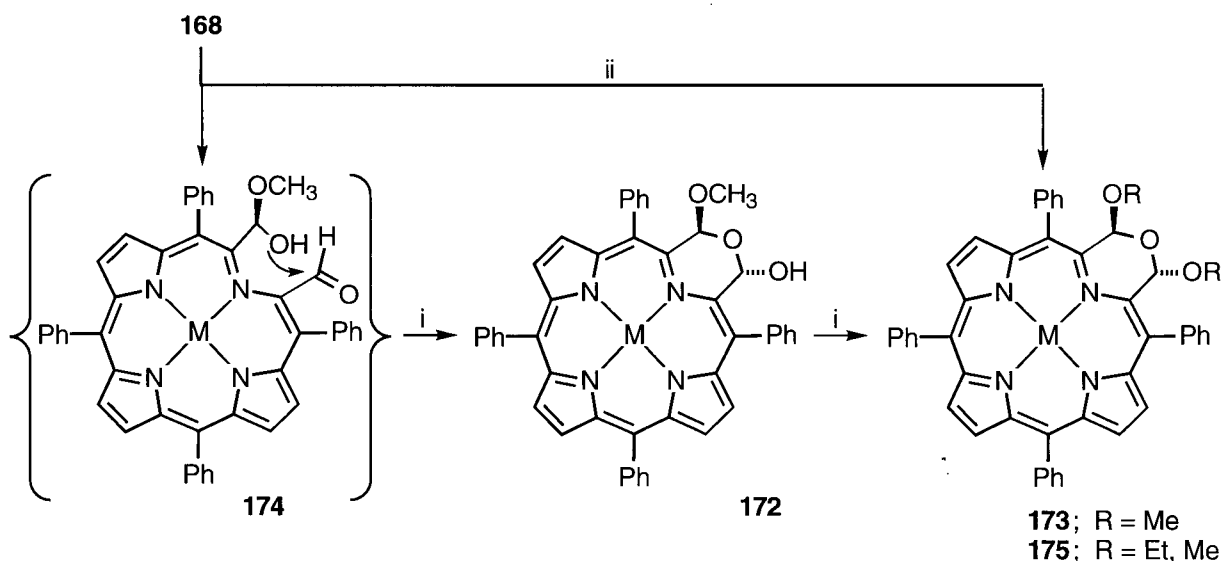


Figure 1-27 Optical spectrum (CH_2Cl_2) of **173**

The formation of **172** is, as seen in the mass spectrum, associated with an increase in mass corresponding to the uptake of methanol in the starting compound, and **173** gained another 15 mu, corresponding to the additional uptake of a methyl group. These changes

are, under the present reaction conditions, best explained by the uptake of two equivalents of methanol with a concomitant loss of water. Hence, these mass spectral results suggest already the formation of an acetal. Inspection of the structure of dialdehyde **167** reveals that it is ideally set up for an intramolecular double acetal formation (Scheme 1-45). Acid-catalyzed reaction of one aldehyde group with methanol forms hemiacetal **174**. The alcohol functionality of this hemiacetal reacts immediately with the second aldehyde functionality to form the isolable intermediate **172**, which upon further acid-treatment converts into the double acetal **173**. The $^1\text{H-NMR}$ spectra of **172** and **173** support this scheme strongly. The expected overall symmetry of the compounds **172** (no mirror plane) and **173** (containing a mirror plane) can be deduced from the coupling patterns of the β -protons. Also the presence of one or two methoxygroups, respectively, and of hydrogens attached to a non-aromatic part of the molecule are visible.



Scheme 1-45

Formation of **172** and **173**.

Reaction conditions: (i) MeOH, catalytic amount of HCl (g); (ii) mixture of MeOH/EtOH, catalytic amount of HCl (g)

In one experiment, **168** was dissolved in chloroform, a drop of methanol was added, and the solution was exhaustively treated with acid as described above. The resulting

pigment **175** was dissolved in chloroform and petroleum ether 40-60 was allowed to diffuse into the solution. Beautiful dark green crystals suitable for X-ray crystal structure analysis were deposited. The optical spectrum of the crystalline material was identical to that for **173**. Surprisingly, though, mass spectral analysis of the crystals showed that in addition to the expected peak ($m/e = 748$), two more peaks with $m/e = 762$ and 776 were present, corresponding to compounds containing one or two more methylene groups. The $^1\text{H-NMR}$ was also unexpectedly complex, and indicated the presence of ethyl groups. Reinvestigation of the experiment revealed that chloroform stabilized with ethanol was used. As a result, the formation of a mixture of ethyl and methyl double acetals (methyl-methyl, methyl-ethyl, as well as ethyl-ethyl) was possible, thus explaining the spectroscopic findings for **175**.

Despite the presence of three species in the crystalline material, it was possible to solve the crystal structure. All three compounds crystallized in the same lattice and largely in the same orientation. The presence of the methoxy-bearing compounds was noticeable only by a partial occupancy for the terminal carbon of the ethoxy side chains. This conservation of one lattice for TPP-based structures is not unusual.³⁶³ An ORTEP representation of **175** is shown in Figure 1-28, a side view and a stereoview of this compound are shown in Figure 1-29. Experimental details of the crystal structure analysis are listed in Table 1-2, final atomic coordinates in Table 1-5, and selected bond lengths in Table 1-6. The crystal structure brings about the final proof for the structure of **175** (and **173**). The presence of the six-membered ring in **175** results a spectacular distortion of the porphyrin 'plane'. This distortion is best described by a roughly 45° twist along the axis passing through N1-Ni-N3. Despite this, the central nickel atom is still coordinated in a square planar fashion and the median Ni-N bond length of 1.895 \AA is almost exactly as long as that found in (porphyrinato)Ni(II) complexes.⁴¹ The alkoxy groups of the double acetal functionality are exclusively arranged transoid to each other. This can be understood using steric and stereoelectronic arguments.

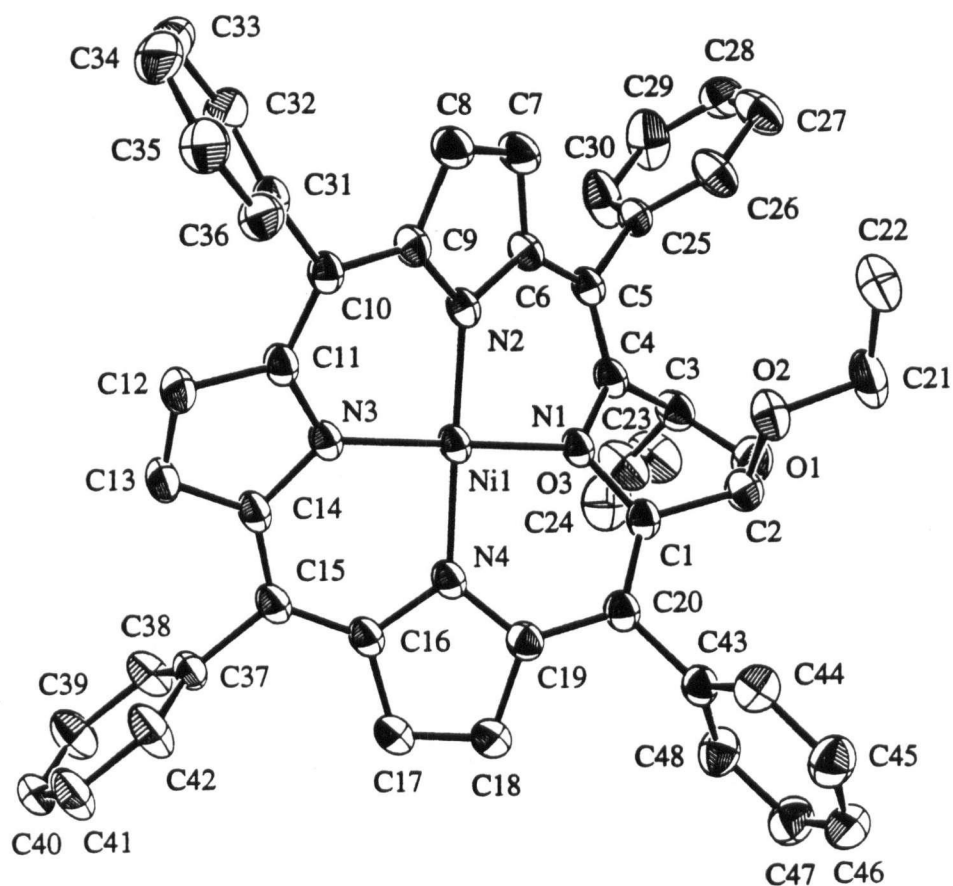


Figure 1-28 ORTEP representation (33% probability level) of **175**. The partially occupied positions have been assigned by the use of non-shaded spheres.

The molecular structures and the ground and excited state dynamics of non-planar porphyrins have been reviewed in 1995.³⁶⁴ The host of structures discussed there are distorted through steric interactions of side chains and groups attached to the outer or inner periphery of the porphyrin macrocycle, resulting in various ruffling modes.³⁶⁵ None of the structures derived their ruffling through the replacement of a pyrrolic unit by, as in **175**, a six-membered or any other sized ring. In fact, we believe that **175** is the first structurally characterized aromatic porphyrinic macrocycle with this intriguing feature. Berlin and Breitmeyer synthesized in 1994 two non-aromatic porphyrinoids in which one pyrrole unit

was replaced by benzene and pyridine, respectively.^{319,320} Bonnett and co-workers reported in 1993 the synthesis of an aromatic pigment in which one pyrrole was formally replaced by a six-membered ring, however, it was not structurally characterized.³⁶² This pigment will be discussed below in more detail. The distortion has, as demonstrated, a pronounced effect on the optical spectrum, and it remains to be elucidated what effect this distortion has on, for example, the electrochemical characteristics of this compound.

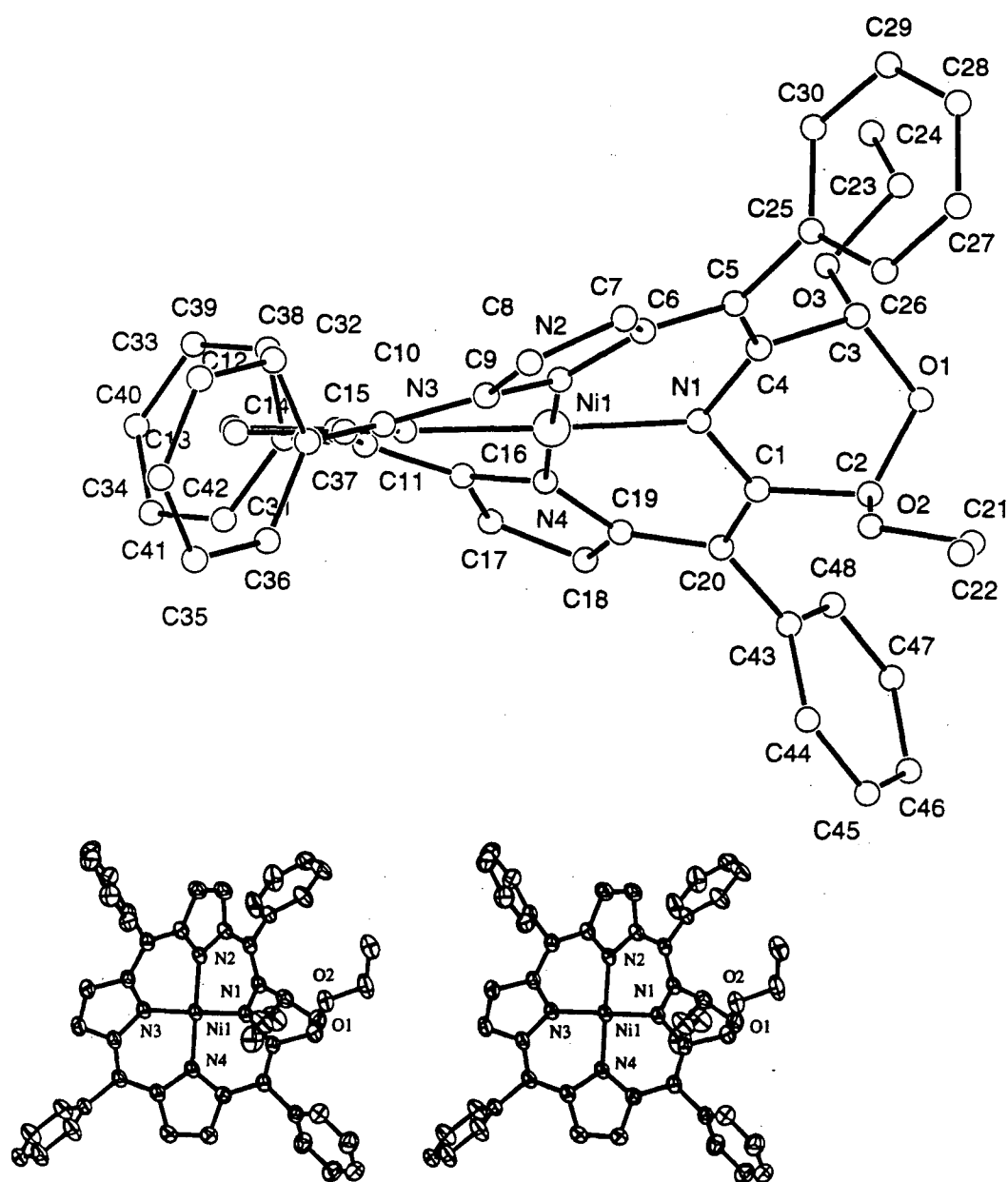
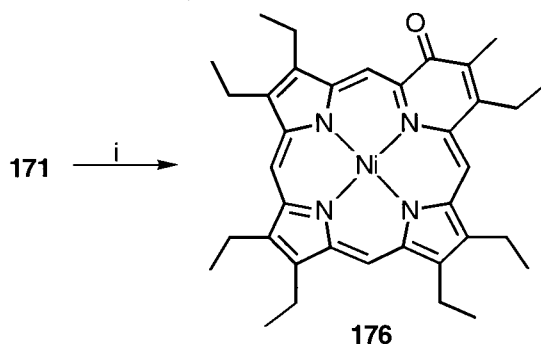


Figure 1-29 Side view and stereoview of the crystal structure of 175

In contrast to dialdehyde **168**, octaethyl diketone **171** contains enolizable hydrogens, and when treated with base, undergoes an intramolecular aldol condensation to form **176** (Scheme 1-46). No crystal structure has been reported for this compound, and no statement about its conformation can be made. However, the presence of an α,β -unsaturated ketone within the six-membered ring suggests a less severe distortion from planarity as found for **175**.



Scheme 1-46 Formation of aldol condensation product **176**³⁶²
Reaction conditions: (i) base

The examples of the reactivity of the diol moiety of the *meso*-tetraphenylchlorins mentioned in the foregoing chapters highlight the use of the osmium tetroxide mediated dihydroxylation not only to confer specific spectroscopic and solubility properties on a potential drug for PDT, but also to introduce functionalities to modify the porphyrin skeleton so as to create unique pigments. The chemistry of these compounds has only started to be explored and it can be safely predicted that more novel pigments will be made by chemical modification of the *meso*-tetraphenyl-2,3-*vic*-dihydroxychlorins and their metal complexes. In particular, the formations of secobacteriochlorins and secoisobacteriochlorins from the tetraols **146** and **149** or their metal complexes seem attractive goals for further research. The oxidation of dialdehyde **167** to the corresponding diacid and its decarboxylation may lead to the formation of the parent secochlorin, an, as yet, elusive compound.

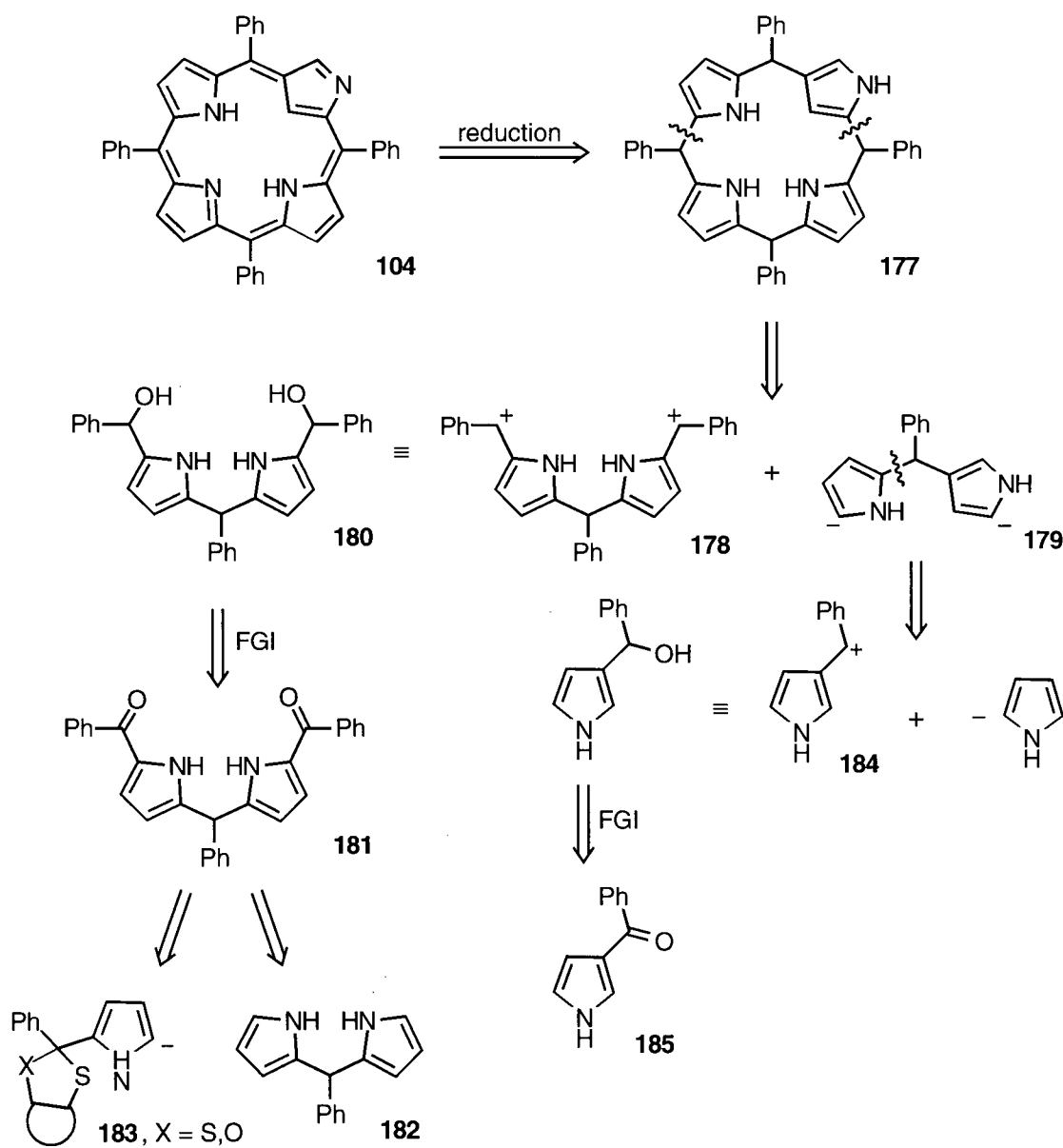
2.2 STUDIES TOWARDS THE DIRECTED SYNTHESIS OF N-CONFUSED TPP

Any in-depth study of N-confused porphyrins requires the preparation of significant amounts of this material. Given the roughly 5% yield of the original, 'random' Rothmund-type syntheses^{268,269} and the laborious multiple chromatography steps involved, a better synthesis of N-confused porphyrin would be desirable. To that end, a directed step-by-step synthesis of N-confused porphyrin was sought. Such directed synthesis may also enable the synthesis of derivatives of N-confused porphyrins such as *meso*-diphenyl-N-confused porphyrin or *meso*-phenyl-di-N-confused porphyrins, which are likely not accessible by the Rothmund-type condensation.

2.2.1 RETROSYNTHETIC ANALYSIS OF N-CONFUSED PORPHYRIN

Retrosynthetic analysis³⁶⁶ of N-confused porphyrin (**104**) suggests, based on the recognition of the availability of a 2 + 2-type approach for its synthesis, a series of structurally simplifying transformations, shown in Scheme 1-46. The first transformation is the conversion of porphyrin **104** into its reduced form, the N-confused porphyrinogen **177**. Compound **177** transforms by cleavage of two C $_{\alpha}$ -C $_{meso}$ bonds into two bipyrrolic synthons, **178** and **179**. The typical nucleophilic reactivity pattern of the pyrrole α -positions in synthon **179** requires in the corresponding synthetic step an electrophilic counterpart in **178**. The typical reagent of such reactivity is the corresponding hydroxy-compound **180**, available by reduction of the bisbenzoyl-*meso*-phenyldipyrromethane (**181**). This compound should be available by direct benzoylation⁵⁶ of the *meso*-phenyldipyrromethane³⁶⁷, a known compound. Alternative pathways are also available.³⁶⁸⁻³⁷⁰ The bipyrrolic unit **179** containing the α -to- β -link transforms into pyrrole, with its usual reactivity at the α -position,

and **184**, which is ultimately derived from β -benzoylpyrrole **185**, a readily available material. From this synthetic plan it follows that the α,β -dipyrromethane is the key intermediate as it has, as a result of the α -to- β pyrrole linkage, the 'N-confused' unit already locked in place. Most importantly, **179** is set up for a 2 + 2 condensation and a regular reactivity pattern is expected for this α,β -dipyrromethane, *i.e.* the positions of highest nucleophilicity are both α -positions.



Scheme 1-47 Retrosynthetic analysis of N-confused porphyrin **104**

2.2.2 THE DIRECTED SYNTHESIS OF N-CONFUSED PORPHYRIN

The synthesis of N-confused porphyrin and its precursors proceeded along the pathways suggested by the retrosynthetic analysis; however, several unforeseen events occurred. On one hand, the synthesis became less straightforward, and on the other hand, it gave serendipitous access to a novel compound (**180**) with a highly interesting structure (Scheme 1-48).

Synthesis of *meso*-Phenyldipyrromethane (**179**) and *meso*-diphenyltripyrane (**180**)

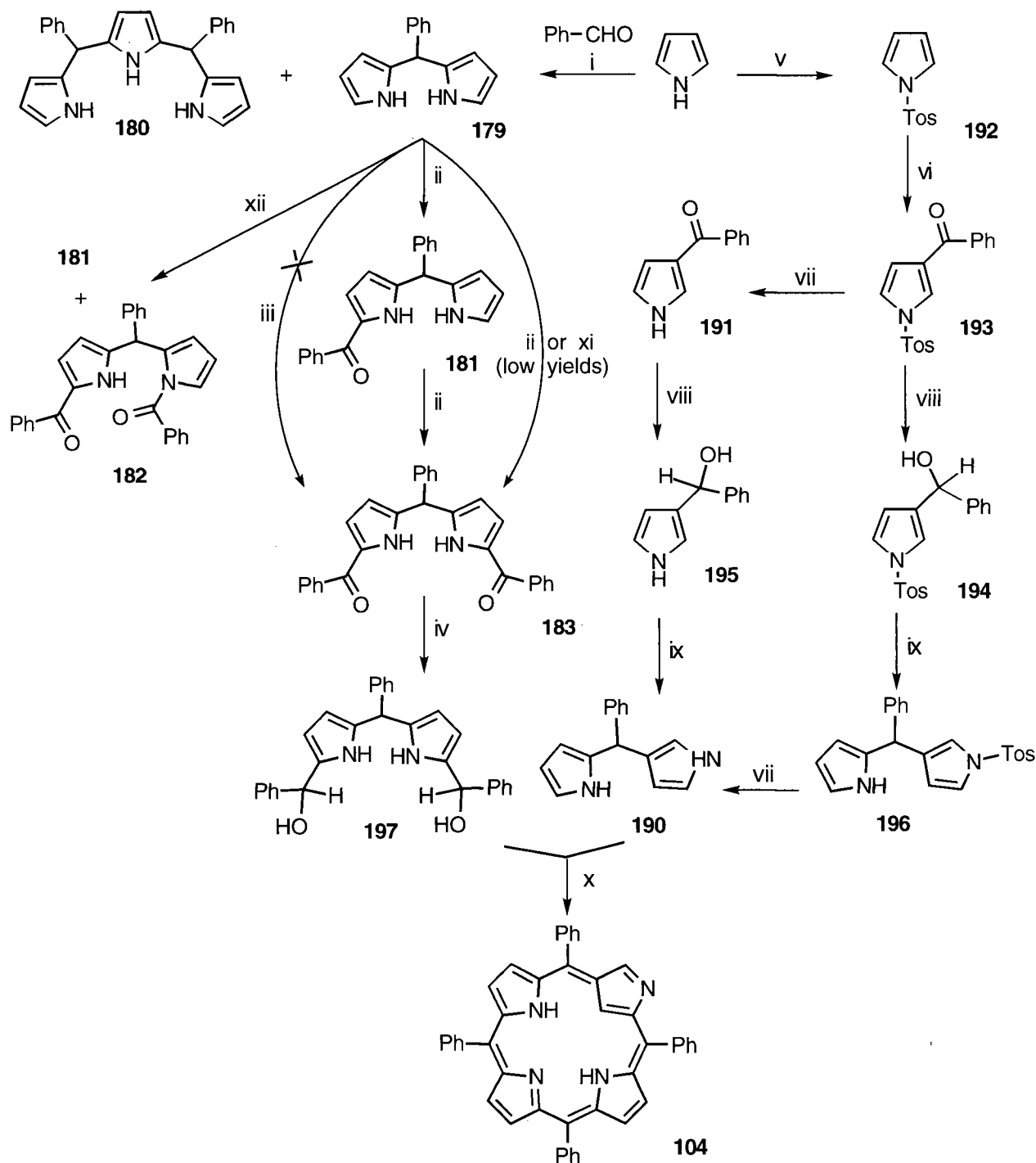
Benzaldehyde and pyrrole were condensed in pyrrole as solvent, catalyzed by trifluoroacetic acid, to produce *meso*-phenyldipyrromethane (**179**) according to a procedure of Lee and Lindsey³⁶⁷ or, alternatively, by a method briefly mentioned in the footnotes of a paper by Rebek and co-workers.³⁷¹ This former procedure calls for a purification step by column chromatography with an unusually large compound to stationary phase ratio. As this makes the synthesis of multi-gram scales of **179** time-consuming, inconvenient and costly, we tested several other methods to separate the main product **179**, the dimeric product from this polycondensation reaction, from other oligomers produced during the reaction. Recrystallization techniques only afforded oils enriched in **179**. When these oils were transferred into a sublimation apparatus and heated (130°C at 0.1 torr), **179** sublimed, to our delight, and crystallized at the cooling finger as colorless or white crystals of analytical purity. Later a protocol was established which enabled us to synthesize more than 10 grams of **179** per day. For another use of **179**, see Part 3 of this thesis.

In runs in which the above oil was prepurified by short column chromatography and treated with the sublimation protocol, the residue left in the bottom of the sublimation apparatus hardened, upon cooling, into a red-orange glass. Analysis of this glass proved that

it contained ~95% *meso*-diphenyltripyrane (**180**). In Lindsey's paper describing the synthesis of **179**, the occurrence of a small amount of an unstable tailing component was mentioned and, based on $^1\text{H-NMR}$ spectroscopy provisionally assigned structure **180**. This tripyrane is, even when ground into a powder, stable in the solid form but could not, in our hands, be further purified by chromatography or crystallization without retrieving it as an unstable oil. Preparative TLC of the crude condensation mixture and mass spectral analysis of the bands tailing the tripyrane confirmed the presence of higher oligomers such as *meso*-triphenyltetrapyrane ($m/e = 531$) and *meso*-tetraphenylpentapyrane ($m/e = 786$). Macroscopic quantities of these compounds could, however, not be isolated and characterized. One successful synthetic application of the tripyrane is in the synthesis of *meso*-phenylsapphyrins, shown in Part 1, section 2.3, and another is shown in Part 3.

Synthesis of 1-Benzoyl-5-phenyldipyrromethane (181), 1,10-dibenzoyl-5-phenyldipyrromethane (182), and 1,9-Dibenzoyl-5-phenyldipyrromethane (183)

Wallace *et al.*⁵⁶ described in 1993 the synthesis of *meso*-tetraarylporphyrins *via* a 2+2 approach. Much like in the present case, a 1,9-di(phenylhydroxymethyl)-5-aryl-dipyrromethane, produced from the reduction of the corresponding dibenzoyl-compound, was condensed with a *meso*-phenyldipyrromethane. The dibenzoyl-compound was synthesized in 39% yield by a Vilsmeier-Haak-type synthesis from dipyrromethane and required a purification step by preparative TLC. In our hands, this reaction could only be reproduced with yields under 20%. The main impediment of the reaction was thought to be the acid-catalyzed decomposition of the dipyrromethane and, consequently, we reasoned that basic reaction conditions would be more appropriate to accomplish the benzylation.

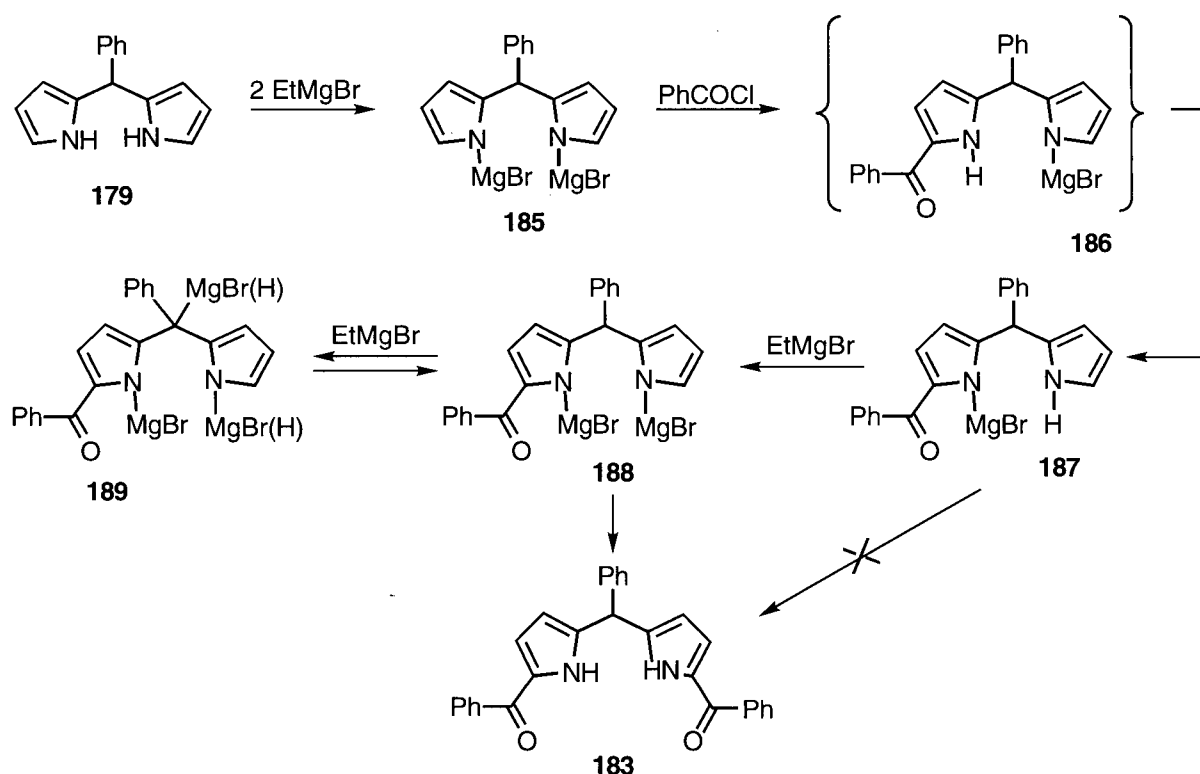


Scheme 1-48

Directed synthesis of N-confused TPP (**104**)

Reaction conditions: (i) pyrrole, cat. TFA; (ii) 1. 2.1 equiv. EtMgBr, 2. 2 equiv. BzOCl; (iii) 1. large excess EtMgBr, 2. BzOCl; (iv) 1. NaBH₄, 2. AcOH; (v) 1. NaH, 2. *p*-TsCl; (vi) BzOCl/AlCl₃; (vii) KOH/dioxane (viii) 1. LiAlH₄, 2. H₂O (ix) 1. cat. *p*-TsOH/toluene/Δ; (x) AcOH/Δ; (xi) 1. POCl₃/BzOCl, 2. AcNa/H₂O; (xii) AlCl₃/BzOCl in 1,2-dichloroethane

We hoped that reaction of dipyrromethane **179**, activated as the Grignard compound with benzoylchloride would, in analogy to the chemistry of pyrrole³⁷², provide the dibenzoyldipyrromethane **183**, and we were surprised to find that 1-benzoyl-5-phenyl-dipyrromethane (**181**) remained the main product and only traces of the dibenzoylated product **183** were formed. Harsher conditions such as performance of the reaction at higher temperatures or the use of a ten-fold excess of ethyl-Grignard resulted in extensive decomposition. These findings are rationalized as shown in Scheme 1-49.



Scheme 1-49 Rationalization of the findings of the benzoylation experiments of **179**

Dipyrromethane **179**, treated with two equivalents of ethyl-Grignard, deprotonates to give the bis-Grignard **185**. Reaction with one equivalent of benzoylchloride benzoylates the α -position and generates, formally, the mono-Grignard **186**.^{*} The proton attached to the

^{*} For the subtleties of the reactivity of the pyrrolyl ambident anion, see Wang and Anderson.³⁷²

nitrogen of the benzoylated pyrrole moiety is now more acidic than that attached to the other pyrrole. Consequently, a proton exchange to form, at least formally, structure **187** takes place. This compound cannot react in the desired way to form the dibenzoyl compound **183**. The addition of large excess of Grignard reagent to deprotonate **187** *in situ* is pointless as this excess of reagent would be quenched quickly by the benzoylchloride added. For that reason, a two-step approach had to be taken: first synthesis of mono-benzoylated **187** and then in a separate second step, addition of two equivalents of ethyl-Grignard to a solution of **187** to generate **188**, and subsequent reaction with benzoylchloride to form the desired dibenzoylated product **183**. A large excess of Grignard reagent has to be avoided during this step as this results in the formation of a multitude of undesired compounds. We explain this with the finding that the *meso*-proton in **187** is acidic enough to be deprotonated by ethyl-Grignard, forming compounds of the general structure **189**, which leads upon reaction with benzoylchloride to the observed by-products. This acidity of the *meso*-proton can be readily tested by the treatment of **187** (and even **179**) with several equivalents of ethyl-Grignard and subsequent quenching with D₂O. The recovered materials shows reduced proton signals for the *meso*-hydrogen in the ¹H-NMR.

In a further attempt to overcome the difficulties of synthesis of **183**, **179** was treated with aluminum trichloride/benzoylchloride. Under rigorously dry conditions, little decomposition is observed and **181** forms in good yields but no **182** forms at all. Instead, the C,N-dibenzoylated product **182** appears in the reaction mixture.

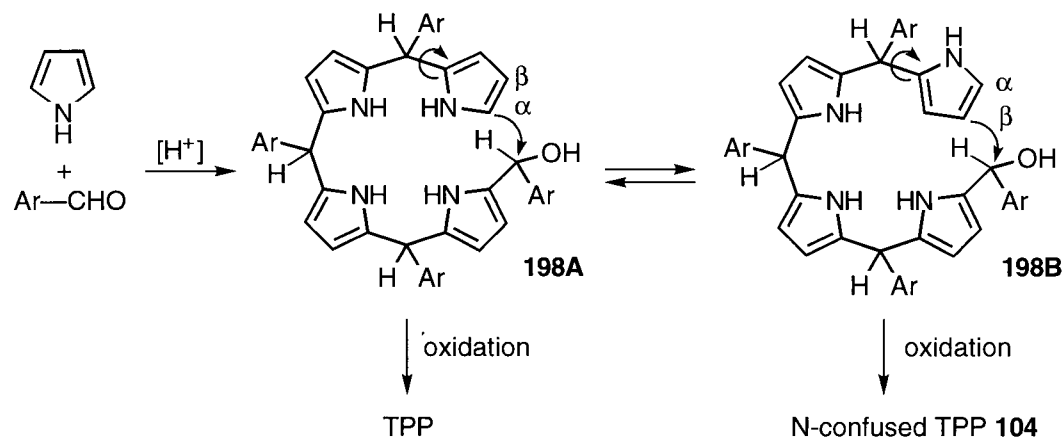
Synthesis of N-Confused *meso*-phenyldipyrromethane **190**

The synthesis of the key intermediate, the α -to- β linked *meso*-phenyldipyrromethane **190** proceeded in a straightforward manner (Scheme 1-48). Synthesis of 3-benzoylpyrrole (**191**) via 1-tosylpyrrole (**192**) is well described.^{368,373-375} Reduction of either the tosylated 3-benzoylpyrrole **193** or its deprotected form generated the desired alcohols **194** or **195**, respectively. Both alcohols are relatively unstable and apart from NMR spectroscopic analyses of the crude mixtures, no further characterization was attempted. Acid-catalyzed condensation of these alcohols with pyrrole produced in good yield the N-confused dipyrromethanes **196** or **190**, respectively. Base induced detosylation converted **196** into **190**. The route with the early detosylation (**193**→**191**→**195**→**190**) was given preference over the alternate route with the late detosylation (**193**→**194**→**196**→**190**). Although α,β -linked dipyrromethanes have been described before, they have been *meso*-unsubstituted and α - and β -alkylated.³⁷⁶ Unlike *meso*-phenyldipyrromethane **179**, **190** was always produced as an oil and attempts to sublime it were unsuccessful.

The final 2 + 2 condensation

The dibenzoyldipyrromethane **183** was reduced to the corresponding alcohol **197**, mixed in several solvents with an equimolar amount of the N-confused dipyrromethane **190** and, after the addition of catalytic amounts of various acids, the reaction mixtures turned dark. After the starting materials had, based on TLC control, disappeared, an oxidant such as DDQ or chloranil was added. To our disappointment, the yield of the desired N-confused porphyrin **104** was invariably low ($\leq 5\%$, in some cases **104** was not detectable at all). Thus, the synthetic effort required to make the preformed units was not balanced with high yield of the desired product. It is interesting to note that the yields of analogous regular tetraarylporphyrin syntheses are relatively low as well, around 12%.⁵⁶

Chmielewski *et al.*²⁶⁹ suggested the following for the mechanism of the formation of N-confused porphyrin *via* the Rothmund-type condensation (Scheme 1-50): Two helical conformations of the intermediate tetrapyrromethane **198**, varying only in the orientation of one terminal pyrrolic unit and interchangeable simply by rotation around an α -*meso*-carbon bond, are present in the reaction mixture (**198A** and **198B**). Nucleophilic attack of the pyrrole α -position leading to ring closure, gives, after oxidation of the initially formed porphyrinogen, regular TPP, while attack of the β -positions gives, after oxidation, the N-confused porphyrin. While the α -position is more reactive towards electrophiles than the β -position,³⁷⁷ there are ample examples in the literature exemplifying the reactivity of the β -positions and the helical conformation of the linear tetrapyrrolic intermediates under similar reaction conditions.^{44,378-383}



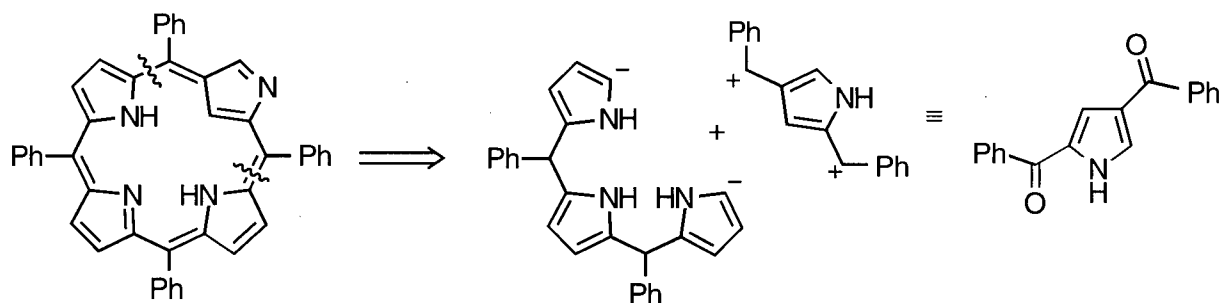
Scheme 1-50 Proposed mechanism of formation of N-confused porphyrin²⁶⁹

In light of this, it is even more surprising that our attempted synthesis did not generate the desired results as the proposed intermediate **189** is very similar to the likely intermediate in the condensation reaction of **179** and **190**. We have no conclusive explanation for this finding. However, the formation of porphyrins using 2 + 2-condensations frequently requires the use of special and carefully controlled conditions unique to a particular system. Furuta and co-workers propose a pronounced anion template

effect directing the formation of the N-confused porphyrin.²⁶⁸ Consequently, a series of experiments with varying acids catalyzing the final condensation may eventually discover the right conditions for the formation of high yields of N-confused porphyrins *via* this attractive 2+2 approach.

Future Work

Future work towards the directed synthesis of N-confused porphyrin **104** may succeed following alternative approaches. One alternative retrosynthetic analysis of **104** is shown in Scheme 1-51. This analysis employs a 3+1-approach utilizing the tripyrrane **190** as starting material. Such a synthesis seems particularly attractive as it offers a very short synthetic route.

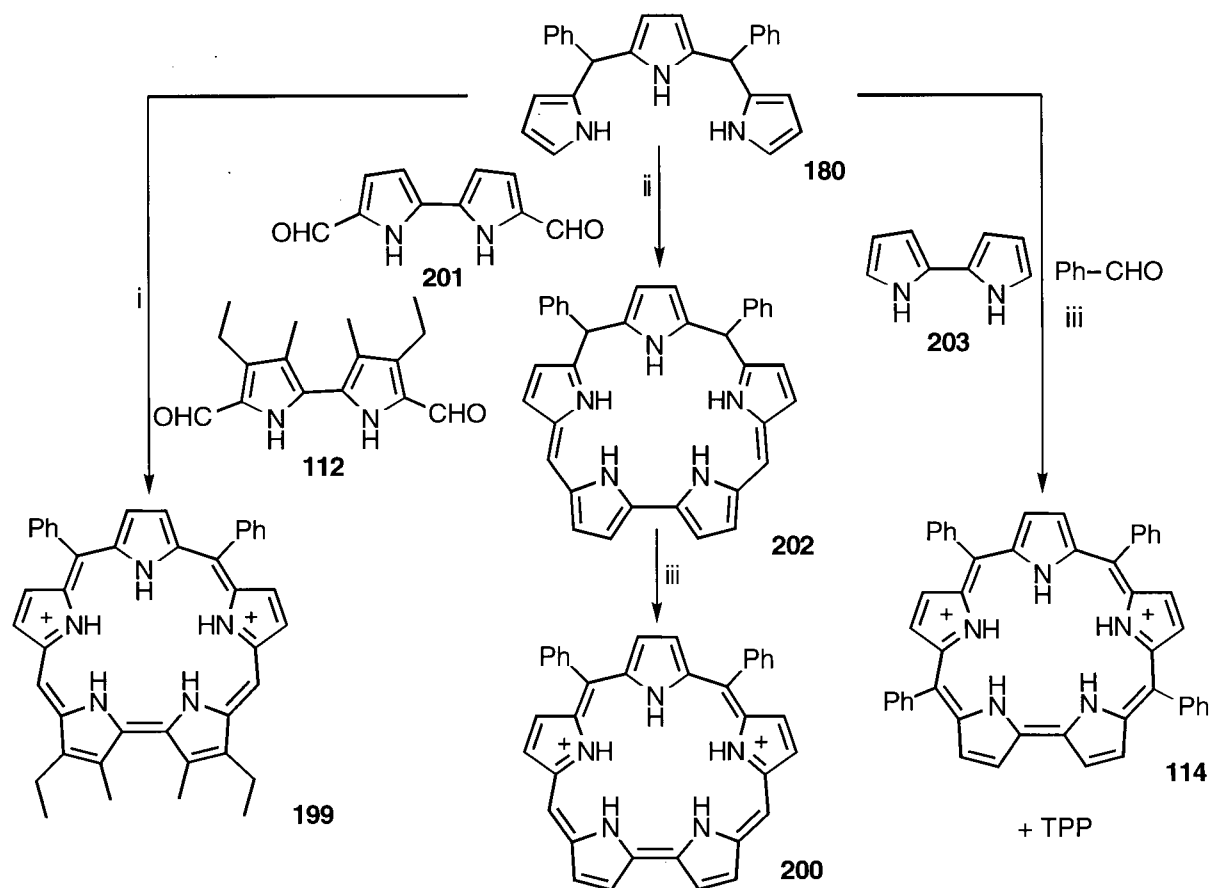


Scheme 1-51 Alternative retrosynthetic analysis of N-confused porphyrin

We have developed efficient strategies to synthesize the acyclic precursors necessary for the directed synthesis of N-confused porphyrin and we anticipate further developments towards high-yielding macrocyclization procedures in the near future.

2.3 THE DIRECTED SYNTHESIS OF *meso*-PHENYLSAPPHYRINS

Sapphyrins are generally prepared by condensation of a tripyrrane with a bipyrrrole dialdehyde (see Section 1.3.5). With the novel *meso*-phenyltripyrrane (**180**) in hand, we had the opportunity to prepare in an analogous fashion *meso*-diphenyl substituted sapphyrins **199**, and **200**, and in a four-component Rothmund-type condensation *meso*-tetraphenyl-sapphyrin **114** (Scheme 1-52). At the time this work was started, no *meso*-phenyl substituted sapphyrins were known, but in the fall of 1995, Sessler, Kodadek and co-workers published the synthesis and structural characterization of **114** *via* the condensation of dipyrrane dialdehyde, benzaldehyde and pyrrole under Lindsey-type conditions³⁸⁴ and, almost at the same time, Latos-Grazynski and co-workers published the isolation of tetraphenylsapphyrin **199** as a side-product from the Rothmund synthesis of TPP.³¹⁵ Both procedures, however, produce the particular sapphyrins in low yields (~10% and 1.1%, respectively) and both require extensive chromatographic work-up (3-4 consecutive column and preparative plate runs). The syntheses to be presented here are short, produce up to 39% yield in the final sapphyrin condensation (for **114**) and, due to the absence of any other porphyrinic by-products, require only minimal chromatographic work-up. While Latos-Grazynski's one-step synthesis is undeniably the shortest possible, our approach is a little longer (a total of 5 steps from pyrrole and benzaldehyde) but still much shorter than any traditional sapphyrin synthesis.²⁹⁵



Scheme 1-52 Synthesis of the *meso*-phenylsapphyrins **114**, **199**, and **200**

The Synthesis of 5,10-Diphenylsapphyrin (**200**)

Bipyrrole dialdehyde (**201**) and tripyrrane **180** were dissolved in ethanol and several equivalents of *p*-toluenesulfonic acid were added. The mixture turned royal blue within minutes (broad bands at λ_{\max} 360 and 580 nm), indicating the formation of, possibly, the partially conjugated pigment **202**. This situation did not change over the course of hours, whether molecular oxygen was bubbled through the solution or not. When oxidants such as DDQ were added, the mixture largely decomposed and, as judged by optical spectroscopy, only traces of sapphyrin-type chromophores could be detected. Evaporation of the solution to dryness over a period of several days produced a black, brittle and insoluble film. Most surprising, trituration of this film with chloroform gave a forest-green solution composed

almost entirely of the dication of 5,10-diphenylsapphyrin **200**. This assignment is based on a series of analytical and spectroscopic techniques, some of which are detailed below. Sapphyrins are basic pigments and are generally isolated and chromatographed as their dications. The present sapphyrin could also be chromatographed on silica gel as its free base. This might suggest a lower basicity for this pigment in comparison to alkylsapphyrins. Sessler and co-workers reported a similar observation for **199**.³⁸⁴ Washing of a chloroform solution with either a dilute hydrochloric acid or a dilute ammonia solution converts **200** into its diprotonated or free base form, respectively.

The interest in alkylsapphyrins as potential photosensitizers to be used in PDT stems from their strong absorptions in the long wavelength region. This strong absorption in the region above 700 nm can also be observed for the *meso*-phenyl substituted variety. The optical spectrum of **200** in its free base and protonated form are shown in Figure 1-30. As for decamethylsapphyrin²⁹⁸, the Soret-band of the free base is split, and singular in the protonated form. The Q-bands are, in both the protonated and non-protonated case, slightly bathochromically shifted as compared to decamethylsapphyrin.

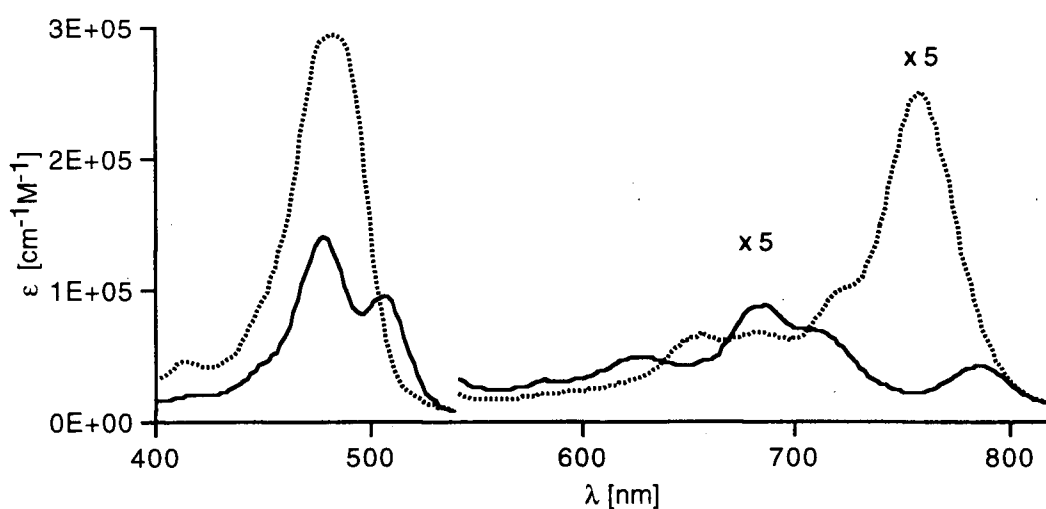


Figure 1-30 Optical spectrum (CH₂Cl₂) of **200** (—) and **200·2HCl** (····)

Sapphyrin **200** is dibasic. Full protonation of this mirror-symmetric molecule is seen in the $^1\text{H-NMR}$ by the presence of three non-equivalent protons in the ratios of 1:2:2 in the high-field region. One complex multiplet centered at 8.0 ppm accounts for the *meta*- and *para*-protons of the phenyl-protons, and the multiplet at 8.65 for the *ortho*-protons. Signals for five non-equivalent β -hydrogens, each integrating for two protons, four of which are doublets and one a singlet are expected, and found. The singlet furthest down-field can be assigned to the *meso*-protons. Their extreme shift is in accord with that observed in decaalkylsapphyrins.²⁹⁵

The $^1\text{H-NMR}$ of **200** as its free base and of its dihydrochloride **200·2HCl** are shown in Figure 1-31. The $^1\text{H-NMR}$ spectrum of, for instance, TPP, changes upon protonation in that it results in doubling of the integration of the signals in the high-field region, assigned to the NH-protons, and thus clearly showing that protonation occurs at the inner nitrogens. Only small shifts are observed for the remaining signals, all of which can be explained by the presence of the dicationic charge. Comparison of the two spectra of **200** and **200·2HCl** reveal that they cannot be rationalized by such a simple protonation-deprotonation reaction. While the spectrum of the diprotonated species is readily assigned, that of the free base is not. The $^1\text{H-NMR}$ spectrum of the free base **200**, on the other hand, displays in the moderate high-field region one very broad and one sharp signal, each integrating for about two hydrogens. In addition, only four typical β -hydrogen signals can be detected and one low-field signal corresponding to one proton and exchangeable with D_2O is present. Integration, peak width and number are inconsistent with the formulation of **200** existing in conformation **200A**, shown in Figure 1-32. All these facts indicate that diphenylsapphyrin folds as shown in Structure **200B**.

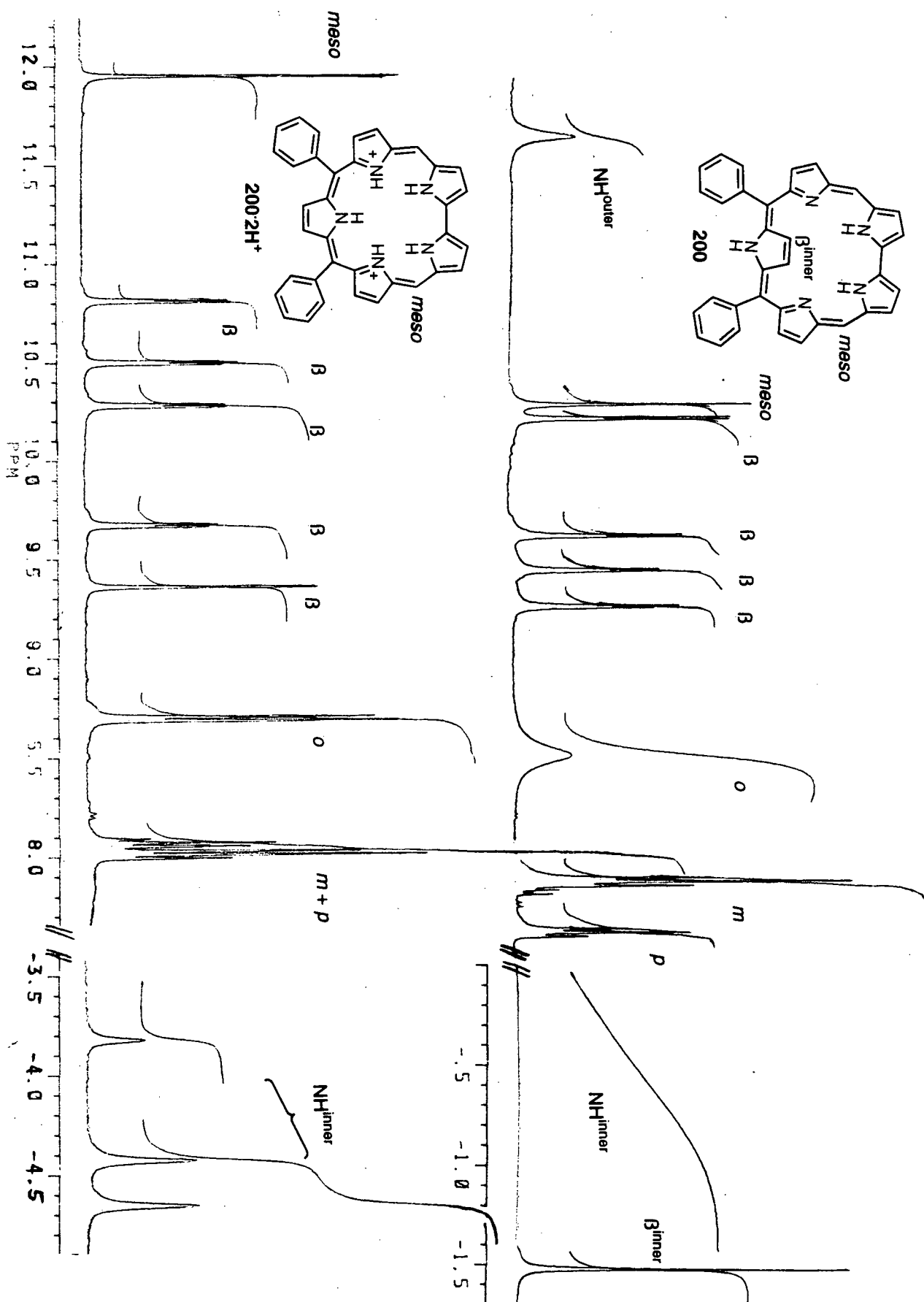


Figure 1-31 ¹H-NMR (400 MHz, CDCl₃) of **200** (top trace) and **200-2HCl** (bottom trace). Note the different axes for the high-field regions.

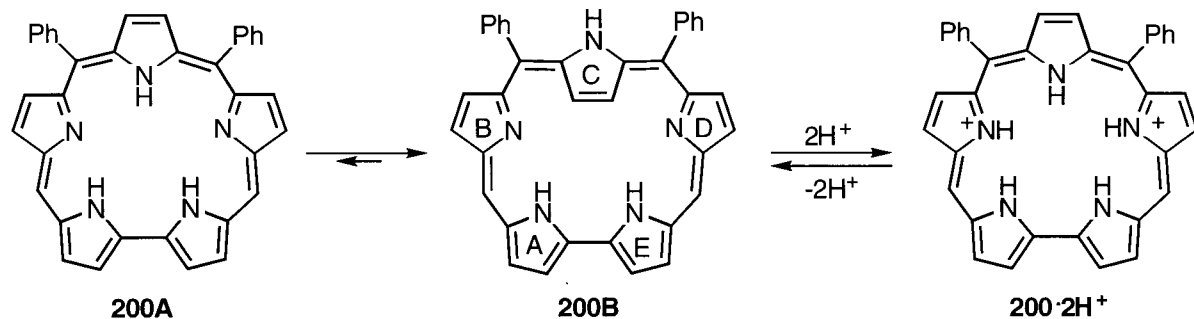


Figure 1-32 Conformation of diphenylsapphyrin **200** as free base and as diprotonated species

Inversion of the pyrrolic unit **C** directs the β -protons towards the middle of the still aromatic macrocycle, and, hence, shields them effectively and directs the NH proton of ring **C** outwards, thus deshielding it. This explains the 1H -NMR spectrum, in particular the finding of the sharp signal at -1.5 and the broad, exchangeable signal at 11.8 ppm, respectively.

Latos-Grazynski and co-workers observed and described very recently an analogous sapphyrin inversion for 5,10,15,20-tetraphenylsapphyrin (**114**).³¹⁵ Another indication for the validity of this assumption can be found in the literature. N-Confused TPP **104** features in a similar way a β -proton in the centre of the macrocycle and an NH proton at the outer periphery. The observed chemical shifts for these protons in **104** are comparable to those found here.^{268,269}

Synthesis of 5,10,15,20-Tetraphenylsapphyrin (**114**)

This sapphyrin was synthesized under Lindsey-type conditions. Benzaldehyde, pyrrole and bipyrrrole (**203**) were dissolved in degassed methylene chloride and treated with catalytic amounts of trifluoroborane etherate. Chloranil was added to this reaction mixture. This mixture of newly formed TPP and sapphyrin **114** was separated by chromatography.

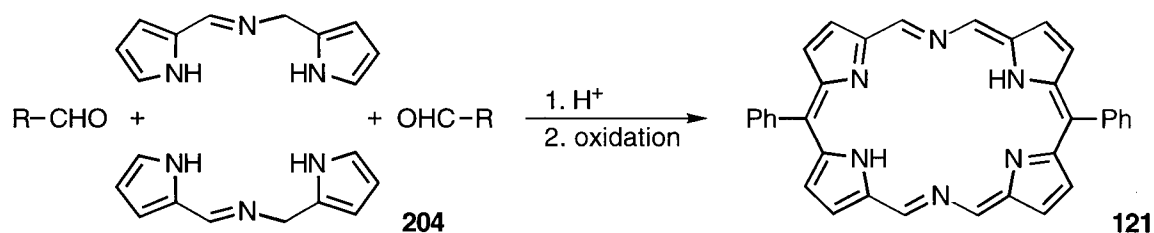
The spectroscopic properties of this sapphyrin were, as expected, similar to those of **200** and identical with those reported by Chmielewski *et al.*³¹⁵ The overall yield of 3.7% is more than three times that reported by the Polish group and we think that this higher yield is due to the use of the preformed building block (dipyrrin), as compared to the synthesis from pyrrole and benzaldehyde, though any findings based on the encountered minimal absolute yields are, at best, inconclusive.

Synthesis of 3,22-Diethyl-2,23-dimethyl-5,10-diphenylsapphyrin (**199**)

This sapphyrin was prepared along the lines described in the benchmark publication by Bauer *et al.* for decaalkylsapphyrins.²⁹⁸ Dipyrrin dialdehyde **112** and tripyrrane **180** were dissolved in absolute alcohol and as molecular oxygen was bubbled through the solution, some *p*-toluenesulfonic acid was added. The mixture turned dark green and the sapphyrin was isolated by standard chromatography techniques. Only traces of TPP (<< 1%) were formed as by-products. The distinct optical and NMR spectra of this compound readily identify it as the desired sapphyrin. All properties proved identical with those reported by Sessler, Kodadek and co-workers for this compound.³⁸⁴ In addition, these authors solved the X-ray crystal structure of the dihydrochloride salt. This largely planar molecule, like its β -alkyl analogs, can act as chloride anion receptor in the solid state.

2.4 THE REDUCTIVE COUPLING OF 2-CYANOPYRROLES

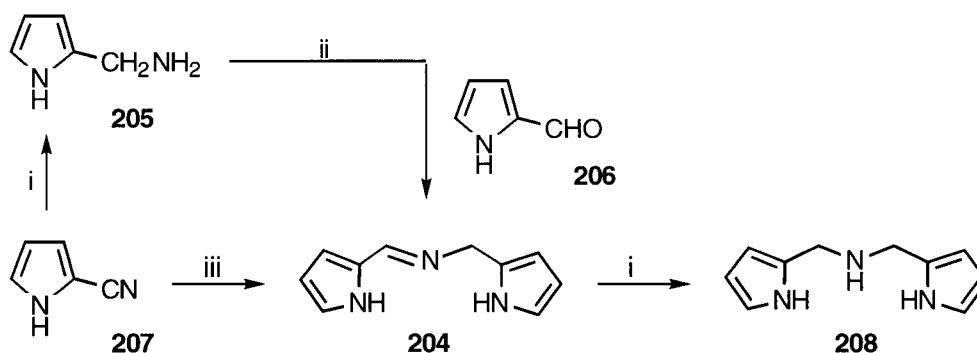
As mentioned in the introductory Chapter (section 1.3.5), the mechanism of the facile formation of porphocyanine *via* the LAH reduction of α,α' -dicyanodipyrromethanes is not entirely clear. Given the favorable photophysical properties of this compound class and its promise for use as a third generation PDT agent, the study of its mechanism of formation with the goal to, perhaps, optimize its preparation seemed worthwhile. Also, an alternative synthesis of this compound class was sought. Scheme 1-52 depicts one alternative possibility, namely the fusion of two imine-linked halves, followed by aromatization of the formed macrocycle. This type of coupling is under investigation by other members of Prof. Dolphin's research group.



Scheme 1-52 Proposed alternative synthetic pathway for the formation of *meso*-phenylporphocyanines

Imine **204** is a known compound.³⁸⁵ Its synthesis is shown in Scheme 1-53. 2-(Aminomethyl)pyrrole (**205**) is reacted with 2-pyrrolealdehyde (**206**) in aqueous solution to form **204**. **205** was reportedly synthesized by the LAH reduction of 2-cyanopyrrole (**207**). When we repeated these procedures, we replaced the dilute sulfuric acid quenching step of the LAH reduction reaction mixture³⁸⁶ by the addition of Glauber's salt ($\text{Na}_2\text{SO}_4 \cdot 10 \text{H}_2\text{O}$). It was found that imine **204** was formed as the sole product. This outcome is exclusive to the use of aluminum hydrides as reductant. Compound **207** is inert to sodium borohydride with

or without the addition of transition metals, but diisobutylaluminum hydride (DIBAL) produces, albeit not as cleanly, **204**. The formation of **204** is also surprising considering that its imine-link is susceptible to reduction by LAH, giving the amine **208**. This provides the first clue that the imine functionality must have formed during the quenching step.



Scheme 1-53 Formation of imine-linked dipyrrolic compound **204**
Reaction conditions: (i) LiAlH₄, then dil. H₂SO₄; (ii) H₂O; (iii) LiAlH₄, then Glauber's salt (Na₂SO₄·10H₂O)

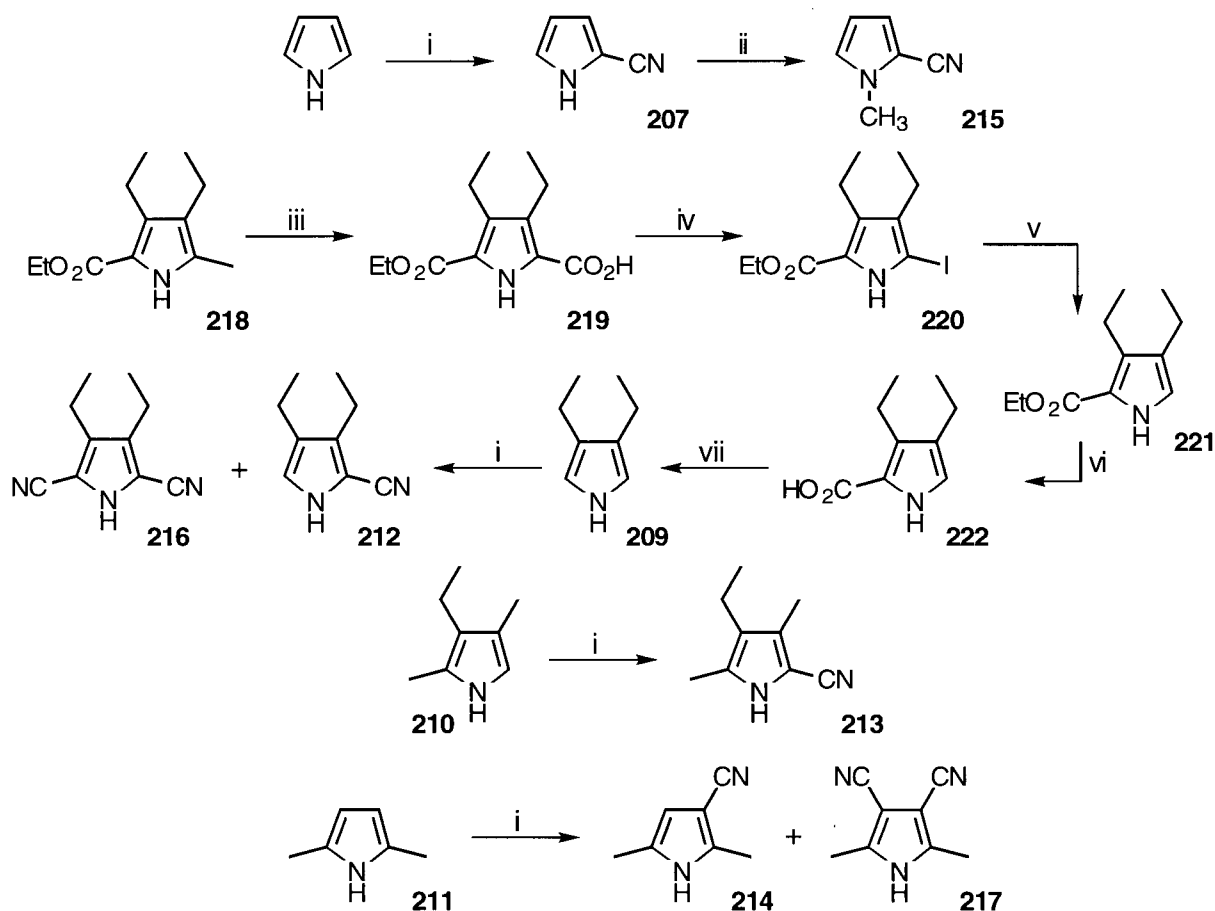
This finding prompts several possible explanations. Partial reduction of the cyano group forms, after hydrolysis of the initially formed imine, an aldehyde functionality which then reacts, according to the above scheme, with an aminomethylpyrrole (**205**), stemming from the full reduction of **207**. A second, and more likely, possibility is, that the initially formed imines condense to form the imine-linkage. There are precedents for such a condensation in the literature. Hydrobenzamide (ArCH(-N=CHAr)₂) can be formed from an aromatic aldehyde and ammonia *via* the imine (ArCH=NH).³²⁴ One drawback of these explanations is, however, that while partial LAH reductions of cyanopyrroles to form pyrrolealdehydes *via* hydrolysis of the imines are known, they require the use of very deactivated 2,4-dicyanopyrroles.^{386,387} This is clearly not the case in the reduction of **207**. This makes proposed mechanisms based on partial reductions of the cyano group unlikely. In turn, this makes *in situ* reductive couplings seem to be more likely. To investigate this

possibility in more detail, several cyanopyrroles were synthesized and their behavior towards the LAH reduction conditions were studied.

Synthesis of Cyanopyrroles

Several possibilities to synthesize cyanopyrroles are available.³⁸⁸⁻³⁹² Possibly the most versatile and convenient strategy is the direct introduction of cyano groups by reaction of a pyrrole with chlorosulfonyl isocyanate (CSI)³⁹³ followed by solvolysis of the intermediate chlorosulfonylamide with DMF.^{386,394-398} This methodology was applied to pyrrole^{386,397}, 3,4-diethylpyrrole (**209**), 3-ethyl-2,4-dimethylpyrrole (**210**), and 2,5-dimethylpyrrole (**211**), to produce the monocyanopyrroles **207**, **212**, **213**, and **214**, respectively. 2-Cyanopyrrole (**207**) was converted to the known 1-methyl-2-cyanopyrrole³⁹⁹ by methylation of the pyrrolic nitrogen. In cases in which two pyrrolic hydrogens could be substituted for cyano groups this was also observed, producing **216** and **217**. By using excess CSI, the doubly cyanated pyrroles could be made the major products of the cyanation reaction. A similar dicyanation has been described for pyrrole.³⁹⁷

The starting pyrroles were either commercially available (pyrrole and **211**), or were synthesized in-house according to standard procedures.^{39,400} One such pyrrole substituent manipulation is exemplified for the synthesis of 3,4-diethylpyrrole (**209**). The methyl group in **218** was oxidized to the corresponding acid function. This group of the resulting **219** was replaced by iodine, which subsequently was removed reductively. Ester hydrolysis of the resultant product **221** then produced the acid **222** which is prone to thermal decarboxylation to α -free pyrrole **209**. This desired pyrrole was isolated by high vacuum distillation and immediately cyanated with either one or two equivalents of CSI, producing the final products **212** or **216**, respectively.

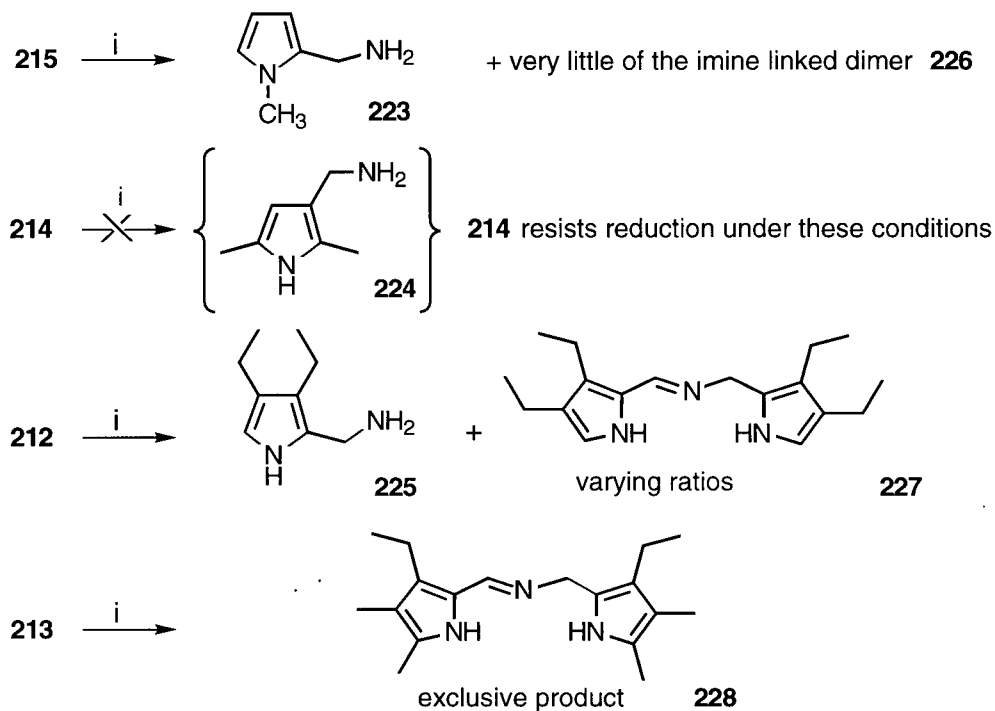


Scheme 1-54

Syntheses of the cyanopyrroles

Reaction conditions: (i) 1 (or 2) equivalents of $\text{CS}_2/\text{DMF}/\text{CH}_3\text{CN}$, respectively, then aqueous workup; (ii) 1. NaH , 2. TosCl ; (iii) 1. $\text{SO}_2\text{Cl}_2/\text{Et}_2\text{O}$, 2. H_2O ; (iv) I_2/KI ; (v) H_2 over PtO_2 ; (vi) $\text{KOH}/\text{H}_2\text{O}$; (vii) Ethyleneglycol/ Δ

With the mono-cyanopyrroles in hand, a series of reductions was performed. Each reduction followed the same protocol. A defined small amount of the cyanopyrrole was dissolved in dry THF and the solution was cooled in an ice-bath and kept under a nitrogen atmosphere. Four equivalents of LAH were added in portions and, after addition was completed, the mixture was stirred for one hour. Glauber's salt was then added until gas evolution ceased, and the resulting slurry was filtered through Celite®. The filtrate was evaporated *in vacuo*, and the residue analyzed by mass, ^1H - and ^{13}C -NMR spectroscopy. The results are presented in Scheme 1-55.



Scheme 1-55 Outcome of the LiAlH_4 reduction of various cyanopyrroles
 Reaction condition: (i) $\text{LiAlH}_4/\text{THF}$ at 0°C , then $\text{Na}_2\text{SO}_4 \cdot 10\text{H}_2\text{O}$

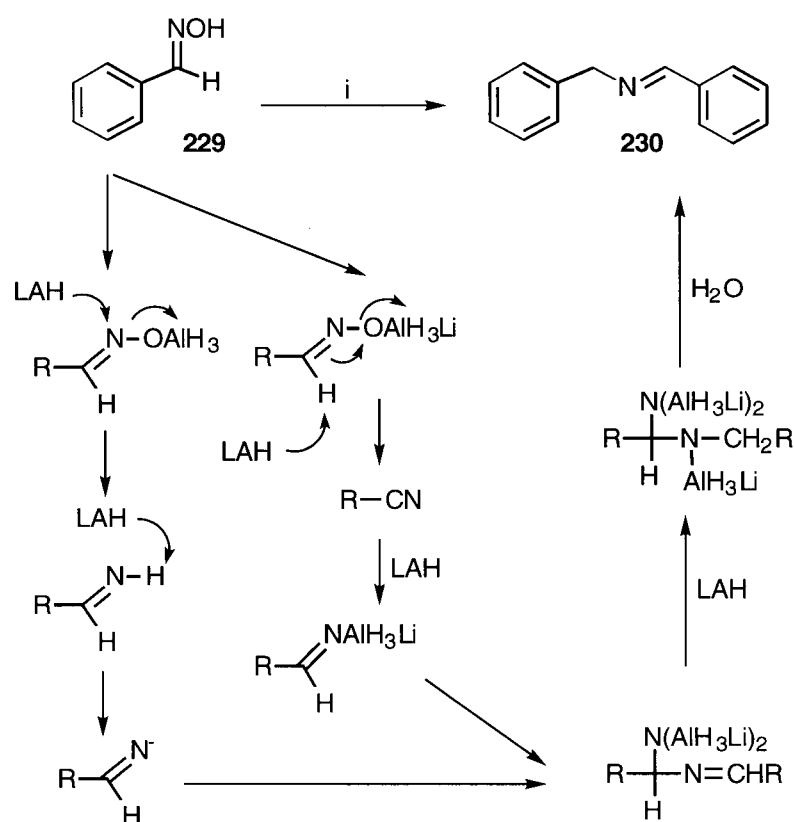
Reduction of cyanopyrrole **215** resulted almost exclusively in the formation of the corresponding aminomethyl compounds **223** (product ratio 13:1 in favor of **223**). β -Cyanopyrrole **214** resisted reduction under the conditions employed and was fully recovered. This unusual stability of β -cyano groups towards nucleophilic attack has precedent in the literature.³⁸⁶ Reduction of the compounds **212** and **213** gave the imine dimers **227** and **228**. The imine was the sole product in the latter case whereas in the former the aminomethyl compound **225** was observed as well. The particular ratio of the two compounds **225** and **227** varied from run to run from 1:2 to 3:1.

Reduction of **207** with lithium aluminum deuteride and subsequent quenching with deuterated water (in the form of deuterated Glauber's salt made by diffusion of deuterated water onto dry sodium sulfate) produced **208-d₈** in which all but the CH-protons of the

methylene-linked ring are deuterated. Quenching with water produced non-deuterated **208**, suggesting that quenching elicits exchange of the protons. This can be understood by the strongly basic nature of LAH and the strongly basic conditions of the quenching procedure.

The major difference in the starting materials is the ability of their pyrrole-nitrogens to participate in, for example, a coordinating action with the reductant. The N-methylated pyrrole **215** cannot form readily chelate-type interactions with aluminum. In order to trace possible aluminum complexes formed by (partially reduced) **207** and LAH, ^{27}Al -NMR spectra^{401,402} of solutions of **207** in THF/benzene- d_6 (19:1) containing various amounts of LAH were measured. With a ratio of **207**:LAH of ~1:3, a strong signal for the LAH and a broad, featureless signal 60-80 ppm upfield of this signal is seen. Increase in the relative amount of **207** strengthens the broad signal at the expense of the LAH signal. At about a 1:1 ratio the LAH signal has entirely vanished. The failure in measuring well defined signals for the presumed aluminum complex is not entirely unexpected. Due to the quadrupole moment of the ^{27}Al -nucleus, only highly symmetric (tetrahedral) complexes give sharp signals.

Study of the literature reveals two closely related publications.^{403,404} The more recent contribution of Wang and Sukeniki describes the reduction of oximes with LAH in HMPA-containing solvents. One particular example, the reduction of benzaldoxime (**229**) resulted in the formation of the imine-linked dimer **230** and the authors rationalize this finding by the mechanism shown in Scheme 1-56. They propose a series of deprotonation and reduction steps. An LAH reduction in the absence of HMPA leads to the formation of benzylamine. Their rationalization for changing of the outcome of the reaction by the presence of HMPA hinges upon the promotion of the basicity of LAH by strong complexation of the lithium ions by this co-solvent.⁴⁰⁴

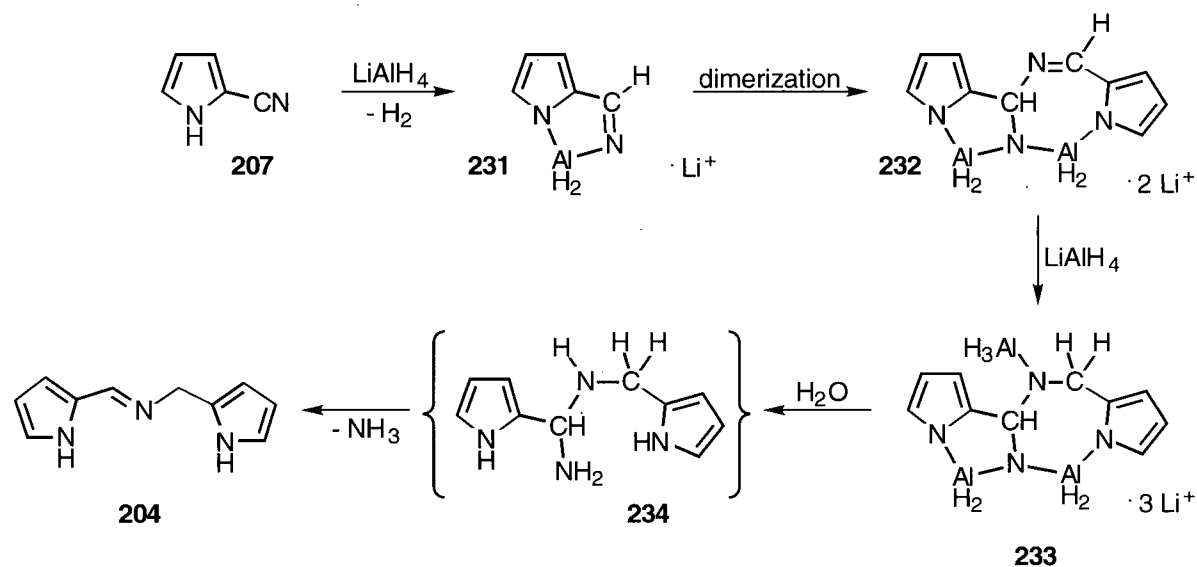


Scheme 1-56 Mechanism of the LAH coupling of benzaldoxime⁴⁰³
 Reaction condition: (i) 1. LAH/THF/HMPA, 2. H₂O

In the case of the reductive coupling of **207**, the co-solvent HMPA is not present and yet a similar reaction can be observed. We propose the sequence shown in Scheme 1-57 as one possible mechanism of the coupling, although it is important to note that we have only just begun to collect evidence for the details, and the work is still in progress. However, this proposal bears some resemblance to known literature mechanisms.

According to this mechanism, the first step would be a combined deprotonation/reduction of **207** to form a chelate of type **231**. Similarly constructed chelates of copper(II) are known for 2-pyrrolealdehyde.⁴²⁰ This chelate may dimerize to give **232**. Its double bond may be reduced by another equivalent of LAH. Hydrolysis would give the labile

species **234** which stabilizes itself by the abstraction of ammonia to produce the final product **204**. And, in fact, the smell of ammonia can be detected during the hydrolysis step. The proposed mechanism may not be the only mechanism occurring as, for instance, the presence of the dimer **227** and the aminomethyl pyrrole **225** indicates.

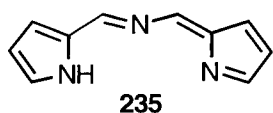


Scheme 1-57 Hypothetical mechanistic scheme of formation of **204** through the LiAlH_4 reduction of cyanopyrrole **207**

It is interesting to note that although we may have been the first group to recognize this coupling, there are indications in the literature that this coupling has been observed before, but went unrecognized. Barnett *et al.* described in 1980 the LAH reduction of 2,4-dicyanopyrroles. Following a workup employing 2.5 M sulfuric acid, they found one product to be 4-cyano-2-pyrrolecarboxaldehyde. They noted “Over half the starting material was not accounted for.”³⁸⁶ In light of our findings this is understandable. The strong acid cleaved the initially formed imine into a stable pyrrolealdehyde fraction and into a very unstable aminomethyl fraction. The latter decomposed and, hence, could not be accounted for.

2.5 THE UNEXPECTED FORMATION OF A TRIPYRROLIC TETRADENTATE NICKEL CHELATE (236)

Our interest in dipyrrens, tripyrrins and other potential metal chelating pyrrolic pigments (see Parts 2 and 3), prompted investigations into whether the unknown imine-linked, fully conjugated pigment is accessible through the oxidation of **204**. Many attempts



to produce an isolable compound failed, but one interesting observation was made. In some experiments the oxidation was tried in the presence

of metal ions. With the addition of nickel(II) as its acetate, the formation of tiny amounts of a brilliantly orange pigment of very low polarity ($R_f = 0.9$ $\text{CHCl}_3/\text{silica}$) was noticed. It later could be shown that under certain conditions this orange pigment could be made the major product. This enabled the synthesis of several hundred milligrams and full characterization of this pigment (**236**). Its analytical and spectroscopic properties were inconsistent with it having structure **235** or being a nickel complex of **235**.

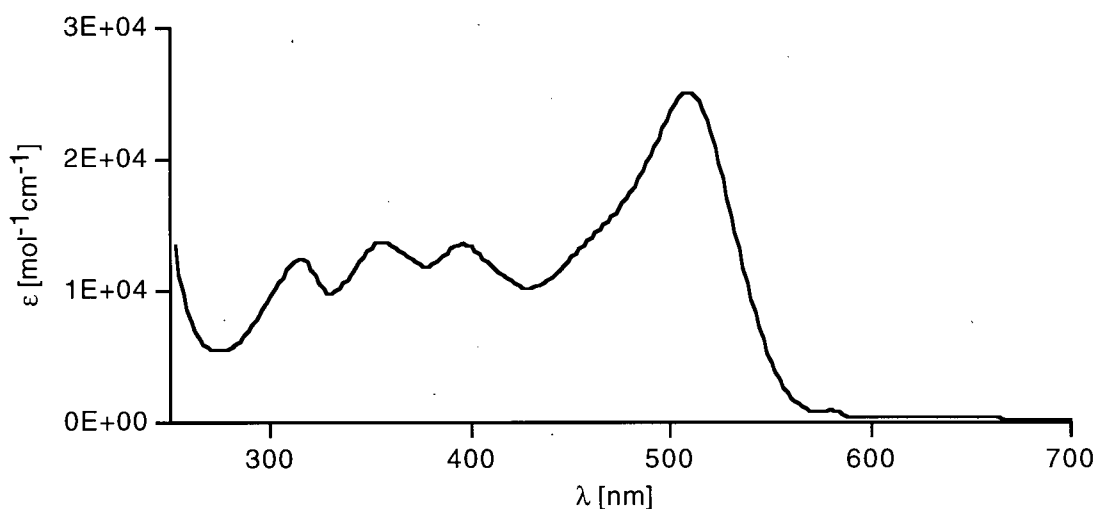


Figure 1-33 Optical spectrum(CHCl_3) of **236**

The UV-visible spectrum of the compound, shown in Figure 1-33, exhibits some characteristics of the (dipyrinato)nickel chromophore (compare to Part 2, section 2.3). The $^1\text{H-NMR}$ shows ten non-equivalent protons in the aromatic region and the signal for the methylene group of the starting material is still present (Figure 1-34). No proton signals indicative of NH protons could be traced, suggesting the formation of a (nickel) complex.

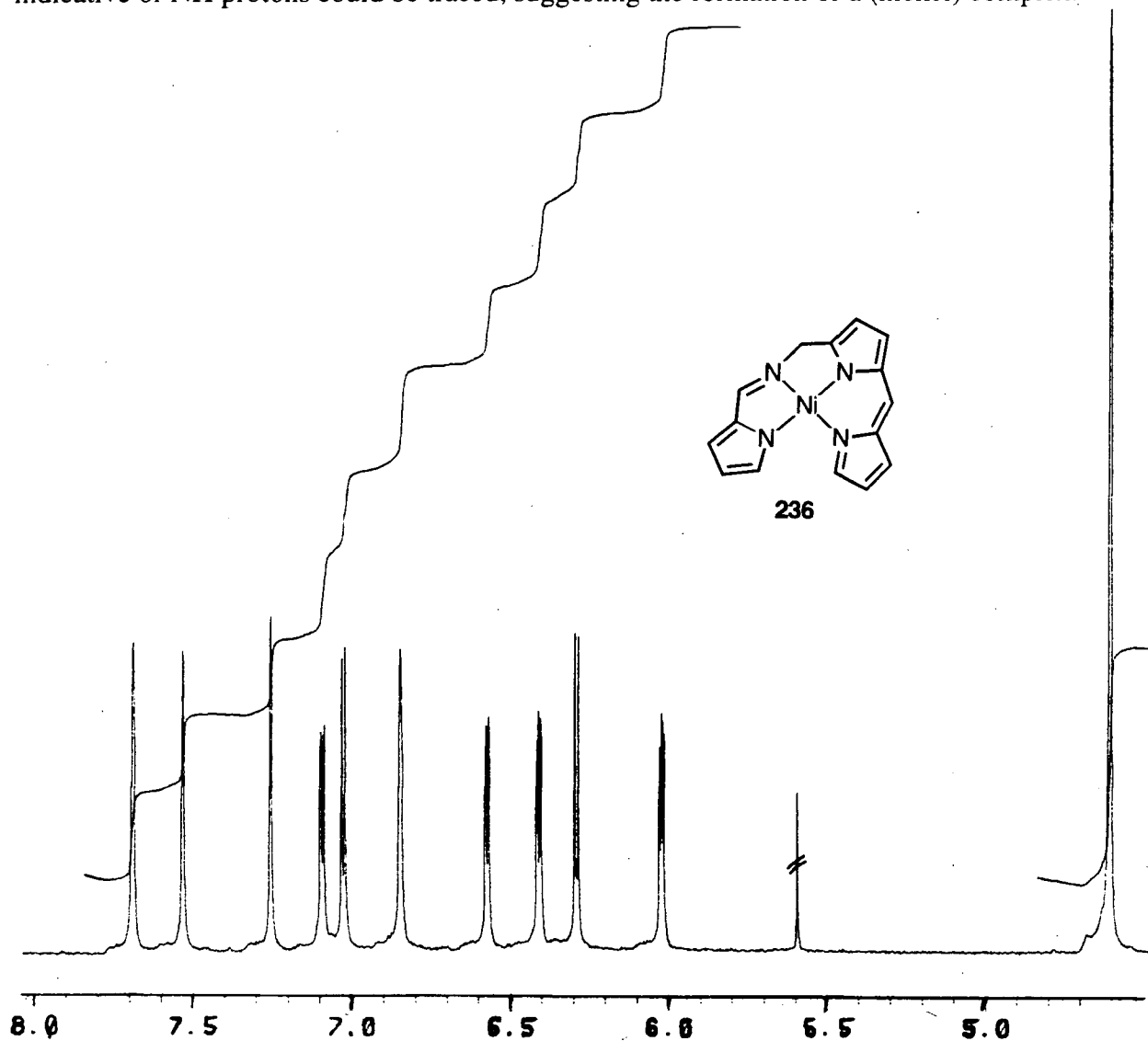
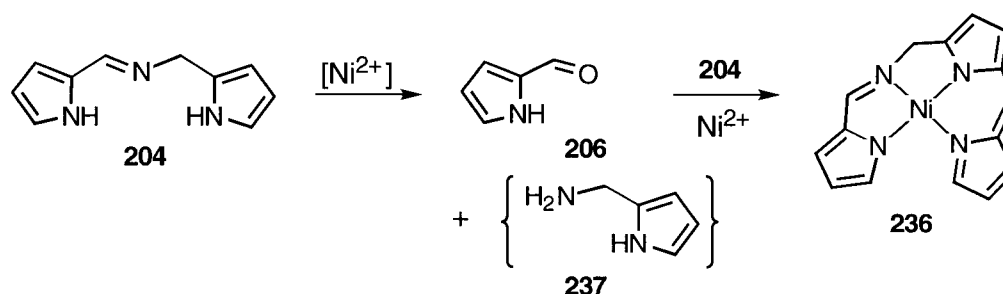


Figure 1-34 $^1\text{H-NMR}$ spectrum (200 MHz, acetone- d_6) of 236

The HR-MS of the compound (*vide supra*) corroborated the presence of a nickel atom, and because the compound, by virtue of its sharp NMR signals, proved to be diamagnetic, a square planar metal complex of nickel(II) had to be assumed.⁴⁰⁵

Based on the potential lability of the imine linkage towards hydrolysis and the reactivity pattern of any pyrrole aldehyde equivalent formed in such a cleavage, the reaction sequence shown in Scheme 1-58, and the structure depicted for the pigment **236** was proposed: Lewis acid catalyzed hydrolysis of **204** gives pyrrole aldehyde **206** and, formally, the unstable aminomethyl pyrrole **237**. The aldehyde **206** reacts with a second equivalent of **204** at its most nucleophilic position (the α -position of the pyrrolic unit which is not deactivated by the imine nitrogen) to form a dipyririn unit. This molecule would be poised to 'wrap around' the nickel atom and to coordinate it in a square planar fashion to finally give **236**. This structure would account for all spectroscopic and analytical data.



Scheme 1-58 Proposed mechanism of formation and structure of **236**

A single crystal X-ray crystal structure of **236** subsequently confirmed the structural assignment, and a mechanistic investigation revealed interesting aspects of the reaction mechanism.

The Molecular Structure of **236**

Slow evaporation of a THF solution of **236** provided coarse red-orange crystals suitable for X-ray crystallography. An ORTEP representation and side view of the structure are shown in Figure 1-35. Experimental details of the structure determination are listed in Table 1-2, the final atomic coordinates are listed in Table 1-7, and selected bond lengths in Table 1-8.

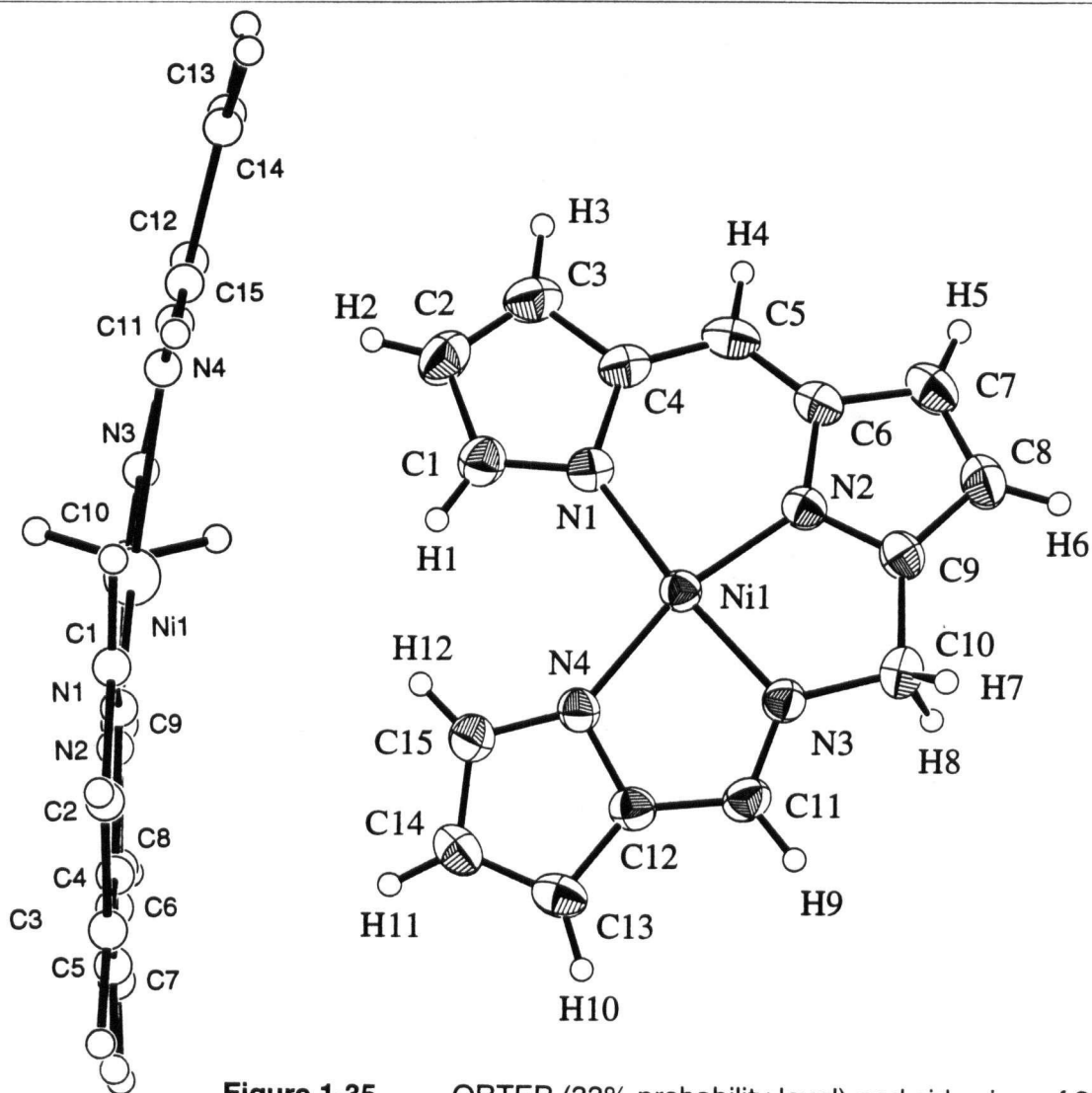


Figure 1-35 ORTEP (33% probability level) and side view of **236**

Most obvious and intriguing in this structure is the pronounced flatness of the open-chain ligand-metal complex. As a result, nickel is coordinated in a perfectly planar fashion by the four nitrogens with bond distances varying from 1.845(2) to 1.893(2) Å. Three types of nitrogens are present in the molecule, two of which are part of a dipyrrole moiety, one is an imine nitrogen and one is a pyrrole nitrogen. The pyrrole and imine nitrogens are in conjugation, and so are the nitrogens in the dipyrrole moiety but the two pairs are isolated from each other by a methylene group. Neither the differences in the metal-nitrogen nor the intra-dipyrrole bond lengths can be, in analogy to the dipyrrole complexes to be described in Part 2, rationalized with a simple resonance description.

The Influence of Various Reaction Conditions in the Formation of **236**

Pigment **236** forms in moderate yields at slightly elevated temperatures (~50°C) upon reacting **204** with nickel(II) in (wet) methanolic or ethanolic solution. Pyrrole aldehyde **206** can be detected by TLC from the onset of the reaction. This suggests that the first step of the reaction is, indeed, the cleavage of the imine moiety in **204**. The hydrolysis is catalyzed by the Lewis acidity of nickel(II) as the compound is perfectly stable under these conditions in the absence of the metal. Other Lewis acids such as zinc(II) as its acetate and Brønsted acids (HCl, HBr, TFA) were shown to catalyze the hydrolysis of the imine linkage under the above described conditions. The highly unstable **237** could not be seen, nor could possible reaction products such as dipyrromethanes from a self-condensation of **204**. Only the occurrence of highly polar and colorful materials in the course of the reaction indicate its polymerization and/or reaction with any other pyrrolic compounds in the reaction mixture. The acid-catalyzed hydrolysis of imines and the instability of any aminomethyl pyrroles is well documented in the literature.⁴¹⁹

The second step of the reaction requires the formation of the final ligand and, possibly concomitant, the formation of complex **236**. An equimolar alcoholic solution of independently synthesized pyrrole aldehyde (**206**) and **204** form in the presence of nickel(II) complex **236** in yields almost double those obtained in the absence of additional aldehyde. This corroborates the assumption that pyrrole aldehyde is the reactive species in the ligand formation derived from cleavage of the imine moiety. The formation of **236** is of particular interest as it is susceptible to a profound metal template effect. Only nickel(II) is capable of forming a complex of type **236**. Some metals (zinc) catalyze only the hydrolysis of the imine step, others (cobalt, iron, copper) form highly colored precipitates with **204**. They are, however, known complexes of the type $(\mathbf{204})_2\mathbf{M}$.^{385,406} A metal-free mixture of 2-pyrrolealdehyde (**206**) and imine **204** does not show any reaction. This mixture treated

with Brønsted acids such as HBr exhibits at first the typical optical spectrum of a dipyrin hydrobromide ($\lambda_{\max} \sim 500$ nm, compare to Part 2), but rapid decomposition sets in and no defined product can be isolated. Neutralization and reaction with nickel(II) yields no isolable products, indicating no formation of, for instance, the free base of **236**. On the other hand, an alcoholic solution of pyrrole and pyrrole aldehyde (**206**) does not form the corresponding dipyrin in the presence of nickel(II), indicating that the presence of ligand **204** is required for the reaction to proceed.

The Mass Spectrum of Complex **236**

The electron impact LR-mass spectrum (180°C) of **236** (A) together with the calculated isotope pattern for $\text{C}_{15}\text{H}_{12}\text{N}_4\text{Ni}$ (B) is shown in Figure 1-36.

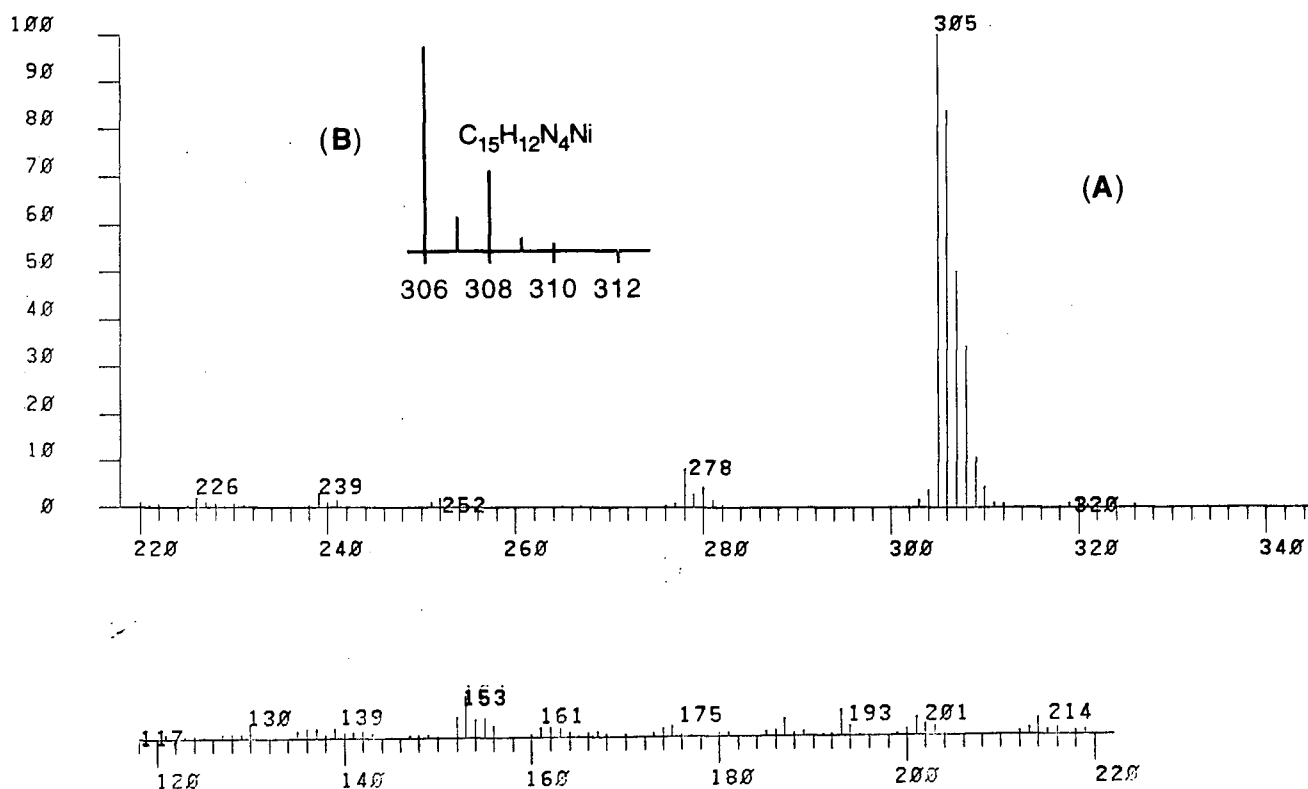
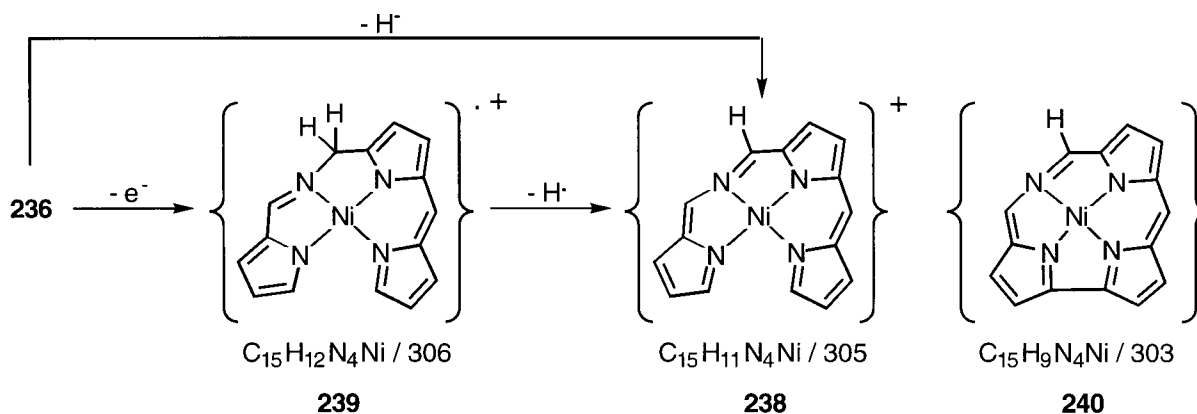


Figure 1-36 Measured (EI, 180°C) (A) and expected (B) mass spectrum of **236**

There are clear discrepancies between the measured and the expected spectrum, both in the value of the molecular peak as well as in the isotope pattern. Instead of the expected molecular ion peak of $m/e = 306$ (or 307 for the often observed MH^+) one molecular peak with $m/e = 305$ is observed. The high resolution mass of 305.03370 mu revealed its composition to be $C_{15}H_{11}N_4Ni$ (expected: 305.03372 mu). This fragmentation pattern, corresponding to a hydride abstraction of complex **236**, finds its explanation in the highly resonance stabilized structure of the resulting cation (**238**) (Scheme 1-59). The computed overlay of a ~1:2 ratio of **239** (resonance stabilized radical cation, $m/e = 306$) and **238** yields the observed spectral pattern. No indications for the formation of a cyclized product such as **240** were found in the mass spectrum. Attempts to form macroscopic amounts of **238** under solution phase conditions failed.



Scheme 1-59 Fragmentation of **236** in the EI mass spectrometer

3. EXPERIMENTAL

3.1 INSTRUMENTATION AND GENERAL MATERIALS

Melting points were determined on a Thomas Model 40 Micro Hot Stage and are uncorrected. The infrared spectra were measured with a Perkin-Elmer Model 834 FT-IR instrument or an a Perkin Elmer 710D. The ^1H -NMR spectra were measured on a Bruker AC-200 spectrometer (200 MHz) or a Bruker WH-400 with data processing on a Bruker data station, or a Varian XL-300 (300 MHz). ^{13}C -NMR spectra were measured on a Bruker AC-200 Fourier-transform spectrometer (50 MHz), a Varian XL-300 (75 MHz) or a Bruker AMX 500 (125 MHz). The NMR spectra are expressed on the δ scale and are referenced to residual solvent peaks. The low and high resolution FAB and EI mass spectra were obtained on a AEI MS902 and a Kratos MS50. The UV-visible spectra were measured on a Hewlett Packard HP 8452A photodiode array spectrophotometer and the data were processed on a microcomputer (CA Cricket Graph III software). Elemental analyses were performed on a Fisons CHN/O Analyzer, Model 1108. For experimental details of the X-ray crystal structure determination, see Table 1-2 (p. 193).

Materials

The silica gel used in the flash chromatographies was Merck Silica Gel 60, 230-400 mesh. R_f -values were measured on Merck silica TLC aluminum sheets (silica gel 60 F₂₅₄), whilst preparative TLC was performed on pre-coated 20x20 cm, 0.5 or 1.0 mm thickness, Whatman or Merck silica gel plates (with or without fluorescence indicator).

TPP and its zinc(II), nickel(II) (**126**), iron(III)Cl (**127**), and copper(II) (**128**) complexes and the variously substituted *meso*-tetraarylporphyrins were synthesized along standard Rothmund-type procedures^{41,44,45} with subsequent metallations.³²⁸ TPC (**18**) and TPCZn (**142**) were synthesized from TPP following the procedure described by Whitlock *et al.*⁸³ DPP (**139**) was produced according to a procedure outlined by Manka *et al.*⁴¹⁷

3-Benzoylpyrrole (**191**)³⁷⁴ has been synthesized from 1-tosylpyrrole (**192**)⁴⁰⁷ following procedures described.

2,2'-Bipyrrole (**203**) was prepared from pyrrole and 2-pyrrolidinone/ POCl_3 , followed by dehydrogenation of the resulting 1-pyrrolyl-2-pyrrole.⁴⁰⁸ Violent pyrrole polymerization was observed in several runs upon the addition of POCl_3 to the reaction mixture. Thus, it was later added slowly (over several hours) with the help of a syringe pump. The dehydrogenation was, in a second variation to the original procedure, performed in trimethyleneglycol dimethylester. An alternative synthesis of **203** by palladium(II) catalyzed coupling of 1-arylpyrrole,⁴⁰⁹ and subsequent hydrolysis of the 1,1'-dibenzoyl-2,2'-bipyrrole proved to be by far not as cost efficient and convenient as the latter synthesis. 2,2'-Bipyrrole dialdehyde (**112**) was prepared from **203** following a standard Vilsmeier-Haak formylation procedure as first described by Bauer *et al.*²⁹⁸ 4,4'-Diethyl-5,5'-diformyl-3,3'-dimethyl-2,2'-bipyrrole⁴¹⁰ (**114**) was prepared by hydrolysis of the corresponding

dicyanovinylgroup⁴¹¹ protected compound. This compound was available from stocks of the research group.

2-Pyrrolealdehyde (**206**) was prepared by Vilsmeier-Haak formylation of pyrrole.⁴¹² 3,4-Dimethyl-4-ethylpyrrole (**210**), and 3,4-diethylpyrrole (**209**) were prepared by standard procedures^{39,413} from in-house pyrrolic starting materials. 2-Cyanopyrrole (**207**) was prepared from pyrrole and chlorosulfonyl isocyanate according to a procedure detailed by Barnett, Anderson, and Loaner.³⁸⁶

All other reagents and solvents were commercially available and of reagent grade or higher, and were, unless specified, used as received.

NOTE OF CAUTION

Some chemicals used throughout this work deserve special attention. H₂S, OsO₄, chlorosulfonyl isocyanate (CSI), and Br₂ are volatile, corrosive and severely toxic chemicals. They must be handled in a well-ventilated fumehood and proper personal protective equipment must be worn. Also, familiarization with the recommendations, warnings, first aid measures and disposal procedures for these chemicals as outlined in the Material Safety Data Sheets (MSDS) should be mandatory before working with these compounds.

3.1 *meso*-ARYL- VIC-DIOLCHLORINS, -BACTERIOCHLORINS AND -ISO-BACTERIOCHLORINS

meso-Tetraphenyl-2,3-osmate ester-2,3-chlorin bispyridine adduct (**124**)

A solution of TPP (160 mg, 0.26 mmol) and OsO₄ (65 mg, 1 equivalent) in pyridine (10 mL) was stirred at room temperature in a tightly stoppered flask for 72 h. The mixture was then evaporated in vacuo at temperatures not exceeding 50°C. The resulting solid was loaded onto column (silica gel, 20x3 cm) and eluted with CH₂Cl₂/MeOH (gradient ranging from 100% CH₂CH₂ to CH₂CH₂/10% MeOH). The first fraction was starting material (50 mg, 31% recovery), and the second main purple fraction the desired compound. Slow evaporation from CH₂CH₂/10% MeOH with the exclusion of light produces **124** as purple microcrystalline material (85 mg, 32% yield).

MW = 1027.15 (bis-pyridine adduct); mp = d. > 120°C; R_f = 0.49 (silica-CH₂Cl₂/5% MeOH); ¹H-NMR (400 MHz, CDCl₃) - 1.72 (br s, exchangeable with D₂O, 2H), 6.99 (s, 2H), 7.30 (m, 6H), 7.51 (tr, *J* = 4.8 Hz, 2H), 7.57 (tr, *J* = 4.5 Hz, 2H), 7.61-7.72 (m, 8H), 7.97 (d, *J* = 4.3 Hz, 2H), 8.05 (d, *J* = 4.3 Hz, 2H), 8.09 (d, *J* = 4 Hz, 4H), 8.26 (d, *J* = 3 Hz, 2H), 8.43 (s, 2H), 8.57 (m, 6H); ¹³C-NMR (75 MHz, CDCl₃) 96.59, 114.06, 121.97, 124.34, 124.71, 126.16, 126.55, 126.88, 127.04, 127.43, 127.47, 132.13, 132.24, 133.86, 134.11, 135.41, 139.82, 140.91, 142.07, 142.22, 149.74, 152.67, 162.95; UV-Visible (CHCl₃) λ_{max} (rel. intensity) 420 (1.0), 520 (0.12), 548 (0.11), 594 (0.05), 646 (0.13) nm; LR-MS (EI, 3-NBA) *m/e* 1159 (<1, MH⁺ + 2 NBA), 1106 (<1, C₄₄H₃₀N₄O₄Os), 631 (10, C₄₄H₃₁N₄O), 615 (21, C₄₄H₃₁N₄); HR-MS (EI, 3-NBA) *m/e* expected for C₅₈H₄₃N₆O₉Os (= C₄₄H₃₀N₄O₃Os·2 matrix·H⁺): 1159.27121, found: 1159.27200.

(meso-Tetraphenyl-2,3-osmate ester-2,3-chlorinato)zinc(II) bispyridine adduct (125)

Prepared from TPPZn in 58% yield according to a procedure analogous to the one described for the preparation of **124**. Column chromatography (silica-Et₂O/CH₂Cl₂ 7:3).

MW = 1091.51; mp = d > 150°C; R_f = 0.41 (3:2-Et₂O:CH₂Cl₂); ¹H-NMR (400 MHz, CDCl₃) δ 6.86 (s, 2H), 7.23 (m, 2H), 7.38 (br s, 4H), 7.45 (tr, *J* = 7Hz, 2H), 7.53 (tr, *J* = 7Hz, 2H), 7.58-7.64 (m, 8H), 7.90-7.96 (m, 4H), 8.0-8.08 (overlapping m and d *J* = 4.5 Hz, 6H), 8.37 (s, 2H), 8.41 (d, *J* = 4.5, 2H), 8.64 (br s, 4H); UV-Visible (CHCl₃) λ_{max} (rel. intensity) 424 (1.0), 570 (sh), 618 (0.18) nm; LR-MS (EI, 3-NBA) *m/e* 932 (< 1, M⁺-2 pyridine), 692, (5, C₄₄H₂₈N₄OZn), 976 (9, C₄₄H₂₈N₄Zn); HR-MS (EI, 3-NBA) *m/e* expected for C₄₄H₂₈N₄O₄⁶⁴Zn¹⁹²Os: 932.09911, found 932.09752; Analysis calc'd for C₅₄H₄₀N₆O₅OsZn (**125**·H₂O): C, 58.51; H, 3.64; N, 7.58; found: C, 58.97; H, 3.68; N, 7.38.

(meso-Tetraphenyl-2,3-osmate ester-2,3-chlorinato)zinc(II) bispyridine-d₅ adduct

Prepared analogous to **124** in 1:9 pyridine-d₅:CHCl₃ as solvent mixture.

¹H-NMR (400 MHz, CDCl₃) δ - 1.73 (s, 2H), 6.99 (s, 2H), 7.33, (br tr, *J* = 7 Hz, 2H), 7.53, (tr, *J* = 7 Hz, 2H), 7.65-7.74 (m, 8H), 7.99 (d, *J* = 4.5 Hz, 2H), 8.43 (s, 2H), 8.57 (d, *J* = 4.5 Hz, 2H).

meso-Tetraphenyl-3,4-vic-dihydroxy-3,4-chlorin (129)**General procedure for the OsO₄ mediated dihydroxylation of meso-arylporphyrins**

TPP (1.0 g, 1.63 x 10⁻³ mol) was dissolved/suspended in freshly distilled, ethanol-stabilized CHCl₃/10% pyridine (200 mL, in general, the least amount of solvent possible) and was treated with OsO₄ (540 mg, 1.3 equivalents). The reaction flask was stoppered and stirred at ambient temperature in the dark until no change could be detected by optical spectroscopy or TLC control (ca. 4 days). The reaction was then quenched by purging with gaseous H₂S for 5 min. Following the addition of MeOH (~20 mL), the precipitated black OsS was filtered off through Celite[®]. The filtrate was evaporated to dryness by a stream of

air or N₂. (FUMEHOOD !!; the use of a rotary evaporator connected to an aspirator is not recommended for the evaporation step as this carries residual H₂S into the waste-water streams, resulting in a pungent stench from the drains. Washings of the organic reaction mixture performed with dilute Na₂CO₃ solutions to extract the H₂S forms, depending on the phenyl substituents, very stable emulsions.) The resulting residue was loaded onto a silica gel column (200 g, 280 - 400 mesh) and eluted with CH₂Cl₂. The first fraction is starting material (400 mg, 40 % recovery). 1.5 % MeOH/CH₂Cl₂ eluted then **125**. Slow evaporation from a MeOH/CH₂Cl₂ mixture gave **125** (520 mg, 8.02 x 10⁻⁴ mol, 49 % yield) as bright purple crystalline material.

Further elution of the column with 5% MeOH/CH₂Cl₂ gave a crude mixture of **145** and **146** (ca. 40 mg, 3.5 %).

MW = 648.76; m.p. > 300°; R_f = 0.68 (silica-CH₂Cl₂/1.5% MeOH); ¹H-NMR (400 MHz, CDCl₃) δ - 1.78 (br s, 2H), 3.14 (s, exchangeable with D₂O, 2H), 6.36 (s, 2H), 7.68 - 7.80 (m, 12H), 7.92 (d, *J* = 8.5 Hz, 2H), 8.09 (br s, 4H), 8.15 (d, *J* = 8.5 Hz, 2H), 8.33 (d, *J* = 4.5 Hz, 2H), 8.48 (s, 2H), 8.63 (d, *J* = 4.5 Hz, 2H); ¹³C-NMR (125 MHz, CDCl₃) δ 73.9, 113.2, 123.1, 124.2, 126.7, 127.5, 127.7, 127.9, 128.1, 132.2, 132.7, 133.9, 134.1, 135.5, 140.6, 141.2, 141.8, 153.2, 161.4; UV-Visible (CHCl₃) λ_{max} (log ε) 408 (5.27), 518 (4.19), 544 (4.19), 592 (3.85), 644 (4.38) nm; fluorescence (CH₂Cl₂) at 649 nm (excitation 512 nm); LR-MS (EI, 300°C) *m/e* 648 (0.5, M⁺), 646 (0.9, M⁺ - 2H), 630 (100, M⁺ - H₂O), 614 (42.7); HR-MS (EI, 300°C) *m/e* calc'd for C₄₄H₃₂N₄O₂: 648.2525, found 648.2525; Analysis calc'd for C₄₄H₃₂N₄O₂ · 1/2 H₂O: C, 80.34; H, 5.06; N, 8.52; found: C, 80.26; H, 4.93; N, 8.46.

(5,10,15,20-Tetraphenyl-*vic*-2,3-dihydroxy-2,3-chlorinato)zinc(II) (**130**)

Prepared in 72% yield from TPPZn following the general procedure. Washing with dilute acetic acid removes coordinated pyridine. Slow evaporation of a CHCl₃ /MeOH solution containing a drop of pyridine produces blue-green crystals of **125** as its pyridine

adduct. Alternatively, refluxing of a solution of **129** in $\text{CHCl}_3/\text{MeOH}$ 9:1 containing excess zinc acetate converts the free base quantitatively into its metallated form **130** within 2 h.

MW = 712.12; mp (d) > 300°; R_f = 0.62 (silica gel-1.5 % $\text{MeOH}/\text{CH}_2\text{Cl}_2$); $^1\text{H-NMR}$ (400 MHz, CDCl_3) δ 5.30 (s, 2H, exchangeable with D_2O), 6.12 (s, 2H), 7.55 - 7.72 (m, 12H), 7.81 (d, J = 7Hz, 2H), 7.94 (d, J = 7Hz, 2H), 7.96- 8.06 (m, 6H), 8.37 (s, 2H), 8.46 (d, J = 4.5 Hz, 2H) (pyridine adduct: additional signals at, 3.8 (m, 2H), 5.9 (br tr, 2H), 6.69 (tr, J = 2.5 Hz, 1H); $^{13}\text{C-NMR}$ (75 MHz, CDCl_3) δ 50.63, 126.48, 126.59, 126.63, 127.23, 127.35, 127.48, 127.68, 127.77, 127.82, 129.31, 132.11, 132.52, 133.63, 133.68, 133.79, 141.73, 142.57, 146.52, 148.04, 154.22, 156.28; UV-Vis ($\text{CH}_2\text{Cl}_2/0.5\%\text{MeOH}$) λ_{max} (log ϵ) 418 (5.41), 524, 564, 596 (sh), 614 (4.71) nm; LR-MS (FAB, 3-NBA) m/e 710 (29.2, M^+), 693 (7.0, $\text{M}^+\text{-OH}$), 676 (3.7, $\text{M}^+\text{-2OH}$); HR-MS (FAB, 3-NBA) m/e calc'd for $\text{C}_{44}\text{H}_{30}\text{N}_4\text{O}_2^{64}\text{Zn}$: 710.16602, found 710.16595; Analysis calc'd for $\text{C}_{44}\text{H}_{30}\text{N}_4\text{O}_2\text{Zn}\cdot\text{C}_5\text{H}_5\text{N}$: C, 74.38; H, 4.46; N, 8.85; found: C, 73.50; H, 4.25; N, 7.87.

(5,10,15,20-Tetraphenyl-*vic*-2,3-dihydroxy-2,3-chlorinato)nickel(II) (**131**)

Prepared in 23% yield from TPPNi following the general procedure. Alternatively, refluxing under nitrogen a solution of **129** ($\text{CHCl}_3/\text{MeOH}$ 9:1) containing excess nickel acetate converts the free base quantitatively into its metallated form **130** within 24 h. Crystallization by slow solvent exchange from CHCl_3 to MeOH gives bright green crystals of **131**.

MW = 705.40; mp (d) > 250°; R_f = 0.48 (silica- $\text{CH}_2\text{Cl}_2/0.5\%\text{MeOH}$); $^1\text{H-NMR}$ (400 MHz, CDCl_3) δ 2.85 (s, 2H, exchangeable with D_2O), 5.81 (s, 2H), 7.55 - 7.65 (m, 12H), 7.70 (m, 4H), 7.82 (m, 4H), 8.22 (overlapping s and d = J , 4H), 8.38 (d, J = 4.5 Hz, 2H); $^{13}\text{C NMR}$ (50 MHz, DMSO-d_6) δ 76.0, 111.4, 123.2, 127.3, 127.5, 128.2, 128.5, 132.2, 132.6, 137.5, 139.1, 139.4, 140.4, 145.8, 148.6; UV/Vis ($\text{CH}_2\text{Cl}_2/0.5\%\text{MeOH}$): λ_{max} (log ϵ) 416 (5.10), 516 (3.66), 552 (sh), 572 (sh), 612 nm (4.30); LR-MS (FAB, thioglycerol) m/e 705 (25.5, MH^+), 704 (20.2, M^+), 693 (18.0, $\text{M}^+\text{-OH}$); HR-MS (FAB, thioglycerol) m/e calc'd for

$C_{44}H_{31}N_4O_2^{58}Ni$: 705.18005, found 705.17945; Analysis calc'd for $C_{44}H_{30}N_4NiO_2 \cdot 1/3 H_2O$: C, 74.29; H, 4.34; N, 7.88; found: C, 74.33; H, 4.06; N, 7.59.

5-(4-hydroxyphenyl)-10,15,20-triphenyl-2,3-vic-dihydroxy-2,3-chlorin (**134**) and 10-(4-hydroxyphenyl)-5,15,20-triphenyl-2,3-vic-dihydroxy-2,3-chlorin (**135**)

Prepared from 5-(4-hydroxyphenyl)-10,15,20-triphenylporphyrin (260 mg, 4.04×10^{-4} mol) according to the general procedure for the dihydroxylation of *meso*-arylporphyrins. The two isomeric products **134** (22% yield) and **135** (16% yield) were separated by preparative TLC (silica- $CH_2Cl_2/1.5\%$ MeOH, multiple developments).

(**134**):

MW = 664.76; $R_f = 0.31$ ($CH_2Cl_2/2.5\%$ MeOH/silica); 1H -NMR (400 MHz, $CDCl_3/10\%$ acetone- d_6) δ -1.96 (br s, 2H), 3.63 (s, 2H), 6.19 (d, $J = 5.1$ Hz, 1H), 6.25, d, $J = 5.1$ Hz, 1H), 7.02 (dd, $J = 7, 23$ Hz, 2H), 7.45-7.60 (m, 12), 7.78 (dd, $J = 7, 23$ Hz, 2H), 7.9-8.0 (m, 4H), 8.18 (d, $J = 4.5$ Hz, 1H), 8.23 (d, $J = 4.5$ Hz, 1H), 8.30 (s, 2H), 8.47 (dd, $J = 4.5, 1.2$ Hz, 1H); UV-visible ($CHCl_3/10\%$ MeOH) λ_{max} 410, 508, 526, 596, 642; LR-MS (EI, thioglycerol) m/e 665 (80, MH^+), 647 (8, $MH^+ - H_2O$); HR-MS (EI, thioglycerol) m/e expected for $C_{44}H_{33}N_4O_3$: 665.25527, found 665.25569.

(**135**):

MW = 664.76; $R_f = 0.55$ ($CH_2Cl_2/2.5\%$ MeOH/silica); 1H -NMR (400 MHz, $CDCl_3/10\%$ acetone- d_6) δ -1.85 (br s, 2H), 3.50 (s, 2H), 7.08 (d, $J = 8.5$ Hz, 2H), 7.52-7.65 (m, 9H), 7.83 (br s, 4H), 7.95-8.08 (m, 4H), 8.20 (d, $J = 4.5$ Hz, 2H), 8.36 (d, $J = 4.5$ Hz, 1H), 8.42 (d, $J = 4.5$ Hz, 1H), 8.51 (d, $J = 4.5$ Hz, 1H), 8.59 (d, $J = 4.5$ Hz, 1H); UV-visible ($CHCl_3/10\%$ MeOH) λ_{max} 410, 508, 526, 596, 642; LR-MS (EI, thioglycerol) m/e 665 (75, MH^+), 647 (4, $MH^+ - H_2O$); HR-MS (EI, thioglycerol) m/e expected: 665.25527; found 665.25681.

meso-Tetra-(3-hydroxyphenyl)-2,3-vic-dihydroxy-2,3-chlorin (137)

Prepared in 33% yield from [*meso*-tetra-(3-hydroxyphenyl)porphyrinato]zinc according to the general procedure. The crude reaction mixture was demetallated with 5%TFA/CH₂Cl₂ and then purified by chromatography (silica-5%MeOH/CH₂Cl₂).

MW = 712.76; R_f = 0.37 (silica-10%MeOH/CH₂Cl₂); ¹H-NMR (400 MHz, DMSO-d₆) δ - 1.98 (br s, 2H), 5.17 (br s, 2H), 6.18 (s, 2H), 7.07 (dd, *J* = 2.2, 7 Hz, 2H), 7.18 (dd, *J* = 2.2, 7 Hz, 2H), 7.30 (m, 2H), 7.39-7.58 (m, 10H), 8.36 (br s, 2H), 8.43 (s, 2H), 8.69 (d, *J* = 4.6 Hz, 2H), 9.75 (br s, 4H); UV-visible (MeOH) λ_{max} (rel. intensities) 414 (1.0), 516 (0.11), 542 (0.10), 592 (0.07), 644 (0.14); LR-MS (EI, thioglycerol/MeOH) *m/e* 713 (16, MH⁺); HR-MS (EI, 3-NBA/CHCl₃) *m/e* calc'd for C₄₄H₃₂N₄O₆: 713.24001, found: 713.23925.

meso-Tetra-(3,4,5-trimethoxyphenyl)-2,3-vic-dihydroxy-2,3-chlorin (138)

138 was prepared in 66% yield from *meso*-tetra(3,4,5-trimethoxyphenyl)porphyrin according to the standard procedure. Chromatography silica-CH₂Cl₂/2.5%MeOH.

MW = 1009.08; mp < 300°C; R_f = 0.72 (silica-CH₂Cl₂/5.0% MeOH); ¹H-NMR (400 MHz, DMSO-d₆) δ - 1.98 (s, 2H), 3.81 (s, 3H), 3.86 (s, 3H), 3.88 (s, 3H), 3.90 (s, 3H), 3.92 (s, 3H), 3.95 (s, 3H), 5.31 (d, 4.8, 2H), 6.19 (d, *J* = 4.8 Hz, 2H), 7.15 (s, 2H), 7.37 (s, 2H), 7.41 (s, 2H), 7.43 (s, 2H), 8.46 (d, *J* = 4.8 Hz, 2H); 8.49 (s, 2H), 8.77 (d, *J* = 4.8 Hz, 2H); ¹³C-NMR (75 MHz, CDCl₃) δ 56.35, 61.26, 74.50, 110.15, 111.7, 112.1, 112.26, 113.20, 123.00, 124.33, 128.19, 132.69, 135.62, 136.15, 137.23, 138.10, 141.00, 141.09, 151.50, 152.34, 152.55, 153.20, 161.80; UV-visible (CH₂Cl₂/0.5% MeOH) λ_{max} 420, 520, 548, 594, 646; LR-MS (FAB, 3-NBA) *m/e* 1009 (60, M⁺), 991 (10, M⁺ - H₂O), 975 (5, M⁺ - 2OH); HR-MS (FAB, 3-NBA) *m/e* calc'd for C₅₆H₅₆N₄O₁₄: 1008.37922, found 1008.38109.

5,10-Diphenyl-2,3-vic-dihydroxy-2,3-chlorin (139)

139 was prepared in 45% yield from 5,10-diphenylporphyrin (49 mg in 10 mL solvent) according to the general procedure. However, the reaction time was considerably

shortened (5h) and the mixture was separated on a preparative TLC (silica-1.5%MeOH/CH₂Cl₂, double development).

MW = 496.57; R_f = 0.28 (silica-CH₂Cl₂/1.5%MeOH); ¹H-NMR (400 MHz, CDCl₃/10%acetone-d₆) δ -2.23 (br s, 1H), -1.88 (br s, 1H), 5.99 (d, *J* = 6.5 Hz, 1H), 6.34 (d, *J* = 6.5 Hz, 1H), 7.62-7.75 (m, 6H), 7.91 (d, *J* = 5.2 Hz, 1H), 8.09 (m, 2H), 8.18 (m, 1H), 8.42 (d, *J* = 4.5 Hz, 1H), 8.64 (d, *J* = 4.5 Hz, 1H), 8.83 (d, *J* = 4.5 Hz, 1H), 8.92 (d, *J* = 4.5 Hz, 1H), 8.97 (d, *J* = 4.5 Hz, 1H), 9.11 (d, *J* = 4.5 Hz, 1H), 9.90 (s, 1H), 9.34 (s, 1H); UV-visible (CHCl₃/5%MeOH) λ_{max} (rel. intensities) 398 (1.0), 502 (0.10), 530 (0.06), 584 (0.04), 636 (0.19); LR-MS (EI, 3-NBA) *m/e* 496 (79, M⁺), 478 (100, M⁺-H₂O); HR-MS (EI, 3-NBA) *m/e* calc'd for C₃₂H₂₄N₄O₂: 496.18993, found 496.18979.

meso-Tetraphenyl-2,3-*vic*-dihydroxy-2,3,12,13-bacteriochlorin (**141**)

Two different methods are available for the synthesis of **141**.

Method 1: The compound was prepared in 53% yield from *meso*-tetraphenylchlorin (50 mg, 8.1 x 10⁻⁵ mol) according to the general osmium tetroxide mediated dihydroxylation procedure.

Method 2: *meso*-Tetraphenylchlorin (100 mg, 1.62 x 10⁻⁴ mol) was dissolved in a suspension of 200 mg dry Na₂CO₃ in dry pyridine (20 mL). The mixture was kept under N₂ and refluxed. *p*-Toluenesulfonylhydrazide (150 mg, 5 equivalents) were added in portions over a period of 4 h. Reflux was continued for another 2 h. The mixture was cooled, filtered, the filtrate evaporated to dryness and the residue was separated on a preparative TLC plate. The pink band of **141** separating from the brown band of **129** (silica, 1.5%MeOH/CH₂Cl₂) was isolated to give, after recrystallization from CH₂Cl₂/CCl₄, **141** in 12 % yield.

MW = 650.78; R_f = 0.78 (silica gel-2.5% MeOH/CH₂Cl₂); ¹H-NMR (400 MHz, CDCl₃) δ -1.58 (s, 2H), 3.00 (s, 2H), 3.94-4.21 (m, 4H), 6.13 (s, 2H), 7.58-7.73 (m, 12H), 7.79 (br tr, *J* = 6.8 Hz, 4H), 7.86 (br d, *J* = 4.4 Hz, 2H), 7.97 (dd, *J* = 4.8, 2 Hz, 2H), 8.13 (2 overlapping

d, $J = 4.5$ Hz, 4H); UV-Vis (CH_2Cl_2) λ_{max} (log ϵ): 378 (4.96), 524 (4.49), 724 (4.71) nm; LR-MS (+ FAB, 3-NBA) m/e 650 (100, M^+), 633 (19.2, $\text{M}^+ - \text{OH}$); HR-MS (+ FAB, 3-NBA) m/e calc'd for $\text{C}_{44}\text{H}_{34}\text{N}_4\text{O}_2$: 650.26818, found 650.27118;

(*meso*-Tetraphenyl-2,3-*vic*-dihydroxy-2,3,7,8-isobacteriochlorinato)zinc(II) (**143**) and *meso*-Tetraphenyl-2,3-*vic*-dihydroxy-2,3,7,8-isobacteriochlorin (**144**)

Prepared in invariably low yields (< 10%) from **142** following either of the two methods described for **141**. The main product appeared to be **130**. In no case, however, was the formation of a bacteriochlorin or metallochlorin chromophore, respectively, observed. The green pigment **143** {HR-MS (FAB, 3-NBA) calc'd m/e for $\text{C}_{44}\text{H}_{32}\text{N}_4\text{O}_2\text{Zn}$: 712.18167; found 712.17630} was directly demetallated by 5% TFA/ CH_2Cl_2 to produce the fuchsia-colored **144**.

144:

MW = 650.78; $R_f = 0.28$ (silica- $\text{CH}_2\text{Cl}_2/0.5\%$ MeOH); $^1\text{H-NMR}$ (400 MHz, $\text{CDCl}_3/4\%$ MeOH- d_4) δ 3.2-3.5 (m, 4H), 5.28 (d, $J = 6.5$ Hz, 1H), 5.34 (d, $J = 6.5$ Hz), 7.38 (d, $J = 4.5$ Hz), 7.4-7.6 (m, 18H), 7.6-7.75 (m, 2H), 7.7-7.8 (m, 2H); UV-Vis (CH_2Cl_2) λ_{max} (log ϵ): 394 (5.02), 480 (sh), 514 (4.03), 546 (4.19), 590 (4.20) nm; LR-MS (+FAB, thioglycerol/ CHCl_3) m/e 651 (38, MH^+), 633 ($\text{MH}^+ - \text{H}_2\text{O}$); HR-MS (+FAB, thioglycerol/ CHCl_3) m/e calc'd for $\text{C}_{44}\text{H}_{34}\text{N}_4\text{O}_2$: 650.26818, found 650.26675.

meso-Tetraphenyl-2,3-12,13-*di-vic*-dihydroxy-2,3,12,13-bacteriochlorin (**145**) and *meso*-Tetraphenyl-2,3-12,13-*trans*-*di-vic*-dihydroxy-2,3,12,13-bacteriochlorin (**146**)

129 (100 mg, 1.54×10^{-4} mol) was dissolved in a minimal amount of CHCl_3 containing 10 % pyridine (ca. 4 mL). OsO_4 (51 mg, 1.3 equivalents) was added and the stoppered solution was stirred at r.t. until the chlorin peak at 644 nm was largely replaced by the bacteriochlorin peak at 708 nm (16 h). The reaction was quenched by bubbling gaseous H_2S through it. After filtering of the solution (Celite[®]) and evaporation of the filtrate, the

mixture was separated on a preparative TLC plate (silica gel, 2 mm, 5 % MeOH in CH₂Cl₂ as eluent, two developments). Yield 19 % and 20% for **145** and **146**, respectively.

(145):

MW = 682.78; mp = d > 150°C; R_f = 0.51 (silica gel-CH₂Cl₂/5.0 % MeOH); ¹H-NMR (300 MHz, DMSO-d₆) δ = -1.65 (s, 2H), 4.99. d (J = 4.9 Hz, 4H), 5.87 (d, J = 4.9 Hz Hz, 4H), 7.6 (br m, 12H), 7.86 (br s, 4H), 7.96 (overlapping s and broad s, 8H); ¹³C-NMR (75 MHz, DMSO-d₆) δ = 73.11, 115.63, 122.88, 127.10, 131.54, 133.85, 136.22, 141.22, 160.07; UV-Vis (CH₂Cl₂) λ_{max} = 376 (5.42), 528 (5.08), 708 (4.89) nm; LR-MS (+ FAB, 3-NBA) m/e 682 (100, M⁺), 665 (31.1, M⁺ - OH), 648 (5.8, M⁺ - 2OH), 613 (6.4, M⁺ - 4OH - H); HR-MS (+ FAB, 3-NBA) m/e calc'd for C₄₄H₃₄N₄O₄: 682.25801, found 682.25470.

(146):

MW = 682.78; mp = d > 150°C; R_f = 0.30 (silica gel-CH₂Cl₂/5.0 % MeOH); ¹H-NMR (400 MHz, DMSO-d₆) δ -1.75 (s, 2H), 5.05 (br s, 4H), 5.95 (s, 4H), 7.65 (br s, 12H), 7.93 (br s, 8H), 8.09 (s, 4H); UV-Vis (CH₂Cl₂) λ_{max} (log ε): 376 (5.40), 528 (5.01), 708 (4.86) nm; LR-MS (+ FAB, 3-NBA) m/e 682 (19.4, M⁺), 665 (7.4, M⁺ - OH), 649 (9.4), 648 (7.5, M⁺ - 2OH), 613 (1.5, M⁺ - 4OH - H).; HR-MS (+ FAB, 3-NBA) m/e calc'd for C₄₄H₃₄N₄O₄: 682.25797, found 682.25518.

(*meso*-Tetraphenyl-2,3,7,8-*cis*-di-*vic*-dihydroxy-2,3,7,8-isobacteriochlorinato)zinc(II) (**147**) and (*meso*-Tetraphenyl-2,3,7,8-*trans*-di-*vic*-dihydroxy-2,3,7,8-isobacteriochlorinato)zinc(II) (**148**)

Prepared in low yields from **130** following the general dihydroxylation procedure. TPPZn treated with 3-4 equivalents of OsO₄ also produces these compounds and they are found, albeit in very small amounts, in the polar material left on the chromatography column used in the preparation of **130**. Their purification was always performed by preparative TLC plate chromatography.

147:

MW = 746.12; R_f = 0.21 (silica-CH₂Cl₂/10%MeOH); LR-MS (+ FAB, 3-NBA/CHCl₃) *m/e* 744 (40, M⁺), 726 (11, M⁺ - H₂O); HR-MS (+ FAB, 3-NBA) *m/e* calc'd for C₄₄H₃₄N₄O₄⁶⁴Zn: 744.17150, found 744.17210.

148:

MW = 746.12; R_f = 0.33 (silica-CH₂Cl₂/10%MeOH); strongly fluorescent purple-green color in solution; ¹H-NMR (400 MHz, CDCl₃/20%acetone-d₆) δ = -2.75 (brs, 4H), 5.68 d (J = 8.8 Hz, 4H), 7.37 (d, J = 4.5 Hz, 2H), 7.48-7.57 (m, 12H), 7.76 (m, 4H), 7.82 (d, J = 4.5 Hz, 2H), 7.83-7.89 (m, 4H); UV-Vis (CH₂Cl₂/0.5%MeOH) λ_{\max} (rel. intensities) 394 (sh), 418 (1.0), 512 (0.07), 558 (0.12), 596 (0.27), 638 (0.04) nm; LR-MS (+ FAB, 3-NBA/CHCl₃) *m/e* 744 (45, M⁺), 727 (13, M⁺ - OH); HR-MS (+ FAB, 3-NBA) *m/e* calc'd for C₄₄H₃₄N₄O₄⁶⁴Zn: 744.17150, found 744.17176.

meso-Tetraphenyl-2,3,7,8-trans-di-vic-dihydroxy-2,3,7,8-isobacteriochlorin (149)

Prepared by demetallation of **148** in 5%TFA/CH₂Cl₂

MW = 682.78; R_f = 0.71 (silica-CH₂Cl₂/5%MeOH); fuchsia color in solution; ¹H-NMR (400 MHz, CDCl₃) δ = 2.55 (br s, 2H), 2.70 (br s, 2H), 4.04 (br s, 2H), 5.49 (d J = 7 Hz, 2H), 5.58 (d, J = 7 Hz, 2H), 7.22 (d, J = 4.5 Hz, 2H), 7.50-7.60 (m, 14H), 7.68-7.78 (m, 6H), 7.82 (dd, J = 4.5, 2 Hz, 2H); UV-Vis (CH₂Cl₂/0.5%MeOH) λ_{\max} (log ϵ) 398 (5.17), 514 (4.12), 548 (4.29), 586 (4.20), 638 (3.56) nm; LR-MS (+ FAB, thioglycerol/CHCl₃) *m/e* 683 (70, MH⁺), 665 (12, M⁺ - H₂O); HR-MS (+ FAB, 3-NBA) *m/e* calc'd for C₄₄H₃₅N₄O₄ 683.26583, found 683.26604.

3.2 REACTIONS OF THE *MESO*-TETRAPHENYL-*VIC*-DIOL-CHLORINS

(*meso*-Tetraphenyl-*vic*-3,4-di-O-isopropylidene-3,4-chlorinato)zinc(II) (**150**)

130 (20 mg, 2.81×10^{-5} mol) dissolved in 20 mL dry acetone containing freshly fused ZnCl_2 (100 mg) was refluxed for 20 min under anhydrous conditions. The reaction mixture was evaporated to dryness. The resulting residue was separated on a preparative TLC plate (silica gel- $\text{CH}_2\text{Cl}_2/20\%\text{CCl}_4$). The main bright green band was isolated after one development, to give **150** in 60% yield. A small amount (~10% yield) of **152** is also formed during this reaction.

MW = 752.19; $R_f = 0.31$ (silica gel- $\text{CH}_2\text{Cl}_2/20\%\text{CCl}_4$); $^1\text{H-NMR}$ (300 MHz, CDCl_3) δ 0.61 (s, 3H), 1.37 (s, 3H), 6.46 (s, 2H), 7.55-7.76 (m, 12H), 8.05 (dd, $J = 8.0, 2.1$ Hz, 4H), 8.12 (m, 4H), 8.16 (d, $J = 4.5$ Hz, 4H), 8.41 (s, 2H), 8.53 (d, $J = 4.5$, 2H); UV-visible (CH_2Cl_2) 418, 520, 564, 594 (sh), 612; LR-MS (+ FAB, 3-NBA) m/e 750 (11, M^+), 693 (23, $\text{MH}^+ - \text{C}_3\text{H}_6\text{O}$); HR-MS (+ FAB, 3-NBA) m/e expected for $\text{C}_{47}\text{H}_{34}\text{N}_4\text{O}_2^{64}\text{Zn}$: 750.19732, found 750.19422.

meso-Tetraphenyl-2-hydroxy-porphyrin (**151**) and (*meso*-tetraphenyl-2-hydroxy-porphyrinato)zinc(II) (**152**)

129 or **130** (0.154 mmol) was dissolved in benzene (10 mL) and refluxed. Three drops of HClO_4 (70% aqueous solution) were added and the reflux was continued for 3 min. The bright green solution was then washed with dilute aqueous ammonia, dried over anhydrous Na_2CO_3 and evaporated to dryness. The resulting solid was chromatographed on a short column (CHCl_3 /silica gel). The main purple fraction was precipitated by solvent exchange with hexanes. Drying (50°C/high vacuum) of the microcrystalline material produces in 85% yield analytically pure **151**. The material was identical to that described by

Crossley *et al.*³⁵² **152** is produced from **151** in quantitative yields by standard metallation with Zn(II)acetate in hot CHCl₃/MeOH.

(meso-Tetraphenyl-2,3-dioxochlorinato)Zn(II) (**157**)

A benzene solution of DDQ (66 mg, 2.94 x 10⁻⁴ mol in 5 mL) was added to **130** (100 mg, 1.40 x 10⁻⁴ mol) dissolved in benzene (10 mL). Stirring at r.t. converted the green starting material quantitatively into the yellow product **157**. Short column chromatography (silica, benzene) separated the excess reagent from the product. Evaporation of the solvent produces **157** as a brown-blue solid in high yield.

MW = 708.10; R_f = 0.8 (silica-CH₂Cl₂/CCl₄ 1:1); ¹H-NMR (300 MHz, CDCl₃) δ 7.6-7.75 (m, 12H), 7.77 (dd, *J* = 8, 2 Hz, 4H), 8.25 (dd, *J* = 8, 2 Hz, 4H), 8.32 (d, *J* = 4.5 Hz, 2H), 8.45 (s, 2H), 8.53 (d, *J* = 4.5 Hz, 2H); UV-visible (CH₂Cl₂) λ_{max} (rel. intensities) 416 (1.0), 496 (0.13), very broad, featureless band centred ~650 nm; LR-MS (EI, 350°C) *m/e* 708 (85, M⁺), 692 (100, M⁺-O).

meso-Tetraphenyl-2-oxa-3-oxo-chlorinato)zinc(II) (**163**) and *meso-tetraphenyl-2-oxa-3-oxo-chlorin* (**164**)

163 is isolated during chromatography of the crude reaction mixture resulting from the treatment of TPPZn with OsO₄/pyridine, followed by reduction with H₂S. It is the band following the separation of the starting material. Slow diffusion of petroleum ether 40-60 into a CHCl₃ solution (green) containing a trace of pyridine of **164** results in the formation of purple X-ray quality crystals. **164** is prepared by acid treatment (10% TFA/CH₂Cl₂) of **163**. Washing of the acidic solution with dilute aqueous NH₃, drying of the isolated organic phase over anhydrous Na₂CO₃ and recrystallization by slow solvent exchange to hexane produces **164** as dark purple powder.

163:

MW = 696.09; mp = d > 200°C; R_f = 0.82 (silica-ethyl acetate/hexane 3:1); ¹H-NMR (300 MHz, CDCl₃) δ 7.65-7.77 (m, 12H), 7.93 (dd, *J* = 7.8, 2 Hz, 2H), 8.05 (dd, *J* = 7.8, 2 Hz, 2H), 8.10 (dd, *J* = 7.8, 2 Hz, 4H), 8.51 (d, *J* = 4.5 Hz, 1H), 8.58 (d, *J* = 4.5 Hz, 1H), 8.65, 8.67, 8.69 (three overlapping d, *J* = 4.5 Hz, 1H), 8.75 (d, *J* = 4.5 Hz, 1H); ¹³C-NMR (75 MHz, CDCl₃) δ 173.5, 154.1, 143.4, 142.1, 142.0, 139.0, 138.0, 134.3, 134.0, 133.8, 132.4, 132.3, 132.2, 132.0, 130.9, 130.7, 130.6, 129.5, 128.8, 127.9, 127.8, 127.7, 127.6, 127.5, 126.7, 126.6; UV-visible (CH₂Cl₂) λ_{max} (log ε) 402 (sh), 422 (5.53), 520 (3.54), 558 (4.07), 602 (4.44); LR-MS (EI, 250°C) *m/e* 694 (30.9, M+), 638 (7.3), 561 (17.4), 483 (3.5), 28 (100); HR-MS (EI, 200°C) *m/e* calc'd for C₄₃H₂₆N₄O₂⁶⁴Zn: 694.1347, found 695.1355. See below for the X-ray crystal structure data.

164:

MW = 632.72; R_f = 0.50 (silica-CCl₄/CH₂Cl₂ 1:1); ¹H-NMR (300 MHz, CDCl₃) δ = -2.05 (s, 1H), -1.82 (s, 1H), 7.66-7.78 (m, 12), 7.97 (m, 2H), 8.00-8.16 (m, 6H), 8.52 (d, *J* = 4.5 Hz, 1H), 8.57 (dd, *J* = 4.5, 15 Hz, 1H) overlapping with 8.59 (d, *J* = 4.5 Hz, 1H), 8.69 (d, *J* = 4.5, 1.5 Hz, 1H), 8.78 (two overlapping dd, *J* = 4.5, 1.5 Hz, 2H); UV-visible (CHCl₃) λ_{max} (log ε) 420 (5.56), 522 (4.15), 558 (4.16), 588 (3.95), 640 (3.66); UV-visible (TFA/CHCl₃) λ_{max} 430, 588 (sh), 614; LR-MS (FAB, 3-NBA) *m/e* 633; HR-MS (FAB, 3-NBA) *m/e* calc'd for C₄₃H₂₈N₄O₂: 632.2212, found 632.2168.

(meso-Tetraphenyl-2,3-secochlorinato-2,3-dialdehyde)Ni(II) (167)

131 (170 mg, 9.94 × 10⁻⁵ mol) dissolved in dry THF (10 mL) were treated with Pb(IV)(acetate)₄ (120 mg, moist). Within 10 min at r.t. the solution turned from green to dark yellow. After no starting material was detectable by TLC (20 min), the solution was then evaporated to dryness *in vacuo* and the resulting residue was purified by flash chromatography (silica, 3x7 cm, CHCl₃). The first yellow fraction was collected and

evaporated to dryness, dissolved in CH_2Cl_2 and solvent exchange to hexane gave **167** in 80% yield as a dark purple-brown powder of analytical purity.

MW = 703.61; mp > 250°C; R_f = 0.88 (silica- CHCl_3 , yellow-brown spot which turns forest-green within a few minutes); $^1\text{H-NMR}$ (400 MHz, DMSO-d_6) δ 7.55-7.60 (m, 12H), 7.70-7.75 (m, 8H), 7.85 (d, J = 4.8 Hz), 7.98 (s, 2H), 8.18 (d, J = 4.8 Hz), 9.50 (s, 2H); the $^1\text{H-NMR}$ in CDCl_3 exhibit additional broad signals at 7.1 (s, 2H), 7.8 (s, 2-4H) and 8.8 (s, 1-2H) which have not found any explanation yet; $^{13}\text{C-NMR}$ (50 MHz, CDCl_3) δ 120.0, 126.7, 127.4, 127.8, 128.2, 128.6, 130.8, 131.4, 132.9, 133.4, 134.0, 134.6, 135.7, 138.8, 140.8, 144.1, 146.9, 188.7; IR (film): ν = 1684 cm^{-1} (C=O); UV/Vis (CH_2Cl_2) λ_{max} (log ϵ) 312 (4.55), 344 (sh), 414 (4.63), 466 (4.78), 686 nm (4.04); LR-MS (EI, 280°C) m/e 702 (4.0, M^+), 700 (3.5, M^+-2H), 686 (33.6, M^+-O), 684 (8.1, $\text{M}^+-\text{H}_2\text{O}$), 673 (100, M^+-CHO); HR-MS (FAB, 3-NBA/ CHCl_3) m/e calc'd for $\text{C}_{44}\text{H}_{29}\text{N}_4^{58}\text{NiO}_2$: 703.16440, found 703.16394; Analysis calc'd for $\text{C}_{44}\text{H}_{28}\text{N}_4\text{NiO}_2$: C, 75.13; H, 4.01; N, 7.96; found: C, 75.04; H, 4.34; N, 7.34.

Pigment **172** and pigment **173**

167 (50 mg, 7.11×10^{-5} mol) dissolved in CHCl_3 (2 mL, pentene stabilized) containing 2% MeOH were fumed carefully with some head space from a conc. HCl bottle applied through a pipette. **172** and **173** appear immediately. The mixture was separated on a preparative TLC plate (silica, CHCl_3). Depending on the intensity of the acid treatment, variable yields of the two green products were produced. Other than the two pigments **172** and **173**, no other pigments or decomposition can be observed. **172** is labile.

172:

MW = 733.45; R_f = 0.45 (silica- CHCl_3); M.p. > 150 °C (d); $^1\text{H-NMR}$ (400 MHz, CDCl_3) δ 2.45 (d, 3J = 7.6 Hz, 1 H), 3.12 (s, 3H), 6.12 (s, 1 H), 6.47 (d, 3J = 7.6 Hz, 1 H), 7.50-7.65 (m, 20 H), 7.78 (d, 3J = 4.6 Hz, 1 H), 7.84 (d, 3J = 4.6 Hz, 1 H), 8.06 (two overlapping d, second order, 2 H), 8.22 (dd, 3J = 4.6, 1.2 Hz, 2 H); $^{13}\text{C-NMR}$ (125 MHz, DMSO-d_6)

δ 54.1, 89.2, 96.7, 110.5, 111.1, 125.3, 125.4, 127.4, 127.7, 127.8, 127.9, 128.0, 128.1, 128.8, 128.8, 129.0, 132.4, 133.1, 137.7, 137.8, 137.9, 138.5, 138.7, 140.8, 141.3, 141.4, 145.5, 145.6; UV/Vis (CH_2Cl_2) λ_{max} ($\log \epsilon$) 430 (4.82), 640 (4.10); LR-MS (EI, 3-NBA/ CHCl_3) m/e 734 (20, MH^+); HR-MS (EI, 3-NBA/ CHCl_3) m/e calc'd for $\text{C}_{45}\text{H}_{32}\text{N}_4^{58}\text{NiO}_3$: 734.18279; found 734.18314.

173:

MW = 749.49; R_f = 0.80 (silica- CHCl_3); M.p. > 200 (d); $^1\text{H-NMR}$ (400 MHz, CDCl_3): δ 3.03 (s, 6 H), 6.08 (s, 2 H), 7.5-7.65 (m, 20 H), 7.81 (d, 3J = 4.5 Hz, 2 H), 8.06 (s, 2 H), 8.22 (d, 3J = 4.5 Hz, 2 H); $^{13}\text{C-NMR}$ (50 MHz, CDCl_3): δ 54.6, 97.4, 111.9, 122.6, 124.4, 125.9, 126.0, 126.2, 127.1, 127.6, 127.7, 127.8, 128.9, 129.2, 132.8, 132.9, 133.3, 138.7, 138.8, 139.0, 139.7, 142.4, 146.5; UV/Vis (CH_2Cl_2) λ_{max} ($\log \epsilon$) 430 (4.81), 640 (4.09); MS (EI, 3-NBA/ CHCl_3) m/e 748 (18, MH^+), 717 (8, M^+-OCH_3); HR-MS (EI, 3-NBA/ CHCl_3) m/z calc'd for $\text{C}_{46}\text{H}_{34}\text{N}_4^{58}\text{NiO}_3$: 748.19844; found 748.19938; Analysis calc'd for $\text{C}_{46}\text{H}_{34}\text{N}_4\text{NiO}_3$: C, 73.73; H, 4.57; N, 7.48; found: C, 73.81; H, 4.63; N, 7.52.

Pigment 175

Prepared analogous to **173** from **167** in $\text{CHCl}_3/\text{MeOH}/\text{EtOH}$. Its UV-visible spectrum is identical to that of **173**. The three components present cannot be separated by TLC. Their presence is indicated by the presence of three strong molecular ion peaks at m/e 748 (corresponding to $\text{C}_{46}\text{H}_{34}\text{N}_4^{58}\text{NiO}_3$), 762 (corresponding to $\text{C}_{47}\text{H}_{36}\text{N}_4^{58}\text{NiO}_3$), and 776 (corresponding to $\text{C}_{48}\text{H}_{38}\text{N}_4^{58}\text{NiO}_3$). The $^1\text{H-NMR}$ (400 MHz, CDCl_3) and $^{13}\text{C-NMR}$ (75 MHz, CDCl_3) have a complex fine structure. Compared to the spectrum of **173**, additional signals at δ 0.8 (two overlaying t) and at 3.5 (m) and at 14.8 and 62.4 are attributed to the presence of the ethyl groups. See below for details of the X-ray crystal structure determination.

3.3 THE DIRECTED SYNTHESIS OF N-CONFUSED TPP

5-Phenyldipyrane (**179**) and 5,10-diphenyltripyrane (**180**)

Method A (adaption from Lindsey and co-worker)³⁶⁷

Benzaldehyde (6.0 mL, 59 mmol) was mixed with pyrrole (150 mL, 2.16 mol) and the mixture was deoxygenated by bubbling dry N₂ through it for 15 min. With the mixture still under nitrogen, TFA (0.45 mL, 5.8 mmol) was added and the mixture was stirred for 15 min at ambient temperature. After this time, the mixture was evaporated under vacuum (5 torr) and slight heating on a rotary evaporator yielded a dark oil. The oil was taken up in a minimal amount of CH₂Cl₂, and loaded onto a flash chromatography column (silica gel, 5.5 x 30 cm, CH₂Cl₂). The colorless, dipyrane **3** and tripyrane **4**, and some minute amounts of unidentified material ($\leq 1\%$) containing fractions (TLC control, upon Br₂-fuming of the TLC spots, **179** turns bright orange, **180** turns beige) were collected and evaporated on a rotary evaporator to yield a tan oil. This oil was transferred into a sublimation apparatus and subjected to high vacuum (0.1 torr). A slow heating rate ($\sim 0.75^\circ\text{C}/\text{min}$) was maintained until visible sublimation set in at 130°C. After further sublimation had ceased, the white crystalline sublimate, consisting of crystalline **179** (7.20 g, 55 % yield), and the orange, glassy sublimation residue (2.45 g, 11 % yield) consisting mainly ($\geq 95\%$, based on ¹H-NMR and analysis of the residue) of **180** were collected.

Method B (adaptation from Carell³⁷¹):

This method is, in principal, useful for the preparation of tripyranes which are not made from unsubstituted pyrroles (as the pyrroles are here not needed as solvent).

Benzaldehyde (12 mL, 0.118 mol) and pyrrole (52 mL, 0.745 mol) are dissolved in toluene (750 mL). A catalytic amount of *p*-toluenesulfonic acid monohydrate (100 mg, 4.9×10^{-4} mol) was added and the mixture was refluxed under N₂ for 1 h. After this time, the

mixture was evaporated on a rotary evaporator to produce a brown oil. This oil was subjected to the same treatment (chromatography, sublimation) as described in Method A to give **179** (44 % yield) and **180** (9.8 %).

179:

Analytical and spectroscopic properties identical to those described in the literature.³⁶⁷

$R_f = 0.78$ (silica- $\text{CH}_2\text{Cl}_2/\text{CCl}_4$ 1:1).

180:

MW = 377.49; mp = 75-80°C, $R_f = 0.63$ (silica $\text{CH}_2\text{Cl}_2:\text{CCl}_4$ 1:1); $^1\text{H-NMR}$ (200 MHz, CD_2Cl_2) δ 5.35 (s, 2H), 5.78 (d, $J = 4$ Hz, 2H), 5.89 (s, 2H), 6.14 (m, 2H), 6.66 (m, 2H), 7.15-7.38 (m, 10H), 7.75 (br s, 1H), 7.88 (br s, 2H); $^{13}\text{H-NMR}$ (50 MHz, CDCl_3) δ 44.1, 107.2, 107.4, 108.4, 117.2, 127.0, 128.4, 128.6, 132.3, 132.5, 142.1; LR-MS (EI, 150°C) m/e 377 (45, M^+), 221 (18), 156 (14), 145 (23), 80 (20), 67 (100); HR-MS (EI, 200°C), expected for $\text{C}_{26}\text{H}_{23}\text{N}_3$: 377.1892, found 377.1881; Analysis calc'd for $\text{C}_{26}\text{H}_{23}\text{N}_3$: C, 82.73; H, 6.14; N, 11.13; found 82.16, 6.03, 10.72.

1-Phenylcarbonyl-5-phenyldipyrromethane (181)

Sublimed **179** (533 mg; 2.40 mmol) was dissolved under anhydrous conditions in dry THF (20 mL). Ethylmagnesium bromide (1.80 mL 3M solution in Et_2O ; 2.2 equiv.) was syringed in, and the mixture was stirred for 15 min at r.t., then refluxed for 10 min and finally cooled to 0°C. The reaction mixture was taken up by a syringe and freshly distilled benzoylchloride (330 μl ; 1.15 equiv.) in dry THF (10 mL) was added to the (now empty) flask. The dipyrromethane-Grignard solution was, under ice cooling, slowly syringed back into the flask. The mixture was stirred at r.t. for 1h and refluxing for an additional 20 min., TLC analysis indicated the disappearance of the starting material. The reaction mixture was quenched with MeOH and subsequently diluted with water (50 mL). The products were extracted with CHCl_3 (3x50 mL) and the combined organic layers were dried over MgSO_4 and evaporated under vacuum to give a yellow oil. Flash column chromatography (silica, 20

x 3 cm, CH₂Cl₂) separated the title compound from traces of starting material and higher polarity materials (containing also traces of **183**). Evaporation of the solvent *in vacuo* afforded **181** as slightly yellow oil which solidified (540 mg, 69 %). The procedure is amenable to a 5-fold scale-up. For an alternative synthesis, see preparation for **182**.

MW = 326.40; mp = 72-77°C; R_f = 0.65 (silica-CH₂Cl₂/5.0% MeOH); ¹H-NMR (400 MHz, CDCl₃) δ 5.65 (s, 1H), 6.03 (s, 1H), 6.17 (s, 2H), 6.61 (m, 1H), 6.86 (m, 1H), 7.18-7.33 (m, 5H), 7.44-7.64 (m, 3H), 7.82 (d, 2H), 8.75 (s, 1H), 10.81 (s, 1H); ¹³C-NMR (75 MHz, CDCl₃) δ 44.17, 107.78, 108.26, 110.88, 117.90, 121.66, 127.14, 128.33, 128.38, 128.64, 129.12, 130.78, 131.23, 131.80, 138.50, 141.06, 142.68, 184.99; LR-MS (EI, 200°C) *m/e* 326 (100, M⁺), 249 (25.4), 221 (71.1), 156 (21.3), 105 (76.2); HR-MS (EI, 150°C) *m/e* calc'd for C₂₂H₁₈N₂O: 326.14191, found 326.14194.

1,9-Diphenylcarbonyl-5-phenyldipyrromethane (**183**)

181 (880 mg, 2.69 mmol) dissolved under anhydrous conditions in dry THF (20 ml) was treated with ethylmagnesium bromide (2.25 mL 3M solution in Et₂O; 2.5 equiv.). The rate of addition was such that a slow reflux was maintained. The mixture was refluxed for an additional 40 min after the completion of the addition. The solution turned red during this time. Benzoylchloride (0.93 mL, 3 equiv.) was added to the cooled solution by syringe at a slow rate. The mixture was then refluxed for an additional 1.5 h. The tan solution was then poured into aqueous ammonium acetate and stirred for 1 h. Extraction with CHCl₃ (4x50 mL), drying of the organic phase over Na₂CO₃ and evaporation of the solvent *in vacuo* provided crude **183**. Purification by flash chromatography (silica, 20x3.5, CH₂Cl₂/0.5% MeOH) and evaporation of the appropriate fractions provided a tan oil which solidified to produce 0.92 g (79% yield) of **182**.

MW = 430.29; no sharp mp; R_f = 0.33 (silica-CH₂Cl₂/5.0% MeOH, spot stains yellow with Br₂); ¹H-NMR (400 MHz, CDCl₃) δ 6.05 (m, 2H), 6.40 (m, 2H), 7.30-7.55 (m, 11H), 7.82 (dd, *J* = 7.5, 2 Hz, 4H), 11.2 (br s, 2H); ¹³C-NMR (75 MHz, CDCl₃) δ 44.9, 11.2, 120.7,

127.6, 128.1, 128.7, 129.0, 129.4, 131.0, 131.7, 138.2, 140.0, 140.5, 184.5; LR-MS (EI, 250°C) *m/e* 430 (57.0, M⁺), 325 (48.9, M⁺-PhCO), 105 (100, PhCO⁺); HR-MS (EI, 200°C) *m/e* calc'd for C₂₉H₂₂N₂O₂: 430.1861, found 430.1674; Analysis calc'd for C₂₉H₂₂N₂O₂: C, 80.91; H, 5.15; N, 6.51; found: C, 80.80; H, 5.13; N, 6.23.

1,10-Diphenylcarbonyl-5-phenyldipyrromethane (**183**)

179 (100 mg, 5.41 x 10⁻⁴ mol) dissolved in 1,2-dichloroethane (5 mL) was added dropwise under anhydrous conditions into a freshly prepared mixture of AlCl₃ (133 mg, 2.2 equiv.) and benzoyl chloride (0.11 mL, 9.0 x 10⁻⁴ mol) in 10 mL of 1,2-dichloroethane. After being stirred for 15 h at r.t., the mixture was quenched by pouring it into aqueous Na-acetate. Extraction with CHCl₃ (3 x 25 mL), drying over Na₂CO₃ and evaporation of the solvent, produced a solid which was chromatographed (silica preparative TLC, 1.5%MeOH/CH₂Cl₂) to give **181** (75 mg, 42 % yield) and **183** (46 mg, 19 % yield).

MW = 430.29; R_f = 0.39 (silica, 2.5%MeOH/CH₂Cl₂); ¹H-NMR (200 MHz, CDCl₃) δ 5.42 (s, 1H), 5.91 (m, 1H), 6.13 (q, *J* = 10Hz), 6.43 (m, 1H), 7.15-7.35 (m, 7H), 7.35-7.50 (m, 4H), 7.75 (dd, *J* = 13, 3 Hz, 2H), 8.10 (dd, *J* = 13, 3 Hz, 2H), 8.59 (br s, 1H); ¹³C-NMR (50 MHz, CDCl₃) δ 43.8, 108.5, 108.9, 117.8, 124.8, 125.6, 127.3, 128.2, 128.4, 128.9, 130.2, 131.4, 133.7, 134.7, 139.8, 141.0, 172.0, 192.3; LR-MS (EI, 180°C) *m/e* 430 (<1, M⁺), 326 (82, M⁺-PhCO), 249 (24), 221 (M⁺-2PhCO), 105 (100, PhCO⁺).

Phenyl-2-pyrrolyl-3-pyrrolymethane (**190**)

Method A (detosylation of **196**):

To a solution of **196** (500 mg, 1.33 mmol) in dioxane (20 mL) was added dropwise concentrated (viscous) aqueous KOH until the resulting mixture started to separate into two layers. The solution was then stirred for 12h at r.t. The reaction was then diluted with H₂O (100 mL) and extracted with Et₂O (4x20 mL). Evaporation of the ether produced **190** (60 mg, 87 % yield) as an oil, which, as judged by NMR, was pure.

Method B (condensation of **195** with pyrrole):

191 (620 mg, 3.62 mmol) dissolved in dry THF (5 mL) was, under anhydrous conditions and cooled by an ice-bath, dropped into a suspension of LAH (150 mg, 1 equiv.) in dry THF (30 mL). After the addition is completed, Glauber's salt was (0.5 g) slowly added to the mixture. The resulting sludge was filtered through Celite® and the filter cake thoroughly extracted with THF. The combined filtrates were evaporated to dryness *in vacuo* and immediately used in the next step. TLC analysis (silica, 5%MeOH/CH₂Cl₂) of the crude mixture exhibits **195** as a spot with low R_f (R_f = 0.1), which stains brown with Br₂ fumes, possibly some starting material (R_f = 0.3) and possibly some low polarity material (R_f = 0.95) which stains bright red with Br₂. This proved to be 3-benzylpyrrole which resulted from an over-reduction of **191** and which is hard to separate from the final product **190**.

195:

MW = 173.21; ¹H-NMR (200 MHz, CDCl₃) δ 2.45 (br s, 1H), 5.81 (s, 1H), 6.16 (m, 1H), 6.55 (m, 1H), 6.68 (m, 1H), 7.20-7.55 (m, 5H), 8.4 (br s, 1H); ¹³C-NMR (50 MHz, CDCl₃) δ 71.0, 107.2, 116.1, 118.5, 126.4, 127.2, 128.2, 128.3, 144.6.

195 (crude mixture from the reduction of 620 mg, 3.62 mmol of **191**) was dissolved in toluene (25 mL) containing 1 drop of acetic anhydride, pyrrole (0.5 mL) and a catalytic amount of *p*-toluenesulfonic acid·4 H₂O. The mixture was refluxed under N₂ for 10 min. No starting material could be detected (TLC) after this time. The mixture was evaporated *in vacuo* to dryness (the facilitate the chromatographic purification, it is important to remove all of the pyrrole) and the resulting oil was purified by flash chromatography (silica, CHCl₃). The first main fraction was collected and evaporated to produce **190** in 52% yield.

190:

MW = 222.29; R_f = 0.76 (silica-CH₂Cl₂), stains brown upon treatment with Br₂; ¹H-NMR (200 MHz, CDCl₃) δ 5.38 (s, 1H), 5.91 (m, 1H), 6.15 (q, *J* = 7 Hz, 1H), 6.43 (m, 1H), 6.66 (m, 1H), 6.77 (q, *J* = 6 Hz, 1H), 7.22-7.35 (m, 5H), 8.00 (br s, 2H); ¹³C-NMR (50 MHz,

CDCl₃) δ 43.5, 106.7, 108.3, 108.8, 116.7, 118.3, 125.6, 126.5, 128.5, 128.6, 128.9, 135.2, 144.7; LR-MS (EI, 180°C) *m/e* 222 (100, M⁺), 156 (20.1, M⁺-pyrrolyl), 154 (20.1, M⁺-pyrrolyl-2H), 145 (65.4, M⁺-phenyl); HR-MS (EI, 150°C) *m/e* calc'd for C₁₅H₁₄N₂: 222.11569; found 222.11571.

3-(phenylhydroxymethyl)-1-tosyl-pyrrole (**194**)

193 (100 mg, 3.08 x 10⁻⁴ mol) dissolved in dry THF (10 mL) was treated under anhydrous conditions with LAH (58 mg, 5 equiv.). No starting material was detectable {TLC, R_f = 0.8 (silica, CH₂Cl₂/0.5 % MeOH)} after 1h at r.t. The reaction was carefully quenched by the addition of Glauber's salt and then some H₂O. The mixture was partitioned between H₂O and CHCl₃ (50 mL each), the organic phase was isolated, dried over Na₂CO₃ and evaporated *in vacuo* to give a colorless oil (90 mg, 90 % yield) which showed partial crystallization upon standing. As judged by NMR, the material thus produced is pure. Although **195** seemed to be stable, it was generally directly used in the next step.

MW = 328.41; R_f = 0.65 (silica-CH₂Cl₂/0.5 % MeOH); ¹H-NMR (200 MHz, CDCl₃) δ 2.25 (s, 3H), 2.75 (br, 1H), 5.05 (s, 1H), 6.06 (overlapping d, 1H), 6.94 (m, 2H), 7.10-7.23 (m, 7H), 7.59 (d, *J* = 8 Hz, 2H); ¹³C-NMR (50 MHz, CDCl₃) δ 21.60, 70.50, 112.76, 117.91, 121.38, 126.89, 127.11, 127.75, 128.26, 130.05, 132.67, 135.95, 143.16, 145.11; LR-MS (EI, 180°C) *m/e* 327 (31), 325 (18), 310 (M⁺-H₂O, 8), 248 (22), 155 (52), 105 (82), 91 (100); HR-MS (EI, 150°C) *m/e* calc'd for C₁₈H₁₈NSO₃: 328.1007; found: 328.0972.

Phenyl-2-pyrrolyl-(1-tosyl-3-pyrrolyl)-methane (**196**)

195 (1.22 g, 3.72 mmol) dissolved in glacial acetic acid (50 mL) containing five drops of acetic anhydride and pyrrole (1.2 mL, 5 eq) was refluxed under anhydrous conditions for 1h. The mixture was evaporated to dryness under high vacuum (it is important to remove all excess pyrrole as it proves hard to separate large amounts of pyrrole from the desired compound by chromatography), and the resulting oil was purified by flash

chromatography (silica-CHCl₃). The fraction containing the least polar compound was isolated. 900 mg (91 % yield) of **196** as an oil were thus produced.

MW = 376.47; R_f = 0.75 (silica-CH₂Cl₂); ¹H-NMR (200 MHz, CDCl₃) δ 2.42 (s, 3H), 5.25 (s, 1H), 5.83 (m, 1H), 6.14 (m, 1H), 6.17 (q, *J* = 1.7 Hz, 1H), 6.65 (m, 1H), 6.86 (m, 1H), 7.10-7.22 (m, 3H), 7.25-7.35 (m, 5H), 7.72 (d, *J* = 8 Hz, 2H), 7.86 (br s, 1H); ¹³C-NMR (50 MHz, CDCl₃) δ 21.66, 43.19, 107.13, 108.23, 114.70, 117.16, 118.93, 121.34, 126.85, 128.43 (br), 128.59, 130.03, 131.45, 133.10, 136.10, 142.57, 145.00.

N-Confused porphyrin (**104**)

183 (125 mg, 2.9 × 10⁻⁴ mol) dissolved in MeOH/CH₂Cl₂ (4 mL of a 1:1 mixture) and NaBH₄ (100 mg, 2.6 mmol) was added in portions over 10 min. After 10 more min. of stirring, brine was added to the solution, the organic phase was separated, the aqueous phase extracted with CH₂Cl₂ (3 × 10 mL) and the combined and the dried (Na₂CO₃) extracts were evaporated to dryness. The presence of the dihydroxy compound **197** was seen by TLC {R_f = 0.2 (silica, CH₂Cl₂/5%MeOH), stains bright red with Br₂}. The freshly prepared **197** was dissolved in CH₂Cl₂ (25 mL) and an equimolar amount of **190** (65 mg) was added. A catalytic amount of *p*-toluenesulfonic acid·H₂O was added and the slowly darkening mixture was stirred at r.t. for 2h. After this time, DDQ (65 mg, 2 equiv.) was added and the mixture was stirred for 2 d. After this time, the optical spectrum of the crude mixture exhibited a Soret-type band at 434 nm and a weaker band at 740 nm. Both bands are indicative for the presence of **104**, however, preparative TLC separation of the mixture did not allow isolation of **104** in larger amounts than 6-9 mg, corresponding to 3-5% yield. No TPP was formed during the reaction.

3.4 THE DIRECTED SYNTHESIS OF SAPPHYRINS

10,15-Diphenylsapphyrin (**200**)

Bipyrrole dialdehyde **201** (94 mg, 5.0×10^{-4} mol) and tripyrrane **180** (188 mg, 1 equivalent) were dissolved, with the help of a heat gun, in a beaker containing dry EtOH (450 mL). To facilitate the dissolution of **201**, it has to be either finely powdered or dissolved in DMSO (0.5-1 mL) first, and this solution is then mixed with the EtOH. *p*-Toluenesulfonic acid monohydrate (380 mg, 2 mmol) dissolved in 1 mL EtOH was slowly added to the vigorously stirred solution. The mixture turned royal blue (broad bands at λ_{\max} 360, 580 nm) over the course of 15 minutes. The mixture was allowed to evaporate completely over several days. The resulting dark crust is collected and broken up (and dried under high vacuum in cases where DMSO had been used to dissolve the dialdehyde), and thoroughly triturated with CHCl_3 (5 x 20 ml). The combined brilliant green extracts were evaporated *in vacuo* and the resulting crude **200** was chromatographed on alumina preparative TLC plates with $\text{CH}_2\text{Cl}_2/0.1\%$ Et_3N as eluent. The main band was isolated, extracted with CH_2Cl_2 and the product was precipitated by solvent exchange with cyclohexane to give 22 mg (8 %) of **200**. Washing of a CHCl_3 solution of **200** with aqueous HCl or HIO_3 converts the green-yellow free base solution into a bright yellow solution of the corresponding protonated form.

MW = 539.58; R_f = 0.18 (silica-5%MeOH/ CH_2Cl_2); $^1\text{H-NMR}$ (400 MHz, CDCl_3) δ -1.52 (s, 2H), -0.1-0 (br s, 2H), 7.15-7.20 (m, 1H); 7.25-7.30 (m, 1H), 7.60 (tr, 3J = 7 Hz, 2H), 7.85 (tr, 3J = 8 Hz, 4H), 8.49 (br s, 4H), 9.24 (d, 3J = 4.5 Hz, 2H), 9.43 (d, 3J = 4.5 Hz, 2H), 9.60 (d, 3J = 4.5 Hz, 2H), 10.20 (d, 3J = 5.0 Hz, 2H), 10.27 (s, 2H); UV-Vis ($\text{CH}_2\text{Cl}_2/\text{trace Et}_3\text{N}$) λ_{\max} (log ϵ) 478 (4.86), 506 (4.71), 626 (3.67), 686 (3.97), 708 (sh), 786 (3.62) nm; LR-MS (EI, 200°) m/e 527 (100, M^+), 450 (14.6, M^+ -phenyl), 264 (M^{++} , 27.9); HR-MS (EI, 180°) m/e calc'd for $\text{C}_{36}\text{H}_{25}\text{N}_5$: 527.21100, found 527.21015.

200·2HCl:

$^1\text{H-NMR}$ (400 MHz, CDCl_3) δ -4.69 (s, 2H), -4.48 (s, 2H), -3.87 (s, 1H), 7.26 (d, $^3J = 8$ Hz, 1H), 7.80 (d, $^3J = 8$ Hz, 1H); 8.65 (d, $^3J = 5$ Hz, 4H), 9.33 (d, $^4J = 0.8$ Hz, 2H), 9.63 (dd, $^3J = 5$ Hz, $^4J = 0.8$ Hz, 2H), 10.25 (dd, $^3J = 5$ Hz, $^4J = 0.8$ Hz, 2H), 10.46 (dd, $^3J = 5$ Hz, $^4J = 0.8$ Hz, 2H), 10.78 (dd, $^3J = 5$ Hz, $^4J = 0.8$ Hz, 2H), 11.92 (s, 2H); $^{13}\text{C-NMR}$ (75 MHz, CDCl_3) δ 145.69, 140.61, 136.45, 131.68, 130.56, 130.28, 129.91, 129.83, 129.79, 128.83, 128.56, 126.75, 124.90, 123.15, 104.22, 102.71; UV-Vis ($\text{CH}_2\text{Cl}_2/\text{trace HCl}$) λ_{max} (log ϵ) 482 (5.47), 656 (4.13), 682 (4.13), 724 (sh), 758 (4.70) nm;

3,22-Diethyl-2,23-dimethyl-5,10-diphenylsapphyrin (199)

Tripyrrane **180** (22.6 mg, 6×10^{-5} mol) and bipyrrrole dialdehyde **112** (16.3 mg, 1 equivalent) were dissolved under anhydrous conditions in absolute EtOH (60 mL). Molecular oxygen was bubbled at r.t. through the solution. *p*-Toluenesulfonic acid monohydrate (45.6 mg, 4 equivalents) was added to this solution, and a slow oxygen bubble was maintained for 12 h. The solution turned from an initial red through aquamarine to green. The dark green solution was evaporated to dryness *in vacuo* and the resulting dark solid was subjected to column chromatography (alumina neutral, activity I-2.5% MeOH/ CH_2Cl_2). The first (purple) fraction (minute amount of TPP) was discarded and the second (green) main fraction was collected. Precipitation from hexane gave 14.3 mg (39% yield) of **199** as dark green powder. It had identical spectroscopic properties to those reported by Sessler, Kodadek and co-workers.³⁸⁴

5,10,15,20-Tetraphenylsapphyrin (114)

Bipyrrrole (**203**) (26.4 mg, 2×10^{-4} mol), tripyrrane **180** (75 mg, 1 equivalent), and benzaldehyde (42 μL , 2 equivalents) were dissolved under anhydrous conditions in dry CH_2Cl_2 (20 mL), and the solution was degassed by bubbling nitrogen through it for 20 min. One drop of BF_3 -etherate was added and the mixture was stirred for 1 h. *p*-Chloranil

(100 mg, 4×10^{-4} mol) was added and the mixture was refluxed for 1 h. After this time, the mixture was evaporated *in vacuo* to dryness and the residue was subjected to flash chromatography (alumina, neutral, activity II- CH_2Cl_2), separating the by-product TPP and a yellow-green fraction containing the sapphyrin. The latter fraction was evaporated to dryness and chromatographed on a preparative plate (alumina- $\text{CH}_2\text{Cl}_2/\text{CCl}_4$ 1:1). The main band was extracted with CH_2Cl_2 and slow evaporation of this solution provided 3.6 mg (3.7%) of dark green sparkly crystals of **114**. It proved identical with the tetraphenylsapphyrin described by Chmielewski *et al.*³¹⁵

3.5 THE PREPARATION OF CYANOPYRROLES

2-Cyano-1-methylpyrrole (215)

This product has been described before by Barnett *et al.*³⁸⁶ These authors prepared it from in 67% from 1-methyl pyrrole and chlorosulfonyl isocyanate. The synthesis to be described here details an alternative synthesis,⁴¹⁴ and complements the analytical data provided by Anderson.³⁹⁹

2-Cyanopyrrole (207) (1.1 g, 11.58 mmol) dissolved in CH₃CN (5 mL) was added dropwise under N₂ into a suspension of KH (~ 700 mg, 1.5 equiv., from a mineral oil suspension, washed with dry CH₃CN) in CH₃CN (25 mL). The suspension was refluxed for 1 h, during which time most of the KH went into solution. The reaction mixture was cooled and methyl iodide (865 mL, 1.2 equivalent) was syringed into the ice-cold solution. The mixture was then refluxed for an additional 1.5 h. The fine white precipitate of KI was then filtered (glass frit-M) from the cooled solution, and the filtrate evaporated *in vacuo* to give a pale yellow oil. This oil was subjected to flash column chromatography (silica gel, 25 x 3 cm, CHCl₃). The first major fraction was collected, to give, after evaporation of the solvent, 745 mg (60.7 %) of a colourless liquid, which, based on the ¹H-NMR, was pure. Due to its low boiling point (72-75°C/9 torr)³⁸⁶, it is likely that some product was lost during the work-up.

MW = 106.13; R_f = 0.71 (silica-CHCl₃); ¹H-NMR (200 MHz,) δ 3.72 (s, 3H), 6.10 (dd, J = 4.0, 4.0 Hz, 1H), 6.78 (dd, J = 4.0, 2.0 Hz, 1H), 6.71 (m, 1H); ¹³C-NMR (50 MHz, CDCl₃) δ 35.2, 104.3, 109.4, 113.8, 119.8, 127.6; MS (EI, 150°C) *m/e* 106 (100, M⁺), 105 (82.0, M⁺-H), 78 (31.0), 64 (12.3), 52 (14.0); HR-MS (EI, 150°C) *m/e* calc'd for C₆H₆N₂: 106.05310, found 106.05302.

3-Cyano-2,5-dimethylpyrrole (214)

General Procedure for the preparation of cyanopyrroles from CSI and the corresponding pyrroles

2,5-Dimethylpyrrole (211) (1.0 g, 10.5 mmol) was dissolved under anhydrous conditions in a mixture of DMF (2 mL) and CH₃CN (10 mL) in a flask equipped with a septum, and was cooled in an icebath to -5°C. Chlorosulfonylisocyanate (CSI) (1 equivalent, 911 mL, 1.48 g) dissolved in dry CH₃CN (5 mL) was syringed into the stirred solution. No starting material was detectable by TLC after 15 min. The orange solution was then quenched by pouring it into aqueous Na₂CO₃ (100 mL, 5 % w/w). After the solution was stirred for 1 h at room temperature, it was extracted with CHCl₃ (3 x 50 mL). The combined organic layers were thoroughly washed with water, dried over Na₂CO₃ and evaporated to dryness. The partially solidified oil was loaded onto a flash chromatography column (silica gel, 25 x 3 cm-CHCl₃). The first major fraction gave after vacuum evaporation of the solvent and drying (20°C/0.2 torr; the compound sublimes easily) the desired compound in 70.5 % (1.25 g) yield as fine, colorless crystals. An analytical sample was sublimed at 70°C/0.2 torr. A second, minor (~ 5%) fraction proved to be 3,4-cyano-2,5-dimethylpyrrole (217):

MW = 120.15; m.p. = 85.0°C; R_f = 0.63 (silica-CH₂Cl₂); ¹H-NMR (200 MHz, CDCl₃) δ 2.18 (s, 3H), 2.35 (s, 3H), 5.95 (d, 1.5 Hz, 1H), 8.40 (br s, 1H); ¹³C-NMR (50 MHz, CDCl₃) δ 12.0, 12.5, 90.0, 107.8, 118.0, 127.7, 136.7; LR-MS (EI, 150°C) 120 (52.5, M⁺), 119 (100), 105 (13.9), 92 (12.4), 78 (9.3), 65 (8.9); HR-MS (EI, 150°C) *m/e* calc'd for C₇H₈N₂: 120.06875, found 120.06822; Analysis calc'd for C₇H₈N₂: C, 69.97; H, 6.71; N, 23.31; found: C, 70.15; H, 6.44; N, 23.18.

3,4-Dicyano-2,5-dimethylpyrrole (**217**)

Either isolated as side (~ 5%) product of the preparation of **214**, or 62 % yield after chromatography from 2,5-dimethylpyrrole following the general procedure, albeit with 2.5 equivalents of CSI:

MW = 145.16; m.p. 242-244° (dried at 80°C/ 0.2 torr, 15 h); R_f = 0.27 (silica-CH₂Cl₂); ¹H-NMR (200 MHz, acetone-d₆) δ 2.35 (s, 6H), 11.2 (v br s, 1H); ¹³C-NMR (50 MHz, acetone-d₆) δ 11.7, 93.00, 114.5, 138.9; LR-MS (EI, 150°C) 145 (46.8, M⁺), 144 (100, M⁺-H), 5.0 (11.7, C₇H₇N₂⁺); HR-MS (EI, 150°C) *m/e* calc'd for C₈H₇N₃: 145.06400, found 145.06332.

2-Cyano-3,5-dimethyl-4-ethylpyrrole (**213**)

Prepared in 69 %yield from 3,4-dimethyl-4-ethylpyrrole (**210**) and 1.2 equivalents of CSI according to the general procedure. The crude product can be filtered off after the hydrolysis step (48 h, 5°C). Either column chromatography (silica-CH₂Cl₂) or sublimation (110°C/760 torr) gives analytical pure material as a white solid or long, colorless needles, respectively.

MW = 148.21; m.p. 133-134° (sublimed material); R_f = 0.31 (silica-CH₂Cl₂/0.5% MeOH); ¹H-NMR (200 MHz, CDCl₃) δ 1.04 (tr, 3.6 Hz, 3H), 2.12 (s, 3H), 2.18 (s, 3H), 2.35 (q, 3.6 Hz, 2H), 8.40 (br s, 1H); ¹³C-NMR (50 MHz, CDCl₃) δ 10.0, 11.4, 15.0, 96.7, 102.8, 115.5, 122.6, 130.4, 131.1; LR-MS (EI, 150°C) *m/e* c 148 (25.3, M⁺), 133 (100, M⁺-CH₃), 32 (63.8); HR-MS (EI, 150°C) *m/e* calc'd for C₉H₁₂N₂: 148.0005, found 148.0001; Analysis calc'd for C₉H₁₂N₂: C, 72.94; H, 8.16; N, 18.90; found: C, 73.17; H, 8.23; N, 19.00.

2-Cyano-3,4-diethylpyrrole (**212**)

Prepared from 3,4-diethylpyrrole (1.165 g, 9.46 mmol) in 76 % yield according the general procedure. Chromatographic (CHCl₃/silica, 12 x 3 cm) workup and evaporation of

the solid *in vacuo* produces **212** as a slightly pink, coarse crystalline solid. An analytical sample was sublimed at 70°C/0.2 torr. Chromatography also yielded a minor amount of **216**.

MW = 148.20; mp = 133-134°C (sublimed material); $R_f = 0.39$ (silica-CH₂Cl₂); ¹H-NMR (300 MHz, CDCl₃) δ 1.98 (two overlaying (separated by 1 Hz) tr, $J = 7.5$ Hz, 6H), 2.41 (d of q, $J = 0.8, 7.5$ Hz, 2H), 2.57 (q, 7.5 Hz, 2H), 6.65 (d, 2.5 Hz, 1H), 8.95 (br s, 1H); ¹³C-NMR (50 MHz, CDCl₃) δ 14.6, 15.0, 18.0, 18.2, 98.6, 115.2, 120.8, 125.8, 136.5; LR-MS (EI, 150°C) 148 (29.8, M⁺), 133 (100, M⁺-CH₃), 118 (20.7, M⁺-C₂H₆), 106 (10.4), 91 (9.9), 77 (16.5); HR-MS (EI, 150°C) m/e calc'd for C₉H₁₂N₂: 148.10005, found 148.10045; Analysis calc'd for C₉H₁₂N₂: C, 72.94; H, 8.16; N, 18.90; found: C, 73.00; H, 8.27; N, 19.02.

2,5-Dicyano-3,4-diethylpyrrole (**216**):

Isolated in small amounts as side-product in the preparation of **212** or prepared from 3,4-diethylpyrrole (**209**) (0.5 g, 4.06 mmol) and excess CSI in 47 % yield according to the general procedure. After the addition of the CSI (0.833 mL, 2.5 equ.), the mixture was refluxed for 1 h. Hydrolysis was accomplished over an extended period of time (12 h) on the steam bath. The crude mixture was purified by flash chromatography (silica, 10 x 3 cm, CH₂Cl₂).

MW = 173.22; $R_f = 0.4$ (silica-CH₂Cl₂/2.5% MeOH); ¹H-NMR (200 MHz, acetone-d₆) δ 1.18 (tr, 7.5 Hz, 6H), 2.56 (q, 7.5 Hz, 4H), 10.9 (br s, 1H); ¹³C-NMR (50 MHz, acetone-d₆) δ 11.7, 93.0, 116.5, 139.8; LR-MS (EI, 150°C) 173 (25.5, M⁺), 158 (100, M⁺-CH₃); HR-MS (EI, 150°C) m/e calc'd for C₁₀H₁₁N₃: 173.09529, found 173.09512; Analysis calc'd for C₁₀H₁₁N₃: C, 69.34; H, 6.40; N, 24.26; found: C, 69.62; H, 6.38; N, 24.30.

3.6 THE REDUCTIVE COUPLING OF 2-CYANOPYRROLES

(2-Pyrrolylmethene)-(2-pyrrolylmethyl)imine (**204**)

General Procedure for the reductive coupling of 2-cyanopyrroles

2-Cyanopyrrole (**207**)(2.0 g, 21.67 mmol) dissolved in dry THF (10 mL) was carefully added dropwise under anhydrous conditions into a cooled (0°C) and vigorously stirred suspension of LAH (960 mg, 24.2 mmol) in THF (30 mL) over 20 min. After completion of the addition, the reaction mixture was stirred for one additional hour at 0°C. To quench the reaction, Glauber's salt (Na₂SO₄ · 10 H₂O, ~2.0 g) was slowly added until gas evolution ceased. The resulting colorless thick slurry was filtered through a pad of Celite® 545 and the filter cake thoroughly rinsed with CHCl₃ (~ 50 mL). The combined filtrates were evaporated to dryness on a rotary evaporator to give the desired imine (1.61 g, 85.5 %) as an off-white solid. Recrystallization from EtOH/H₂O gives **204**, after drying at high vacuum at 50°C, as analytically pure shiny plates. If fumed with Br₂, the colorless spot of this compound on a silica gel TLC plate turns slowly and characteristically into a yellow spot with purple edges.

MW = 173.22; mp = 155-157°C³⁸⁵; R_f = 0.16 (silica-CH₂Cl₂/5% MeOH); ¹H-NMR (200 MHz, acetone-d₆) δ 4.59 (s, 2H), 5.93 (s, 1H), 5.98 (t, *J* = 2.0 Hz, 1H), 6.14 (dd, *J* = 2.0, 2.0 Hz, 1H), 6.42 (dd, *J* = 1.9, 2.0 Hz, 1H), 6.67 (narrow m, 1H), 6.91 (narrow m, 1H), 9.85 (br s, 1H), 10.65 (br s, 1H); ¹³C NMR (50 MHz, CDCl₃) δ = 56.7, 106.2, 108.5, 110.0, 115.3, 117.6, 122.5, 129.3, 129.8, 152.9; LR-MS (EI, 150°C) *m/e* 173 (63.6, M⁺), 96 (86.1), 92 (89.2), 80 (100, C₅H₆N⁺), 68 (50.5); HR-MS (EI, 150°C) *m/e* calc'd for C₁₀H₁₁N₃: 173.09529, found 173.09535.

Bis(2-pyrrolylmethyl)amine (208)

204 (0.1 g, 5.8×10^{-4} mol) dissolved in THF (10 mL) was added under anhydrous conditions and at 0°C to a suspension of LAH (44 mg, 2 equivalents) in dry THF (5 mL). The reaction mixture was quenched with Glauber's salt ($\text{Na}_2\text{SO}_4 \cdot 10 \text{H}_2\text{O}$, 0.2 g) and the resulting slurry filtered through a pad of Celite®. The filtrate was evaporated on a rotary evaporator to give the desired amine as a colourless and odorless oil. It was, based on $^1\text{H-NMR}$, $\geq 95\%$ pure. The amine is not visible under a UV lamp if spotted on a TLC plate (with fluorescence indicator), however, Br_2 fumes make it visible.:

MW = 175.26; $R_f = 0.1$ (silica- $\text{CH}_2\text{Cl}_2/7\%$ MeOH); $^1\text{H-NMR}$ (200 MHz, CDCl_3) δ 2.65 (br s, 1H), 6.08 (s, 2H), 6.15 (s, 2H), 6.68 (s, 2H), 8.70 (br s, 2H); $^{13}\text{C-NMR}$ (50 MHz, CDCl_3) δ 45.6, 106.9, 108.2, 117.6, 129.9; LR-MS (EI, 180°C) m/e 175 (30.1, M^+), 158 (37.8), 108 (57.9, M^+ -pyrrole), 95 (93.8, $\text{C}_5\text{H}_7\text{N}^+$), 80 (100, $\text{C}_5\text{H}_6\text{N}^+$), 68 (63.1, $\text{C}_4\text{H}_6\text{N}^+$); HR-MS (EI, 180°C) m/e calc'd for $\text{C}_{10}\text{H}_{13}\text{N}_3$: 175.11095, found 175.11107.

The Reduction Experiments of Cyanopyrroles 212, 213, and 215

Following the general procedure, ca. 100 mg of the respective cyanopyrroles were reduced. The crude reaction mixtures were evaporated to dryness and dried under high vacuum at ambient temperature. The resulting oils or solids were taken up in CDCl_3 and the success of the experiments was judged, in addition to the evaluation of the LR-MS of the crude mixtures, by the resulting $^1\text{H-}$ and $^{13}\text{C-NMRs}$. The product ratios are determined by the integration of the $^1\text{H-NMR}$.

Reduction of 2-cyano-3,4-diethylpyrrole (212)

This reduction produces 2-(aminomethyl)-3,4-diethylpyrrole (**225**) and the imine linked dimer **227** in variable ratios between 3:2 and 2:1. $^1\text{H-NMR}$ (200 MHz, CDCl_3) δ 1.3-1.4 (m, $-\text{CH}_2\text{CH}_3$ of **225** and **227**), 2.25-2.65 (m, $-\text{CH}_2\text{CH}_3$ of **225** and **227**), 3.2 (br s, $-\text{NH}_2$

of **225**), 3.82 (s, $-\text{CH}_2\text{NH}_2$ of **225**), 4.78 (s, $=\text{N}-\text{CH}_2-$ of **227**), 6.5-6.6 (pyrrole-H of **225** and **227**), 8.30 (s, $-\text{C}_\text{H}=\text{N}$ of **227**), 8.80 (br s, pyrrolylmethyl-NH of **227**, the corresponding signal for the pyrrolylmethene-NH is observed at shifts >12 ppm), 9.1 (br s, NH of **225**).

Reduction of 2-cyano-4-ethyl-3,5-dimethylpyrrole **213**

This reduction leads to the exclusive formation of the imine linked dimer **228**. ^1H -NMR (200 MHz, CDCl_3) δ 1.05-1.2 (m, 6H), 2.03 (s, 3H), 2.07 (s, 3H), 2.10 (s, 3H), 2.19 (s, 3H), 2.35-2.47 (m, 4H), 4.62 (s, 2H), 8.20 (s, 1H); ^{13}C -NMR (50 MHz, CDCl_3) δ 8.8, 9.1, 10.7, 11.1, 15.5, 15.8, 17.3, 17.7, 55.4, 113.2, 120.7, 121.8, 122.7, 123.0, 124.1, 126.7, 127.9, 150.6; LR-MS (EI, 200°C) m/e 283 (23, M^+2H), 179 (20), 163 (82), 136 (100).

Reduction of 2-cyano-1-methylpyrrole (**215**)

This reduction gives 2-(aminomethyl)-1-methylpyrrole (**223**) and a second product (imine linked dimer (?)) ^1H -NMR (200 MHz, CDCl_3) δ 1.2, 3.8, 4.6, 6.5, 6.6, 8.2; $m/e = 201$ in the ratio of 1:13 as judged by ^1H -NMR). However, this second product could not be produced in a large enough quantity to undoubtedly determine its structure.

223:

^1H -NMR (200 MHz, CDCl_3) δ 3.61 (s, 3H), 3.82 (s, 2H), 5.95-6.1 (m, 2H), 6.58 (m, 1H); ^{13}C -NMR (50 MHz, CDCl_3) δ 33.6, 38.1, 106.3, 106.6, 122.2, 134.2; LR-MS (EI, 200°C) m/e 110 (53, M^+), 94 (100, M^+-NH_2).

3.7 THE FORMATION OF COMPLEX 236

[SP-4]-[(2-dipyrinato- κ^2 N,N'-methyl)(2-pyrrolylmethenato- κ N"-)imine- κ N''']nickel(II)
(236)

Imine **204** (200 mg, 1.16 mmol), 2-pyrrolealdehyde (**206**) (110 mg, 1.16 mmol) and nickel(II) acetate tetrahydrate (500 mg, 2.0 mmol), dissolved in a 2:1 mixture of EtOH and CHCl₃ (15 mL), were heated at reflux temperature for 1h. The initially pale green color of the solution turned time dark orange during that time. Evaporation *in vacuo* of the reaction mixture gave a solid which was triturated with CHCl₃ (4x5 mL). The volume of the dark orange solution was reduced and chromatographed (silica gel, 2x12 cm, CHCl₃). The first major orange band was collected and evaporated to dryness. The resulting solid was dissolved in CH₂Cl₂, and slow solvent exchange with cyclohexane resulted in the formation of analytically pure **236** as shiny metallic green dichroic short needles (125 mg, 35%). For the details of the X-ray crystal structure determination see below.

MW = 306.98; m.p. = 184 °(drying conditions 50°C at 0.1 torr); R_f = 0.90 (silica-CHCl₃); ¹H-NMR (400 MHz, acetone-d₆) δ = 4.60 (s, 2H), 6.01 (dd, *J* = 2.0 Hz, 3.8H, 1H), 6.29 (d, *J* = 4.2 Hz, 1H), 6.41 (dd, *J* = 4.2, 1.7 Hz, 1H), 6.57 (dd, *J* = 3.7, 0.8 Hz, 1H), 7.02 (d, *J* = 4.2 Hz, 1H), 7.09 (dd, *J* = 4.1, 1.1 Hz, 1H), 7 (25, s, 1H), 7.53 (s, 1H), 7.69 (s, 1H); ¹³C-NMR (50 MHz, CDCl₃/10% acetone-d₆) δ 54.0 (=C-), 111.3 (=C-), 112.8 (=C-), 117.0 (=C-), 117.8 (=C-), 129.7 (=C-), 129.9 (=C-), 131.6 (=C-), 133.5 (=C=), 136.9 (=C-), 139.7 (=C=), 146.2 (=C=), 151.1 (=C-), 158.9 (=C-), 162.9 (=C=); UV-Vis (CH₂Cl₂) λ_{\max} (log ϵ) 314 (4.08), 354 (4.11), 394 (4.12), 508 (4.40) nm; LR-MS (EI, 150°C) *m/e* : 311 (1.1), 310 (4.5), 309 (10.5), 308 (34.2), 307 (50.0), 306 (83.9), 305 (100.0); HR-MS (EI, 150°C) *m/e* calc'd for C₁₅H₁₂N₄⁵⁸Ni: 306.04153, found 306.04013; Analysis calc'd for C₁₅H₁₂N₄Ni: C, 58.69; H, 3.94; N, 18.25; found: C, 58.51; H, 3.74; N, 18.00.

3.8 CRYSTAL STRUCTURE ANALYSES OF 163-PYRIDINE, 175 AND 236

The crystals of **163** (**175** and **236**) were mounted on a glass fibre and all measurements were made at $21 \pm 1^\circ\text{C}$ on a Rigaku AFC6S diffractometer. Selected crystallographic data appear in Table 1-2. The final unit-cell parameters were obtained by least-squares on the setting angles for 25 reflections in the range $93.9 < 2\theta < 104.9^\circ$ ($80.6 < 2\theta < 97.5$, and $34.1 < 2\theta < 38.8$). Of the 9000 (7834 and 5135) reflections which were collected, 8602 (7492 and 5014) were unique ($R_{\text{int}} = 0.020, 0.017$ and 0.032). The intensities of three standard reflections, measured every 200 reflections throughout the data collections, decreased by 1.2% in **236**. A linear correction factor was applied to the data to account for this phenomenon. No decay correction was applied for **163** and **175**. The data were processed and corrected for Lorentz and polarization effects. All structures were solved by the heavy atom Patterson method and expanded using Fourier techniques. Hydrogens were refined isotropically. Neutral atom scattering factors for all atoms and anomalous dispersion corrections for the non-hydrogen atoms were taken from the *International Tables for X-Ray Crystallography*.⁴¹⁸ Final atomic coordinates and equivalent isotropic thermal parameters of and selected bond lengths in **163-pyridine**, **175** and **236** appear in Tables 1-3 to 1-8.

There is one molecule of pyridine in **163-pyridine** in the asymmetric unit. The lactone group in **163-pyridine** was modeled as disordered over five states. The site occupancies of the carbonyl oxygen atoms were constrained to total of 1.0 and were adjusted as the refinement progressed to yield approximately equal equivalent isotropic thermal parameters. The associated ring atoms were treated as part C and part O, based on the appropriate carbonyl oxygen populations.

The crystal of **175** is a solid solution of four different compounds differing only in the alkoxy groups OR and OR': R = R' = Me; R = Me, R' = Et; R = Et, R' = Me; R = R' = Et.

Table 1-2 Crystallographic data for **163-pyridine**, **175**, and **236**

compound	163-pyridine	175	236
crystal	purple prism	green prism	red prism
dimensions, mm	0.17x0.28x0.35	0.20x0.25x0.30	0.35x0.35x0.50
empirical formula	C ₅₃ H ₃₆ N ₆ O ₂ Zn	C ₄₇ H ₃₆ N ₄ NiO ₃	C ₁₅ H ₁₂ N ₄ Ni
MW	854.29	763.53	306.99
crystal system	triclinic	triclinic	monoclinic
space group	<i>P</i> $\bar{1}$ (#2)	<i>P</i> $\bar{1}$ (#2)	C2/c (#15)
a, Å	13.2954(8)	13.447(2)	21.461(1)
b, Å	14.899(2)	13.950(1)	5.362(1)
c, Å	11.226(2)	11.015 (2)	22.0841(9)
α, deg	93.46(1)	102.180(9)	
β, deg	104.728(8)	112.768(9)	92.748(4)
γ, deg	99.707(7)	94.074(9)	
V, Å ³	2107.4(4)	1835.4(4)	2538.4(4)
Z	2	2	8
D _{calc} , g/cm ³	1.346	1.381	1.606
radiation	CuK α	CuK α	MoK α
λ, Å	1.54178	1.54178	0.71069
μ, cm ⁻¹	12.08	11.57	15.22
Transmission factors			0.921-1.00
R; R ω	0.036, 0.038	0.044; 0.042	0.032; 0.024
gof	2.46	1.13	1.68

Table 1-3 Atomic coordinates and $B_{eq.}[\text{\AA}^2]^a$ for **163**-pyridine

Atom ^b	x	y	z	$B_{eq.}$	Occupancy
Zn(1)	0.16039(2)	0.21047(2)	0.42785(3)	3.724(7)	
O(1) ^a	0.2056(2)	-0.0285(1)	0.2341(2)	5.04(5)	
O(2)	0.0581(4)	-0.1160(3)	0.1476(4)	7.1(1)	0.45
O(2a)	0.2265(7)	-0.0872(7)	0.1718(9)	7.3(3)	0.22
O(2b)	0.1002(7)	0.4675(6)	0.7549(10)	7.2(3)	0.21
O(2c)	-0.242(3)	0.157(2)	0.486(3)	8.1(8)	0.07
O(2d)	0.270(3)	0.497(3)	0.794(4)	6.4(9)	0.05
N(1)	0.1583(1)	0.0813(1)	0.3458(2)	3.78(4)	
N(2)	0.0080(1)	0.1624(1)	0.4393(2)	3.79(4)	
N(3)	0.1721(1)	0.3150(1)	0.5631(2)	3.70(4)	
N(4)	0.3232(1)	0.2314(1)	0.4723(2)	3.71(4)	
N(5)	0.1165(2)	0.2750(1)	0.2615(2)	4.30(5)	
N(6)	0.652(2)	0.2261(8)	-0.0199(7)	18.2(4)	
C(1)	0.2405(2)	0.0527(1)	0.3139(2)	3.77(5)	
C(2) ^b	0.0946(2)	-0.0510(1)	0.2153(2)	4.86(5)	
C(3)	0.0685(2)	0.0191(1)	0.2879(2)	3.86(5)	
C(4)	-0.0332(2)	0.0205(1)	0.2967(2)	3.76(5)	
C(5)	-0.0597(2)	0.0853(2)	0.3737(2)	3.97(5)	
C(6) ^c	-0.1623(2)	0.0816(2)	0.3923(2)	5.02(6)	
C(7)	-0.1579(2)	0.1567(2)	0.4688(2)	4.92(6)	
C(8)	-0.0509(2)	0.2081(2)	0.4968(2)	4.05(5)	
C(9)	-0.0143(2)	0.2927(2)	0.5697(2)	3.95(5)	
C(10)	0.0911(2)	0.3399(1)	0.6026(2)	3.85(5)	
C(11) ^d	0.1310(2)	0.4199(2)	0.6912(2)	4.78(6)	
C(12) ^e	0.2386(2)	0.4406(1)	0.7046(2)	4.74(5)	
C(13)	0.2625(2)	0.3751(1)	0.6255(2)	3.84(5)	
C(14)	0.3651(2)	0.3717(1)	0.6194(2)	3.77(5)	
C(15)	0.3925(2)	0.3041(1)	0.5486(2)	3.77(5)	
C(16)	0.4987(2)	0.2983(2)	0.5481(2)	4.38(5)	
C(17)	0.4944(2)	0.2229(2)	0.4719(2)	4.45(6)	
C(18)	0.3837(2)	0.1806(2)	0.4258(2)	3.83(5)	
C(19)	0.3470(2)	0.0968(1)	0.3493(2)	3.77(5)	
C(20)	-0.1223(2)	-0.0503(1)	0.2162(2)	3.73(5)	

C(21)	-0.1672(2)	-0.0347(2)	0.0962(2)	5.08(6)
C(22)	-0.2513(2)	-0.0969(2)	0.0207(2)	5.58(7)
C(23)	-0.2904(2)	-0.1757(2)	0.0626(2)	5.10(6)
C(24)	-0.2454(2)	-0.1927(2)	0.1799(3)	5.85(7)
C(25)	-0.1609(2)	-0.1303(2)	0.2564(2)	5.31(6)
C(26)	-0.0923(2)	0.3350(2)	0.6171(2)	4.16(5)
C(27)	-0.1235(2)	0.3080(2)	0.7195(3)	5.81(7)
C(28)	-0.1960(3)	0.3489(3)	0.7614(3)	7.24(10)
C(29)	-0.2372(3)	0.4175(3)	0.7016(4)	7.6(1)
C(30)	-0.2089(3)	0.4433(2)	0.5992(4)	7.24(10)
C(31)	-0.1363(2)	0.4031(2)	0.5575(3)	5.57(7)
C(32)	0.4534(2)	0.4424(2)	0.7016(2)	4.09(5)
C(33)	0.5025(2)	0.4258(2)	0.8190(2)	6.11(7)
C(34)	0.5838(2)	0.4912(2)	0.8956(3)	6.93(8)
C(35)	0.6169(2)	0.5720(2)	0.8565(3)	6.46(8)
C(36)	0.5691(3)	0.5892(2)	0.7401(4)	7.58(9)
C(37)	0.4875(2)	0.5252(2)	0.6628(3)	6.34(7)
C(38)	0.4245(2)	0.0527(2)	0.3037(2)	3.96(5)
C(39)	0.4781(2)	0.0950(2)	0.2255(2)	4.97(6)
C(40)	0.5486(2)	0.0530(2)	0.1811(3)	6.16(8)
C(41)	0.5672(2)	-0.0309(2)	0.2151(3)	6.40(8)
C(42)	0.5160(3)	-0.0722(2)	0.2947(3)	6.07(8)
C(43)	0.4445(2)	-0.0318(2)	0.3385(2)	4.89(6)
C(44)	0.1257(3)	0.2419(2)	0.1538(3)	6.16(8)
C(45)	0.0940(3)	0.2801(3)	0.0457(3)	7.06(9)
C(46)	0.0500(3)	0.3549(3)	0.0471(3)	7.12(9)
C(47)	0.0376(3)	0.3896(2)	0.1556(3)	8.2(1)
C(48)	0.0724(3)	0.3476(2)	0.2611(3)	6.64(8)
C(49)	0.6010(7)	0.275(1)	0.042(2)	15.7(4)
C(50)	0.642(2)	0.3018(6)	0.146(2)	15.5(5)
C(51)	0.733(2)	0.2885(8)	0.2044(7)	16.2(4)
C(52)	0.7850(7)	0.240(1)	0.153(2)	16.0(4)
C(53)	0.748(2)	0.2107(7)	0.038(2)	15.7(5)

$${}^a B_{eq} = (8/3)\pi^2 \sum \sum U_{ij} a_i^* a_j^* (\mathbf{a}_i \cdot \mathbf{a}_j).$$

^b Superscripts refer to C/O ratios: ^a 55/45, ^b 78/22, ^c 93/7, ^d 95/5, ^e 79/21

Table 1-4. Selected bond lengths [Å] in **163-pyridine** with estimated standard deviations in parentheses

Bond	Distance [Å]	Bond	Distance [Å]
Zn(1)–N(1)	2.075(2)	Zn(1)–N(2)	2.071(2)
Zn(1)–N(3)	2.066(2)	Zn(1)–N(4)	2.058(2)
Zn(1)–N(5)	2.146(2)	O(1)–C(1)	1.397(3)
O(1)–C(2)	1.415(2)	O(2)–C(2)	1.148(4)
O(2a)–O(1)	1.198(9)	O(2c)–C(7)	1.18(4)
O(2d)–C(12)	1.21(4)	N(1)–C(1)	1.357(3)
N(1)–C(3)	1.366(3)	N(2)–C(5)	1.373(3)
N(2)–C(8)	1.370(3)	N(3)–C(10)	1.360(3)
N(3)–C(13)	1.368(3)	N(4)–C(15)	1.381(2)
N(4)–C(18)	1.365(3)	N(5)–C(44)	1.320(3)
C(1)–C(19)	1.402(3)		
C(2)–C(3)	1.427(3)	C(3)–C(4)	1.384(3)
C(4)–C(5)	1.404(3)	C(4)–C(20)	1.501(3)
C(5)–C(6)	1.425(2)	C(6)–C(7)	1.352(3)
C(7)–C(8)	1.444(3)	C(8)–C(9)	1.400(3)
C(9)–C(10)	1.403(3)	C(9)–C(26)	1.490(3)
C(10)–C(11)	1.437(2)	C(11)–C(12)	1.378(3)
C(12)–C(13)	1.410(3)	C(13)–C(14)	1.392(3)
C(14)–C(15)	1.397(3)	C(14)–C(32)	1.501(3)
C(15)–C(16)	1.431(3)	C(16)–C(17)	1.354(3)
C(17)–C(18)	1.447(3)	C(18)–C(19)	1.409(3)

Table 1-5 Atomic coordinates and B_{eq} . [\AA^2]^a for 175

Atom	x	y	z	B_{eq} .	Occupancy
Ni(1)	0.19083(3)	0.28677(4)	0.30436(5)	3.926(10)	
O(1)	-0.1932(2)	0.2892(2)	0.0787(2)	6.37(6)	
O(2)	-0.1273(2)	0.3209(2)	0.3132(2)	6.37(6)	
O(3)	-0.1145(2)	0.2233(2)	-0.0649(3)	7.81(8)	
N(1)	0.0380(2)	0.2880(2)	0.2233(2)	4.08(5)	
N(2)	0.1644(2)	0.1698(2)	0.3562(2)	4.07(5)	
N(3)	0.3433(2)	0.2837(2)	0.3794(2)	4.08(5)	
N(4)	0.2171(2)	0.4065(2)	0.2593(2)	4.22(5)	
C(1)	-0.0077(2)	0.3725(2)	0.2232(3)	4.30(6)	
C(2)	-0.1255(2)	0.3566(2)	0.2030(3)	5.15(7)	
C(3)	-0.1427(2)	0.2102(3)	0.0428(3)	5.37(8)	
C(4)	-0.0393(2)	0.2025(2)	0.1608(3)	4.42(6)	
C(5)	-0.0278(2)	0.1157(2)	0.1979(3)	4.15(6)	
C(6)	0.0675(2)	0.1064(2)	0.3060(3)	4.37(6)	
C(7)	0.0767(2)	0.0348(3)	0.3837(4)	5.85(8)	
C(8)	0.1788(2)	0.0560(3)	0.4844(3)	5.63(8)	
C(9)	0.2362(2)	0.1376(2)	0.4631(3)	4.39(6)	
C(10)	0.3483(2)	0.1701(2)	0.5233(3)	4.34(6)	
C(11)	0.3980(2)	0.2336(2)	0.4734(3)	4.36(6)	
C(12)	0.5122(2)	0.2498(2)	0.5026(4)	5.34(8)	
C(13)	0.5252(2)	0.3065(2)	0.4222(4)	5.36(8)	
C(14)	0.4211(2)	0.3304(2)	0.3487(3)	4.41(6)	
C(15)	0.4030(2)	0.4014(2)	0.2741(3)	4.40(6)	
C(16)	0.3083(2)	0.4418(2)	0.2401(3)	4.56(7)	
C(17)	0.2940(3)	0.5333(2)	0.2029(4)	5.55(8)	
C(18)	0.1995(3)	0.5566(2)	0.2072(4)	5.75(8)	
C(19)	0.1500(2)	0.4758(2)	0.2381(3)	4.55(7)	
C(20)	0.0448(2)	0.4646(2)	0.2376(3)	4.43(7)	
C(21)	-0.2313(3)	0.3056(4)	0.3207(6)	10.0(2)	
C(22)	-0.224(1)	0.246(1)	0.422(2)	12.7(6)	0.38
C(23)	-0.2025(7)	0.1775(8)	-0.2001(9)	9.1(3)	0.65

C(23a)	-0.132(2)	0.159(1)	-0.171(2)	9.2(5)	0.35
C(24)	-0.177(1)	0.184(1)	-0.305(2)	10.0(5)	0.31
C(24a)	-0.161(4)	0.051(4)	-0.238(5)	10.4(9)	0.11
C(25)	-0.1214(2)	0.0298(2)	0.1344(3)	4.41(6)	
C(26)	-0.1933(3)	0.0208(3)	0.1930(3)	6.29(9)	
C(27)	-0.2813(3)	-0.0568(3)	0.1358(4)	7.3(1)	
C(28)	-0.2971(3)	-0.1246(3)	0.0213(5)	6.78(10)	
C(29)	-0.2291(3)	-0.1163(3)	-0.0378(5)	8.9(1)	
C(30)	-0.1400(3)	-0.0398(3)	0.0180(4)	7.9(1)	
C(31)	0.4203(2)	0.1324(2)	0.6387(3)	4.68(7)	
C(32)	0.4363(3)	0.0343(3)	0.6211(4)	6.07(9)	
C(33)	0.5059(3)	0.0026(3)	0.7299(5)	7.3(1)	
C(34)	0.5594(3)	0.0679(3)	0.8551(4)	7.2(1)	
C(35)	0.5447(3)	0.1649(3)	0.8750(4)	6.65(9)	
C(36)	0.4760(2)	0.1975(2)	0.7667(3)	5.51(8)	
C(37)	0.4941(2)	0.4428(2)	0.2442(3)	4.59(7)	
C(38)	0.5017(3)	0.4030(3)	0.1239(4)	6.13(9)	
C(39)	0.5859(3)	0.4417(3)	0.0958(4)	7.1(1)	
C(40)	0.6626(3)	0.5204(3)	0.1880(5)	6.36(10)	
C(41)	0.6566(3)	0.5591(3)	0.3072(5)	7.5(1)	
C(42)	0.5734(3)	0.5206(3)	0.3364(4)	7.3(1)	
C(43)	-0.0096(2)	0.5546(2)	0.2446(3)	4.49(7)	
C(44)	-0.0167(3)	0.6001(3)	0.3642(3)	5.82(9)	
C(45)	-0.0637(3)	0.6859(3)	0.3754(4)	7.0(1)	
C(46)	-0.1055(3)	0.7242(3)	0.2654(5)	7.1(1)	
C(47)	-0.1008(3)	0.6794(3)	0.1452(5)	7.3(1)	
C(48)	-0.0530(3)	0.5947(3)	0.1349(4)	6.19(9)	

$${}^a B_{eq} = (8/3)\pi^2 \sum \sum U_{ij} a_i^* a_j^* (\mathbf{a}_i \cdot \mathbf{a}_j).$$

Table 1-6. Selected bond lengths [Å] in **175** with estimated standard deviations in parentheses

Bond	Distance [Å]	Bond	Distance [Å]
Ni(1)–N(1)	1.900(2)	Ni(1)–N(2)	1.892(2)
Ni(1)–N(3)	1.898(2)	Ni(1)–N(4)	1.887(2)
O(1)–C(2)	1.399(4)	O(1)–C(3)	1.401(4)
O(2)–C(2)	1.414(4)	O(2)–C(21)	1.436(4)
O(3)–C(3)	1.419(4)	O(3)–C(23)	1.468(9)
O(3)–C(23a)	1.24(1)	N(1)–C(1)	1.368(4)
N(1)–C(4)	1.379(3)	N(2)–C(6)	1.363(3)
N(2)–C(9)	1.388(4)	N(3)–C(11)	1.375(4)
N(3)–C(14)	1.380(3)	N(4)–C(16)	1.398(3)
N(4)–C(19)	1.363(4)	C(1)–C(2)	1.505(4)
C(1)–C(20)	1.368(4)	C(3)–C(4)	1.521(4)
C(4)–C(5)	1.358(4)	C(5)–C(6)	1.409(4)
C(5)–C(25)	1.503(4)	C(6)–C(7)	1.429(4)
C(7)–C(8)	1.352(4)	C(8)–C(9)	1.440(4)
C(9)–C(10)	1.386(4)	C(10)–C(11)	1.393(4)
C(10)–C(31)	1.494(4)	C(11)–C(12)	1.431(4)
C(12)–C(13)	1.355(4)	C(13)–C(14)	1.424(4)
C(14)–C(15)	1.392(4)	C(15)–C(16)	1.379(4)
C(15)–C(37)	1.495(4)	C(16)–C(17)	1.424(4)
C(17)–C(18)	1.350(4)	C(18)–C(19)	1.435(4)
C(19)–C(20)	1.411(4)	C(20)–C(43)	1.499(4)
C(21)–C(22)	1.51(2)	C(23)–C(24)	1.35(2)
C(23a)–C(24a)	1.47(5)	C(25)–C(26)	1.366(4)

Table 1-7 Atom Coordinates and B_{eq} [\AA^2] for 236

Atom	x	y	z	B_{eq}
Ni(1)	0.13527(1)	0.17533(6)	0.34572(1)	3.298(7)
N(1)	0.07988(8)	-0.0955(4)	0.35457(9)	3.63(5)
N(2)	0.14371(9)	0.2216(4)	0.42848(8)	3.61(5)
N(3)	0.19076(8)	0.4435(4)	0.34637(9)	3.57(5)
N(4)	0.13797(9)	0.2095(4)	0.25883(8)	3.60(5)
C(1)	0.0550(1)	-0.2484(5)	0.3124(1)	4.46(7)
C(2)	0.0153(1)	-0.4260(6)	0.3368(2)	5.29(8)
C(3)	0.0159(1)	-0.3822(6)	0.3967(2)	5.17(8)
C(4)	0.0562(1)	-0.1788(5)	0.4095(1)	4.30(6)
C(5)	0.0728(1)	-0.0775(6)	0.4654(1)	4.78(7)
C(6)	0.1140(1)	0.1151(5)	0.4763(1)	4.14(6)
C(7)	0.1348(2)	0.2438(6)	0.5297(1)	5.16(8)
C(8)	0.1755(1)	0.4221(6)	0.5139(1)	4.88(7)
C(9)	0.1800(1)	0.4056(5)	0.4505(1)	3.89(6)
C(10)	0.2137(1)	0.5477(6)	0.4049(1)	4.30(7)
C(11)	0.2012(1)	0.5403(5)	0.2943(1)	4.22(7)
C(12)	0.1725(1)	0.4173(5)	0.2443(1)	3.83(6)
C(13)	0.1698(1)	0.4561(6)	0.1820(1)	4.57(7)
C(14)	0.1334(1)	0.2685(6)	0.1573(1)	4.63(7)
C(15)	0.1146(1)	0.1229(5)	0.2049(1)	4.39(7)

$${}^a B_{eq} = (8/3)\pi^2 \sum \sum U_{ij} a_i^* a_j^* (\mathbf{a}_i \cdot \mathbf{a}_j).$$

Table 1-8 Bond lengths in **236** [Å]

Bond	Distance [Å]	Bond	Distance [Å]
Ni(1)–N(1)	1.893(2)	Ni(1)–N(2)	1.845(2)
Ni(1)–N(3)	1.867(2)	Ni(1)–N(4)	1.931(2)
N(1)–C(1)	1.332(3)	N(1)–C(4)	1.409(3)
N(2)–C(6)	1.384(3)	N(2)–C(9)	1.334(3)
N(3)–C(10)	1.470(3)	N(3)–C(11)	1.291(3)
N(4)–C(12)	1.384(3)	N(4)–C(15)	1.352(3)
C(1)–C(2)	1.402(4)	C(2)–C(3)	1.343(4)
C(3)–C(4)	1.412(4)	C(4)–C(5)	1.381(4)
C(5)–C(6)	1.373(4)	C(6)–C(7)	1.419(4)
C(7)–C(8)	1.352(4)	C(8)–C(9)	1.411(3)
C(9)–C(10)	1.480(4)	C(11)–C(12)	1.405(4)
C(12)–C(13)	1.390(3)	C(13)–C(14)	1.371(4)
C(14)–C(15)	1.387(4)		

4. REFERENCES

- (1) Dolphin, D. *Can. J. Chem.* **1994**, *72*, 1005.
- (2) Brown, S. B.; Truscott, T. G. *Chem. Brit.* **1993**, *11*, 955.
- (3) Bonnett, R. *Chem. Soc. Rev.* **1995**, 19.
- (4) North, J.; Coombs, R.; Levy, J. In *Photodynamic Therapy and Biomedical Lasers*; P. Spinelli, M. Dal Fante and R. Marchesini, Ed.; Elsevier Science Publishers: The Netherlands, 1992; pp 103.
- (5) Edelson, M. F. *Sci. Am* **1988**, *68*, 259.
- (6) Raab, O. *Infusoria. Z. Biol.* **1900**, *39*, 524.
- (7) Jesionek, A.; Tappeiner, V. H. *Muench. Med. Wochenschr.* **1903**, *47*, 2024.
- (8) Policard, A. *C. R. Hebd. Soc. Biol. 91*, **1925**, 1422.
- (9) *The Physiological Effects of Radiation Energy*; Laurens, H., Ed.; Tudor Press: New York, 1933.
- (10) Meyer-Betz, F. *Deutsches Arch. Klin. Med.* **1913**, *112*, 476.
- (11) Lipson, R. L.; Baldes, E. J. *Arch. Dermatol.* **1960**, *82*, 508.
- (12) Lipson, R. L.; Baldes, E. J.; Olson, E. M. *J. Natl. Cancer Inst.* **1961**, *26*, 1.
- (13) Dougherty, T. J. *J. Natl. Cancer Inst.* **1974**, *51*, 1333.
- (14) Dougherty, T. J.; Grindey, G. E.; Fiel, R.; Weishaupt, K. R.; Boyle, D. G. *J. Natl. Cancer Inst.* **1975**, *55*, 115.
- (15) Dougherty, T. J.; Kaufman, J. E.; Goldfarb, A.; Weishaupt, K. R.; Boyle, D. G.; Mittleman, A. *Cancer Res.* **1978**, *38*, 2628.
- (16) Berenbaum, M. C.; Bonnett, R.; Scourides, P. A. *Br. J. Cancer* **1982**, *45*, 571.
- (17) Wilson, P. C. *Photosensitizing Compounds: Their Chemistry, Biology and Clinical Use*; Wiley Interscience: Chichester, 1989, pp 73.
- (18) Gomer, C. J.; Dougherty, T. J. *Cancer Res.* **1979**, *39*, 146.

- (19) Sternberg, E.; Dolphin, D. In *Photodynamic Therapy and Biomedical Lasers*; P. Spinelli, M. Dal Fante and R. Marchesini, Ed.; Excerpta Medica: Amsterdam, London, New York, Tokyo, 1992; pp 470-474.
- (20) Allison, B. A.; Waterfield, E.; Richter, A. M.; Levy, J. *J. Photochem. Photobiol.* **1991**, *54*, 709.
- (21) Richter, A. M.; Kelly, B.; Chow, J.; Liu, D. J.; Towers, G. H. N.; Dolphin, D.; Levy, J. *G. J. Natl. Cancer Inst.* **1987**, *79*, 1327.
- (22) Morgan, A. R.; Garbo, G. M.; Keck, R. G.; Skalkos, G.; Selman, S. H. *Photochem. Photobiol.* **1990**, *51*, 589.
- (23) Bonnett, R.; White, R. D.; Winfield, U.-J.; Berenbaum, M. C. *Biochem. J.* **1989**, *261*, 277.
- (24) Wöhrle, D.; Shopova, M.; Müller, S.; Milev, A. D.; Manatareva, V. N.; Krastev, K. *J. Photochem. Photobiol., B. Biol.* **1993**, *21*, 155.
- (25) *The Science of Photobiology*; Smith, K. C., Ed.; Plenum Press: New York, 1989.
- (26) van Lier, J. E. In *Photodynamic Therapy of Neoplastic Disease*; D. Kessel, Ed.; CRC Press: Boca Raton, 1990; Vol. 1; pp 279-291.
- (27) Lee See, K.; Forbes, I. J.; Betts, W. H. *J. Photochem. Photobiol.* **1984**, *39*, 631.
- (28) van Lier, J. E. In *Photobiological Techniques*; D. P. Valenzo, R. H. Pottier, P. Mathis and R. H. Douglas, Ed.; Plenum Press: New York, London, 1991; Vol. 216; pp 85-98.
- (29) Adams, K. R.; the late Berenbaum, M. C.; Bonnett, R.; Nizhnik, A. N.; Salgado, A.; Asunción Vallés, M. *J. Chem. Soc., Perkin Trans. 1* **1992**, 1465.
- (30) *The Porphyrins*; Dolphin, D., Ed.; Academic Press: New York, 1978; Vol. VII.
- (31) Fischer, H.; Orth, H. *Die Chemie des Pyrrols*; Akademische Verlagsgesellschaft (Johnson Reprint, New York 1968): Leipzig, 1937; Vol. II, pp 59-60.
- (32) Nicholas, R. E. H.; Rimington, C. *Biochem. J.* **1951**, *50*, 194.
- (33) Baker, E. W.; Palmer, S. E. In *The Porphyrins*; D. Dolphin, Ed.; Academic: New York, 1978; Vol. I.
- (34) Drabken, D. L. In *The Porphyrins*; D. Dolphin, Ed.; Academic: New York, 1978; Vol. 1; pp 29-83.
- (35) Fuhrhop, J.-H.; Smith, K. M. *Laboratory Methods in Porphyrin and Metalloporphyrin Research*; Elsevier: Amsterdam, 1975.
- (36) DiNello, R. K.; Chang, C. K. In *The Porphyrins*; D. Dolphin, Ed.; Academic Press: New York, 1978; Vol. I; pp 290-340.

-
- (37) Fischer, H.; Orth, H. *Die Chemie des Pyrrols*; Akademische Verlagsgesellschaft: Leipzig, 1937; Vol. II, pp 269 pp.
- (38) Smith, K. M.; Cavaleiro, J. A. S. *Heterocycles* **1987**, *26*, 1947.
- (39) Paine III, J. B. In *The Porphyrins*; D. Dolphin, Ed.; Academic Press: New York, 1978; Vol. 1; pp 101-234.
- (40) Rothmund, P. *J. Am. Chem. Soc.* **1936**, *61*, 2912.
- (41) Treibs, A.; Häberle, N. *Liebigs Ann. Chem.* **1968**, *718*, 183.
- (42) Adler, A. D.; Longo, F. R.; Finarelli, J. D.; Goldmacher, J.; Assour, J.; Korsakoff, L. *J. Org. Chem.* **1967**, *32*, 476.
- (43) Rocha Gonsalves, A. M. d.; Varejão, J. M. T. B.; Reireira, M. M. *J. Heterocyclic Chem.* **1991**, *28*, 635.
- (44) Lindsey, J. S.; Schreimann, I. C.; Hsu, H. C.; Kearney, P. C.; Marguerettaz, A. M. *J. Org. Chem.* **1987**, *52*, 827.
- (45) Lindsey, J. S.; MacCrum, K. A.; Tyhonas, J. S.; Chuang, Y.-Y. *J. Org. Chem.* **1994**, *59*, 579.
- (46) Lindsey, J. S. In *Metalloporphyrin Catalyzed Oxidations*; F. Montanari and L. Casella, Ed.; Kluwer Academic Publishers: Netherlands, 1994; pp 49-86.
- (47) Dolphin, D. *J. Heterocyclic Chem.* **1970**, *7*, 275.
- (48) Little, R. G. *J. Heterocyclic Chem.* **1981**, *18*, 833.
- (49) Kuroda, Y.; Murase, H.; Suzuki, Y.; Ogoshi, H. *Tetrahedron Lett.* **1989**, *30*, 2411.
- (50) Bruix, M.; Elguero, J.; Meutermans, W. *J. Chem. Research (S)* **1992**, 370.
- (51) Lindsey, J. S.; Prathapan, S.; Johnson, T. E.; Wagner, R. W. *Tetrahedron* **1994**, *50*, 8941.
- (52) Kihn-Botulinski, M.; Meunier, B. *Inorg. Chem.* **1988**, *27*, 209.
- (53) Oulmi, D.; Maillard, P.; Guerquin-Kern, J.-L.; Huel, C.; Momenteau, M. *J. Org. Chem.* **1995**, *60*, 1554.
- (54) Onaka, M.; Shinoda, T.; Izumi, Y.; Nolen, E. *Chem. Lett.* **1993**, 117.
- (55) Petit, A.; Loupy, A.; Mailard, P.; Momenteau, M. *Synth. Comm.* **1992**, *22*, 1137.
- (56) Wallace, D. M.; Leung, S. H.; Senge, M. O.; Smith, K. M. *J. Org. Chem.* **1993**, *58*, 7245.
- (57) Ema, T.; Kuroda, Y.; Ogoshi, H. *Tetrahedron Lett.* **1992**, *32*, 4529.
- (58) Robinson, B. C.; Morgan, A. R. *Tetrahedron Lett.* **1993**, *34*, 3711.

- (59) Chandrasekar, P.; Lash, T. D. In *210 th ACS National Meeting*; Chicago, IL, 1995; Aug. 20.-24., Organic Chemistry Paper No. 79.
- (60) Lash, T. D.; Novak, B. H. *Angew. Chem., Int. Ed. Engl.* **1995**, *34*, 683.
- (61) Lash, T. D.; Novak, B. H. *Tetrahrdon Lett.* **1995**, *36*, 4381.
- (62) Clezy, P. S.; Mirza, A. H. *Aust. J. Chem.* **1982**, *35*, 197.
- (63) Chaudhry, I. A.; Clezy, P. S. *Aust. J. Chem.* **1982**, *35*, 1185.
- (64) Bonnett, R.; McManus, K. A. *J. Chem. Soc., Chem. Commun.* **1994**, 1129.
- (65) Bender, C. O.; Bonnett, R.; Smith, R. G. *J. Chem. Soc. (C)* **1970**, 1251.
- (66) Fayer, J. *Chem. Ind.* **1991**, 869.
- (67) Gouterman, M. In *The Porphyrins*; D. Dolphin, Ed.; Academic Press: New York, San Francisco, London, 1978; Vol. III; pp 1-165.
- (68) Chang, C. K.; Hanson, L.; Richardson, P. F.; Young, R.; Fayer, J. *Proc. Natl. Acad. Sci. US* **1981**, *78*, 2652.
- (69) Fajer, J.; Davis, M. S. In *The Porphyrins*; D. Dolphin, Ed.; Academic Press: New York, 1978; Vol. IV; pp 197-256.
- (70) Ma, L. Ph.D. Thesis, University of British Columbia, 1995.
- (71) Willstätter, R.; Stoll, A. *Investigations on Chlorophyll*; Science Press: Lancaster, OH, 1928.
- (72) Scheer, H.; Inhoffen, H. H. In *The Porphyrins*; D. Dolphin, Ed.; Academic Press: New York, San Francisco, London, 1978; Vol. II; pp 45.
- (73) *Chlorophylls*; Scheer, H., Ed.; CRC: Boca Raton, 1991.
- (74) Stevens, R. V. In *B12*; D. Dolphin, Ed.; John Wiley & Sons: New York, Toronto, 1982; Vol. 1, Chemistry; pp 169-200.
- (75) Woodward, R. B.; Ayer, W. A.; Beaton, J. M.; Bickelhaupt, F.; Bonnett, R.; Buchschacher, P.; Closs, G. L.; Dutler, H.; Hannah, J.; Hauck, F. P.; Ito, S.; Langemann, A.; LeGoff, E.; Leimgruber, W.; Lwowski, W.; Sauer, J.; Valenta, Z.; Volz, H. *Tetrahedron* **1990**, *46*, 7599.
- (76) Woodward, R. B.; Ayer, W. A.; Beaton, J. M.; Bickelhaupt, F.; Bonnett, R.; Buchschacher, P.; Closs, G. L.; Dutler, H.; Hannah, J.; Hauck, F. P.; Ito, S.; Langemann, A.; LeGoff, E.; Leimgruber, W.; Lwowski, W.; Sauer, J.; Valenta, Z.; Volz, H. *J. Am. Chem. Soc.* **1960**, *82*, 3800.
- (77) Dutton, C. J.; Fookes, C. J. R.; Battersby, A. R. *J. Chem. Soc., Chem. Commun.* **1983**, 1237.
- (78) Montforts, F.-P.; Schwartz, U. M. *Angew. Chem., Int. Ed. Engl.* **1985**, *24*, 775.

-
- (79) Battersby, A. R.; Westwood, S. W. *J. Chem. Soc., Perkin Trans. 1* **1987**, 1679.
- (80) Montforts, F.-P.; Gerlach, B.; Höper, F. *Chem. Rev.* **1994**, *94*, 327.
- (81) Ball, R. H.; Dorrough, G. D.; Calvin, M. *J. Am. Chem. Soc.* **1946**, *68*, 2278.
- (82) Rousseau, K.; Dolphin, D. *Tetrahedron Lett.* **1974**, *48*, 4251.
- (83) Whitlock, J., H.W.; Hanamer, R.; Oester, M. Y.; Bower, B. K. *J. Am. Chem. Soc.* **1969**, *91*, 7485.
- (84) Eisner, U. *J. Chem. Soc.* **1957**, 854.
- (85) Tabushi, I.; Sakai, K.; Yamamura, K. *Tetrahedron Lett.* **1978**, 1821.
- (86) Ulman, A.; Gallucci, J.; Fisher, D.; Ibers, J. A. *J. Am. Chem. Soc.* **1980**, *102*, 6852.
- (87) Burns, D. H.; Caldwell, T. M.; Burden, M. W. *Tetrahedron Lett.* **1993**, *34*, 2883.
- (88) Closs, G. L.; Closs, L. E. *J. Am. Chem. Soc.* **1963**, *85*, 818.
- (89) Buchler, J. W.; Schneehage, H. H. *Tetrahedron Lett.* **1972**, *36*, 3803.
- (90) Whitlock, J. W.; Oester, M. Y. *J. Am. Chem. Soc.* **1973**, *95*, 5738.
- (91) Inhoffen, H. H.; Buchler, J. W.; Thomas, R. *Tetrahedron Lett.* **1969**, *14*, 1145.
- (92) Pastro, D. J. In *Comprehensive Organic Chemistry*; D. Barton and W.D. Ollis, Ed.; Pergamon Press: Oxford, New York, Toronto, Sydney, Paris, Frankfurt 1979, Chapter 3.3.
- (93) Smith, J. R. L.; Calcin, M. *J. Am. Chem. Soc.* **1966**, *88*, 4500.
- (94) Scheer, H.; Svec, W. A.; Cope, P. T.; Studier, M. H.; Scott, R. G.; Katz, J.J. *J. Am. Chem. Soc.* **1974**, *96*, 3714.
- (95) Berenbaum, M. C.; Akande, S. L.; Bonnett, R.; Kaur, H.; Ioannou, S.; White, R. D.; Winfield, U.-J. *Br. J. Cancer* **1986**, *54*, 717.
- (96) Bonnett, R.; Ioannou, S.; White, R. D.; Winfield, U.-J.; Berenbaum, M. C. *Photobiochem. Photobiophys. Suppl.* **1987**, 45.
- (97) Berenbaum, M. C.; Bonnett, R.; Chevretton, E. B.; Akande-Adebakin, S. L.; Ruston, M. *Lasers Med. Sci.* **1993**, *8*, 235.
- (98) Bonnett, R.; McGarvey, D. J.; Harriman, A.; Land, E. J.; Truscott, T. G.; Winfield, U.-J. *Photochem. Photobiol.* **1988**, *48*, 271.
- (99) Ris, H.-B.; Altermatt, H. J.; Stewart, C. M.; Schaffner, T.; Wang, Q.; Lim, C. K.; Bonnett, R.; Althaus, U. *Int. J. Cancer* **1993**, *55*, 245.
- (100) Savary, J.-F.; Monnier, P.; Wagnières, G.; Braichotte, D.; Fontolliet, C.; van der Berg, H. *Proc. SPIE* **1994**, 2078, 330.

-
- (101) Ris, H.-B.; Altermatt, H. J.; Inderbitzi, R.; Hess, R.; Nachbur, B.; Stewart, C. M.; Wang, Q.; Lim, C. K.; Bonnett, R.; Berenbaum, M. C.; Althaus, U. *Br. J. Cancer* **1991**, *64*, 1116.
- (102) Wolf, H.; Scheer, H. *Liebigs Ann. Chem.* **1973**, 1740.
- (103) Wolf, H.; Scheer, H. *Liebigs Ann. Chem.* **1973**, 1710.
- (104) Smith, K. M.; Simpson, D. J. *J. Chem. Soc., Chem. Commun.* **1987**, 613.
- (105) Crossley, M. J.; King, L. G. *J. Org. Chem.* **1993**, *58*, 4370.
- (106) Shine, H. J.; Padilla, A. G.; Wu, S.-M. *J. Org. Chem.* **1979**, *44*, 4069.
- (107) Baldwin, J. E.; Crossley, M. J.; DeBernardis, J. *Tetrahedron* **1982**, *38*, 685.
- (108) Catalano, M. M.; Crossley, M. J.; Harding, M. M.; King, L. G. *J. Chem. Soc., Chem. Commun.* **1984**, 1535.
- (109) Severin, T.; Schmitz, R.; Temme, H.-L. *Chem. Ber.* **1963**, *96*, 2499.
- (110) Kniel, P. *Helv. Chim. Acta* **1968**, *51*, 371.
- (111) Flitsch, W. *Adv. Heterocycl. Chem.* **1988**, *43*, 73.
- (112) Fuhrhop, J.-H. In *The Porphyrins*; D. Dolphin, Ed.; Academic Press: New York, San Francisco, London, 1978; Vol. 2; pp 131-159.
- (113) Inhoffen, H. H.; Brockmann jr., H.; Bliesener, K.-M. *Liebigs Ann. d. Chem.* **1969**, *730*, 173.
- (114) Morgan, A. R.; Scherrer Pangka, V.; Dolphin, D. *J. Chem. Soc., Chem. Commun.* **1984**, 1047.
- (115) Callot, H. L.; Johnson, A. W.; Sweeney, A. *J. Chem. Soc., Perkin Trans. 1* **1973**, 1424.
- (116) Scherrer Pangka, V.; Morgan, A. R.; Dolphin, D. *J. Org. Chem.* **1986**, *51*, 1094.
- (117) Morgan, A. R.; Garbo, G. M.; Keck, R. W.; Miller, R. A.; Selman, S. H.; Skalkos, D. *J. Med. Chem.* **1990**, *33*, 1258.
- (118) Pandey, R. K.; Shiau, F.-Y.; Ramachandran, K.; Dougherty, T. J.; Smith, K. M. *J. Chem. Soc., Perkin Trans. 1* **1992**, 1377.
- (119) DiNello, R. K.; Dolphin, D. *J. Org. Chem.* **1980**, *45*, 5196.
- (120) Cavaleiro, J. A. S.; Jackson, A. H.; Neves, M. G. P. M. S.; Rao, K. R. n. *J. Chem. Soc., Chem. Commun.* **1985**, 776.
- (121) DiNello, R. K.; Chang, C. K. In *The Porphyrins*; D. Dolphin, Ed.; Academic Press: New York, San Francisco, London, 1986; Vol. 1; pp 289-339.

- (122) Aveline, B.; Hasan, T.; Redmond, R. W. *Photochem. Photobiol.* **1994**, *59*, 328.
- (123) Richter, A. M.; Waterfield, E.; Jain, A. K.; Sternberg, E. D.; Dolphin, D.; Levy, J. G. *Photochem. Photobiol.* **1990**, *52*, 495.
- (124) Richter, A. M.; Cerruti-Sola, S.; Sternberg, E. D.; Dolphin, D.; Levy, J. G. *J. Photochem. Photobiol., B* **1990**, *5*, 231.
- (125) Tovey, A. M.Sc. Thesis, University of British Columbia, Canada, 1995.
- (126) Callot, H. *Bull. Chem. Soc. Chim. Fr.* **1972**, *11*, 4387.
- (127) Morgan, A. R. In *Photodynamic Therapy - Basic Principles and Clinical Applications*; B. W. Henderson and T. J. Dougherty, Ed.; Marcel Dekker, Inc.: New York, 1992; pp 157.
- (128) Arnold, D. P.; Gaete-Holms, R.; Johnson, A. W.; Smith, A. R. P.; Williams, G. A. *J. Chem. Soc., Perkin Trans. 1* **1978**, 1660.
- (129) Morgan, A. R.; Tertel, N. C. *J. Org. Chem.* **1986**, *51*, 1347.
- (130) Morgan, A. R.; Rampersaud, A.; Garbo, G. M.; Keck, R. W.; Selman, S. H. *J. Med. Chem.* **1989**, *32*, 904.
- (131) Morgan, A. R.; Gupta, S. *Tetrahedron Lett.* **1994**, *35*, 4291.
- (132) Gunter, M. J.; Robinson, B. C. *Aust. J. Chem.* **1990**, *43*, 1839.
- (133) Vicente, M. G. H.; Rezzano, I. N.; Smith, K. M. *Tetrahedron Lett.* **1990**, *31*, 1365.
- (134) Morgan, A. R.; Garbo, G. M.; Keck, R. W.; Skalkos, D.; Selman, S. H. In *Photodynamic Therapy: Mechanisms. Proc. SPIE1989*; Vol. 1065; pp 146.
- (135) Gunter, M. J.; Robinson, B. C.; Gulbis, J.M.; Tiekink, E.R.T. *Tetrahedron* **1991**, *47*, 7853.
- (136) Selman, S. H.; Hapton, J. A.; Morgan, A. R.; Keck, R. W.; Balkany, A. D.; Skalkos, D. *Photochem. Photobiol.* **1993**, *57*, 681.
- (137) Morgan, A. R.; Gupta, S. *Tetrahedron Lett.* **1994**, *35*, 5347.
- (138) Montforts, F.-P.; Zimmermann, G. *Angew. Chem., Int. Ed. Engl.* **1986**, *25*, 458.
- (139) Haake, G.; Meier, A.; Montforts, F.-P.; Scheurich, G.; Zimmermann, G. *Liebigs Ann. d. Chem.* **1992**, 325-336.
- (140) Sherman, G.; Volcker, A.; Siekel, K.; Schmidt, R.; Brauer, H.-D.; Montforts, F.-P. *Photochem. Photobiol.* **1990**, *51*, 45.
- (141) Montforts, F.-P.; Meier, A.; Scheurich, G.; Haake, G.; Bats, J. W. *Angew. Chem., Int. Ed. Engl.* **1992**, *31*, 1592.

-
- (142) Montforts, F.-P.; Mai, G.; Romanowski, F.; Bats, J. W. *Tetrahedron Lett.* **1992**, *33*, 765.
- (143) Kusch, D.; Töllner, E.; Lincke, A.; Montforts, F.-P. *Angew. Chem., Int. Ed. Engl.* **1995**, *34*, 784.
- (144) Schröder, M. *Chem. Rev.* **1980**, *80*, 187.
- (145) Makowka, O. *Chem. Ber.* **1908**, *41*, 943.
- (146) Lewis, D. E. *J. Chem. Ed.* **1994**, *71*, 39.
- (147) Hofmann, K. A. *Chem. Ber.* **1912**, *41*, 3329.
- (148) Criegee, R. *Liebigs Ann. d. Chem.* **1936**, *522*, 75.
- (149) Ref. 165, 2538.
- (150) Marzilli, L. G.; Hanson, B. E.; Kistenmacher, T. J.; Epps, L. A.; Stewart, R. C. *Inorg. Chem.* **1976**, *15*, 1661.
- (151) Collin, R. J.; Jones, J.; Griffith, W. P. *J. Chem. Soc., Dalton Trans. 1* **1974**, 1094-1097.
- (152) Riemersma, J. C. *Biochem. Biophys. Acta* **1968**, *152*, 718.
- (153) Cartwright, B. A.; Griffith, W. P.; Schröder, M.; Skapski, A. C. *Inorg. Chim. Acta* **1981**, *53*, L192.
- (154) Herrmann, W. A.; Eder, S. J.; Scherer, W. *Chem. Ber.* **1993**, *126*,
- (155) Subbaraman, L. R.; Subbaraman, J.; Behrman, E. J. *Inorg. Chem.* **1972**, *11*, 2621.
- (156) Herrmann, W. A.; Edre, S. J. *Chem. Ber.* **1993**, *126*, 31.
- (157) Herrmann, W. A.; Eder, S. J.; Scherer, W. *Angew. Chem., Int. Ed. Engl.* **1992**, *31*, 1345.
- (158) Herrmann, W. A.; Weichelbaumer, G.; German Patent (Offenlegung) DE 3920917 A1, 3 Jan. 1991 (*Chem. Abs.* 114(13): 121466n).
- (159) Akashi, K.; Palermo, R. E.; Sharpless, K. B. *J. Org. Chem.* **1978**, *43*, 2063.
- (160) Eames, J.; Mitchell, H. J.; Nelson, A.; O'Brien, P.; Warren, S.; Wyatt, P. *Tetrahedron Lett.* **1993**, *36*, 1719.
- (161) Sharpless, K. B.; Amberg, W.; Bennani, Y. L.; Crispino, G. A.; Hartung, J.; Jeong, K.-S.; Kwong, H.-L.; Morikawa, K.; Wang, Z.-M.; Xu, D.; Zhang, X.-L. *J. Org. Chem.* **1992**, *57*, 2768.
- (162) Nakajima, M.; Tomioka, K.; Iitaka, Y.; Koga, K. *Tetrahedron* **1993**, *49*, 10793.

- (163) Berrisford, D. J.; Bolm, C.; Sharpless, K. B. *Angew. Chem., Int. Ed. Engl.* **1995**, *34*, 1059.
- (164) *Organic Synthesis by Oxidation with Metal Compounds*; Singh, H. S., Ed.; Plenum: New York, 1986, pp 187-213.
- (165) Kolb, H. C.; Van Nieuwenhze, M. S.; Sharpless, K. B. *Chem. Rev.* **1994**, *94*, 2483.
- (166) Göbel, T.; Sharpless, K. B. *Angew. Chem., Int. Ed. Engl.* **1993**, *32*, 1329.
- (167) Buschmann, H.; Scharf, H.-D.; Hoffmann, N.; Esser, P. *Angew. Chem., Int. Ed. Engl.* **1991**, *30*, 477.
- (168) Zelikoff, M.; Taylor, H. A. *J. Am. Chem. Soc.* **1950**, *72*, 5039.
- (169) Sharpless, K. B.; Teranishi, A. Y.; Bäckvall, J. E. *J. Am. Chem. Soc.* **1977**, *99*, 3120.
- (170) Patrick, D. W.; Truesdale, L. K.; Biller, S. A.; Sharpless, K. B. *J. Org. Chem.* **1978**, *43*, 2628.
- (171) Schoental, R. *Nature* **1948**, *161*, 237.
- (172) Criegee, R.; Marchand, B.; Wannowius, H. *Liebigs Ann. Chem.* **1942**, *550*, 99.
- (173) Badger, G. M.; Reed, R. I. *Nature* **1948**, *161*, 238.
- (174) Badger, G. M. *J. Chem. Soc.* **1949**, 456.
- (175) Badger, G. M.; Lynn, K. R. *J. Chem. Soc.* **1950**, 1726.
- (176) Cook, J. W.; Schoental, R. *J. Chem. Soc.* **1948**, 170.
- (177) Cook, J. W.; Schoental, R. *Nature* **1948**, *161*, 237.
- (178) Cook, J. W.; Schoental, R. *J. Chem. Soc.* **1950**, 47.
- (179) Oberender, F. G.; Dixon, J. A. *J. Org. Chem.* **1959**, *24*, 1226.
- (180) Wallis, J. M.; Kochi, J. K. *J. Am. Chem. Soc.* **1988**, *110*, 8207.
- (181) Amic, D.; Trinajstic, N. *J. Chem. Soc., Perkin Trans. 2* **1990**, 1595.
- (182) Dias, J. R. *J. Chem. Educ.* **1989**, *66*, 1012.
- (183) Dewar, M. J. S.; Dougherty, R. C. *The PMO Theory of Organic Chemistry*; Plenum Press: New York, 1975.
- (184) Hirsch, A. *Angew. Chem., Int. Ed. Chem.* **1993**, *32*, 1138.
- (185) Hawkins, J., M. *Acc. Chem. Res.* **1992**, *25*, 150.

- (186) (a) Hawkins, J. M.; Lewis, T. A.; Loren, S.; Meyer, A.; Heath, J. R.; Shibato, Y.; Saykally, R. J. *J. Org. Chem.* **1990**, *55*, 6250. (b) Hawkin, J. M.; Meyer, A.; Lewis, A. F.; Loren, S.; Hollander, F. J.; *Science* **1991**, 312.
- (187) Wudl, F. *Acc. Chem. Res.* **1992**, *25*, 157.
- (188) Knop, J. V.; Fuhrhop, J.-H. *Z. Naturforsch. Teil B.* **1970**, *25*, 729.
- (189) Fischer, H.; Eckoldt, H. *Liebigs Ann. d. Chem.* **1940**, *543*, 138.
- (190) Fischer, H.; Pfeiffer, H. *Liebigs Ann. d. Chem.* **1944**, *556*, 131.
- (191) Wenderoth, H. *Liebigs Ann. d. Chem.* **1947**, *558*, 53.
- (192) Chang, C. G.; Sotiriou, C.; Weishih, W. *J. Chem. Soc., Chem. Comm.* **1986**, 1213.
- (193) Pandey, R. K.; Shiau, F. Y.; Isaac, M.; Ramaprasad, S.; Dougherty, T. J.; Smith, K. M. *Tetrahedron Lett.* **1992**, *33*, 7815.
- (194) Johnson, A. W.; Oldfield, D. *J. Chem. Soc.* **1965**, 4303.
- (195) Bonnett, R.; Nizhnik, A. N.; Berenbaum, M. C. *J. Chem. Soc., Chem. Comm.* **1989**, 1822.
- (196) Bonnett, R.; Berenbaum, M. In *Photosensitizing Compounds: their Chemistry, Biology and Clinical Use*; Wiley: 1989.
- (197) Bonnett, R.; Nizhnik, A. N.; White, S. G.; Berenbaum, M. C. *J. Photochem. Photobiol., B* **1990**, *6*, 29.
- (198) Kessel, D.; Emith, K. M.; Pandey, R. K.; Shiau, F.-Y.; Henderson, B. *Photochem. Photobiol.* **1993**, *58*, 200.
- (199) *Photodynamic Therapy and Biomedical Lasers*; Smith, K. M.; Lee, S.-J.; Shiau, F.-Y.; Pandey, R. K.; Jagerovic, N., Ed.; Elsevier: Netherlands, 1992, pp 769.
- (200) Smith, K. M.; Goff, D. A. *J. Am. Chem. Soc.* **1985**, *107*, 4954.
- (201) Gerzevske, K. R.; Pandey, R. K.; Smith, K. M. *Heterocycles* **1994**, *39*, 439.
- (202) Meunier, I.; Pandey, R. K.; Walker, M. M.; Senge, M. O.; Dougherty, T. J.; Smith, K. M. *Bioorg. Medicin. Chem. Lett.* **1992**, *2*, 1575.
- (203) Chang, C. G.; Sotiriou, C. *J. Heterocyclic Chem.* **1985**, *22*, 1739.
- (204) Chang, C. G.; Sotiriou, C. *J. Org. Chem.* **1987**, *52*, 926.
- (205) Inhoffen, H. H.; Jäger, P.; Mählich, R.; Mengler, C.-D. *Liebigs Ann. d. Chem.* **1967**, *704*, 188.
- (206) Inhoffen, H. H.; Jäger, P.; Mählich, R. *Liebigs Ann. d. Chem.* **1971**, *749*, 109.
- (207) Barrett, J. *Nature (London)* **1959**, *183*, 1185.

- (208) Inhoffen, H. H.; Bliesener, C.; Brockmann jr., H. *Tetrahedron Lett.* **1966**, 3779.
- (209) Inhoffen, H. H. *Pure Appl. Chem.* **1968**, 17, 443.
- (210) Bonnett, R.; Dolphin, D.; Johnson, A. W.; Oldfield, D.; Stephenson, G. F. *Proc. Chem. Soc. London* **1964**, 371.
- (211) Fischer, H.; Halbig, P.; Walach, B. *Liebigs Ann. Chem.* **1927**, 452, 268.
- (212) Fischer, H.; Gebhardt, H.; Rothhaas, A. *Liebigs Ann. d. Chem.* **1930**, 482, 1.
- (213) Inhoffen, H. H.; Nolte, W. *Tetrahedron Lett.* **1967**, 23, 2185.
- (214) Inhoffen, H. H.; Nolte, W. *Liebigs Ann. d. Chem.* **1969**, 725, 167.
- (215) Chauhan, S. M. S.; Vijayarahavan *Indian. J. Chem.* **1991**, 30B, 1104.
- (216) Chang, C. K.; Wu, W. *J. Org. Chem.* **1986**, 51, 2134.
- (217) Mylrajan, M.; Andersson, L. A.; Loehr, T. M.; Wu, W.; Chang, C. K. *J. Am. Chem. Soc.* **1991**, 113, 5000.
- (218) Connick, P. A.; Haller, K. J.; Macor, K. A. *Inorg. Chem.* **1993**, 32, 3256.
- (219) Stolzenberg, A. M.; Glazer, P. A.; Foxman, B. M. *Inorg. Chem.* **1986**, 25, 983.
- (220) Ozawa, S.; Sakamoto, E.; Watanabe, Y.; Morishima, I. *J. Chem. Soc., Chem. Commun.* **1994**, 935.
- (221) Connick, P. A.; Macor, K. A. *Inorg. Chem.* **1991**, 30, 4654.
- (222) Inhoffen, H. H.; Buchler, J. W.; Jäger, P. *Prog. Chem. Org. Nat. Prod.* **1968**, 26, 284.
- (223) Inhoffen, H. H.; Müller, N. *Tetrahedron Lett.* **1969**, 3209.
- (224) Grigg, R.; Johnson, A. W.; Shelton, K. W. *J. Chem. Soc. (C)* **1969**, 655.
- (225) Hamilton, A.; Johnson, A. W. *J. Chem. Soc. (C)* **1971**, 3879.
- (226) Chang, C. K.; Wu, W.; Chern, S.-S.; Peng, S.-M. *Angew. Chem., Int. Ed. Engl.* **1992**, 31, 70.
- (227) Chatfield, M. J.; La Mar, G. N.; Lecomte, J. T. J.; Balch, A. L.; Smith, K. M.; Langry, K. C. *J. Am. Chem. Soc.* **1986**, 108, 7108.
- (228) Chatfield, M. J.; La Mar, G. N.; Parker, W. O., Jr.; Smith, K. M.; Leung, H.-K.; Morris, I. K. *J. Am. Chem. Soc.* **1988**, 110, 6352.
- (229) Iakovides, P.; Smith, K. M. *Tetrahedron Lett.* **1990**, 31, 3853.
- (230) Clezy, P. S. In *The Porphyrins*; D. Dolphin, Ed.; Academic Press: New York, San Francisco, London, 1978; Vol. 2; pp 103-130.

-
- (231) *The Porphyrins*; Clezy, P. S., Ed.; Academic Press: New York, San Francisco, London, 1978; Vol. 2, pp 103-130.
- (232) Bonnett, R.; Dimsdale, M. J.; Stephenson, G. F. *J. Chem. Soc. (C)* **1969**, 564.
- (233) Clezy, P. S.; Liepa, A. J. *Aust. J. Chem.* **1970**, 23, 2477.
- (234) Clezy, P. S.; Nichol, A. W. *Aust. J. Chem.* **1965**, 11, 1835.
- (235) Chiu, J. T.; Loewen, P. C.; Switala, J.; Gennis, G. R.; Timkovich, R. *J. Am. Chem. Soc.* **1989**, 111, 7046.
- (236) Timkovich, R.; Cork, M. S.; Gennis, R. B.; Johnson, P. Y. *J. Am. Chem. Soc.* **1985**, 107, 6069.
- (237) Chang, C. K.; Wu, W. *J. Biol. Chem.* **1986**, 261, 8593.
- (238) Chang, C. K. *J. Biol. Chem.* **1985**, 260, 9520.
- (239) Micklefield, J.; Mackman, R. L.; Aucken, C. J.; Beckmann, M.; Block, M. H.; Leeper, F. J.; Battersby, A. R. *J. Chem. Soc., Chem. Commun.* **1993**, 275.
- (240) Chang, C. K.; Sotiriou, C. *J. Org. Chem.* **1985**, 50, 4989.
- (241) (a) Chang, C. K.; Barkigia, K. M.; Hanson, L. K.; Fajer, J. *J. Am. Chem. Soc.* **1986**, 108, 1352 (b) Barkigia, K. M.; Chang, C. K.; Fajer, J. *J. Am. Chem. Soc.* **1991**, 113, 7445.
- (242) Prinsep, R. M.; Caplan, F. R.; Moore, R. E.; Patterson, G. M. L.; Smith, C. D. *J. Am. Chem. Soc.* **1992**, 114, 385.
- (243) Prinsep, M. R.; Patterson, G. M. L.; Larsen, L. K.; Smith, C. D. *Tetrahedron* **1995**, 51, 10523.
- (244) Sotiriou, C.; Chang, C. K. *J. Am. Chem. Soc.* **1988**, 110, 2264.
- (245) Wu, W.; Chang, C. K. *J. Am. Chem. Soc.* **1987**, 109, 3149.
- (246) Borman, S. In *Chem. Eng. News*; Washington, D.C., 1995; pp 30-31.
- (247) Sessler, J. L. *Angew. Chem., Int. Ed. Engl.* **1994**, 33, 1348.
- (248) Waluk, J.; Michl, J. *J. Org. Chem.* **1991**, 56, 2729.
- (249) Vogel, E.; Köcher, M.; Schmickler, H.; Lex, J. *Angew. Chem., Int. Ed. Engl.* **1986**, 25, 257.
- (250) Callot, H. J.; Rohrer, A.; Tschamber, T.; Metz, B. *New J. Chem.* **1995**, 19, 155.
- (251) Aukauloo, M. A.; Guillard, R. *New J. Chem.* **1994**, 18, 1205.
- (252) Sessler, J. L.; Brucker, E. A.; Weghorn, S. J.; Kisters, M.; Schäfer, M.; Lex, J.; Vogel, E. *Angew. Chem., Int. Ed. Engl.* **1994**, 33, 2308.

- (253) Vogel, E.; Koch, P.; Hou, X.-L.; Lausmann, M.; Kisters, M.; Aukauloo, M. A.; Richard, P.; Guillard, R. *Angew. Chem., Int. Ed. Engl.* **1993**, *32*, 1600.
- (254) Vogel, E.; Balci, M.; Pramod, K.; Koch, P.; Lex, J.; Ermer, O. *Angew. Chem., Int. Ed. Engl.* **1987**, *26*, 928.
- (255) Chang, C. K.; Morrison, I.; Wu, W.; Chern, S.-S.; Peng, S.-M. *J. Chem. Soc., Chem. Commun.* **1995**, 1173.
- (256) Renner, M. W.; Forman, A.; Wu, W.; Chang, C. K.; Fajer, J. *J. Am. Chem. Soc.* **1989**, *111*, 8618.
- (257) Lausmann, M.; Zimmer, I.; Lex, J.; Lueken, H.; Wieghardt, K.; Vogel, E. *Angew. Chem., Int. Ed. Engl.* **1994**, *33*, 736.
- (258) Aramendia, P. F.; Redmond, R. W.; Nonell, S.; Schuster, W.; Braslavsky, S. E.; Schaffner, K.; Vogel, E. *Photochem. Photobiol.* **1986**, *44*,
- (259) Mártire, D. O.; Jux, N.; Aramedía, P. F.; Negri, R. M.; Lex, J.; Braslavsky, S. E.; Schaffner, K.; Vogel, E. *J. Am. Chem. Soc.* **1992**, *114*, 9969.
- (260) Waluk, J.; Müller, M.; Swiderek, P.; Köcher, M.; Vogel, E.; Hohlneicher, G.; Michl, J. *J. Am. Chem. Soc.* **1991**, *113*, 5511.
- (261) Wehrle, B.; Limbach, H.-H.; Köcher, M.; Ermer, O.; Vogel, E. *Angew. Chem., Int. Ed. Engl.* **1987**, *26*, 934.
- (262) Berman, A.; Michaeli, A.; Feitelson, J.; Bowman, M. K.; Norris, J. R.; Levanon, H.; Vogel, E.; Koch, P. *J. Phys. Chem.* **1992**, *96*, 3041.
- (263) Schlüpmann, J.; Huber, M.; Toporowicz, M.; Köcher, M.; Vogel, E.; Levanon, H.; Möbius, K. *J. Am. Chem. Soc.* **1988**, *110*, 8566.
- (264) Gisselbrecht, J. P.; Gross, M.; Köcher, M.; Lausmann, M.; Vogel, E. *J. Am. Chem. Soc.* **1990**, *112*, 8618.
- (265) Bernard, C.; Gisselbrecht, J. P.; Gross, M.; Vogel, E.; Lausmann, M. *Inorg. Chem.* **1994**, *33*, 2393.
- (266) Vogel, E.; Köcher, M.; Balci, M.; Teichler, I.; Lex, J.; Schmickler, H.; Ermer, O. *Angew. Chem., Int. Ed. Engl.* **1987**, *26*, 931.
- (267) Nonell, S.; Bou, N.; Teixido, J.; Villanueva, A.; Juarranz, A.; Cañete, M. *Tetrahedron Lett.* **1995**, *36*, 3405.
- (268) Furuta, H.; Asano, T.; Ogawa, T. *J. Am. Chem. Soc.* **1994**, *116*, 767.
- (269) Chmielewski, P. J.; Latos-Grazynski, L.; Rachlewicz, K.; Glowiak, T. *Angew. Chem., Int. Ed. Engl.* **1994**, *33*, 779.
- (270) Adams, K. R. Ph.D. Thesis, London, GB, 1969.
- (271) Arduengo, A. J.; Harlow, R. L.; Kline, M. *J. Am. Chem. Soc.* **1991**, *113*, 361.

- (272) Arduengo, A. J., III; Dias, H. V. R.; Harlow, R. L.; Kline, M. *J. Am. Chem. Soc.* **1992**, *114*, 5530.
- (273) Arduengo, A. J., III; Bock, H.; Chen, H.; Denk, M.; Dixon, D. A.; Green, J. C.; Herrmann, W. A.; Jones, N. L.; Wagner, M.; West, R. *J. Am. Chem. Soc.* **1994**, *116*, 6641.
- (274) Enders, D.; Breuer, K.; Raabe, G.; Runsink, J.; Teles, J. H.; Melder, J.-P.; Ebel, K.; Brode, S. *Angew. Chem., Int. Ed. Engl.* **1995**, *34*, 1021.
- (275) Gosh, A. *Angew. Chem., Int. Ed. Engl.* **1995**, *34*, 1028.
- (276) Chmielewski, P. J.; Latos-Grazynski *J. Chem. Soc., Perkin Trans. 2* **1995**, 503.
- (277) Woodward, R. B. *Ind. Chim. Belg.* **1962**, *27*, 1293.
- (278) Dolphin, D.; Felton, R. H.; Borg, D. C.; Fajer, J. *J. Am. Chem. Soc.* **1970**, *92*, 734.
- (279) Guzinski, J. A.; Felton, R. H. *J. Chem. Soc., Chem. Commun.* **1973**, 715.
- (280) Kadish, K. M.; Rhodes, R. K. *Inorg. Chem.* **1981**, *20*, 2961.
- (281) Harriman, A.; Porter, G.; Walters, P. *J. Chem. Soc., Faraday Trans. 1* **1983**, *76*, 1335.
- (282) Hinman, A. S.; Pavelich, B. J.; Kondo, A. E. *J. Electroanal. Chem.* **1987**, *234*, 145.
- (283) Gold, A.; Ivey, W.; Toney, G. E.; Sangaiah, R. *Inorg. Chem.* **1984**, *23*, 2932.
- (284) Lee, W. A.; Bruice, T. C. *Inorg. Chem.* **1986**, *25*, 131.
- (285) Richoux, M. C.; Neta, P.; Christensen, P. A.; Harriman, A. *J. Chem. Soc., Faraday Trans. 2* **1986**, *82*, 235.
- (286) Takeda, Y.; Takahara, S.; Kobayashi, Y.; Misawa, H.; Sakuragi, H.; Takumaru, K. *Chem. Lett.* **1990**, *11*, 2103.
- (287) Cavaleiro, J. A. S.; Evans, B.; Smith, K. M. In *Porphyrin Chemistry Advances*; F. R. Longo, Ed.; Ann Arbor Science: Ann Arbor, 1979; p 375.
- (288) Xie, H.; Smith, K. M. *Tetrahedron Lett.* **1992**, *33*, 1197.
- (289) Young, S. W. *Magnetic Resonance Imaging: Basic Principles*; Raven Press: New York, 1988, pp 1-282.
- (290) Lauffer, R. B. *Chem. Rev.* **1987**, *87*, 901.
- (291) Bell, J. D.; Sadler, P. J. In *Chemistry in Britain*; 1993; 597.
- (292) Sessler, J. L. *Top. Curr. Chem.* **1991**, *161*, 177.
- (293) Asat, A. M.Sc. Thesis, University of British Columbia, 1995.

- (294) Woodward In *Aromaticity: An International Symposium*; The Chemical Society London: Sheffield, 1966.
- (295) Sessler, J. L.; Cyr, M.; Burrell, A. K. *Tetrahedron* **1992**, *48*, 9661.
- (296) Broadhurst, M. J.; Grigg, R.; Johnson, A. W. *J. Chem. Soc., Chem. Commun.* **1969**, 23.
- (297) Broadhurst, M. J.; Grigg, R.; Johnson, A. W. *J. Chem. Soc., Perkin Trans. 1* **1972**, 2111.
- (298) Bauer, V. J.; Clive, D. L. J.; Dolphin, D.; Paine III, J. B.; Harris, F. L.; King, M. M.; Loder, J.; Wang, S.-W. C.; Woodward, R. B. *J. Am. Chem. Soc.* **1983**, *105*, 6429.
- (299) Sessler, J. L.; Mody, T. M.; Lynch, V. *J. Am. Chem. Soc.* **1993**, *115*, 3346.
- (300) Sessler, J. L.; Cyr, M.; Furuta, H.; Král, V.; Mody, T.; Morishima, T.; Shionoya, M.; Weghorn, S. *Pure Appl. Chem.* **1993**, *65*, 393.
- (301) Iverson, B. L.; Shreder, K.; Král, V.; Sessler, J. L. *J. Am. Chem. Soc.* **1993**, *115*, 11022.
- (302) Iverson, B. L.; Thomas, R. E.; Král, V.; Sessler, J. L. *J. Am. Chem. Soc.* **1994**, *116*, 2663.
- (303) Iverson, B. L.; Shreder, K.; Kral, V.; Smith, D. A.; Smith, J.; Sessler, J. L. *Pure Appl. Chem.* **1994**, *66*, 845.
- (304) Broadhurst, M. J.; Grigg, R.; Johnson, A. W. *J. Chem. Soc., Perkin Trans. 1* **1972**, 1124.
- (305) Sessler, J. L.; Hoehner, M. In *210 th American Chemical Society National Meeting*; Chicago, IL, 1995.
- (306) Weghorn, S. J.; Lynch, V.; Sessler, J. L. *Tetrahedron Lett.* **1995**, *36*, 4713.
- (307) Rexhausen, H.; Gossauer, A. *J. Chem. Soc., Chem. Commun.* **1983**, 275.
- (308) Gossauer, A. *Bull. Soc. Chim. Belg.* **1983**, *92*, 793.
- (309) Gossauer, A. *Chimia* **1984**, *37*, 341.
- (310) Gossauer, A. *Chimia* **1984**, *38*, 45.
- (311) Burrell, A. K.; Hemmi, G.; Lynch, V.; Sessler, J. L. *J. Am. Chem. Soc.* **1991**, *113*, 4690.
- (312) Tovey, A., M.Sc. Thesis, University of British Columbia, 1995.
- (313) Charrière, R.; Jenny, T. A.; Rexhausen, H.; Gossauer, A. *Heterocycles* **1993**, *36*, 1561.
- (314) Sessler, J. L.; Cyr, M. J.; Burrell, A. K. *Synlett* **1991**, 127.

- (315) Chmielewski, P. J.; Latos-Grazynski, L.; Rachlewicz, K. *Eur. J. Chem.* **1995**, *1*, 68.
- (316) Rothemund, P. *J. Am. Chem. Soc.* **1936**, *58*, 625.
- (317) Rothemund, P. *J. Am. Chem. Soc.* **1939**, *61*, 2912.
- (318) Sessler, J. L.; Hemmi, G.; Mody, T. D.; Murai, T.; Burrell, A.; Young, S. W. *Acc. Chem. Res.* **1994**, *27*, 43.
- (319) Berlin, K.; Breitmaier, E. *Angew. Chem., Int. Ed. Engl.* **1994**, *33*, 219.
- (320) Berlin, K.; Breitmaier, E. *Angew. Chem., Int. Ed. Engl.* **1994**, *33*, 1246.
- (321) Sessler, J. L.; Mody, T. D.; Ford, D.; Lynch, V. *Angew. Chem., Int. Ed. Engl.* **1992**, *31*, 452.
- (322) Dolphin, D.; Rettig, S. J.; Tang, H.; Wijesekera, T.; Xie, L. Y. *J. Am. Chem. Soc.* **1993**, *115*, 9301.
- (323) Xie, L. Y.; Dolphin, D. *J. Chem. Soc., Chem. Commun.* **1994**, 1475.
- (324) Crowell, T. I.; McLeod, R. K. *J. Org. Chem.* **1967**, *32*, 4030.
- (325) Boyle, R. W.; Xie, L. Y.; Dolphin, D. *Tetrahedron Lett.* **1994**, *35*, 5377.
- (326) Buchler, J. W.; Dreher, C.; Künzel, F. M. *Struct. Bonding (Berlin)* **1995**, *84*, 1.
- (327) Sharpless, K. B.; Amberg, W.; Bennani, Y. L.; Crispino, G. A.; Hartung, J.; Jeong, K.-S.; Kwong, H.-L.; Morikawa, K.; Wang, Z.-M.; Xu, D.; Zhang, X.-L. *J. Org. Chem.* **1992**, *57*, 2768.
- (328) Buchler, J. W. In *The Porphyrins*; D. Dolphin, Ed.; Academic Press: New York, 1978; Vol. 1; Chapter 10.
- (329) Brückner, C. Diplomarbeit, Rheinisch-Westfälische Technische Hochschule, Aachen, Germany, 1991.
- (330) Lavalley, D. K. *The Chemistry and Biochemistry of N-substituted Porphyrins*; VCH: Weinheim, New York, 1987.
- (331) NMR", Caleo Scientific Software Publishers, USA, 1989.
- (332) Senge, M. O.; Medforth, C. J.; Sparks, L. D.; Shelnut, J. A.; Smith, K. M. *Inorg. Chem.* **1993**, *32*, 1716 and references cited therein.
- (333) Computational results obtained using Discover[®] 2.9.5./94.0 (ESFF 91 force field) from Biosym Technologies, San Diego, U.S.A. on a SGI Personal Iris work station.
- (334) Savoie, H.; Dolphin, D., unpublished results.
- (335) Al-Laith, M.; Matthews, E. K. *Biochem. Pharmacol.* **1993**, *46*, 567.
- (336) Al-Laith, M.; Matthews, E. K. *Br. J. Cancer* **1994**, *70*, 893.

-
- (337) Matthews, E. K.; Cui, C. J. *Br. J. Cancer* **1990**, *61*, 695.
- (338) Matthews, E. K.; Cui, Z. J. *Biochem. Pharmacol.* **1990**, *39*, 1445.
- (339) Mang, T. S.; Wieman, T. J. *Proc. SPIE* **1988**, *847*, 116.
- (340) Matthews, E. K.; Mesber, D. E. *Br. J. Pharmacol.* **1984**, *83*, 555.
- (341) Fleischer, E. B. *Acc. Chem. Res.* **1970**, *3*, 105.
- (342) Radonovich, L. J.; Bloom, A.; Hoard, J. L. *J. Am. Chem. Soc.* **1972**, *94*, 2073.
- (343) Gottwald, L. K.; Ullman, E. F. *Tetrahedron Lett.* **1969**, *36*, 3071.
- (344) Rose, E.; Quelquejeu, M.; Pochet, C.; Julien, N.; Kossany, A.; Hamon, L. *J. Org. Chem.* **1993**, *58*, 5030.
- (345) Nishino, N.; Sakamoto, T.; Kiyota, H.; Mihara, M.; Yanai, T.; Fujimoto, T. *Chem. Lett.* **1993**, 279.
- (346) Hayashi, T.; Asai, T.; Hokazono, H.; Ogoshi, H. *J. Am. Chem. Soc.* **1993**, *115*, 12210.
- (347) Eaton, S. S.; Eaton, G. R. *J. Chem. Soc., Chem. Commun.* **1974**, 576.
- (348) Eaton, S. S.; Eaton, G. R. *J. Am. Chem. Soc.* **1975**, *97*, 3660.
- (349) Eaton, S. S.; Eaton, G. R. *J. Am. Chem. Soc.* **1977**, *99*, 6594.
- (350) Eaton, S. S.; Eaton, G. R. *Inorg. Chem.* **1978**, *17*, 1542.
- (351) Green, T. W.; Wuts, P. G. M. *Protective Groups in Organic Synthesis*; 2nd ed.; John Wiley & Sons: New York, 1991.
- (352) Crossley, M. J.; Harding, M. M.; Sternhell, S. *J. Org. Chem.* **1988**, *53*, 1132.
- (353) Catalano, M. M.; Crossley, M. J.; King, L. G. *J. Chem. Soc., Chem. Commun.* **1984**, 1537.
- (354) Crossley, M. J.; King, L. G.; Pyke, S. M. *Tetrahedron* **1987**, *43*, 4569.
- (355) Crossley, M. J.; King, L. G. *J. Chem. Soc., Chem. Commun.* **1984**, 920.
- (356) Crossley, M. J.; Burn, P. L.; Langford, S. J.; Pyke, S. M.; Stark, A. G. *J. Chem. Soc., Chem. Commun.* **1991**, 1567.
- (357) Crossley, M. J.; Burn, P. L.; Chew, S. S.; Cuttance, F. B.; Newsom, I. A. *J. Chem. Soc., Chem. Commun.* **1991**, 1564.
- (358) Crossley, M. J.; Govenlock, L. J.; Prashar, J. K. *J. Chem. Soc., Chem. Commun.* **1995**, 2379.

- (359) Meyer Jr., E. F.; Cullen, D. L. In *The Porphyrins*; D. Dolphin, Ed.; Academic Press: New York, 1978; Vol. III; pp 513-529.
- (360) Hassner, A.; Stumer, C. *Organic Syntheses Based on Name Reactions and Unnamed Reactions*; Elsevier: Oxford, 1994; Vol. 11, pp 82, 240.
- (361) Mani, S. N.; Beall, L. S.; White, A. J. P.; Williams, D. J.; Barrett, A. G. M.; Hoffman, B. M. *J. Chem. Soc., Chem. Commun.* **1994**, 1943.
- (362) Adams, K. R.; Bonnett, R.; Burke, P. J.; Salgado, A.; Vallés, M. A. *J. Chem. Soc., Chem. Commun.* **1993**, 1860.
- (363) Byrn, M. P.; Curtis, C. J.; Hsiou, Y.; Khan, S. I.; Sawin, P. A.; Tendick, S. K.; Terzis, A.; Strouse, C. E. *J. Am. Chem. Soc.* **1993**, *115*, 9480.
- (364) Ravikanth, M.; Chandrashekar, T. K. *Struct. Bond.* **1995**, *82*, 107.
- (365) Medford, C. J.; Senge, M. O.; Smith, K. M.; Sparks, L. D.; Shelnut, J. A. *J. Am. Chem. Soc.* **1992**, *114*, 9859.
- (366) Corey, E. J.; Cheng, X.-M. *The Logic of Chemical Synthesis*; John Wiley & Sons: New York, 1989.
- (367) Lee, C.-H.; Lindsey, J. S. *Tetrahedron* **1994**, *50*, 11427.
- (368) Cadamuro, S.; Degani, I.; Dughera, S.; Fochi, R.; Gatti, A.; Piscopo, L. *J. Chem. Soc., Perkin Trans. 1* **1993**, 273.
- (369) Barbero, M.; Cadamuro, S.; Degani, I.; Fochi, R.; Gatti, A.; Regondi, V. *Synthesis* **1986**, *12*, 1074.
- (370) Barbero, M.; Cadamuro, S.; Degani, I.; Fochi, R.; Gatti, A.; Regondi, V. *J. Org. Chem.* **1988**, *53*, 2245.
- (371) Carell, T., Ph.D. thesis, Ruprechts-Karl-Universität Heidelberg 1994. referenced in: Shipps Jr., G.; Rebek Jr., J. *Tetrahedron Lett.* **1994**, *35*, 6823.
- (372) Wang, N.-C.; Anderson, H. J. *Can. J. Chem.* **1977**, *55*, 4103.
- (373) Kakushima, M.; Hamel, P.; Frenette, R.; Rokach, J. *J. Org. Chem.* **1983**, *48*, 3214.
- (374) Rokach, J.; Hamel, P.; Kakushima, M.; Smith, G. M. *Tetrahedron Lett.* **1981**, *22*, 4901.
- (375) Anderson, H. J.; Loader, C. *Synthesis* **1985**, 353.
- (376) Fischer, H.; Orth, H. *Die Chemie des Pyrrols*; Akademische Verlagsgesellschaft (Johnson Reprint, New York 1968): Leipzig, 1934; Vol. I, pp 349-350.
- (377) *Pyrroles, Part 1*; Jones, R. A., Ed.; John Wiley & Sons: New York, Chichester, Brisbane, Toronto, Singapore, 1990; Vol. 48.
- (378) Lindsey, J. S.; Hsu, H. C.; Schreiman, I. C. *Tetrahedron Lett.* **1986**, *27*, 4969.

-
- (379) Lindsey, J. S.; Wagner, R. W. *J. Org. Chem.* **1989**, *54*, 828.
- (380) Franck, B. *Angew. Chem., Int. Ed. Engl.* **1982**, *21*, 343.
- (381) Schumacher, K.-H.; Franck, B. *Angew. Chem., Int. Ed. Engl.* **1989**, *28*, 1243.
- (382) Battersby, A. R.; Baker, M. G.; Broadbent, H. A.; Fookes, J. R.; Leeper, F. J. *J. Chem. Soc., Perkin Trans. 1* **1987**, 2027.
- (383) Battersby, A. R.; Leeper, F. J. *Chem. Rev.* **1990**, *90*, 1261.
- (384) Sessler, J. L.; Lisowski, L.; Boudreaux, K.A.; Lynch, V.; Barry, J. Kodadek, T.J. *J. Org. Chem.* **1995**, *60*, 5975.
- (385) Tanaka, H.; Yamauchi, O. *Chem. Pharm. Bull.* **1962**, *10*, 435.
- (386) Barnett, G. H.; Anderson, H. J.; Loader, C. E. *Can. J. Chem.* **1980**, *58*, 409.
- (387) Málek, R. *J. Org. React.* **1988**, *36*, 249.
- (388) Bringmann, G.; Schneider, S. *Synthesis* **1983**, 138.
- (389) Friedman, L.; Shecter, H. *J. Org. Chem.* **1961**, *26*, 2522.
- (390) Streith, J.; Fizet, C.; Fritz, H. *Helv. Chim. Acta* **1976**, *59*, 2786.
- (391) Yoshida, K. *J. Am. Chem. Soc.* **1977**, *99*, 6111.
- (392) Adamcyk, M.; Reddy, R. E. *Tetrahedron Lett.* **1995**, *36*, 7983.
- (393) Szabo, W. A. *Aldrichimica Acta* **1977**, *10*, 23.
- (394) Lohaus, G. *Chem. Ber.* **1967**, *100*, 2719.
- (395) Vorbrüggen, H. *Tetrahedron Lett.* **1968**, *13*, 1631.
- (396) Mehta, G.; Dhar, D. N.; Suri, S. C. *Synthesis* **1978**, 374.
- (397) Loader, C. E.; Anderson, H. *Can. J. Chem.* **1981**, *59*, 2673.
- (398) Boyle, R. W.; Karunaratne, V.; Jasat, A.; Mar, E. K.; Dolphin, D. *Synlett* **1994**, 939.
- (399) Anderson, H. J. *Can. J. Chem.* **1959**, *37*, 2053.
- (400) Paine III, J. B. Ph. D. Thesis, Harvard University, Cambridge, 1973.
- (401) Nöth, H.; Rurländer, R.; Wolfgardt, P. *Z. Naturforsch.* **1980**, *35b*, 31.
- (402) Akitt, J. W. *Progress in NMR Spectroscopy* **1989**, *21*, 1.
- (403) Wang, S. S.; Sukeniki, C. N. *J. Org. Chem.* **1986**, *50*, 5448.
- (404) Yoon, N. M.; Brown, H. C. *J. Am. Chem. Soc.* **1968**, *90*, 2927.

-
- (405) Cotton, F. A.; Wilkinson, G. *Advanced Inorganic Chemistry*; 5th ed.; John Wiley & Sons: New York, 1988.
- (406) Tanaka, H.; Yamauchi, O. *Chem. Pharm. Bull.* **1961**, *9*, 588.
- (407) Papadopoulos, E. P.; Haidar, N. F. *Tetrahedron Lett.* **1968**, *14*, 1721.
- (408) Rapoport, H.; Castagnoli, N., Jr. *J. Am. Chem. Soc.* **1962**, *84*, 2178.
- (409) Itahara, T. *J. Chem. Soc., Chem. Commun.* **1980**, 49.
- (410) Grigg, R.; Johnson, A. W.; Wasley, J. W. F. *J. Chem. Soc.* **1963**, 359.
- (411) Paine, J. B., III; Woodward, R. B.; Dolphin, D. *J. Org. Chem.* **1976**, *41*, 2826.
- (412) Silverstein, R. M.; Ryskiewicz, E. E.; Willard, C. *Org. Synth. Coll. Vol.* **1963**, *4*, 831.
- (413) Wijesekera, T. Ph.D. Thesis, University of British Columbia, 1980.
- (414) Ramasamy, K.; Robins, R. K.; Revankar, G. R. *J. Heterocyclic Chem.* **1987**, *24*, 863.
- (415) Korth, H. G.; Ingold, K. U.; Sustmann, R.; de Groot, H.; Sies, H. *Angew. Chem., Int. Ed. Engl.* **1992**, *31*, 891.
- (416) Cheng, R.-J.; Chen, Y.-R.; Chuang, C.-E. *Heterocycles* **1992**, *34*, 1.
- (417) Manka, J.S.; Lawrence, D.S. *Tetrahedron Lett.* **1989** *30(50)* 6989.
- (418) (a) *International Tables for X-Ray Crystallography*; Kynoch Press: Birmingham, UK, 1974; Vol. IV, pp 99-102, 149-150. (b) *International Tables for Crystallography*; Kluwer Academic Publishers: Boston, 1992; Vol. C, pp 219-222.
- (419) Kim, J. B.; Adler, A. D.; Longo, F. R. In *The Porphyrins*; D. Dolphin, Ed.; Academic Press: New York, 1978; Vol. 1; pp 85-100.
- (420) Adams, H.; Bailey, N.A.; Fenton, D.E.; Moss, S.; Rodriguez de Barbarin, C.O.; Jones, G. *J. Chem. Soc., Dalton Trans.*, **1986**, 693.

PART 2

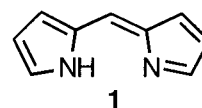
***meso*-PHENYLDIPYRRINS -
SYNTHESIS
AND
METAL COMPLEX FORMATION**

1 INTRODUCTION

As described in Part 1, the synthesis of large quantities of *meso*-phenyl-dipyrromethane and *meso*-diphenyltripyrane became feasible. Aside from their main use as starting material for the directed synthesis of 'N-confused' and *meso*-diphenyl porphyrins etc., their oxidation to the corresponding unsaturated novel *meso*-phenyl substituted dipyrrens and tripyrrins, and a study of their metal-complexing properties appeared to be an interesting goal.

1.1 ALKYLDIPYRRINS AND THEIR METAL COMPLEXES

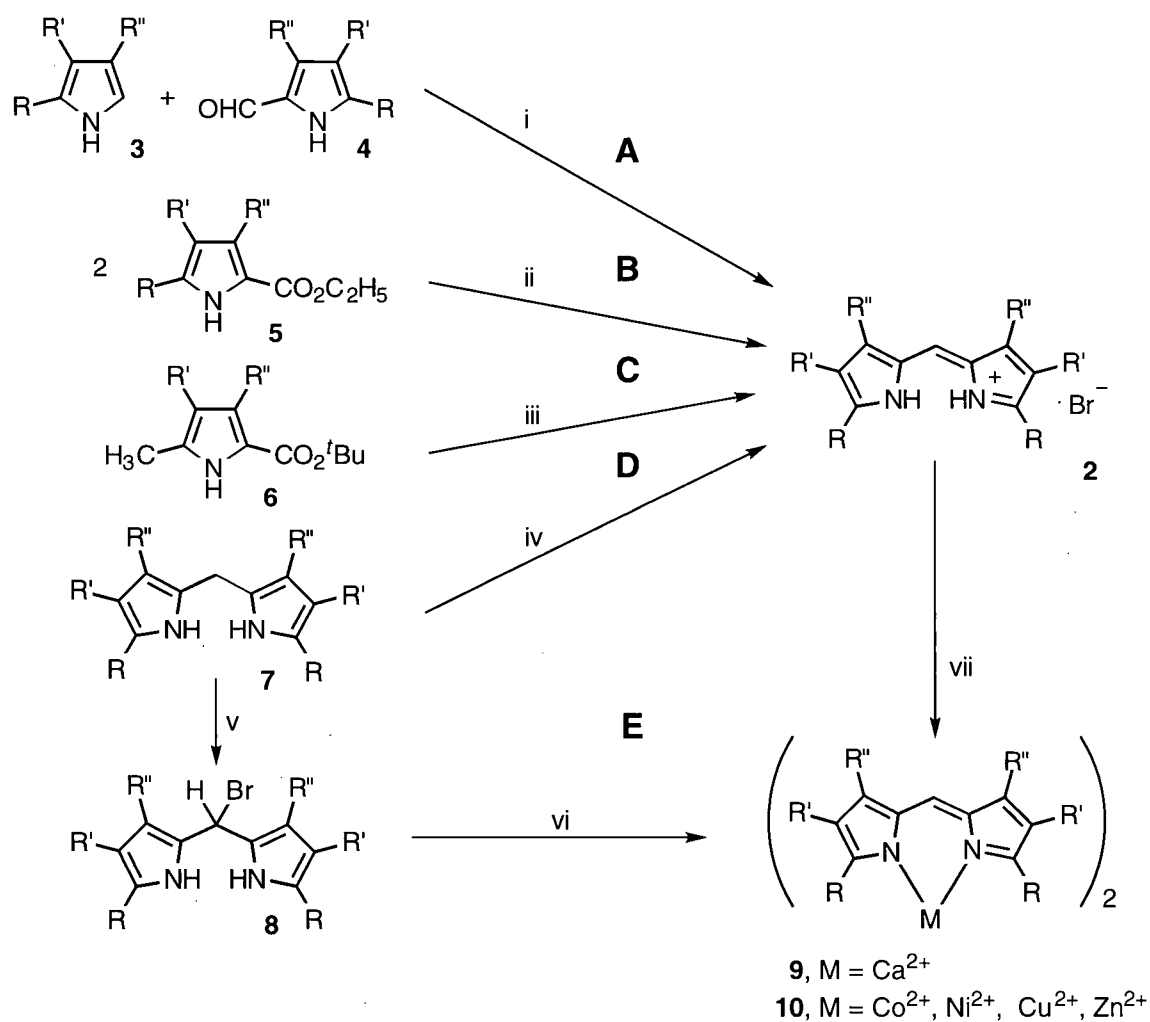
Dipyrrens (**1**) are basic, brightly colored, fully conjugated and flat bipyrrrolic pigments. Their propensity to strongly chelate transition metals has long been recognized.¹ Scheme 2-1 outlines the principal pathways for the synthesis of alkyldipyrrens (**2**) and their chelate type mode of metal complex formation.² Five main synthetic pathways can be distinguished:



A The 'classic' and most versatile reaction is the acid catalyzed condensation of an α,β -alkyl- α' -free pyrrole (**2**) with a trialkylpyrrole- α -aldehyde (**3**)¹⁻³

B The reaction of an α,β -alkyl- α' -ethyloxycarbonylpyrrole (**5**) in concentrated formic acid induces the cleavage of the ester, spontaneous decarboxylation to the α -unsubstituted pyrrole, and subsequent fusion by formic acid of two units to form the desired dipyrin⁴

C The halogenation of an α -unsubstituted α' -methylpyrrole (**6**) induces a head-to-tail condensation of two molecules of the initially formed α -(halomethyl)- α -unsubstituted pyrrole to give **2** ($R = \text{Br}, \text{CH}_2\text{Br}$)^{1,2}



Scheme 2-1

Synthetic pathways towards dipyrrens

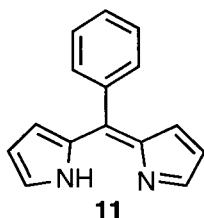
Reaction conditions: (i) HBr/EtOH ; (ii) HCOOH conc.; (iii) Br_2/AcOH ; (iv) oxidation by a variety of oxidants; (v) Br_2 ; (vi) 1. CaO , 2. M(II)X_n ; (vii) M(II)X_2

D The oxidation of hexaalkyldipyrromethanes (**7**) by a wide variety of oxidants, *e.g.* ferric chloride¹, or DDQ⁵

The dipyrins prepared by methods **A-D** are generally isolated as their stable and well crystallizable hydrobromide or hydrochloride salts.

E The *meso*-bromination of a dipyrromethane to yield the *meso*-bromo-dipyrromethane **8**, and subsequent reaction with calcium oxide to form the calcium complex **9**, yield directly a metal chelate. This calcium chelate can easily be transmetallated with a variety of transition metals.⁶⁻⁸

In all other cases, reaction of dipyrin **2** with a divalent transition metal salt yields the corresponding dipyrinato complexes **10**. None of the methods **A**, **B**, **C** or **E** have the potential to give access to *meso*-substituted, α,β -free dipyrins such as, for instance, **11**.



Only route **D** offers access to the title compounds by oxidation of a *meso*-phenyldipyrromethane⁹. As will be outlined later in detail, this route was, indeed, successful in providing the title compounds.

Hexaalkyldipyrins, such as **2**, have been of interest because of their relation to the biological important porphyrins and bile pigments and, consequently, their use as intermediates in the synthesis of them.^{10,11} In fact, dipyrins were the obligatory intermediates in Fischer's porphyrin synthesis, historically the first discovered method for preparing these macrocycles.¹² It was also Fischer who pointed out the strong sternutatory (causing sneezing) effect of these compounds, which were particularly strong of β -free dipyrin hydrobromides.^{2,13,14} Luckily, this effect could not be detected in the β,β' -unsubstituted *meso*-phenyldipyrins or its salts.

1.2 *meso*-SUBSTITUTED 4,6-DIPYRRINS

meso-Alkyl substituted dipyrrens are less common.^{1,15,16} This can, perhaps, be explained by the fact that most naturally occurring porphyrins are *meso*-unsubstituted. In the case of *meso*-substituents containing an α -hydrogen atom the dipyrren salt (**12**) will tautomerize, upon deprotonation, to yield the corresponding *meso*-ylidenedipyrrens (**13**) (Figure 2-1).^{10,17,18} One such example of this class was recently described by Xie *et al.*¹⁹

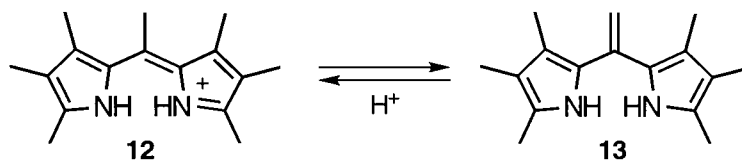
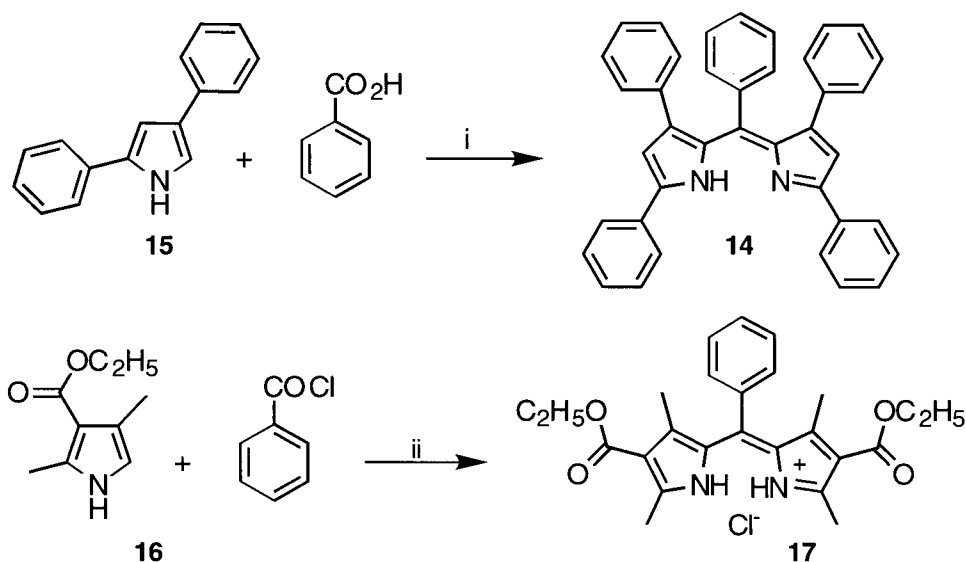


Figure 2-1 *meso*-Methyldipyrren - *meso*-ylidenedipyrrene equilibrium

Reports of *meso*-phenyl substituted dipyrrens are even rarer. In fact, the author is aware of only three previous syntheses, two of which are shown in Scheme 2-2. Rogers confirmed in 1943 a finding from 1908²⁰, which described the formation of **14** by reaction of 2,4-diphenylpyrrole (**15**) with *in situ* generated benzoylchloride.^{21,22} In a similar approach, Treibs and co-worker reacted pyrrole **16** with benzoylchloride to yield the hexasubstituted *meso*-phenyldipyrren hydrochloride **17**.⁴ It is noteworthy that in both instances the pyrroles were substituted, particularly at one α - and at least one β -position. This prevents polymerization of the pyrroles during the harsh reaction conditions. Consequently, these methods are not options to synthesize *meso*-phenyl, α -unsubstituted dipyrrens. A disadvantage of the protecting α -phenyl moieties is that they introduce severe steric inter-ligand interactions upon metal complex formations. Moreover, *meso*-phenyl substitution concomitant with β -substituents introduces intra-ligand steric interactions which can, for

instance in the case of **14**, lead to deviations from planarity and even chemical instability.²³ No report was given on the metal complexation properties of either **14** or **17**.



Scheme 2-2 Formation of *meso*-phenyldipyrins
Reaction conditions: (i) POCl₃/Δ; (ii) Δ

In 1985 an X-ray structure of bis[1-(2,6-dichlorobenzyl)-5-(2,6-dichlorophenyl)-dipyrinato]-zinc(II) was reported.²⁴ This *meso*-phenyl and α -substituted dipyrin complex was the kinetic product in the Rothmund-type condensation of the sterically hindered 2,6-dichlorobenzaldehyde with pyrrole, and its isolation was unexpected and fortuitous. Thus, this synthetic pathway towards *meso*-phenyl dipyrins and their metal complexes cannot be generalized. Recently some reports appeared in the literature in which *meso*-phenyl substituted dipyrin moieties were integral parts of larger molecules. The BF₂-complex of an α -methyl-*meso*-phenyl-dipyrin unit was the input unit of a molecular photonic wire²⁵ and an α -thiophenyl and β -alkyl substituted *meso*-phenyldipyrin was synthesized in the course of research towards polyheterocyclic ligands²⁶; however, neither the complexing properties nor the conformation of this compound was reported.

The stereochemistry of these ligands around the metal is dependent on the bulkiness of the substituents in the α - and α' -position, and has found interest²⁷ since Porter²⁸ called attention to this phenomenon. However, only limited structural data are available.^{27,29,30} Few α -unsubstituted dipyrinato complexes have been prepared³¹⁻³⁴ and in no case has a crystal structure been described. Therefore, it was interesting to investigate the complex geometry of the α,α' -unsubstituted *meso*-phenyldipyrin ligands of type **2** and to contrast these findings with published data. This and the general interest for novel ligand classes for use in transition metal catalysis,³⁵ photometric metal detection³⁶ or biomedical purposes³⁷ prompted the investigation of the synthesis and the metal complexing properties of α,β -unsubstituted *meso*-phenyldipyrins.

Other more distantly related *meso*-substituted pigments have been described. For instance, Wagner *et al.*³⁸ reported the crystal structure of a 10-aryl-bilatriene-*abc*. Structurally related to dipyrins are 1,9-dioxodipyrins (propentdyopent). For their synthesis see Bonnett and co-workers³⁹, and for the structure of a bis(1,9-dioxodipyrinato)Cu(II) complex see Balch and co-workers⁴⁰.

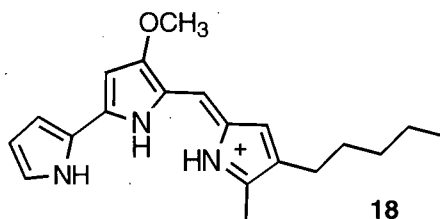
1.3 4,7-DIPYRRINS

Reports on α - β -linked 4,7-dipyrins (as well as on β,β' -linked dipyrins)⁴¹ are scarce. They are reportedly fairly unstable⁴² and this might be the reason that they are not well characterized. As the α - β -linked isomer to **20**, *meso*-phenyl-2,3'-dipyrromethane, was synthesized in due course of the studies described in Part 1, section 2.2.2, attempts to oxidize this compound to the corresponding 4,7-*meso*-phenyldipyrin suggested itself. However, all experiments led to no avail.

1.4 TRIPYRRINS AND RELATED TRIPYRROLIC PIGMENTS

Although the biosynthetic pathway for all tetrapyrrolic pigments involves the porphobilinogen deaminase catalyzed tetramerization of porphobilinogen to a porphyrinogen *via*, undoubtedly, a tripyrrane intermediate, these tripyrrolic compounds have received only little attention, as have their dehydro species.⁴³⁻⁴⁵ Also in comparison to the wealth of knowledge on linear tetrapyrrolic compounds such as bilanes, biladienes, bilines and bilones, the knowledge about the tripyrrolic congeners is minimal.¹⁰ To the best of our knowledge, only one tripyrrinone has been structurally characterized.⁴⁶ Coordination compounds of tripyrrinones have been investigated⁴⁷ and used in intriguing carrier mediated proton driven countertransport chains in which metal ions are transported across a liquid membrane against a concentration gradient.⁴⁸

Apparently the only tripyrrolic pigments of wider interest are those related to prodigiosene (**18**), the first isolated member of a class of naturally occurring pigments with strong antimicrobial and cytotoxic properties, all possessing the 2-pyrrolyldipyrin skeleton.^{49,50}



As outlined in Part 1, section 2.2.2, no *meso*-phenyl substituted tripyrrane was previously known. It was, therefore, interesting to study the oxidation of this tripyrrane in order to see whether the corresponding *meso*-phenyltripyrin, similarly not described before, could be derived. Section 2.4 of this Part describes the results of these studies.

2.2 PREPARATION AND CHARACTERIZATION OF *meso*-PHENYLDIPYRRINS

Dehydrogenations with DDQ have found wide application in the synthesis of pyrrolic pigments.⁵¹ In particular, DDQ is useful in the conversion of any type of reduced porphyrins (*e.g.* porphyrinogens or chlorins) to the corresponding fully unsaturated porphyrins.⁵² Porphyrinogens are intermediates in the TPP synthesis according to the methods of Adler⁵³ or Lindsey⁵⁴, *i.e.* the acid catalyzed cyclization of pyrrole and benzaldehyde. Hence, it was not unexpected that the reaction of *meso*-phenyl- α,α' -dipyrins **19** or **20** with one equivalent of DDQ smoothly formed the desired dipyrins **23** and **11**, respectively (Scheme 2-3). *p*- and *o*-Chloranil are equally well suited to perform the conversion. Reduction of **11** or **23** with NaBH₄ in MeOH regenerates the leuko form **20** or **19**. In dilute solution, the oxidation products are bright yellow in color. The optical spectrum of **20** under acidic and basic conditions is shown in Figure 2-2.

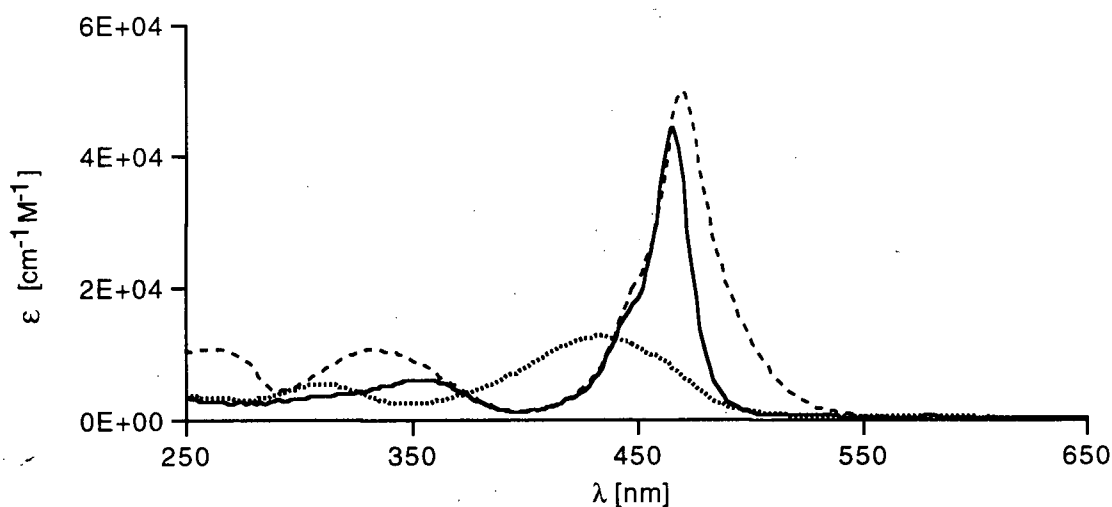


Figure 2-2 UV-visible spectrum of **11** in MeOH/trace NH₃ (.....), and in MeOH/trace HCl (—), and **23** in MeOH/trace HCl (----)

The two-band pattern of the protonated species is analogous to that of 3,3',4,4',5,5'-tetramethyldipyrin¹⁵, but ~14 nm hypsochromically shifted, with slightly lower extinction coefficients. The bands have been assigned to $\pi^* \leftarrow \pi$ transitions and are indicative of the marked planarity of these fully conjugated aromatic systems. Addition of acid protonates the basic imine-type nitrogen of the *2H*-pyrrole unit and this removal of non-degeneracy of the linear resonator in combination with the presence of a positive charge induces a bathochromic shift of 42 nm and a doubling of the extinction coefficient.⁵⁵ For steric reasons, it can be inferred that the phenyl moiety is approximately perpendicular to the plane of the dipyrin. Consequently, the phenyl group is not in full conjugation with the pyrrolic system and substituents on the phenyl group minimally influence the π -cloud of the dipyrin. This explains the close similarity of the optical spectrum of **11** and its *p*-nitro-derivative **23**; a similar situation is also found in variously phenyl substituted TPPs.⁵⁶ The optical spectrum of **11** is more similar to that of the hexamethyldipyrin than to the spectrum of **14** which is about 110 nm bathochromically shifted²³, possibly reflecting the extended conjugation (and distortion) of the system by the α -phenyl groups. The *p*-nitro compound **23** and its metal complexes exhibit an additional band at ~258 nm which can be attributed to the *p*-nitrophenyl moiety.

The observed numbers of signals in the ¹H and ¹³C-NMR of the *meso*-phenyl- α,α' -dipyrins indicate a plane of symmetry. This is consistent with formulating the dipyrins as adopting a planar conformation and a rapid tautomeric exchange of the NH-proton between the two nitrogens. As a result of this fast exchange, the proton is lodged between the two nitrogens, indicated by the low field resonance of 12.5 ppm for this strongly hydrogen-bonded proton.* It can be concluded that *meso*-phenyldipyrins have the above shown Z

* For the energetics of the tautomeric exchange, see Falk and Hofer⁴²; for the energetics of the conformational interchanges see Falk and Müller⁵⁷.

configuration (based on the *exo*-cyclic double bond) and *syn* conformation (based on the *exo*-cyclic single bond).¹⁰ The ¹H-NMR spectrum shifts for the β-protons of **11** of 6.39 and 6.47 ppm and for the α-protons of 7.78 ppm attest to the aromatic character of these compounds.

Alkyldipyrrens of type **2** are, owing to their basicity, generally isolated and purified as their hydrobromide or hydrochloride salts.¹ Although conditions for thin-layer and column chromatography of dipyrren hydrobromides have been described it is not a common practice. Their free bases are also reportedly less stable. Hence, it was surprising to find that in the case of the *meso*-phenyldipyrrens, column chromatography (CH₂Cl₂/silica gel) of their free bases posed no difficulty.

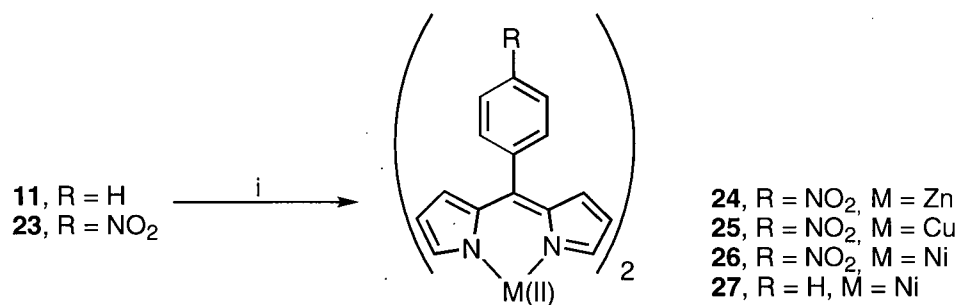
It should also be noted that, as assessed by UV-visible spectroscopy, the oxidation of several α- and β-substituted *meso*-Phenyldipyrromethanes such as 2,2'-dicarbonylethoxy-5-phenyl-3,3',4,4'-tetramethyldipyrromethane, with DDQ, to their corresponding dipyrrens is possible.

2.3 FORMATION AND CHARACTERIZATION OF TRANSITION METAL CHELATES OF *meso*-PHENYLDIPYRRINS

2.3.1 THE COMPLEXES OF Ni(II), Cu(II), AND Zn(II)

General Data and Synthesis

A concentrated MeOH-solution of the *meso*-phenyldipyrins **11** or **23** when mixed with a methanolic solution of the divalent metal ions Co^{2+} , Ni^{2+} , Cu^{2+} , and Zn^{2+} as their acetates, yields the corresponding highly colored metal complexes (Scheme 2-4). The nickel, copper, and zinc complexes are stable and do not require any special handling. The cobalt complexes are characterized by some special features, and are discussed in a separate chapter (Section 2.3.3). Analyses confirmed the stoichiometry of the precipitates as $\text{M}(\text{Ligand})_2$. The metal complexes formed X-ray quality dichroic (metallic dark green/red) crystals.



Scheme 2-4

Formation of dipyrinato complexes from dipyrins
Reaction conditions: (i) $\text{M}(\text{II})(\text{acetate})_2/\text{MeOH}/(\text{base})$

IR Spectra

The vibrational spectrum of the metal complexes are similar to those of their ligands. This is not unexpected as conjugation is already attained in the planar ligand moiety before coordination to a metal. Thus, intraligand vibrations will undergo only minor shifts upon metal chelation. This has been rationalized before for the metal complexes of hexaalkyldipyrins.⁵⁹

Optical Spectra

The optical properties of the metal compounds are strongly dependent on the central metal and, as expected, the spectra of the two nickel chelates **26** and **27** are very similar. (Figure 2-3 and 2-4). In solution, they are brilliant orange in color.

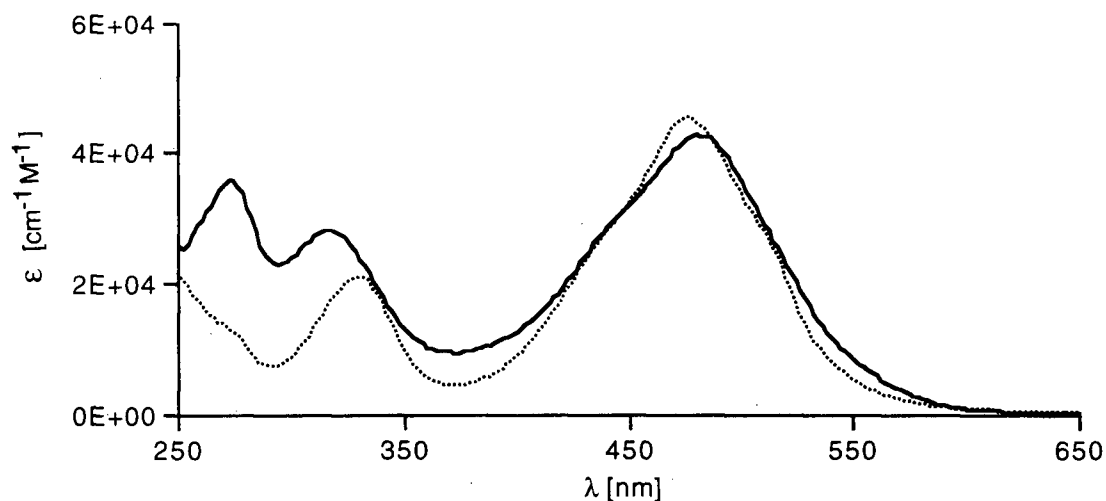


Figure 2-3 UV-visible spectra of **27**(.....) and **26** (—) in CH₂Cl₂

This similarity, particularly with respect to λ_{\max} and $\log \epsilon$, is indicative of a very similar stereochemistry of these two compounds. The optical spectrum of the zinc chelate **24** (bright yellow color) resembles that of the protonated ligand suggesting the absence of any metal \rightarrow metal transitions (Figure 2-4). However, charge transfer ligand \rightarrow metal transitions

are generally observed in this energy region and they cannot be excluded.²⁷ However, other authors⁶⁰ have assigned this band exclusively to intraligand $\pi^* \leftarrow \pi$ transitions and the bands in the 320-350 nm region to charge transfer transitions. The electronic spectra of the nickel and copper chelates **26**, **27**, and **25** follow the same pattern as that of **24**. The optical spectra of the metal chelates are nearly indistinguishable in non- or weakly coordinating solvents such as benzene, methanol, methylene chloride or chloroform but show changes in pyridine, most noticeable for the zinc chelate **24**, as also shown in Figure 2-4. Table 2-1 lists selected optical data of some known dipyrinato-metal complexes (shown below) and of the novel compounds **24**, **25** and **26**.

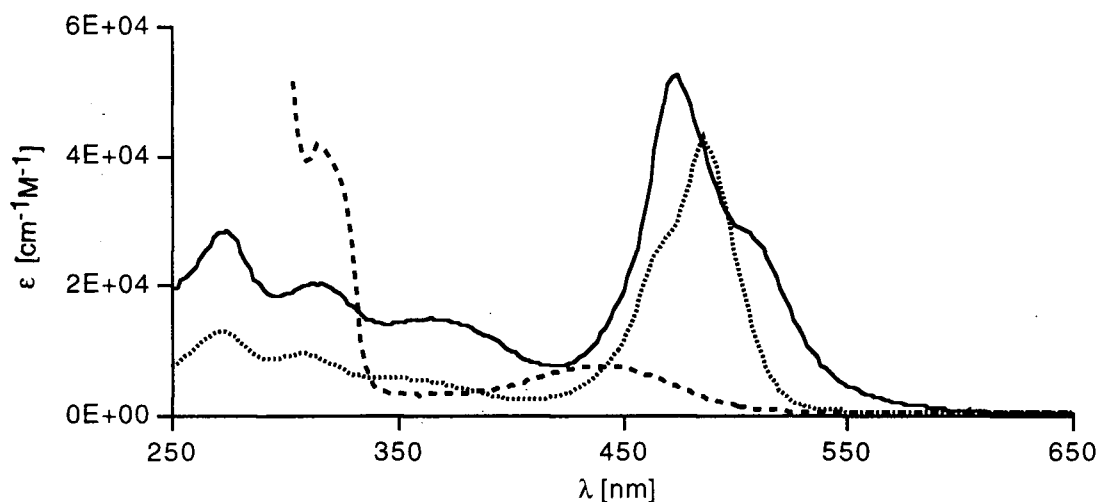
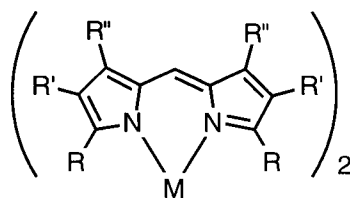


Figure 2-4 UV-visible spectra of **25** (—) and **24** (.....) in CH_2Cl_2 , and of **24** (-----) in $\text{CH}_2\text{Cl}_2/20\%$ pyridine

When comparing the longest wavelength absorption of the zinc chelate **24** at 486 nm against the equivalent transitions of the alkyl substituted analogies **27-34**, it is remarkable that the *meso*-phenyldipyrin chromophore is distinguished by the highest energy transition. An equivalent trend can be seen in the nickel (**26** vs. **35-38**) and copper (**25** vs. **39-42**) chelate series. Hyperconjugation effects have been suggested for the progressive bathochromic shift with increasing methyl-substitution.³² Extended π -conjugation can be

evoked for the bathochromically shifted optical spectrum in case of dipyrins **30** and **34**. The absence of both effects in the zinc, nickel and copper chelates **24-27** rationalizes their relatively high transition energies. The introduction of a *meso*-methyl substituent in chelates **31** and **32** leads, when compared to their *meso*-unsubstituted analogies **29** and **30**, to a relatively small change in the energy of the longest wavelength transition, however, their extinction coefficients significantly decrease. This, based on theoretical considerations, may be taken as a sign of distortion from planarity.²³



	R	R'	R''	R _{meso}	M ²⁺
19	-H	-H	-H	-Ph ^C	Zn
25	-H	-Me	-Me	-H	Zn
26	-Me	-H	-Me	-H	Zn
27	-Me	-Me	-Me	-H	Zn
28	-Me	-CO ₂ Et	-Me	-H	Zn
29	-Me	-CO ₂ Et	-Me	-Me	Zn
30	-Me	-Me	-Me	-Me	Zn
31	-CO ₂ Et	-Cl	-Cl	-H	Zn
32	-Ph	-H	-H	-H	Zn
22	-H	-H	-H	-Ph	Ni
33	-Me	-H	-Me	-H	Ni
34	-Me	-Me	-Me	-H	Ni
35	-Me	-CO ₂ Et	-Me	-H	Ni
36	-Ph	-H	-H	-H	Ni
21	-H	-H	-H	-Ph ^C	Cu
37	-H	-Me	-Me	-H	Cu
38	-Me	-Me	-Me	-H	Cu
39	-Me	-CO ₂ Et	-Me	-H	Cu
40	-Ph	-H	-H	-H	Cu

Based on the foregoing, the high extinction coefficients of the metal chelates of the *meso*-phenyldipyrins seem to indicate that the ligands are flat. In the absence of any β -substituent and hence any intraligand steric crowding, and in analogy to the conformation of TPPs⁶¹, this appears to be a reasonable assumption. As will be detailed later, the single crystal X-ray structure of **27** (and of **48**) shows that the assumption of planarity is, in fact, valid.

Table 2-1 UV-visible data and dihedral angles of literature known and novel dipyrinato-complexes

	λ_{\max} (log ϵ) ^a [nm]	dihedral angle [°] ^b	reference
19	486 (4.97) ^d	90 ^g	this work
25	500 (5.08) ^e , 483 (4.97)	90 ^g	27
26	488 (4.22) ^e , 469, sh	90 ^g	27
27	505 (4.93) ^e , 487 (5.07)	90 ^g	27
28	490 (5.33) ^e , 446, sh	90 ^g	27
29	501 (5.05) ^f		15
30	505 (4.06) ^f		15
31	537 (5.13) ^e		8,62
32	552 (4.93) ^e , 510 (5.06)	90 ^g	27
22	484 (4.63) ^d	42 ^h , 38.5 ⁱ	this work
33	512 (4.85) ^e	76.3 ⁱ	29,59
34	531 (4.70) ^e , 462 (4.57)		59
35	495 (4.99) ^e		60
36	540 (4.85) ^e	≤ 60 ^j , 66 ^h	31
21	474 (4.72) ^e	48 ^h	this work
37	471 (4.85) ^e , 409 (4.61)	50 ^h , 63 ^j	31
38	525 (4.65) ^e , 471 (4.76)	68 ^j	59
39	495 (5.05) ^e	66 ^j	30,60
40	564 (4.93) ^e , 509 (4.70)	90 ^h , 73 ^j	31

^aof longest wavelength $\pi^* \leftarrow \pi$ transition, ^bbetween planes formed by the ligands, ^c*p*-NO₂-phenyl; ^din CH₂Cl₂; ^ein CHCl₃; ^fsolvent not specified; ^gassumed angle; ^hcalculated according to Motekaitis and Martell⁸ ⁱfrom X-ray crystal structure; ^jbased on ligand field transition analysis³¹

The stereochemistry of the ligands around the central metal is strongly dependent on the metal type. The preference of zinc(II) for a tetrahedral and of nickel(II), and, even more so, of copper(II) for a square planar coordination sphere is well documented.⁶³ Regardless of the α -substituents present in the dipyrin ligands, the realization of a tetrahedral coordination sphere poses no inter-ligand steric interactions. Consequently, and in analogy to the stereochemistry of the zinc chelates of alkyldipyrins, compound **24** can be assigned a tetrahedral structure.^{8,27,32,60} The picture is more complex for the nickel and copper chelates. It has been found in previous studies that α -substituents prevent square planar coordination due to inter-ligand crowding. This forces the complex into a distorted tetrahedral structure in which the two approximately planar α -methyldipyrinato ligands are inclined (as determined by X-ray crystal structure analysis) at an angle (referred to as dihedral angle) of 76.3° for the nickel chelate **35**²⁹ and 66° for the copper chelate **41**³⁰. With hydrogen as the sole α -substituents no *a priori* statement can be made about the stereochemistry around the metal. It has been suggested that some electronic interaction exists between the π -systems of the two dipyrin units coordinated to the same metal ion in the 'tetrahedral' cobalt(II) and copper(II) complexes.⁶⁴ Martell and co-worker presented an MO theory model and derived a relationship (Equation 2-1) where the intensity of the longest wavelength transition is assumed to change with the tetrahedral angle Θ between the ligands:⁸

$$\frac{\epsilon^{\Theta}}{\epsilon^{90}} = \sin^2 \Theta \quad \text{Equation 2-1}$$

Θ is the tetrahedral angle, ϵ^{90} is the extinction coefficient of a reference compound known to be tetrahedral, *i.e.* $\Theta = 90^\circ$, and ϵ^{Θ} is the extinction coefficient of a similar compound whose geometry is to be determined. According Equation 2-1, the calculated tetrahedral angle in nickel complex **26** would be 42°, and in the copper complex **25**, 48°.

There are, though, precautions to be taken when applying Martell's methodology for determination of the inter-ligand dihedral angle. The prerequisite that the ligands are flat and coordinate in exactly the same MN_4 -fashion to the complexes to be compared must be strictly fulfilled. Fergusson and co-workers, for instance, published a crystal structure analysis of the palladium chelate of 3,3',5,5'-tetramethyl-4,4'-diethoxycarbonyldipyrin in which the dipyrin unit was not planar. The tendency for palladium to achieve square planar coordination geometry is strong enough to distort the planar ligand and to enforce a stepped arrangement of the ligands around the metal centre.²⁷ With little change in transition energy, the extinction coefficients were reduced compared to the analogous tetrahedral cadmium, mercury or zinc complexes and, consequently, the application of equation 2-1 gives incorrect results when compared to the actual structure. A second example can be derived from examination of the literature. Based on the extinction coefficient of **33**, Martell and co-worker determined the dihedral angle of the copper analog to be 40° .⁸ However, considering the steric requirement of the ethoxycarbonyl moiety and setting it against the crystallographically determined dihedral angle of 66° for **41**, or values determined for the complexes **39** - **42**, this value appears to be considerably too low. Murakami *et al.* investigated the IR spectrum and the ligand-field bands of this complex and proposed the involvement of the carbonyl oxygen in this copper chelate, giving a CuN_4O_2 coordination.⁶² In light of this it becomes apparent that the dihedral angle predicted by Martell's method had to be in error. In the present case, however, the prerequisites of similarly flat ligands forming in all cases of an MN_4 coordination sphere is most likely fulfilled and, consequently, the theoretically determined values may be significant. Indeed, an X-ray crystal structure analysis for the nickel complex **27** proved the value determined by Martell's method to be fairly accurate (3.5° deviation, Table 2-1). As for the copper chelate, a final experimental proof of the calculated value is still awaited, but the value of 48° is in agreement with the calculated value of one other α -unsubstituted copper chelate **39**, and, as expected, is significantly smaller than for the α -alkylsubstituted chelates. The calculated

values for copper chelates have to be taken with some reservation as shown by the discrepancies of the values determined by ligand field transition band analysis and by Martell's method.

The change of the optical spectrum of **24** upon the addition of pyridine (Figure 2-4) results from an expansion of the Zn-coordination sphere from tetrahedral ZnN_4 to a (distorted tetragonal) pyramid ZnN_5 . This forces the dipyrin ligands to take up a smaller dihedral angle, which probably accounts for the observed spectrum. The nickel chelate UV-visible spectrum shows only a slight change upon addition of pyridine. This is consistent with the reluctance of the square planar nickel(II)porphyrins to expand their coordination sphere and the small changes in their optical spectra associated with any coordination.⁶⁵ This effect is even more pronounced in the case of the Jahn-Teller ion copper(II).

NMR-Spectroscopy

The ^1H - and ^{13}C -NMR data of the diamagnetic metal chelates **24**, **26** and **27** are largely as expected, and are similar to the spectra of the protonated ligands. One noticeable exception is a large low field shift of the α -protons in the nickel chelates **26** and **27** (Figure 2-5), *i.e.* a shift of +2.48 ppm for **26** as compared to the zinc analog **24**. This is also evidence of the small dihedral angle of the ligand mean planes in the nickel complex. The α -protons experience shielding effects of both the aromatic dipyrinato systems and thus are more shielded when compared to the tetrahedral zinc complex, where such 'double' shielding cannot occur.

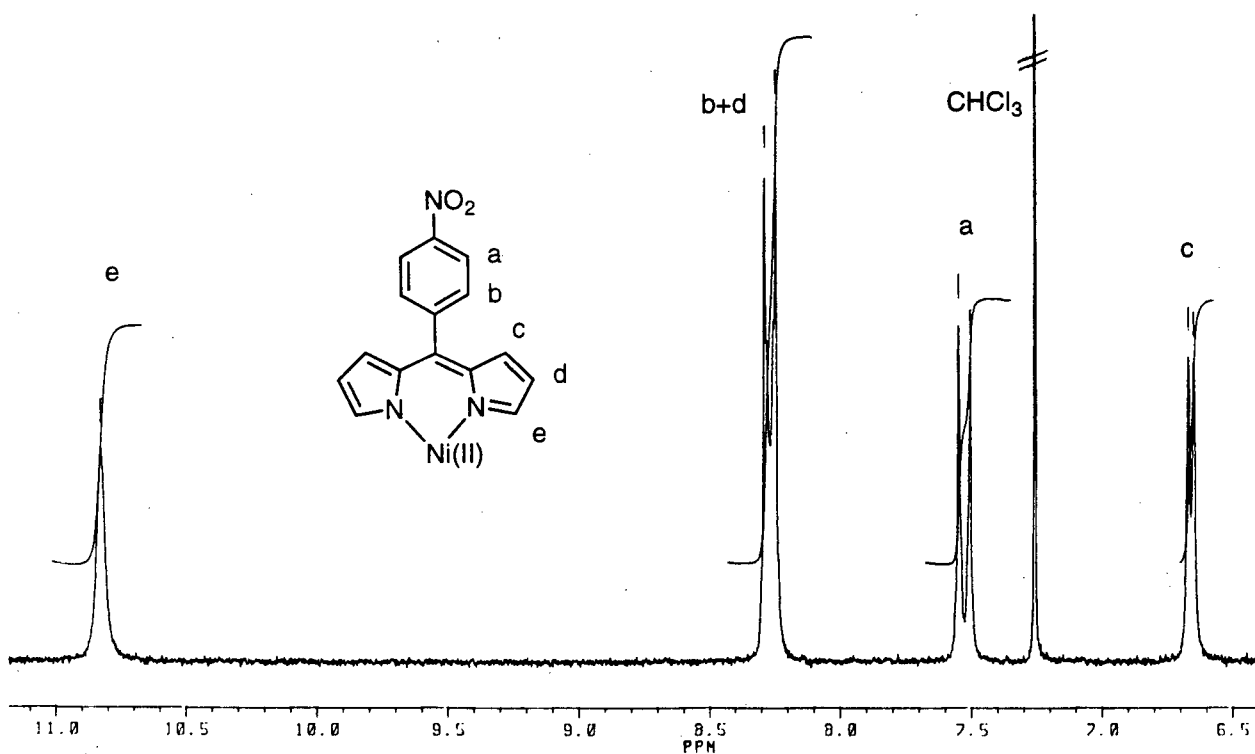
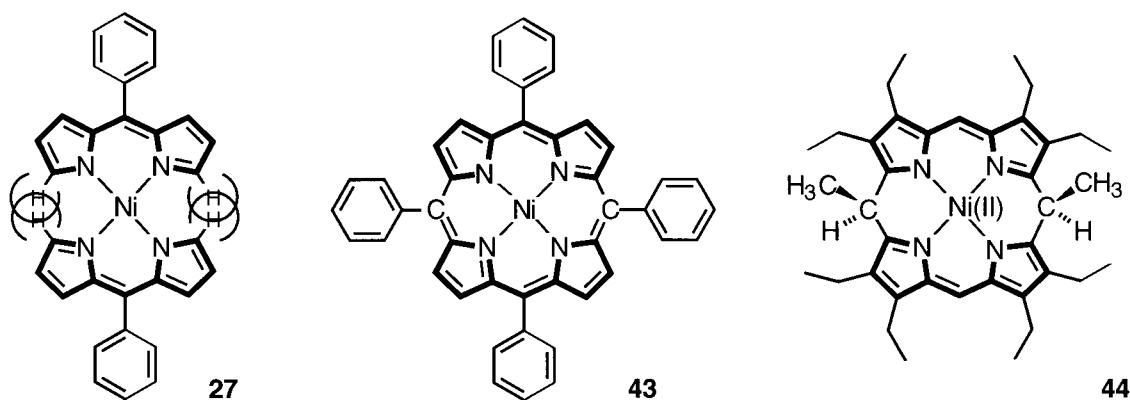


Figure 2-5 ^1H -NMR (200 MHz, CDCl_3) of **26**

Magnetic Properties

The magnetic properties of the nickel(II) complexes having N-donor ligands may allow conclusions regarding their coordination geometry: square planar complexes are typically diamagnetic, and tetrahedral complexes paramagnetic.⁶³ Nickel(II) chelates of α -substituted dipyrins have been described as paramagnetic^{8,60} and, therefore, their description as distorted tetrahedral rather than distorted square planar is plausible regardless of the actual dihedral angle between the ligands. It was, therefore, surprising, that the nickel chelates **26** and **27**, as judged by their sharp ¹H- and ¹³C-NMR spectra, proved to be diamagnetic. This suggests that they are (distorted) square planar. On the basis of a comparison of the steric interactions in the cyclic and planar [*meso*-tetraphenylporphyrinato]nickel(II) (**43**) or the cyclic and saddle shaped [5,15-dimethyl-5,15-dihydro-octaethylporphyrinato]nickel(II) (**44**)⁶⁶ it becomes clear that a planar coordination can be excluded since despite the absence of any α -substituents, the two α -hydrogens of the opposing ligands would occupy the same space (given standard Ni-N bond lengths) in case of square planar coordination.



To unambiguously answer the question about the dihedral angles in the nickel chelate, an X-ray crystal structure analysis of a single crystal of **27** was undertaken.

2.3.2 CRYSTAL STRUCTURE ANALYSIS OF BIS[*meso*-PHENYL-DIPYRRINATO]Ni(II) (27)

The ORTEP representation of **27** as it exists in the crystal together with the numbering system employed is shown in Figure 2-6. Table 2-2 lists selected bond lengths. The atom coordinates are listed in Table 2-4 (Experimental Section).

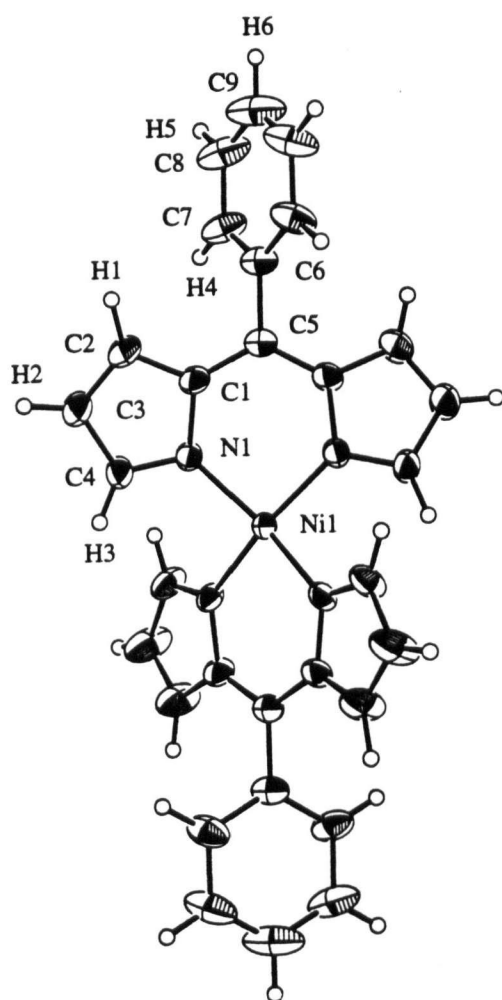
The molecule has an D_2 -symmetry, which makes the two ligands equivalent and endows an C_2 -axis passing through the *p*-hydrogens of the *meso*-substituent, the methine carbons and the central metal. The planes of the two essentially planar dipyrin ligands enclose a dihedral angle of 38.5° , in close agreement with the calculated value of 42° . The equivalent angle in [3,3',5,5'-tetramethyldipyrinato]nickel(II) (**35**) is, as mentioned above, 76.3° .²⁹ The small angle results directly from the smaller size of the α -H as compared to the α -methyl group.

The bite angle N–Ni–N_a of the ligand is 94.3° , which is, within the experimental uncertainty, equal to the bite angle observed for **35**. The N–Ni–N_b angle is 152.5° . Unlike in the latter structure, no distortion in the sense of a deviation of co-linearity of the two local two-fold axes of each Ni-ligand group can be detected. The four Ni–N distances are equal (1.879(2) Å) and unusually short for complexes of this kind. We regard this effect partially due to the reduced ionic radius of the d^8 low spin ion vs. the high spin congener⁶⁷ (**35**), and partially due to the reduced inter-ligand steric interactions. The extent of the steric effect becomes perceptible if the bond length is compared to those in related nickel complexes **35**,

nickel porphyrin (**43**), a ruffled nickel porphyrin (**45**), and a 5,10-dihydroporphyrin system **44** as listed in Table 2-3.

Table 2-2 Selected bond distances in **27**

Atoms	Distance [Å]
Ni(1)–N(1)	1.879(2)
N(1)–C(5)	1.336(3)
C(1)–C(5)	1.390(3)
C(3)–C(4)	1.396(4)
C(6)–C(7)	1.374(3)
C(8)–C(9)	1.355(4)
N(1)–C(1)	1.404(3)
C(1)–C(2)	1.405(4)
C(2)–C(3)	1.360(4)
C(5)–C(6)	1.505(4)
C(7)–C(8)	1.400(4)



Symmetry operations:
 (a) $1/4-x, 1/4-y, z$ (b) $x, 1/4-y, 5/4-z$
 (c) $1/4-x, y, 5/4-z$

Figure 2-6 ORTEP representation (33% probability level) of **27**

Symmetry operations:
(a) $1/4-x, 1/4-y, z$ (b) $x, 1/4-y, 5/4-z$
(c) $1/4-x, y, 5/4-z$

Table 2-3 Nickel-nitrogen bond length in selected tetrapyrrolic pigments

compound #	Ni-N bond length [Å]	reference
27	1.879(2)	this work
35	1.952(7) (averaged)	29
44	1.904(5) (3 out of 4)	66
45	1.929	68,69
43	1.93-1.96 ^a	70

^a octaalkylporphyrin nickel(II) complexes

The quasi-rigid porphyrin core (in complex **43**) resists undue radial expansions or contractions in the equatorial plane of the core. Therefore, the metal-porphyrin nitrogen bond lengths are restricted relative to the normal range of values that are found in metal-monodentate nitrogen ligand bond length, which results in a 'stretched' bond length of up to 1.96 Å.⁶⁶ Ruffled nickel porphyrins can reduce the bond length by about 0.03 Å; in the saddle shaped **44**, which is essentially a strapped bis(dipyrinato)Ni(II) compound, the bond length is a further 0.025 Å shorter. The removal of the ligand strap concomitant with the introduction of α -methyl groups introduces severe steric interactions in **35** but allows for a large dihedral angle. Nonetheless, a long Ni-N bond length is recorded for this class of complexes. Removal of a large portion of this interaction by the replacement of the methyl groups with hydrogens in **26** allows the two ligands to achieve 'pseudo-planarity' and results in the shortest Ni-N bond length of its class.

Inspection of the intraligand bond lengths reveals that two types of C–N bonds exist, a short C_{α} –N bond and a long $C_{\alpha'}$ –N bond. The differences can be accounted for in terms of a resonance description of the π -electrons in the ligand molecule. Figure 2-7 shows the two limiting resonance structures and the associated bond lengths.

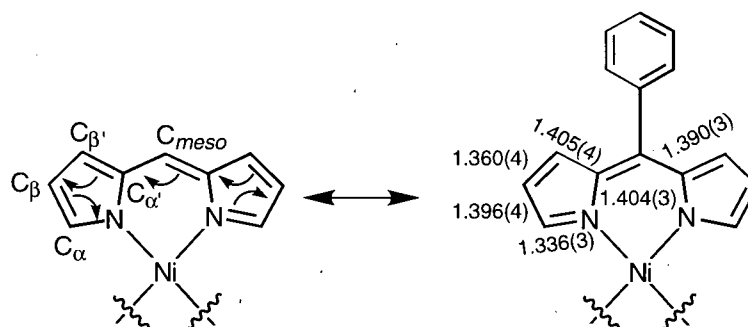


Figure 2-7 Limiting resonance forms of the dipyrinato ligands. Bond distances are given in Å.

According to this simplified picture, the C_{α} –N bond would receive partial π -contribution, the $C_{\alpha'}$ –N bond would not. The difference in double bond character explains the observed bond length differences in a qualitative way. The deviation of the $C_{\alpha'}$ –N bond length from the expected 1.42 Å for a C–N single bond reflects the aromatic character of the pyrrole unit itself, albeit the analogous bond length in pyrrole is about 0.04 Å shorter.⁷¹ The $C_{\alpha'}$ – C_{meso} bond and the C_{α} – C_{β} bond have a formal bond order of 1.5, and hence their bond lengths are as expected. The mean plane of the *meso*-phenyl group is tilted 58.1° with respect to the mean plane of the dipyrin unit. This deviation from the, perhaps, expected orthogonal finds its parallels in the structure of TPPs.

2.3.3 THE COMPLEXES OF COBALT(II) AND COBALT(III)

Both α - and β -alkyl substituted dipyrinato complexes of cobalt(II) have been described frequently, and in all the reports they have been described as air-stable.^{1,15,27,31,59,60,62} Their spectroscopic data are consistent with a (distorted) tetrahedral structure. Following the above outlined metal coordination protocol, it was found that, as expected, a solution of cobalt(II) acetate in methanol yielded an orange precipitate. Mass spectral analysis indicated the formation of the anticipated product bis(*meso*-phenyldipyrinato)cobalt(II) (**46**). The optical spectrum of a freshly prepared sample of **46** is shown in Figure 2-8.

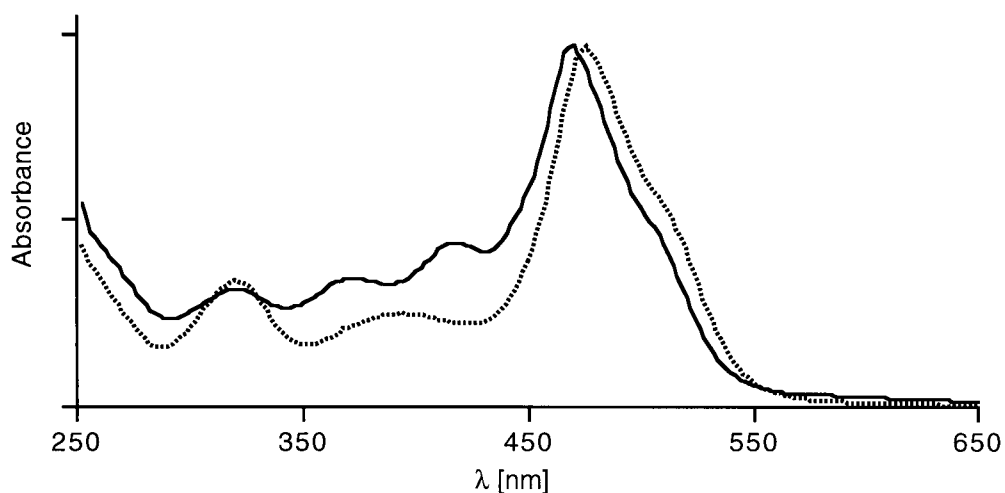


Figure 2-8 Optical spectrum of **46** (.....) and **48** (—) in CHCl_3

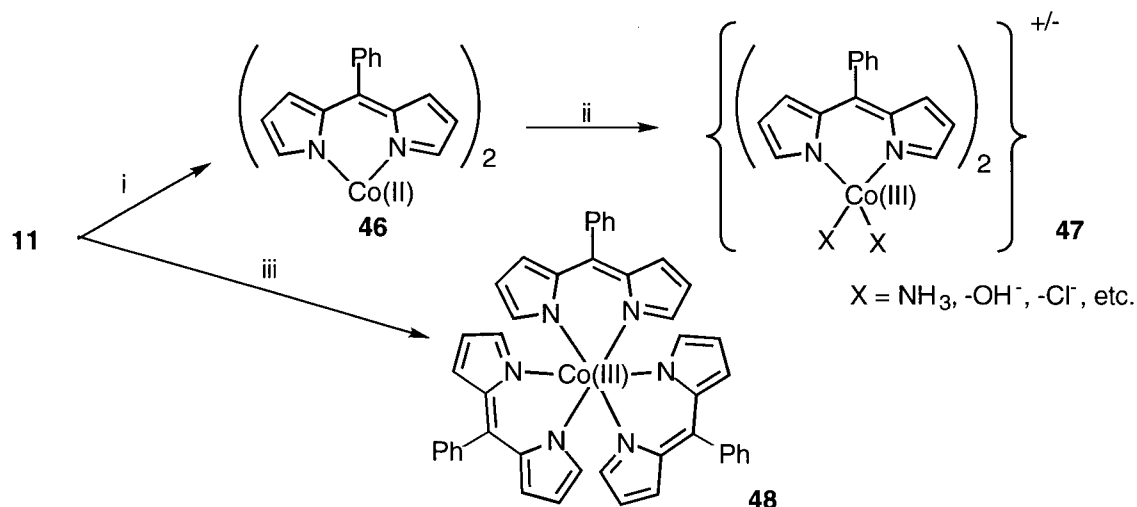
Comparison to the spectrum of the corresponding tetrahedral zinc complex **24** shows a clear resemblance in shape and values, again, indicating the formation of **24**. It was, hence, surprising that unlike the nickel (**26**), copper (**25**) or zinc (**24**) complexes, the cobalt complex (**46**) seemed to be exceedingly difficult to purify. Column chromatography of the initially low polarity material resulted in extensive decomposition, visible at large amounts of bright

orange material (with a very similar optical spectrum as **46**) tightly adsorbed onto the solid phase. Attempted recrystallizations also led to extensive decomposition and only tarry products.

Cobalt(III) shows a particular affinity for nitrogen donor atoms, in fact, the preferred oxidation state of cobalt in the presence of nitrogen donor ligands is +III, and examples of this type of complexes are numerous.^{63,72} In light of this, all of the previously stable cobalt(II) complexes of the N,N-chelating dipyrins have to be regarded as exemptions to this rule. It has been noted by Murakami *et al.*⁷³ that the bulkiness of the α -substituents in dipyrinato complexes of iron and manganese determines their preferred oxidation states. Methyl substitution resulted in the formation of divalent metal complexes in a 1:2 metal to ligand molar ratio, while the lack of any substituents at these positions led to the stable formation of trivalent metal complexes with a 1:3 metal to ligand molar ratio. Similarly, chromium(III) formed, based on ligand-field band analysis, a complex with an α -methyl dipyrin in which two dipyrinato ligands and one acetate coordinate the central metal in a distorted octahedral fashion.⁷³ In other words, the ligand, by allowing or disallowing a certain coordination geometry, stabilizes the metal in an oxidation state which is most suited for the coordination geometry provided.

Upon mixing of *meso*-phenyldipyrin (**11**) with a large excess of cobalt(II) a 1:2 metal to ligand complex forms. Dipyrin **11** is α -unsubstituted and, therefore, it is assumed that it allows the metal to achieve a (distorted) octahedral coordination sphere and, thereby, by air oxidation, achieve the oxidation state +III. This would result in the formation of a charged (bisdipyrinato)cobalt(III) complex (**47**) (Scheme 2-5). With no specific ligand offered, amine, hydroxo, methoxo, or acetato complexes could be formed under the condition provided. This would rationalize the 'decomposition' of the initially formed complex **46**. This string of rationalizations prompts the question whether it is possible to

form a 1:3 cobalt(III):*meso*-phenyldipyrinato complex if either excess ligand **11** is provided during the aerial oxidation of **46**, or if **11** is directly complexed to cobalt(III). The answer is yes. Cobalt(II) can be oxidized by air in the presence of ammonia. Thus cobalt(III) (as its hexamino complex) reacts with **11** to form a stable, low polarity pigment with an optical spectrum very similar to that of **48** (Figure 2-5). Elemental analysis and mass spectral data are consistent with its formulation as tris(*meso*-phenyldipyrinato)Co(III). Should the steric requirements of the ligand indeed allow an octahedral coordination sphere, this would certainly be achieved by this cobalt(III) complex.

**Scheme 2-5**

Formation of cobalt (II) and cobalt (III) dipyrinato complexes

Reaction conditions: (i) Co(II) acetate, MeOH; (ii) O₂ (air); (iii) 1. Co(II) acetate, NH₃/O₂ (air), MeOH, 2. ligand addition

A crystal suitable for X-ray crystallography could be grown and its analysis, fully confirming the proposed octahedral structure of **48**, is reported below.

2.3.4 CRYSTAL STRUCTURE ANALYSIS OF TRIS[*meso*-PHENYL-DIPYRRINATO]COBALT(III) (**48**)

The ORTEP representation of **48** as it exists in the crystal together with the numbering system employed is shown in Figure 2-9. The atom coordinates are listed in Table 2-5 (Experimental Section). Crystals of complex **48**, grown by slow evaporation of an acetone solution, contain one equivalent acetone as solvate in a 1:1 disordered position, with the terminal carbon atoms C(26) and C(27) located on the twofold axis.

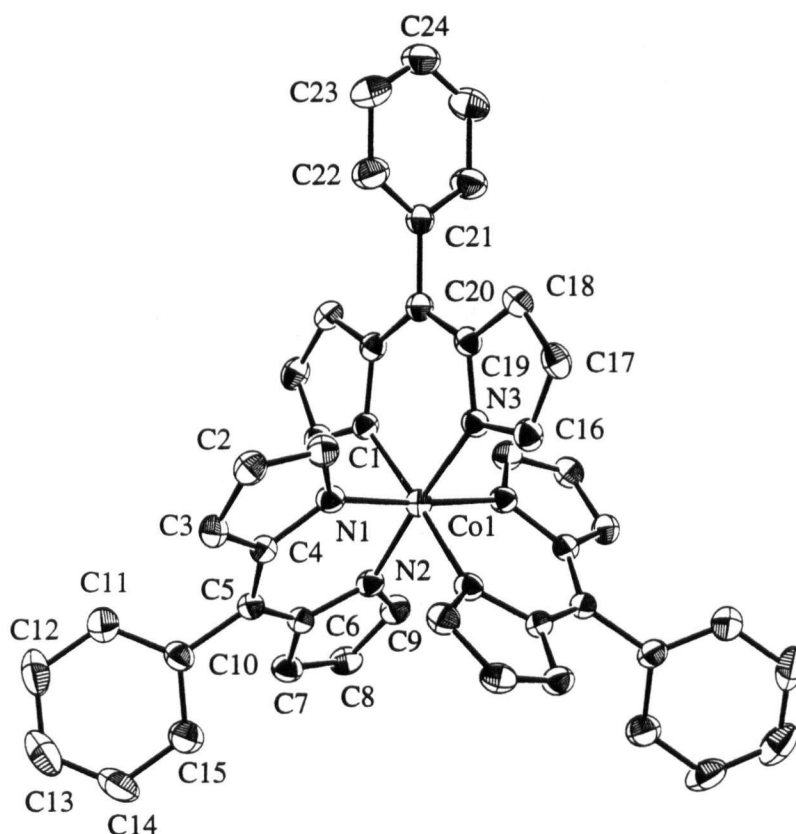


Figure 2-9 ORTEP representation (33% probability level) and numbering scheme of **48**. Solvate molecule (acetone) omitted for clarity

The six coordinating nitrogens in complex **48** form an almost perfect octahedral coordination sphere around the central metal. This is in contrast to the previously described tris(2,3,7-trimethyldipyrinato) complexes of iron(III) and manganese (III). They have been described, based on ligand field band analysis, as trigonally distorted octahedral and Jahn-Teller distorted octahedral, respectively.^{33,34} The complex **48** has exact C_2 -symmetry. The distortion from the, perhaps, expected C_3 -symmetry is, however, very small. The *meso*-phenyldipyrinato ligand molecules are flat and they enclose dihedral angles of only 1.1 and 2.2° off the ideal 90° and the cobalt-nitrogen bond lengths (1.945(2) Å) are, within the experimental uncertainty, equal and within the expected range. The bite angles of the two non-equivalent ligands are 87.25(9) and 92.04(9)°. The trend in the bond length differences of the two pyrrolic C_α - C_β bond lengths is equivalent to those observed in the structure of **27**, and they find the same explanation.

Remarkable is the short distance (2.42 Å) from the α -Hs to the nitrogens of the opposing ligands, for instance from H1 (attached to C1) to N3. This short distance is a result of the octahedral arrangement of the ligands and the given length of the metal-nitrogen bond. However, the lack of any appreciable distortion within the ligands, or within the arrangement of the ligands around the central metal to prevent such a close contact, allows speculations about the existence of a stabilizing hydrogen-bond-like interaction between these atoms.

2.4 THE DDQ-OXIDATION OF *meso*-DIPHENYLTRIPYRRANE (49)

Encouraged by successful DDQ oxidation of *meso*-phenyldipyrromethane to the corresponding dipyrin, *meso*-phenyltripyrane (49) was subjected to equivalent conditions. The mixture turned immediately dark and, based on TLC, the bulk of the starting material was consumed after a short period of time. TLC analysis of the mixture revealed, aside from numerous dark, ill resolved (polymeric ?) compounds, the presence of a small amount of a distinctly red pigment (50), which then was isolated by preparative TLC. The optical spectrum of 50 is shown in Figure 2-10. The simple two-band spectrum, significantly bathochromical shifted as compared to that of the dipyrins is, along the notion of Falk's simplified "free electron in a box model"¹⁰ predicted for tripyrrolic conjugated pigments, and thus seems to support the assumption of having prepared the desired compound 51. However, the finding that upon TFA addition the spectrum did not dramatically change (solution color went from pale red to purple), raised doubts whether the desired compound was, in fact, in hand.

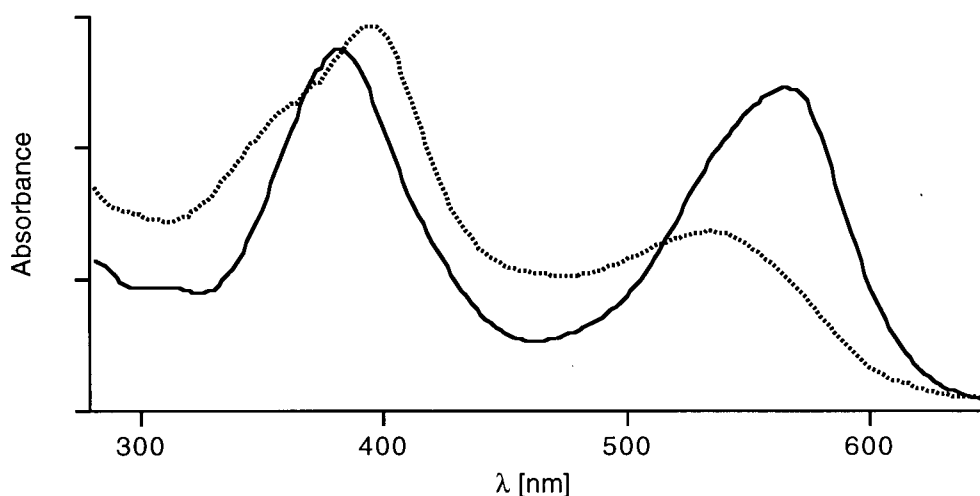


Figure 2-10 Optical spectrum of equal concentrations of 50 in $\text{CHCl}_3/1\% \text{Et}_2\text{NH}$ (.....) and in $\text{CHCl}_3/1\% \text{TFA}$ (—)

The mass spectrum of the compound ($m/e = 389$, corresponding to $C_{26}H_{19}N_3O$) indicated the presence of one oxygen and, moreover, the number of signals in the 1H -NMR of the compound indicated a compound less symmetric than envisioned compound **51** (Figure 2-11).

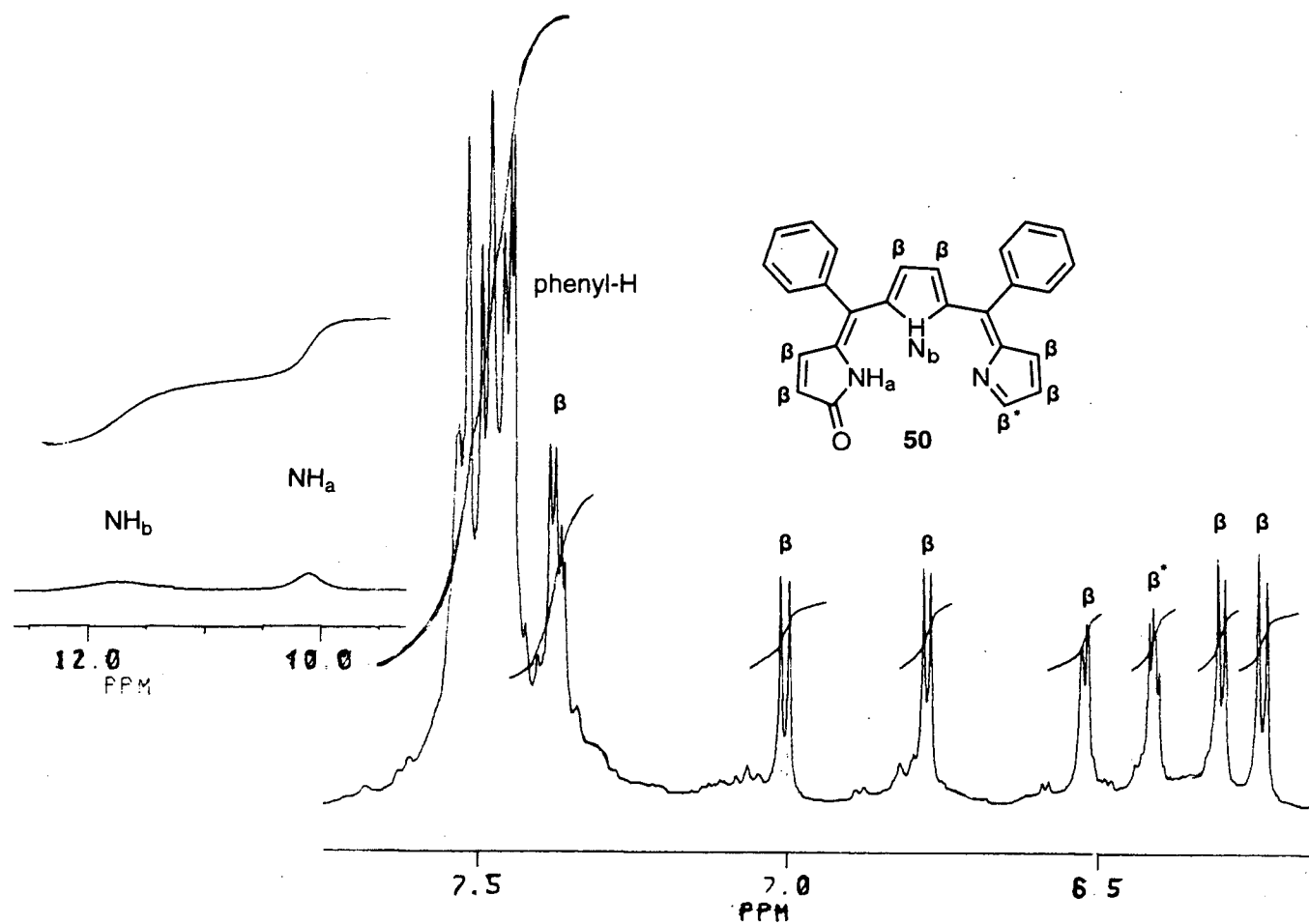
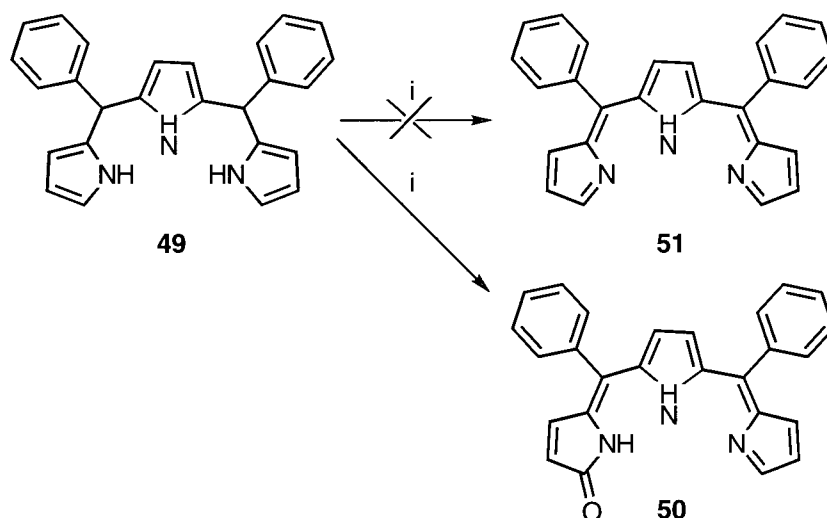


Figure 2-11 1H -NMR (CD_2Cl_2 , 200 MHz) of **50**

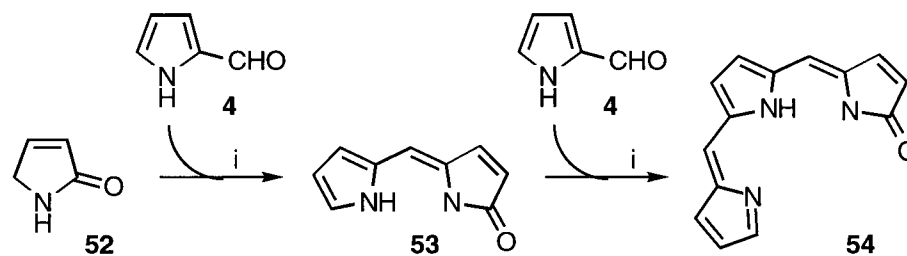
The spectrum shows, besides the multiplet for the phenyl groups, seven doublets and one triplet (doublet of doublet) of equal intensity in the chemical shift range and with coupling constants typical for pyrrole- β -protons, and two broad signals of equal intensity in

the pyrrolic NH region. The spectroscopic data can be assigned to a *meso*-phenyl-tripyrin-1-one (**50**). Further proof for the existence of the amide-type carbonyl functionality stems from the IR (1695 cm^{-1}) and the ^{13}C -NMR (197 ppm) of this compound. The spectral data compare well with those of known alkyl-substituted tripyrrinones.^{47,48,74-76}



Scheme 2-6 DDQ oxidation of *meso*-diphenyltripyrane (**49**)
Reaction condition: (i) 2 equiv. DDQ/benzene/r.t.

It is assumed that the introduced oxygen atom is derived from water present in the reaction mixture as no precautions were taken to attain anhydrous conditions. The introduction of a keto-functionality in dipyrins by oxidation (hydrolysis/oxidation of the corresponding 1-bromodipyrins in the presence of silver salts)⁷⁷ is long known, albeit this pathway was abandoned with the emergence of the reaction sequence shown in Scheme 2-7.^{78,79} Pyrrole aldehyde **4** reacts in an vinylogous aldol reaction with pyrroline-2-ones (**52**) to give dipyrinones (**53**). This is the starting material for the synthesis of (β -alkyl substituted) tripyrrinone (**54**) as they are, unlike dipyrins, susceptible to a second condensation with **4**.



Scheme 2-7 Classic method for the synthesis of tripyrrinones. Alkyl substituents have been omitted for clarity.
Reaction condition: (i) H^+

Analogous to the situation described in the previous chapters, this condensation methodology is not suited to generate *meso*-phenyl substituted tripyrrinones, and consequently, the present method of oxidizing the parent tripyrrane with DDQ is, as of yet, the only entrance towards this class of compounds. No attempts were undertaken to optimize the reaction conditions, thus an improvement in yield can be expected from further research on these interesting compounds.

A remarkable specificity in the DDQ oxidation of *meso*-phenyldi- and tripyrranes becomes evident. No indication of the presence of the desired compound **51** was ever found when oxidizing tripyrrane **49** with DDQ, and, conversely, the corresponding dipyrinones could not be detected in the oxidation of the dipyrromethanes. No explanation for this specificity can be offered as of now.

3. CONCLUSIONS

The *meso*-phenyl-4,6-dipyrins can be conveniently prepared from the corresponding dipyrromethanes. They exhibit properties similar to previously described alkyl-substituted dipyrins with the exception that they exhibit a significantly higher $\pi^* \leftarrow \pi$ transition energy as judged by their hypsochromically shifted UV-visible spectra. The *meso*-phenyldipyrins form metal complexes with nickel(II), copper(II), zinc(II), cobalt(II) and cobalt(III). Their spectroscopic data can be rationalized in the context of the previously described dipyrinato complexes. However, the lack of a bulky α -substituent allows for unique properties with this class of ligands. The nickel complex can be described as distorted square planar. The structure of the nickel complex was determined by single crystal X-ray structure analysis to have the smallest dihedral angle and the shortest Ni-N bond length recorded for nickel dipyrinato complexes. As a consequence of this, and in contrast to previously described bis(dipyrinato)nickel(II) complexes, they are diamagnetic. The cobalt(II) complex, presumably of tetrahedral structure, appears to be oxidatively unstable. This as well is unlike previously described cobalt(II) dipyrinato complexes and is assumed also to be due to the small steric bulk of the ligand, allowing the cobalt(II) to oxidize and to expand its coordination sphere. The unique properties of the title compounds are also highlighted by the formation of an octahedral tris(*meso*-phenyldipyrinato)Co(III) complex, the first structurally characterized example of its class.

Oxidation of a *meso*-phenyl substituted tripyrrane resulted in the formation of a novel *meso*-phenyltripyrin-1-one.

4. EXPERIMENTAL SECTION

Instrumentation

Melting points were determined on a Thomas Model 40 Micro Hot Stage and are uncorrected. The infrared spectra were measured with a Perkin-Elmer Model 834 FT-IR instrument. The NMR spectra were measured with a Bruker AC-200 Fourier-transform spectrometer (200 MHz for ^1H -NMR, 50 MHz for ^{13}C -NMR) and are expressed in the δ scale with residual solvent as internal standard. The low and high resolution mass spectra were obtained on a AEI MS9 and a Kratos MS 50, respectively. The electronic spectra were measured on a Hewlett Packard HP 8452A photodiode array spectrophotometer (instrumental precision ± 2 nm). Elemental analyses were performed on a Fisons CHN/O Analyzer, Model 1108. For instrumental details of the X-ray crystal structure determination, see Table 2-4.

Materials

meso-Phenyldipyrromethane (**20**) was synthesized according to the modified procedure of Lee and Lindsey⁹ and purified as described in Part 1. All other reagents and solvents were commercially available and of reagent grade or higher, and were, unless otherwise specified, used as received. The silica gel used in the flash chromatographies was Merck Silica Gel 60, 230-400 mesh. R_f -values were measured on Merck silica TLC aluminum sheets (silica gel 60 F₂₅₄, Art. 5554). Preparative TLC plates were 20x20 cm precoated silica Gel 60 F₂₅₄ plates (0.5 mm) supplied by Merck.

4.1 DIPYRRROMETHANES, DIPYRRINS AND THEIR METAL COMPLEXES

5-(4-Nitro-phenyl)-4,6-dipyrromethane (**19**)

4-Nitrobenzaldehyde (3.0 g, 19.87 mmol) was dissolved in freshly distilled pyrrole (44.0 g, 0.662 mol). The mixture was degassed by bubbling with N₂ for 10 min. TFA (0.15 mL, 0.1 equiv based on the benzaldehyde) was added and the mixture was stirred under N₂ until no starting aldehyde could be detected by TLC (ca. 15 min.). The volume of the slightly yellow mixture was reduced under high vacuum at 50°C to a viscous oil. This oil was dissolved in CH₂Cl₂ (100 mL) and cyclohexane (50 mL) was added. Without heating, the mixture was reduced on the rotary evaporator until precipitation just began. Scratching with a glass rod caused rapid crystallization of a slightly greenish solid which, after drying at 50°C/0.2 mm for 24 h gave 3.85 g (71.2%) of analytically pure compound **19**. A second crop of lesser purity was obtained from the mother liquor upon further evaporation (0.55 g, 10.3%).

MW = 265.27; mp = 158°C; R_f = 0.36 (CHCl₃-silica gel); ¹H-NMR (200 MHz, CDCl₃) δ 5.58 (s, 1H), 5.87 (m, 2H), 6.18 (dd, *J* = 11.8, 2.5 Hz, 2H), 6.74 (m, 2H), 7.37 (d, 2H, *J* = 11.8 Hz), 7.95 (br s, 2H), 8.14 (d, 2H, *J* = 11.8 Hz); ¹³C-NMR (50 MHz, CDCl₃) δ 43.8, 107.8, 108.8, 118.0, 123.8, 129.2, 130.8, 146.9, 149.7; UV-visible (MeOH) λ_{max} (rel. intensity): 222 (1.0), 266 (0.77) nm; LR-MS (EI, 180°C) *m/e* = 267 (100.0, M⁺), 220 (9.7, MH⁺-NO₂), 201 (16.3, M⁺-C₄H₄N), 154 (9.7), 145 (47.3, MH⁺-Ph-NO₂); HR-MS (EI, 180°C) calc'd. for C₁₅H₁₃N₃O₂: 267.10078; found: 267.10080; Analysis calc'd. for C₁₅H₁₃N₃O₂: C 67.41, H 4.9, N 15.72; found: C 67.23, H 4.98, N 15.62.

5-phenyl-4,6-dipyrin (11)

meso-Phenyldipyrromethane (**20**) (500 mg, 2.25 mmol) was dissolved with the help of a heat gun in benzene (25 mL). A solution of DDQ (537 mg, 2.35 mmol) dissolved in benzene (5 mL) was added and the mixture stirred until no starting material could be detected by TLC (1 h). The black precipitate was filtered off and air-dried to provide 440 mg (85 %) of crude **11** which was used for metal complex formation. An analytical sample was purified by column chromatography (silica gel, 25 g, 1% MeOH in CHCl₃). The bright yellow main fraction was collected and evaporated to dryness. The yellow film was dissolved in acetone (20 mL) and precipitated by diffusion of cyclohexane into this solution to yield a yellow-brown precipitate in 55.0 % yield based on crude material.

MW = 220.26; mp = 184 °C; R_f = 0.39 (CH₂Cl₂-silica gel); ¹H-NMR (200 MHz, acetone-d₆) δ 6.39 (m, 2H), 6.47 (d, *J* = 3.5 Hz, 2H), 6.39-6.47 (m, 5H), 7.78 (s, 2H), ~12.5 (s, very broad, 1H); ¹³C-NMR (50 MHz, acetone-d₆) δ 118.3, 128.5, 129.2, 129.7, 131.3, 135.0, 138.0, 144.6; IR (neat): 1555, 1450, 1435, 1340, 1055 cm⁻¹; UV-visible (MeOH/trace NH₄OH) λ_{max} (log ε): 312 (3.75), 430 (4.10) nm; UV-visible (MeOH/trace HCl) λ_{max} (log ε): λ_{max} (log ε): 362 (4.02), 474 (4.53) nm; LR-MS (EI, 180°C) *m/e* = 220 (77, M⁺); 219 (100, M⁺-H); HR-MS (EI, 180°C) calc'd for C₁₅H₁₂N₂: 220.10005; found: 220.10012.

5-(4-Nitro-phenyl)-4,6-dipyrin (23)

This compound was prepared by a method analogous to that used for compound **11**. Yield after chromatography: 59%.

MW = 265.27; mp = 189-191°; R_f = 0.83 (CH₂Cl₂-silica gel); ¹H-NMR (200 MHz, acetone-d₆) δ 6.21 (m, 2H), 6.40 (m, 2H), 7.36 (d, *J* = 8 Hz, 2H), 7.55 (s, 2H), 7.96 (d, *J* = 8 Hz, 2H), ~12.0 (very broad, 1H); ¹³C-NMR (50 MHz, acetone-d₆) δ 119.0, 123.7, 128.8, 128.9, 132.4, 139.5, 140.9, 144.6, 145.6; IR (neat): 1555, 1520, 1515, 1510, 1450, 1340, 1050 cm⁻¹; UV-visible (MeOH/trace NH₃) λ_{max} (log ε): 264 (3.99), 300 (4.08), 434 (4.38) nm; UV-

visible (MeOH/trace HCl) λ_{\max} (log ϵ): 258 (4.16), 336 (4.17), 470 (4.74) nm; LR-MS (EI, 150°C) m/e = 265 (100, M^+); 234 (18.8, $MH^+ - 2O$), 228 (68.2), 218 (96.5, $M^+ - HNO_2$); HR-MS (EI, 150°C) calc'd for $C_{15}H_{11}O_2N_3$: 265.0851; found: 265.08501.

Bis[5-(4-nitro-phenyl)-4,6-dipyrinato]Zn(II) (**24**)

To a solution of dipyrin **23** (100 mg, 3.77×10^{-4} mol) in MeOH (10 mL) was added zinc acetate dihydrate (420 mg, 5 equiv) in MeOH (10 mL) and the mixture was heated on a water bath for 4 h. The mixture was evaporated to dryness on the rotary evaporator and the remaining solids were triturated with $CHCl_3$. The resulting bright orange-yellow solution was filtered through a short plug of silica gel and allowed to slowly evaporate. Compound **24** as dark orange lumps with a bright green metallic lustre, was obtained, which was, after drying (0.1 mm/50°C), analytically pure (180 mg, 81%).

MW = mp $\leq 300^\circ$; R_f = 0.39 (CH_2Cl_2 -silica); 1H -NMR (200 MHz, $CDCl_3$) δ 6.45 (dd, J = 0.8, 4.2 Hz, 1H), 6.59 (dd, J = 0.8, 4.2 Hz, 1H), 7.59 (s, 1H), 7.75 (d, 9.2 Hz, 1H), 8.35 (d, 1H, 9.2 Hz); IR (neat): 1590, 1541, 1515, 1405, 1372, 1335, 1243, 1190, 1025, 995 cm^{-1} ; UV-visible (CH_2Cl_2) λ_{\max} (log ϵ): 486 (4.97), 352 (4.08), 308 (4.30), 272 (4.42) nm; UV-visible (pyridine) λ_{\max} (rel. intensity): 440 (0.2), 316 (1.0) nm; LR-MS (EI) m/e = 592 (40.3, M^+), 295 (88.8), 280 (48.7), 265 (100, Ligand $^+$); Analysis calcd. for $C_{30}H_{20}N_6O_4Zn$: C, 60.63, H 3.39, N 14.1; found: C 60.71, H 3.3, N 14.00.

Bis[5-(4-nitro-phenyl)-4,6-dipyrinato]Ni(II) (**26**)

Compound **26** was prepared using the procedure for the preparation of **24**. Slow evaporation of a $CHCl_3$ /1% MeOH solution of **26** yielded a dark brown-orange microcrystalline material which was, after drying (0.1 mm/50°C), analytical pure.

MW = 587.22; mp = 230°C; R_f = 0.83 (CH_2Cl_2 -silica gel); 1H -NMR (200MHz, $CDCl_3$) δ 6.66 (d, J = 4.1 Hz, 1H), 7.52 (d, J = 8.6 Hz, 1H), 8.26 (2 overlapping d, 2H), 10.83 (s, 1H); IR (neat): 1595, 1555, 1520, 1335, 1370, 1240, 1040, 1020, 995 cm^{-1} ; UV-visible (CH_2C_2)

λ_{\max} (log ϵ): 274 (4.58), 318 (4.47), 484 (4.63) nm; UV-visible (MeOH) λ_{\max} (rel. intensities): 272 (0.47), 292, sh (0.45), 466, sh (0.96), 482 (1.0) nm; UV-visible (pyridine) λ_{\max} (rel. intensities): 316 (1.0), 456, br (0.43), 486 (0.48) nm; LR-MS (EI, 180°C) m/e = 586 (48.3, M^+), 539 (15.6, $M^+ - \text{HNO}_2$), 464 (15.3, $M^+ - \text{Ph-NO}_2$); HR-MS (EI) calc'd for $\text{C}_{30}\text{H}_{20}\text{N}_6\text{NiO}_4$: 586.08997, found 586.08992; Analysis calc'd for $\text{C}_{30}\text{H}_{20}\text{N}_6\text{NiO}_4$: C 61.36, H 3.43, N 14.31; found: C 61.57, H 3.36, N 14.20.

Bis[5-(4-nitro-phenyl)-4,6-dipyrinato]Cu(II) (**25**)

Dipyrin (**23**) (100 mg, 3.77 mmol) was dissolved in minimal warm MeOH (~5 ml) and, under stirring, a solution of copper acetate monohydrate (380 mg, 5 equiv) in MeOH (5 mL) and conc. ammonia (0.5 mL) was added. The metal complex precipitated from the dark orange solution almost instantaneously. The precipitate was filtered off after stirring for 12 h at room temperature, dried and chromatographed on a short (10 x 2.5 cm, 1% MeOH- CHCl_3) column of silica gel. The first intensely orange band was collected and slow evaporation of the solvent furnished 160 mg (72%) of the metal complex **25** as black needles with a green metallic lustre. Alternatively, repeated recrystallization from $\text{CHCl}_3/\text{MeOH}$ yields dark green, dichroic microcrystals with a metallic lustre. After drying (0.1 mm/50°C) an analytically pure sample was obtained.

MW = 592.07; mp = no melting $\leq 300^\circ\text{C}$; R_f = 0.80 (CHCl_3 -silica gel); UV-visible (CHCl_3) λ_{\max} (log ϵ): 274 (4.52), 314 (4.21), 368 (4.26), 474 (4.72) nm; UV-visible (MeOH) λ_{\max} (rel. intensities): 268 (0.72), 308 (0.47), 374 (0.39), 468 (1.0), 502, sh (0.53) nm; LR-MS (EI) m/e = 591 (6.6, M^+), 295 (100), 280 (68.6), 264 (44.3), 248 (26.5), 234 (49.0); HR-MS (EI, 240°C) calc'd for $\text{C}_{30}\text{H}_{20}\text{O}_4\text{N}_6^{65}\text{Cu}$: 593.08240, found: 593.08305; Analysis calc'd for $\text{C}_{30}\text{H}_{20}\text{CuN}_6\text{O}_4$: C 60.63, H 3.39, N 14.15; found: C 60.70, H 3.54, N 14.03.

Bis[5-phenyl-4,6-dipyrinato]Ni(II) (27)

Prepared from nickel(II) acetate and dipyrin **11** in 76 % yield in an analogous fashion as described for **24**. Slow evaporation of an acetone solution gave **27** as dichroic crystals.

MW = 497.21; mp = dec: 240°; $R_f = 0.22$ (CH₂Cl₂-silica gel); ¹H-NMR (300 MHz, CDCl₃) δ 6.73 (d, $J = 4.6$ Hz, 4H), 7.38-7.46 (m, 10H), 7.60 (d, $J = 4.5$ Hz, 4H), 9.63 (s, 4H); ¹³C-NMR (50 MHz, CDCl₃) δ 127.4, 129.1, 130.7, 134.5, 136.8, 139.4, 143.7, 147.7, 173.0; IR (neat): 1575, 1535, 1505, 1410, 1380, 1345, 1245, 1035, 1030, 1000 cm⁻¹; UV-visible (CHCl₃) λ_{max} (log ϵ): 324 (4.33), 472 (462) nm; UV-visible (MeOH) λ_{max} (rel. intensity) 264 (0.18), 314 (0.23), 458 (0.83), 478 (1.0) nm; LR-MS (EI, 200°C) $m/e = 496$ (100, M⁺), 430 (18.8), 419 (18.2), 219 (74.8); HR-MS (EI, 200°C) calc'd for C₃₀H₂₂N₄Ni: 496.11978, found: 496.12071; Analysis calc'd for C₃₀H₂₂N₄Ni: C 72.47, H 4.46, N 11.27; found: C 72.33, H 4.70, N 11.3.

Bis[5-phenyl-4,6-dipyrinato]Co(II) (46)

Prepared from cobalt(II) acetate and dipyrin **11** in an analogous fashion as described for **24**. Chromatographic purification (CHCl₃-silica gel) of **46** yields a very broad orange band. Crystallizations failed in a variety of solvent systems. Extensive handling caused progressive decomposition, to be seen by TLC as a large amount of bright orange base line material:

MW = 497.47; UV-visible (CHCl₃) λ_{max} (rel. intensity): 320 (0.37), 400 (0.36), 476 (1.0), 508 (sh) nm; LR-MS (EI, 220°C) $m/e = 497$ (100, M⁺), 219 (5.0, M⁺-ligand); HR-MS (EI, 220°C) calc'd for C₃₀H₂₂N₄Co: 497.11765, found: 497.11713;

Tris[5-phenyl-4,6-dipyrinato]Co(III) (48)

Air was bubbled for 12 h through a solution of cobalt(II) acetate in methanol (50 mL), containing conc. aqueous ammonia (5 mL). Crude dipyrane **11** (200 mg, $\sim 7.0 \times 10^{-4}$ mol) dissolved in MeOH (2 mL) was added to the grey solution. (Loss of MeOH due to evaporation was compensated for). The resulting orange solution was evaporated to dryness and the resulting oil was taken up in CHCl₃ (50 mL), washed repeatedly with water, dried over Na₂SO₄, reduced and loaded onto a silica gel column (3x25 cm, CHCl₃ as eluent). The first orange band was collected and evaporated to give a film of 11 mg ($\sim 6\%$) of **48**. Slow evaporation of an acetone solution of **48** yielded coarse dark-orange chunks with a metallic shine.

MW = 717.03; R_f = 0.95 (CHCl₃-silica); UV-visible (CHCl₃) λ_{\max} (rel. intensity): 320 (34.4), 370 (37.5), 418 (46.0), 468 (1.0) nm; LR-MS (EI, 250°C) *m/e* = 716 (1.05, M⁺), 497 (72.42, M⁺-ligand), 219 (100.0, M⁺-2 ligands); HR-MS (EI, 250°C) calc'd for C₄₅H₃₃N₆Co: 716.20984, found: 716.20800; Analysis calc'd for C₄₅H₃₃N₆Co·C₃H₆O: C 74.41, H 5.07, N 10.85; found: C 74.73, H 4.90, N 11.31.

5,10-Diphenyl-15*H*,17*H*-tripyrin-1-one (50)

meso-Phenyltripyrane (**49**) (125 mg, 3.33×10^{-4} mol) dissolved in benzene (5 mL) were treated with DDQ (151 mg, 6.66×10^{-4}). Immediately a black precipitate separated from a dark supernatant. After being stirred at r.t. for an additional 30 min., the mixture was evaporated to dryness, redissolved in CH₂Cl₂/0.5%MeOH (10 mL), filtered through Celite[®], and, after reduction of the volume, loaded onto a preparative TLC plate (0.5 mm, silica gel). After two consecutive developments (CHCl₃:hexane, 8:2) the only distinct product, a bright red-purple band, was isolated. Recrystallization by slow solvent exchange (from CH₂Cl₂ to hexane) yielded 12 mg **50** as dark purple powder (9 % yield).

MW = 389.46; mp = d < 250°C; R_f = 0.60 (silica-CH₂Cl₂/1.5%MeOH); ¹H-NMR (400 MHz, CDCl₃) δ 6.23 (d, 1H, J = 6 Hz), 6.30 (d, 1H, J = 6 Hz), 6.35 (dd, 1H), 6.52 (d, 1H, J = 5 Hz), 6.77 (d, 1H, J = 6 Hz), 7.00 (d, 1H, J = 6 Hz), 7.36-7.39 (m, 2H), 7.4-7.5 (m, 10H), 10.1 (br s, 1H, exchangeable with D₂O), 11.4 (br s, 1H, exchangeable with D₂O), ¹³C-NMR (50 MHz, CDCl₃) δ 197 (a spectrum with well resolved peaks in the aromatic region could, due to lack of compound, not be obtained within a typical 4k scan experient); IR (film): 1695 cm⁻¹, other peaks were not indicative or ill resolved; UV-visible (CHCl₃, 1% EtN₂NH) λ_{max} (rel. intensity): 396 (1.0), 534 (0.46) nm; UV-visible (CHCl₃, 1% TFA) λ_{max} (rel. intensity): 382 (1.0), 566 (0.88) nm; LR-MS (EI, 150°C) m/e = 389 (17.5, M⁺), 360 (5.0); HR-MS (EI, 150°C) calc'd for C₂₆H₁₉N₃O: 389.15280, found: 389.15181.

4.2 CRYSTAL STRUCTURE ANALYSIS OF BIS(5-PHENYL-4,6-PYRRINATO)NI(II) (27) AND TRIS(5-PHENYL-4,6-DIPYRRINATO)CO(III) (48)

Crystallographic data appear in Table 2-4. The final unit-cell parameters were obtained by least-squares on the setting angles for 25 reflections with $2\theta = 23.3\text{--}33.6^\circ$. The data were processed, corrected for Lorentz and polarization effects, decay, and absorption (empirical, based on azimuthal scans for three reflections). The structure was solved by direct methods, the coordinates of the non-hydrogen atoms being determined from an *E*-map or from subsequent difference Fourier syntheses.⁸⁰ The molecules have exact *D*₂ (27) or exact *C*₂ symmetry (48). Non-hydrogen atoms were refined with anisotropic thermal parameters and hydrogen atoms were fixed in calculated positions with C-H = 0.98 Å and BH = 1.2 *B* bonded atom. No correction for secondary extinction were necessary. Neutral atom scattering factors for all atoms and anomalous dispersion corrections for the non-hydrogen atoms were taken from the *International Tables for X-Ray Crystallography*.⁸¹ Final atomic coordinates and equivalent isotropic thermal parameters, appear in Tables 2-5 (27) and 2-6, respectively (48).

Tabel 2-4 Crystallographic data^a of compound 27 and 48

Compound	27	48 (acetone solvate)
Formula (MW)	C ₃₀ H ₂₂ N ₄ Ni (497.23)	C ₄₈ H ₃₉ N ₆ CoO (774.81)
Crystal system	Orthorhombic	Monoclinic
Space group	<i>Fddd</i> (#70)	<i>C2/c</i> (#15)
<i>a</i> , Å	17.156(3)	13.539(2)
<i>b</i> , Å	35.217(1)	22.348(2)
<i>c</i> , Å	7.886(1)	13.467(1)
<i>V</i> , Å ³	4764.4(9)	3882.7(8)
<i>Z</i> ; <i>D</i> _{calc} , g/cm ³	8; 1.386	4; 1.325
<i>F</i> (000)	2064	1616
μ , cm ⁻¹	8.41 (MoK α)	4.88 (MoK α)
Crystal size, mm	0.20 x 0.30 x 0.40	0.35 x 0.40 x 0.45
Transmission factors	0.877-1.000	
Scan type	ω -2 θ	ω -2 θ
Scan range, deg in ω	0.94 + 0.35 tan θ	1.25 + 0.35 tan θ
Scan speed, deg/min	16 (up to 8 rescans)	32 (up to 9 rescans)
Data collected	+ <i>h</i> , + <i>k</i> , + <i>l</i>	
2 θ _{max} , deg	70	60
Crystal decay, %	2.3	5.24
Total (unique) reflections	2874 (2874)	6017 (5786)
Reflections with $I \geq 3\sigma(F_2)$	1058	2309
No. of variables	82	266
<i>R</i> , <i>R</i> _w	0.040, 0.031	0.039, 0.033
<i>gof</i>	2.00	1.59
Max <i>D</i> / <i>s</i> (final cycle)	0.0002	0.0008
Residual density e ⁻ /Å ³	-0.44 to 0.42	-0.28 to 0.35

^a Temperature 294 K, Rigaku AFC6S diffractometer, Mo *K* α radiation ($\lambda = 0.71069$ Å), graphite monochromator, takeoff angle 6.0°, aperture 6.0 x 6.0 mm at a distance of 285 mm from the crystal, stationary background counts at each end of the scan (scan/background time ratio 2:1), $\sigma^2(F_2) = [S^2(C + 4B)]/Lp^2$ (*S* = scan rate, *C* = scan count, *B* = normalized background count), function minimized $S\omega(I|F_{ol}-|F_{cl}|)^2$ where $\omega = 4F_{o2}/\sigma^2(F_{o2})$, $R = \sum |F_{ol}-|F_{cl}||/\sum |F_{ol}|$, $R_w = (\sum \omega(I|F_{ol}-|F_{cl}|)^2/S\omega F_{o2})^{1/2}$, and $gof = [\sum \omega(I|F_{ol}-|F_{cl}|)^2/(m-n)]^{1/2}$. Values given for *R*, *R*_w, and *gof* are based on those reflections with $I \geq 3\sigma(F_2)$.

Table 2-5 Atom Coordinates and B_{eq} [\AA^2] for 27

atom	x	y	z	B_{eq}
Ni(1)	0.12500	0.12500	0.62500	3.07(1)
N(1)	0.0990(1)	0.16201(5)	0.4630(2)	3.61(5)
C(1)	0.0985(1)	0.20166(7)	0.4808(3)	3.91(6)
C(2)	0.0592(2)	0.21708(8)	0.3404(4)	6.72(9)
C(3)	0.0340(2)	0.18773(9)	0.2426(4)	8.0(1)
C(4)	0.0592(2)	0.15443(8)	0.3215(3)	5.29(7)
C(5)	0.1250	0.22034(9)	0.6250	3.50(7)
C(6)	0.1250	0.26307(9)	0.6250	4.18(8)
C(7)	0.1658(2)	0.28288(8)	0.5040(4)	5.70(8)
C(8)	0.1666(2)	0.32263(8)	0.5060(6)	7.5(1)
C(9)	0.1250	0.3416(1)	0.6250	8.6(2)

$$B_{eq} = \frac{8}{3} \pi^2 (U_{11}(aa^*)^2 + U_{22}(bb^*)^2 + U_{33}(cc^*)^2 + 2U_{12}aa^*bb^*\cos\gamma + 2U_{13}aa^*cc^*\cos\beta + 2U_{23}bb^*cc^*\cos\alpha)$$

Table 2-6 Atom Coordinates and B_{eq} [\AA^2] for 48

atom	x	y	z	B_{eq}
Co(1)	0.5000	0.24994(3)	0.7500	2.73(1)
O(1)	0.4289(5)	0.0350(3)	0.3447(6)	9.6(2)
N(1)	0.5052(2)	0.2528(1)	0.6073(1)	2.86(5)
N(2)	0.6039(2)	0.18703(9)	0.7868(2)	2.86(6)
N(3)	0.3911(2)	0.31020(10)	0.7169(2)	2.72(6)
C(1)	0.4484(2)	0.2881(1)	0.5311(2)	3.36(7)
C(2)	0.4646(2)	0.2751(1)	0.4354(2)	3.57(7)
C(3)	0.5343(2)	0.2291(1)	0.4537(2)	3.28(7)
C(4)	0.5613(2)	0.2152(1)	0.5616(2)	2.88(7)
C(5)	0.6291(2)	0.1709(1)	0.6149(2)	2.80(6)
C(6)	0.6510(2)	0.1583(1)	0.7208(2)	2.88(7)
C(7)	0.7267(2)	0.1181(1)	0.7816(2)	3.45(7)

C(8)	0.7248(2)	0.1222(1)	0.8815(2)	3.49(7)
C(9)	0.6483(2)	0.1647(1)	0.8819(2)	3.41(7)
C(10)	0.6808(2)	0.1331(1)	0.5542(2)	3.31(7)
C(11)	0.7495(3)	0.1568(1)	0.5063(3)	4.44(8)
C(12)	0.7933(3)	0.1211(2)	0.4467(3)	5.6(1)
C(13)	0.7697(3)	0.0610(2)	0.4354(3)	6.1(1)
C(14)	0.7040(3)	0.0368(1)	0.4838(3)	5.7(1)
C(15)	0.6593(3)	0.0725(1)	0.5427(3)	4.54(9)
C(16)	0.2888(2)	0.3004(1)	0.6841(2)	3.39(7)
C(17)	0.2333(2)	0.3542(1)	0.6624(2)	3.55(7)
C(18)	0.3051(2)	0.3993(1)	0.6848(2)	3.29(7)
C(19)	0.4040(2)	0.3722(1)	0.7192(2)	2.83(7)
C(20)	0.5000	0.4008(2)	0.7500	2.82(9)
C(21)	0.5000	0.4677(2)	0.7500	3.1(1)
C(22)	0.4963(3)	0.4991(1)	0.6610(2)	4.71(9)
C(23)	0.4964(3)	0.5613(2)	0.6612(3)	5.5(1)
C(24)	0.5000	0.5914(2)	0.7500	5.5(2)
C(25)	0.4734(6)	0.0372(4)	0.2841(7)	6.1(3)
C(26)	0.5000	0.0962(3)	0.2500	6.1(2)
C(27)	0.5000	-0.0198(3)	0.2500	8.6(2)

$$B_{eq.} = \frac{8}{3} \pi^2 (U_{11}(aa^*)^2 + U_{22}(bb^*)^2 + U_{33}(cc^*)^2 + 2U_{12}aa^*bb^* \cos \gamma + 2U_{13}aa^*cc^* \cos \beta + 2U_{23}bb^*cc^* \cos \alpha)$$

5. LIST OF REFERENCES

- (1) Fischer, H.; Orth, H. *Die Chemie des Pyrrols*; (Reprint by Johnson Reprint Corporation, New York:1968); Akademische Verlagsgesellschaft: Leipzig, 1940; Vol. 2, erste Hälfte pp 1-151 and references therein.
- (2) Gossauer, A.; Engel, J. In *The Porphyrins*; D. Dolphin, Ed.; Academic: New York, 1987; Vol. 2; Chapter 7.
- (3) Corwin, A. H.; Andrews, J. S. **1936**, 58, 1086.
- (4) Treibs, A.; Strell, M.; Strell, I.; Grimm, D.; Gieren, A.; Schanda, F. *Liebigs Ann. Chem.* **1978**, 289.
- (5) Jacobi, P. A.; Guo, J. *Tetrahedron Lett.* **1995**, 36, 2717.
- (6) Brunnings, K.; Corwin, A. *J. Am. Chem. Soc.* **1944**, 66, 331.
- (7) Fischer, H.; Nussler, R. *Liebigs Ann. Chem.* **1931**, 491, 167.
- (8) Motekaitis, R. J.; Martell, A. E. *Inorg. Chem.* **1970**, 9, 1832.
- (9) Lee, C.-H.; Lindsey, J. S. *Tetrahedron* **1994**, 50, 11427.
- (10) Falk, H. *The Chemistry of Linear Oligopyrroles and Bile Pigments*; Springer: Wien, New York, 1989 and references therein.
- (11) Meyer, E. F., Jr.; Cullen, D. R. In *The Porphyrins*; D. Dolphin, Ed.; Academic: New York, 1978; Vol. 3; Chapter 11.
- (12) Fischer, H.; Klarer, J. *Liebigs Ann. Chem.* **1926**, 448, 178.
- (13) Fischer, H.; Kirstahler, A. *Liebigs Ann. Chem.* **1928**, 466, 179.
- (14) Fischer, H. *Chem. Ber.* **1914**, 47, 3274.
- (15) Johnson, A. W.; Kay, I. T.; Markham, E.; Price, R.; Shaw, K. B. *J. Chem. Soc.* **1959**, 3416.
- (16) Treibs, A.; Hintermeier, K. *Liebigs Ann. Chem.* **1955**, 592, 11.
- (17) Treibs, A.; Herrman, E.; Meissner, E.; Kuhn, A. *Liebigs Ann. Chem.* **1957**, 602, 153.

- (18) Treibs, A.; Reitsam, F. *Liebigs Ann. Chem.* **1958**, 611, 194.
- (19) Xie, H.; Lee, D. A.; Senge, M. O.; Smith, K. M. *J. Chem. Soc., Chem. Comm.* **1994**, 791.
- (20) Gabriel *Chem. Ber.* **1908**, 14, 1138.
- (21) Rogers, M. A. T. *J. Chem. Soc.* **1943**, 596.
- (22) Rogers, M. A. T. *J. Chem. Soc.* **1943**, 598.
- (23) Jeffreys, R. A.; Knott, E. B. *J. Chem. Soc.* **1951**, 1028.
- (24) Hill, C. L.; Williamson, M. M. *J. Chem. Soc., Chem. Commun.* **1985**, 1228.
- (25) Wagner, R. W.; Lindsey, J. S. *J. Am. Chem. Soc.* **1994**, 116, 9759.
- (26) Carré, F. H.; Corriu, R. J. P.; Bolin, G.; Moreau, J. J. E.; Vernhet, C. *Organometallics* **1993**, 12, 2478.
- (27) March, F. C.; Couch, D. A.; Emerson, K.; Fergusson, J. E.; Robinson, W. T. *J. Chem. Soc. (A)* **1971**, 440.
- (28) Porter, R. C. *J. Chem. Soc.* **1938**, 368.
- (29) Cotton, F. A.; DeBoer, B. G.; Pipal, J. R. *Inorg. Chem.* **1970**, 9, 783.
- (30) Elder, M.; Penfold, B. R. *J. Chem. Soc. (A)* **1969**, 2556.
- (31) Murakami, Y.; Matsuda, Y.; Sakata, K. *Inorg. Chem.* **1971**, 10, 1728.
- (32) Murakami, Y.; Sakata, K. *Bull. Chem. Soc. Jpn.* **1974**, 47, 3025.
- (33) Murakami, Y.; Matsuda, Y.; Sakata, K.; Harada, K. *Bull. Chem. Soc. Jpn.* **1974**, 47, 458.
- (34) Murakami, Y.; Sakata, K.; Harada, K.; Matsuda, Y. *Bull. Chem. Soc. Jpn.* **1974**, 47, 3021.
- (35) Pfaltz, A. *Acc. Chem. Res.* **1993**, 26, 339 and references therein.
- (36) Irving, H. M. N. H. In *Comprehensive Coordination Chemistry*; G. Wilkinson, Ed.; Pergamon: Oxford, 1987; Vol. 1; Chapter 10 and references therein.
- (37) Howard-Lock, H. E.; Lock, C. J. L. In *Comprehensive Coordination Chemistry*; G. Wilkinson, Ed.; Pergamon: Oxford, 1987; Vol. 6, Chapter 62.2.
- (38) Wagner, U.; Kratky, C.; Falk, H.; Wöss, H. *Monatsh. Chem.* **1991**, 122, 749.
- (39) Bonnett, R.; Dimsdale, R. J.; Stephenson, G. F. *J. Chem. Soc., Perkin Trans. 1* **1987**, 439.

- (40) Balch, A. L.; Mazzanti, M.; Noll, B. C.; Olmstead, M. M. *J. Am. Chem. Soc.* **1993**, *115*, 12206.
- (41) Falk, H.; Hofer, O. *Monatsh. Chem.* **1975**, *106*, 97.
- (42) Falk, H.; Hofer, O. *Monatsh. Chem.* **1974**, *105*, 995.
- (43) Scott, A. I. *Angew. Chem., Int. Ed. Engl.* **1993**, *32*, 1223 and references therein.
- (44) Battersby, A. R.; McDonald, E. *Acc. Chem. Res.* **1979**, *12*, 14 and references therein.
- (45) Battersby, A. R. *Acc. Chem. Res.* **1993**, *26*, 15 and references therein.
- (46) Cullen, D. J.; Meyer Jr., E. F.; Eivazi, F.; Smith, K. M. *J. Chem. Soc., Perkin Trans. 2* **1978**, 259.
- (47) Munder, S.; Pfaff, E.; Plieninger, H.; Sander, W. *Liebigs Ann. Chem.* **1980**, 2031.
- (48) Eichinger, D.; Falk, H. *Monatsh. Chem.* **1987**, *118*, 261.
- (49) Brown, D.; Griffith, D.; Rider, M. E.; Smith, R. C. *J. Chem. Soc., Perkin Trans. 1* **1986**, 455.
- (50) Boger, D. L.; Patel, M. *J. Org. Chem.* **1988**, *53*, 1405 and references therein.
- (51) Lindsey, J. S. In *Metalloporphyrins Catalyzed Reactions*; F. Montanari and L. Casella, Ed.; Kluwer: Netherlands, 1994; pp 49-86.
- (52) Barnett, G. H. *Tetrahedron Lett.* **1973**, *30*, 2887.
- (53) Adler, A. D.; Longo, F. R.; Finarelli, J. D.; Goldmacher, J.; Assour, J.; Korsakoff, L. *J. Org. Chem.* **1966**, *32*, 476.
- (54) Lindsey, J. S.; Wagner, R. W. *J. Org. Chem.* **1989**, *54*, 828.
- (55) Brooker; Sprague *J. Am. Chem. Soc.* **1941**, *63*, 3203.
- (56) Treibs, A.; Häberle, N. *Liebigs Ann. Chem.* **1968**, *718*, 183.
- (57) Falk, H.; Müller, N. *Tetrahedron* **1983**, *39*, 1875.
- (58) Paine III, J. B. In *The Porphyrins*; D. Dolphin, Ed.; Academic: New York, 1978; Vol. 1; pp 101-234.
- (59) Murakami, Y.; Sakata, K. *Inorg. Chim. Acta* **1968**, *2*, 273.
- (60) Fergusson, J. E.; Ramsay, C. A. *J. Chem. Soc. (A)* **1965**, 5222.
- (61) Scheidt, W. R. In *The Porphyrins*; D. Dolphin, Ed.; Academic: New York, 1978; Vol. 3; Chapter 10.
- (62) Murakami, Y.; Matsuda, Y.; Sakata, K.; Martell, A. E. *J. Chem. Soc., Dalton Trans.* **1973**, 1729.

-
- (63) Cotton, F. A.; Wilkinson, G. *Advanced Inorganic Chemistry*; 5th ed.; John Wiley & Sons: New York, 1988.
- (64) Eley, D.; Spivey, D. *Trans. Faraday Soc.* **1962**, 58, 405.
- (65) Buchler, J. W. In *The Porphyrins*; D. Dolphin, Ed.; Academic: New York, 1978; Vol. 1; pp 389-483.
- (66) Dwyer, P. N.; Buchler, J. W.; Scheidt, W. R. *J. Am. Chem. Soc.* **1974**, 96, 2789.
- (67) Shannon, R. D. *Acta Crystallogr.* **1976**, A32, 751.
- (68) Meyer Jr., E. F. *Acta Crystallogr., Sect. B* **1972**, 28, 2162.
- (69) Renner, M. W.; Buchler, J. W. *J. Phys. Chem.* **1995**, 99, 8045.
- (70) Collins, D. M.; Scheidt, W. R.; Hoard, J. L. *J. Am. Chem. Soc.* **1972**, 94, 6689.
- (71) *Pyrroles: The Synthesis and the Physical and Chemical Properties of the Pyrrole Ring*; Jones, A., Ed.; John Wiley & Sons: New York, 1990; Vol. 48 Part 1, pp 22-23.
- (72) Levason, W.; McAuliffe, C. A. *Coord. Chem. Rev.* **1974**, 12, 151.
- (73) Murakami, Y.; Matsuda, Y.; Iiyama, K. *Chem. Lett.* **1972**, 1069.
- (74) Falk, H.; Grubmayer, K. *Monatsh. Chem.* **1977**, 18, 625.
- (75) Eichinger, D.; Falk, H. *Monatsh. Chem.* **1987**, 118, 91.
- (76) Khan, S. A.; Plieninger, H. *Chem. Ber.* **1975**, 108, 2475.
- (77) Fischer, H.; Fröwis, H. *Hoppe Seyler's Z. Physiol. Chem.* **1931**, 195, 49.
- (78) Plieninger, H.; Lichtenwald, H. *Hoppe Seyler's Z. Physiol. Chem.* **1942**, 273, 206.
- (79) Plieninger, H.; Decker, P. *Liebigs Ann. Chem.* **1956**, 598, 198.
- (80) (a) Altomare, A.; Burla, M.C.; Camalli, M.; Cascarano, M.; Giacovazzo, C.; Guagliardi, A.; Polidori, G. *J. Appl. Cryst.*, in preparation. (b) Beurskens, P.T.; Admiraal, G.; Beurskens, G.; Bosman, W.P.; Garcia-Granda, S.; Gould, R.O; Smits, J.M.M.; Smykala, C. The DIRDIF program system, *Technical Report of the Crystallography Laboratory*, 1992, University of Nijmegen, The Netherlands.
- (81) (a) *International Tables for Crystallography*, The Kynoch Press: Birmingham, UK (Present distributor: Kluwer: Boston, MA), 1974, Vol. IV, pp. 99-102; (b) *International Tables for Crystallography*, Kluwer: Boston, MA, 1992, Vol. C; pp 219-222.

PART 3

2-PYRROLYLTHIONES

AS

N,S-BIDENTATE

CHELATORS

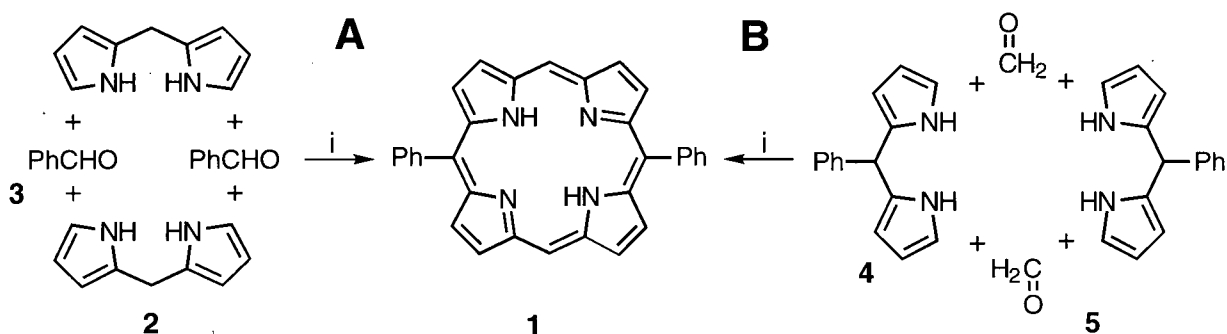
1. INTRODUCTION

1.1 2-PYRROLYLTHIONES AS COMMON PRECURSORS USED IN A PORPHYRIN SYNTHESIS

5,10-*meso*-Diphenylporphyrin (**1**) is an interesting porphyrin in that it combines some features of TPP, namely the unsubstituted β -positions and the *meso*-phenyl groups, with some features of OEP, namely the unsubstituted *meso*-positions, without being as difficult to prepare as porphine¹. The chemical properties peculiar to this molecule are only beginning to be explored. Some of these have already allowed the synthesis of novel ethynyl linked porphyrin arrays as models of light harvesting antenna systems² and the development of a bioconjugation method³. Principally, there are two ways to access porphyrin **1**, both involve the condensation of a dipyrrolic moiety with a single carbon unit to form a porphyrinogen, followed by oxidation to the corresponding porphyrin (Scheme 3-1).

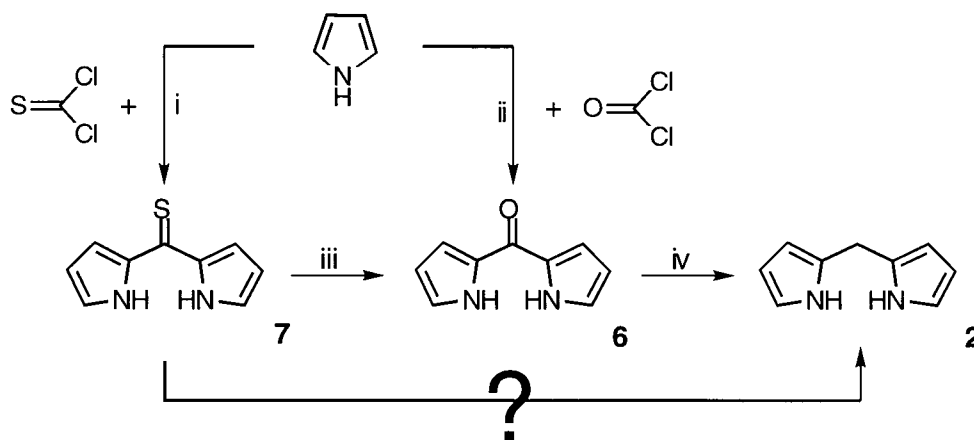
A The acid catalyzed condensation of di-2-pyrromethane (**2**) with benzaldehyde (**3**). This 'classical' synthesis for **1** is analogous to the Rothmund-type synthesis of TPP.^{4,5}

B The condensation of phenyldi(2-pyrrolyl)methane (**4**) with formaldehyde (**5**). This possibility became viable with the ability to synthesize **4** in multi-gram quantities (cf. Part 1). This novel approach is now under development by Dolphin, James and co-workers.⁶



Scheme 3-1 Principal pathways for the formation of 5,10-*meso*-diphenylporphyrin **1**
Reaction conditions: (i) 1. H^+ , 2. DDQ

The common synthesis of di-2-pyrromethane **2** is *via* the reduction of di-2-pyrrolylketone (**6**)^{7,8}, which itself is either derived from the hydrogen peroxide oxidation of the corresponding thione⁹ **7**, or, in low yields, directly from pyrrole, activated as its Grignard salt, and phosgene¹⁰ (Scheme 3-2).



Scheme 3-2 Synthesis of di-2-pyrromethane
Reaction Conditions: (i) Et_2O , 0°C , 1 min; (ii) 1. EtMgBr , 2. phosgene; (iii) $\text{H}_2\text{O}_2/\text{KOH}$, MeOH ; (iv) 1. BH_3 , 2. steam distillation.

Although phosgene is being used on a very large scale in industry, this violently toxic gas is difficult to handle in the laboratory. Attempts to replace phosgene by triphosgene, a crystalline material introduced in 1987 by Eckert and Foster, and advertised as being able to

replace phosgene in virtually all applications¹¹, were, due to the formation of relatively large amounts of 2-trichloromethoxycarbonylpyrrole as by-product and the relatively high molar costs of triphosgene, unsatisfactory in our experience (see Chapter 3.2 for details). The sulfur congener of phosgene, thiophosgene, used to synthesize thione **7** from pyrrole is a liquid. Owing to its lower volatility it is easier to handle. The condensation of thiophosgene and pyrrole produces thione **7** in good yields as beautiful red crystals with a metallic shine, and, most importantly, this compound can be prepared with little effort in large scale.⁹ The overall laborious three step reaction sequence - preparation of thione **7**, oxidation to the corresponding ketone **6**, followed by its reduction to give dipyrromethane (**2**) - has an overall yield of ~30%. We believed that it could be made shorter and the yield improved by a direct hydrodesulfurization of the thione.

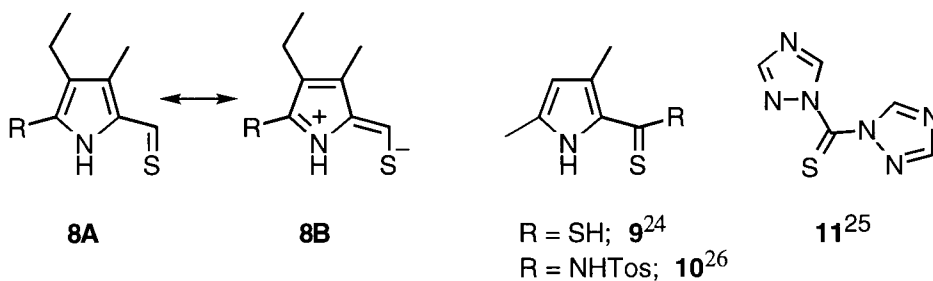
Hydrodesulfurizations of thiones, thioethers, thioalcohols and compounds such as thiophenes are commercially interesting reactions as the so called 'sweetening' of hydrocarbon fossil fuels is such a process. Although the commercially interesting reaction types are typically high temperature (gas phase) reactions catalyzed over solid catalyst surfaces, many liquid phase model reactions have been reported. Among the wide variety of reagents used in these studies¹²⁻¹⁶, the hydrogenation over Raney nickel¹⁷ appeared to be the most promising as it is the most simple, economical and versatile method. In fact, Raney nickel is known to desulfurize every substrate containing C-S bonds, with a range of yields, from low to excellent.^{13,18}

In anticipation of some results to be described in the following sections, hydrogen over Raney-nickel did lead in fair yields to the expected hydrodesulfurization, and, consequently, we achieved the primary goal of improving the original reaction sequence to access multi-gram quantities of dipyrromethane (**2**) by a simple pathway. More remarkable in the context of unexpected results, however, was the formation of small amounts of brown-

orange material with a low polarity (as based on its R_f -value on silica gel TLC plates) upon mixing the thione **7** with Raney nickel in the absence of hydrogen. The nature of this pigment is the central topic of this Part 3. First, however, it will be illustrative to review briefly the properties of thiones, their metal complexes in biological and synthetic systems, and the general properties of N,S-(heterocyclic)-bidentate ligands and the metal complexes derived from them.

1.2 THIOCARBONYL COMPOUNDS

The chemistry of thiones has been reviewed extensively.¹⁹ Whereas simple dialkylthiones are unstable compounds and were until recently known exclusively as cyclic trimers, diarylthiones are found to form fairly stable monomeric species. In 1960 Woodward and co-workers used a stable 2-pyrrolylthioaldehyde (**8A**) in their total synthesis of chlorophyll *a*.^{20,21} The membership of this and closely related classes of compounds has since been extended.^{22,23} Some examples based on pyrrole (**9,10**) and triazole (**11**) are shown below.



Their stability undoubtedly arises from a considerable resonance contribution of polarized forms such as **8B**, indicated by the longer wavelength of the C=S stretching frequency as compared to, for example, diphenylthione.¹⁹

Direct methods, such as a thio-analog to the Vilsmeier-Haak formylation,^{22,23} have been devised for the synthesis of thiocarbonyl compounds, however, most thiocarbonyls are prepared by conversion of their oxo-analogs with a variety of reagents.^{19,27} Phosphorus pentasulfide^{28,29}, Lawesson's reagent (2,4-bis(4-methoxyphenyl)-1,3-dithia-2,4-phosphetane-2,4-disulfide)³⁰ under various conditions³¹ or hydrogen sulfide (with an acid catalyst)³² are the most widely used reagents for this purpose.

The comparatively softer character of sulfur, coupled with the high polarizability of the C=S bond, gives rise to important differences in reactivity between thiones and ketones. Thiones, in general, are highly colored compounds and possess strong absorption bands in the visible region. A comparison of the optical spectra of the colorless 2-pyrrolylketone (**6**) and its red thio-analog 2-pyrrolylthione (**7**) illustrates this most impressively (Figure 3-1).

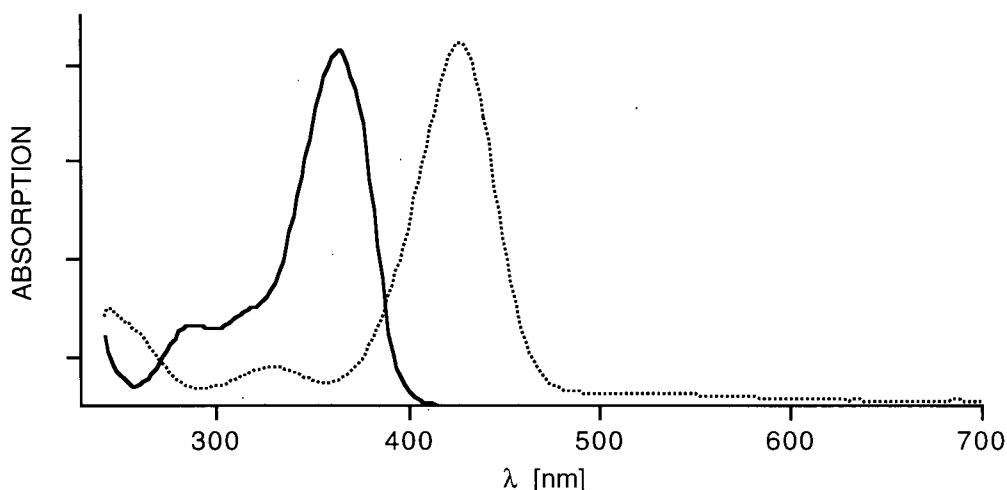


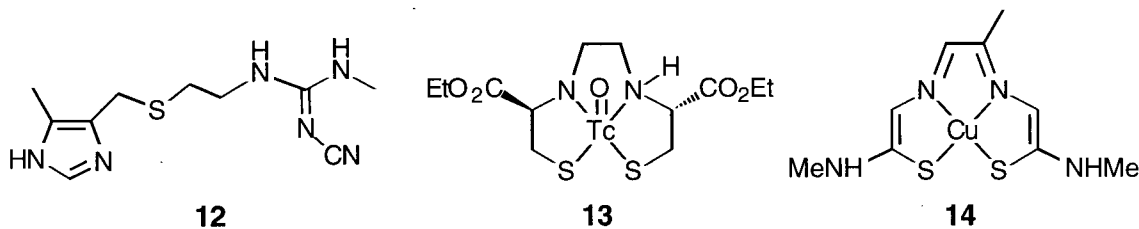
Figure 3-1 Normalized optical spectra (MeOH) of 2-pyrrolylketone (**6**) (—) and 2-pyrrolylthione (**7**) (.....)

The photochemistry of thiones has also been studied extensively.³³⁻³⁷ While there are similarities in the primary photoprocesses between carbonyl and thiocarbonyl compounds, significant differences exist in the final products obtained. Their use in synthesis is, with notable exceptions (*vide infra*), by far not as well established as it is for ketones.

1.3 SULFUR DONOR-METAL COMPLEXES IN BIOLOGICAL SYSTEMS

The above mentioned softness of sulfur donor groups leads to a stronger binding to class (b) metals than do oxygen donors, and sulfur ligands occupy a late position in the nephelauxic series.³⁸ These properties are, perhaps, what prompted 'Nature' to utilize sulfur donor ligands (cystein derived thiolates, sulfides) in some metalloenzymes (such as the [NiFe] hydrogenase³⁹, the blue copper proteins⁴⁰, aconitases⁴¹, and the cytochromes P₄₅₀⁴² to fine-tune the electronic properties of the metals involved. This phenomenon led to the synthesis of innumerable non-natural sulfur containing ligands for modeling certain aspects of these enzymes. This modeling of the reactive centers of enzymes is a core theme of the burgeoning field of bioinorganic (biomimetic) chemistry.⁴³⁻⁴⁷

Sulfur rich proteins, known as metallothioneins, play a crucial role in the biological transport and storage of certain metals such as zinc, copper, cadmium, mercury, and lead.⁴⁸ A sulfur containing drug, cimetidine (**12**) (trade name Tagamet), used for the treatment of peptic ulcers, is proposed to exist as a copper(II) chelate under *in vivo* conditions.⁴⁹ Carcinostatic and antiviral properties of N,S-donor ligands have been reported on several occasions and it has been suggested that their mode of action is the sequestering of metal ions which are involved in carcinogenesis.⁵⁰ Be that as it may, metal complexes of certain ligands have been shown to be cytotoxic as well.³⁸



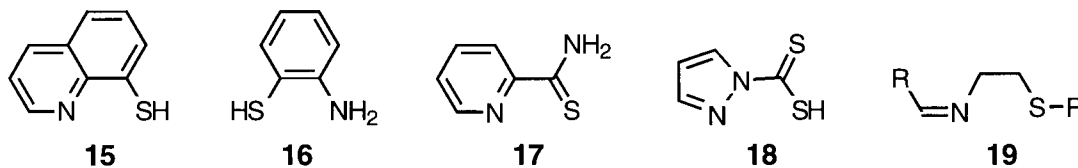
Other drugs containing sulfur ligands, such as compounds **13**⁵¹ and **14**⁵², are being used to shuttle radioactive metals such as technetium (^{99m}Tc) or copper (⁶²Cu) for radioimaging purposes into (and out of) of patients.⁵³

The design of ligands for gadolinium(III) or manganese(III) to be used as contrast agents for magnetic resonance imaging (MRI)^{54,55} could also employ sulfur donor ligands. Ligands with sulfur donors usually confer some lipid solubility on the metal complex and they form complexes with therapeutically important metals such as palladium or platinum.³⁸

1.4 SULFUR-NITROGEN CHELATING AGENTS AND THEIR METAL COMPLEXES

A review pertaining to this specific topic has been published by Akbar Ali and Livingston in 1974.³⁸ More recent reviews cover bidentate ligands in general⁵⁶ or certain sulfur containing ligands,^{57,58} all three including bidentate N,S- and N,O-ligands. An exhaustive review of the reactivity of the metal ion-sulfur bond was published by Kuehn and Isied in 1980,⁵⁹ also covering a large number of S,N- and S,O-chelates. Reviews covering the metal complexes of electron-rich sulfur-nitrogen rings and cages,⁶⁰ simple sulfur-nitrogen ligands,⁶¹ metal thiolate complexes,⁶² and inorganic sulfur-nitrogen ligands have been published.⁶³ In the present context, a review covering heterocyclic nitrogen donor ligands by Reedijk⁶⁴ and one by Foulds⁶⁵ summarizing the coordination chemistry of nickel are of interest as well.

The structures shown below, or combinations thereof, represent the bulk of the described N,S donor bidentate ligands. The nitrogen is either part of a heterocycle (**15**⁵⁶, **17**³⁸, **18**⁶⁶), an imine nitrogen (**19**⁵⁶ R = alkyl or aryl) or an amine (**16**⁶⁷⁻⁶⁹). The sulfur is either a thiol (**15**, **16**), thioether (**19**), or thiocarbonyl of a thioester (**18**) or -amide (**17**). Although thiophene is known as a sulfur donor, it is less common as such.⁷⁰



In the complexed form, the ligand can be neutral (**17-19**), monoanionic (**15**, **18**), or even dianionic (**16**) and the formed metallacycles are typically five- or six-membered.

To the best of our knowledge, 2-pyrrolylthiones and related thiones have not been described as metal complexing agents before, although in 1969 Clezy and Smythe mentioned in a paper describing the synthesis of di-2-pyrrolylthione (**7**) that,

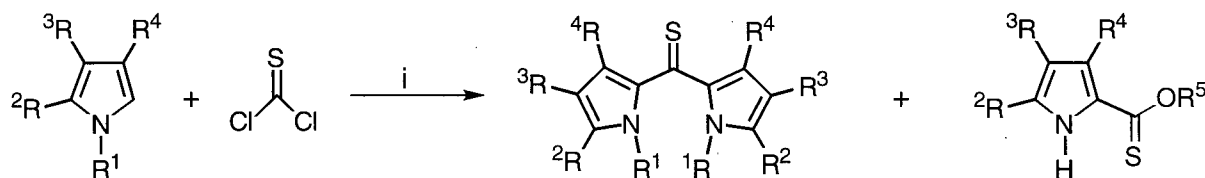
“Like other members of the thione class [Andrieu, C., Mollier, Y., Lozac’h, N. *Bull. Soc. chim. Fr.*, **1965**, 2457.] the dipyrrolylthiones form complexes with mercuric chloride.”⁷¹

without, however, giving an analysis or estimate of the nature of the complexes .

2. RESULTS AND DISCUSSION

2.1 SYNTHESIS OF DI-2-PYRROLYLTHIONES

The syntheses of 2-pyrrolylthiones **7** and **21-24** from thiophosgene and the corresponding pyrroles were performed according to the general procedures described in the literature.⁹ However, they were slightly modified in that dry methanol or ethanol was used to quench the reaction, instead of the aqueous methanolic solutions used by Clezy and Smythe.



R ¹	R ²	R ³	R ⁴		R ¹	R ²	R ³	R ⁴		R ²	R ³	R ⁴	R ⁵
-H	-H	-H	-H		-H	-H	-H	-H	7				
-Me	-H	-H	-H		-Me	-H	-H	-H	21				
-H	-H	-Me	-Me		-H	-H	-Me	-Me	22				
-H	-Me	-Me	-Me		-H	-Me	-Me	-Me	23	-Me	-Me	-Me	-Me
-H	-Me	-Et	-Me		-H	-Me	-Et	-Me	24				
-H	-CO ₂ Bz	-Me	-Me	27						-CO ₂ Bz	-Me	-Me	-Et

Scheme 3-3

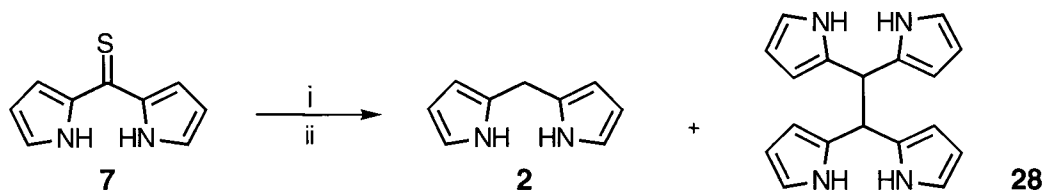
Formation of dipyrrylthiones and pyrrolylthioneesters

Reaction conditions: (i) 1. benzene/Et₂O, r.t., 10 min.; 2. MeOH or EtOH.

The consequence of this was that the thiocarbonyl ester **25** and **26** could be isolated. Whereas **25** was a side product of the condensation, **26** was obtained as the sole reaction product of the deactivated pyrrole **27** with thiophosgene. Precise adherence to the original procedures would have resulted in the formation of the corresponding thioacids, which presumably, would have been adsorbed tightly onto the solid phase during the column chromatography (silica gel/benzene/chloroform) of the crude reaction mixtures. The reaction of the parent unsubstituted pyrrole was, based on the original procedure, scaled up considerably (ten-fold, yielding ~20 grams of crystalline material) without any problems in reaction control or loss of yield.

2.2 HYDRODESULFURIZATION OF DI-2-PYRROLYLTHIONES

Refluxing thione **7** in solvents as tetrahydrofuran, methanol, ethanol or acetone with a large excess of commercially available Raney-nickel and in the presence of a small amount of an amine base (ammonia or triethyl amine) produces small amounts of the desired reduced species **2**, and, as will be expanded on later, a brown pigment. Application of hydrogen at normal pressure to the reaction at ambient temperatures results in total and fast hydrodesulfurization of the starting material, visible by the decolorization of the initially dark orange solution (Scheme 3-4).



Scheme 3-4

Desulfurization of **7**

Reaction condition: (i) EtOH, drop Et₃N, Raney-nickel/H₂ 1 atm., r.t.;

Removal of the solids by filtration, evaporation of the solvent and either steam distillation, high vacuum distillation or column chromatography produce the dipyrromethane as colorless crystals in yields typically over 60%. A TLC of the crude mixture, stained with bromine fumes, shows the presence of several pyrrolic side products which were, with the exception of the tetrapyrrolic compound **28**⁶, not identified. A radical mechanism is assumed for this type of reduction, and the fate of the sulfur (possibly elemental sulfur, possibly nickel sulfide) is not discussed in the standard literature.¹³ The occurrence of the dimer **28** attests to the radical nature of the hydrodesulfurization.

This reduction method can also, in varying yields, be applied to thiones **21** to **24** to give the corresponding dipyrromethanes. The advantage of this method to prepare dipyrromethanes lies in the ease of the procedure and the simplicity of the purification, the high purity of the resulting product, all in combination with an acceptable yield. The procedure is also amenable to any increase of scale. The disadvantages of this reduction method are intrinsic to the use of Raney-nickel:¹³ Firstly, the reduction is not a catalytic reduction as the nickel is used in a very large excess and most likely binds the sulfur irreversibly. Secondly, nickel is mildly toxic, is known to be a strong allergen and is, in its form as Raney-nickel, pyrophoric. This necessitates the special disposal of large amounts of spent nickel. Thirdly, the speed and yield of the reduction is sharply dependent on the activity of the Raney-nickel, and varied in our hands from almost instantaneous to requiring one night, and from 40% with plenty of side products to over 90% with very few side products. Finally, the unpredictable deactivation on aging, and the practical difficulty in determining accurately the weight of nickel used due to the necessity of keeping this pyrophoric solid in a slurry of aqueous base, create some difficulties in the reliable reproduction of this capricious reaction.

2.3 THE REACTION OF DI-2-PYRROLYLTHIONE (7) WITH NICKEL(II)

Upon mixing and refluxing an acetone or methanol solution of thione **7** with Raney-nickel, the appearance of a small amount of brown pigment with an R_f -value slightly higher than that of the thione was observed. Neither a solution of 1,1'-dimethyldipyridylthione **21** nor of dipyrroketone **6** gave such a reaction, indicating the involvement of the pyrrolic nitrogen and the sulfur in the formation of this pigment. It was also noticed that the amount of pigment formed correlated with the age of the Raney-nickel and, during the above described early experiments, the length of time the nickel suspension was refluxed in the presence of oxygen (air). The longer it was refluxed and the more aged the Raney-nickel, the more pigment formed. No pigment was detected in the experiments performed under hydrogen. These findings pointed towards the involvement of oxidized forms of nickel, most likely nickel(II). And indeed, a mixture of a methanolic solution of thione **7** with nickel(II) as its acetate results in the quantitative conversion of the thione into this brown pigment (**29**). Recrystallization gave dark green crystals with a metallic sheen. The optical spectrum of the orange solution of complex **29** is shown in Figure 3-2.

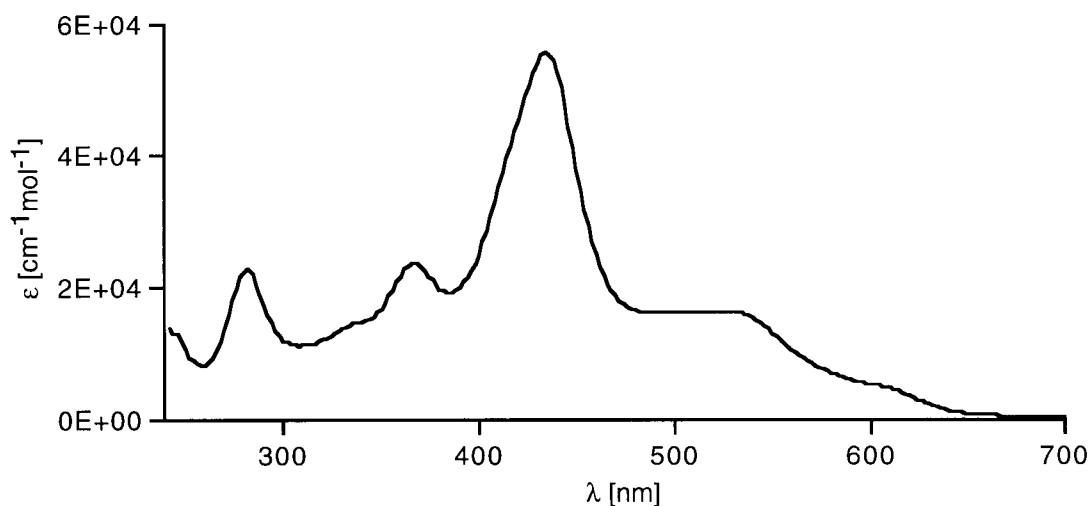
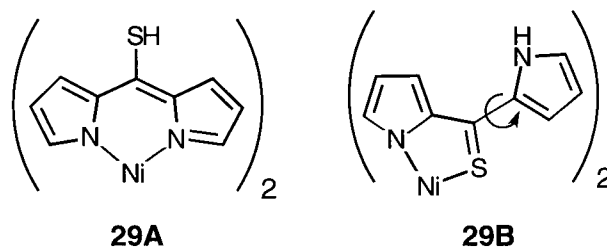


Figure 3-2 Optical spectrum (CH_2Cl_2) of **29**

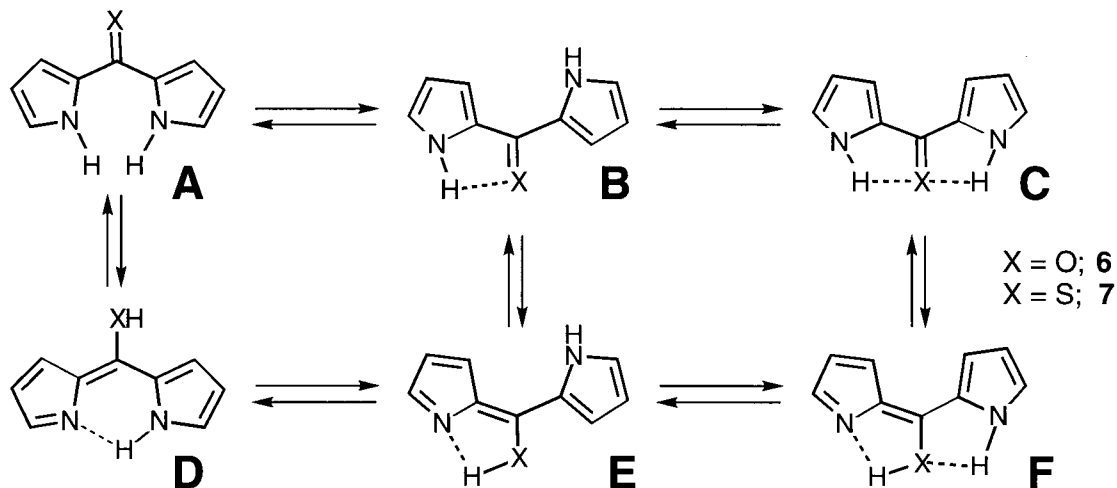
The mass spectrum and the elemental analysis of the pigment indicated the composition $C_{18}H_{14}N_4NiS_2$. This is consistent with the formulation of it as a neutral nickel(II) complex with two thione ligands in their anionic form. Two modes of chelation could be attained by thiones of type **29**, namely **29A**, in which the thio-enolate form of **7** chelates like a dipyrinato moiety, or **29B**, in which the thione tautomer coordinates as an N,S-bidentate chelate.



Other non-chelating coordination modes are conceivable, however they are, in light of the propensity of nickel(II) to form tetra-coordinated complexes and the thermodynamic drive towards the formation of chelates *versus* non-chelates, unlikely. To further deduce the structure from spectroscopic and analytical data, it is illustrative at this point to discuss first the solution and solid state conformation of 2-pyrrolylthiones in general, and of **7** and its oxo-analog **6** in particular.

2.4. SOLUTION AND SOLID STATE CONFORMATION OF DI-2-PYRROLYLTHIONE (7) AND -KETONE (6)

Structural work on benzoylpyrrole, di-2-pyrrolylketone and their sulfur analogs is limited.⁷²⁻⁷⁴ Theoretically, they could, as shown in Scheme 3-5, exist in various interconvertible conformations with several tautomeric forms, each of which will in practice be populated to a different degree. Dipole moment studies of di-2-pyrrolylketone (6) and di-2-pyrrolylthione (7) have shown that the preferred solution state conformation in several non-polar solvents is an uniplanar conformation in which the carbonyl group is on the same side of the molecule as the nitrogens, represented by structures C and F.⁷⁴ The oxo-compound is stabilized by hydrogen bonds not available to the thio-compound and thus a much higher proportion of it is in this conformer compared to the thio-compound.



Scheme 3-5 Possible conformers and tautomers of di-2-pyrrolylcarbonyl compounds

Simple thiones are often found to exist predominantly in the enthiol tautomer. Conjugated thiones are more stable as their thione tautomer¹⁹, however exceptions are known and understood.^{75,76} Of the possible tautomeric structures, structures A-C are dominant in both the oxo- and the thio-compound. Structures D-F incorporate a dipyrin chromophore and

thus are expected to be colored. The ketone **6** is, in solution and the solid state, colorless; thione **7** is red, however its bathochromically shifted spectrum, compared to **6**, has been attributed to the electronic properties of the thione moiety itself, in other words, without the implication of any dipyrin-like tautomer (Figure 3-1).⁹

This string of arguments singles out conformation **C** as the preferred conformation of the two 2-pyrrolyl compounds **6** and **7** in solution, and this conformation is also found in the solid phase. This was shown conclusively by single crystal X-ray crystal structure analysis (Figures 3-3 and 3-4). Crystallographic data and experimental details are found in Table 3-1, the final atomic coordinates are listed in Tables 3-3 and 3-4, and selected bond lengths in Tables 3-8 and 3-9. Both compounds are essentially planar (24.36° for oxo and 31.94° angle between the mean plane of the pyrrolic units) with all heteroatoms on the same side of the molecule. The bond lengths measured for the thione and the ketone are essentially the same and the small deviations in the two N-C α bond lengths in each molecule ($\Delta = 0.028 \text{ \AA}$ in **7**; $\Delta = 0.026 \text{ \AA}$ in **6**) can be rationalized by a small contribution of **F**-like tautomers. In neither case was an intramolecular hydrogen bond found, again underlining the minor importance of any enol or enthiol tautomeric contribution to the structures. Interesting are the intermolecular interactions as seen in the architecture of the unit cells, also shown in Figures 3-3 and 3-4. 2/3 of the thiones **7** in a unit cell are stacked in pairs, undoubtedly held together by π - π interactions. Some molecules of ketone **6**, on the other hand, display an intermolecular hydrogen-bond from the carbonyl oxygen to an NH-proton.

On the basis of the above facts, isomer **29B** is given preference over isomer **29A** for the description of the dithionato nickel(II) complex (**29**), as it allows the ligands to adopt a conformation very similar to the solution and solid state conformation of the ligand in its non-complexed state. More support for this can be gleaned from the spectroscopic properties of complex **29**.

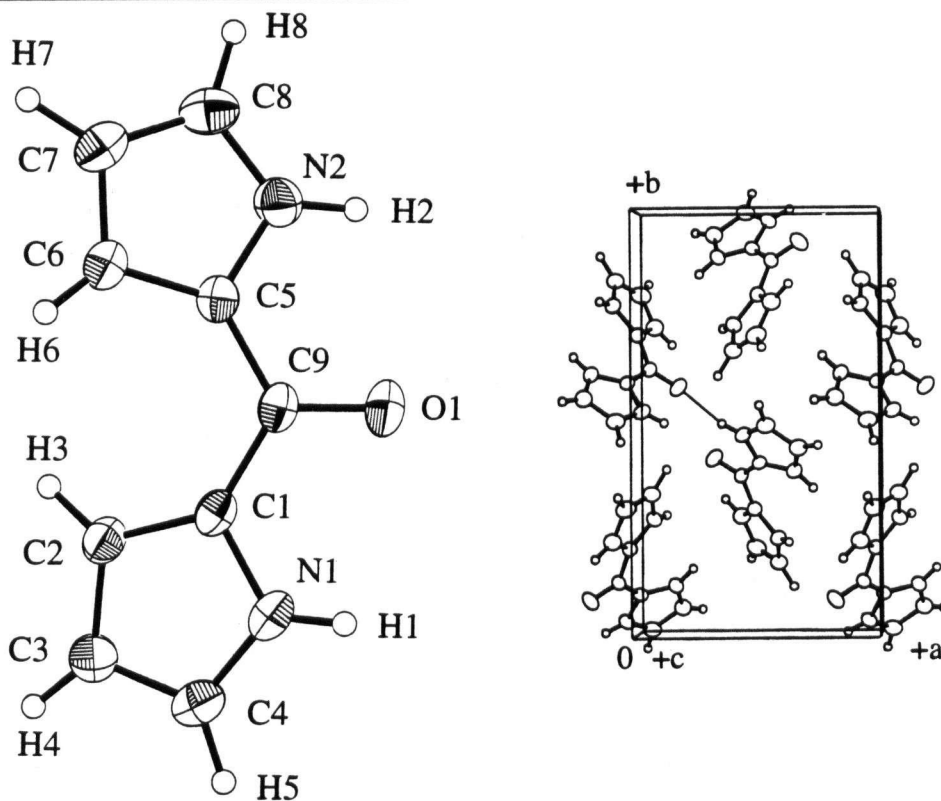


Figure 3-3 ORTEP representation (33% probability level) and unit cell of 6

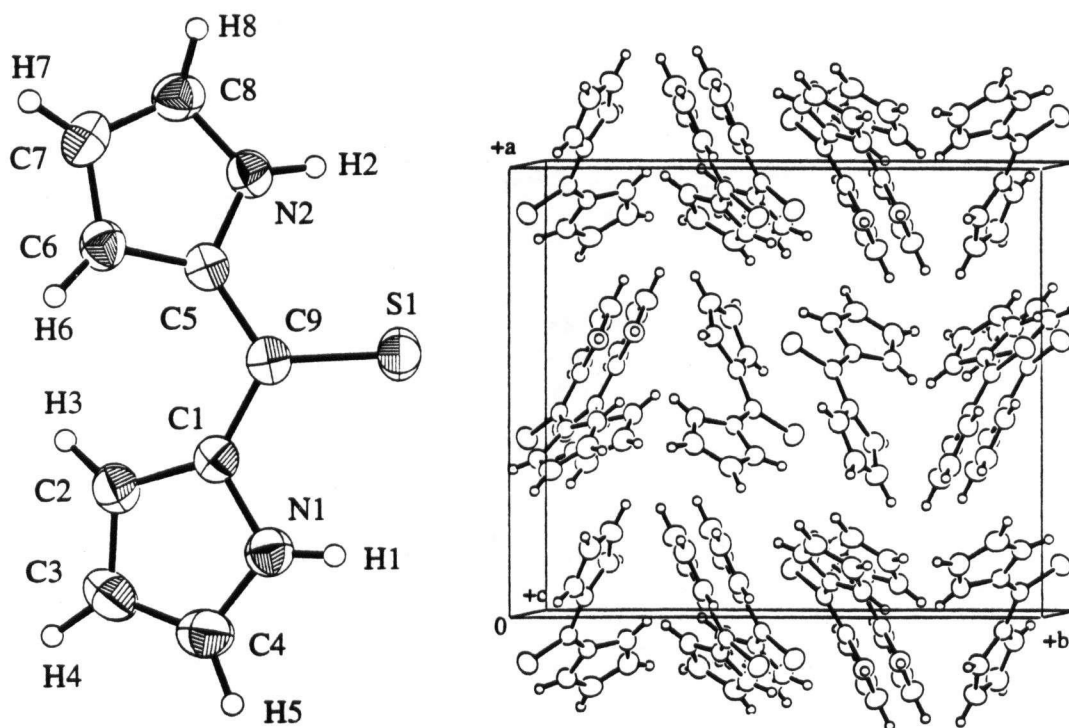


Figure 3-4 ORTEP representation (33% probability level) and unit cell of 7

2.5 SPECTROSCOPIC PROPERTIES OF COMPLEX 29

The optical spectrum (Figure 3-2) of compound **29** does not show definitively which structural possibility is present, however, it supports the isomer **29B** as follows: Its strongest absorption ($\log \epsilon$) at 434 nm (4.75) corresponds poorly with the strongest absorption of bis(*meso*-phenyldipyrinato)nickel(II) at 484 nm (4.63) (Part 2), consequently this does not indicate the presence of a dipyrinato chromophore. Furthermore, additional broad bands at longer wavelengths are visible in the spectrum, but it must also be realized that the influence of a *meso*-thiol on the optical spectrum of a dipyrinato ligand is hard to predict.

Finally, the ^1H - and ^{13}C -NMR allow the clear distinction between the isomers of choice to represent the correct structure of **29**. The C,H-COSY spectrum of this complex is shown in Figure 3-5. The presence of seven non-equivalent hydrogens in the aromatic region, split into two groups not joined by any 3J coupling (H,H-COSY), one proton (exchangeable with D_2O) at 11.2 ppm (acetone- d_6), and the presence of three quaternary and six tertiary carbons (APT) clearly excludes structure **29A** and supports **29B**. The two sets of hydrogen signals belong to the two pyrrolic units, the exchangeable proton is the NH proton and the number of carbon signals corresponds to the number of carbons present in each ligand. The higher symmetry of the structural alternative **29A** would have resulted in a spectrum showing only three coupled hydrogens and one exchangeable proton.

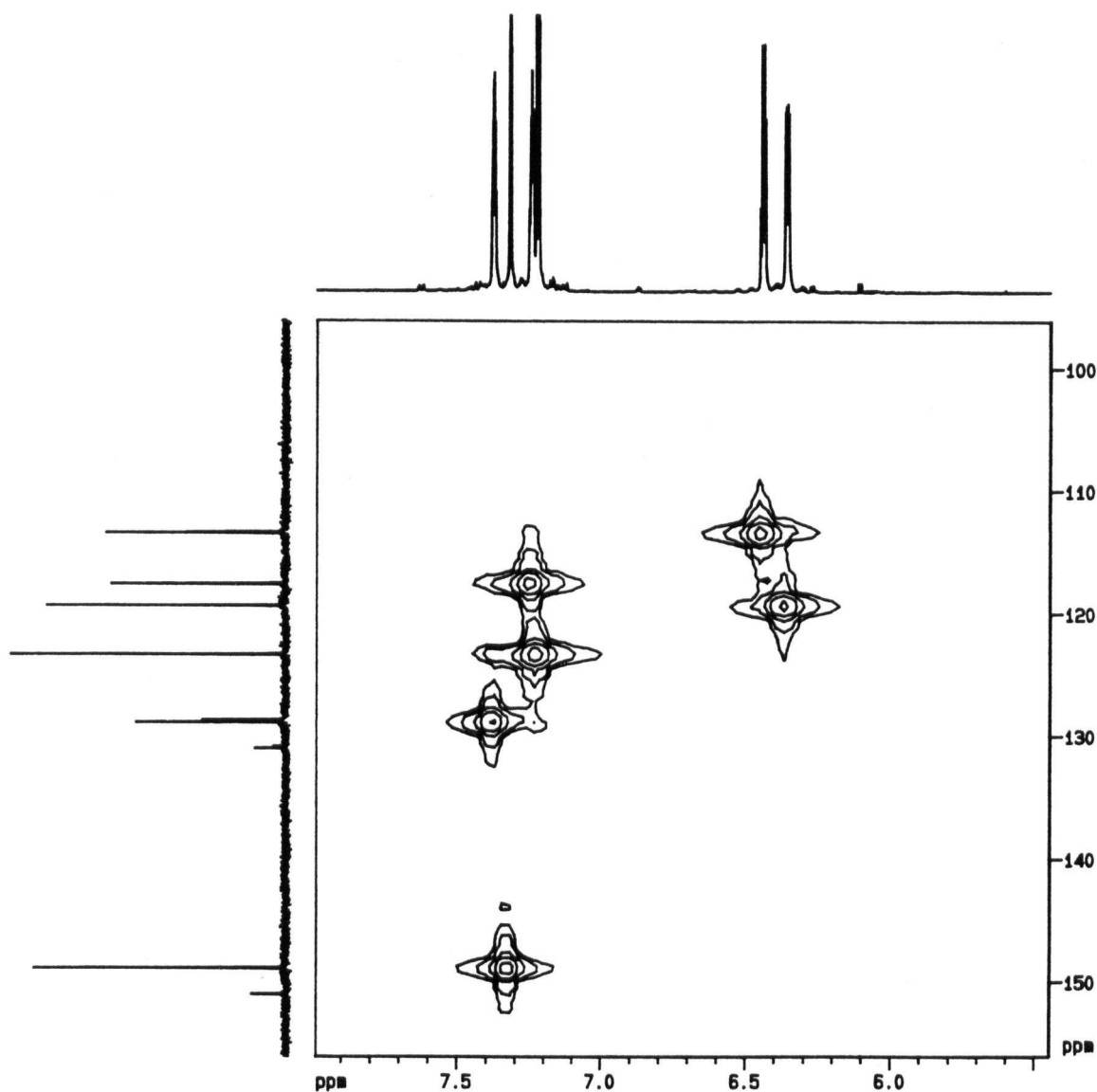
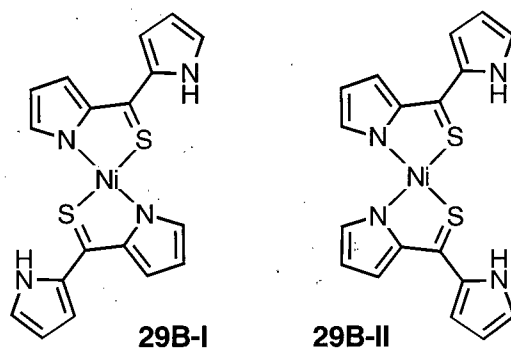


Figure 3-5 C,H-COSY (500 MHz, acetone- d_6) of **29**

The NMR data based assignment of the structure as **29B** assumes equivalency of both ligands in the complex. This is a likely circumstance for all coordination modes ranging from tetrahedral to square planar. Sharp NMR signals of this nickel(II) complex were obtained, corroborating the diamagnetic low-spin configuration of the nickel(II) ion. This allows the classification of the complex as square planar (cf. to Part 2). However, two square planar nickel(II) complexes of type **29B** are possible, **29B-I** and **29B-II**.



Steric considerations, similar to those for the dipyrinato complexes discussed in Part 2 (i.e. possible inter-ligand steric interactions of the α,α' -hydrogens in a square planar arrangement) and possible *trans*-effects exercised by the donor atoms make structure **29B-I** the most likely and, indeed, X-ray crystal structure analysis confirms this.

2.6 STRUCTURAL CHARACTERIZATION OF COMPLEX 29

A crystal suitable for X-ray crystallography was grown by slow evaporation of an acetone solution of the nickel complex **29**. Crystal data with some experimental details, the final atomic coordinates and selected bond distances are listed in Tables 3-2, 3-5 and 3-10, respectively. The ORTEP representation of the complex is shown in Figure 3-6. As expected, pigment **29** is an almost perfectly square planar N,S-donor chelate of nickel(II) and both ligands are arranged in the *trans*-configuration. The conformation of the monodeprotonated ligands in this complex is very similar to that of the free ligand (cf. to Figure 3-4).

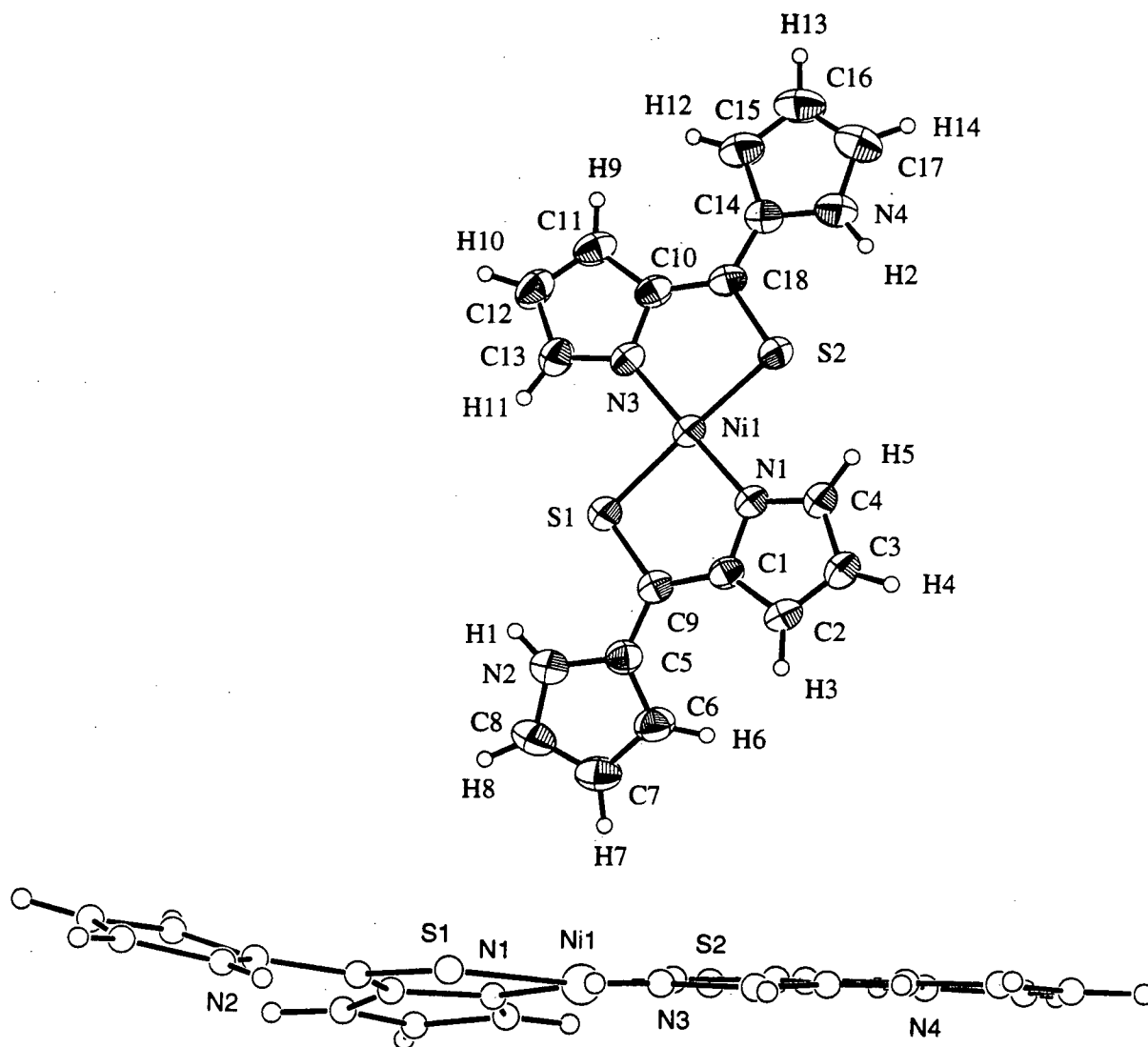


Figure 3-6 ORTEP representation (33% probability level), numbering system used and side view of the complex **29**

Upon metallation, the coordinating pyrrolic units underwent some bond length changes, outlined in Figure 3-7, which can be rationalized by the increased weight of the limiting resonance structure indicated. The bond lengths in the non-coordinating pyrrolic unit remain unchanged upon metal complex formation. It appears, thus, that it is non-participating in the operation of the complexation, although its co-planarity with the planar complexing system allows resonance interactions.

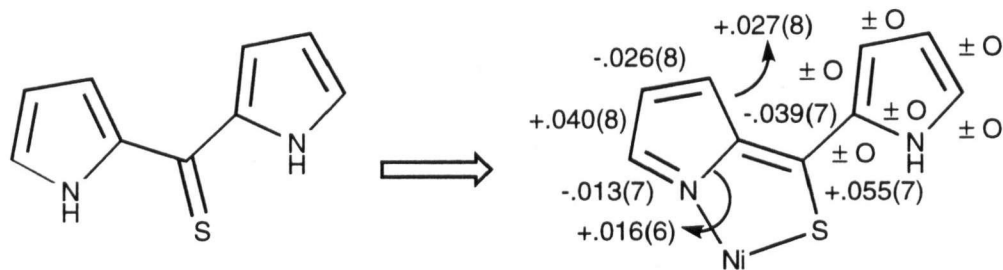


Figure 3-7 Bond lengths and angle changes of the ligand upon metallation. The changes were determined by comparison with the average bond length in the solid state structure of the corresponding molecules **7** and **29**.

With its NH proton, the non-coordinating unit forms an intermolecular hydrogen bond to the rim of the aromatic system of a coordinated pyrrolic unit, shown in Figure 3-8.

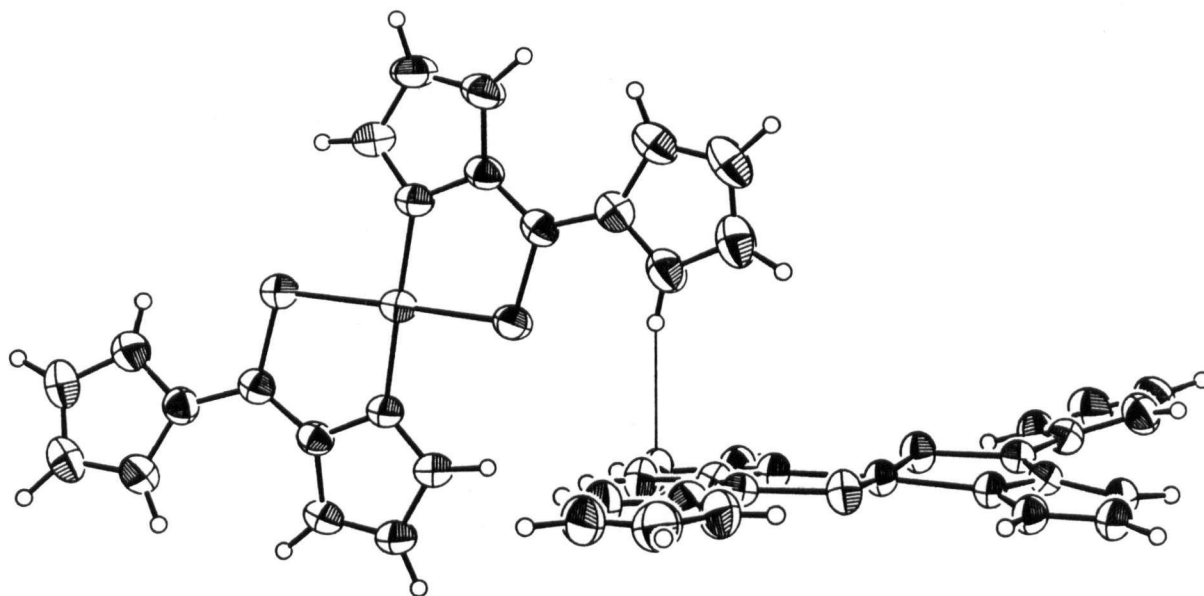


Figure 3-8 Intermolecular interaction as seen in the crystal of **29**

The elementary factors controlling the strength of the coordination interaction have been recognized:⁷⁷

- the topological (or linking) factor
- the metric (or relative size) factor
- the geometric (or shape) factor
- the rigidity factor
- the complementarity factor.

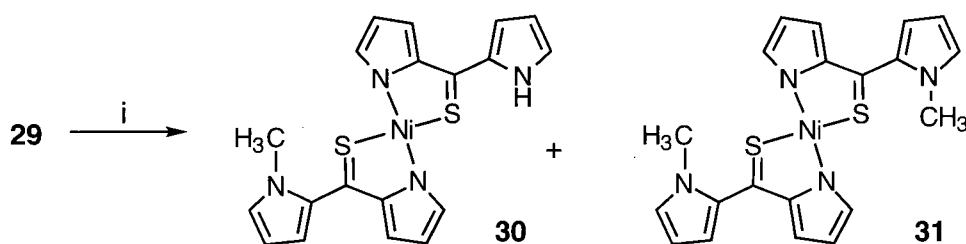
Judged by the similarity of the free and complexed ligand conformation and the restricted number of possible rotations around bonds in the free ligand, the present complex fulfills the criteria of the above list particularly well. These favorable binding interactions likely translate into a high thermodynamic stability of the complex.

2.7 TRANSFORMATIONS OF COMPLEX 29

Complex **29** is a coordinatively saturated, air- and water-stable compound. This stability not only facilitates the investigation of this and many other complexes to be described below, but it also implies that the complex will be relatively inert to chemical transformations.

N-Methylation

The 'by-standing' role of the non-complexing pyrrolic unit raises several questions. One is whether it is possible to chemically modify this unit without disturbing the complexation, and another is whether this unit could be omitted altogether. The first question will be addressed in this chapter, and the latter in Chapter 2-10. Deprotonation of complex **29** with BuLi and subsequent reaction with one or two equivalents of MeI results cleanly in the formation of the products **30** and **31**, respectively. These N-methylated compounds are almost indistinguishable by UV-visible spectroscopy from their starting compounds and show in the mass spectrum the expected mass gain of 14 and 28 mu, respectively. The compounds could also be unambiguously identified by their ¹H-NMR spectra.



Scheme 3-6

N-methylation of complex **29**

Reaction conditions: (i) 1. 2.1 equiv. BuLi in THF, -40°C, 2. 1 or 2.2 equiv. MeI

The C_2 symmetry of **31** is reflected in a simple, starting material-like spectrum with an additional signal for the methyl groups, and the spectrum of the compound carrying two non-equivalent ligands is correspondingly more complex. It can be inferred from steric arguments that the methylated pyrrole moiety is likely co-planar with the rest of the molecule, and the identity of the optical spectra may indicate this.

Reduction

The nickel complex is, at ambient temperature and normal pressure inert to hydrogen. However, it smoothly converts to the dipyrromethane (**2**) after the addition of Raney-nickel. No attempts were undertaken to reduce (or oxidize) the central metal.

Protonation

Reaction of a chloroform solution of complex **29** with trifluoroacetic acid results in the formation of a metal free, polar yellow pigment with a spectrum typical for a dipyrin ($\lambda_{\text{max}} = 402 \text{ nm}$). The conversion can be followed by UV-visible spectroscopy and well defined isobestic points at 362 and 434 nm can be detected, suggesting a 'one-step' conversion into a well defined product. The $^1\text{H-NMR}$ (acetone- d_6) shows three proton signals in the region expected for pyrrolic hydrogens and no signals typical for NH-protons. The mass spectrum of the compound ($M^+ = 208$) corresponds to a mass expected for the ligand **7** + **32**. Elemental analysis shows the presence of only carbon, hydrogen and nitrogen. No structural assignment could be made for this compound.

2.8 THE REACTION OF DI-2-PYRROLYLTHIONE (7) WITH VARIOUS METAL IONS, AND STRUCTURAL CHARACTERIZATION OF SELECTED COMPLEXES

To examine the ability of ligand **29** to complex to metals other than nickel(II), a series of experiments with an arbitrarily chosen range of metals was conducted, in which, unless other conditions are specified, a methanolic metal solution was mixed with a methanolic solution of the potential ligand. Success or failure of the complexations was judged by the changes of the optical spectrum and mass spectrometry of precipitates or products isolated by chromatography. In several cases (*e.g.* with cobalt(III) and mercury(II)) the products were structurally characterized. The investigations to be described in this chapter will focus primarily on the nickel(II) and cobalt(III) and to some extent on mercury(II) complexes of 2-pyrrolylthiones. Other metals have been considered but a thorough study has been left for future investigations.

2.8.1 REACTION OF THIONE 7 WITH MERCURY(II)

Mercury was chosen for its known thiophilicity, and for its propensity to form tetrahedral complexes. The reaction yielded a fine, bright yellow crystalline precipitate (**32**) giving an elemental analysis for $C_{18}H_{14}N_4HgS_2$ which corresponds to a complex with a ligand:metal stoichiometry of 2:1. Its solubility in solvents such as acetone or methylene chloride was lower, as compared to the nickel complex, and the optical spectrum of the bright yellow solution, shown in Figure 3-9, differed significantly as well.

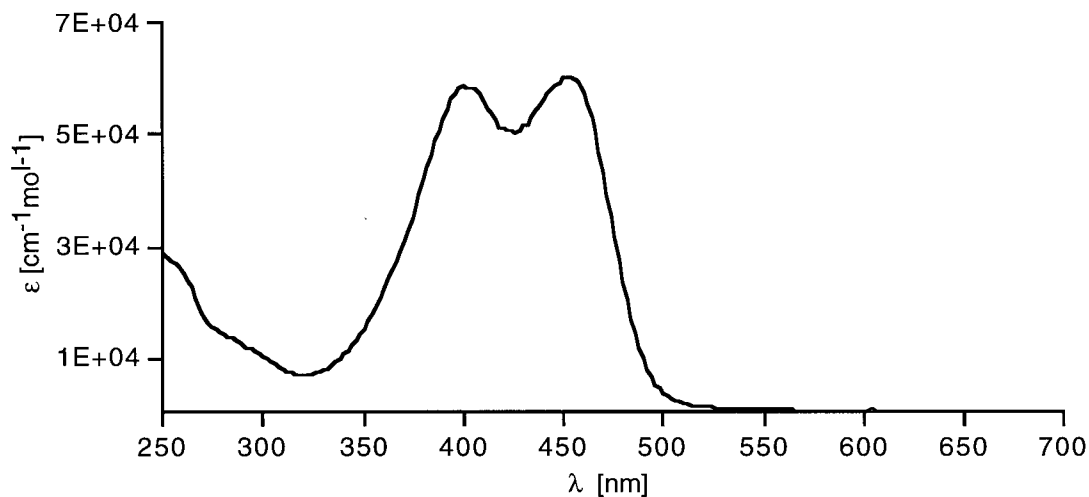


Figure 3-9 Optical spectrum (CH_2Cl_2) of mercury complex **32**

The complex dissolved in DMSO in sufficient concentrations for analysis by NMR spectroscopy. The pattern for one set of equivalent ligands was readily apparent. The results suggested the expected formation of a tetrahedral complex with two chelating ligands around the central metal. However, a polymeric structure with bridging ligands of the same ligand:metal stoichiometry could not be excluded, consequently crystals were grown by allowing a dilute solution of **32** in methylene chloride to evaporate slowly. Crystallographic and experimental data are listed in Table 3-2 and the final atomic coordinates in Table 3-6. A stereoview of an ORTEP representation of the molecule is shown in Figure 3-10. The structural analysis showed the molecule as a (distorted) tetrahedral complex, with a dihedral angle of 62.1° between the planes defined by the mercury, the coordinated nitrogen and the sulfur atom of the respective ligands. The intraligand bond lengths and bond angles are, with one exemption, equivalent to those observed in the nickel complex. The two pyrrolic units of the ligands are not uniplanar but angled by about 40° , a value close to that of the free ligand (32°). It may be speculated that this distortion and a similar interligand orbital interaction of the chromophores, as seen in the dipyrin metal complexes (Part 2), alter the optical spectra in the observed way.

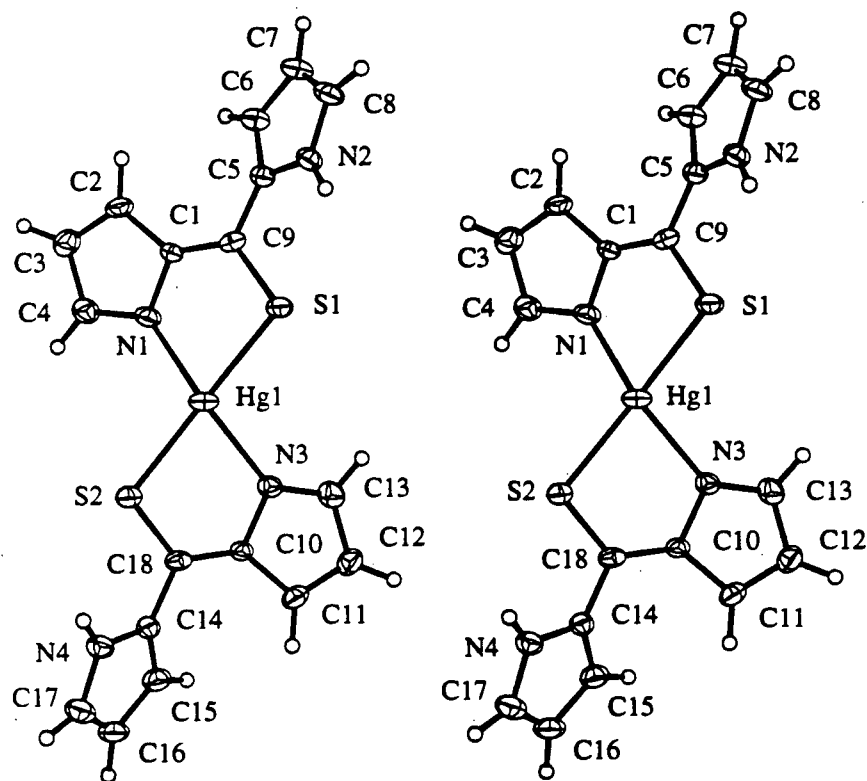


Figure 3-10 Stereoscopic view of the mercury complex 32

2.8.2 REACTION OF THIONE 7 WITH COBALT(II) AND (III)

To further evaluate thione **7** as a ligand, cobalt(II) was reacted with thione **7**. This caused rapid precipitation of a dark solid, which upon chromatography, proved to be a mixture of two orange low-polarity compounds (**33-I** and **33-II**) in the ratio of ~4:6. Both complexes had very similar optical spectra, shown in Figure 2-11.

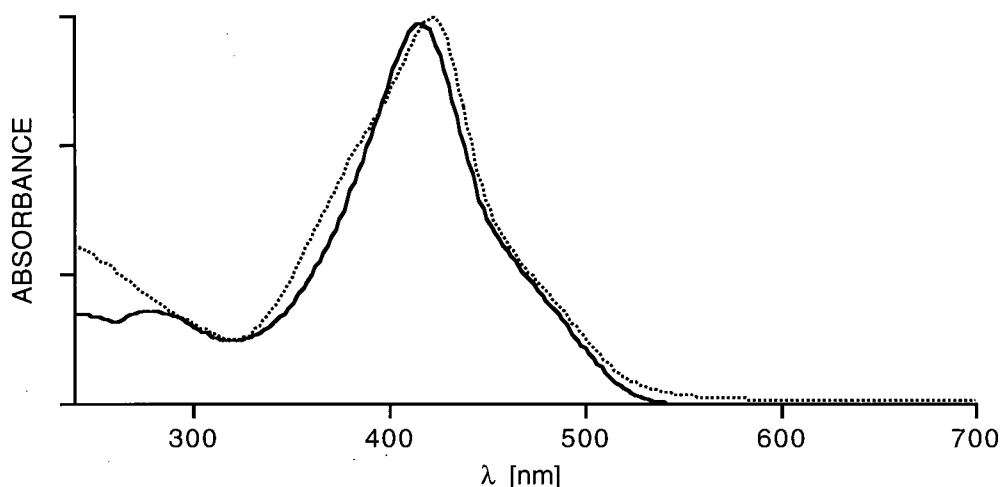


Figure 3-11 Optical spectra (CH_2Cl_2) of the cobalt complexes **33-I** (—) and **33-II** (.....)

Both compounds have identical mass spectra ($M^+ = 584$) corresponding to a molecular formula of $\text{C}_{27}\text{H}_{21}\text{N}_6^{59}\text{CoS}_3$, *i.e.* to a complex of the ligand:metal stoichiometry of 1:3. The low polarity of the complex and its high solubility in non-polar organic solvents indicated the presence of an electro-neutral complex of cobalt(III). The facile aerial oxidation of cobalt(II) to cobalt(III) in the presence of (amine) ligands is well known, and thus all findings could be rationalized by the formation of an (octahedral) cobalt(III) tris-chelate. Complexes **33-I** and **33-II** also form by a ligand exchange reaction with cobalt(III)(acac)₃ and **7** in refluxing phenol. This underscores the thermodynamic stability of the complexes.

Unsymmetrical bidentate ligands (i.e. ligands with two different ends, here, N and S) forming octahedral complexes may form two stereoisomeric complexes. These isomers, the so called *fac*- (carrying all equivalent donor atoms on one face of the coordination polyhedron) and the *mer* isomer (carrying the equivalent donor atoms along a meridian of the coordination polyhedron) can be, in this case, clearly distinguished by their differing symmetries. Octahedral complexes of cobalt(III) are typically in a diamagnetic d^6 low spin configuration and consequently regular ^1H - and ^{13}C -NMR spectra can be obtained. The ^1H -NMR spectra of both isomers are shown below.

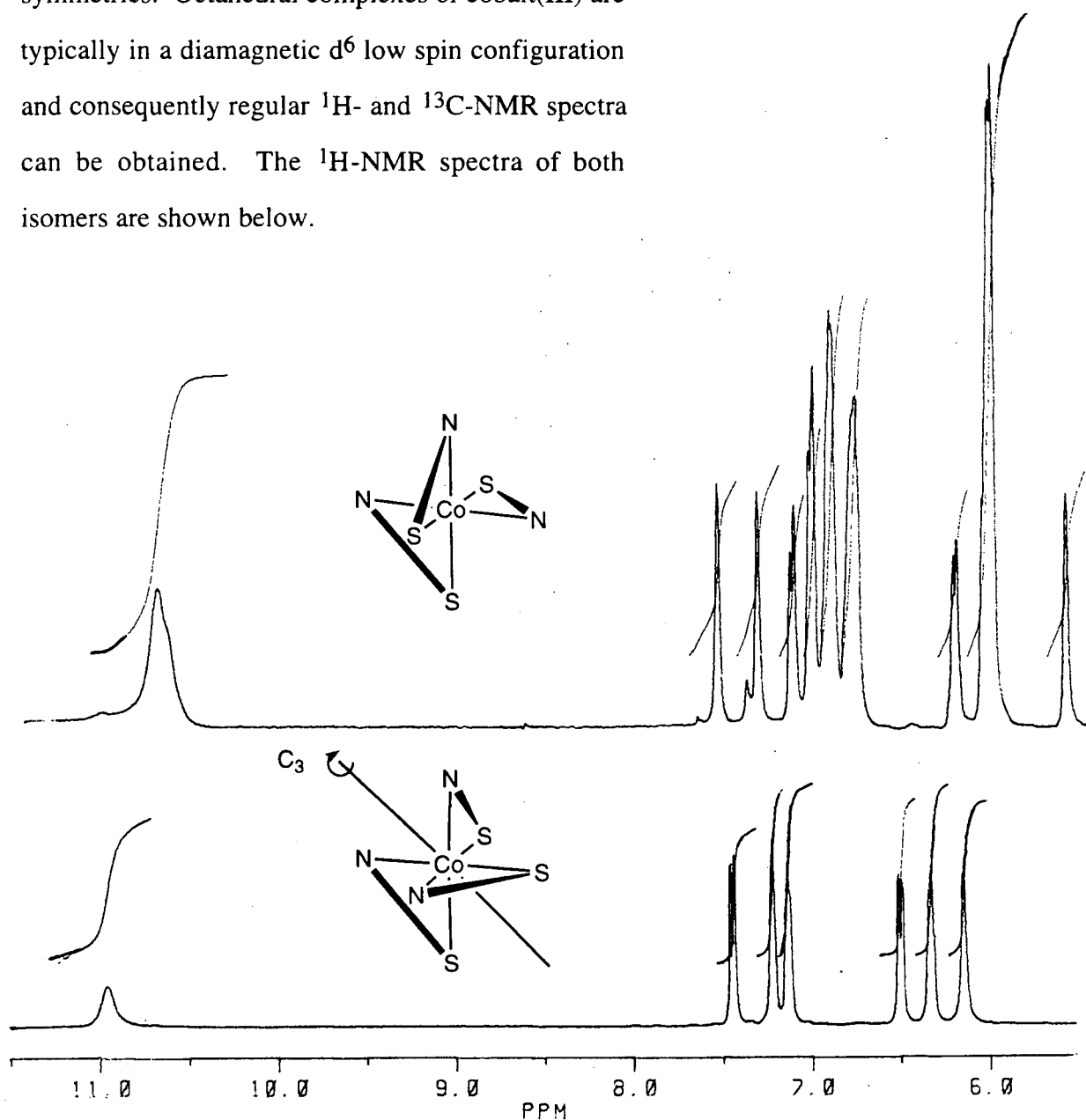


Figure 3-12 ^1H -NMR (200 MHz, acetone- d_6) of the isomeric complexes 40-I and 40-II

The $^1\text{H-NMR}$ spectrum of the isomer of higher polarity (**33-II**) is very similar to that exhibited by the nickel(II) complex **29**, *i.e.* six signals of equal intensity are visible in the aromatic region with associated couplings typical for pyrrolic hydrogens, with a seventh broad signal at 11.0 ppm. The symmetry of *fac*-isomers (point group S_3) bestow a C_3 -axis onto the complex, rendering all three ligands equivalent. Consequently, **33-II** could be assigned the *fac*-type stereochemistry. The *mer*-isomer contains no such high symmetry element in the complex, and this renders all three ligands non-equivalent. This is clearly visible in the more complex $^1\text{H-NMR}$ spectrum of the of lower polarity pigment **33-I**.

The final proof of this assignment was provided by a single crystal X-ray structure analysis of **33-I** (as its acetone solvate), shown in Figure 3-13. Crystal data and some experimental details are listed in Table 3-2 and the final atomic coordinates are listed in Table 3-7. The donor atoms in the essentially planar ligands form an almost perfect octahedron around the central metal. All deviations in bond length as compared to the uncoordinated ligand are equivalent to those observed in the nickel(II) (**29**) and the mercury(II) complex **32**. The deviation from co-planarity within the ligands (average 25°) is again similar to that observed in the free ligand and the mercury complex. The propensity of the NH-protons to undergo hydrogen bonding is, in this structure, highlighted by the incorporation of one hydrogen bonded molecule of acetone into the crystal.

Recent investigations of the dihedral angles observed in the structures of variously substituted biphenyls reveal a delicate electronic control of the dihedral angle by the substituents. To what extent electronic and crystal packing effects are responsible for the dihedral angle observed in the thionato complexes remains unclear.

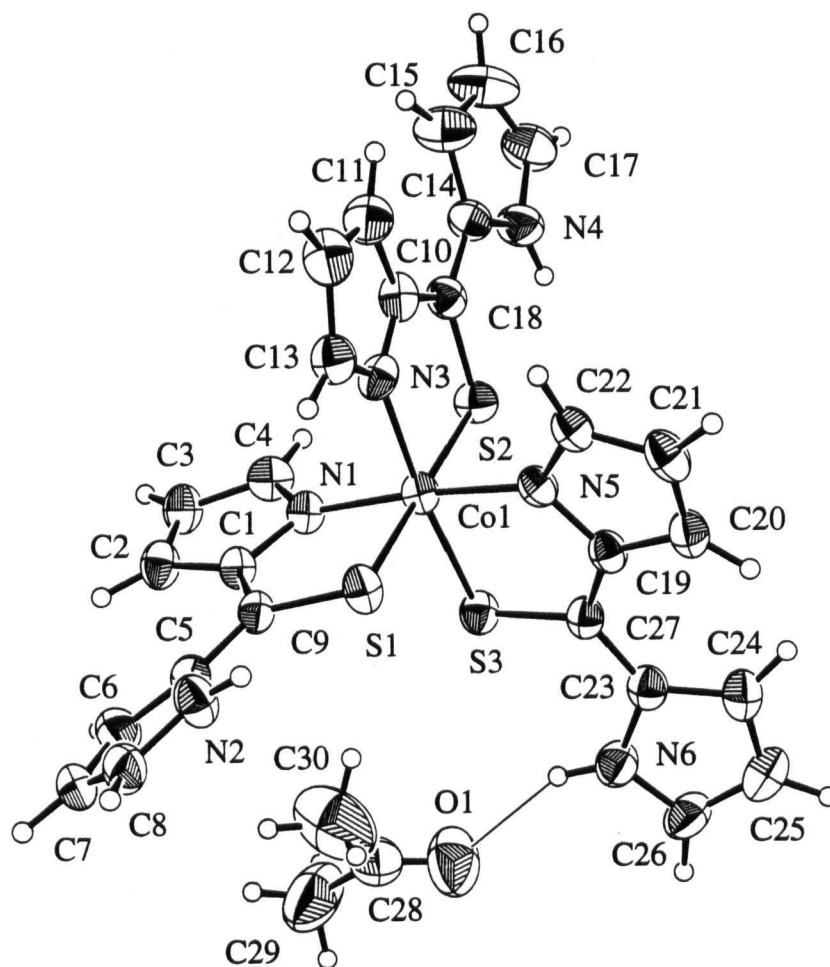


Figure 3-13 ORTEP representation (33% probability level) and numbering scheme used of **33-I** (as its acetone solvate)

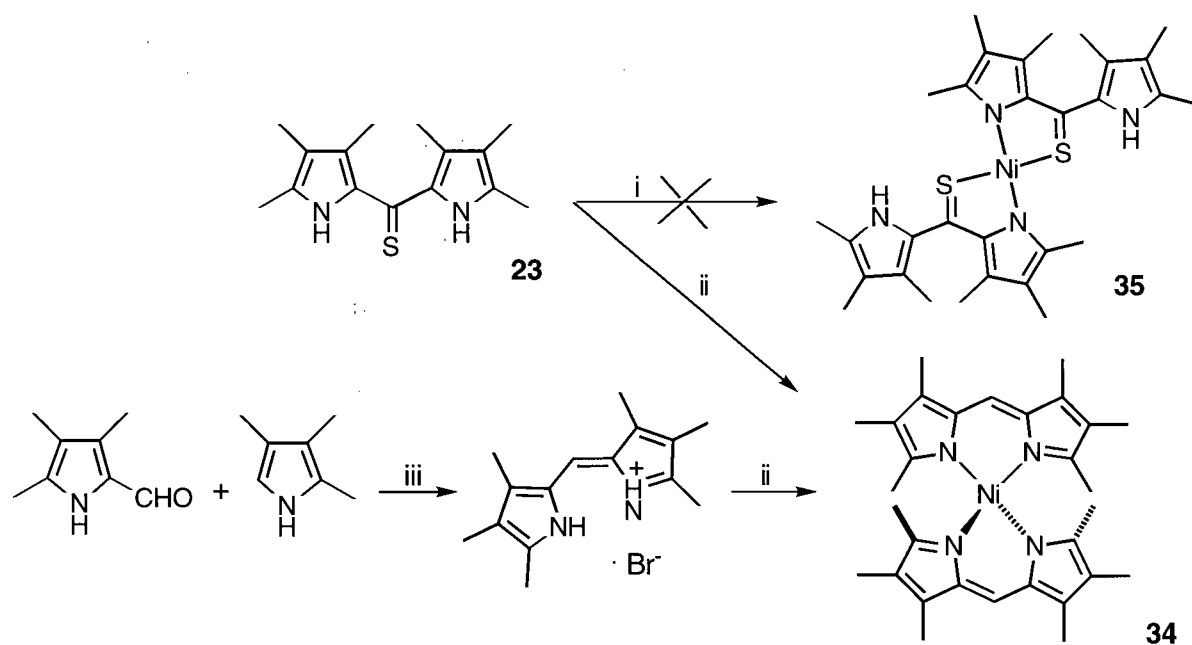
2.8.3 REACTION OF THIONE 7 WITH VARIOUS METAL IONS

The following entries summarize the results of a number of experiments involving attempted chelation of thione **7** with a random selection of metal ions under various conditions:

- Reflux of chromic(acac)₃ in phenol in the presence of the ligand was unsuccessful in generating an isolable complex.
- Manganese(III) as its acetate resulted in extensive decomposition of the ligand.
- Iron(II) as its trichloride reacted in the presence of oxygen with the ligand to form only one major product (black crystals) with a ligand to metal stoichiometry of 3:1 (mass, elemental analysis). The formation of an octahedral iron(III) complex is assumed.
- The reaction of **7** with copper(II) resulted in the formation of a dark yellow, non-crystalline precipitate which, due to its paramagnetism and insolubility in most common solvents and low tendency to crystallize, could not be characterized.
- Zinc(II) has been characterized as moderately thiophilic.⁴⁶ It was, consequently, surprising to find that zinc(II) yielded no visible reaction with thione **7**.
- The reaction of silver(I) as its nitrate resulted in the formation of a bright yellow solution. Solubility and polarity suggested the formation of a salt, likely of a tetrahedral [(ligand)₂Ag(I)]⁻. This is also consistent with the ¹H-NMR (MeOH-d₄) of the compound.
- The reaction with cadmium(II) acetate yields a light red precipitate with analytical, physical and spectroscopic properties similar to that of the mercury(II) complex **32** and, thus, a structure similar to complex **32** is assumed.

2.9 ESTABLISHMENT OF THE STERIC REQUIREMENTS OF THE 2-PYRROLYLTHIONATO MOIETY

In an early attempt to prepare complexes of thiones other than **7**, hexamethyl thione **23** was refluxed with Raney-nickel (in the absence of hydrogen), producing, after extended reaction times, a small amount of a bright red pigment. This could be identified as the bis(hexamethyldipyrinato)nickel(II) (**34**). The assignment of this paramagnetic pigment was confirmed by an independent synthesis, shown in Scheme 3-7 (see also Part 2). To our surprise, however, not a trace of the expected complex **35** could be detected. An equivalent set of reactions has been performed with the di(2,4-dimethyl-3-ethyl)thione (**24**), essentially reproducing the above results.



Scheme 3-7

Attempted formation of complex **35** and the formation of **34**

Reaction conditions: (i) Raney-Ni/acetone/ Δ ; (ii) Ni(II)acetate, MeOH; (iii) HBr/EtOH

In later experiments, peralkylated thiones **23** and **24** were mixed with nickel(II)-acetate in MeOH, but again, the expected complex could not be found, in fact, no reaction at all occurred, and the starting thione could be recovered quantitatively.

Due to the electronic similarity of the ligands, as judged by their similar optical spectra, electronic arguments do not seem adequate to explain these findings. However, two explanations involving steric arguments could be evoked. The interaction of the β -methyl groups prevent intramolecular co-planarity of the pyrrole moieties, and this might prevent the formation of the complex. However, considering the previously discussed by-stander role of the non-coordinating pyrrole, this argument seems unlikely. The key to understanding the finding may lie in the steric interaction of the α -substituents. Based on the X-ray crystal data of nickel complex **29**, a computer generated model, in which the α -hydrogens of structure **29** have been replaced with methyl groups, is shown in Figure 3-14.

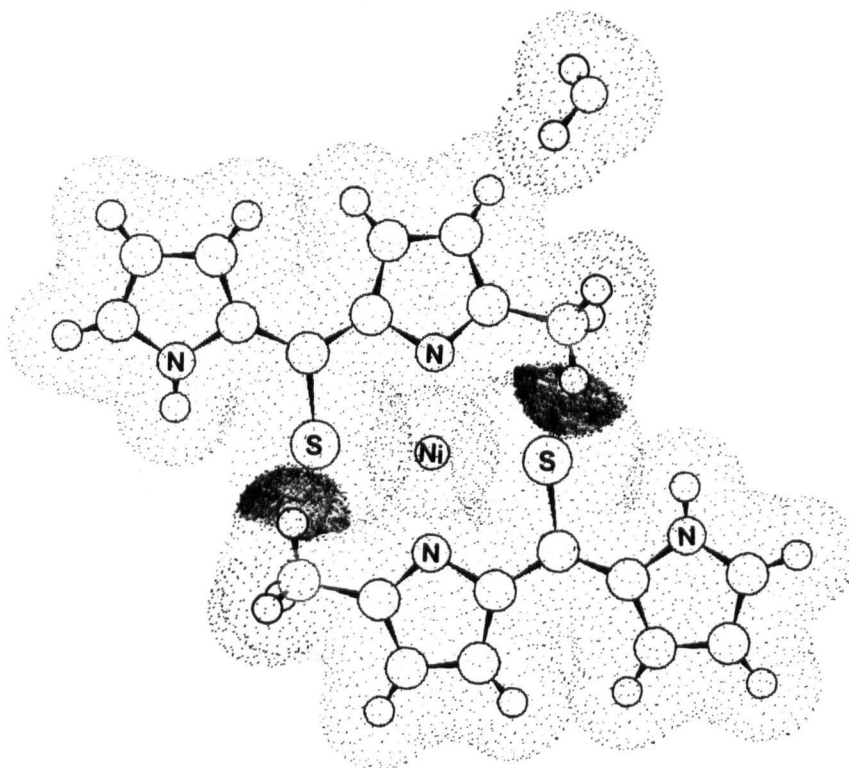
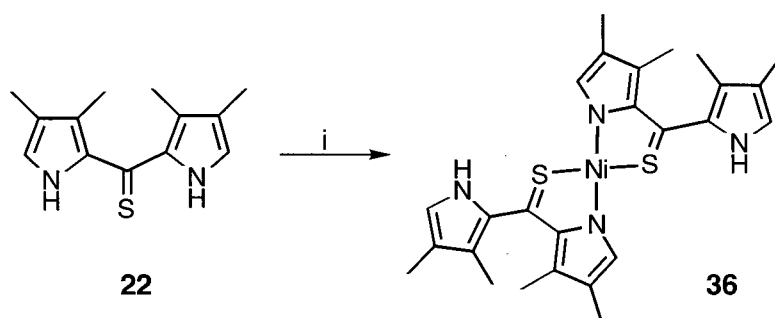


Figure 3-14 Computer generated model⁷⁸ of a hypothetical nickel(II) complex with an α -methyl-thionato ligand

As indicated by the large overlap of the van der Waals radii of the α -methyl groups and the sulfur of the opposing ligand, a square planar arrangement cannot be achieved. Interestingly, the formation of a tetrahedral complex cannot be observed either, likely due to an equivalent interaction.

The hypothesis that the formation of complex **35** is prevented by the bulk of the α -substituent is proven by the smooth complexation of nickel(II) by the α -unsubstituted β,β' -dimethyl thione **22** to give the corresponding complex **36**.

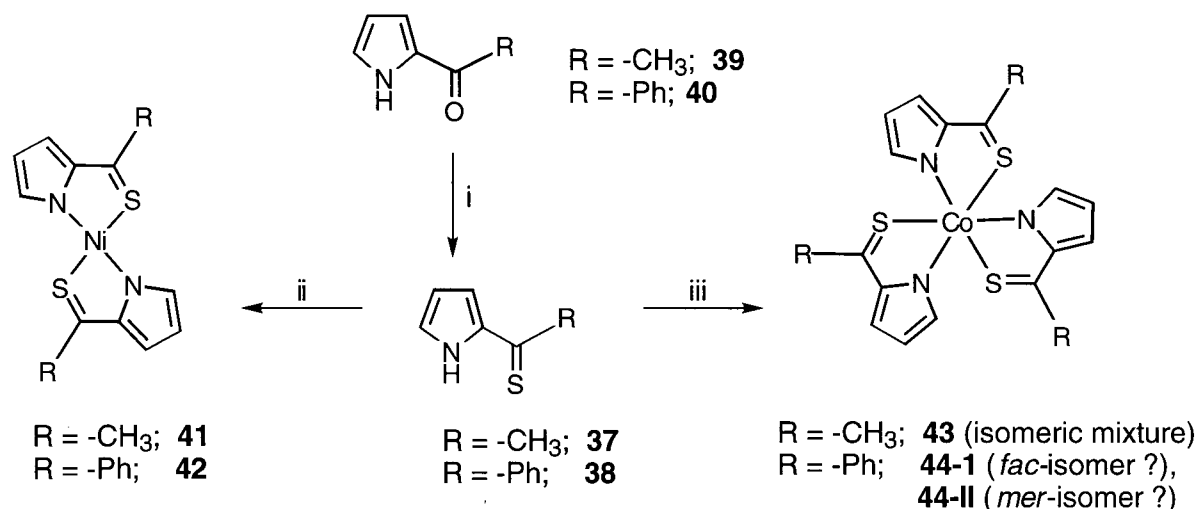


Scheme 3-8 Formation of nickel(II) complex **36**

The spectroscopic data of complex **36** are largely as expected. The wavelength of absorption of the strongest band in the optical spectrum is 10 nm hypsochromically shifted as compared to the complex **29**. As suggested above, and as can be clearly seen in a computerized model, a coplanar conformation of the two pyrrolic units of the ligand cannot be achieved in the presence of methyl substituents at C3. Consequently, the resulting diminished electronic interaction of the non-coordinating pyrrole moiety with the chromophore may explain this shift.

2.10 SYNTHESIS OF 2-THIOACETYL- (37) AND 2-THIOBENZOYL-PYRROLE (38), AND FORMATION OF THE NICKEL(II) AND COBALT(III) COMPLEXES THEREOF

The recognition of the by-stander role of the non-complexing pyrrolic unit in all of the dipyrrolylthionato complexes so far described prompts the question whether molecules containing solely the 2-pyrrolylthione moiety would be capable of forming complexes as well. Compounds of this class are, for instance, 2-thioacetylpyrrole (37)³¹ and 2-thiobenzoyl-pyrrole (38)⁷⁴. While both compounds have been described in the literature, the latter was ill characterized and described as an oil. We find it is, in fact, a crystalline solid. Both thiones can be prepared from their corresponding oxo-analogs (39 and 40) by reaction with phosphorus pentasulfide under reflux in acetonitrile, benzene or pyridine or by sonication at slightly elevated temperatures. (Scheme 3-9)



Scheme 3-9

Synthesis of 2-pyrrolylthiones **37** and **38**, and their Ni(II) and Co(III) complex formation

Reaction conditions: (i) P₄S₁₀ in benzene, Δ or sonication; (ii) Ni(II)acetate/ MeOH; (iii) Co(II)acetate/MeOH/O₂

The nickel(II) complexes **41** and **42** form in high yield upon simple mixing of methanolic solutions of the reactants. Their spectroscopic and analytical data allow for their formulation as square planar complexes with a ligand : metal ratio of 2:1. By analogy to the dipyrrolylthionato complex **29**, it is assumed that the ligands are arranged in an anti-parallel manner. The different electronic influence of the methyl or phenyl group on the rest of the complex as compared to the pyrrolyl group in **29** is demonstrated by their significantly varying optical spectra, shown in Figure 3-15. Both spectra exhibit the same pattern, with that of the phenyl substituted complex being ~25 nm bathochromically shifted. The purple thiobenzoylpyrrolato complex was distinguished by a very low solubility in non-coordinating solvents, whereas the red thioacetyl analog was freely soluble in a variety of solvents.

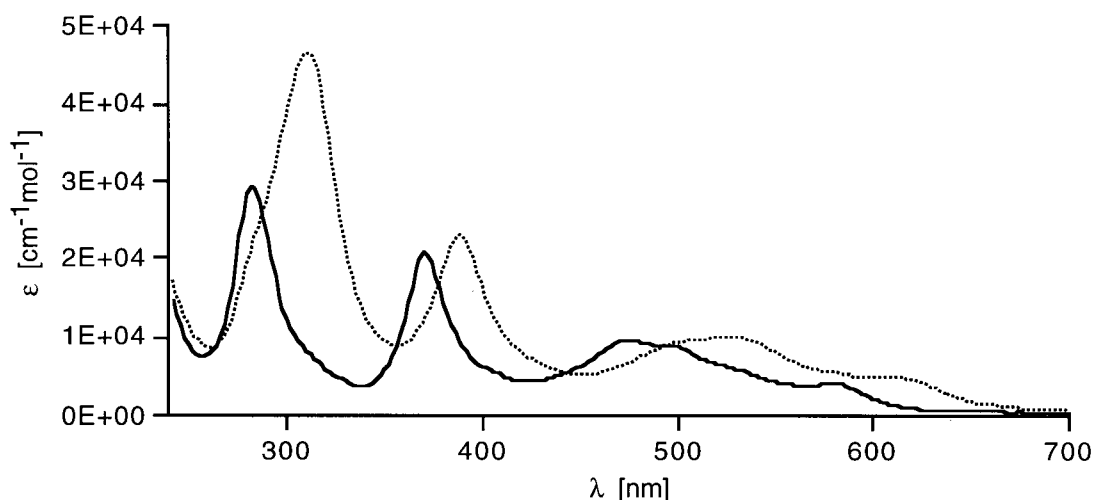


Figure 3-15 Optical spectrum(CH_2Cl_2) of **41** (—) and **42** (.....)

The corresponding cobalt(III) complexes **43** and **44** formed equally smoothly under the general complex forming conditions. The yellow-orange 2-thioacetylpyrrolato complex **43** could not be separated into its *fac*- and *mer*-stereoisomers, which, however, were clearly present based on NMR data. Certain peaks in the ^{13}C -NMR were quadrupled. We assigned one peak to one carbon in the set of three equivalent ligands in the *fac*-isomer, and the other

three peaks to the corresponding carbons in the three non-equivalent ligands in the *mer*-isomer. The separation of these isomers by chromatography posed no problem in the case of the 2-thiobenzoylpyrrolato complex **44**. Mass spectral and analytical data proved their composition to be $M(\text{Ligand})_3$, however, whereas one of the isomers (**44-II**) has expectedly a complex ^1H - and ^{13}C -NMR spectrum (and thus was tentatively assigned to be the *mer*-isomer), the proton spectrum of the other isomer is not as simple as expected for the *fac*-isomer of **44**. Whether this is due to a distorted octahedral geometry or due to a totally unexpected coordination geometry cannot be decided. Crystals seemingly suitable for X-ray crystallography have been grown but the results of the diffraction have not been obtained at the time of writing of this thesis.

The optical spectra are significantly different from those of their dipyrrolylthione congeners. As well, the phenyl-substituted complex is characterized by a bathochromically shifted spectrum as compared to that of the methyl-substituted analog (Figure 3-16).

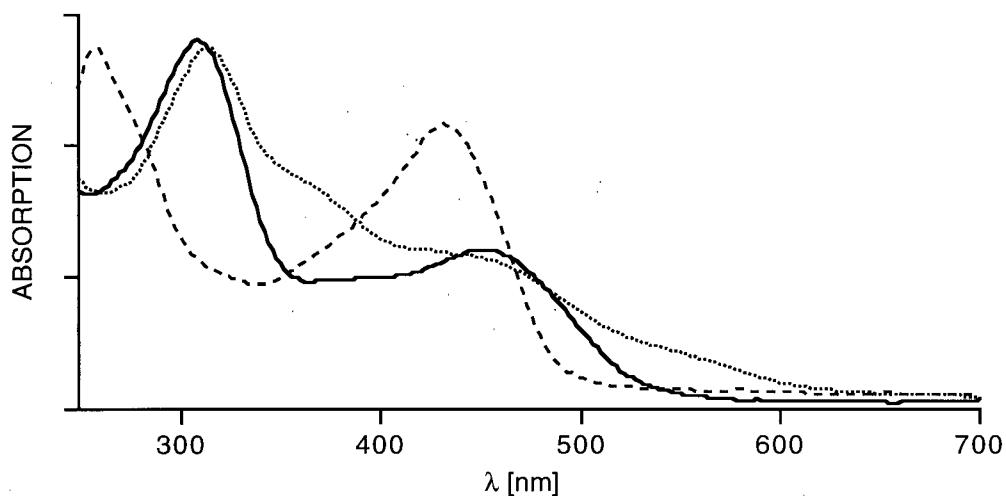
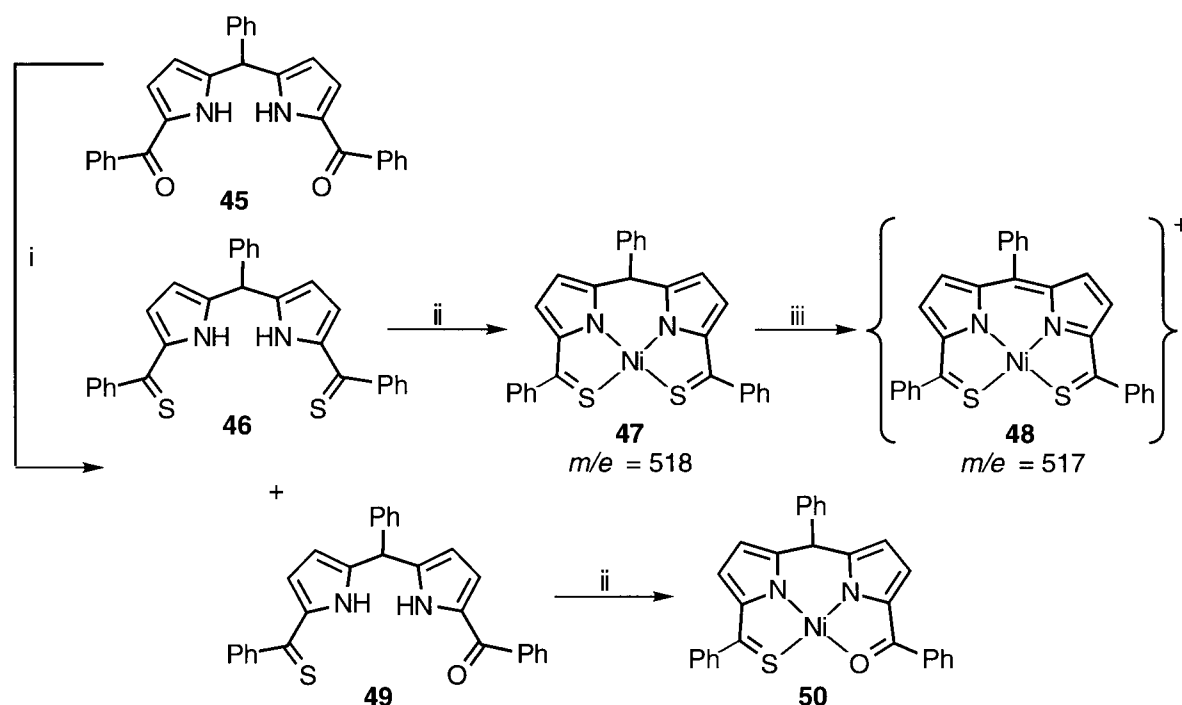


Figure 3-16 Normalized optical spectra (CH_2Cl_2) of **44-I** (—), **44-II** (⋯), and **43** (---)

2.11 PRELIMINARY REPORTS ON THE FORMATION OF TETRADENDATE LIGANDS CONTAINING THE 2-PYRROLYLTHIONE MOTIF, AND THEIR NICKEL(II) COMPLEXES

An anti-parallel square planar arrangement of the ligands along the metal centre was inferred for complex **29**. The synthesis of a complex with the corresponding parallel arrangement would be desirable for comparative reasons. Section 2.2 of Part 1 described the synthesis of the bisbenzoyldipyrrolylmethane **45** and its likely conformation. The procedures to convert benzoylpyrroles into their thio-analogs outlined in the preceding chapter were also found to be applicable to the bisbenzoyldipyrromethane **45**, generating dithione **46** (Scheme 3-10).



Scheme 3-10 Formation of tetradentate 2-pyrrolylthione and -ketone ligands, and their Ni(II) complexes
Reaction conditions: (i) P_4S_{10} in benzene, Δ or sonication; (ii) Ni(II)acetate/ MeOH (iii) conditions of EI mass spectral analysis

Thus, conversion of dibenzoyl **45** results in the formation of an orange pigment (**46**) with the expected mass for the shown dithione structure. Attempts to purify this dithione led to large losses of compound, consequently, it was used crude in later experiments. Thus, a potential pathway to create a complex with parallel ligand arrangement emerges, given of course, that the tetradentate thione ligand **47** complexes in an analogous way to nickel(II) as with **7** (Scheme 3-10), an assumption also supported by computer-generated⁷⁸ models. When dithione **46** was reacted with nickel(II) as its acetate, a non-polar auburn pigment (**47**) with an optical spectrum unlike that of nickel complex **29** was produced (Figure 3-17).

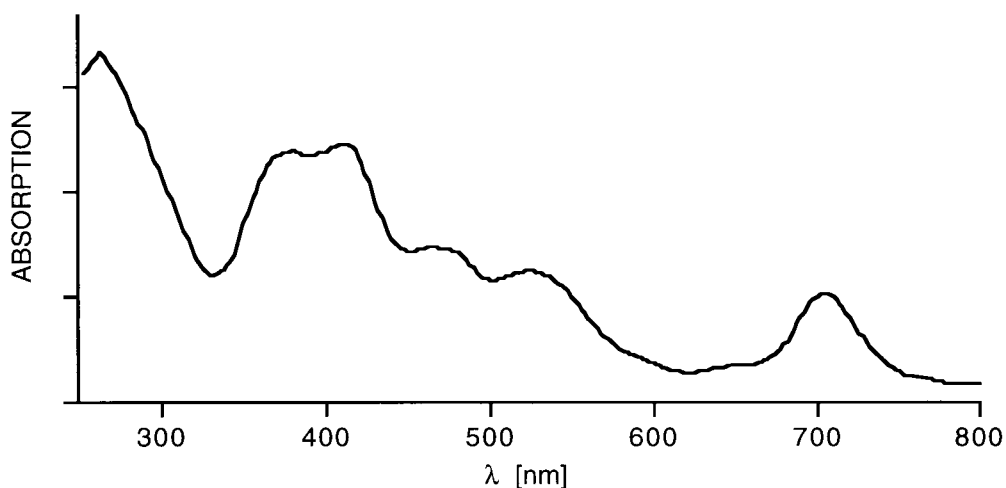


Figure 3-17 Optical spectrum (CH_2Cl_2) of **47**

Its mass spectrum ($m/e = 518$) is as expected for a nickel complex of structure **47**. Moreover, the fragmentation pattern of this pigment gives some insight into its structure. Most noticeably, the fragmentation pattern is very simple. The strongest peak (100%) in the mass spectrum is a peak corresponding to $M^+ - 1$. We attribute this to the creation of the fully conjugated complex **48** which could only have formed from the anticipated complex **47**. Other than one relatively weak peak corresponding to M^+ -phenyl, no other peaks above $m/e = 77$ are of significant intensity, attesting to the stability of the initially formed structure **48**. The complexes of type **29**, on the other hand, exhibited rich fragmentation patterns.

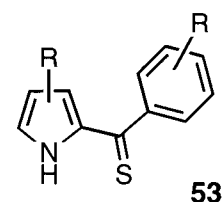
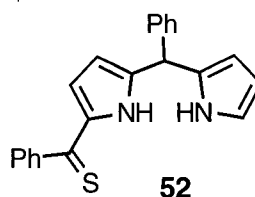
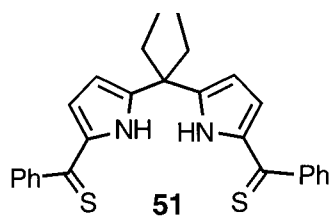
No $^1\text{H-NMR}$ spectrum of this compound could be obtained suggesting the compound is paramagnetic. That, in turn, suggests a radically different coordination sphere from the square planar coordination in **29**. The exact nature of this compound is still under investigation.

The oxo- to thio-conversion of the two ketone functionalities in **45** occurs in two separate steps. Hence, it was not surprising to observe the formation of a lesser amount of a product (**49**) with an R_f -value between that of starting compound **45** and the dithione **46**, and a molecular mass suggesting the presence of one oxygen and one sulfur. We assigned it structure **49**. Surprisingly, however, was the fact that this compound also formed, based on mass spectral analysis, a nickel(II) complex, assigned the structure **50**. As the diketone **46** does not form any complex with nickel(II) under the conditions investigated, this pronounced change in reactivity can be attributed to the presence of the thione moiety, underlining the strength of the nickel(II)-sulfur interaction.

3 CONCLUSION AND FUTURE WORK

In conclusion, 2-pyrrolylthiones are novel bidentate, planar N,S-donor chelators which form, in fair to high yields, strongly colored complexes with a variety of metals. The solid state conformation of the ligand in the complexes is very similar to that of the free ligand. The complexes are stable, coordinatively saturated compounds with a high tendency to crystallize. The present study has shown that 2-pyrrolylthiones are versatile ligands, however, the scope of their applicability in biomimetic or pharmaceutical chemistry remains to be investigated. To further evaluate their potential use, more data need to be acquired and more compounds synthesized.

Electrochemical investigations on whether the ligand is capable of stabilizing unusual oxidation states of the central metal would be useful. Multidentate ligands containing hard-soft donor sets have been of interest for the understanding of the fundamental factors governing the action of various metalloenzymes.⁷⁹ The 2-pyrrolylthione motif could be built into a series of structurally related and rigid potential ligands (*e.g.* **49**) to study these factors. Di-*meso*-substituted ligands (**51**), tridentate ligands (**52**), and tetradentate monoanionic ligands such as **48** also seem to be attractive synthetic targets for these studies. Finally, the investigation of the biodistribution of metal complexes of variously substituted thiones such as **53** would give some insight into the potential of this ligand type to be used in biological applications.



4. EXPERIMENTAL

3.1 INSTRUMENTATION AND MATERIALS

Melting points were determined on a Thomas Model 40 Micro Hot Stage and are uncorrected. The infrared spectra were measured with a Perkin-Elmer Model 834 FT-IR instrument or an a *Perkin Elmer* 710D. The ^1H -NMR spectra were measured on a Bruker AC-200 spectrometer (200 MHz) with data processing on a Bruker data station, or a Varian XL-300 (300 MHz). ^{13}C -NMR spectra were measured on a Bruker AC-200 Fourier-transform spectrometer (50 MHz) or a Varian XL-300 (75 MHz). A C,H-COSY spectrum was taken on a Bruker AMX 500 (500/125 MHz). The NMR spectra are expressed on the δ scale and were referenced to residual solvent peaks. The low and high resolution mass spectra were obtained on a AEI MS9 and a Kratos MS 50, respectively. The electronic spectra were measured on a Hewlett Packard HP 8452A photodiode array spectrophotometer and the data were processed on a microcomputer (CA Cricket Graph III software). Elemental analyses were performed on a Fisons CHN/O Analyzer, Model 1108. For experimental details of the X-ray crystal structure determination, see Tables 3-1 and 3-2. Sonication experiments were performed in a Cole Model 8845-6 cleaning bath with unspecified sonication power output.

Materials

The silica gel used in the flash chromatographies was Merck Silica Gel 60, 230-400 mesh. R_f -values were measured on Merck silica TLC aluminum sheets (silica gel 60 F₂₅₄)

whilst preparative TLC was performed on pre-coated 20x20 cm, 0.5 or 1.0 mm thickness, Whatman or Merck silica gel plates (with or without fluorescence indicator). 2-Acetylpyrrole (**37**)⁸⁰ and 2-benzoylpyrrole (**38**)⁸¹ were prepared according to literature procedures. 2,2'-Dibenzoyl-5-phenyldipyrromethane (**45**) was synthesized as described in Part 1. Dipyrrolylthiones **7** and **21 - 24** were prepared according to Clezy and Smythe.⁹ The data for the previously prepared dipyrrolylthiones included here were either not reported in the original paper (¹³C-NMR, high field FT ¹H-NMR), or are included for comparison. The Raney-nickel used was purchased from Aldrich (#22,167-8) as a 50% slurry in water pH > 9. All other reagents and solvents were commercially available and of reagent grade or higher, and were used as received.

NOTE OF CAUTION

Some chemicals used throughout this work deserve special attention. Thiophosgene and Br₂ are volatile, corrosive and severely toxic chemicals. They must be handled in a well-ventilated fumehood and proper personal protective equipment must be worn. Raney-nickel is pyrophoric and a suspected carcinogen. Special care should be taken in handling and disposing of this material. Familiarization with the recommendations, warnings, first aid measures and disposal procedures for these chemicals as outlined in the Material Safety Data Sheets (MSDS) should be mandatory before working with these compounds.

3.2 2-PYRROLYLKETONES

2-Trichloromethoxycarbonylpyrrole and di-2-pyrrolylketone (**6**)

Pyrrole (0.42 g, 6.27 mmol) dissolved in dry THF (20 mL) was stirred under anhydrous conditions with triphosgene (1.86 g, 6.27 mmol) for 24 h at 30°C. The reaction mixture was quenched with MeOH (5 mL), stirred for an additional 2 h, diluted with CH₂Cl₂ and washed with an aqueous carbonate solution. The organic layer was separated and reduced on a rotary evaporator to give a dark oil which was submitted to flash chromatography (silica gel-CH₂Cl₂/4x20 cm). The first band eluted yielded, after removal of the solvent, 2-trichloromethoxycarbonylpyrrole as a white solid in 4.9% yield (70 mg, 3.08 x 10⁻⁴ mol). The second major band, yielded, after removal of the solvent, ketone **6** (130 mg, 8.12 x 10⁻⁴ mol, 26 % yield).

2-Trichloromethoxycarbonylpyrrole:

MW = 228.46; R_f = 0.7 (CH₂Cl₂); ¹H-NMR (300 MHz, CDCl₃) δ 6.38 (m, 1H), 6.92 (m, 1H), 6.99 (m, 1H), 9.2 (br s, 1H); LR-MS (EI, 150°C) m/e = 227 (18.0, M⁺), 148 (23.5), 117 (55.3, CCl₃⁺), 94 (100, pyrrolylCO⁺), 66 (72.2, pyrrolyl⁺).

6⁹:

MW = 160.18; R_f 0.29 (CH₂Cl₂); ¹H-NMR (300 MHz, CDCl₃) δ 5.85 (m, 2H), 6.60 (m, 2H), 6.68 (m, 2H), 9.65 (br s, 2H); ¹³C-NMR (75 MHz, CDCl₃) δ 110.96, 116.16, 124.15, 130.50, 172.64; UV-visible (CH₂Cl₂) λ_{max} (rel intensity) = 2.54 (0.2), 334 (1.0) nm.

3.3 2-PYRROLYLTHIONES

2-Ethoxythiocarbonyl-3,4,5-trimethylpyrrole (**25**)

Isolated in ~ 5% yield by column chromatography (silica gel/CHCl₃) as a side product from the preparation of di(2,3,4-dimethyl-2-pyrrolyl)thio ketone (**23**) according to the (modified) procedure of Clezy and Smythe⁹, in which the reaction mixture is quenched with MeOH. Pale yellow transparent scales (recrystallized 2x from EtOH/H₂O).

MW = 197.29; R_f = 0.79 (CH₂Cl₂:CCl₄ 1:1/silica); mp = 92-93°; ¹H-NMR (300 MHz, CDCl₃) δ 1.44 (tr, *J* = 7.2 Hz, 3H), 1.89 (s, 3H), 2.17 (s, 3H), 2.23 (s, 3H), 4.64 (q, *J* = 7.2 Hz, 2H), 9.12 (br s, 1H); ¹³C-NMR (50 MHz, CDCl₃) δ 8.67, 11.80, 12.05, 66.35, 119.04, 128.47, 134.41, 199.30; UV-Vis (CH₂Cl₂) λ_{max} (rel. intensity) 260 (0.30), 288 (0.18), 360 (1.00) nm; LR-MS (EI, 150°C) *m/e* 197 (69.4, M⁺), 169 (10.1, M⁺-C₂H₅), 152 (53.0, M⁺-OC₂H₅), 136 (100.0, M⁺-C₂H₅-S), 120 (22.8, M⁺-OC₂H₅-S), 108 (18.0, M⁺-CSOC₂H₅); HR-MS (EI, 150°C) *m/e* calc'd for C₁₀H₁₅NOS: 197.08740, found 197.0873; Analysis calc'd for C₁₀H₁₅NOS: C, 60.88; H, 7.66; N, 7.10; S, 16.25; found: C, 60.62; H, 7.59; N, 6.98; S, 16.42.

2-Benzoyloxycarbonyl-3,4-dimethyl-5-methoxythiocarbonylpyrrole (**26**)

Isolated in small yield (<5%) from the attempted preparation of di(5-benzyloxycarbonyl-3,4-dimethyl-2-pyrrolyl)thio ketone from 2-benzyloxycarbonyl-3,4-dimethylpyrrole with thiophosgene according to a procedure of Clezy and Smythe.⁹ This product (pale yellow crystalline solid) was the only isolated product after the quenching of the reaction mixture with methanol.

MW = 303.38; R_f = 0.82 (CH₂Cl₂:CCl₄ 1:1/silica); mp = 65°; ¹H-NMR (200 MHz, CDCl₃) δ 2.27 (s 3H, 3- or 4-CH₃), 4.24 (s, 3H, -OCH₃), 5.34 (s, 2H, -CH₂Ph), 7.15-7.25 (m, 5H, Ph-H), 9.88 (br s, 1H, NH); ¹³C-NMR (50 MHz, CDCl₃) δ 10.18, 11.46, 57.88, 66.38,

123.13, 124.95, 128.02, 128.28, 128.47, 128.65, 131.05, 135.88, 160.68, 201.47; UV-Vis (CH₂Cl₂) λ_{\max} (rel. intensity) 244 (0.97), 270 (0.36), 348 (1.00) nm; LR-MS (EI, 150°C) 303 (29.2, M⁺), 228 (1.5, M⁺-CSOCH₃), 212 (13.6, M⁺-C₇H₇), 194 (22.3), 169 (8.4, MH⁺-CO₂-C₇H₇), 91 (100); HR-MS (EI, 150°C) *m/e* calc'd for C₁₆H₁₇NO₃S: 303.09291, found 303.0928; Analysis calc'd for C₁₆H₁₇NO₃S: C, 63.35; H, 5.65; N, 4.62; S, 10.57; found: C, 63.36; H, 5.65; N, 4.56; S, 10.70;

Di-2-pyrrolylthione (**7**)

MW=176.17; R_F 0.50 (1:1 CCl₄/CH₂Cl₂); ¹H-NMR (300 MHz, CDCl₃) δ 6.37 (m, 2H), 7.02 (m, 2H), 7.15 (m, 2H); (all multiplets are distinguished by a very narrow peak width due to unusually small coupling constants), 9.9 (br s, 2H); ¹³C-NMR (100 MHz, CDCl₃) δ 112.35, 114.71, 127.58, 138.26, 192.97; IR (Nujol) 3365, 3320 (NH), 1087, 1055 (C=S) cm⁻¹; UV-visible (CHCl₃) λ_{\max} (log ϵ) = 303 (3.47), 406 (4.56) nm.

Di(4-ethyl-3,5-dimethyl-2-pyrrolyl)thione (**24**)

MW = 288.45; ¹H-NMR (200 MHz, CDCl₃) δ 1.03 (tr, *J* = 9 Hz, 6H), 1.95 (s, 6H), 2.21 (s, 6H), 2.40 (q, *J* = 9 Hz, 4H), 9.0 (br s, 2H); ¹³C-NMR (50 MHz, CDCl₃) δ = 10.86, 11.69, 14.97, 17.45, 125.49, 126.63, 134.61, 136.20, 189.46.

Di(3,4,5-trimethyl-2-pyrrolyl)thione (**23**)

MW = 260.40; ¹H-NMR (200 MHz, CDCl₃) δ 1.90 (s, 3H), 1.98 (s, 3H), 2.21 (s, 3H), 8.90 (br s, 2H); ¹³C-NMR (75 MHz, CDCl₃) δ 9.03, 11.34, 11.82, 120.01, 126.20, 134.96, 136.04, 189.35.

Di(1-methyl-2-pyrrolyl)thione (**21**)

MW = 203.28; ¹H-NMR (200 MHz, CDCl₃) δ 3.95 (s, 6H), 6.10 (dd, *J* = 4, 4 Hz, 2H), 6.54 (dd, *J* = 4, 4 Hz, 2H), 6.98 (m, 2H); ¹³C-NMR (50 MHz, CDCl₃) δ 37.33, 107.80,

120.10, 133.50, 142.72, 197.38; IR (Nujol) = 1060, 1045 cm^{-1} ; UV-Vis (CHCl_3) λ_{max} ($\log \epsilon$) = 320 (3.36), 393 (4.36) nm.

2-Thioacetyl-pyrrole (**37**)

Acetylpyrrole (**41**) (500 mg, 4.63 mmol) was dissolved in benzene (50 mL) and phosphorus pentasulfide (2.0 g, 4.50 mmol) was added in portions to the refluxing mixture. The entire mixture was loaded, after no starting material could be detected by TLC (~30 min), onto a wide, short column (8x10 cm) of silica gel, which was topped by a layer of Celite[®]. The column was eluted with benzene and the first, bright red fraction was collected and evaporated on the rotary evaporator to yield **37** as an red-orange oil (140 mg, 1.12 mmol, 24.6% yield). As this compound proved to decompose at ambient temperature and in the presence of oxygen within days, it was generally prepared and used immediately.

MW = 125.19; mp < 4°C (74-75°C lit.³¹); R_f = 0.75 ($\text{CH}_2\text{Cl}_2/\text{CCl}_4$ 1:1), red color; $^1\text{H-NMR}$ (200 MHz, CDCl_3) δ 2.99 (s, 3H, - CH_3), 6.45 (m, 1H), 7.08 (m, 1H), 7.26 (m, 1H), 9.8 (br m, 1H); $^{13}\text{C-NMR}$ (50 MHz, CDCl_3) δ 34.64, 112.98, 114.89, 129.99, 142.18, 217.79; UV-Vis (MeOH) λ_{max} (rel. intensity): 256 (0.13), 290 (0.14), 374 (1.0) nm; LR-MS (EI, 150°C) m/e : 125 (100, M^+), 110 (57.4, $\text{M}^+ - \text{CH}_3$), 92 (63.5, $\text{M}^+ - \text{SH}$), 83 (18.5), 67 (17.7), 65 (23.8).

2-Thiobenzoylpyrrole (**38**)

This compound has been prepared by the ultrasonic-assisted conversion of 2-benzoylpyrrole (**42**) by phosphorus pentasulfide.⁷⁴ However, the authors of this paper describe the compound as a liquid, report no yields and give no indication about the purity of the compound characterized the compound only by low field $^1\text{H-NMR}$ and IR.

4.0 g (23.24 mmol) 2-Benzoylpyrrole were refluxed under N_2 in benzene (100 mL). 5 g (11.25 mmol) Powdered phosphorus pentasulfide was added in 5 portions over 30 min. The

mixture was also repeatedly sonicated for several minutes in a commercially available cleaning bath. The resulting dark mixture was filtered through Celite[®], the filtrate was reduced under vacuum and finally chromatographed on silica gel (3x12 cm) with benzene as eluent. The bright orange main fraction was collected and evaporated to dryness to afford 2.92 g (15.56 mmol, 67 % yield) of dark red oil which crystallized upon standing.

MW=187.18; mp \leq 40°C; R_f = 0.85 (CH₂Cl₂/CCl₄ 1:1), red-orange color; ¹H-NMR (200 MHz, benzene-d₆) δ 5.75-5.85 (m, 1H), 6.20-6.25 (m, 1H), 6.30-6.40 (m, 1H), 6.83-7.05 (m, 3H), 7.50-7.60 (m, 2H), 9.1 (br s, 1H); ¹³C-NMR (50 MHz, benzene-d₆) δ 112.30, 117.15, 127.69, 128.20, 129.74, 130.31, 142.03, 146.67, 213.00; IR (KBr pellet) = 3360, 1520, 1400, 1380, 1255, 1220, 1097 (C=S), 1048, 1032 cm⁻¹; UV-Vis (MeOH) λ_{max} 310 (4.41), 390 (4.75), 536 (2.33) nm; LR-MS (EI, 150° C) m/e : 187 (85, M⁺), 154 (100, M⁺-SH), 110 (30), 77 (18); HR-MS (EI, 150° C) calc'd for C₁₁H₉NS: 187.0456, found 187.0455; Analysis calc'd for C₁₁H₉NS: C, 70.56; H, 4.84; N, 7.48; found: C, 70.28; H, 4.72; N, 7.33.

3.4 2-PYRROLYLTHIONATO-METAL COMPLEXES

(SP-4- *trans*)-Bis(2-pyrrolyl-2'-pyrrolylato- κ N-thione- κ S)nickel(II) (**29**)

General Procedure for the preparation of 2-pyrrolylthionato metal complexes

Thione **7** (0.5 g, 2.84 mmol) dissolved in MeOH (10 mL) was mixed with a solution of nickel(II) acetate tetrahydrate (2.5 g, 6.02 mmol) in MeOH (20 mL) and aqueous concentrated ammonia (0.2 mL). Rapid precipitation of a dark solid occurred. The mixture was stirred for an additional 12 h, the solid filtered off, dried under vacuum (50°C) and purified either by means of column chromatography (silica gel with CHCl₃ as eluent), or by repeated (2-3 times) recrystallization on a rotary evaporator by slow solvent exchange from CH₂Cl₂ to hexane or by slow evaporation of an acetone solution. Depending on the method chosen, up to 450 mg (78%) of an analytically pure dark green crystalline material was obtained.

MW = 409.15; mp = 273°C (d); R_f = 0.45 (1:1 CCl₄/CH₂Cl₂), brown color; ¹H-NMR (500 MHz, acetone-d₆) δ 6.36 (dd, *J* = 1.6, 5.8 Hz, 1H), 6.44 (m, 1H), 7.22 (dd, *J* = 0.9, 4.5 Hz, 1H), 7.24 (m, 1H), 7.32 (tr, 1.4 Hz, 1H), 7.37 (m, 1H), 11.2 (br s, 1H, exchangeable with D₂O); ¹³C-NMR (75 MHz, acetone-d₆) δ 113.4 (-CH=), 117.6 (-CH=), 119.4 (-CH=), 123.3 (-CH=), 128.8 (-CH=), 131.0 (=C=), 148.9 (-CH=), 151.0 (=C=), 175.9 (C=S); UV-Vis (acetone) λ_{\max} (log ϵ) 366 (4.38), 434 (4.75), 530 (4.23) nm; MS (EI, 220°) *m/e* 408 (100, M⁺), 374 (17.2), 341 (8.5), 288 (76.3), 176 (55.4, Ligand⁺); Analysis calc'd for C₁₈H₁₄N₄NiS₂: C, 52.84; H, 3.45; N, 13.69; S, 15.67; found: C, 53.10; H, 3.46; N, 13.35; S, 14.83.

(SP-4-*trans*)-(2-pyrrolyl-2'-pyrrolylato- κ N-thione- κ S)[2-(1-methyl)pyrrolyl-2'-pyrrolylato- κ N-thione- κ S]nickel(II) (**30**) and (SP-4-*trans*)-bis[2-(1-methyl)pyrrolyl-2'-pyrrolylato- κ N-thione- κ S]-nickel(II) (**31**)

Nickel complex **29** (200 mg, 3.94×10^{-4}) was suspended under anhydrous conditions in dry THF (25 mL). A 1.6 M solution of n-BuLi in THF (300 mL, 1.2 equivalents) was syringed into the cooled (-78°C) solution, upon which all remaining solids dissolved. After being stirred for 1h, the solution was allowed to warm up to 0°C , and was cooled again to -78°C . MeI (30 μL , 1.2 equivalents) was injected and the solution was allowed to warm up to r.t. The solution was quenched with MeOH (1 mL), diluted with CHCl_3 (50 mL), washed with water, dried over Na_2SO_4 and subjected to preparative TLC (silica gel, 1:3 mixture of CH_2Cl_2 and CCl_4). Three brown bands became visible. They were isolated, eluted with CH_2Cl_2 and evaporated to dryness. The least polar compound was starting material (30 mg, 15% recovery), the second band was the mono-N-methylated product **30** (125 mg, 61% yield), and the third, least polar compound, was the bis-N-methylated product **31** (20 mg, 9%). The outcome was changed to: **29** (5% recovery), **30** (22%), and **31** (55%) if, under otherwise identical conditions, 2.4 equivalents of n-BuLi and MeI were used.

(30):

MW = 437.20; mp ≥ 220 (d); $R_f = 0.65$ (1:1 $\text{CH}_2\text{Cl}_2/\text{CCl}_4$), brown color; $^1\text{H-NMR}$ (200 MHz, CDCl_3) δ 4.01 (s, 6H), 6.23 (s, 2H), 6.32 (s, 2H), 6.68 (s, 2H), 6.85 (s, 2H), 7.00 (s, 2H), 7.47 (s, 2H) (the splittings observed in the 500 Mhz spectrum of the parent compound **29**, and which are also expected to be present in **30** could not be resolved at 200 MHz, 32 scans); $^{13}\text{C-NMR}$ (50 MHz, CDCl_3) δ 33.2, 105.1, 114.1, 120.8, 127.8, 131.2, 146.2, 149.9, 151.1, 178.0; UV-Vis (CH_2Cl_2) λ_{max} (rel. intensity) 368 (0.53), 432 (1.0), 543 (0.39) nm; LR-MS (EI, 150°C) m/e 436 (100, M^+), 421 (9.2, M^+-CH_3), 403 (6.2), 248 (25.6, M^+ -ligand), 189 (ligand $^+$); HR-MS (EI, 150°C) m/e calc'd for $\text{C}_{20}\text{H}_{18}\text{N}_4\text{NiS}_2$: 436.0326, found 436.0328.

(31):

MW = 423.17; mp $\geq 200^\circ\text{C}$ (d); $R_f = 0.55$ (1:1 $\text{CCl}_4/\text{CH}_2\text{Cl}_2$), brown color; $^1\text{H-NMR}$ (200 MHz, CDCl_3) δ 4.07 (s, 3H), 6.23 (s, 1H), 6.25-6.4 (m, 2H), 6.45 (s, 1H), 6.68 (s, 1H), 6.85-7.0 (m, 3H), 7.11 (s, 1H), 7.20 (s, 1H), 7.40-7.45 (m, 2H), 9.6 (br s, 1H) (the splittings observed in the 500 Mhz spectrum of the parent compound **29**, cannot be resolved at 200 MHz, 32 scans); UV-Vis (CHCl_3) λ_{max} (rel. intensity) 368 (0.47), 434 (1.0), 534 (0.33) nm; LR-MS (EI, 200°) m/e 422 (100, M^+), 408 (36, M^+-CH_2), 246 (28), 189 (88, methylated ligand), 176 (63, non-methylated ligand); HR-MS (EI, 200°) m/e calc'd for $\text{C}_{18}\text{H}_{14}\text{N}_4\text{NiS}_2$: 422.0170, found 422.0157.

(SP-4-*trans*)-Bis[2-(3,4-dimethyl)pyrrolyl-2'-(3,4-dimethyl)pyrrolylato- κN -thione- κS]-nickel(II) (**36**)

This complex was prepared from tetramethylthione **22** and nickel acetate in 30% yield as described in the general procedure for the preparation of 2-pyrrolylthionato complexes.

MW = 521.36; $R_f = 0.33$ (1:1 $\text{CCl}_4/\text{CH}_2\text{Cl}_2$); $^1\text{H-NMR}$ (200 MHz, CDCl_3) δ 1.80 (s, 3H), 1.85 (s, 3H), 2.02 (s, 3H), 2.10 (s, 3H), 6.76 (s, 1H), 6.78 (s 1H), 7.30 (s, 1H), 8.12 (s, 1H), 9.3 br s (1H); UV-Vis (CHCl_3) λ_{max} (rel. intensity) 360 (sh), 424 (1.0), 508 (0.52); LR-MS (EI, 200°C) m/e 520 (12.6, M^+), 505 (0.9, M^+-CH_3), 459 (9.1), 424 (7.8, M^+ -dimethylpyrrole), 410 (4.4), 337 (9.1, M^+ -ligand), 322 (7.6, M^+ -ligand- CH_3), 232 (45.1), 184 (100, ligand $^+$); HR-MS (EI, 200°C) m/e calc'd for $\text{C}_{26}\text{H}_{30}\text{N}_4^{58}\text{NiS}_2$: 520.1265, found 520.1259.

(OC-6-*mer*)- (**33-I**) and (OC-6-*fac*)-Tris(2-pyrrolyl-2'-pyrrolylato- κN -thione- κS)-cobalt(III) (**33-II**)

Prepared in 22 % (**33-I**) and 19% (**33-II**) yield from thione **7** and cobalt(II) acetate in the presence of oxygen according to the general procedure for the preparation of

2-pyrrolylthionato complexes. The column chromatographically (silica-CHCl₃) prepurified metal complex mixture was further separated on a preparative TLC plate (1 mm silica gel, CH₂Cl₂:CCl₄ 1:3, multiple developments).

(33-I):

Slow evaporation of an acetone solution of **33-I** yielded dark ruby-red X-ray quality crystals: MW = 584.62; m.p. $\geq 150^\circ\text{C}$ (d)^o; R_f = 0.25 (CH₂Cl₂/CCl₄) dark brown-orange color; ¹H-NMR (300 MHz, acetone-d₆) δ 5.95 (s, 1H), 6.35-6.42 (m, 6H), 6.56 (dd, *J* = 1.2, 4.2 Hz, 1H), 7.10-7.20 (m, 3H), 7.24-7.30 (m, 2H), 7.34-7.37 (m, 2H), 7.46 (dd, *J* = 1.2, 4.5 Hz, 1H), 7.67 (s, 1H), 7.91 (s, 1H), 11.0 (br s, 3H); ¹³C-NMR (50 MHz, acetone-d₆) δ 112.1, 112.2, 112.3, 114.8, 114.9, 115.4, 120.4 (multiplet), 120.7, 123.3, 124.1 (multiplet), 126.9, 127.0 (multiplet), 131.6 (multiplet), 145.8, 147.7, 147.9, 151.1, 151.2, 151.4, 178.2, 178.4, 178.7; UV-Vis (CHCl₃) λ_{max} 416 nm; LR-MS (FAB, 3-NBA matrix) 643 (3.5, M⁺+Co), 585 (5.3, MH⁺), 409 (100, M⁺-ligand), 343 (23.0), 234 (78.1); LR-MS (FAB, 3-NBA matrix) *m/e* calc'd for C₂₇H₂₁N₆⁵⁹CoS₃: 584.03218, found 584.03505; Analysis calc'd for C₂₇H₂₁N₆CoS₃·1/2 H₂O: C, 54.63; H, 3.74; N, 14.16; found: C, 54.34; H, 3.66; N, 13.84.

(33-II):

MW = 584.62; m.p. $\geq 170^\circ\text{C}$ (d)^o; R_f = 0.12 (CH₂Cl₂/CCl₄), dark orange color; ¹H-NMR (200 MHz, acetone-d₆) δ 5.37 (s, 3H), 5.57 (m, 3H), 5.72 (dd, *J*=1.5, 4.2 Hz, 3H), 6.35 (m, 3H), 6.44 (s, 3H), 6.66 (d, 4.2H, 3H), 11.0 (br s, 3H); UV-Vis (CHCl₃) λ_{max} 424 nm; LR-MS (FAB, 3-NBA matrix) *m/e* 643 (4.1, M⁺+Co), 584 (3.5, MH⁺), 584 (3.3, M⁺), 409 (100, M⁺-ligand), 343 (23.2), 234 (76.1); HR-MS (FAB, 3-NBA matrix) *m/e* calc'd for C₂₇H₂₁N₆⁵⁹CoS₃: 584.03280, found 584.03184; Analysis calc'd for C₂₇H₂₁N₆CoS₃: C, 55.47; H, 3.62; N, 14.38; found: C, 55.04; H, 3.72; N, 14.11.

(T-4)-Bis(2-pyrrolyl-2'-pyrrolylato- κ N-thione- κ S)mercury(II) (32)

Prepared from mercury acetate and thione **7** according to the general procedure for the preparation of 2-pyrrolylthionato complexes. The crude metal complex precipitate was filtered, dried and loaded onto a short column of silica gel and eluted with CH_2Cl_2 . Slow evaporation of the fluorescent yellow CH_2Cl_2 solution yielded **32** as analytically pure shiny yellow hexagonal plates (33 % yield). The product is quite soluble only in polar solvents such as acetic acid, pyridine or DMSO.

MW = 551.05; mp = 181°C (d)^o; R_f = 0.45 (CH_2Cl_2), brilliant yellow color; ¹H-NMR (300 MHz, DMSO-*d*₆) δ 4.39 (s, 2H), 6.71 (d, *J* = 2.7 Hz, 2H), 6.98 (s, 2H), 7.30 (s, 2H), 7.38 (d, *J* = 3.3 Hz, 2H), 7.58 (s, 2H), 11.95 (s, 2H); ¹³C-NMR (75 MHz, pyridine-*d*₅) δ 112.3, 118.4, 121.8, 127.0, 127.0, 127.7, 146.9, 151.2, 173.4; UV-Vis (CH_2Cl_2) λ_{max} 402 (4.77), 452 (4.78) nm; Analysis calc'd for C₁₈H₁₄N₄HgS₂: C, 39.23; H, 2.56; N, 10.17; found: C, 38.88; H, 2.61; N, 9.85.

(SP-4)-Bis(2-pyrrolylato- κ N-thiobenzoyl- κ S)nickel(II) (42)

Prepared in 80% yield from thione **38** (100 mg) and nickel acetate in the presence of oxygen. Chromatography on a short column of silica gel with CH_2Cl_2 as eluent was used to purify the complex. The first purple fraction was collected and evaporated *in vacuo* to yield **42** as analytically pure microscopically fine dark purple needles. This complex is distinguished by a low solubility in polar and non-polar solvents, making NMR studies of the compound difficult. THF and dioxane dissolve sufficient material for ¹H-NMR, but not for ¹³C-NMR (typical 4k experiment).

MW = 431.19; R_f = 0.92 (1:1 $\text{CH}_2\text{Cl}_2/\text{CCl}_4$), dark purple color; mp = 234°C (d); ¹H-NMR (200 MHz, dioxane-*d*₈) δ 6.45 (dd, *J* = 4.0, 1.5 Hz, 2H), 6.90 (dd, *J* = 4.0, 1.5 Hz, 2H), 7.45-7.60 (m, 6H), 7.68 (s, 2H), 7.85 (dd, *J* = 8.0, 2 Hz, 4H); UV-Vis (CH_2Cl_2) λ_{max} (log ϵ) 312 (4.68), 390 (4.38), 506 (sh), 524 (4.00), 604 (sh) nm; LR-MS (EI, 150°C) 430 (100, M⁺),

397 (19.5), 308 (17.0), 245 (19.1, MH⁺-ligand), 186 (33.6, ligand), 154 (64.3); HR-MS (EI, 150°C) *m/e* calc'd for C₂₂H₁₆N₂⁵⁹NiS₂: 430.0108, found 430.0104; Analysis calc'd for C₂₂H₁₆N₂NiS₂: C, 61.28; H, 3.74; N, 6.50; found: C, 61.17; H, 3.53; N, 6.42.

(44-I) and **(44-II)** Tris(2-pyrrolylato-κN-thiobenzoyl-κS)cobalt(III) (tentative)

Prepared in 32 % **(44-I)** and 22 % **(44-II)** yield from thione **7** (200 mg) and cobalt(II) acetate in the presence of oxygen according to the general procedure for the preparation of 2-pyrrolylthionato complexes. The column chromatographically (silica-CHCl₃) prepurified metal complex mixture was further separated on a preparative TLC plate (1 mm silica gel-CH₂Cl₂:CCl₂ 1:2).

(44-I):

MW = 617.69; mp = 165°C (d); R_f = 0.89 (1:1 CH₂Cl₂/CCl₄), orange color; UV-Vis (CH₂Cl₂) λ_{max} 306 (4.78), 452 (4.39) nm; ¹H-NMR (200 MHz, CDCl₃) δ 6.09 (s, 1H), (d of t, *J* = 2, 6 Hz, 3H), 6.48 (d of t, *J* = 2, 6 Hz, 2H), 6.90 (t, *J* = 7 Hz, 2H), 6.99 (t, *J* = 7 Hz, 2H), 7.25-7.40 (m, 9H), 7.62-7.88 (m, 1H), 7.88 (s, 1H); ¹³C-NMR (50 MHz, CDCl₃) δ suggests the presence of 3(?) non-equivalent ligands; LR-MS (EI, 200°C) 617 (31.6, M⁺), 431 (96.1, M⁺-ligand), 308 (27.4, M⁺⁺), 187 (27.5, ligand), 154 (83.4); HR-MS (EI, 200°C) *m/e* calc'd for C₃₃H₂₄N₃⁵⁹CoS₃: 617.0464, found 617.0472; Analysis calc'd for C₃₃H₂₄N₃CoS₃: C, 64.17; H, 3.92; N, 6.80; found: C, 63.90; H, 4.14; N, 6.62.

(44-II):

MW = 617.69; mp = 185-190°C, upon cooling and reheating of the orange film, no melting is observed ≤ 240°C; R_f = 0.73 (1:1 CH₂Cl₂/CCl₄), brown color; the ¹H-NMR of this compound is due to the presence of (at least) 18 non-equivalent protons in the aromatic region, convoluted: ¹H-NMR (200 MHz, acetone-d₆) δ 6.30 (d, *J* = 5 Hz, 1H), 6.58 (d, *J* = 5 Hz, 1H), 6.67 (d, *J* = 5 Hz, 1H), 6.78 (d, *J* = 5 Hz, 1H), 6.8-7.2 (m, 10H), 7.2-7.5 (m, 6H),

7.5-7.7 (m, 4H); UV-Vis (CH₂Cl₂) λ_{\max} 312 (4.89), 446 (sh) nm; LR-MS (EI, 200°C) 617 (32.0, M⁺), 431 (100, M⁺-ligand), 308 (22.7, M⁺⁺), 187 (43.6, ligand), 154 (90.1); HR-MS (EI, 200°C) *m/e* calc'd for C₃₃H₂₄N₃⁵⁹CoS₃: 617.0464, found 617.0478.

(SP-4)-Bis[2-pyrrolylato- κ N-thioacetyl- κ S]nickel(II) (**41**)

Prepared in 81% yield from thione **37** and nickel acetate according to the general procedure. Slow evaporation of a MeOH solution yields fine long dark red needles.

MW = 307.05; mp = 212-214°C (phase transition - as seen through the microscope - at 177°C); R_f = 0.90 (CHCl₃), deep red color; ¹H-NMR (200 MHz, CDCl₃) δ 2.84 (s, 3H), 6.25 (d, 4.4H, 1H), 6.81 (m, 1H), 7.42 (s, 1H); ¹³C-NMR (50 MHz, CDCl₃) δ 22.7, 119.3, 123.5, 152.3, 155.6, 191.7; UV-Vis (log ϵ) λ_{\max} 370 (4.32), 282 (4.48), 474 (3.99), 496 (sh), 578 (3.58) nm; LR-MS (EI, 150°C) *m/e* = 306 (100, M⁺), 291 (15.6, M⁺-CH₃), 246 (18.3), 182 (27.8), 92 (67.0); HR-MS (EI, 150°C) *m/e* calc'd for C₁₂H₁₂N₂⁵⁸NiS₂: 305.9795, found 305.9803; Analysis calc'd for C₁₂H₁₂N₂NiS₂: C, 46.94; H, 3.94; N, 9.12; found: C, 47.13; H, 3.69; N, 8.92.

(OC-6)-Tris[2-pyrrolylato- κ N-thioacetyl- κ S]cobalt(III) (**43**)

This complex was prepared in 30% yield from thione **38** and cobalt(II) acetate in the presence of oxygen (air) analogous to the general procedure. Various chromatography systems could not detect or even separate the two isomers of the complex. Consequently, this compound was characterized as the 1:1 mixture (based on the integration of the ¹H-NMR) of its isomers.

MW = 431.47; R_f = 0.76 (1:1 CH₂Cl₂/CCl₄), bright yellow color; UV-Vis λ_{\max} 434 nm; ¹H-NMR (200 MHz, CDCl₃) δ 2.7-2.9 (m, 12H), 5.95 (s, 1H), 6.25-6.65 (m, 5H), 7.00-7.40 (m, 4H), 7.65 (s, 1H), 7.93 (s, 1H); ¹³C-NMR (75 MHz, CDCl₃) δ 22.7, 23.1, 23.2, 120.1, 120.2, 120.3, 122.6, 122.9, 123.5, 123.7, 147.6, 147.7, 149.7, 149.9, 154.0, 154.3, 154.7, 190.9,

191.1, 192.4; LR-MS (EI, 220°C) m/e = 431 (43.0, M⁺), 306 (100, M⁺-ligand), 291 (9.2, M⁺-ligand-CH₃), 184 (50.4), 149 (14.9), 125 (ligand⁺), 92 (85.0); HR-MS (EI, 220°C) m/e calc'd for C₁₈H₁₈N₃⁵⁹CoS₃: 430.9995, found 430.9987; Analysis calc'd for C₁₈H₁₈N₃CoS₃: C, 50.11; H, 4.20; N, 9.74; found: C, 50.34; H, 4.12; N, 9.63.

[2,10-dithiobenzoyl-κS,S'-5-phenyl-dipyrromethanato-κN,N']nickel(II) (**47**)

2,10-Dibenzoyldipyrromethane (**45**) (100 mg, 2.35 x 10⁻⁴ mol) dissolved in benzene was mixed with phosphorus pentasulfide (200 mg) and sonicated for 1h. As judged by TLC analysis, the reaction proceeded at first cleanly with little side products, but later produced a host of colored materials. Filtration followed by column chromatography (benzene/silica) produced an impure orange material (**46**), which was immediately dissolved in MeOH (5 mL) and mixed with an excess of nickel(II) acetate dissolved in a little MeOH. A brown precipitate formed which was filtered, dried and chromatographed (preparative plate, 0.5 mm, silica, 1:1 CH₂Cl₂:CCl₄). The major low polarity product of aubergine-brown color was isolated.

MW = 519.30, R_f = 0.77 (1:1 CH₂Cl₂/CCl₄), auburn; UV-Vis (rel. intensity) λ_{max} 266 (1.0), 378 (0.75), 410 (0.75), 466 (0.47), 524 (0.40), 702 (0.32) nm; LR-MS (EI, 180°C) m/e = 517 (100, M-H⁺), 518 (78.2, M⁺), 441 (23.2, M⁺-phenyl); HR-MS (EI, 180°C) m/e calc'd for C₂₉H₂₀N₂⁵⁸NiS₂: 518.04211, found 518.04181; paramagnetic as judged by the severe line broadening in the ¹H-NMR.

3.5 THE HYDRODESULFURIZATION OF 2-PYRROLYLTHIONES

2-Pyrrolylmethane (**2**)

2-Pyrrolylthione (1.0 g, 5.68 mmol) was dissolved in ethanol or THF (50 mL) containing conc. aqueous NH_3 or Et_3N (0.5 mL) and a 50% slurry of Raney nickel in water pH > 9 (4-10 mL) were added. The flask with the rapidly stirred mixture was connected at ambient temperature to a standard normal pressure hydrogenation apparatus. Alternatively, hydrogen was bubbled through the solution. Hydrodesulfurization set in instantaneously and was, depending on the activity of the Raney nickel, completed within 20 min to 12 h. In cases TLC analysis (or visual inspection; thione is orange, the product colorless) revealed the presence of starting material after several hours, more Raney nickel was added until all thione was consumed, upon which the Raney nickel was filtered off (! CAUTION !) and the solution reduced *in vacuo* to an oil. The oil was taken up in CHCl_3 and chromatographed on silica gel. The first fraction was collected and evaporated to dryness to yield up to 60% of **2** as crystalline, color- and odorless analytically pure material. The second fraction was identified as tetrapyrrolylethane **28**.

NOTE: At best, the reaction can be described as capricious. Rule of thumb, however, proved to be that the more active (the fresher) the Raney nickel and thus the faster the reaction, the better the yield and the less side-products were formed. The reaction was successfully scaled up to the reduction of 5.0 g of thione. Dipyrromethanes can be made visible on a TLC plate by fuming the plate with Br_2 vapors. Bright red spots indicate dipyrromethanes.⁸²

1,1',2,2'-tetrapyrrolylethane (28)

Isolated by column chromatography (2nd fraction) in low yield as a side product from the hydrodesulfurization of thione **7**.

MW = 290.37; R_f = 0.78 (CHCl₃/silica); ¹H-NMR (200 MHz, CDCl₃) δ 4.80 (s, 1H), 5.88 (m, 2H), 6.09 (dd, J = 4,3 Hz, 2H), 6.75 (m, 2H), 7.6 (br s, 2H); ¹³C-NMR (75 MHz, CDCl₃) δ 42.6, 107.4, 108.5, 112.2, 117.3, 131.2; LR-MS (EI, 220°C) m/e = 290 (10.0, M⁺), 288 (20, M⁺-2H), 222 (12.1, M⁺-pyrrolyl), 145 (MH₂⁺⁺-4H).

3.6 CRYSTAL STRUCTURE ANALYSES OF 6, 7, 29, 33-I, AND 32

Selected crystallographic data appear in Table 3-1 and 3-2. The final unit-cell parameters were obtained by least-squares on the setting angles for 25 reflections with $2\theta = 52.9\text{--}76.5^\circ$ for **7**, $99.7\text{--}115.0^\circ$ for **6**, $57.6\text{--}75.6^\circ$ for **29**, $23.0\text{--}31.3^\circ$ for **33-I**, and $26.1\text{--}38.2^\circ$ for **32**. The intensities of three standard reflections, measured every 200 reflections throughout the data collections, decayed linearly by 2.7% for **7** and remained constant for the four other compounds. The data were processed and corrected for Lorentz and polarization effects, decay (for **7**), and absorption (empirical, based on azimuthal scans).⁸³

The structures of **6**, **7**, **29**, were solved by direct methods and those of **33-I** and **32** were solved by conventional heavy atom methods; the heavy atom coordinates being determined from the Patterson function and those of the remaining non-hydrogen atoms from subsequent difference Fourier syntheses. The structure analyses of **29** and **32** were initiated in the centrosymmetric space groups $R\bar{3}$ and $P\bar{1}$, respectively, on the basis of the E -statistics and the appearances of the Patterson functions. These choices were confirmed by the subsequent successful solutions and refinements of the structures. Crystals of **29** contain 0.28 water molecules per nickel complex, located on the threefold axis. The population parameter for the oxygen atom was refined. Complex **33-I** crystallizes as an acetone solvate.

All non-hydrogen atoms were refined with anisotropic thermal parameters. The hydrogen atoms in **6** and **7** were refined with isotropic thermal parameters and those in the metal complexes **29**, **32**, and **33-I** were fixed in calculated positions ($N\text{--}H = 0.91 \text{ \AA}$, $C\text{--}H = 0.98 \text{ \AA}$, $B_H = 1.2 B_{\text{bonded atom}}$). The hydrogen atoms associated with the water molecule in **29** were not included in the model. Secondary extinction corrections (Zachariasen type 2 isotropic) were applied where appropriate, the final values of the extinction coefficient being

$4.60(11) \times 10^{-6}$ for **7**, $2.27(3) \times 10^{-4}$ for **6**, and $2.6(3) \times 10^{-6}$ for **32**. Neutral atom scattering factors for all atoms and anomalous dispersion corrections for the non-hydrogen atoms were taken from the *International Tables for X-Ray Crystallography*.^{84,85} Final atomic coordinates and equivalent isotropic thermal parameters of **6**, **7**, **29**, **32**, and **33-I**, and selected bond lengths in compounds **6**, **7**, and **29** appear in Tables 3-3 - 3-10.

Table 3-1 Crystallographic data for **6** and **7**

compound	7	6
formula	C ₉ H ₈ N ₂ S	C ₉ H ₈ N ₂ O
MW	176.24	160.18
crystal system	orthorhombic	orthorhombic
space group	Pbca (#61)	P2 ₁ 2 ₁ 2 ₁ (#19)
a, Å	13.9380(8)	8.6496(4)
b, Å	16.559(1)	15.0622(5)
c, Å	7.3620(9)	5.9536(7)
V, Å ³	1699.1(2)	775.65(8)
Z	8	8
ρ_{calc} , g/cm ³	1.378	1.372
T, °C	21	21
radiation	Cu	Cu
λ , Å	1.54178	1.54178
μ , cm ⁻¹	28.85	7.56
Transmission factors	0.79-1.00	0.77-1.00
R (F)	0.031	0.025
R ω (F)	0.028	0.026

Table 3-2 Crystallographic data for 29, 33-I, and 32

compound	29·0.28 H ₂ O	33-I·Me ₂ CO	32
formula	C ₁₈ H ₁₄ N ₄ NiS ₂ · 0.28 H ₂ O	C ₂₇ H ₂₁ CoN ₆ S ₃ · C ₃ H ₆ O	C ₁₈ H ₁₄ HgN ₄ S ₂
MW	414.25	642.70	551.05
crystal system	trigonal	monoclinic	triclinic
space group	R $\bar{3}$	P21/n	PT
a, Å	18.467(1)	9.569(1)	8.443(2)
b, Å	18.467(1)	23.152(1)	14.278(1)
c, Å	26.404(2)	13.659(1)	7.445(1)
α , deg	90	90	90.561(9)
β , deg	90	100.882(8)	97.64(1)
γ , deg	120	90	104.250(9)
V, Å ³	7797(1)	2971.6(5)	861.3(2)
Z	18	4	2
ρ_{calc} , g/cm ³	1.588	1.436	2.125
T, °C	21	21	21
radiation	Cu	Mo	Mo
λ , Å	1.54178	0.71069	0.71069
μ , cm ⁻¹	39.47	8.11	92.10
Transmission factors	0.77-1.00	0.93-1.00	0.40-1.00
R (F)	0.032	0.043	0.042
R ω (F)	0.033	0.038	0.040

Table 3-3 Atomic coordinates and $B_{eq.} [\text{\AA}^2]^a$ for **7**

atom	x	y	z	$B_{eq.}$
S(1)	0.39455(5)	0.48484(4)	0.74769(11)	5.21(3)
N(1)	0.5661(2)	0.38847(14)	0.8750(4)	4.9(1)
N(2)	0.3543(2)	0.43749(14)	0.3585(3)	4.5(1)
C(1)	0.5402(2)	0.38073(14)	0.6952(3)	4.0(1)
C(2)	0.6163(2)	0.3411(2)	0.6127(4)	5.0(1)
C(3)	0.6857(2)	0.3264(2)	0.7428(6)	6.2(2)
C(4)	0.6534(3)	0.3562(2)	0.9033(5)	5.9(2)
C(5)	0.4203(2)	0.39185(14)	0.4509(3)	3.9(1)
C(6)	0.4385(2)	0.3254(2)	0.3415(4)	4.8(1)
C(7)	0.3842(2)	0.3328(2)	0.1849(4)	5.5(2)
C(8)	0.3327(2)	0.4031(2)	0.1978(4)	5.2(2)
C(9)	0.4536(2)	0.41585(13)	0.6275(3)	3.9(1)

$$^a B_{eq.} = (8/3)\pi^2 \sum \sum U_{ij} a_i^* a_j^* (\mathbf{a}_i \cdot \mathbf{a}_j).$$

Table 3-4 Atomic coordinates and $B_{eq.} [\text{\AA}^2]^a$ for **6**

atom	x	y	z	$B_{eq.}$
O(1)	0.31440(13)	0.41645(8)	0.3281(2)	4.77(6)
N(1)	0.4453(2)	0.47233(8)	0.7272(3)	3.89(6)
N(2)	0.4197(2)	0.27586(10)	0.0795(3)	4.28(6)
C(1)	0.5083(2)	0.40582(9)	0.5977(3)	3.22(5)
C(2)	0.6511(2)	0.38657(10)	0.6926(3)	3.76(6)
C(3)	0.6720(2)	0.44165(12)	0.8778(3)	4.44(8)
C(4)	0.5423(2)	0.49391(11)	0.8949(3)	4.31(7)
C(5)	0.4791(2)	0.29469(9)	0.2873(3)	3.28(5)
C(6)	0.5767(2)	0.22508(10)	0.3415(3)	3.81(6)
C(7)	0.5746(2)	0.16511(10)	0.1631(3)	4.39(7)
C(8)	0.4782(2)	0.19864(12)	0.0031(3)	4.69(8)
C(9)	0.4280(2)	0.37489(9)	0.4014(3)	3.30(6)

$$^a B_{eq.} = (8/3)\pi^2 \sum \sum U_{ij} a_i^* a_j^* (\mathbf{a}_i \cdot \mathbf{a}_j).$$

Table 3-5 Atomic coordinates and B_{eq} . [\AA^2]^a for **29**

atom	x	y	z	B_{eq} .
Ni(1)	0.49475(3)	0.07878(3)	0.07322(2)	4.56(2)
S(1)	0.58538(5)	0.17915(5)	0.12261(3)	5.39(3)
S(2)	0.39574(5)	-0.02117(5)	0.02920(3)	5.41(3)
O(1) ^b	1/3	-1/3	0.2043(4)	29.6(9)
N(1)	0.50356(15)	0.00355(15)	0.11670(9)	4.5(1)
N(2)	0.7004(2)	0.2433(2)	0.21370(10)	6.2(1)
N(3)	0.4889(2)	0.1527(2)	0.02731(9)	5.0(1)
N(4)	0.2779(2)	-0.0929(2)	-0.05750(10)	6.8(1)
C(1)	0.5556(2)	0.0334(2)	0.15896(11)	4.6(1)
C(2)	0.5559(2)	-0.0356(2)	0.18252(11)	5.2(1)
C(3)	0.5046(2)	-0.1050(2)	0.15545(12)	5.6(1)
C(4)	0.4732(2)	-0.0788(2)	0.11482(11)	5.0(1)
C(5)	0.6470(2)	0.1580(2)	0.21166(12)	5.2(1)
C(6)	0.6495(2)	0.1274(2)	0.25880(13)	6.4(2)
C(7)	0.7052(2)	0.1946(3)	0.28848(13)	7.1(2)
C(8)	0.7363(2)	0.2651(3)	0.26016(14)	7.0(2)
C(9)	0.5973(2)	0.1184(2)	0.16772(11)	4.7(1)
C(10)	0.4341(2)	0.1228(2)	-0.01337(11)	5.0(1)
C(11)	0.4485(3)	0.1918(3)	-0.04331(13)	6.5(2)
C(12)	0.5112(3)	0.2615(2)	-0.02111(14)	7.1(2)
C(13)	0.5342(2)	0.2355(2)	0.02250(13)	6.0(2)
C(14)	0.3230(2)	-0.0072(2)	-0.05608(12)	5.5(1)
C(15)	0.2988(2)	0.0189(3)	-0.09895(13)	7.0(2)
C(16)	0.2410(3)	-0.0510(3)	-0.12473(14)	8.1(2)
C(17)	0.2283(2)	-0.1198(3)	-0.0988(2)	8.0(2)
C(18)	0.3820(2)	0.0355(2)	-0.01720(10)	4.9(1)

^a $B_{eq} = (8/3)\pi^2 \sum \sum U_{jj} a_j^* a_j^* (\mathbf{a}_i \cdot \mathbf{a}_j)$. ^b Occupancy 0.28(?).

Table 3-6 Atomic coordinates and $B_{eq.}$ [\AA^2] for 32

atom	x	y	z	$B_{eq.}$
Hg(1)	0.58772(5)	0.28497(2)	0.47148(5)	3.982(9)
S(1)	0.5259(3)	0.1566(1)	0.6879(3)	3.71(5)
S(2)	0.7658(3)	0.3895(1)	0.2812(3)	3.39(5)
N(1)	0.3547(8)	0.1834(4)	0.3044(9)	3.1(2)
N(2)	0.3828(8)	-0.0473(4)	0.7831(9)	2.9(1)
N(3)	0.6162(7)	0.4310(4)	0.6256(9)	2.6(1)
N(4)	0.9970(8)	0.5781(4)	0.2049(9)	3.1(2)
C(1)	0.3089(9)	0.0926(5)	0.380(1)	2.5(2)
C(2)	0.2143(9)	0.0269(5)	0.237(1)	3.2(2)
C(3)	0.209(1)	0.0766(6)	0.083(1)	3.7(2)
C(4)	0.297(1)	0.1736(6)	0.129(1)	3.5(2)
C(5)	0.2953(9)	-0.0133(5)	0.641(1)	2.6(2)
C(6)	0.1426(10)	-0.0768(5)	0.610(1)	3.3(2)
C(7)	0.137(1)	-0.1493(6)	0.735(1)	3.9(2)
C(8)	0.290(1)	-0.1305(5)	0.837(1)	3.7(2)
C(9)	0.3656(9)	0.0751(5)	0.555(1)	2.8(2)
C(10)	0.7246(9)	0.5089(5)	0.550(1)	2.5(2)
C(11)	0.7639(10)	0.5871(5)	0.686(1)	3.1(2)
C(12)	0.687(1)	0.5561(6)	0.828(1)	3.5(2)
C(13)	0.5976(10)	0.4599(6)	0.783(1)	3.3(2)
C(14)	0.8812(9)	0.5835(5)	0.311(1)	2.7(2)
C(15)	0.866(1)	0.6780(5)	0.311(1)	3.6(2)
C(16)	0.980(1)	0.7294(6)	0.204(1)	4.4(2)
C(17)	1.059(1)	0.6669(7)	0.144(1)	3.9(2)
C(18)	0.7860(9)	0.4995(5)	0.393(1)	2.5(2)

$$^a B_{eq.} = (8/3)\pi^2 \sum \sum U_{ij} a_i^* a_j^* (a_i a_j)$$

Table 3-7 Atomic coordinates and B_{eq} [\AA^2]^a for 33-I

atom	x	y	z	B_{eq}
Co(1)	0.20859(6)	0.11862(3)	0.28419(5)	3.91(3)
S(1)	0.10078(12)	0.07503(5)	0.14303(9)	4.62(5)
S(2)	0.31742(12)	0.16215(5)	0.42579(9)	4.85(6)
S(3)	0.42120(11)	0.09826(5)	0.24821(9)	4.55(5)
O(1)	0.6569(5)	0.0822(2)	0.0432(4)	11.5(3)
N(1)	0.1973(3)	0.18775(15)	0.2045(3)	4.0(2)
N(2)	-0.0616(4)	0.0771(2)	-0.0705(3)	5.5(2)
N(3)	0.0336(3)	0.1364(2)	0.3307(3)	4.5(2)
N(4)	0.3177(4)	0.2161(2)	0.6264(3)	6.1(2)
N(5)	0.2243(3)	0.0460(2)	0.3515(2)	4.0(2)
N(6)	0.6566(4)	0.0135(2)	0.2263(3)	5.5(2)
C(1)	0.1344(4)	0.1859(2)	0.1043(3)	4.0(2)
C(2)	0.1294(5)	0.2424(2)	0.0642(4)	5.0(2)
C(3)	0.1896(5)	0.2777(2)	0.1409(4)	5.3(3)
C(4)	0.2299(5)	0.2430(2)	0.2256(4)	4.9(2)
C(5)	0.0216(4)	0.1240(2)	-0.0389(3)	4.4(2)
C(6)	0.0342(5)	0.1544(2)	-0.1233(4)	5.5(3)
C(7)	-0.0446(6)	0.1262(2)	-0.2049(4)	6.1(3)
C(8)	-0.1031(5)	0.0790(2)	-0.1714(4)	6.0(3)
C(9)	0.0839(4)	0.1319(2)	0.0642(3)	4.0(2)
C(10)	0.0384(5)	0.1616(2)	0.4181(4)	4.6(2)
C(11)	-0.1032(5)	0.1641(2)	0.4391(4)	6.1(3)
C(12)	-0.1902(5)	0.1393(2)	0.3608(5)	6.5(3)
C(13)	-0.1012(5)	0.1232(2)	0.2920(4)	5.6(3)
C(14)	0.1873(5)	0.2057(2)	0.5691(4)	4.8(2)
C(15)	0.0912(6)	0.2315(3)	0.6214(5)	7.7(3)
C(16)	0.1692(8)	0.2553(3)	0.7081(5)	8.9(4)
C(17)	0.3101(7)	0.2455(3)	0.7100(4)	7.3(3)
C(18)	0.1693(5)	0.1779(2)	0.4755(4)	4.5(2)
C(19)	0.3444(5)	0.0112(2)	0.3534(3)	4.0(2)
C(20)	0.3267(5)	-0.0404(2)	0.4046(3)	5.0(2)

C(21)	0.1979(6)	-0.0358(2)	0.4332(3)	5.6(3)
C(22)	0.1357(5)	0.0166(2)	0.3987(3)	4.7(2)
C(23)	0.5756(5)	0.0007(2)	0.2974(4)	4.8(2)
C(24)	0.6491(5)	-0.0426(2)	0.3553(4)	6.0(3)
C(25)	0.7692(6)	-0.0555(2)	0.3180(5)	7.1(3)
C(26)	0.7726(5)	-0.0208(2)	0.2380(5)	6.5(3)
C(27)	0.4494(4)	0.0322(2)	0.3044(3)	4.1(2)
C(28)	0.5762(8)	0.1099(3)	-0.0140(6)	8.7(4)
C(29)	0.6254(9)	0.1547(3)	-0.0774(7)	14.4(6)
C(30)	0.4243(8)	0.1043(5)	-0.0258(6)	16.1(7)

$${}^a B_{eq} = (8/3)\pi^2 \sum \sum U_{ij} a_i^* a_j^* (\mathbf{a}_i \cdot \mathbf{a}_j)$$

Table 3-8 Selected bond lengths in **7** with estimated standard deviations in parentheses

Bond	Length	Bond	Length
S(1)—C(9)	1.663(2)	C(2)—C(3)	1.382(4)
N(1)—C(1)	1.378(3)	C(3)—C(4)	1.357(4)
N(1)—C(4)	1.346(4)	C(5)—C(6)	1.387(3)
N(2)—C(5)	1.370(3)	C(5)—C(9)	1.437(3)
N(2)—C(8)	1.348(3)	C(6)—C(7)	1.384(4)
C(1)—C(2)	1.387(4)	C(7)—C(8)	1.372(4)
C(1)—C(9)	1.430(3)		

Table 3-9. Selected bond lengths in **6** with estimated standard deviations in parentheses

Bond	Distance [Å]	Bond	Distance [Å]
O(1)—C(9)	1.244(2)	C(2)—C(3)	1.392(2)
N(1)—C(1)	1.376(2)	C(3)—C(4)	1.375(2)
N(1)—C(4)	1.344(3)	C(5)—C(6)	1.384(2)
N(2)—C(5)	1.369(2)	C(5)—C(9)	1.455(2)
N(2)—C(8)	1.348(2)	C(6)—C(7)	1.394(2)
C(1)—C(2)	1.389(2)	C(7)—C(8)	1.363(3)
C(1)—C(9)	1.437(2)		

Table 3-10. Selected bond lengths in **29** with estimated standard deviations in parentheses

Bond	Distance [Å]	Bond	Distance [Å]
Ni(1)—S(1)	2.1988(9)	C(1)—C(9)	1.380(4)
Ni(1)—S(2)	2.1740(9)	C(2)—C(3)	1.355(4)
Ni(1)—N(1)	1.871(2)	C(3)—C(4)	1.416(4)
Ni(1)—N(3)	1.869(2)	C(5)—C(6)	1.377(4)
S(1)—C(9)	1.724(3)	C(5)—C(9)	1.432(4)
S(2)—C(18)	1.711(3)	C(6)—C(7)	1.391(4)
N(1)—C(1)	1.394(3)	C(7)—C(8)	1.356(5)
N(1)—C(4)	1.332(3)	C(10)—C(11)	1.408(4)
N(2)—C(5)	1.379(4)	C(10)—C(18)	1.408(4)
N(2)—C(8)	1.357(4)	C(11)—C(12)	1.360(5)
N(3)—C(10)	1.387(4)	C(12)—C(13)	1.392(4)
N(3)—C(13)	1.332(4)	C(14)—C(15)	1.389(4)
N(4)—C(14)	1.372(4)	C(14)—C(18)	1.415(4)
N(4)—C(17)	1.349(4)	C(15)—C(16)	1.376(5)
C(1)—C(2)	1.420(4)	C(16)—C(17)	1.356(5)

5. LIST OF REFERENCES

- (1) Kim, J. B.; Adler, A. D.; Longo, F. R. In *The Porphyrins*; D. Dolphin, Ed.; Academic Press: New York, 1978; Vol. 1; pp 85-100.
- (2) Lin, V. S.-Y.; DiMagno, S. G.; Therien, M. J. *Science* **1994**, *264*, 1105.
- (3) Boyle, R. W.; Johnson, C. K.; Dolphin, D. H. *J. Chem. Soc., Chem. Comm.* **1995**, 527.
- (4) Treibs, A.; Häberle, N. *Liebigs Ann. Chem.* **1968**, *718*, 183.
- (5) Manka, J. S.; Lawrence, D. S. *Tetrahedron Lett.* **1989**, *30*, 6989.
- (6) Boyle, R. W.; Brückner, C.; Posakony, J.; James, B. R.; Dolphin, D. H. manuscript in preparation.
- (7) Ballantine, J. A.; Jackson, A. H.; Kenner, G. W.; McGillivray, G. *Tetrahedron, Supplement 1* **1966**, *22*, 241.
- (8) Biswas, K. M.; Houghton, L. E.; Jackson, A. H. *Tetrahedron, Supplement 7* **1966**, *22*, 261.
- (9) Clezy, P. S.; Smythe, G. A. *Aust. J. Chem.* **1969**, *22*, 239.
- (10) Fischer, H.; Orth, H. *Die Chemie des Pyrrols*; Akademische Verlagsgesellschaft: Leipzig, 1937; Vol. I, pp 335.
- (11) Eckert, H.; Foster, B. *Angew. Chem., Int. Ed. Engl.* **1987**, *26*, 894.
- (12) In *Comprehensive Organic Chemistry*; D. Barton and W.D. Ollis, Ed.; Pergamon Press: Oxford, New York, Toronto, Sydney, Paris, Frankfurt, 1979; Vol. 3.
- (13) Caubère, P. and Coutrot, P. In *Comprehensive Organic Synthesis*; B. M. Trost and I. Fleming, Ed.; Pergamon Press: Oxford, New York, Seoul, Tokyo, 1991; Vol. 8., Chapter 4.3.
- (14) Garcia, J. J.; Maitlis, P. M. *J. Am. Chem. Soc.* **1993**, *115*, 12200.
- (15) Kuimelis, R. G.; Nambiar, K. P. *Tetrahedron Lett.* **1993**, *34*, 3813.

- (16) Luo, S.; Ogilvy, A. E.; Rauchfuss, T. B.; Rheingold, A. L.; Wilson, S. R. *Organometallics* **1991**, *10*, 12192.
- (17) Hauptmann, H.; Walter, W. F. *Chem. Rev.* **1962**, *62*, 347.
- (18) Farnier, M.; Soth, S.; Fournari, P. *Can. J. Chem.* **1976**, *54*, 1083.
- (19) Duus, F. In *Comprehensive Organic Chemistry*; D. Barton and W. D. Ollis, Ed.; Pergamon Press: Oxford, New York, Toronto, Sydney, Paris, Frankfurt, 1979; Vol. 3; pp 374.
- (20) Woodward, R. B.; Ayer, W. A.; Beaton, J. M.; Bickelhaupt, F.; Bonnett, R.; Buchschacher, P.; Closs, G. L.; Dutler, H.; Hannah, J.; Hauck, F. P.; Ito, S.; Langemann, A.; LeGoff, E.; Leimgruber, W.; Lwowski, W.; Sauer, J.; Valenta, Z.; Volz, H. *J. Am. Chem. Soc.* **1960**, *82*, 3800.
- (21) Woodward, R. B.; Ayer, W. A.; Beaton, J. M.; Bickelhaupt, F.; Bonnett, R.; Buchschacher, P.; Closs, G. L.; Dutler, H.; Hannah, J.; Hauck, F. P.; Ito, S.; Langemann, A.; LeGoff, E.; Leimgruber, W.; Lwowski, W.; Sauer, J.; Valenta, Z.; Volz, H. *Tetrahedron* **1990**, *46*, 7599.
- (22) Reid, D. H.; McKenzie, S. *J. Chem. Soc. (C)* **1970**, 145.
- (23) Mackie, R. K.; McKenzie, S.; Reid, D. H.; Webster, R. G. *J. Chem. Soc., Perkin Trans. 1* **1973**, 657.
- (24) Treibs, A. *Liebigs Ann. Chem.* **1969**, 723, 129.
- (25) Jensen, K. A.; Anthoni, U.; Kägi, B.; Larsen, C.; Pedersen, T. C. *Acta Chem. Scand.* **1968**, *22*, 1.
- (26) Treibs, A.; Schulze, L.; Kreuzer, F.-H.; Kolm, H.-G. *Liebigs Ann. Chem.* **1973**, 207.
- (27) Steliou, K.; Mrani, M. *J. Am. Chem. Soc.* **1982**, *104*, 3104.
- (28) Scheeren, J. W.; Ooms, P. H. J.; Nivard, R. J. F. *Synthesis* **1973**, *3*, 149.
- (29) Machiguchi, T. *Tetrahedron* **1995**, *51*, 1133.
- (30) Cava, M. C.; Levinson, M. I. *Tetrahedron* **1985**, *22*, 5061.
- (31) Murase, M.; Yoshida, S.; Hosaka, T.; Tobinaga, S. *Chem. Pharm. Bull.* **1991**, *39*, 489.
- (32) Paquer, D. *Internat. J. Sulfur Chem.* **1973**, *8*, 173.
- (33) de Mayo, P. *Acc. Chem. Res.* **1976**, *9*, 52.
- (34) Coyle, J. D. *Tetrahedron* **1985**, *41*, 5393.
- (35) Maciejewski, A.; Steer, R. P. *Chem. Rev.* **1993**, *93*, 67.

-
- (36) Pushkara Rao, V.; Nageshwer Rao, B.; Ramamurthy, V. In *CRC Handbook of Organic Photochemistry and Photobiology*; W. M. Horspool and P.-S. Song, Ed.; CRC Press: Boca Raton, New York, London, Tokyo, 1995; pp 793-803.
- (37) Ramamurthy, V.; Nageshwer Rao, B.; Pushkara Rao, V. In *CRC Handbook of Organic Photochemistry and Photobiology*; W. M. Horspool and P.-S. Song, Ed.; CRC Press: Boca Raton, New York, London, Tokyo, 1995; pp 775-792.
- (38) Akbar Ali, M.; Livingstone, S. E. *Coord. Chem. Rev.* **1974**, *13*, 101.
- (39) Halcrow, M. A. *Angew. Chem., Int. Ed. Engl.* **1995**, *34*, 1193.
- (40) Fee, J. *Struct. Bond.* **1975**, *23*, 1.
- (41) Emptage, M. H. In *Metal Clusters in Proteins*; L. Que, Ed.; American Chemical Society: Washington, 1988; Vol. 372.
- (42) Dawson, J. H.; Sono, M. *Chem. Rev.* **1987**, *87*, 1255.
- (43) Williams, R. J. P. *Coord. Chem. Rev.* **1990**, *100*, 573.
- (44) Gray, H. B.; Malstrøm, B. G. *Biochemistry* **1989**, *28*, 7499.
- (45) *Bioinorganic Chemistry*; Bertini, I.; Gray, H. B.; Lippard, S. J.; Valentine, J., Ed.; University Science Books: Mill Valley, CA, 1994.
- (46) Kaim, W.; Schwederski, B. *Bioanorganische Chemie*; Teubner: Stuttgart, 1991.
- (47) Cowan, J. A. *Inorganic Biochemistry: An Introduction*; VCH: New York, Weinheim, Cambridge, 1993.
- (48) Theil, E. C.; Raymond, K. N. In *Bioinorganic Chemistry*; Bertini, I.; Gray, H.B.; Lippard, S.J. and Valentine, J., Ed.; University Science Books: Mill Valley, CA, 1991; pp 1-35.
- (49) Greenaway, F. T.; Brown, L. M.; Dabrowiak, J. C.; Thompson, M. R.; Day, V. M. *J. Am. Chem. Soc.* **1980**, *102*, 7782.
- (50) French, F. A.; Blanz, E. J. *J. Med. Chem.* **1966**, *9*, 585.
- (51) Jurisson, S. *Inorg. Chem.* **1986**, *25*, 543.
- (52) John, E. K.; Green, M. A. *J. Med. Chem.* **1990**, *33*, 1704.
- (53) Parker, D. *Chem. Br.* **1994**, *10*, 818.
- (54) Lauffer, R. B. *Chem. Rev.* **1987**, *87*, 901.
- (55) Bell, J. D.; Sadler, P. J. *Chemi Bri.* **1993**, 597.
- (56) Vagg, R. S. In *Comprehensive Coordination Chemistry*; G. Wilkinson, R. D. Gillard and J. A. McCleverty, Ed.; Pergamon Press: Oxford, 1987; Vol. 2; pp 793-812.

- (57) Livingstone, S. E. In *Comprehensive Coordination Chemistry*; G. Wilkinson, R. D. Gillard and J. A. McCleverty, Ed.; Pergamon Press: Oxford, 1987; Vol. 2; pp 633-660.
- (58) McAuliffe, C. A. *Adv. Inorg. Chem. Radiochem.* **1975**, *17*, 165.
- (59) Kuehn, C. A.; Isied, S. S. *Prog. Inorg. Chem.* **1980**, *27*, 153.
- (60) Chivers, T. *Chem. Rev.* **1985**, *85*, 341.
- (61) Kelly, P. F.; Woollins, J. D. *Polyhedron* **1986**, *5*, 607.
- (62) Dance, I. G. *Polyhedron* **1986**, *5*, 1037.
- (63) Chivers, T.; Edelman, F. *Polyhedron* **1986**, *5*, 1661.
- (64) Reedijk, S. E. In *Comprehensive Coordination Chemistry*; G. Wilkinson, R. D. Gillard and J. A. McCleverty, Ed.; Pergamon Press: Oxford, 1987; Vol. 2; pp 73-98.
- (65) Foulds, G. A. *Coord. Chem. Rev.* **1990**, *98*, 1.
- (66) Trovimenko, S. *Chem. Rev.* **1972**, *72*, 497.
- (67) Hieber, W.; Brück, R. *Z. Anorg. Allg. Chem.* **1952**, *269*, 13.
- (68) Livingstone, S. E. *J. Chem. Soc.* **1956**, 437.
- (69) Livingstone, S. E. *J. Chem. Soc.* **1956**, 1042.
- (70) Amari, C.; Pelizzi, C.; Pelizzi, G.; Predieri, G.; Sartori, G. *Inorg. Chim. Acta* **1994**, *223*, 97.
- (71) Clezy, P. S.; Smythe, G. A. *Aust. J. Chem.* **1969**, *22*, 242.
- (72) Cheng, C. L.; John, I. G.; Ritchie, G. L. D.; Gore, P. H. *J. Chem. Soc., Perkin Trans. 2* **1974**, 1318.
- (73) English, R. B.; McGillivray, G.; Smal, E. *Acta Crystallogr., Sect. B* **1980**, *36*, 1136.
- (74) Lumbroso, H.; Liégeois, C.; Pappalardo, G. C.; Andrieu, C. G. *J. Mol. Struct.* **1984**, *112*, 85.
- (75) Klose, G.; Arnold, K.; Eckelmann, U.; Uhlemann, E. *Tetrahedron* **1972**, *28*, 6019.
- (76) Carlsen, L.; Duus, F. *J. Am. Chem. Soc.* **1978**, *100*, 281.
- (77) Busch, D. H.; Stephenson, N. A. *Coord. Chem. Rev.* **1990**, *11*, 119.
- (78) Computational results obtained using *Discover*[®] 2.9.5./94.0 (ESFF 91 force field) from Biosym Technologies, San Diego, U.S.A. on a SGI Personal Iris work station.
- (79) James, T. L.; Smith, D. M.; Holm, R. H. *Inorg. Chem.* **1994**, *33*, 4869.

-
- (80) Schweizer, E. E.; Light, K. K. *J. Org. Chem.* **1966**, *31*, 2912.
- (81) White, J.; McGillivray, G. *J. Org. Chem.* **1977**, *42*, 4248.
- (82) Paine III, J. B. In *The Porphyrins*; D. Dolphin, Ed.; Academic Press: New York, 1978; Vol. 1; pp 101-234.
- (83) In Molecular Structure Corporation: The Woodlands, TX, 1985 & 1992.
- (84) (a) *International Tables for X-Ray Crystallography*; Kynoch Press: Birmingham, UK, 1974; Vol. IV, pp 99-102, 149-150. (b) *International Tables for Crystallography*; Kluwer Academic Publishers: Boston, 1992; Vol. C, pp 219-222.